Volume 13, Issue 3, September 2023
pISSN 2158-0510 eISSN 2158-0529

IJBM

International Journal of BIOMEDICINE

www.ijbm.org

IJBM

INTERNATIONAL JOURNAL OF BIOMEDICINE

Aims and Scope: *International Journal of Biomedicine* (IJBM) is an open access journal. IJBM publishes peer-reviewed articles on aspects of basic, applied, and translational research in biology and medicine. Authors are invited to submit Original clinical and experimental research studies, Review articles, Case reports, Perspectives, and Viewpoints. All research studies involving animals must have been conducted following animal welfare guidelines such as the National Institutes of Health (NIH) Guide for the Care and Use of Laboratory Animals, or equivalent documents. Studies involving human subjects or tissues must adhere to the Declaration of Helsinki and Title 45, US Code of Federal Regulations, Part 46, Protection of Human Subjects, and must have received approval from the appropriate institutional committee charged with oversight of human studies. Informed consent must be obtained.

International Journal of Biomedicine endorses and behaves in accordance with the codes of conduct and international standards established by the Committee on Publication Ethics (COPE).

International Journal of Biomedicine (ISSN 2158-0510) is published four times a year by International Medical Research and Development Corp. (IMRDC), 442 5th Avenue #1196, Manhattan, NY 10018, USA

Customer Service: International Journal of Biomedicine, 442 5th Avenue #1196, Manhattan, NY 10018, USA; Tel: 1-917-740-3053; E-mail: editor@ijbm.org

Manuscript Submission: Original works will be accepted with the understanding that they are contributed solely to the Journal, are not under review by another publication, and have not previously been published except in abstract form. Accepted manuscripts become the sole property of the Journal and may not be published elsewhere without the consent of the Journal. A form stating that the authors transfer all copyright ownership to the Journal will be sent from the Publisher when the manuscript is accepted; this form must be signed by all authors of the article. All manuscripts must be submitted through the International Journal of Biomedicine`s online submission and review website. Authors who are unable to provide an electronic version or have other circumstances that prevent online submission must contact the Editorial Office prior to submission to discuss alternate options (editor@ijbm.org).

IJBM

INTERNATIONAL JOURNAL OF BIOMEDICINE

Human Genetics Asia 2023

68th Annual Meeting of the Japan Society of Human Genetics (JSHG)
14th Asia Pacific Conference on Human Genetics (APCHG)
22nd Annual meeting of East Asian Union of Human Genetics Societies (EAUHGS)

Dates
October 11-14, 2023

Venue **Toshi Center Hotel Tokyo / Zenkoku Toshi Kaikan, JAPAN**

President **Kenjiro Kosaki**
Professor, Center for Medical Genetics,
Keio University School of Medicine

Secretariat
c/o Congrès Inc.
Onward Park Bldg., 3-10-5 Nihonbashi, Chuo-ku Tokyo 103-8276, JAPAN
Email: jshg2023@congre.co.jp

Asia Pacific Society of Human Genetics
EAUHGS

IJBM

INTERNATIONAL JOURNAL OF BIOMEDICINE

www.ijbm.org

Volume 13 Issue 3 September 2023

CONTENTS

CONTENTS

CONTINUED


2024
IESS
dubai
1ST
INTERNATIONAL EPILEPSY
SURGERY SOCIETY CONGRESS
IESS DUBAI 2024
19 - 21 January 2024
Conrad Hotel, Dubai, UAE
SAVE THE DATE
www.IESSCongress.org

60th ANNUAL MEETING

EASD

9-13 SEPTEMBER 2024

MADRID

WWW.EASD.ORG

International Journal of Biomedicine 13(3) (2023) 9-16
http://dx.doi.org/10.21103/Article13(3)_RA1

REVIEW ARTICLE

INTERNATIONAL JOURNAL OF BIOMEDICINE

Acute Vascular Events: Cellular and Molecular Mechanisms

Varun HK Rao[1], Rasika T. Shankar[1], Gundu H. R. Rao[2*]

[1]*South Asian Society on Atherosclerosis and Thrombosis, India*
[2]*Lillehei Heart Institute, University of Minnesota, Minneapolis, Minnesota, USA*

Abstract

Cardiovascular diseases (CVDs) are the leading cause of death worldwide. An estimated 17.9 million individuals died from CVDs in 2019, representing 32% of all global deaths. Of these deaths, 85% were due to heart attack and stroke. Cardiometabolic risks, such as hypertension, excess weight, obesity, type 2 diabetes, and vascular diseases, contribute significantly to the progression of coronary artery disease. Known sequelae of events that lead to these cardiometabolic diseases include oxidative stress, inflammation, development of dysfunction of vascular adipose tissue, altered blood pressure and blood lipids, altered glucose metabolism, hardening of the arteries, endothelial dysfunction, development of atherosclerotic plaques, and activation of platelet and coagulation pathways. The Framingham Heart Study Group has developed a Risk Score that estimates the risk of developing heart disease in a 10-year period. This group of experts has developed mathematical functions for predicting clinical coronary disease events. These prediction capabilities are derived by assigning weights to major CVD risk factors such as sex, age, blood pressure, total cholesterol, low-density lipoprotein, high-density lipoprotein cholesterol, smoking behavior, and diabetes status.

Currently, there is a growing interest in the use of artificial intelligence and machine learning applications. AI-based mimetic pattern-based algorithms seem to be better than the conventional Framingham Risk Score, in predicting clinical events related to CVDs. However, there are limitations to these applications as they do not have access to data on the specific factors that trigger acute vascular events, such as heart attack and stroke.

This overview briefly discusses some salient cellular and molecular mechanisms involved in precipitating thrombotic conditions. Further improvements in emerging technologies will provide greater opportunities for patient selection and treatment options. Several clinical studies have demonstrated that most CVDs can be prevented by addressing behavioral risk factors such as tobacco use, unhealthy diet and obesity, physical activity, and harmful use of alcohol. Early detection and better management of the modifiable risks seem to be the only way to reduce, reverse, or prevent these diseases. (**International Journal of Biomedicine. 2023;13(3):9-16.**)

Keywords: cardiovascular disease • artificial intelligence • thrombosis • risk factors

For citation: Rao VHK, Shankar RT, Rao GHR. Acute Vascular Events: Cellular and Molecular Mechanisms. International Journal of Biomedicine. 2023;13(3):9-16. doi:10.21103/Article13(3)_RA1

Abbreviations

AI, artificial intelligence; **AA**, arachidonic acid; **CVD**, cardiovascular disease; **CAD**, coronary artery disease; **CCTA**, coronary computed tomography angiography; **CRP**, C-reactive protein; **FRS**, Framingham Risk Score; **ML**, machine learning; **T2D**, type 2 diabetes; **VT**, venous thrombosis.

Introduction

Metabolic diseases, such as hypertension, excess weight, obesity, T2D, and vascular diseases, have increased in incidence and prevalence to epidemic proportions worldwide in the last four decades.[1-3] Metabolic diseases are a cluster of disease conditions or related risk factors of altered metabolism that contribute to the development of atherosclerotic vascular diseases.[4] Despite the advances in diagnosing the risk factors and managing various metabolic diseases, atherosclerotic cardiovascular disease (CVD) outcome remains the leading cause of morbidity and mortality.[5] CVDs are the leading cause of death globally, taking an estimated 17.9 million lives each year.[6] According to a 'News Release' from the American Heart Association (July 21, 2021), heart diseases are likely to remain the number one killer in the U.S. indefinitely due to long-term

COVID-19 impact. The trend is likely to continue for years to come, as the long-term impact of the novel coronavirus will directly affect vascular health.[7-11] This trend can be disrupted by developing early diagnostic capabilities for the modifiable risks and introducing robust management of identified risks.[12]

The Framingham Risk Score (FSR) is a simplified tool for the assessment of risk level for developing CVD over a 10-year period.[13] The FRS considers six coronary risk factors: age, gender, total cholesterol (TC), high-density lipoproteins cholesterol (LDL), smoking habits, and systolic blood pressure. FRS seems to be the most applicable method for predicting a person's chance of developing CVD in the long term.[14-16] An international team of experts studied the effect of each additional risk-modifying characteristic using Fine and Gray models and reported that the coronary calcium score was the single strongest added predictor of risk.[17] There is considerable interest in the level of C-reactive protein (CRP), as a valuable test for predicting the risk of atherosclerotic vascular disease.[18] Amplifying this finding, a news report had the following headline, "The Heart Disease Test That Could Save Your Life." Furthermore, the article described CRP as an "easy new way to help predict your risk of heart attack and stroke." However, a recent study by Hickam and associates from the University of Toronto concludes, "the evidence base supporting the inclusion of CRP in vascular disease risk assessment is tenuous, incomplete, and conflicting."[19] We agree with this conclusion.

A search on the internet on the topic of: "Acute Vascular Events", reveals a few reports, one on the use of heart rate variability by Wang and associates from China,[20] and the other on using machine learning (ML), using the MESA study data.[21] The authors of the MESA study concluded that ML in conjunction with deep phenotyping improves prediction accuracy in cardiovascular event prediction in an initially asymptomatic population. They, too, concluded that artificial intelligence (AI) approaches and deep learning applications will improve risk prediction through multimodal data integration. A multinational research team has identified several limitations in this approach, such as difficulties incorporating AI into clinical practice and the lack of standardization in clinical health data.[22] Having said that, we would like to inform the readers that it is not that simple to predict acute vascular events, as the data processed by such advanced applications assume that all the biomarkers needed for risk stratification and risk prediction are available. Let us just ask the same question we asked on the internet, -'Risk Factors for Prediction of Acute Vascular Events', to the 'all-knowing' ChatGPT (Open AI). The answer lists 10 risk factors: age, gender, smoking, blood pressure, cholesterol, diabetes, family history, obesity, physical inactivity, and stress. None of these risk factors trigger the acute events, although they all contribute their share to the progression of vascular disease. This overview will briefly review the cellular and molecular mechanisms that promote acute vascular events, such as heart attacks and stroke.

Metabolic Diseases and Atherosclerotic Vascular Disease

The fact that in 2014, 6090, and 2015, 5524 articles were published related to metabolic vascular syndrome indicates the role of metabolic diseases in promoting atherosclerotic vascular disease.[23] The metabolic syndrome has been described as a cluster of five pre-morbid metabolic-vascular risk factors or diseases (with the 'deadly quartet' - hyperglycemia, visceral obesity, dyslipidemia, and hypertension) associated with increased CVD. However, the sequelae of risks that promote atherosclerotic CVD include oxidative stress, inflammation, hyperglycemia, dyslipidemia, hypertension, excess weight, obesity, T2D, narrowing of the arteries, endothelial dysfunction, subclinical atherosclerosis, activation of platelets and coagulation pathways. In routine clinical settings, hyperglycemia, visceral obesity, dyslipidemia, and hypertension provide the basis for integrated diagnostics, management, and prevention of these disorders. The exact mechanisms involved in how these metabolic diseases initiate and promote atherosclerosis of the vasculature are not clear at this time. However, oxidative stress, increased reactive oxygen species, and low-grade inflammation, especially in dysfunctional adipose tissue of the vessels, seem to play a very important role in the pathophysiology of atherosclerosis. A pro-inflammatory state and dysfunctional adipose tissue shift the endothelium toward reduced vasodilation and consequent thrombotic condition.[24]

Historical Perspective of Platelet Activation

Blood platelets interact with various soluble agonists, such as epinephrine, adenosine diphosphate, and many insoluble cell matrix components, including collagen, laminin, and biomaterials used to construct invasive medical devices. These interactions stimulate specific receptors and glycoprotein-rich domains (integrins and nonintegrin) on the plasma membrane and lead to the activation of intracellular effective enzymes. Most of the regulatory events appear to require free calcium. Ionized calcium is the primary bioregulator, and a variety of biochemical mechanisms are modulated by the level and availability of free calcium. Major enzymes regulating free calcium levels via second messengers include phospholipase C, phospholipase A2, and phospholipase D, together with adenylyl cyclase and guanylyl cyclases (Fig 1A). G-Protein beta gamma dependent activation of phospholipase C results in the hydrolysis phosphatidyl inositol 4, 5 bisphosphate and formation of second messengers 1, 2-diacylyglycerol and inositol 1, 4, 5 trisphosphates (IP3), Diglyceride induces activation protein kinase C, whereas IP3 mobilizes calcium from internal membrane stores.

Elevation of cytosolic calcium stimulates phospholipase A2 and liberates arachidonic acid. Free arachidonic acid is transformed to a novel metabolite thromboxane A2 by fatty acid synthetase (COX-1, cyclooxygenase). Thromboxane A2 is the major endogenous metabolite of this pathway and plays a critical role in platelet recruitment, granule mobilization, and secretion of granule contents (Figure 1 A & B). Secretion of granules promotes p-selectin expression (adhesion protein) on the platelet membrane. In addition, activation of platelets also promotes the expression of acidic lipids on the membrane and tissue factor expression, thus making these cells procoagulant. Although platelets that are not activated can bind surface-bound fibrinogen, they cannot bind circulating soluble fibrinogen. Agonist-mediated activation of platelets promotes the expression of an epitope on glycoprotein IIb/IIIa receptors.

Activation of this receptor is essential for the binding of circulating fibrinogen. Fibrinogen forms a bridge between individual platelets and facilitates thrombus formation. Von Willebrand factor (vWF) binds platelet GP Ib-IX complex under high shear conditions. Up-regulation of signaling pathways will increase the risk for clinical complications associated with acute coronary events. In a short overview like this, it is hard to cover all aspects of platelet activation mechanisms, and readers are urged to refer to comprehensive reviews on this topic.[25-31]

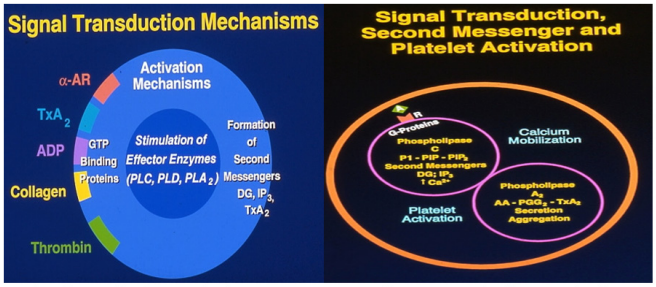

A. *Signal transduction mechanisms.* **B.** *Second messengers leading to activation.*

Fig. 1. *Platelet activation mechanisms.*

Factors Promoting Thrombotic Events

An Internet search on 'risk factors for arterial thrombosis' lists the following risks: smoking, diabetes, high blood pressure, high cholesterol, lack of activity and obesity, and family history of arterial thrombosis. Arterial thrombosis is the cause of myocardial infarction and stroke, while venous thrombosis (VT) leads to venous thromboembolism. Furthermore, arterial thrombi are rich in platelets, and venous thrombi are rich in fibrin. Arterial thrombosis occurs in places of high shear flow, while VT occurs in areas of low shear blood flow.[32] Even when one searches response for 'risk factors that trigger heart attack and stroke, ' the information on the internet does not cover the mechanisms that promote these acute events. The internet response is that 'leading risk factors for heart disease and stroke are high blood pressure, high low-density lipoprotein (LDL) cholesterol, diabetes, smoking, obesity, unhealthy diet, and physical inactivity." We asked the same question to ChatGPT. The reply was the same ten risks that we mentioned in the introduction. Since I was to provide my input, I mentioned. "Your Open AI is not ready to answer such complex questions. It is still looking at half a century-old Framingham Risk Score. None of the above ten risk factors trigger acute vascular events such as heart attack or stroke. Narrowing of the artery, atherosclerotic plaque buildup, vascular dysfunction, and activation of platelet and coagulation pathways are some of the major contributors to acute vascular events". I got an apology, and the chat assistant rephrased what I listed as probable causes for acute vascular events.

Cellular and Molecular Mechanisms that Promote Acute, Arterial, and Vascular Events

The endothelium, a monolayer of endothelial cells, covers the entire inner surface of the blood vessels and, as such, is in contact with the blood and the circulating cells (Fig 2). The surface of the endothelium is covered by glycocalyx, a mosaic of glycoproteins, proteoglycans, and glycosaminoglycans. The vessel wall is covered with more than a trillion endothelial cells. The wall of blood vessels is comprised of three layers: a) the innermost tunica intima, made up of endothelial cells and sub-endothelial connective tissue; b) the intermediate, tunica media, mainly made up of smooth muscle cells; and c) the outer, tunica adventitia, made up of collagen. Principal endothelial-derived procoagulant molecules include thrombin, vWF, tissue factor expression, vascular cell adhesion molecule-1(VCAM-1), altered CD39/CD73 expression, plasmin activator inhibitor-1(PAI-1), ADAMTS-13. Anticoagulant molecules include nitric oxide, prostacyclin, thrombomodulin, heparin sulfate, urokinase plasmin activator (u-PA), tissue plasminogen activator (t-PA), C-terminal metalloproteinase with multiple functions (ADAMTS-18), endothelial protein C receptor (EPCR) and tissue factor pathway inhibitor (TFPI).

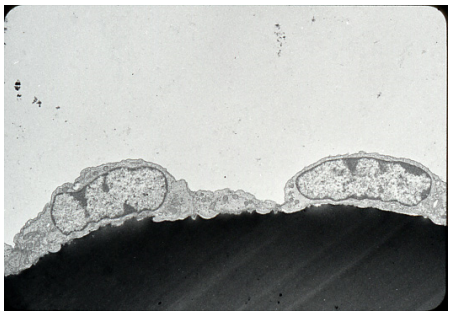

Fig. 2. *Scanning electron micrograph of endothelial cells. (Courtesy: Professor (Late) James G White, University of Minnesota)*

Endothelium prevents the development of thrombotic conditions by providing a surface that discourages the attachment of platelets and clotting proteins (Fig. 3).

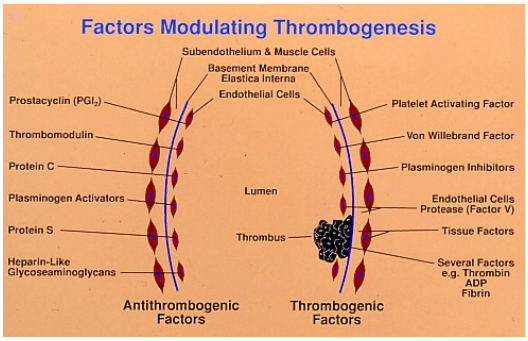

Fig. 3. *Molecular mechanisms involved in thrombogenesis. (Personal collection; source unknown)*

Following endothelial injury or dysfunction of endothelial cells, circulating platelets get activated and promote expression of cell surface adhesion molecules. These conditions also promote leukocyte rolling and tethering onto the endothelium, which initiates inflammatory responses that promote thrombosis. Alteration in the production of vessel wall prostacyclin (PGI_2)

or increased thromboxane production by circulating platelets, as well as lowered nitric oxide (NO) production, induce endothelial dysfunction. Vessel wall damage due to atherosclerosis, hypertension, vascular abnormalities, or dysfunction enhances platelet adhesion and interaction with the endothelium (Fig 4). Endothelial dysfunction is common in hypertensive subjects, diabetics, and metabolic syndrome.

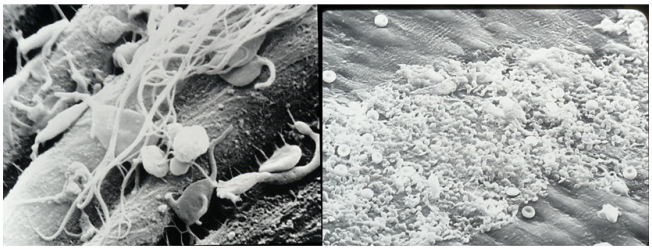

Fig. 4. *Platelet Interaction with dysfunctional (A) and denuded endothelium (B).*

(Courtesy: Professor (Late) James G White, University of Minnesota)

The activated renin-angiotensin system, together with increased oxidized lipids, may play a role in the enhanced vascular oxidative stress. These events promote the development of inflammation of the vasculature. Inflammation enhances the formation of reactive oxygen species (ROS), damaging the vessel walls. In an earlier study, we demonstrated the role of hyperglycemia in precipitating acute vascular events.[33] In brief, the pathogenesis of arterial thrombosis involves damage of the vessel wall, alterations in the production of vasodilators and vasoconstrictor molecules, development of atherosclerosis, plaque formation, and activation of platelet and coagulation pathways. To maintain an antithrombotic surface, the healthy endothelium secretes various anticoagulant molecules. However, when the surface is damaged or dysfunctional, it releases procoagulant molecules.

The endothelial barrier to prevent platelet interactions with the subendothelium depends upon the stable cell-cell junctions (Fig. 2). ACE2 on the endothelium converts angiotensin II to angiotensin-(1–7), which, as a ligand, binds to the G-protein-coupled receptor MAS, thus modulating anti-inflammatory and antithrombotic signaling pathways. Furthermore, as we have described earlier, it produces natural anticoagulant and anti-fibrinolytic molecules. A healthy endothelium produces PGI2 and nitric oxide to prevent platelet adhesion and activation.

In an earlier section, we have described molecular mechanisms involved in platelet activation. In brief, agonists interact with preferred receptors on the plasma membrane. In Figure 5 above, we have used thrombin as the agonist, interacting at the specific receptor site and inducing activation of phospholipase C, which in turn promotes the formation of active biological molecules, inositol trisphosphate (IP_3), and diglyceride (DG). Inositol trisphosphate mobilizes cytosolic calcium from membrane stores, and diglyceride activates protein kinase C. Elevation of cytosolic calcium stimulates phospholipase A2 and induces the release of arachidonic acid (AA) from membranes. Free AA is converted to prostaglandin endoperoxides G2 and H2 by cyclooxygenase (COX1). These endoperoxide molecules are further converted to thromboxane A2 (TxA2) by platelets and to prostacyclin (PGI_2) by vessel wall enzymes. Thromboxane A2 is the most potent platelet agonist, and PGI_2 is a potent antagonist. Endogenously generated thromboxanes act at the specific receptor sites on the platelet membranes and activate the GP IIb /IIIa receptors. Activated GPIIb/IIIa receptors recognize soluble fibrinogen and interact with other activated platelets to form platelet aggregates (Fig 6).

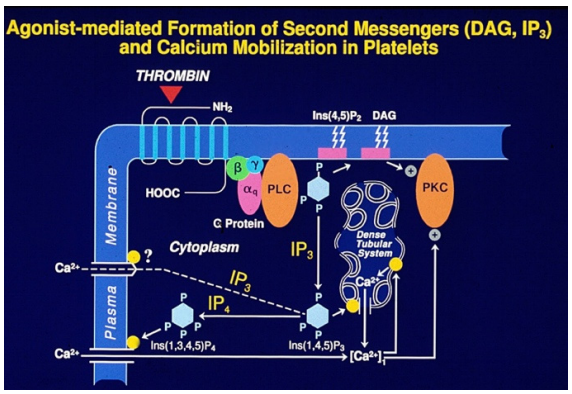

Fig. 5. *Molecular mechanisms involved in platelet activation.*

(Personal Collection: Prepared by University of Minnesota Artists)

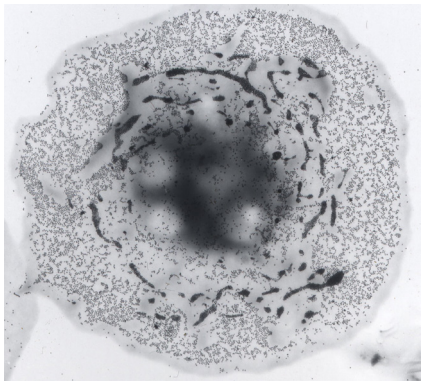

Fig. 6. *Scanning electron micrograph of spread platelets showing fibrinogen binding to activated platelets (Arteriosclerosis.1990;10:738-744).*

(Courtesy; Professor (Late) James G White, University of Minnesota)

Studies at the University of Minnesota by Professor James White and Gines Escolar demonstrated that fibrinogen gold (Fgn/Au) and platelet glycoproteins (GPIIb /IIIa) receptor complexes were moved from peripheral margins toward centers of surface-activated platelets.[27] The authors concluded that "GP11b-111a receptors remain randomly dispersed from the edge on fully activated spread platelets".

To study the role of free fatty acids in platelet physiology and pharmacology, we did a one-of-a-kind study in 1980 using a drug-induced diabetic rat model. Diabetic subjects are known to have hyperfunctional platelets. In these studies, rats were rendered diabetic by injection of streptozotocin. We followed the ability of platelets and vessel wall tissues to make prostanoids using radiolabeled AA in the control and diabetic rats. We evaluated the release and conversion of free fatty

acids to thromboxane and prostacyclin by monitoring their stable metabolites. A schematic pathway of results obtained in these studies is presented in Figure 7. Conversion of AA to pro-aggregatory thromboxane was higher in the diabetic rats. Whereas the levels of vasoactive prostacyclin were lower in the diabetic rats compared to control rats, suggesting a shift to a prothrombotic state.[34] The changes observed in platelet and vessel wall arachidonic acid were normalized by pancreatic islet cell transplantation to these diabetic animals (data not shown). For the first time, these studies demonstrated the differential effect of hyperglycemia on vascular and platelet prostaglandin production. In this overview, we have limited our discussions to the role of platelets in thrombosis. We have not discussed the role of coagulation pathways in this complex process.

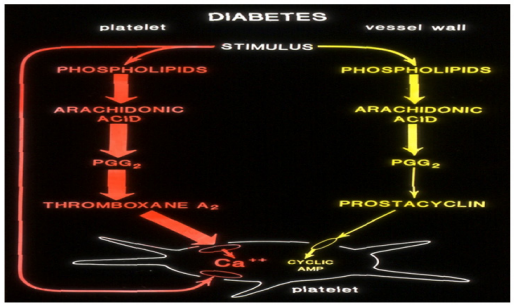

Fig. 7. *Altered platelet and vessel wall prostaglandin production in diabetes rats.*

(Courtesy: Professor John Gerrard. University of Minnesota)

Biomarkers Indicating Platelet Activation and Prothrombotic State

Circulating preactivated platelets and a prothrombotic phenotype can be detected as a marker of platelet activation.[35] Activated platelets shed P-selectin, an adhesion molecule, which is expressed on the platelet membrane.[36] Circulating platelets with p-selectin and soluble p-selectin in the blood indicate platelet activation. Activated platelets also express CD40L(CD154).[37] Activation of platelets leads to an increase in soluble CD40L(sCD40L). High-affinity fibrinogen binding sites on GPIIb/IIIa can be detected by PAC-1, a mouse monoclonal antibody.[38] Therefore, PAC-1 binding on the platelet surface is indicative of platelet activation. Similarly, even fibrinogen binding on platelets itself is indicative of activated platelets. Monitoring elevated cytosolic calcium with appropriate calcium-specific fluorophores will also indicate the activation state of blood platelets. Platelet activation also can be determined by the expression of CD62, CD63, CD41, CD42, and activated GPIIb/IIIa. Stable metabolites of thromboxane B2 in blood and urine can be used as markers of platelet activation.[39] Platelet-derived microparticles, which are strongly procoagulant, also indicate platelet activation. In addition to these markers, the international normalized ratio (INR), which measures how quickly the blood clots or prothrombin time (PT), can also be used to monitor the prothrombotic status of the blood. Readers are urged to refer to comprehensive monographs for additional information on platelet activation.[25-35]

Discussion

CVDs are the most common cause of morbidity and mortality worldwide. Despite the impressive improvements in patient diagnosis and robust risk factor management, they have been ranked the number one killer for decades and will continue to occupy this position for decades. INTERHEART study by the multicountry investigators demonstrated that modifiable risk factors, such as smoking, hypertension, blood apoproteins, diabetes, waist-hip ratio, dietary patterns, physical activity, consumption of alcohol, and psychosocial factors, account for most of the risk for myocardial infarction worldwide, and management of these risks significantly prevents premature mortality due to myocardial infarction.[40] In a similar study on stroke in 32 countries, the authors concluded, "The potentially modifiable risk factors are collectively associated with about 90% of stroke in each major region of the world, among ethnic groups, in men and women, and all ages."[41] Commenting on the results of these studies, Zeng and associates wondered whether the study might have overestimated the role of ten potentially modifiable risk factors, whereas factors such as social status, metabolic syndrome, and nutrition are important risk factors for ischemic stroke.[42]

Some authors claim the decline in mortality from CAD and stroke as the success story of the past four decades.[43] Models have shown that this remarkable decline has been fueled by rapid progress in both prevention and treatment, declines in smoking, improvements in hypertension treatment, and widespread use of statins, development, and use of thrombolytic agents and stents for acute coronary syndromes. However, recent evidence suggests that long-term decline in CVD mortality may have stagnated and even reversed in younger populations.[44] A large study from the Imperial College of London reported that although CVD mortality has declined in industrial countries, diabetes mortality has increased.[45] A multicountry study concluded, "Across four studies involving 55,685 participants, genetic and lifestyle factors were independently associated with susceptibility to coronary artery disease. Among participants at high genetic risk, a favorable lifestyle was associated with a nearly 50% lower relative risk of coronary artery disease."[46] What is clear from these studies is that early diagnosis of various risk factors for CVDs and robust management of the identified risks changes in lifestyle, including healthy diet and exercise, will significantly lower premature mortality due to coronary artery disease. Despite these encouraging studies, the growing prevalence of cardiovascular risk factors and better prognosis of patients with CVDs have increased the global CVD burden.[47,48]

There is great interest in using AI and ML techniques to improve the diagnosis and treatment of vascular diseases.[49-52] These techniques have many applications in cardiovascular drug therapy, pharmacogenomics, diagnosis, and treatment planning. These approaches can be used for improving risk prediction, monitoring various clinical complications, and developing AI technology compatible with smartphones and high-tech diagnostic tools. According to British researchers, cardiology seems to be at the forefront of AI/ML applications.[53] There seems to be a great opportunity for developing accurate methods for predicting CVD outcomes, noninvasive diagnosis of CAD, detection of

malignant arrhythmias through wearables, and the development of diagnosis and treatment strategies and predictions for heart failure patients. Researchers from Australia have demonstrated that an AI-based, fully automated coronary artery calcium scoring model shows high accuracy and low analysis time.[54] CCTA has been used to predict long-term outcomes. Researchers used data from the CONFIRM study to predict 5-year all-cause mortality by combining 44 CT variables. This study included 10,000 patients with suspected coronary disease. Compared to FRS and CCTA-based risk models (segment stenosis score, segment involvement score), the model combining CCTA and clinical variables was far better in predicting 5-year all-cause mortality.[55] An editorial in *JAMA* rightly suggests that new ways to identify groups at increased risk, beyond conventional risk factors and current estimate models, are required and warrant investigation.[56]

AI, ML, software analytics, and chatGPT are growing rapidly in all fields of public health. In healthcare, where patient well-being is paramount, it is recommended to subject AI and ML analytics to clinical validation before widespread acceptance and adoption. It typically involves evaluating the performance of the technology on large and diverse populations, comparing it to existing standards or gold standards, and assessing its impact on patient outcomes. Thereby ensuring that the technology meets standards of accuracy, reliability, and safety. Clinical validation helps to verify the performance of the AI/ML model in real-world scenarios. It ensures that the results are consistent and clinically meaningful. AI/ML applications may play a significant role in improving diagnosis and opting for treatment plans. Such risk assessment tools are critical in the current approach to primary prevention of atherosclerotic CVDs.[57] A recent review by multicountry researchers covers state-of-the-art AI applications across various noninvasive imaging modalities to quantify cardiovascular risk in CAD.[58,59] A recent study published in the European Heart Journal evaluated the ability of a deep-learning-based CVD marker, Reti-CVD, to identify individuals with intermediate – and high-risk for CVD by existing risk assessment tools, including FRS.[60] Despite such findings, AI-ML-GPT-related fears have emerged with the rise of language learning models, exemplified by Open AI's GPT. The emerging technologies and their applications have left clinicians, and scientists wondering how these analytics might be used in the future and what risks these technologies pose for patients and clinicians.[61]

FRS was developed using conventional risk factors to predict the 10-year risk for developing CVDs and not for predicting acute vascular events. Researchers have used data from the CONFIRM study to predict 5-year all-cause mortality by combining 44CT variables. Coronary artery calcium is currently assessed manually. A novel AI-based model showed high levels of correlation and agreement with standard measurement. Such emerging technologies could be incorporated to develop AI and ML-based analytics for risk stratification, risk prediction, and management. What other risk scores can be included to enhance risk stratification and risk prediction? Circulating CRP seems to help to estimate the risk for cardiovascular events.[62] Researchers from Germany used CRP data to improve FRS and concluded that CRP significantly enhances global coronary risk as assessed by FRS, especially in intermediate-risk groups. Classical risk factors used to compute FRS do not account for all incident coronary events, especially those associated with acute occlusive arterial events. Such observations have led to the search and inclusion of biomarkers involved in cellular and molecular mechanisms that trigger acute vascular events. This overview briefly covered some salient mechanisms that play a significant role in platelet-dependent acute vascular events. Having said that, we must remind readers that this is only a partial story, as we have not discussed the role of coagulation pathways in these acute events. We hope future studies will include emerging risk factors that modulate the activation of platelet and coagulation pathways in computing CVD-related risk stratification and risk prediction equations.

Conclusion

Heart attacks and strokes are acute vascular events mainly caused by a blood clot that blocks and prevents the blood flow to the heart or brain. Coronary atherosclerosis is the underlying condition for these acute vascular events. Multiple risk factors are involved in the initiation, progression, and precipitation of these acute events, although the exact cause that triggers these events remains elusive. The Framingham Heart Study Group described modifiable risk factors that play a role in the development of vascular diseases. Several clinical studies have demonstrated that identifying these conventional risk factors and managing these risks significantly prevents premature mortality due to myocardial infarction. According to the experts from the Division of Preventive Cardiology, Cleveland Clinic, "90 percent of the heart disease is preventable through healthier diet, regular exercise and not smoking". Despite such good news and the encouraging results of multiple clinical studies, the global burden of CVDs has increased in incidence and prevalence. The prevalence of total CVDs nearly doubled from 271 million in 1990 to 523 million in 2019, while deaths steadily increased from 12.1 million in 1990 to 18.6 million in 2019. Metabolic diseases such as hypertension, excess weight, obesity, and T2D increase the risk of coronary artery disease. Every major clinical trial has demonstrated that management of modifiable risk factors for CVD and lifestyle changes significantly reduces premature mortality. Yet, we do not see an overall reduction in CVD incidence and prevalence worldwide. Maybe it is time to focus on reducing, reversing, or preventing metabolic diseases rather than focusing on just CVD risk management. In this overview, we have briefly discussed some salient cellular and molecular mechanisms involved in precipitating thrombotic conditions. We have speculated that including emerging risk factors in computing the risk stratification may improve risk predictability for acute vascular events.

Competing Interests

The authors declare that they have no competing interests.

References

1. Rao GHR. Global Syndemic of Metabolic Diseases: Editorial Comments. J Diab. Clin Res.2019;1(1):2-4.
2. Chong B, Kong G, Shankar K, Chew HSJ, Lin C, Goh R, et al. The global syndemic of metabolic diseases in the young adult population: A consortium of trends and projections from the Global Burden of Disease 2000-2019. Metabolism. 2023 Apr;141:155402. doi: 10.1016/j.metabol.2023.155402.
3. Chew NWS, Ng CH, Tan DJH, Kong G, Lin C, Chin YH, et al. The global burden of metabolic disease: Data from 2000 to 2019. Cell Metab. 2023 Mar 7;35(3):414-428.e3. doi: 10.1016/j.cmet.2023.02.003.
4. Grundy SM, Cleeman JI, Daniels SR, Donato KA, Eckel RH, Franklin BA, et al.; American Heart Association; National Heart, Lung, and Blood Institute. Diagnosis and management of the metabolic syndrome: an American Heart Association/ National Heart, Lung, and Blood Institute Scientific Statement. Circulation. 2005 Oct 25;112(17):2735-52. doi: 10.1161/ CIRCULATIONAHA.105.169404. Erratum in: Circulation. 2005 Oct 25;112(17):e297. Erratum in: Circulation. 2005 Oct 25;112(17):e298.
5. Roth GA, Mensah GA, Johnson CO, Addolorato G, Ammirati E, Baddour LM, et al.; GBD-NHLBI-JACC Global Burden of Cardiovascular Diseases Writing Group. Global Burden of Cardiovascular Diseases and Risk Factors, 1990-2019: Update From the GBD 2019 Study. J Am Coll Cardiol. 2020 Dec 22;76(25):2982-3021. doi: 10.1016/j. jacc.2020.11.010. Erratum in: J Am Coll Cardiol. 2021 Apr 20;77(15):1958-1959.
6. Arnett DK, Blumenthal RS, Albert MA, Buroker AB, Goldberger ZD, Hahn EJ, et al. 2019 ACC/AHA Guideline on the Primary Prevention of Cardiovascular Disease: A Report of the American College of Cardiology/American Heart Association Task Force on Clinical Practice Guidelines. Circulation. 2019 Sep 10;140(11):e596-e646. doi: 10.1161/ CIR.0000000000000678. Erratum in: Circulation. 2019 Sep 10;140(11):e649-e650. Erratum in: Circulation. 2020 Jan 28;141(4):e60. Erratum in: Circulation. 2020 Apr 21;141(16):e774.
7. Rao GHR. Number one Killer: Vascular Disease. Ann Clin Diab. Endocrionol.2018; 1(1):1008.
8. Rao GHR. Coronavirus Disease and Acute Vascular Events. Clin Appl Thromb Hemost. 2020 Jan-Dec;26:1076029620929091. doi: 10.1177/1076029620929091.
9. Rao GHR. Coronavirus (COVID-19), Comorbidities, and Acute Vascular Events; Guest Editorial. ECCMC EC Clinical Case Reports. 3.6 (2020):87-91.
10. Rao GHR. Coronavirus Disease (Covid-19), Comorbidities, and Clinical Manifestations. Guest Editorial. EC Diab, Met Res. 4.6 (2020): 27-33.
11. Rao GHR. Coronavirus Disease (Covid-19): A Disease of the Vascular Endothelium. Ser. Cardiol. Res. 2020;2(1): 23-27.
12. Rao GHR. Prevention or reversal of cardiometabolic diseases. J Clin & Prevent. Cardiol. 2018 (7): 22-28.
13. Jahangiry L, Farhangi MA, Rezaei F. Framingham risk score for estimation of 10-years of cardiovascular diseases risk in patients with metabolic syndrome. J Health Popul Nutr. 2017 Nov 13;36(1):36. doi: 10.1186/s41043-017-0114-0.
14. Gordon T, Kannel WB, Halperin M. Predictability of coronary heart disease. J Chronic Dis. 1979;32(6):427-40. doi: 10.1016/0021-9681(79)90103-6.
15. Gordon T, Kannel WB. Multiple risk functions for predicting coronary heart disease: the concept, accuracy, and application. Am Heart J. 1982 Jun;103(6):1031-9. doi: 10.1016/0002-8703(82)90567-1.
16. Wilson PW, D'Agostino RB, Levy D, Belanger AM, Silbershatz H, Kannel WB. Prediction of coronary heart disease using risk factor categories. Circulation. 1998 May 12;97(18):1837-47. doi: 10.1161/01.cir.97.18.1837.
17. Hageman SHJ, Pennells L, Pajouheshnia R, et al. The value of additional risk factors for improving 1-year cardiovascular risk prediction in apparently healthy people. Euro Heart J. 2022; 43(2):ehac544.2277.
18. Ridker PM, Rifai N, Rose L, Buring JE, Cook NR. Comparison of C-reactive protein and low-density lipoprotein cholesterol levels in the prediction of first cardiovascular events. N Engl J Med. 2002 Nov 14;347(20):1557-65. doi: 10.1056/NEJMoa021993.
19. Comarow A. A message from the heart. US News World Rep. 2002 Nov 25;133(20):54-6, 59-60, 61.
20. Wang J, Wu X, Sun J, Xu T, Zhu T, Yu F, et al. Prediction of major adverse cardiovascular events in patients with acute coronary syndrome: Development and validation of a non-invasive nomogram model based on autonomic nervous system assessment. Front Cardiovasc Med. 2022 Nov 3;9:1053470. doi: 10.3389/fcvm.2022.1053470.
21. Ambale-Venkatesh B, Yang X, Wu CO, Liu K, Hundley WG, McClelland R, et al. Cardiovascular Event Prediction by Machine Learning: The Multi-Ethnic Study of Atherosclerosis. Circ Res. 2017 Oct 13;121(9):1092-1101. doi: 10.1161/ CIRCRESAHA.117.311312.
22. Cabral BP, Braga LAM, Syed-Abdul S, Mota FB. Future of Artificial Intelligence Applications in Cancer Care: A Global Cross-Sectional Survey of Researchers. Curr Oncol. 2023 Mar 16;30(3):3432-3446. doi: 10.3390/curroncol30030260.
23. Hanefeld M, Pistrosch F, Bornstein SR, Birkenfeld AL. The metabolic vascular syndrome - guide to an individualized treatment. Rev Endocr Metab Disord. 2016 Mar;17(1):5-17. doi: 10.1007/s11154-016-9345-4.
24. Elyaspour Z, Zibaeenezhad MJ, Razmkhah M, Razeghian-Jahromi I. Is It All About Endothelial Dysfunction and Thrombosis Formation? The Secret of COVID-19. Clin Appl Thromb Hemost. 2021 Jan-Dec;27:10760296211042940. doi: 10.1177/10760296211042940.
25. Rao GH. Physiology of blood platelet activation. Indian J Physiol Pharmacol. 1993 Oct;37(4):263-75. PMID: 8112802.
26. Rao GHR. Handbook of Platelet Physiology and Pharmacology. Kluwer Academic Publishers, Boston. 1999.
27. Rao GHR. Manual of Blood Platelets: Morphology, Physiology and Pharmacology. Jaypee Medical Publishers, New Delhi, India. 2019.hol
28. Rao GHR, Gerrard JM, Cohen I, et al: Origin and role of calcium in platelet activation -contraction-secretion coupling. Cell Calcium Metabolism (Ed Gary Fiskum) Plenum Publishing Corp, 1989.
29. Rao GHR. Physiology and Pharmacology of Platelets. Int J prog. Cardiovasc. Sci. 1995;2:108-110.
30. Rao GH. Signal transduction, second messengers, and platelet function. J Lab Clin Med. 1993 Jan;121(1):18-20.
31. Rao GHR. Signa transduction, second messengers and platelet pharmacology. Pharmacol (Life sci) 1994;13:39-44.
32. Koupenova M, Kehrel BE, Corkrey HA, Freedman JE. Thrombosis and platelets: an update. Eur Heart J. 2017 Mar 14;38(11):785-791. doi: 10.1093/eurheartj/ehw550.
33. Rao GHR: Altered Glucose Metabolism and Acute

Vascular Events. J Clin Cardiol and Diag. 4(1): 9-16, 2022
34. Gerrard JM, Stuart MJ, Rao GH, Steffes MW, Mauer SM, Brown DM, White JG. Alteration in the balance of prostaglandin and thromboxane synthesis in diabetic rats. J Lab Clin Med. 1980 Jun;95(6):950-8.
35. Rao GH. Platelet hyperfunction as risk factor for chronic and acute coronary events. Toxicol Mech Methods. 2005;15(6):425-31. doi: 10.1080/15376520500194759.
36. Massaguer A, Engel P, Tovar V, March S, Rigol M, Solanes N, et al. Characterization of platelet and soluble-porcine P-selectin (CD62P). Vet Immunol Immunopathol. 2003 Dec 15;96(3-4):169-81. doi: 10.1016/s0165-2427(03)00163-6.
37. Yun SH, Sim EH, Goh RY, Park JI, Han JY. Platelet Activation: The Mechanisms and Potential Biomarkers. Biomed Res Int. 2016;2016:9060143. doi: 10.1155/2016/9060143.
38. Shattil SJ, Cunningham M, Hoxie JA. Detection of activated platelets in whole blood using activation-dependent monoclonal antibodies and flow cytometry. Blood. 1987 Jul;70(1):307-15.
39. Szczuko M, Kozioł I, Kotlęga D, Brodowski J, Drozd A. The Role of Thromboxane in the Course and Treatment of Ischemic Stroke: Review. Int J Mol Sci. 2021 Oct 28;22(21):11644. doi: 10.3390/ijms222111644.
40. Yusuf S, Hawken S, Ounpuu S, Dans T, Avezum A, Lanas F, et al.; INTERHEART Study Investigators. Effect of potentially modifiable risk factors associated with myocardial infarction in 52 countries (the INTERHEART study): case-control study. Lancet. 2004 Sep 11-17;364(9438):937-52. doi: 10.1016/S0140-6736(04)17018-9.
41. O'Donnell MJ, Chin SL, Rangarajan S, Xavier D, Liu L, Zhang H, et al.; INTERSTROKE investigators. Global and regional effects of potentially modifiable risk factors associated with acute stroke in 32 countries (INTERSTROKE): a case-control study. Lancet. 2016 Aug 20;388(10046):761-75. doi: 10.1016/S0140-6736(16)30506-2.
42. Zeng X, Deng A, Ding Y. The INTERSTROKE study on risk factors for stroke. Lancet. 2017 Jan 7;389(10064):35. doi: 10.1016/S0140-6736(16)32620-4.
43. Mensah GA, Wei GS, Sorlie PD, Fine LJ, Rosenberg Y, Kaufmann PG, et al. Decline in Cardiovascular Mortality: Possible Causes and Implications. Circ Res. 2017 Jan 20;120(2):366-380. doi: 10.1161/CIRCRESAHA.116.309115.
44. Lopez AD, Adair T. Is the long-term decline in cardiovascular-disease mortality in high-income countries over? Evidence from national vital statistics. Int J Epidemiol. 2019 Dec 1;48(6):1815-1823. doi: 10.1093/ije/dyz143.
45. Di Cesare M, Bennett JE, Best N, Stevens GA, Danaei G, Ezzati M. The contributions of risk factor trends to cardiometabolic mortality decline in 26 industrialized countries. Int J Epidemiol. 2013 Jun;42(3):838-48. doi: 10.1093/ije/dyt063.
46. Khera AV, Emdin CA, Drake I, Natarajan P, Bick AG, Cook NR, et al. Genetic Risk, Adherence to a Healthy Lifestyle, and Coronary Disease. N Engl J Med. 2016 Dec 15;375(24):2349-2358. doi: 10.1056/NEJMoa1605086.
47. Conrad N, Judge A, Tran J, Mohseni H, Hedgecott D, Crespillo AP, et al. Temporal trends and patterns in heart failure incidence: a population-based study of 4 million individuals. Lancet. 2018 Feb 10;391(10120):572-580. doi: 10.1016/S0140-6736(17)32520-5.
48. Nowbar AN, Gitto M, Howard JP, Francis DP, Al-Lamee R. Mortality From Ischemic Heart Disease. Circ Cardiovasc Qual Outcomes. 2019 Jun;12(6):e005375. doi: 10.1161/CIRCOUTCOMES.118.005375.
49. Joshi M, Melo DP, Ouyang D, Slomka PJ, Williams MC, Dey D. Current and Future Applications of Artificial Intelligence in Cardiac CT. Curr Cardiol Rep. 2023 Mar;25(3):109-117. doi: 10.1007/s11886-022-01837-8.
50. Krittanawong C, Zhang H, Wang Z, Aydar M, Kitai T. Artificial Intelligence in Precision Cardiovascular Medicine. J Am Coll Cardiol. 2017 May 30;69(21):2657-2664. doi: 10.1016/j.jacc.2017.03.571.
51. Paraskevas KI, Saba L, Suri JS. Applications of Artificial Intelligence in Vascular Diseases. Angiology. 2022 Aug;73(7):597-598. doi: 10.1177/00033197221087779.
52. Mathur P, Srivastava S, Xu X, Mehta JL. Artificial Intelligence, Machine Learning, and Cardiovascular Disease. Clin Med Insights Cardiol. 2020 Sep 9;14:1179546820927404. doi: 10.1177/1179546820927404.
53. Karatzia L, Aung N, Aksentijevic D. Artificial intelligence in cardiology: Hope for the future and power for the present. Front Cardiovasc Med. 2022 Oct 13;9:945726. doi: 10.3389/fcvm.2022.945726.
54. Ihdayhid AR, Lan NSR, Williams M, Newby D, Flack J, Kwok S, et al. Evaluation of an artificial intelligence coronary artery calcium scoring model from computed tomography. Eur Radiol. 2023 Jan;33(1):321-329. doi: 10.1007/s00330-022-09028-3.
55. Patel B, Sengupta P. Machine learning for predicting cardiac events: what does the future hold? Expert Rev Cardiovasc Ther. 2020 Feb;18(2):77-84. doi: 10.1080/14779072.2020.1732208.
56. Berger JS. Aspirin for Primary Prevention-Time to Rethink Our Approach. JAMA Netw Open. 2022 Apr 1;5(4):e2210144. doi: 10.1001/jamanetworkopen.2022.10144.
57. Lloyd-Jones DM, Braun LT, Ndumele CE, Smith SC Jr, Sperling LS, Virani SS, Blumenthal RS. Use of Risk Assessment Tools to Guide Decision-Making in the Primary Prevention of Atherosclerotic Cardiovascular Disease: A Special Report From the American Heart Association and American College of Cardiology. Circulation. 2019 Jun 18;139(25):e1162-e1177.
58. Lin A, Kolossváry M, Motwani M, Išgum I, Maurovich-Horvat P, Slomka PJ, Dey D. Artificial Intelligence in Cardiovascular Imaging for Risk Stratification in Coronary Artery Disease. Radiol Cardiothorac Imaging. 2021 Feb 25;3(1):e200512. doi: 10.1148/ryct.2021200512.
59. Pal M, Parija S, Panda G, Dhama K, Mohapatra RK. Risk prediction of cardiovascular disease using machine learning classifiers. Open Med (Wars). 2022 Jun 17;17(1):1100-1113. doi: 10.1515/med-2022-0508.
60. Yi JK, Rim TH, Park S, Kim SS, Kim HC, Lee CJ, et al. Cardiovascular disease risk assessment using a deep-learning-based retinal biomarker: a comparison with existing risk scores. Eur Heart J Digit Health. 2023 Mar 28;4(3):236-244. doi: 10.1093/ehjdh/ztad023.
61. Haupt CE, Marks M. AI-Generated Medical Advice-GPT and Beyond. JAMA. 2023 Apr 25;329(16):1349-1350. doi: 10.1001/jama.2023.5321.
62. Wilson PW, Pencina M, Jacques P, Selhub J, D'Agostino R Sr, O'Donnell CJ. C-reactive protein and reclassification of cardiovascular risk in the Framingham Heart Study. Circ Cardiovasc Qual Outcomes. 2008 Nov;1(2):92-7.

***Contact Information:** Emeritus Professor Gundu H. R. Rao, Laboratory Medicine and Pathology, Director, Thrombosis Research, Lillehei Heart Institute, University of Minnesota. E-mail: gundurao9@gmail.com*

International Journal of Biomedicine 13(3) (2023) 17-30
http://dx.doi.org/10.21103/Article13(3)_RA2

REVIEW ARTICLE

INTERNATIONAL JOURNAL OF BIOMEDICINE

Radiosensitization: Studies and Modern Approaches to Cellular Radiosensitivity

Juan C. Alamilla-Presuel*

The University of Málaga, Málaga, Spain

Abstract

Even though radiation therapy has achieved great success, there is still an unsolved task of increasing radiation damage to tumor tissue and reducing side effects on healthy tissues. There is a wide variety of obstacles that reduce the efficiency of radiotherapy. Mechanisms of radioresistance involve tumor-specific oncogenic signalling pathways, tumor metabolism and proliferation, tumor microenvironment/hypoxia, and genomics. Radiosensitizers are promising agents that enhance injury to tumor tissue by accelerating DNA damage. Several strategies have been used recently to develop highly effective radiosensitizers with low toxicity. In this review, we considered the use of radiosensitizers, including small molecules and nanomaterials, in various malignant tumors and the problems and prospects for their clinical use in cancer therapy.(**International Journal of Biomedicine. 2023;13(3):17-30.**)

Keywords: ionizing radiation • radiosensitizer • cellular radiosensitivity • tumor tissue • DNA damage

For citation: Alamilla-Presuel JC. Radiosensitization: Studies and Modern Approaches to Cellular Radiosensitivity. International Journal of Biomedicine. 2023;13(3):17-30. doi:10.21103/Article13(3)_RA2

Abbreviations

DSBs, double-strand breaks; **EC**, esophageal cancer; **EAC**, esophageal adenocarcinoma; **ESCC**, esophageal squamous cell carcinoma; **HCC**, hepatocellular carcinoma; **HDAC**, histone deacetylase; **HER2**, human epidermal growth factor receptor 2; **HNSCC**, head and neck squamous cell carcinoma; **IR** ionizing radiation; **KRAS**, Kirsten rat sarcoma viral oncogene homologue; **LC**, lung cancer; **PAR**, poly(ADP-ribose); **PARP**, PAR polymerase; **PCa**, prostate cancer; **RR**, ribonucleotide reductase; **ROS**, reactive oxygen species; **SCC**, squamous cell carcinoma; **SCLC**, small cell lung cancer.

Introduction

Radiation therapy is one of the most common forms of cancer treatment. Ionizing radiation (IR) takes effect by indirect or direct action. In direct action, radiation damages molecules such as proteins, lipids, and, particularly, DNA, resulting in the ending of cell division and proliferation as well as necrosis or apoptosis. The indirect action destroys the molecules through free radicals, principally by ROS, which are derived from the radiolysis of water (Image 1).[1] There is a wide variety of obstacles that reduce the efficiency of radiotherapy. Hypoxia is one of the main ones. For most tumors, a significant proportion of tumor cells are exposed to hypoxic conditions and, consequently, are prone to radioresistance.[2] The dependency of cellular responses to IR on the oxygen level has been recognized for almost a century.[3,4] IR causes DNA damage either by direct ionization or indirectly by DNA interaction of radicals formed by ionization of water surrounding DNA, resulting in DNA single- or double-strand breaks.[5] The probability of permanent IR-induced DNA damage is higher in the presence of oxygen than in its absence. In the presence of oxygen, ROS are formed, which increase the overall concentration of DNA-damaging agents. Numerous studies are focusing on elucidating the underlying mechanisms of hypoxia-induced radioresistance and developing strategies

***Correspondence:** Juan C. Alamilla-Presuel. Department of Radiology and Physical Medicine. Medical Faculty. The University of Málaga, Málaga, Spain E-mail: alamillajc@uma.es*

for radiosensitization. Several studies have demonstrated that acute hypoxia increases cell survival and autophagy, selecting for cancer cells with stem cell characteristics, and making them resistant to radiotherapy.[6-8] To limit hypoxia-induced radioresistance, several strategies are exploited, such as increasing oxygen availability by enhancing blood flow, mimicking oxygen, and targeting hypoxic tumor cells.[9]

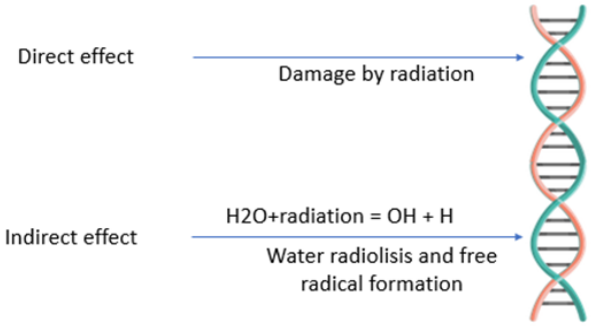

Image 1. *Radiation damage to DNA.*

Improving radio response with radiosensitizers is a promising approach in radiotherapy. Radiosensitizers are promising agents that enhance injury to tumor tissue in IR. A pioneer in this field, G. Adams,[10] classified radiosensitizers into five groups based on the mechanisms of their action: (1) suppressors of intracellular thiols, or other endogenous radioprotective substances, (2) cytotoxic substances formed by radiolysis of the radiosensitizer, (3) inhibitors of DNA repair, (4) thymine analogs that can incorporate into DNA and (5) oxygen mimetics that can imitate the action of oxygen. However, the continuous development and innovation of new technologies and strategies of radiosensitization forced the introduction of a new classification into three categories based on sensitizer structures: (1) small molecules, (2) macromolecules, and (3) nanomaterials.(1)

Mechanisms of radioresistance involve tumor-specific oncogenic signalling pathways, tumor metabolism and proliferation, tumor microenvironment/hypoxia, and genomics. Most adenocarcinomas and sarcomas, advanced HNSCC, melanoma, non-SCLC, and gliomas are considered radioresistant. Radiosensitive tumors include myeloma, SCLC, germ cell tumors, PCa, and breast cancer.

In this review, we considered the use of radiosensitizers, including small molecules and nanomaterials, in various malignant tumors and the problems and prospects for their clinical use in cancer therapy.

Materials and Methods

We reviewed published data on radiotherapy and radiosensitization methods up to 2021, searching through PubMed, and references from relevant articles, using search terms with suitable keywords. The search terms were “cancer,” “ionizing radiation,” “cellular radiosensitivity,” “tumor tissue,” “DNA damage,” and “radioresistance.”

Drugs as Radiosensitizers in Different Types of Cancer

Breast cancer

Breast cancer is the most common cancer in women. Triple-negative breast cancer (TNBC) accounts for 10%-15% of all breast cancers. TNBC cells, characterized by the lack of estrogen and progesterone receptor expression, as well as HER2 amplification, are unresponsive to anti-ER or HER2 targeting agents. TNBC is the most aggressive subtype of breast cancer. Radioresistance and stemness are substantial obstacles to TNBC treatment. Lehmann et al. identified a LAR (luminal androgen receptor) subtype of TNBC, which included patients with decreased relapse-free survival and was characterized by androgen receptor (AR) signaling. LAR cell lines were uniquely sensitive to bicalutamide (an AR antagonist). AR is expressed in 15%–35% of all TNBC.[11] Michmerhuizen et al.[12] studied whether seviteronel (INO-464), a novel CYP17 lyase inhibitor and AR antagonist, can radiosensitize AR-positive (AR+) TNBC models. The authors reported that seviteronel could selectively radiosensitize AR+ TNBC models in vitro and in vivo. Radiosensitization was mediated, at least in part, through the delayed repair of dsDNA breaks. The results indicate AR as a mediator of radioresistance in AR+TNBC models and seviteronel as a radiosensitizing agent in AR+TNBC.

Lung cancer (LC)

Epigenetic alterations can be considered potential targets for radiosensitization. This can be achieved through the regulation of chromatin structure modifications or through epigenetic manipulations of genes involved in the cell cycle, apoptosis, or DNA repair. The available data on the association between epigenetics and radiosensitivity are sparse and are mostly based on in vitro or in vivo data.

A study by Kang et al.[13] aimed to elucidate the radiosensitizing effect and underlying mechanism of MA-17, a new kind of DNA methyltransferase (DNMT) inhibitor derived from a phthalimido alkanamide structure. DNMT expressions were confirmed in cultured human LC (A549) cells. MA-17 significantly radiosensitized A549 cells. Pretreatment with MA-17 increased sub-G1 fractions and inhibited the repair of double-strand breaks (DSBs) in DNA induced by irradiation. MA-17 also down-regulated DNA homologous recombination and the Fanconi anemia pathway (FANCA, BRCA1, and RAD51C) in A549 cells. DNMT inhibitor MA-17 possessed both biostability and favorable and substantial radiosensitizing effects by augmenting apoptosis or inhibiting DNA damage repair.

SCLC, a high-grade neuroendocrine carcinoma, makes up about 15% of LC cases. As an aggressive malignancy, SCLC has a critical need for novel therapies. Laird and colleagues[14] studied whether PARP inhibition could sensitize SCLC cells to IR. For radiosensitization, poly-ADP-ribose polymerases (PARP1/2) inhibitors veliparib and talazoparib were examined. Short-term viability assay and clonogenic survival assays were used to assess radiosensitization in 6 SCLC cell lines. Both PARP inhibitors effectively sensitize SCLC cell lines and PDXs to IR. However, talazoparib exhibited greater PARP-trapping activity that was associated with superior radiosensitization, and an increased number of

DNA DSBs. Thus, PARP inhibitors, especially those with high PARP-trapping activity, may improve the efficacy of radiotherapy in SCLC.

PARP1 and PARP2 are important DNA damage sensors as they bind rapidly at the site of DNA damage and help in resealing single-stranded DNA breaks during break excision repair and for the repair of the topoisomerase-1 cleavage complex.[15,17] Since PARP plays an important role in response to DNA damage, and radiation leads to double-stranded breaks, examining whether PARP inhibitors act synergistically with radiation is relevant.

Hastak et al.[18] examined the effects of a new PARP inhibitor, LT626, in combination with IR in lung and pancreatic cancers. The combination of LT626 with IR was more effective in inhibiting growth in lung and pancreatic cancer cell lines than either treatment used alone. Using in vivo LC xenograft models, the researchers demonstrated that LT626 functioned as an effective radiosensitizer during fractionated radiation treatment. Overall, in vitro and in vivo studies showed that LT626 acted synergistically with radiation in lung and pancreatic cancers.

Esophageal cancer

Esophageal cancer (EC) is divided into two subtypes, esophageal adenocarcinoma (EAC) and squamous cell carcinoma (SCC). Altered mitochondrial function is linked with radioresistance in EAC. Buckley et al.[19] identified compounds with antiangiogenic and antimetabolic activity targeting oxidative phosphorylation to improve radiosensitivity in EAC cells from pyrazinib (P3)-containing molecules. The results show that in addition to reducing metabolic rates and levels of ROS in EAC, P3 improved radiosensitivity in an isogenic model of this cell type. P3, which had shown an antiangiogenic and antimetabolic effect in zebrafish, showed a reduction tested survival fraction of the cells. Furthermore, P3 also reduced the secretion of interleukins in cells with EAC. Further studies with P3 via EAC biopsies or other non-in vitro methods are important to elucidate the therapeutic potential of P3 further.

The enzyme ribonucleotide reductase (RR) contains the RRM2 subunit, whose overexpression is related to the cellular response to DNA damage, and this can lead to angiogenesis, metastasis, tumor progression, and drug resistance or radioresistance. Osalmid has been shown to inhibit RRM2 by binding to the latter's hydrogen bond. However, its radiosensitizing effects are unknown. In a study by Tang et al.,[20] RRM2 was found to be associated with acquired radioresistance in EC, and osalmid exerted direct cytotoxicity on EC cells. Immunofluorescence assays showed that osalmid treatments alone induce DNA DSBs. Moreover, an analysis by western blot showed that the combination of osalmid and IR induced many DSBs. Colony formation assays showed that osalmid treatment increased radiosensitivity in EC cells. Furthermore, the osalmid and irradiation combination significantly increased the apoptosis rate of EC cells, compared to irradiation or osalmid. Osalmid was identified to have antitumor effects and improved the therapeutic efficacy of radiation in EC.

Human epidermal growth factor receptor 2 (HER2) is involved in many types of cancer, including EC. Pirotinib is an irreversible inhibitor of HER2 that, in a novel experimental setting, has shown an antitumor effect in breast xenograft models that overexpress HER2. However, whether this drug can have an antitumor effect on the esophagus is still unknown. To this purpose, Lian et al.[21] performed a study to analyze the effect of pirotinib combined with radiotherapy on EC cells that were HER2-positive. The results showed that, unlike treatment with radiation alone, irradiated cells combined with pirotinib showed notably reduced colony formation; this indicated that pirotinib enhanced the radiation-inhibitory effect on colony formation in cell lines used. Pirotinib sensitized HER2-positive EC cells to radiation, which enhanced the antiproliferative effect of radiation. These findings are expected to provide a new strategy for the application of new drugs to treat EC.

ESCC tumors develop resistance to radiotherapy; this explains the metastasis, high recurrence, and poor five-year survival of patients with this condition. There are study reports that astaxanthin (ATX), a carotenoid family member, is a beneficial agent for therapy in many kinds of diseases due to its strong antioxidant property. It has had good results in treating various types of cancer. However, there still needs to be more information regarding the ATX effect on ESCC cells' radiosensitivity, and there are no reports yet on the exact mechanisms. To this end, a study by Qian et al.[22] was designed to discover if ATX could improve ESCC cells' sensitivity to irradiation and the possible mechanism in vitro, showing important evidence for this drug as a radiosensitizer in ESCC radiotherapy. ESCC cell lines were exposed to irradiation in the presence or absence of ATX treatment. It was shown that ATX improved the radiosensitivity of ESCC cells and induced apoptosis and G2/M arrest via inhibiting Bcl2, CyclinB1, Cdc2, and promoting Bax expression. ATX appears to be a novel radiosensitizer with promising results for the treatment of ESCC, and further research is warranted.

Sunitinib is a highly selective, multidirectional, receptor tyrosine kinase inhibitor; it has direct apoptotic and antiproliferative effects against various tumors. But there is very little information regarding radiosensitization in EC. Ding et al.[23] investigated the radiosensitive effects of sunitinib on human ESCC cells and the underlying mechanisms. ESCC cells were exposed to hypoxia and, before IR, were treated with sunitinib at different concentrations. Sunitinib enhances radiation-induced apoptosis in both normoxic and hypoxic ESCC cells. Compared with that of the hypoxia and IR groups, the apoptosis rate of the group treated with sunitinib increased dose-dependently. The authors found that the sunitinib radiosensitivity effect was associated with the downregulation of HIF-1α and VEGF expression and concluded that sunitinib could be a promising radiosensitizer for EC radiotherapy.

Prostatic cancer (PCa)

Genistein is a tyrosine-specific protein kinase inhibitor, the best-characterized bioflavonoid-based topoisomerase II poison, which inactivates EGFR, IGF1R, and Akt-mediated signaling. Type II topoisomerases generate double-stranded DNA breaks as part of their reaction mechanism.[24-27] Tyrosine kinase inhibitor (tyrphostin) AG1024 is a specific IGF1R inhibitor, and it has been reported that this inhibitor radiosensitizes prostate and breast cancer cells. Nevertheless, there is not

much information about PCa cells' radiosensitivity to combined treatment with AG1024 and genistein. To this end, Tang et al.[28] studied the synergistic effect of combined therapy with genistein and AG1024 on the PCa cell's radiosensitivity. Genistein treatment suppressed the homologous recombination (HRR) and the non-homologous end joining (NHEJ) pathways by inhibiting the expression of Rad51 and Ku70, and AG1024 treatment only inhibited the NHEJ-pathway via the inactivation of Ku70 detected in western blot analysis. Before irradiation, PCa cells were treated with AG1024, genistein, and a combination. The results show that the combined treatment with genistein and AG1024 improves X-radiation-induced apoptosis in the human PCa cell lines PC3 and DU145. Using western blot analysis, the authors detected the increased expression of ATM(Ser1981), Bax, and active caspase-3 and decreased expression of p-IGF1R(Tyr1135) and Bcl-2 in PC3 and DU145 cells treated with genistein (30 μM) and/or AG1024 (10 μM) plus X-irradiation. The results obtained suggest that both genistein and AG1024 induced apoptosis of PCa cells via the activation of apoptosis-related pathways, which may be associated with the inactivation of IGF1R, and the combination of genistein and AG1024 exhibited a synergistic effect on the radiosensitivity of PCa cells by suppressing the HRR and NHEJ pathways.

Colon cancer

Imidazoacridinone C-1311 is a multipurpose therapeutic agent tested in patients with advanced solid tumors. It was found that C-1311 possesses an acceptable toxicity profile. C-1311 inhibits topoisomerase, leading to subsequent DNA strand breaks and the formation of cleavable complexes of DNA-topoisomerase II complexes. Skwarska et al.[29] conducted a study to assess the effect of the p53 tumor suppressor on the biological response to C-1311 using the genetically matched pair of human colon carcinoma cell lines, HCT116p53+/+ and HCT116p53−/−. Using human colon cancer cell lines, the authors provided a molecular analysis of the response to C-1311 exposure and showed that cells with wild-type p53 underwent p53-mediated G2 phase arrest and, ultimately, senescence; in contrast, cells lacking p53, despite an initial arrest in G2, entered mitosis and underwent mitotic catastrophe and apoptosis. In addition, cells in hypoxic conditions also responded to C-1311 in a p53-dependent manner. The most important result was that C-1311 can be effectively combined with radiation to improve the radiosensitivity of a panel of cancer cell lines.

Lithium chloride (LiCl) is a specific glycogen synthase kinase (GSK)3β inhibitor. This medicine is helpful in treating neurological diseases, cancer, and inflammation. Cammarota et al.[30] investigated the effect of LiCl treatment on the viability of primary colon cancer cells exposed to 7 Gy delivered by highenergy photon beams. To achieve this aim, the viability of irradiated T88 cells, mesenchymal colon cancer cells, was compared with that of irradiated T88 cells pretreated with LiCl. The authors demonstrated that T88 mesenchymal colon cancer cells are resistant to radiotherapy, and LiCl sensitizes these cells to apoptosis in response to high-energy photons. The decrease in cell viability was greater with combined therapy than with irradiation alone. The authors concluded that LiCl could be used to increase the sensitivity of resistant colon cancer cells to radiotherapy.

Celecoxib is a nonsteroidal anti-inflammatory drug, specifically a COX-2 inhibitor. Celecoxib showed anti-cancer effects in both COX-2 dependent and independent pathways and is used as a radiosensitizing enhancer. BI-69A11 is an ATP-competitive AKT inhibitor. Because both COX-2 and AKT inhibitors can enhance the effects of radiation on cancer cells, it is believed that combined treatment of both inhibitors may significantly radiosensitize cancer cells. Pal and colleagues[31] did research in which the effects of combined treatment with celecoxib and BI-69A11 on the colon cancer cells' radiosensitivity were evaluated to define whether this combination is beneficial for patients treated with radiotherapy. Triple therapy treatment led to the induced activation of apoptotic pathways. The authors revealed the therapeutic potential of triple combination therapy in the prevention of radioresistance and demonstrated the cytotoxic effects of triple combination therapy in colon cancer.

Pancreatic ductal adenocarcinoma (PDAC)

Gemcitabine is an antineoplastic agent currently used to treat several types of cancer, including pancreatic cancer. The use of gemcitabine as a radiosensitizer has shown promising results. In different experimental models, the p38 MAPK signaling pathway has been shown to be a major determinant in the cellular response to gemcitabine. However, the molecular mechanism implicated in gemcitabine-associated radiosensitivity remains to be investigated. A study by Pascual-Serra et al.[32] showed that the specific knockdown of MAPK11 (p38β) induced a total loss of the radiosensitivity associated with gemcitabine, as well as a marked increase in the resistance to the drug. The authors identified p38β as a major determinant of the radiosensitizing potential of gemcitabine.

Gemcitabine is widely used as a radiosensitizer for PDAC treatment and is known to induce S-phase arrest of tumor cells, which is a cell cycle phase known to sensitize cells to DNA damage, one of the mechanisms of cell death induced by radiotherapy**.** Waissi et al.[33] performed an in vivo study and a whole-transcriptome analysis to determine whether treatment with gemcitabine, combined with proton therapy and reinforced by DNA-damage radiosensitization using a PARP inhibitor, olaparib, is a viable strategy to improve the treatment of PDAC. NMRI mice bearing MIA PaCa-2 xenografts were treated with olaparib and/or gemcitabine and irradiated with 10Gy photon or proton. The results obtained showed that the association of gemcitabine, olaparib, and proton therapy significantly enhanced tumor response and progression-free survival in a heterotopic xenografts mice model.

Vance et al.[34] demonstrated that combined inhibition of homologous recombination repair mediated by checkpoint kinase-1 [Chk1] via AZD7762 and PARP1 [via olaparib (AZD2281)] selectively radiosensitizes p53 mutant pancreatic cancer cells.

Nasopharyngeal carcinoma (NPC)

Salinomycin is a monocarboxylic polyether antibiotic that kills many types of microorganisms. It has also shown

great efficacy in killing cancer stem cells. However, the information on radiosensitivity is rare. A study by Zhang et al.[35] aimed to explore the radiosensitivity of salinomycin on human NPC cell line CNE-2. CNE-2 cells were treated with salinomycin or irradiation, alone or in combination. DSB levels were determined by γ-H2AX foci immunofluorescence staining in CNE-2 cells at different time points after X-ray exposure. The combination of salinomycin treatment and 4-Gy X-rays increased γ-H2AX nuclear foci formation, compared with X-rays alone. Nuclear foci without salinomycin increased due to DBS repair. Salinomycin induced apoptosis and G2/M arrest, increased Bax and cleaved caspase3, decreased Bcl-2 expression, and increased the formation of γ-H2AX nuclear foci. The authors concluded that salinomycin may be a radiosensitizer for NPC radiotherapy.

Liver cancer

HCC is the most common form of liver cancer and the third most common cause of cancer deaths worldwide. Some studies have reported that chemotherapy agents can be used as radiation sensitizers in the treatment of HCC.[36,37] The phenanthroline derivatives and their metal complexes have been recognized as potential anticancer candidates because they have a strong affinity with DNA and are safer and more efficient for further cancer therapy.[38] Liu et al.[39] synthesized a phenanthroline derivative, 2-phenyl-imidazo [4, 5 f] [1, 10] phenanthroline (L02), and combined it with X-ray radiation to investigate whether it can enhance the radiosensitivity in inhibiting HCC cells. The radiosensitization of L02 combined with IR was evaluated by the sensitivity enhancement ratio and isobolographic analysis. L02 sensitized HCC cells to IR by inducing apoptosis, increasing the expression of apoptosis markers, and enhancing radiation-induced DNA damage. The authors concluded that L02 may be a novel radiosensitizer for HCC.

Apatinib, a highly selective inhibitor of the vascular endothelial growth factor receptor-2 (VEGFR2) tyrosine kinase, has a good inhibitory effect on advanced HCC.[40] In HCC, apatinib can induce cell cycle arrest at the G2/M phase, promoting apoptosis of HCC cells in vitro, and its inhibitory effect is related to the expression level of VEGFR.[41] In SMMC-7721 cells, apatinib promoted apoptosis by inhibiting the phosphorylation level of PI3K/AKT.[42] The combination of this drug with chemotherapy and immunotherapy has shown progress. Liao et al.[43] investigated the potential clinical utility of apatinib as a radiosensitizer in the treatment of HCC. The findings revealed that apatinib enhanced the radiosensitivity of HCC cell lines, suppressed the repair of radiation-induced DNA DSBs, and increased IR-induced apoptosis. Apatinib radiosensitized HCC via suppression of the IR-induced PI3K/AKT pathway. In an in vivo study, apatinib combined with irradiation significantly decreased xenograft tumor growth. Apatinib showed therapeutic potential as a radiosensitizer in HCC suppressing PI3K/AKT signaling pathway.

Head and neck cancer

Most head and neck cancers are squamous cell cancers. Human papillomavirus (HPV) is a known risk factor for head and neck squamous cell carcinoma (HNSCC). p16 immunohistochemistry is a widely used method to detect HPV positivity in cancer. The tumor suppressor gene p16, encoding a specific inhibitor of cyclin-dependent kinase (CDK) 4 and 6, is found to be altered in various cancers. It is thought that expression of p16 in HPV-positive HNSCC mediates radiosensitivity via inhibition of CDK 4/6. Göttgens and colleagues[44] used a clinically approved CDK4/CDK6 inhibitor, palbociclib, and assessed its effect on radiosensitivity in HPV-negative and HPV-positive HNSCC cell lines. The study results showed that only HPV-negative HNSCC cells were radiosensitized by palbociclib, which was dependent on the presence of hyperphosphorylated retinoblastoma protein. Palbociclib was an effective radiosensitizer at hypoxia levels that are associated with radiation resistance. The combination of IR and palbociclib was highly effective, leading to the loss of cell viability and a failure to repair IR-induced DNA damage and subsequent mitotic catastrophe. The combination of palbociclib and IR may be an effective therapeutic strategy for treating HPV-negative HNSCC.

Bladder cancer (BC)

Approximately 70% of bladder tumors are nonmuscle-invasive BC; the rest are muscle-invasive BCs. Muscle-invasive BC (MIBC) is more aggressive than non-invasive disease, and approximately 50% of patients with this disease will experience distant recurrence following therapy. Inhibitors of HDAC have been identified as an effective strategy to enhance cancer radiotherapy HDAC inhibitors (HDACi) decrease the ability of tumor cells to repair radiation-induced DNA damage by interfering with DNA damage signalling and repair pathways.[45] In a study by Tsai et al.,[46] the selective HDAC6i enhanced BC radiosensitization and effectively inhibited IR-induced oncogenic CXCL1-Snail-signalling.

Paillas et al.[47] studied the HDAC class I-selective agent romidepsin as a radiosensitizer in bladder tumors. In vitro, romidepsin effectively radiosensitized different BC cells. Romidepsin in combination with IR resulted in a significant delay in tumor growth and did not increase the severity of acute (3.75 days) and late toxicity (at 29 weeks). of normal intestinal tissues. The authors suggest that the disruption of DNA repair pathways caused by romidepsin is a key mechanism for its radiosensitizing effect in BC cells.

Several studies have indicated that tumor survival and growth in advanced cancers are related to autophagy. Autophagy helps tumor cells to overcome stressful conditions, including hypoxia and nutrient deprivation. The inhibition of autophagy or knockdown of autophagy genes can result in tumor-cell death.[48,49] The relationship between radiotherapy and autophagy has not been studied in depth. As apoptosis only accounts for 20% or less of radiation-induced cell death, other cell death pathways, including autophagy, should also be studied.[50]

A study performed by Wang et al.[51] aimed to investigate the radiosensitizing effect of chloroquine in BC, with an emphasis on autophagy inhibition and apoptosis induction. BC cell lines were irradiated with or without chloroquine. The apoptosis rate was measured using Annexin V-FITC/PI double staining. To evaluate the activity of autophagy, the LC3 II and p62 levels were detected with western blotting analysis. Radiation-induced DNA DSBs were measured by

the staining of γ-H2AX. Chloroquine alone inhibited the proliferation of BC cells in a dose-dependent manner. Low cytotoxic concentrations of chloroquine enhanced the radiation sensitivity of BC cells. Chloroquine also decreased the repair of radiation-induced DNA damage. The accumulation of LC3 II and p62 protein levels in BC cell lines was increased by chloroquine treatment. After irradiation, the expression of LC3 II increased, whereas the p62 protein level decreased, which suggested that irradiation activated autophagy. The expression levels of LC3 II and p62 in the combined treatment group were higher than in irradiation alone, indicating that chloroquine inhibited autophagy induced by irradiation in BC. Inhibiting autophagy and activating apoptosis, chloroquine might be a promising radiosensitizer in the radiation therapy of BC.

Anticancer drugs and the mechanism of their action at the cellular/molecular level are summarized in Table 1.

Nanoparticles and small molecule inhibitors

In the past decade, there has been considerable interest in radiosensitization using high atomic number (high-Z) metal nanoparticles (NPs).[52,53] Since high-Z metal NPs have a higher stopping power for IR than soft tissue, they enhance radiotherapy efficacy.[54,55] An enhanced therapeutic effect by radiosensitization mediated by high-Z metal NPs has been reported in multiple preclinical tumor models, including glioblastoma multiforme.[55] Stewart et al.[56] provided the first proof for the novel application of bismuth oxide (Bi2O3) as a radiosensitizer on the highly radioresistant 9L gliosarcoma cell line. The results showed that Bi2O3 NPs increase the radiosensitivity of 9L gliosarcoma tumor cells for both kVp and MV energies.

Saberi et al.[57] evaluated the effect of gold nanoparticles (GNPs) on radiosensitization enhancement of HT-29 human colorectal cancer cells at megavoltage (MV) X-ray energy.

Table 1.

Anticancer agents and the mechanism of their action at the cellular/molecular level.

Agents	Action	Source
Huaier	G0/G1 phase cell cycle arrest	Ding et al. (2016) [78]
Seviteronel	Accumulation of DNA DSBs	Michmerhuizen et al. (2020) [13]
MA-17	Inhibition of DNMT	Kang et al. (2019) [14]
Talazoparib	Enzyme inhibition and PARP trapping	Laird et al. (2018) [15]
Tanshinone I	Differential protein expression	Yan et al. (2018) [93]
Diosmetin	Inhibition the activated Akt signaling pathway	Xu et al. (2017) [97]
Pyrazinib	Reduction of ROS levels	Buckley et al. (2019) [20]
Osalmid	Induction of DNA DSBs	Tang et al. (2020) [21]
Sunitinib	Downregulation of HIF-1α and VEGF expression	Ding et al. (2016) [24]
Pirotinib	Innhibition of HER2	Lian et al. (2020) [22]
Astaxanthin	Antioxidant property, G2/M phase cell cycle arrest	Qian et al. (2017) [23]
Genistein	Activation of apoptotic pathways, suppression of the HRR and NHEJ pathways	Tang et al. (2018) [29]
Sinomenine hydrochloride	Suppression of expression of double-strand break repair protein Ku80 and Rad51 and enhancing Chk1 activation	Zhang et al. (2018) [80]
Imidazoacridinone C-1311	Topoisomerase inhibition	Skwarska et al. (2017) [30]
lithium chloride	GSK-3β inhibition, induction of apoptosis	Cammarota et al. (2020) [31]
Celecobix	COX2 inhibition, activation of apoptotic pathways	Pal et al. (2016) [32]
BI-69A11	ATP-competitive AKT inhibitor	Pal et al. (2016) [32]
Kaemferol	Reduction of clonogenic survival	Kuo et al. (2015) [94]
Gencitabine	Tumor cell's S-phase arrest	Pascual-Serra et al. (2021) [33]
Salinomycin	Induction apoptosis and G2/M phase cell cycle arrest	Zhang et al. (2016) [36]
Phenanthroline L02	Induction apoptosis	Liu et al. (2019) [40]
Apatinib	Suppression of IR-induced PI3K/AKT pathway	Liao et al. 2019 [44]
Mesima	Induction of apoptosis, impairment of cell cycle regulation, reduction of IR-induced DNA damage repair.	Jeong et al. (2020) [92]
Palbociclib	CDK4/6 inhibition	Göttgens et al. (2019) [45]
Romidepsin	Disruption of DNA repair pathways	Paillas et al. (2020) [48]
Valproate	HDAC inhibition	Stritzelberger et al. 2020 [98]
Chloroquine	Inhibition of autophagy and activation of apoptosis	Wang et al. (2018) [52]
Lys05	Lysosomal membrane permeabilization and mitochondrial depolarization.	Zhou et al. (2020) [99]
PI-103	Inhibition of Hsp90	Djuzenova et al. (2012) [105]

The findings showed that the cell viability was not influenced by exposure to different concentrations of GNPs (10-100 μM). GNPs alone did not affect the cell cycle progression and apoptosis. In contrast, GNPs, in combination with 9MV radiation, induced more apoptosis. The interaction of GNPs with MV energy resulted in a significant radiosensitization enhancement, compared with IR alone. The authors concluded that GNPs can act as a bioinert material on NT-29 cancer cells, and enhancing radiosensitization may be associated with an increase in the absorbed radiation dose.

Habiba et al.[58] developed a new type of silver nanoparticle composite, PEGylated graphene quantum dot (GQD)-decorated Silver Nanoprisms (pGAgNPs), that show excellent in vitro intracellular uptake and radiosensitization in radiation-sensitive HCT116 and relatively radiation-resistant HT29 colorectal cancer cells. Treatment with nanoparticles and a single radiation dose of 10Gy significantly reduced the growth of colorectal tumors in nude mice and increased the survival time compared to treatment with radiation only.

The development of safe nanoparticle-based drug carriers to administer the drug directly into tumors and keep it there longer is of great interest. Mirjolet et al.[59] investigated titanate nanotubes (TiONts) to develop a TiONts-docetaxel (DTX) nanocarrier and to evaluate its radiosensitizing efficacy in vivo in a PCa mouse model. Tumor growth was significantly slowed by TiONts-DTX with IR, compared with free DTX in the same conditions. These results suggest that TiONts-DTX improved radiotherapy efficacy in PCa.

Over the past few decades, small molecule inhibitors (SMIs) have gained acceptance as new therapeutic strategies in cancer. SMIs are compounds less than 500Da, targeting any part of the molecule, regardless of the location of the target in the cell.[60] Flap endonuclease 1 (FEN1), a structure-specific metallonuclease, is a typical member of the Rad2 nuclease family. FEN1 plays a critical role in the maturation of the Okazaki fragment of DNA replication. It is essential to DNA repair pathways, such as base excision repair and the polymerase α error editing (AEE) pathway.[61-64] FEN1 is overexpressed in many forms of cancer, and FEN1 inhibitor has been reported to enhance the effect of DNA damage-related chemotherapy.[65-66] The purpose of a study conducted by Li et al.[67] was to determine whether FEN1 inhibitor SC13 could enhance the therapeutic effect of IR therapy in cervical cancer. The results revealed that FEN1 is overexpressed in HeLa cells and can be upregulated further by IR. It was demonstrated that FEN1 inhibitor SC13 enhances IR sensitivity of cervical cancer in vitro and in vivo, and the beneficial effect was mainly due to the impairment of the DNA damage repair mechanism resulting from FEN1 inhibition, leading to apoptosis of cancer cells.

To date, evidence has been accumulated that small non-coding RNAs, microRNAs (miRNAs), are involved in regulating tumor initiation and progression.[68-72] Some studies demonstrated that miRNAs can be used as radiosensitizers.[72,73] Baek et al.[74] showed that overexpression of miR-374 sensitized human pancreatic cancer cell lines PANC1 and MIA PaCa-2 toward carbon ion beam radiation. miRNA miR-374 can potentially be a new radiosensitizer for carbon ion beam radiotherapy.

The mechanisms of the actions of nanoparticles (NP) and small molecule inhibitors (SMI) are summarized in Table 2.

Table 2.

Nanoparticles (NP) and small molecule inhibitors (SMI) and the mechanism of their action.

NP/SMI	Action	Source
Bi2O3	Increasing sensitivity for both kVp and MV energies	Stewart et al. (2016) [57]
miR-374	Increasing sensitivity to carbon ion beam radiation	Baek et al. (2016) [76]
Gold NPs	Increasing the absorbed radiation dose.	Saberi et al. (2017) [58]
TiONts	Reducing tumor growth	Mirjolet et al. (2017) [60]
Silver NPs (pGAgNPs)	Reducing tumor growth	Habiba et al. (2019) [59]
FEN1 inhibitor SC13	Impairment of the DNA damage repair	Li et al. (2019) [69]

Actions of certain drugs toward apoptotic pathways and cellular mechanisms linked to cancer, as well as targets of drugs and compounds are presented in Images 2 and 3.

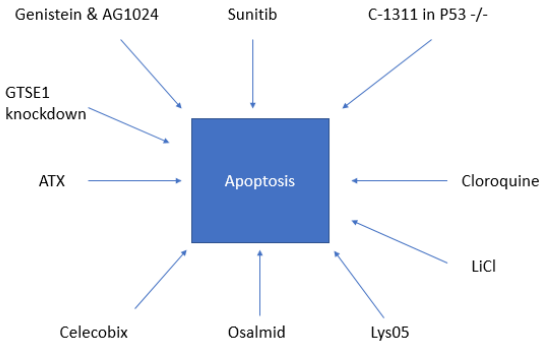

Image 2. *Actions of anticancer drugs toward apoptotic pathways and cellular mechanisms linked to malignant tumors.*

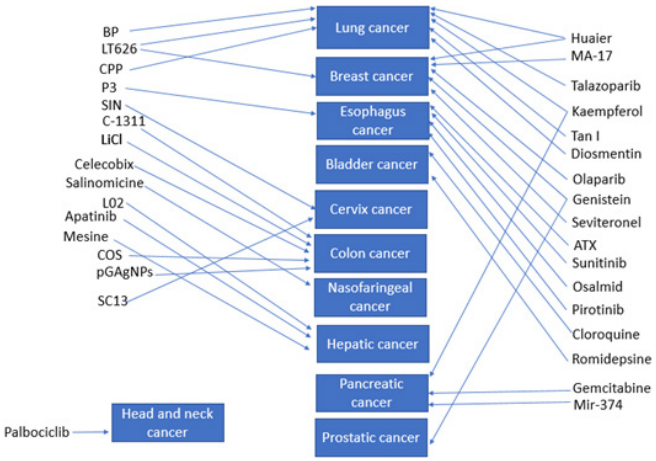

Image 3. *Targets of anticancer drugs and compounds.*

Medicinal plants and traditional Chinese medicine

Recently, several natural products showed promising anticancer properties. Huaier (*Trametes robiniophila Murr*) is a medicinal fungus of traditional Chinese medicine with more than 1500 years of history of clinical application. In recent years, potent antitumor effects of Huaier have been noted in various neoplastic diseases, including breast cancer, HCC, lung cancer, and gastrointestinal cancer.[75] Ding and colleagues[76] conducted a study to evaluate the combined effects of radiotherapy and Huaier on breast cancer. Using HTA 2.0 transcriptome microarray assay, the researchers found that Huaier downregulates genes related to the cell cycle, cell division, cell cycle phases, and DNA repair. The findings obtained suggest that Huaier causes G0/G1 arrest through downregulation of cell cycle-regulating proteins in MCF-7 and MDA-MB-468 cells, prolongs the persistence of γ-H2Ax foci after radiotherapy, and interferes with the homologous recombination pathway of DNA repair by downregulating RAD51. Thus, Huaier may be a promising radiosensitizer for treating breast cancer.

N-Butylidenephthalide (BP), extracted from traditional Chinese medicine *Radix Angelica Sinensis* (*Danggui*), shows antitumor activity against various cancer cell lines. Su et al.[77] studied BP's cytotoxic and radiosensitizing effects in human breast cancer cells. The terminal deoxynucleotidyl transferase dUTP nick end labeling staining (TUNEL assay) detected that BP induces apoptosis in breast cancer cells. BP increased the radiosensitivity of breast cancer cells as measured by colony formation assay and comet assay. The authors concluded that BP could be a potential chemotherapeutic and radiosensitizing agent for the treatment of breast cancer.

Sinomenium acutum has been used in the treatment of neuralgia and rheumatoid arthritis in Asia since ancient times. Sinomenine (SIN), a bioactive alkaloid extracted from the Chinese medicinal plant *Sinomenium acutum*, has many healing properties both in vivo and in vitro. However, the SIN anticancer effects and its water-soluble form, sinomenine hydrochloride (SH), have been recently characterized. Zhang D. and collaborators [78] assessed the sensitizing efficacy of SH in human cervical cancer cells to irradiation, and demonstrated it is a potential radiosensitizer. The results of the study showed that SH treatment affects the DNA DSB response in cells. Likewise, SH was found to suppress the DSB repair protein Ku80 and Rad51 expression and enhance Chk1 activation induced by irradiation. The results showed that SH was useful in radiosensitization through dual pathways, regulation of cell cycle checkpoint, and DNA repair.

Zhang et al.[80] investigated the radiosensitizing effect and underlying mechanisms of *Cyclocarya paliurus* (CP) polysaccharide (CPP) on hypoxic A549 and H520 human nonsmall cell lung carcinoma cells. CP is a member of the Juglandaceae family. CPP is a heteropolysaccharide that possesses antioxidant and hypoglycemic effects and antitumor activity.[80-82] The study's results suggested that CPP markedly inhibited the viability of hypoxic A549 and H520 cells. Combined treatment with CPP and IR enhanced apoptosis of hypoxic A549 and H520 cells, suppressed cell proliferation, modified the expression levels of hypoxiainducible factor1α, survivin, cleaved caspase3, and affected the mammalian target of rapamycin (mTOR)/Akt/phosphatidylinositol4,5bisphosp hate 3kinase (PI3K) pathway. The potential radiosensitizing effects of CPP suggest its efficacy in the combined treatment of non-small cell lung carcinoma.

Phellinus linteus (Mesima), a tropical basidiomycete fungus, is used extensively as a traditional medicine in China, Korea, and other Asian countries to treat different diseases, including many human malignancies.[83,84] The main biological functions of *P. linteus* include anticancer, antioxidant, anti-inflammatory, hypoglycemia, and anti-fibrotic.[85-89] Jeong et al.[90] examined its potential as a radiosensitizer in HCC radiotherapy using human HCC Hep3B and HepG2 cell lines and xenograft tumors. Mesima pretreatment significantly enhanced HCC cell radiosensitivity in vitro, and Mesima+IR significantly reduced xenograft tumor growth and size in vivo compared to those with single treatments. Mesima significantly enhanced radiotherapy efficiency by inhibiting tumor cell survival, inducing apoptosis, impairing cell cycle regulation, and reducing radiation-induced DNA damage repair. The cell viability rate was reduced significantly for cells treated with Mesima before irradiation than those without Mesima. The authors demonstrated that the combined treatment likely regulated the apoptotic process, including intracellular caspase signaling. These findings support the radiosensitizing effects of Mesima on HCC cells.

Tanshinone I (Tan I) is a natural product from *Salvia miltiorrhiza*, showing a broad spectrum of bioactivities, including antitumor activity. Yan et al.[91] identified Tan I as a potential radiation sensitizer in LC cells. Tan I significantly inhibited cell proliferation and clone formation by increasing radiosensitivity in radioresistant LC cells, H358-IR and H157-IR. Tan I suppressed the expression of the pro-oncogenic protein phosphoribosyl pyrophosphate aminotransferase (PPAT) in H358-IR and H157-IR cells and integrated well into the active pocket of the PPAT structure, acting as a potential PPAT inhibitor and improving radiation efficiency.

Kaempferol is a flavonol in the flavonoid category and is widely distributed in various plant genera, such as delphinium, camellia, barberry, and citrus fruits, Kaempferol has been reported to be effective against human non-small cell lung carcinoma, pancreatic cancer, and glioma cells. Nevertheless, the combination of kaempferol and radiation against cancer is still being evaluated. Kuo et al.[92] studied the potential radiosensitization ability of kaempferol in LC in vitro and in vivo. After administering kaempferol, cells were exposed to 0 to 12Gys of radiation. Treatment of cells with radiation alone was found to have a minimal effect on clonogenic survival. However, when kaempferol was administered before irradiation, the surviving fraction significantly decreased. In an in vivo study, it was observed that the volume of the tumor decreased when there was a combination of kaempferol and irradiation. This study provided strong evidence that kaempferol has potential as a radiosensitizer.

The protein kinase B signaling pathway (PKB/Akt), hyperactivated during oncogenesis, is a candidate target for cancer therapy.[93] Akt, as an important intracellular signaling molecule, is critical for cell survival and growth, especially

during cancer progression and radioresistance.[94] Xu et al.[95] showed that diosmetin, the aglycone of the flavonoid glycoside from olive leaves, citrus fruits, and some medicinal herbs, has a promising effect on radiotherapy sensitization. Diosmetin could induce G1 phase arrest and thus enhance the radiosensitivity of radioresistant A549/IR LC cells. Diosmetin also restrains the IR-induced DNA damage repair by inhibiting the activated Akt signaling pathway, acting as a potential drug for treating radioresistant LC cells.

Miscellaneous

Valproate (VPA) is an antiepileptic that, in addition to its anticonvulsant properties, is an effective HDACi, which participates in the modulation of chromatin structure and gene expression. VPA increases radiation sensitivity in various tumor cells in vitro. However, clinical data on the possible improvement of tumor control by adding VPA to tumor therapy is controversial. To determine individual radiosensitivity, Stritzelberger et al.[96] analyzed blood samples of individuals taking VPA. Ex vivo irradiated blood samples of 31 adult individuals with epilepsy were studied using 3-color fluorescence in situ hybridization. Aberrations in chromosomes 1, 2, and 4 were analyzed. Radiosensitivity was determined by the mean number of breaks per metaphase (B/M) and compared with healthy donors of the same age. The average B/M value was higher in the patient group than in healthy individuals (0.480±0.09 vs. 0.415±0.07; P=0.001). The portion of radiosensitive (B/M>0.500) and distinctly radiosensitive (B/M>0.600) individuals was increased in the VPA group (54.9% vs. 11.3% and 9.7% vs. 0.0%; P<0.001). The authors confirmed that patients treated with VPA had an increased radiosensitivity, compared to the control group.

Hydroxychloroquine (HCQ) is a drug that shows effectiveness in many types of tumors. Lys05, dimeric chloroquine, is a newly synthetic lysosomotropic agent that accumulates in the lysosome and blocks autophagy more potently than hydroxychloroquine. Zhou and colleagues [97] studied whether Lys05 has anti-glioma activity. The researchers found that Lys05 decreased cell viability and reduced cell growth of glioma U251 and LN229 cells. After Lys05 treatment, autophagic flux was inhibited and lysosome function was impaired. In addition, Lys05 caused lysosomal membrane permeabilization (LMP) and mitochondrial depolarization. It was concluded that Lys05 increased radiosensitivity in an LMP-dependent manner.

Over the last decade, heat-shock protein 90 (Hsp90) has gained increasing interest as a promising anticancer drug target.[98,99] Hsp90 inhibitors can enhance the sensitivity of tumor cells to the effect of IR in vitro. Several studies have identified Hsp90 as a potential molecular target for radiosensitization.[100,101] Stingl et al.[102] showed that NVP-AUY922, a novel inhibitor of Hsp90, enhances the effect of IR on tumor cells under normoxic conditions. In a study by Djuzenova CS et al.,[103] the clonogenic assay revealed that in lung carcinoma A549 and glioblastoma SNB19 cell lines, NVP-AUY922 enhanced the radiotoxicity under hypoxic exposure to a level like that observed under oxic conditions. These findings may have implications for the combined modality treatment of solid tumors.

Kudryavtsev et al.[104] studied the role of the inducible Hsp70 in the cellular response to radiosensitizing treatments with the Hsp90 inhibitors. Cell lines derived from solid tumors of different origins were treated with the Hsp90 inhibitors or/and γ-photon radiation. The authors found that the Hsp90 inhibitors yielded considerable radiosensitization only when they caused early and pronounced Hsp70 induction; moreover, a magnitude of radiosensitization was positively correlated with the level of Hsp70 induction. It is obvious that targeting the Hsp70 induction in Hsp90 inhibitor-treated cancer cells may enhance the radiosensitivity of tumor cells.

There are many reports on the anticancer effects of chitooligosaccharides (COS);[105-108] however, there is very little information on their radiosensitizing effects. Han et al.(109) investigated the anti-proliferation and radiosensitization effect of COS on human colon cancer cell line SW480. The RAY+COS group was treated with 1.0mg/mL of COS for 48h; the RAY and RAY+COS groups were exposed to X-ray at 0, 1, 2, 4, 6, and 8Gy, respectively. The apoptosis rate was significantly higher in the RAY+COS group than in the RAY group. The percentage of cells in the G2/M phase was higher, and the percentage of cells in the S phase and G0/G1 phase was lower in the RAY+COS group than in the RAY group. The study indicated that COS can enhance the radiosensitization of SW480 cells, inducing apoptosis and G2/M phase arrest.

Alternative diagnostic approaches and new therapeutic strategies in cancer treatment

Over time, more evidence has been discovered that radiosensitizing effects may be genotype-dependent, requiring predictive biomarkers for proper patient selection. Unfortunately, survival clonogenic assays are not suitable for the large cell lines that would be needed to identify tumor genotypes correlated with sensitivity to IR/drug combinations due to the poor ability of the human cancer cell lines to form colonies and the paucity of resources to conduct these assays. Liu Q. et al.[110] hypothesized that short-term assays could provide a change measure of the change in cellular radiosensitivity caused by a targeted drug if the drug, within a few days following irradiation, alters the cell inactivation mode, such as senescence, apoptosis, or autophagy. The authors conducted screening of 32 cancer cell lines using 18 targeted therapeutic agents with known or putative radiosensitizing properties. The cell number remaining after drug exposure with or without radiation was assessed by nonclonogenic assays. To genetically screen for mechanisms of radiosensitization of the multi-kinase inhibitor midostaurin, the drug was administered to 5 LC cell lines. Four of the top 5 cell lines radiosensitized by midostaurin (SRF2Gy of 1.02–1.13) harbored KRAS mutations in codons 12 and 13. In contrast, cells with wild-type KRAS did not show radiosensitization. KRAS mutations (codons 12/13) were found to be a biomarker of radiosensitization by midostaurin in LC. Data highlight the potential clinical significance of this type of screening.

Cyclin-dependent kinases (CDKs) are key regulatory enzymes involved in cell proliferation. They regulate cell cycle checkpoints and transcriptional events in response to extracellular and intracellular signals. The crucial function of

CDKs in cell cycling and DNA damage repair and frequent aberrations of their activities in cancer encouraged an intensive screening for small-molecule CDK inhibitors. CDK9 is one of the most important transcription regulatory members of the CDK family. Storch et al.[111] evaluated the significance of CDK9 inhibition using siRNA technology and a multi-target tumor growth inhibitor ZK 304709 for the radioresponse in a panel of HNSCC cell lines. Upon either CDK9 small interfering RNA knockdown or treatment with ZK304709, the authors examined colony formation, DNA DSBs, apoptosis, cell cycling, and expression and phosphorylation of major cell cycle and DNA damage repair proteins. The results indicated that CDK9 overexpression mediated radioprotection; in contrast, CDK9 depletion enhanced the radiosensitivity of HNSCC cells without induction of apoptosis. ZK304709 showed concentration-dependent cytotoxicity but failed to radiosensitize HNSCC cells. The authors suggested a potential role of CDK9 in the radiation response of HNSCC cells.

G2 and S phase-expressed 1 (GTSE1), a cell cycle-related protein regulating G1/S cell cycle transition,[112] is also closely associated with DNA repair. The response of GTSE1 to IR remains uncovered. A study by Lei et al.[113] aimed to elucidate the radiosensitizing effects in non-SCLC via knockdown GTSE1 expression. The researchers found that radiation could induce GTSE1 to be recruited to DSB site and initiate DNA damage response. The knockdown of GTSE1 expression in non-SCLC cells by siRNA significantly inhibited the proliferation, promoted apoptosis after IR, and enhanced radiosensitivity in NSCLC, impairing the DNA damage repair process.

Conclusion

Recently, radiotherapy has developed rapidly, taking on an increasingly prominent role and position in cancer treatment. Improving radio response with radiosensitizers is a promising approach. Several strategies have been used to develop highly effective and low toxicity radiosensitizers, including small molecules, macromolecules, and nanomaterials. Manipulation of genes involved in radiation resistance represents an important approach to therapeutic intervention in cancer. The combination of radiotherapy with gene therapy provides a promising strategy to modify the radiation response and overcome the radioresistance of tumor cells. However, despite significant advances in the development of radiosensitizers, there is a need to search for new targets for radiotherapy and new mechanisms of sensitization, as well as the development of more effective radiosensitizing drugs.

Competing Interests

The author declares that there is no conflict of interest.

References

1. Wang H, Mu X, He H, Zhang XD. Cancer Radiosensitizers. Trends Pharmacol Sci. 2018 Jan;39(1):24-48. doi: 10.1016/j.tips.2017.11.003.

2. Telarovic I, Wenger RH, Pruschy M. Interfering with Tumor Hypoxia for Radiotherapy Optimization. J Exp Clin Cancer Res. 2021 Jun 21;40(1):197. doi: 10.1186/s13046-021-02000-x.

3. Crabtree HG, Cramer W. The action of radium on cancer cells. II.—Some factors determining the susceptibility of cancer cells to radium. Proc R Soc Lond Ser B Contain Pap Biol Character. 1933;113(782):238–50. doi.org: 10.1098/rspb.1933.0044.

4. GRAY LH, CONGER AD, EBERT M, HORNSEY S, SCOTT OC. The concentration of oxygen dissolved in tissues at the time of irradiation as a factor in radiotherapy. Br J Radiol. 1953 Dec;26(312):638-48. doi: 10.1259/0007-1285-26-312-638.

5. Moeller BJ, Richardson RA, Dewhirst MW. Hypoxia and radiotherapy: opportunities for improved outcomes in cancer treatment. Cancer Metastasis Rev. 2007 Jun;26(2):241-8. doi: 10.1007/s10555-007-9056-0.

6. Rofstad EK, Gaustad JV, Egeland TA, Mathiesen B, Galappathi K. Tumors exposed to acute cyclic hypoxic stress show enhanced angiogenesis, perfusion and metastatic dissemination. Int J Cancer. 2010 Oct 1;127(7):1535-46. doi: 10.1002/ijc.25176.

7. Bhaskara VK, Mohanam I, Rao JS, Mohanam S. Intermittent hypoxia regulates stem-like characteristics and differentiation of neuroblastoma cells. PLoS One. 2012;7(2):e30905. doi: 10.1371/journal.pone.0030905.

8. Martinive P, Defresne F, Bouzin C, Saliez J, Lair F, Grégoire V, et al. Preconditioning of the tumor vasculature and tumor cells by intermittent hypoxia: implications for anticancer therapies. Cancer Res. 2006 Dec 15;66(24):11736-44. doi: 10.1158/0008-5472.CAN-06-2056.

9. Minassian LM, Cotechini T, Huitema E, Graham CH. Hypoxia-Induced Resistance to Chemotherapy in Cancer. Adv Exp Med Biol. 2019;1136:123-139. doi: 10.1007/978-3-030-12734-3_9.

10. Adams GE. Chemical radiosensitization of hypoxic cells. Br Med Bull. 1973 Jan;29(1):48-53. doi: 10.1093/oxfordjournals.bmb.a070956.

11. Proverbs-Singh T, Feldman JL, Morris MJ, Autio KA, Traina TA. Targeting the androgen receptor in prostate and breast cancer: several new agents in development. Endocr Relat Cancer. 2015 Jun;22(3):R87-R106. doi: 10.1530/ERC-14-0543.

12. Michmerhuizen AR, Chandler B, Olsen E, Wilder-Romans K, Moubadder L, Liu M, et al. C. Seviteronel, a Novel CYP17 Lyase Inhibitor and Androgen Receptor Antagonist, Radiosensitizes AR-Positive Triple Negative Breast Cancer Cells. Front Endocrinol (Lausanne). 2020 Feb 11;11:35. doi: 10.3389/fendo.2020.00035.

13. Kang HC, Chie EK, Kim HJ, Kim JH, Kim IH, Kim K, et al. A phthalimidoalkanamide derived novel DNMT inhibitor enhanced radiosensitivity of A549 cells by inhibition of homologous recombination of DNA damage. Invest New Drugs. 2019 Dec;37(6):1158-1165. doi: 10.1007/s10637-019-00730-6.

14. Laird JH, Lok BH, Ma J, Bell A, de Stanchina E, Poirier JT, Rudin CM. Talazoparib Is a Potent Radiosensitizer in Small Cell Lung Cancer Cell Lines and Xenografts. Clin Cancer Res. 2018 Oct 15;24(20):5143-5152. doi: 10.1158/1078-0432.CCR-18-0401.

15. Helleday T, Petermann E, Lundin C, Hodgson B, Sharma RA. DNA repair pathways as targets for cancer therapy. Nat Rev Cancer. 2008 Mar;8(3):193-204. doi: 10.1038/nrc2342.
16. Lord CJ, Ashworth A. The DNA damage response and cancer therapy. Nature. 2012 Jan 18;481(7381):287-94. doi: 10.1038/nature10760.
17. Ray Chaudhuri A, Hashimoto Y, Herrador R, Neelsen KJ, Fachinetti D, Bermejo R, et al. M. Topoisomerase I poisoning results in PARP-mediated replication fork reversal. Nat Struct Mol Biol. 2012 Mar 4;19(4):417-23. doi: 10.1038/nsmb.2258.
18. Hastak K, Bhutra S, Parry R, Ford JM. Poly (ADP-ribose) polymerase inhibitor, an effective radiosensitizer in lung and pancreatic cancers. Oncotarget. 2017 Apr 18;8(16):26344-26355. doi: 10.18632/oncotarget.15464.
19. Buckley AM, Dunne MR, Lynam-Lennon N, Kennedy SA, Cannon A, Reynolds AL, et al. Pyrazinib (P3), [(E)-2-(2-Pyrazin-2-yl-vinyl)-phenol], a small molecule pyrazine compound enhances radiosensitivity in oesophageal adenocarcinoma. Cancer Lett. 2019 Apr 10;447:115-129. doi: 10.1016/j.canlet.2019.01.009.
20. Tang Q, Wu L, Xu M, Yan D, Shao J, Yan S. Osalmid, a Novel Identified RRM2 Inhibitor, Enhances Radiosensitivity of Esophageal Cancer. Int J Radiat Oncol Biol Phys. 2020 Dec 1;108(5):1368-1379. doi: 10.1016/j.ijrobp.2020.07.2322.
21. Lian X, Zhu C, Lin H, Gao Z, Li G, Zhang N, et al. Radiosensitization of HER2-positive esophageal cancer cells by pyrotinib. Biosci Rep. 2020 Feb 28;40(2):BSR20194167. doi: 10.1042/BSR20194167.
22. Qian X, Tan C, Yang B, Wang F, Ge Y, Guan Z, Cai J. Astaxanthin increases radiosensitivity in esophageal squamous cell carcinoma through inducing apoptosis and G2/M arrest. Dis Esophagus. 2017 Jun 1;30(6):1-7. doi: 10.1093/dote/dox027.
23. Ding YQ, Zhu HC, Chen XC, Sun XC, Yang X, Qin Q, et al. Sunitinib modulates the radiosensitivity of esophageal squamous cell carcinoma cells in vitro. Dis Esophagus. 2016 Nov;29(8):1144-1151. doi: 10.1111/dote.12440.
24. Vann KR, Oviatt AA, Osheroff N. Topoisomerase II Poisons: Converting Essential Enzymes into Molecular Scissors. Biochemistry. 2021 Jun 1;60(21):1630-1641. doi: 10.1021/acs.biochem.1c00240.
25. Deweese JE, Osheroff N. The DNA cleavage reaction of topoisomerase II: wolf in sheep's clothing. Nucleic Acids Res. 2009 Feb;37(3):738-48. doi: 10.1093/nar/gkn937.
26. Pommier Y, Leo E, Zhang H, Marchand C. DNA topoisomerases and their poisoning by anticancer and antibacterial drugs. Chem Biol. 2010 May 28;17(5):421-33. doi: 10.1016/j.chembiol.2010.04.012.
27. Pendleton M, Lindsey RH Jr, Felix CA, Grimwade D, Osheroff N. Topoisomerase II and leukemia. Ann N Y Acad Sci. 2014 Mar;1310(1):98-110. doi: 10.1111/nyas.12358.
28. Tang Q, Ma J, Sun J, Yang L, Yang F, Zhang W, Li R, et al. Genistein and AG1024 synergistically increase the radiosensitivity of prostate cancer cells. Oncol Rep. 2018 Aug;40(2):579-588. doi: 10.3892/or.2018.6468.
29. Skwarska A, Ramachandran S, Dobrynin G, Leszczynska KB, Hammond EM. The imidazoacridinone C-1311 induces p53-dependent senescence or p53-independent apoptosis and sensitizes cancer cells to radiation. Oncotarget. 2017 May 9;8(19):31187-31198. doi: 10.18632/oncotarget.16102.
30. Cammarota F, Conte A, Aversano A, Muto P, Ametrano G, Riccio P, et al. Lithium chloride increases sensitivity to photon irradiation treatment in primary mesenchymal colon cancer cells. Mol Med Rep. 2020 Mar;21(3):1501-1508. doi: 10.3892/mmr.2020.10956.
31. Pal I, Dey KK, Chaurasia M, Parida S, Das S, Rajesh Y, et al. Cooperative effect of BI-69A11 and celecoxib enhances radiosensitization by modulating DNA damage repair in colon carcinoma. Tumour Biol. 2016 May;37(5):6389-402. doi: 10.1007/s13277-015-4399-6.
32. Pascual-Serra R, Fernández-Aroca DM, Sabater S, Roche O, Andrés I, Ortega-Muelas M, et al. p38β (MAPK11) mediates gemcitabine-associated radiosensitivity in sarcoma experimental models. Radiother Oncol. 2021 Mar;156:136-144. doi: 10.1016/j.radonc.2020.12.008.
33. Waissi W, Nicol A, Jung M, Rousseau M, Jarnet D, Noel G, et al. Radiosensitizing Pancreatic Cancer with PARP Inhibitor and Gemcitabine: An In Vivo and a Whole-Transcriptome Analysis after Proton or Photon Irradiation. Cancers (Basel). 2021 Jan 30;13(3):527. doi: 10.3390/cancers13030527.
34. Vance S, Liu E, Zhao L, Parsels JD, Parsels LA, Brown JL, et al. Selective radiosensitization of p53 mutant pancreatic cancer cells by combined inhibition of Chk1 and PARP1. Cell Cycle. 2011 Dec 15;10(24):4321-9. doi: 10.4161/cc.10.24.18661.
35. Zhang Y, Zuo Y, Guan Z, Lu W, Xu Z, Zhang H, et al. Salinomycin radiosensitizes human nasopharyngeal carcinoma cell line CNE-2 to radiation. Tumour Biol. 2016 Jan;37(1):305-11. doi: 10.1007/s13277-015-3730-6.
36. Geng CX, Zeng ZC, Wang JY, Xuan SY, Lin CM. Docetaxel shows radiosensitization in human hepatocellular carcinoma cells. World J Gastroenterol. 2005 May 21;11(19):2990-3. doi: 10.3748/wjg.v11.i19.2990.
37. Lee IJ, Seong J. Radiosensitizers in hepatocellular carcinoma. Semin Radiat Oncol. 2011 Oct;21(4):303-11. doi: 10.1016/j.semradonc.2011.05.008.
38. Nath M, Mridula, Kumari R. Microwave-assisted synthesis of mixed ligands organotin(IV) complexes of 1,10-phenanthroline and l-proline: Physicochemical characterization, DFT calculations, chemotherapeutic potential validation by in vitro DNA binding and nuclease activity. J Photochem Photobiol B. 2017 Sep;174:182-194. doi: 10.1016/j.jphotobiol.2017.07.017.
39. Liu HM, Wu Q, Cao JQ, Wang X, Song Y, Mei WJ, Wang XC. A phenanthroline derivative enhances radiosensitivity of hepatocellular carcinoma cells by inducing mitochondria-dependent apoptosis. Eur J Pharmacol. 2019 Jan 15;843:285-291. doi: 10.1016/j.ejphar.2018.10.031.
40. Zhang XH, Cao MQ, Li XX, Zhang T. Apatinib as an alternative therapy for advanced hepatocellular carcinoma. World J Hepatol. 2020 Oct 27;12(10):766-774. doi: 10.4254/wjh.v12.i10.766.
41. Yang C, Qin S. Apatinib targets both tumor and endothelial cells in hepatocellular carcinoma. Cancer Med. 2018 Sep;7(9):4570-4583. doi: 10.1002/cam4.1664.
42. Zhang H, Cao Y, Chen Y, Li G, Yu H. Apatinib promotes apoptosis of the SMMC-7721 hepatocellular carcinoma cell line via the PI3K/Akt pathway. Oncol Lett. 2018 Apr;15(4):5739-5743. doi: 10.3892/ol.2018.8031.
43. Liao J, Jin H, Li S, Xu L, Peng Z, Wei G, et al. Apatinib potentiates irradiation effect via suppressing PI3K/AKT signaling pathway in hepatocellular carcinoma. J Exp Clin Cancer Res.

2019 Nov 6;38(1):454. doi: 10.1186/s13046-019-1419-1.
44. Göttgens EL, Bussink J, Leszczynska KB, Peters H, Span PN, Hammond EM. Inhibition of CDK4/CDK6 Enhances Radiosensitivity of HPV Negative Head and Neck Squamous Cell Carcinomas. Int J Radiat Oncol Biol Phys. 2019 Nov 1;105(3):548-558. doi: 10.1016/j.ijrobp.2019.06.2531.
45. Groselj B, Sharma NL, Hamdy FC, Kerr M, Kiltie AE. Histone deacetylase inhibitors as radiosensitisers: effects on DNA damage signalling and repair. Br J Cancer. 2013 Mar 5;108(4):748-54. doi: 10.1038/bjc.2013.21.
46. Tsai YC, Wang TY, Hsu CL, Lin WC, Chen JY, Li JH, et al. Selective inhibition of HDAC6 promotes bladder cancer radiosensitization and mitigates the radiation-induced CXCL1 signalling. Br J Cancer. 2023 May;128(9):1753-1764. doi: 10.1038/s41416-023-02195-0.
47. Paillas S, Then CK, Kilgas S, Ruan JL, Thompson J, Elliott A, Smart S, Kiltie AE. The Histone Deacetylase Inhibitor Romidepsin Spares Normal Tissues While Acting as an Effective Radiosensitizer in Bladder Tumors in Vivo. Int J Radiat Oncol Biol Phys. 2020 May 1;107(1):212-221. doi: 10.1016/j.ijrobp.2020.01.015.
48. White E. Deconvoluting the context-dependent role for autophagy in cancer. Nat Rev Cancer. 2012 Apr 26;12(6):401-10. doi: 10.1038/nrc3262.
49. Wei H, Wei S, Gan B, Peng X, Zou W, Guan JL. Suppression of autophagy by FIP200 deletion inhibits mammary tumorigenesis. Genes Dev. 2011 Jul 15;25(14):1510-27. doi: 10.1101/gad.2051011.
50. Schleicher SM, Moretti L, Varki V, Lu B. Progress in the unraveling of the endoplasmic reticulum stress/autophagy pathway and cancer: implications for future therapeutic approaches. Drug Resist Updat. 2010 Jun;13(3):79-86. doi: 10.1016/j.drup.2010.04.002.
51. Wang F, Tang J, Li P, Si S, Yu H, Yang X, et al. Chloroquine Enhances the Radiosensitivity of Bladder Cancer Cells by Inhibiting Autophagy and Activating Apoptosis. Cell Physiol Biochem. 2018;45(1):54-66. doi: 10.1159/000486222.
52. Liu Y, Zhang P, Li F, Jin X, Li J, Chen W, Li Q. Metal-based *NanoEnhancers* for Future Radiotherapy: Radiosensitizing and Synergistic Effects on Tumor Cells. Theranostics. 2018 Feb 12;8(7):1824-1849. doi: 10.7150/thno.22172.
53. Vines JB, Yoon JH, Ryu NE, Lim DJ, Park H. Gold Nanoparticles for Photothermal Cancer Therapy. Front Chem. 2019 Apr 5;7:167. doi: 10.3389/fchem.2019.00167.
54. Lu VM, McDonald KL, Townley HE. Realizing the therapeutic potential of rare earth elements in designing nanoparticles to target and treat glioblastoma. Nanomedicine (Lond). 2017 Oct;12(19):2389-2401. doi: 10.2217/nnm-2017-0193.
55. Kobayashi K, Usami N, Porcel E, Lacombe S, Le Sech C. Enhancement of radiation effect by heavy elements. Mutat Res. 2010 Apr-Jun;704(1-3):123-31. doi: 10.1016/j.mrrev.2010.01.002.
56. Stewart C, Konstantinov K, McKinnon S, Guatelli S, Lerch M, Rosenfeld A, et al. First proof of bismuth oxide nanoparticles as efficient radiosensitisers on highly radioresistant cancer cells. Phys Med. 2016 Nov;32(11):1444-1452. doi: 10.1016/j.ejmp.2016.10.015.
57. Saberi A, Shahbazi-Gahrouei D, Abbasian M, Fesharaki M, Baharlouei A, Arab-Bafrani Z. Gold nanoparticles in combination with megavoltage radiation energy increased radiosensitization and apoptosis in colon cancer HT-29 cells. Int J Radiat Biol. 2017 Mar;93(3):315-323. doi: 10.1080/09553002.2017.1242816.
58. Habiba K, Aziz K, Sanders K, Santiago CM, Mahadevan LSK, Makarov V, et al. Enhancing Colorectal Cancer Radiation Therapy Efficacy using Silver Nanoprisms Decorated with Graphene as Radiosensitizers. Sci Rep. 2019 Nov 19;9(1):17120. doi: 10.1038/s41598-019-53706-0.
59. Mirjolet C, Boudon J, Loiseau A, Chevrier S, Boidot R, Oudot A, et al. Docetaxel-titanate nanotubes enhance radiosensitivity in an androgen-independent prostate cancer model. Int J Nanomedicine. 2017 Aug 30;12:6357-6364. doi: 10.2147/IJN.S139167.
60. Lavanya V, Adil M, Ahmed N, Rishi AK, Jamal S. Small molecule inhibitors as emerging cancer therapeutics. Integr Cancer Sci Ther. 2014;1:39–46. doi: 10.15761/ICST.1000109.
61. Balakrishnan L, Bambara RA. Flap endonuclease 1. Annu Rev Biochem. 2013;82:119-38. doi: 10.1146/annurev-biochem-072511-122603.
62. Zheng L, Jia J, Finger LD, Guo Z, Zer C, Shen B. Functional regulation of FEN1 nuclease and its link to cancer. Nucleic Acids Res. 2011 Feb;39(3):781-94. doi: 10.1093/nar/gkq884.
63. Shen B, Singh P, Liu R, Qiu J, Zheng L, Finger LD, Alas S. Multiple but dissectible functions of FEN-1 nucleases in nucleic acid processing, genome stability and diseases. Bioessays. 2005 Jul;27(7):717-29. doi: 10.1002/bies.20255.
64. Liu S, Lu G, Ali S, Liu W, Zheng L, Dai H, et al. Okazaki fragment maturation involves α-segment error editing by the mammalian FEN1/MutSα functional complex. EMBO J. 2015 Jul 2;34(13):1829-43. doi: 10.15252/embj.201489865.
65. He L, Zhang Y, Sun H, Jiang F, Yang H, Wu H, et al. Targeting DNA Flap Endonuclease 1 to Impede Breast Cancer Progression. EBioMedicine. 2016 Dec;14:32-43. doi: 10.1016/j.ebiom.2016.11.012.
66. Zou J, Zhu L, Jiang X, Wang Y, Wang Y, Wang X, Chen B. Curcumin increases breast cancer cell sensitivity to cisplatin by decreasing FEN1 expression. Oncotarget. 2018 Jan 10;9(13):11268-11278. doi: 10.18632/oncotarget.24109.
67. Li JL, Wang JP, Chang H, Deng SM, Du JH, Wang XX, et al. FEN1 inhibitor increases sensitivity of radiotherapy in cervical cancer cells. Cancer Med. 2019 Dec;8(18):7774-7780. doi: 10.1002/cam4.2615.
68. Baek SJ, Ishii H, Tamari K, Hayashi K, Nishida N, Konno M, et al. Cancer stem cells: The potential of carbon ion beam radiation and new radiosensitizers (Review). Oncol Rep. 2015 Nov;34(5):2233-7. doi: 10.3892/or.2015.4236.
69. Calin GA, Dumitru CD, Shimizu M, Bichi R, Zupo S, Noch E, et al. Frequent deletions and down-regulation of micro- RNA genes miR15 and miR16 at 13q14 in chronic lymphocytic leukemia. Proc Natl Acad Sci U S A. 2002 Nov 26;99(24):15524-9. doi: 10.1073/pnas.242606799.
70. He L, Thomson JM, Hemann MT, Hernando-Monge E, Mu D, Goodson S, et al. A microRNA polycistron as a potential human oncogene. Nature. 2005 Jun 9;435(7043):828-33. doi: 10.1038/nature03552.
71. Ma L, Teruya-Feldstein J, Weinberg RA. Tumour invasion and metastasis initiated by microRNA-10b in breast cancer. Nature. 2007 Oct 11;449(7163):682-8. doi: 10.1038/nature06174. Epub 2007 Sep 26. Erratum in: Nature. 2008 Sep 11;455(7210):256.

72. Zhang P, Wang L, Rodriguez-Aguayo C, Yuan Y, Debeb BG, Chen D, et al. miR-205 acts as a tumour radiosensitizer by targeting ZEB1 and Ubc13. Nat Commun. 2014 Dec 5;5:5671. doi: 10.1038/ncomms6671.
73. Huang F, Tang J, Zhuang X, Zhuang Y, Cheng W, Chen W, et al. MiR-196a promotes pancreatic cancer progression by targeting nuclear factor kappa-B-inhibitor alpha. PLoS One. 2014 Feb 4;9(2):e87897. doi: 10.1371/journal.pone.0087897.
74. Baek SJ, Sato K, Nishida N, Koseki J, Azuma R, Kawamoto K, et al. MicroRNA miR-374, a potential radiosensitizer for carbon ion beam radiotherapy. Oncol Rep. 2016 Nov;36(5):2946-2950. doi: 10.3892/or.2016.5122.
75. Qi T, Dong Y, Gao Z, Xu J. Research Progress on the Anti-Cancer Molecular Mechanisms of Huaier. Onco Targets Ther. 2020 Dec 8;13:12587-12599. doi: 10.2147/OTT.S281328.
76. Ding X, Yang Q, Kong X, Haffty BG, Gao S, Moran MS. Radiosensitization effect of Huaier on breast cancer cells. Oncol Rep. 2016 May;35(5):2843-50. doi: 10.3892/or.2016.4630.
77. Su YJ, Huang SY, Ni YH, Liao KF, Chiu SC. Anti-Tumor and Radiosensitization Effects of N-Butylidenephthalide on Human Breast Cancer Cells. Molecules. 2018 Jan 25;23(2):240. doi: 10.3390/molecules23020240.
78. Zhang D, Dong Y, Zhao Y, Zhou C, Qian Y, Hegde ML, et al. Sinomenine hydrochloride sensitizes cervical cancer cells to ionizing radiation by impairing DNA damage response. Oncol Rep. 2018 Nov;40(5):2886-2895. doi: 10.3892/or.2018.6693.
79. Zhang F, Fan B, Mao L. Radiosensitizing effects of Cyclocarya paliurus polysaccharide on hypoxic A549 and H520 human non-small cell lung carcinoma cells. Int J Mol Med. 2019 Oct;44(4):1233-1242. doi: 10.3892/ijmm.2019.4289.
80. Xie JH, Xie MY, Nie SP, Shen MY, Wang YX and Li C. Isolation, chemical composition and antioxidant activities of a water-soluble polysaccharide from Cyclocarya paliurus (Batal.) Iljinskaja. Food Chem. 2010;119:1626–1632.
81. Xie JH, Liu X, Shen MY, Nie SP, Zhang H, Li C, et al. Purification, physicochemical characterisation and anticancer activity of a polysaccharide from Cyclocarya paliurus leaves. Food Chem. 2013 Feb 15;136(3-4):1453-60. doi: 10.1016/j.foodchem.2012.09.078.
82. Li S, Li J, Guan XL, Li J, Deng SP, Li LQ, et al. Hypoglycemic effects and constituents of the barks of Cyclocarya paliurus and their inhibiting activities to glucosidase and glycogen phosphorylase. Fitoterapia. 2011 Oct;82(7):1081-5. doi: 10.1016/j.fitote.2011.07.002.
83. Sliva D. Medicinal mushroom Phellinus linteus as an alternative cancer therapy. Exp Ther Med. 2010 May;1(3):407-411. doi: 10.3892/etm_00000063.
84. Li YG, Ji DF, Zhong S, Liu PG, Lv ZQ, Zhu JX, et al. Polysaccharide from Phellinus linteus induces S-phase arrest in HepG2 cells by decreasing calreticulin expression and activating the P27kip1-cyclin A/D1/E-CDK2 pathway. J Ethnopharmacol. 2013 Oct 28;150(1):187-95. doi: 10.1016/j.jep.2013.08.028.
85. Zong A, Cao H, Wang F. Anticancer polysaccharides from natural resources: a review of recent research. Carbohydr Polym. 2012 Nov 6;90(4):1395-410. doi: 10.1016/j.carbpol.2012.07.026.
86. Park BJ, Lim YS, Lee HJ, Eum WS, Park J, Han KH, et al. Anti-oxidative effects of Phellinus linteus and red ginseng extracts on oxidative stress-induced DNA damage. BMB Rep. 2009 Aug 31;42(8):500-5. doi: 10.5483/bmbrep.2009.42.8.500.
87. Kim BC, Jeon WK, Hong HY, Jeon KB, Hahn JH, Kim YM, et al. The anti-inflammatory activity of Phellinus linteus (Berk. & M.A. Curt.) is mediated through the PKCdelta/Nrf2/ARE signaling to up-regulation of heme oxygenase-1. J Ethnopharmacol. 2007 Sep 5;113(2):240-7. doi: 10.1016/j.jep.2007.05.032.
88. Zhao C, Liao Z, Wu X, Liu Y, Liu X, Lin Z, Huang Y, Liu B. Isolation, purification, and structural features of a polysaccharide from Phellinus linteus and its hypoglycemic effect in alloxan-induced diabetic mice. J Food Sci. 2014 May;79(5):H1002-10. doi: 10.1111/1750-3841.12464.
89. Wang H, Wu G, Park HJ, Jiang PP, Sit WH, van Griensven LJ, Wan JM. Protective effect of Phellinus linteus polysaccharide extracts against thioacetamide-induced liver fibrosis in rats: a proteomics analysis. Chin Med. 2012 Oct 18;7(1):23. doi: 10.1186/1749-8546-7-23.
90. Jeong YK, Oh JY, Yoo JK, Lim SH, Kim EH. The Biofunctional Effects of Mesima as a Radiosensitizer for Hepatocellular Carcinoma. Int J Mol Sci. 2020 Jan 29;21(3):871. doi: 10.3390/ijms21030871.
91. Yan Y, Su W, Zeng S, Qian L, Chen X, Wei J, et al. Effect and Mechanism of Tanshinone I on the Radiosensitivity of Lung Cancer Cells. Mol Pharm. 2018 Nov 5;15(11):4843-4853. doi: 10.1021/acs.molpharmaceut.8b00489.
92. Kuo WT, Tsai YC, Wu HC, Ho YJ, Chen YS, Yao CH, Yao CH. Radiosensitization of non-small cell lung cancer by kaempferol. Oncol Rep. 2015 Nov;34(5):2351-6. doi: 10.3892/or.2015.4204.
93. Mundi PS, Sachdev J, McCourt C, Kalinsky K. AKT in cancer: new molecular insights and advances in drug development. Br J Clin Pharmacol. 2016 Oct;82(4):943-56. doi: 10.1111/bcp.13021.
94. Mayer IA, Arteaga CL. The PI3K/AKT Pathway as a Target for Cancer Treatment. Annu Rev Med. 2016;67:11-28. doi: 10.1146/annurev-med-062913-051343.
95. Xu Z, Yan Y, Xiao L, Dai S, Zeng S, Qian L, et al. Radiosensitizing effect of diosmetin on radioresistant lung cancer cells via Akt signaling pathway. PLoS One. 2017 Apr 17;12(4):e0175977. doi: 10.1371/journal.pone.0175977.
96. Stritzelberger J, Lainer J, Gollwitzer S, Graf W, Jost T, Lang JD, Mueller TM, Schwab S, Fietkau R, Hamer HM, Distel L. Ex vivo radiosensitivity is increased in non-cancer patients taking valproate. BMC Neurol. 2020 Oct 24;20(1):390. doi: 10.1186/s12883-020-01966-z.
97. Zhou W, Guo Y, Zhang X, Jiang Z. Lys05 induces lysosomal membrane permeabilization and increases radiosensitivity in glioblastoma. J Cell Biochem. 2020 Feb;121(2):2027-2037. doi: 10.1002/jcb.29437.
98. Neckers L. Heat shock protein 90: the cancer chaperone. J Biosci. 2007 Apr;32(3):517-30. doi: 10.1007/s12038-007-0051-y.
99. Mahalingam D, Swords R, Carew JS, Nawrocki ST, Bhalla K, Giles FJ. Targeting HSP90 for cancer therapy. Br J Cancer. 2009 May 19;100(10):1523-9. doi: 10.1038/sj.bjc.6605066.
100. Bull EE, Dote H, Brady KJ, Burgan WE, Carter DJ, Cerra MA, Oswald KA, Hollingshead MG, Camphausen K, Tofilon PJ. Enhanced tumor cell radiosensitivity and abrogation of G2 and S phase arrest by the Hsp90 inhibitor

17-(dimethylaminoethylamino)-17-demethoxygeldanamycin. Clin Cancer Res. 2004 Dec 1;10(23):8077-84. doi: 10.1158/1078-0432.CCR-04-1212.
101. Dote H, Burgan WE, Camphausen K, Tofilon PJ. Inhibition of hsp90 compromises the DNA damage response to radiation. Cancer Res. 2006 Sep 15;66(18):9211-20. doi: 10.1158/0008-5472.CAN-06-2181.
102. Stingl L, Stühmer T, Chatterjee M, Jensen MR, Flentje M, Djuzenova CS. Novel HSP90 inhibitors, NVP-AUY922 and NVP-BEP800, radiosensitise tumour cells through cell-cycle impairment, increased DNA damage and repair protraction. Br J Cancer. 2010 May 25;102(11):1578-91. doi: 10.1038/sj.bjc.6605683.
103. Djuzenova CS, Blassl C, Roloff K, Kuger S, Katzer A, Niewidok N, et al. Hsp90 inhibitor NVP-AUY922 enhances radiation sensitivity of tumor cell lines under hypoxia. Cancer Biol Ther. 2012 Apr;13(6):425-34. doi: 10.4161/cbt.19294.
104. Kudryavtsev VA, Khokhlova AV, Mosina VA, Selivanova EI, Kabakov AE. Induction of Hsp70 in tumor cells treated with inhibitors of the Hsp90 activity: A predictive marker and promising target for radiosensitization. PLoS One. 2017 Mar 14;12(3):e0173640. doi: 10.1371/journal.pone.0173640.
105. Zhao M, Gu L, Li Y, Chen S, You J, Fan L, Wang Y, Zhao L. Chitooligosaccharides display anti-tumor effects against human cervical cancer cells via the apoptotic and autophagic pathways. Carbohydr Polym. 2019 Nov 15;224:115171. doi: 10.1016/j.carbpol.2019.115171.
106. Kim EK, Je JY, Lee SJ, Kim YS, Hwang JW, Sung SH, Moon SH, Jeon BT, Kim SK, Jeon YJ, Park PJ. Chitooligosaccharides induce apoptosis in human myeloid leukemia HL-60 cells. Bioorg Med Chem Lett. 2012 Oct 1;22(19):6136-8. doi: 10.1016/j.bmcl.2012.08.030.
107. Luo Z, Dong X, Ke Q, Duan Q, Shen L. Downregulation of CD147 by chitooligosaccharide inhibits MMP-2 expression and suppresses the metastatic potential of human gastric cancer. Oncol Lett. 2014 Jul;8(1):361-366. doi: 10.3892/ol.2014.2115.
108. Vo TS, Ngo DH, Kim SK. Gallic acid-grafted chitooligosaccharides suppress antigen-induced allergic reactions in RBL-2H3 mast cells. Eur J Pharm Sci. 2012 Sep 29;47(2):527-33. doi: 10.1016/j.ejps.2012.07.010.
109. Han FS, Yang SJ, Lin MB, Chen YQ, Yang P, Xu JM. Chitooligosaccharides promote radiosensitivity in colon cancer line SW480. World J Gastroenterol. 2016 Jun 14;22(22):5193-200. doi: 10.3748/wjg.v22.i22.5193.
110. Liu Q, Wang M, Kern AM, Khaled S, Han J, Yeap BY, Hong TS, Settleman J, Benes CH, Held KD, Efstathiou JA, Willers H. Adapting a drug screening platform to discover associations of molecular targeted radiosensitizers with genomic biomarkers. Mol Cancer Res. 2015 Apr;13(4):713-20. doi: 10.1158/1541-7786.MCR-14-0570.
111.Storch K, Cordes N. The impact of CDK9 on radiosensitivity, DNA damage repair and cell cycling of HNSCC cancer cells. Int J Oncol. 2016 Jan;48(1):191-8. doi: 10.3892/ijo.2015.3246.
112. Xu T, Ma M, Chi Z, Si L, Sheng X, Cui C, Dai J, Yu S, Yan J, Yu H, Wu X, Tang H, Yu J, Kong Y, Guo J. High G2 and S-phase expressed 1 expression promotes acral melanoma progression and correlates with poor clinical prognosis. Cancer Sci. 2018 Jun;109(6):1787-1798. doi: 10.1111/cas.13607.
113. Lei X, Du L, Zhang P, Ma N, Liang Y, Han Y, Qu B. Knockdown GTSE1 enhances radiosensitivity in non-small-cell lung cancer through DNA damage repair pathway. J Cell Mol Med. 2020 May;24(9):5162-5167. doi: 10.1111/jcmm.15165.

International Journal of Biomedicine 13(3) (2023) 31-45
http://dx.doi.org/10.21103/Article13(3)_RA3

REVIEW ARTICLE

INTERNATIONAL JOURNAL OF BIOMEDICINE

Role of p53, Cancer Stem Cells, and Cellular Senescence in Radiation Response

Juan C. Alamilla-Presuel*

The University of Málaga, Málaga, Spain

Abstract

Currently, radiotherapy has been identified as the most common cancer treatment. However, the efficacy of this treatment modality is low in several malignancies due to the resistance of cancer to radiation. Multiple mechanisms, including cell-cycle checkpoint function, DNA repair, and cell death pathways, modulate the radio-responsiveness of cancer cells. This review considered the role of p53, cancer stem cells (CSCs), and cellular senescence in radiation response.(**International Journal of Biomedicine. 2023;13(3):31-45.**)

Keywords: p53 • cancer stem cells • cellular senescence • radioresistance

For citation: Alamilla-Presuel JC. Role of p53, Cancer Stem Cells, and Cellular Senescence in Radiation Response. International Journal of Biomedicine. 2023;13(3):31-45. doi:10.21103/Article13(3)_RA3

Abbreviations

CSCs, cancer stem cells; **DSB**, double-strand break; **EMT**, epithelial-mesenchymal transition; **HCC**, hepatocellular carcinoma; **IR** ionizing radiation; **ROS**, reactive oxygen species; **SASP**, senescent-associated secretory phenotype.

Introduction

Currently, radiotherapy has been identified as the most common cancer treatment. However, the efficacy of this treatment modality is low in several malignancies due to the resistance of cancer to radiation. Multiple mechanisms, including cell-cycle checkpoint function, DNA repair, and cell death pathways, modulate the radio-responsiveness of cancer cells. This review considered the role of p53, cancer stem cells (CSCs), and cellular senescence in radiation response.

We reviewed published data on the role of p53, cancer stem cells, and cellular senescence in radiation response up to 2022, searching through PubMed, and references from relevant articles, using search terms with suitable keywords. The search terms were "cancer," "ionizing radiation," "cancer stem cells," "tumor protein p53," "DNA damage," "cellular senescence," and "radioresistance."

***Correspondence:** Juan C. Alamilla-Presuel. Department of Radiology and Physical Medicine. Medical Faculty. The University of Málaga, Málaga, Spain. E-mail: alamillajc@uma.es*

Role of TP53 mutations in human cancer and resistance to radiotherapy

In cancer, the *TP53* (tumor protein p53) gene is one of the most mutated genes, and it is essential to find out the role that this gene plays in radioresistance. The *TP53* gene encodes a tumor suppressor protein, p53, a transcription factor, regulating downstream genes involved in cell-cycle arrest, DNA repair, and programmed cell death (apoptosis) (Image 1). Regulation of the apoptotic function of p53 is associated with selective activation of apoptotic target genes. p53 is considered the "guardian of the genome" to prevent the accumulation of oncogenic mutations that lead to malignant tumors.[2] *TP53* mutations occur in about half of all human cancers, almost always resulting in the expression of a mutant p53 (mutp53) protein.[3,4] Mutational inactivation is considered one of the most common molecular mechanisms behind the dysfunction of p53. *TP53* mutations are distributed in all coding exons of the *TP53* gene; 95% of mutations have been detectable within the genomic region (exons 5–8) encoding the DNA-binding domain of p53.[5] Of the mutations in this domain, the six amino acid residues are most

frequently mutated in human cancers, including Arg-175, Gly-245, Arg-273, and Arg-282.[6] These mutations found within the DNA-binding domain of p53 disrupt its proper conformation, and thus the mutp53 is defective in the sequence-specific transcriptional activation and has oncogenic potential.[7,8] While wild-type p53 is a very short-lived protein in the absence of stress, these missense mutations result in the production of a full-length, altered p53 protein with a long half-life.[9] Mutp53 acts as a dominant-negative inhibitor toward wild-type p53.[8]

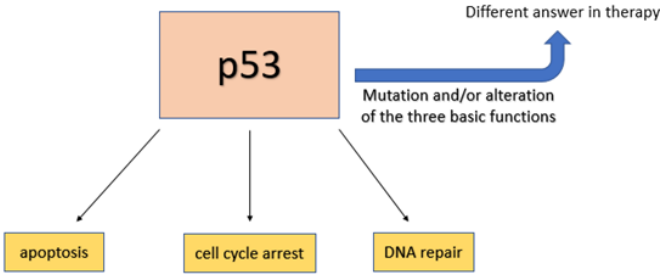

Image 1. *Three essential functions of a tumor suppressor protein p53.*

Mutp53 exhibits a radioresistant phenotype. Mutp53 proteins regulate the expression of several radioresistant genes.[10] Mutp53 activates the expression of NRF2, which is known to confer both chemo- and radioresistance.[11,12] Furthermore, in cells with wild-type p53, DNA damage caused by radiation therapy and most chemotherapeutic agents can lead to p53 accumulation and apoptosis. Loss of p53 function confers impaired apoptosis. Some Mutp53s have been reported to inhibit caspase-9 and p63/73-dependent induction of Bax and Noxa, contributing to the anti-apoptotic effects of mutp53 and the insensitivity of mutp53-containing cells to radiotherapy and chemotherapy.[13-15] Mutp53 proteins play a vital role in the formation and maintenance of CSCs,[16] which are known to play an important role in the development of radioresistance.[17,18] Wild-type p53 has been reported to repress the expression of several CSC markers, including CD44, c-KIT, NANOG, and OCT4. In contrast, mutp53 is associated with loss of repression of these CSC markers, subsequent CSC transformation, and increased radio- and chemoresistance.[19] Thus, the *TP53* gene is an important marker in determining the fate of cells before applying radiotherapy or some other treatment.

p53 molecular interactions

Melanoma is a type of cancer considered radioresistant. However, radiotherapy can be used as a complementary treatment for patients with advanced nodal disease, and that could reduce the risk of tumor prolapse. Melanoma resistance to radiotherapy can occur due to activation of the constitutive MAPK signaling pathway. Another cause of cancer radioresistance is p53 inactivation since wild-type p53 plays an important role in radiosensitization. In melanoma, p53 is rarely mutated, but the WT p53 is inactivated frequently. The melanoma cells' resistance to radiotherapy may very well be related to the MAPK pathway constitutive activation and/or to the p53 inactivation in approximately 90% of melanomas. Krayem et al.[20] carried out a study to evaluate in vitro and in vivo the effect of combining reactivation of p53 with MAPK inhibition on the efficacy of RT in BRAF-mutated melanoma with intrinsic and acquired resistance to BRAF inhibitors. To evaluate the benefit of combining RT with p53 activation and MAPK inhibition, a workflow was designed where melanoma cells were irradiated one day after drug exposure with one single dose of 2 Gy, 5 Gy, or 10 Gy. Protein analysis was done one day after irradiation to assess the direct effect of irradiation and effectors (vemurafenib and PRIMA-1Met). The combination of BRAF inhibition (vemurafenib, which completely shuts down the MAPK pathway) with p53 reactivation (PRIMA-1Met) significantly enhanced the radiosensitivity of BRAF-mutant melanoma cells. In contrast, radiation alone markedly promoted ERK and Akt phosphorylation, thus contributing to radioresistance. The combination of vemurafenib and PRIMA-1Met caused the inactivation of both MAPK kinase and PI3K/Akt pathways, and in combination with radiotherapy, it was able to significantly enhance melanoma cell radiosensitivity. The authors concluded that combining MAPK inhibition with p53 reactivation significantly enhances the radiosensitivity of melanoma both in vitro and in vivo.

In radiotherapy, using radioprotectors and radiosensitizers is an interesting strategy for alleviating adverse effects on normal tissues and reducing tumor resistance. Melatonin is a natural human hormone that shows protective properties against the toxic effects of chemotherapy and radiotherapy. Farhood et al.[21] conducted a review to clarify the mechanisms by which melatonin acts as a radioprotectant and radiosensitizer. Some in vitro studies have shown that melatonin has potent antitumor activity when used in conjunction with radiation. The mechanisms of its radiosensitive effect obviously involve activation of p53 by inhibition of MDM2, changes in the metabolism of tumor cells, suppression of DNA repair responses, and a number of other mechanisms. Additionally, SIRT1 suppression by melatonin is another pathway for p53-mediated apoptosis. The inhibition of COX-2 by melatonin plays an important role in p53-mediated apoptosis. During inflammation due to exposure to radiation, the expression of COX-2 and apoptotic genes such as iNOS and NF-kappaB is increased. The inhibition of these genes can sensitize tumor cells to radiotherapy. Melatonin can help to heal acute reactions during radiotherapy in organs like bone marrow, skin, and the gastrointestinal tract.

Human mitochondrial transcription factor A (TFAM) is needed for mitochondrial DNA replication and transcription, which are essential for mitochondrial biogenesis.[22,23] Inhibition of TFAM in OSC-2 cells leads to a decrease in cell viability and a pronounced induction of apoptosis after gamma irradiation.[24] P53 interacts with the TFAM promoter to activate TFAM transcription and binds to TFAM, thereby regulating cell death.[25-27] TFAM may influence ROS production and further influence cell proliferation and death by directly regulating mitochondrial electron transport chain (ETC) proteins.[28] TIGAR (TP53-induced glycolysis and apoptosis regulator)

promotes the pentose phosphate pathway and helps reduce intracellular ROS.[29,30] Jiang et al.[31] investigated how TFAM affects the sensitivity of tumor cells to IR and found that attenuated expression of TFAM slows tumor cell proliferation by causing G1/S phase arrest. A decrease in TFAM expression led to the inhibition of p53/TIGAR signaling, which further led to an increase in mitochondrial superoxide production and DSB DNA levels in irradiated tumor cells, regulating the sensitivity of tumor cells to radiation.

The aberrant gain of function identified in mtp53 has been shown to promote tumorigenesis; however, many downstream effects of mtp53 are still unknown.[32] A study by Gomes et al.[33] showed that the insulator protein CTCF (CCCTC-binding factor) plays a key role in suppressing the apoptotic p53 response by acting as a gene-specific repressor. Qu et al.[34] demonstrated that otopetrin 2 (*otop2*) plays an important role in the development of colorectal cancer (CRC). The authors determined that *otop2* is an important functional candidate in CRC oncogenesis and demonstrated that p53 plays an important role in governing the *otop2* transcription process by reprogramming the CTCF binding status and altering chromatin architecture.

Wu et al.[35] found an interaction between p53 and RAD18, a central regulator of translesion DNA synthesis, which is highly expressed in glioma cells and reduced cell radiosensitivity to ionizing.[36] Investigating the effects and mechanism of RAD18 in the radiation resistance of glioma and studying the role of p53 in this process, researchers showed that RAD18 functions as a promoter in glioma progression and reduces glioma cells' sensitivity to radiation through down-regulating P53. At the same time, cell growth promotion and cell apoptosis inhibition induced by RAD18 up-regulation were impaired when P53 expression was upregulated under radiation conditions.

Succinate dehydrogenase 5 (SDH5) has been reported to contribute to the development of several types of cancer.[37,38] Zong et al.[39] conducted a study showing that SDH5 can be detected not only in tumors but also in plasma by qRT-PCR, indicating its predictive effect in radiotherapy. The researchers showed that SDH5 modulates radiosensitivity by directly binding p53 and promoting phosphorylation of cytoplasmic p53 at Ser315, which ultimately accelerates the degradation of p53 via the ubiquitin/proteasome pathway and affects radiosensitivity. In SDH5 knockout mice, lung epithelial cells showed increased DNA damage after irradiation. Apoptosis and cell-cycle detection showed that decreased expression of SDH5 resulted in an apparent increase in apoptosis and a cell-cycle arrest in G2/M. SDH5 knockdown decreased p53 phosphorylation predominantly in the cytoplasm and increased its accumulation in the nucleus. SDH5 depletion inhibited p53 degradation via the ubiquitin/proteasome pathway, which promoted apoptosis and increased radiosensitivity in non-small cell lung cancer. Thus, the authors concluded that SDH5 is a novel regulator of p53 and that the loss of SDH5 enhances radiosensitivity by reducing p53 phosphorylation and delaying p53 degradation in lung cancer.

The significance of reducing p53 phosphorylation and degradation to increase radiosensitivity was also analyzed in a study by Xie et al.[40] who investigated the role of CDK16 in the radioresistance of human lung cancer cells. CDK16 negatively modulates p53 signaling pathway to promote radioresistance. CDK16, a member of the cyclin-dependent kinases family (CDK),[41] has demonstrated an essential role in tumorigenesis. A number of studies suggest that CDK16 may act as an oncoprotein in some types of cancer. In particular, the downregulation of CDK16 suppressed cell growth and proliferation in prostate, breast, and CRCs.[42-44] Xie et al.[40] found that CDK16, which is overexpressed in lung cancer and predicts poor prognosis in patients, binds to and phosphorylates p53 at the Ser315 site to trigger p53 degradation via the ubiquitin/proteasome pathway, and CDK16 depletion enhances radiosensitivity in a p53-dependent manner in lung cancer cells. In this regard, CDK16 is a possible target for cancer radiotherapy.

Radiation therapy always causes DNA damage, and cells repair the damaged DNA by activating the cell-cycle checkpoint signaling pathway and stopping the cell cycle to maintain the stability of the genome and the accuracy of chromosome inheritance.[45] Cell-cycle arrest is a common and direct response of most tumor cells affected by radiation.[46] Among the molecules involved in processes of DNA damage repair, the p53-binding protein 1 (53BP1) and mediator of DNA damage checkpoint 1 (MDC1) are distinguished. Following radiation-induced DNA damage, both MDC1 and 53BP1 could transmit the DNA damage signals to the downstream molecules such as cell-cycle checkpoint kinases CHK1 and CHK2. p53 is also involved in the modulation of the cell cycle and the regulation of the cell-cycle checkpoints. A study by Yang et al.[47] aimed to investigate the effects of MDC1 and p53 binding protein 1 (53BP1) silencing on p53, cell-cycle checkpoint kinases (CHK1 and CHK2), and CHK2-T68 expression in the epithelial cell line of human esophageal carcinoma (Eca-109). 53BP1 downregulation significantly reduced p53 and enhanced CHK1 and CHK2 expression in Eca-109 cells. 53BP1 downregulation also significantly regulated CHK1, CHK2, and p53 in xenograft nude mice models exposed to γ-ray irradiation, compared to the untreated group, with p53 negatively correlated with CHK1 and CHK2. The data obtained showed that 53BP1 regulates the cell-cycle arrest by modulating the expression of p53, CHK1 and CHK2 in both Eca-109 cells and xenograft nude mouse models.

The gene associated with retinoid-interferon-induced mortality-19 (GRIM-19) is a tumor suppressor that mediates cell apoptosis in multiple cancer types. A study by Chen et al.[48] investigated the role and underlying mechanism of GRIM-19 in the progression of osteosarcoma, one of the most aggressive types of primary bone cancer that frequently responds poorly to radiotherapy. Overexpression of GRIM-19 accelerated radiation-induced osteosarcoma cell apoptosis by p53 stabilization ex vivo and in vivo.The forced expression of GRIM-19 diminishes the activity of MDM2, a specific p53 protease, resulting in the accumulation of p53 and activation of p53-mediated apoptosis. So, restoring p53 function by inhibiting its interaction with MDM2 is a promising therapeutic strategy for cancer. Yi et al.[49] analyzed the capability of APG-115 to enhance radiation response in gastric cancer in vitro

and in vivo. The authors found that APG-115 radiosensitized p53 wild-type gastric cancer cells. Increasing apoptosis and cell-cycle arrest were observed after the administration of APG-115 and radiation.

In a clinical study performed by Wang et al.,[50] the p53 protein expression in cervical cancer after RT was significantly correlated with cervical space-occupying lesions and tumor size shown in transvaginal color Doppler ultrasound, providing helpful clinical data for monitoring cervical cancer.

p53 molecular interactions are summarized in Table 1.

Table 1.

p53 molecular interactions

Gene/ Protein	Action	Source
MAPK	Inactivation of both MAPK kinase and PI3K/Akt pathways with p53 reactivation significantly enhances the radiosensitivity of melanoma	Krayem et al. (2019) [20]
SIRT1	SIRT1 suppression by melatonin induces p53-mediated apoptosis	Farhood et al. (2019) [21]
TFAM	A decreased TFAM expression led to the inhibition of p53/TIGAR signaling, elevated mitochondrial superoxide and DSB DNA production, and arrest in the G1/S phase.	Jiang et al. (2019) [31]
otop2	p53 governs the transcription process of otop2, a functional candidate in colorectal cancer oncogenesis, by reprogramming the CTCF binding status and altering chromatin architecture.	Qu et al. (2019) [34]
RAD18	p53 upregulation weakens the role of RAD18 in inhibiting apoptosis	Wu et al. (2019) [35]
SDH5	The loss of SDH5 enhances radiosensitivity by reducing p53 phosphorylation and delaying p53 degradation in lung cancer.	Zong et al. (2019) [39]
53BP1	53BP1 downregulation significantly reduced p53 and enhanced CHK1 and CHK2 expression in Eca-109 cells.	Yang et al. (2019) [47]
GRIM19	Overexpression of GRIM-19 diminishes the activity of MDM2, a specific p53 protease, resulting in the accumulation of p53 and activation of p53-mediated apoptosis.	Chen et al. (2018) [48]
APG-115	APG-115 radiosensitizes p53 wild-type gastric cancer cells, increasing apoptosis.	Yi et al. (2018) [49]
CDK16	CDK16 binds to and phosphorylates p53 at Ser315 site to inhibit the transcriptional activity of p53.	Xie et al. (2018) [40]

Sensitizing drugs and modulation of adverse effects of radiotherapy

Cell-cycle checkpoints play a critical role in cell survival after exposure to radiation.[51,52] Most types of cancer have defects in cell-cycle checkpoints, which contribute to the development of radioresistance.[53] Targeting cell-cycle checkpoint defects is the anticancer therapy of the future.[54-57] For example, it was reported that three human cholangiocarcinoma (CCA) cell lines with various cell-cycle defects differ markedly in their sensitivity to radiation. The different radiation sensitivities were associated with existing G1 or G2 checkpoint defects in analyzed cells.[55] CCA cells with a defective G1 checkpoint but an intact G2 checkpoint were the most radioresistant cells. In addition, inhibition of checkpoint kinase 1/2 (Chk1/2) selectively increased the radiation sensitivity of CCA cells with G1 checkpoint defect.

Cancer cells frequently contain G1 checkpoint defects due to loss of p53 function, resulting in radioresistance.[58] A study by Hematulin et al.[59] evaluated the radiosensitizing potential of etoposide, widely used as an antitumor chemotherapy drug,[60] in p53-defective CCA KKU-M055 and KKU-M214 cell lines with G1 checkpoint defects, which differ in G2 checkpoint status. KKU-M055 cells had an effective G2 checkpoint with marked accumulation of cells in the G2/M phase, together with induction of Chk2, Wee1 and Cdc2 phosphorylation after irradiation, and without the activation of the p53-p21 axis in response to radiation. In contrast, a defective G2 checkpoint was demonstrated in KKU-M214 cells, which failed to arrest the cell cycle in the G2/M phase after irradiation. The observed induction of p53 phosphorylation did not contribute to the induction of cell-cycle arrest in KKU-M214 cells in the G2/M phase. Treatment with etoposide increased the sensitivity of two p53-defective CCA cell lines to radiation, regardless of the function of the G2 checkpoint, and G2/M arrest was not the determining mechanism for the radiosensitization activity of etoposide. It was found that apoptosis was the dominant mode of death for KKU-M055 cells with an intact G2 checkpoint, while mitotic catastrophe was the dominant mode of death for KKU-M214 cells with a G2 checkpoint defect. Thus, etoposide can be used as a tumor radiosensitizer regardless of the functionality of the tumor's G2 checkpoints.

Histone deacetylase inhibitors (HDACi) are a group of agents that target histone deacetylase, which affects chromatin structure resulting in gene expression regulation. Radiosensitization by HDACi has been demonstrated in numerous preclinical and clinical studies.[61-64] Moreover, HDACi can also modulate cellular functions independent of gene expression by acting on non-histone protein deacetylation. Thus, HDACi are involved in regulating different altered pathways in cancer, such as apoptosis, cell cycle, and DNA repair.

Valproate (VPA) is an antiepileptic that, in addition to its anticonvulsant properties, is an effective HDACi. A study by Terranova-Barberio et al.[65] examined the combination of VPA with capecitabine metabolite 5′-deoxy-5-fluorouridine (5′-DFUR) in combination with radiotherapy on CRC cells: HCT-116 (p53-wild-type), HCT-116 p53−/−(p53-null), SW620 and HT29 (p53-mutant), which also made it possible to study the role of p53 in the combination setting. Combined treatment with equipotent doses of VPA and 5′-DFUR resulted in synergistic effects in CRC lines expressing p53 (wild-type or mutant). In HCT-116 p53-null−cells, antagonist effects were observed. Radiotherapy further potentiated the antiproliferative, pro-

apoptotic, and DNA damage effects induced by 5′-DFUR/VPA combination in p53 expressing cells.

As noted earlier, in human cancer, more than 50% of tumors contain a mutation or deletion of the *TP53* gene, which increases the likelihood of uncontrolled cell division,[4] since *TP53* plays a central role in mediating the response to DNA damage through the transactivation of numerous genes that inhibit growth or apoptosis, including *p21* gene.[66] Therefore, establishing the dependence of the activity of antitumor drugs on the cellular expression of p53 is of great importance. A study performed by Choo et al.[67] demonstrated the in vitro radiosensitizing effects of VPA on the human breast cancer MCF7 cell line and also revealed that VPA increased the level of DNA breakage, apoptosis, and senescence. VPA also induced tumor suppressor protein p53 and p21 expression and activated checkpoint kinase 2 (CHK2) in MCF7 cells. The treatment with VPA also increased p21 levels and CHK2 activity in p53-null colon cancer HCT116 cells, suggesting that VPA may be used to treat various types of cancer with altered p53 status. VPA-induced radiosensitization was largely dependent on the activity of CHK2. Thus, VPA may exhibit clinical utility concerning increasing the anticancer efficacy of radiotherapy by affecting the level of p53; in addition, the treatment with VPA and irradiation may enhance the radiosensitivity of p53-altered types of cancer.

Recent studies have shown that simvastatin, a 3-hydroxy-3-mehtylglutaryl-coenzyme A (HMG-CoA) reductase inhibitor often used to treat lipid disorders, exhibits anticancer effects by regulating proliferation, apoptosis, and metastasis in various tumors,[68-71] and also enhances radiosensitization by suppressing BIRC5 (survivin) and CTGF (connective tissue growth factor) in gastric cancer and colorectal cancer.[72] Lee et al.[73] investigated whether the combination of simvastatin and IR would radiosensitize HCT116 p53+/+ and p53-/- colon cancer cells. Simvastatin potently stimulated radiosensitization of HCT116 p53-/- cells and xenograft tumors. The combination of simvastatin with IR decreased G2/M arrest and delayed the repair of IR-induced DNA damage, and no differences between the HCT116 p53+/+ and p53-/- cells were evident. Simvastatin also exhibited MDM2 suppression, regardless of p53 status, resulting in inducing radiosensitization. In addition, simvastatin caused accumulations of the FOXO3a, E-cadherin, and tumor suppressor protein p21, downstream factors of MDM2, in HCT116 p53-/- cells. Thus, these findings suggest the possibility of applying simvastatin as an MDM2 inhibitor and radiosensitizer for p53-deficient colorectal tumor treatments.

Nutlin-3, a small molecular weight cis-imidazoline analog, was designed to compete with Mdm2 for binding to p53.[74] Nutlin-3 induces the regulation and activation of the p53 pathway and is found to be effective and non-genotoxic in stabilizing p53 and enhancing apoptosis using experimental models in tumors expressing wild-type p53.[75]

Taste disturbance is one of the most common complications after radiation therapy, leading to decreased appetite and quality of life in patients with head and neck cancer. Faccion et al.[76] showed that checkpoint kinase 2 (Chk2) deficiency reduces p53 expression and inhibits cell apoptosis, partly contributing to the radioprotective effect on taste cells. In particular, Chk2 −/− mice showed less loss of type II and type III taste cells, lower expression of p53, caspase-3, and cleaved caspase-3, and lower levels of apoptosis. However, Chk2 deficiency did not alter oxidative stress levels, antioxidant capacity, and oxidative DNA damage in taste receptors. Chk2 appears to be a new target for correcting radiation-induced taste dysfunction.

Sensitizing drugs and modulation of adverse effects of radiotherapy are summarized in Table 2.

Table 2.

Sensitizing drugs and modulation of adverse effects of radiotherapy

Drug	Action	Source
Etoposide	Etoposide radiosensitizes p53-defective cholangiocarcinoma cell lines regardless of the functionality of the tumor's G2 checkpoint.	Hematulin et al. (2018) [59]
Valproate (VPA)	VPA is HDACi. Valproate up-regulates wild-type p53 and down-regulates mutp53 levels.	Terranova-Barberio et al. (2017) [65]
Simvastatin	Simvastatin exhibits MDM2 suppression, regardless of p53 status, inducing radio-sensitization	Lee et al. (2018) [73]
Nutlin-3	Nutlin-3 induces the regulation and activation of the p53 pathway and enhances apoptosis in tumors expressing wild-type p53.	Yee-Lin et al. (2018) [75]

Response predictive molecular markers

Various studies have shown that wild-type p53, but not mutant p53, can repress survivin expression at the transcriptional level[77] and that loss of survivin function partially mediates a p53-dependent apoptosis pathway.[78] Survivin is the smallest member of the apoptosis inhibitor protein family that plays a key role in regulating cell division and inhibiting apoptosis by blocking caspase activation. Overexpression of survivin in human lung cancer cells blocks p53-dependent apoptosis in a dose-dependent manner,[78] suggesting that survivin regulates (at least in part) the p53-dependent apoptosis pathway. Faccion et al.[76] found that high p53 expression levels and nuclear survivin localization correlated with the subtype of anaplastic astrocytoma, whereas cytoplasmic survivin localization correlated with the glioblastoma subtype. In addition, patients carrying tumors with a high cytoplasmic survivin expression, a high nuclear survivin expression, or a high p53 expression and who did not receive radiotherapy exhibited poorer short-term and long-term survival rates. Hence, patients whose tumors overexpress these proteins may benefit from radiotherapy, irrespective of age and/or histological classification.

Currently, there is no method to predict tumor response to chemoradiotherapy. Stojanovic-Rundic et al.[79] evaluated whether p21 and p53 expressions could be reliable predictors of pathological response to chemoradiotherapy in patients

with locally advanced rectal cancer. Tumor regression was assessed according to Dvorak (tumor regression grade [TRG] scores) and Wheeler (rectal cancer regression grade [RCRG] scores) classification systems. Locally advanced rectal cancer patients with immune expression of p21 had a significantly higher percentage of complete regression than patients with low expression of p21. In contrast, correlations between p53 expression and histopathological, as well as regression, grades were not found. Thus, the results suggested that p53 expression did not predict pathological response to preoperative chemoradiotherapy, but p21 expression did. In general, it can be assumed that the evaluation of several markers will identify a certain group of patients with a better response to radiotherapy.

It should be emphasized that the most crucial role of the p53 gene in radiosensitivity is quite apparent. Nevertheless, today it is necessary to conduct research to correct mutational changes in the gene, increase the sensitivity of cancer cells against the background of T53 activation in them, and radioprotection of healthy tissues against the background of p53 deactivation in them. Thus, the TP53 gene is an essential marker for determining cell fate before radiotherapy.

Cancer stem cells and radioresistance

Currently, there is an increased interest in investigating CSCs, which are the cause of neoplastic phenotypic and functional heterogeneity. CSCs are neoplastic cells with an indefinite potential for self-renewal and, therefore, oncogenic capacity. Recent investigations report that a fraction of these neoplastic cells are considered CSCs, which explains the continuous resistance to the treatment and tumoral recurrence.[80]

The oncogenic capability of CSCs (Image 2) is due to the accumulation of mutations throughout their life, indefinite proliferation, resistance to apoptosis, evasion of anti-growth signaling, expression of telomerase activity, immune destruction, and increased cell motility.[81] If CSCs survive after IR, they are able to cause tumor recurrence (Image 3). It is well known that CSCs mediate radiation resistance of tumors through tumor-specific factors such as the number of CSCs before treatment and repopulation or reoxygenation during fractionated radiotherapy. Recent clinical evidence suggests that stem cell-associated surface markers can be directly used as predictors of radiocurability of tumors with comparable risk factors such as histology and size.[82]

Mesenchymal stem cells (MSCs) have been investigated for use in treating cancers as they can both preferentially home in on tumors and become incorporated into their stroma. This process increases after radiation therapy. A study by de Araújo Farias et al.[83] showed that in vitro, MSCs, when activated with a low dose of radiation, were a source of antitumor cytokines that decrease the proliferative activity of tumor cells, producing a potent cytotoxic synergistic effect on them. In vivo administration of unirradiated mesenchymal cells together with radiation led to an increased efficacy of radiotherapy. The authors concluded that IR and MSCs have a synergistic effect when they are applied together for tumor treatment.

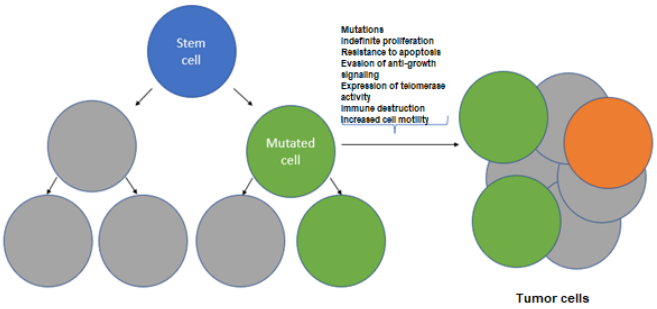

***Image 2**. Oncogenic capability of cancer stem cells (CSCs)*

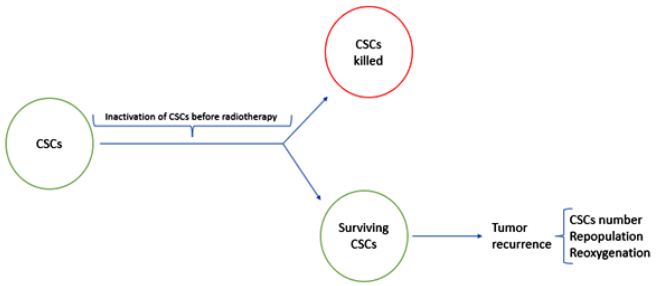

***Image 3.** CSCs surviving after IR and tumor recurrence.*

The NOTCH signaling pathway is critical in tissue development and is involved in malignant transformation. In preclinical lung cancer models, NOTCH inhibition has been shown to improve response to radiotherapy by targeting tumor stem cells. Giuranno et al.[84] showed that NOTCH signaling is active in both primary human models and in murine airway epithelial stem cell models, and, in combination with radiation inhibition of NOTCH, provokes a decrease in S phase and an increase in G1-phase arrest. NOTCH inhibition in irradiated lung basal stem cells resulted in more potent activation of DNA damage checkpoint kinases pATM and pCHK2 and led to an increase in the level of residual 53BP1 foci in irradiated lung basal stem cells, reducing their ability to self-renew.

Zamulaeva et al.[85] evaluated the prognostic significance of the proportion of CSCs in cervical scrapings from 38 patients with cervical cancer treatment and after irradiation at a total dose of 10 Gy. The results were assessed by the degree of tumor regression at 3-6 months after treatment. CSCs were identified as cells with the CD44+CD24low immunophenotype using flow cytometry. The proportion of CSCs in patients with complete tumor regression decreased by an average of 2.2±1.1% after irradiation, while in patients with partial regression, this indicator increased by an average of 3.3±2.3% (P=0.03). Multiple regression analysis revealed two independent indicators that affect tumor regression: the stage of the disease and the change in the proportion of CSCs after the first irradiation sessions. The proportion of CSCs before treatment had no prognostic value.

There is evidence that radiation-induced cells do not die immediately.[86] Contact of surviving tumor and non-tumor cells with the internal and external environment through

various signaling pathways and/or gene expression leads to the production of various chemokines, cytokines, growth factors, and protein hormones. The mechanism of how these close cellular interactions influence the tumor response to radiation is currently an important area of research. MSCs play an important role in non-tumor cells. Recent studies have shown that MSCs have an inhibitory effect on HCC, suggesting that they have potential as a novel therapeutic agent.[87,88] Adipose tissue-derived mesenchymal stem cells (AT-MSCs) are one of the most promising types of MSCs that can be easily obtained using minimally invasive procedures and can differentiate into numerous cell lines.[89] Wu et al.[90] showed that AT-MSCs can enhance the inhibitory effect of radiotherapy on reducing the growth, migration, and invasion of HCC cells in both in vitro and in vivo experiments. RNA-sequencing analysis revealed a noticeable interferon-induced transmembrane 1 (IFITM1)-induced tumor gene signature. Gain and loss mechanistic studies indicated that the mechanism was associated with decreased expression of signal transducer and transcription activator 3 (STAT3) and matrix metallopeptidases (MMPs) and increased expression of P53 and caspases. These data suggest that AT-MSCs can enhance the therapeutic effects of radiotherapy in HCC.

Compared to regularly proliferating cancer cells, CSCs have unique gene profiles and intracellular constitution, and also express specific membrane markers. Current therapeutic strategies targeting CSCs include CSC surface/intrinsic markers or signaling pathways, as well as CSC metabolism or the microenvironment, using antibodies, aptamers, peptide ligands, small molecules, or RNA-based therapeutics.[91-93] Among these strategies, therapeutic antibodies targeting CSC surface markers and small molecule inhibitors targeting CSC signaling pathways have already been investigated in clinical trials.

CD147 has been reported to be associated with CSC characteristics such as epithelial-mesenchymal transition (EMT) [94] and resistance to chemoradiotherapy.[95,96] Metuximab, the anti-CD147 drug, has been successfully used to prevent tumor recurrence after liver transplantation or radiofrequency ablation in patients with advanced HCC.[97,98] Fan et al.[99] demonstrated that anti-CD147 HAb18IgG sensitizes pancreatic cancer cells to chemoradiotherapy by reducing colony and sphere formation in a dose-dependent manner. In addition, HAb18IgG reduced the pancreatic CSC subpopulation and the expression of stem cell transcription factors OCT4, SOX2, and NANOG. Mechanically, HAb18IgG inhibited CSCs by blocking CD44s-pSTAT3 signaling. These results led the authors to suggest a promising therapeutic role for anti-CD147 HAb18IgG in suppressing pancreatic tumor initiation and overcoming relapses after chemoradiotherapy through direct targeting of CSCs.

A study by Konířová et al.[100] was focused on evaluating the response to IR of neural stem cells derived from mouse brains and grown in vitro. Under IR, neural stem cells expressed high mRNA levels of the stemness markers nestin and Sox2, and also showed high expression of Mki67 and Mcm2, markers associated with cell proliferation. The data obtained showed increased transcriptional activity of p53 targets, including Gadd45a, and proliferation arrest after irradiation. Moreover, most of the cells did not undergo apoptosis after irradiation, but stopped proliferation and started the differentiation program. The induction of differentiation and the demonstrated ability of irradiated cells to differentiate into neurons may represent a mechanism by which damaged neural stem cells circumvent the effects of cumulative DNA damage.

Dose-dependent radiation damage to intestinal stem cells (ISCs) is the main cause of radiation-induced gastrointestinal syndrome (RIGS). Self-renewal and proliferation of ISCs and thus maintenance of homeostasis and repair of the intestinal epithelium is primarily dependent on Wnt-β-catenin signaling.[101,102]

Bhanja et al.[103] demonstrated that a small molecular agent BCN057 (3-[(Furan-2-ylmethyl)-amino]-2-(7-methoxy-2-oxo-1,2-dihydro-quinolin-3-yl)-6-methyl-imidazo[1,2-a] pyridin-1-ium) activates canonical Wnt-β-catenin signaling, mitigates RIGS, and improves survival when applied 24 h after a lethal dose of radiation exposure. In an ex vivo crypt organoid model developed from human and mouse intestinal epithelium, BCN057 was shown to rescue ISC from radiation toxicity and induce epithelial repair with activation of Wnt-β-catenin signaling. However, BCN057 did not show any radioprotective effect in tumor tissue. Thus, BCN057 may be a potential emollient against RIGS and may be useful in abdominal radiotherapy.

Damage to heart, lung, and bone marrow (BM) tissues is one of the most important side effects of radiation therapy for breast cancer, which limits the success of tumor treatment.[104-106] Several studies have demonstrated the protective effects of radio-detoxified (gamma irradiation-fragmented) lipopolysaccharide (RD-LPS), also called tolerin,[107] in reducing radiation-induced tissue damage.[108] A study by Hegyesi et al.[109] examined the effects of RD-LPS in a model of cardiotoxicity. The authors focused on endothelial progenitor cells (EPCs) and BM cell-derived small extracellular vesicles (sEVs) as potential biomarkers of the effect of RD-LPS. The effects of local irradiation were studied in a model of cardiac injury in mice with chest irradiation. The researchers found increased mortality after irradiation at a dose of 16Gy. Treatment with RD-LPS significantly extended survival. Using flow cytometry, it was shown that with the introduction of RD-LPS, the number of BM-EPCs increased in the bone marrow and, in particular, in the bloodstream. In addition, mass spectrometric analysis showed that RD-LPS altered the proteomic composition of sEVs derived from BM cells. Treatment with RD-LPS increased the expression of interferon-induced transmembrane protein-3 (IFITM3) in BM cells and in BM cell-derived sEVs. In conclusion, it was noted that treatment with RD-LPS induced an increase in the number of circulating EPCs in parallel with a decrease in radiation-related mortality.

Evidence shows that tissue stem cells with accumulated DNA damage can lead to cancer.[110,111] IR-related DNA damage can be accumulated in the pools of tissue stem cells.[112-114] High-dose-rate radiation has been found to recruit Lgr5+ colonic stem cells, while low-dose-rate radiation does not.[115] Leucine-rich repeat-containing G-protein-coupled receptor 5 (Lgr5) was first identified as a molecular marker on stem cells that could

develop into tumors as cells of origin in cancer.[116] The small and large intestines contain Lgr5+ stem cells in the bottom of crypts. ISCs expressing Lgr5 are cycling stem cells necessary for maintaining tissue in a steady state. Otsuka et al.[117] compared the effects of high-dose-rate (30 Gy/h) and low-dose-rate (0.003 Gy/h) radiation on the replenishment of colonic Lgr5+ stem cells. In Lgr5+ stem cells irradiated with high dose rates, pathways associated with DNA damage response, cell growth, cell differentiation, and cell death were found to be upregulated. In Lgr5+ stem cells irradiated with low dose rates, pathways associated with apical junctions and extracellular signaling were upregulated. High-dose-rate radiation-induced a considerable reduction in cell numbers in the colonic crypts and a dramatic increase in mitosis, which may stimulate the replenishment of the stem cell pool and the accumulation of genetic mutations in tissue stem cells.

CSCs exhibit a range of genetic and cellular adaptations that confer radioresistance. Among the mechanisms, one should take into account efficient DNA repair, the role of the CSC microenvironment and hypoxia,[118] and resistance to apoptosis via activation of the Akt pathway.[119] Cell-cycle phase also determines radiosensitivity, with cells most radiosensitive in the G2-M phase.[120] In addition, microRNAs are well known to play a critical role in the cellular response to IR.[121-125] Griñán-Lisón et al.[126]studied how IR affects the expression of miRNAs associated with stemness in various molecular subtypes of breast cancer (BC). Irradiation of BC cells at doses of 2, 4, or 6Gy affected their phenotype, functional characteristics, pluripotency gene expression, and oncogenic capacity in vivo. The effect of IR on the expression of eight miRNAs associated with stemness and radioresistance (miR-210, miR-10b, miR-182, miR-142, miR-221, miR-21, miR-93, miR-15b) varied depending on subpopulations of cell lines and clinical and pathological features of BC patients. The authors concluded that miRNAs related to BC stem cell subpopulations could provide a valuable method to predict and monitor tumor radio-response depending on the molecular BC subtype.

Malignant tumor cells, including laryngeal cancer cells, mainly obtain energy via the glycolysis of glucose, even under aerobic conditions. This aerobic glycolysis is called the Warburg effect,[127,128] and is believed to be involved in the development of cancer radioresistance.[128-130] Glucose transporter-1 (GLUT-1), localized on the cell membrane and acting as a channel protein for glucose uptake by cancer cells, is a key regulator of the Warburg effect.[128,131] GLUT-1 is expressed at high levels in radioresistant laryngeal cancer.[132-134] Inhibition of GLUT-1 using GLUT-1 small interfering RNA (siRNA) may enhance the radiosensitivity of laryngeal cancer cells.[135] Zhong et al.[136] created the CD133+-Hep-2R cell line and used in vitro and in vivo models of laryngeal cancer to test the radiosensitizing effect of GLUT-1 siRNA on CD133+-Hep-2R cells, exploring the cellular mechanisms underlying radiosensitivity enhancement, using RT-PCR, Western blotting, CCK-8 assay, colony formation assay, and Transwell assay in vitro and in a xenograft tumor model in nude mice. Transfection with GLUT-1 siRNA through inhibition of GLUT-1 expression led to inhibition of proliferation and invasive ability of CD133+-Hep-2R cells, which caused cell-cycle redistribution (a higher proportion of cells in the G0/G1 phase and a lower ratio in the S and G2/M phases). It was also found that suppressing RAD51 and DNA-PKcs expression increased the apoptosis rate and reduced DNA repair capability. Hence, GLUT-1 siRNA can enhance the radiosensitivity of CD133+-Hep-2R cells by inducing a redistribution of cell-cycle phases, inhibiting DNA repair capability, and increasing apoptosis.

Stem cells and the molecules they produce are summarized in Table 3.

Table 3.

Stem cells and the molecules they produce.

Stem cells	Molecules produced by stem cells	Source
MSCs	TRAIL and DKK3	de Araújo Farias et al. (2015) [83]
Basal airway stem cells	NOTCH	Giuranno et al. (2019) [84]
Cervical CSCs	CD44, CD24, and CD45	Zamulaeva et al. (2019) [85]
AT-MSCs	IFITM1	Wu et al. (2019) [90]
Pancreatic CSCs	CD147	Fan et al. (2019) [99]
Neural stem cells	Sox2, MKi67 and MCM2	Konířová et al. (2019) [100]
Intestinal stem cells	Wnt-β-catenin	Bhanja et al. (2019) [103]
Bone marrow-derived endothelial progenitor cells	IFITM3	Hegyesi et al. (2019) [109]
Intestinal stem cells	Lgr5	Otsuka et al. (2017) [117]

Cellular senescence, cancer and cellular radiosensitivity

Cellular senescence is an extremely stable form of cell-cycle arrest and constitutes a strong natural tumor suppressor mechanism. Senescent cells have rather heterogeneous phenotypes and can exhibit both antitumor and tumor-promoting features. Data on the role of cellular senescence in cancer and radioresistance are sometimes ambiguous and even contradictory. Studies published in the past decade have demonstrated that malignant and non-malignant cells with lastingly persistent senescence can acquire pro-tumorigenic properties in certain conditions.

B lymphoma Mo-MLV insertion region 1 homolog (Bmi-1) is a polycomb group protein that regulates cell proliferation and is upregulated in various human cancer types, suggesting a potential role of Bmi-1 as an oncogene [137-140] that can induce anti-senescence in tumor cells. A study by Ye et al.[141] investigated the response of U87 glioma cells to radiation exposure and the role of Bmi-1 in the response following radiotherapy. It was found that X-ray radiation inhibits U87 cell proliferation by inducing senescence rather

than apoptosis. Following radiation exposure, the expression of Bmi-1 was upregulated, particularly when a dose of ≥6 Gy was administered. Bmi-1 may be significant in increasing the radioresistance of glioma cells by enabling cell senescence. Overexpression of Bmi-1 may reduce the expression of p16 and p19Arf, which induce anti-senescence in tumor cells.[142]

SHP-1, a cytosolic protein tyrosine phosphatase, can play either negative or positive roles in regulating signal transduction pathways and is differentially expressed in a number of cancer cell lines,[143-145] having different roles and mechanisms in regulating cell cycle and cell proliferation in different types of tumors. A study by Sun et al.[146] aimed to assess the role of SHP-1 in the radioresistance and senescence of nasopharyngeal carcinoma (NPC) cells. SHP-1 downregulation increased senescence, radiosensitivity, and a higher proportion of cells in G0/G1. Furthermore, SHP-1 overexpression resulted in radioresistance, inhibition of cellular senescence, and cell-cycle arrest in the S phase. Thus, SHP-1 had a critical role in radioresistance, cell- cycle progression, and senescence of NPC cells.

Although cellular senescence is a normal consequence of aging, there is increasing evidence showing that the radiation-induced senescence in both tumor and adjacent normal tissues contributes to tumor recurrence, metastasis, and resistance to therapy, while chronic senescent cells in the normal tissue and organ are a source of many late damaging effects. There is a growing body of evidence suggesting that senescence is associated with the disruption of the tissue microenvironment and the development of a pro-oncogenic environment.[147] Cellular senescence is characterized by irreversible cell-cycle arrest in response to various stress stimuli, resistance to apoptosis and senescent-associated secretory phenotype (SASP). SASP is a phenotype associated with senescent cells wherein those cells secrete a complex mixture containing hundreds of proteins, including pro-inflammatory cytokines/chemokines, immune modulators, tissue-damaging proteases, factors that can adversely affect stem and progenitor cell function, homeostatic factors, ceramides, bradykinins, and growth factors.[148-151] Cancer cells can be equally induced to cellular senescence through a variety of stress and damage signals, including irradiation. Senescent cells exhibit apoptosis resistance, metabolic activity, and secretion of pro-inflammatory and proliferative molecules. The effect of the SASP is highly dependent on context and cell type and is variable during the different stages of cancer progression.[152,153] Acute induction of cellular senescence is considered important for cancer prevention by stimulating the immune system to rapidly eliminate the genetically unstable cells, while chronic cellular senescence due to persistent stress signals (ROS, chronic inflammation) and the accumulation of dysfunctional senescent cells cannot be removed by immune cells; chronic cellular senescence creates a tumor-promoting environment through a secretion of SASP, including IL-1 alpha/beta, IL-6/8, MMPs, VEGF, TGF-beta, HFH, etc. Foregoing factors contribute to the increase in tumor radioresistance.[152,154]

IR is known to induce stress-induced, premature senescence (SIPS) in both normal and cancer cell types after exposure to relatively high doses (10 Gy) of radiation.[155-159] IR-induced senescence, apoptosis resistance, and EMT are three major mechanisms by which radioresistance develops. In a study by Yu et al.,[160] acute IR exposure induced cancer cell senescence and apoptosis, but after long-term IR exposure, cancer cells exhibited radioresistance. The proliferation of radioresistant cells was retarded, and most cells were arrested in G0/G1 phase. The radioresistant cells simultaneously showed resistance to further IR-induced apoptosis, premature senescence, and EMT. Acute IR exposure steadily elevated CDC6 protein levels, one of a group of proteins known as the pre-replication complex, an essential regulator of DNA replication. The ectopic overexpression of CDC6 leads to DNA hyper-replication, DNA damage, and genomic instability.[161] CDC6 overexpression has been detected in a number of cancer types, and high levels of CDC6 correlated with poor prognosis in cancer patients[161,162] and radioresistance in cancer cells.[163] CDC6 ectopic overexpression in CNE2 cells resulted in apoptosis resistance, G0/G1 cell-cycle arrest, premature senescence, and EMT, similar to the characteristics of radioresistant CNE2-R cells. Targeting CDC6 with siRNA promoted IR-induced senescence, sensitized cancer cells to IR-induced apoptosis, and reversed EMT. Furthermore, CDC6 depletion synergistically repressed the growth of CNE2-R xenografts when combined with IR. The authors concluded that CDC6 is a novel radioresistance switch regulating senescence, apoptosis, and EMT.

Genes and proteins involved in cellular senescence and radiation response are presented in Table 4.

Table 4.

Genes/proteins involved in cellular senescence and radiation response.

Gene/ Protein	Action	Source
CDC6	DNA hyper-replication, DNA damage, and genomic instability	Borlado et al. (2008) [161]
Bmi-1	Reduction of p16 and p19Arf expression	Bruggeman et al. (2007) [142]
SHP-1	Downregulated: increased cellular senescence and radiosensitivity Overexpression: decreased cellular senescence and radiosensitivity	Sunet al. (2015) [146]

Conclusion

Radiotherapy has been identified as the most common cancer treatment over the past decades. Unfortunately, the efficacy of this treatment modality is low in several malignancies due to the resistance of cancer to radiation. Multiple mechanisms, including cell-cycle checkpoint function, DNA repair, and cell death pathways, modulate the radio-responsiveness of cancer cells. Recently, increasing interest has focused on the role of p53 in the regulation of cellular growth induced by intense oncogenic signals or replicative stress.[164] Upon stimulation, p53 regulates the

expression of a large number of target genes involved in cell-cycle arrest, DNA repair, senescence, and apoptosis.[165] Numerous studies have shown that p53 plays a critical role in maintaining genomic integrity through its role in DNA damage response.[166] Loss of p53 function promotes (directly and indirectly) chromosomal instability, inducing cells to enter either senescence or apoptosis.[167] A deep understanding of the mechanisms by which p53 is implicated in regulating cellular senescence is of great interest for the development of new therapeutic strategies.

Currently, there is an increased interest in investigating CSCs, which are the cause of neoplastic phenotypic and functional heterogeneity. Emerging evidence suggests that CSCs exhibit a range of genetic and cellular adaptations that confer radioresistance and play a critical role in tumor initiation, malignant progression, disease relapse, and distant metastasis.

Cellular senescence is an extremely stable form of cell-cycle arrest and constitutes a strong natural tumor suppressor mechanism. Studies published in the past decade have demonstrated that, in certain conditions and contexts, malignant and non-malignant cells with lastingly persistent senescence can acquire pro-tumorigenic properties. Senescent cells may have a role in oncogenesis mainly through the SASP, which produces an immunosuppressive environment. A rising number of studies point out that spontaneous senescence and therapy-induced senescence play a substantial role in cancer aggressiveness. Ambiguous and even controversial data on the role of cellular senescence in cancer and radioresistance require further research.

Competing Interests

The author declares that there is no conflict of interest.

References

1. TP53 tumor protein p53 [Homo sapiens (human)] https://www.ncbi.nlm.nih.gov/gene/7157
2. Lane DP. Cancer. p53, guardian of the genome. Nature. 1992 Jul 2;358(6381):15-6. doi: 10.1038/358015a0.
3. Nigro JM, Baker SJ, Preisinger AC, Jessup JM, Hostetter R, Cleary K, et al. Mutations in the p53 gene occur in diverse human tumour types. Nature. 1989 Dec 7;342(6250):705-8. doi: 10.1038/342705a0.
4. Hollstein M, Sidransky D, Vogelstein B, Harris CC. p53 mutations in human cancers. Science. 1991 Jul 5;253(5015):49-53. doi: 10.1126/science.1905840.
5. Vousden KH, Lu X. Live or let die: the cell's response to p53. Nat Rev Cancer. 2002 Aug;2(8):594-604. doi: 10.1038/nrc864.
6. Joerger AC, Fersht AR. Structure-function-rescue: the diverse nature of common p53 cancer mutants. Oncogene. 2007 Apr 2;26(15):2226-42. doi: 10.1038/sj.onc.1210291.
7. Chen PL, Chen YM, Bookstein R, Lee WH. Genetic mechanisms of tumor suppression by the human p53 gene. Science. 1990 Dec 14;250(4987):1576-80. doi: 10.1126/science.2274789.
8. Ozaki T, Nakagawara A. Role of p53 in Cell Death and Human Cancers. Cancers (Basel). 2011 Mar 3;3(1):994-1013. doi: 10.3390/cancers3010994
9. Strano S, Dell'Orso S, Di Agostino S, Fontemaggi G, Sacchi A, Blandino G. Mutant p53: an oncogenic transcription factor. Oncogene. 2007 Apr 2;26(15):2212-9. doi: 10.1038/sj.onc.1210296.
10. Zhu G, Pan C, Bei JX, Li B, Liang C, Xu Y, Fu X. Mutant p53 in Cancer Progression and Targeted Therapies. Front Oncol. 2020 Nov 6;10:595187. doi: 10.3389/fonc.2020.595187.
11. Rojo de la Vega M, Chapman E, Zhang DD. NRF2 and the Hallmarks of Cancer. Cancer Cell. 2018 Jul 9;34(1):21-43. doi: 10.1016/j.ccell.2018.03.022.
12. Jeong Y, Hoang NT, Lovejoy A, Stehr H, Newman AM, Gentles AJ, et al. Role of KEAP1/NRF2 and TP53 Mutations in Lung Squamous Cell Carcinoma Development and Radiation Resistance. Cancer Discov. 2017 Jan;7(1):86-101. doi: 10.1158/2159-8290.CD-16-0127.
13. Chee JL, Saidin S, Lane DP, Leong SM, Noll JE, Neilsen PM, et al. Wild-type and mutant p53 mediate cisplatin resistance through interaction and inhibition of active caspase-9. Cell Cycle. 2013 Jan 15;12(2):278-88. doi: 10.4161/cc.23054.
14. Liu K, Ling S, Lin WC. TopBP1 mediates mutant p53 gain of function through NF-Y and p63/p73. Mol Cell Biol. 2011 Nov;31(22):4464-81. doi: 10.1128/MCB.05574-11.
15. Tchelebi L, Ashamalla H, Graves PR. Mutant p53 and the response to chemotherapy and radiation. Subcell Biochem. 2014;85:133-59. doi: 10.1007/978-94-017-9211-0_8.
16. Shetzer Y, Solomon H, Koifman G, Molchadsky A, Horesh S, Rotter V. The paradigm of mutant p53-expressing cancer stem cells and drug resistance. Carcinogenesis. 2014 Jun;35(6):1196-208. doi: 10.1093/carcin/bgu073
17. Schulz A, Meyer F, Dubrovska A, Borgmann K. Cancer Stem Cells and Radioresistance: DNA Repair and Beyond. Cancers (Basel). 2019 Jun 21;11(6):862. doi: 10.3390/cancers11060862.
18. Najafi M, Farhood B, Mortezaee K. Cancer stem cells (CSCs) in cancer progression and therapy. J Cell Physiol. 2019 Jun;234(6):8381-8395. doi: 10.1002/jcp.27740.
19. Olivos DJ, Mayo LD. Emerging Non-Canonical Functions and Regulation by p53: p53 and Stemness. Int J Mol Sci. 2016 Nov 26;17(12):1982. doi: 10.3390/ijms17121982.
20. Krayem M, Sabbah M, Najem A, Wouters A, Lardon F, Simon S, et al. The Benefit of Reactivating p53 under MAPK Inhibition on the Efficacy of Radiotherapy in Melanoma. Cancers (Basel). 2019 Aug 1;11(8):1093. doi: 10.3390/cancers11081093.
21. Farhood B, Goradel NH, Mortezaee K, Khanlarkhani N, Salehi E, Nashtaei MS, et al. Melatonin as an adjuvant in radiotherapy for radioprotection and radiosensitization. Clin Transl Oncol. 2019 Mar;21(3):268-279. doi: 10.1007/s12094-018-1934-0.
22. Picca A, Lezza AM. Regulation of mitochondrial biogenesis through TFAM-mitochondrial DNA interactions: Useful insights from aging and calorie restriction studies. Mitochondrion. 2015 Nov;25:67-75. doi: 10.1016/j.mito.2015.10.001.
23. Hillen HS, Morozov YI, Sarfallah A, Temiakov D, Cramer P. Structural Basis of Mitochondrial Transcription Initiation. Cell. 2017 Nov 16;171(5):1072-1081.e10. doi: 10.1016/j.cell.2017.10.036.
24. Ueta E, Sasabe E, Yang Z, Osaki T, Yamamoto T. Enhancement of apoptotic damage of squamous cell carcinoma cells by inhibition of the mitochondrial DNA repairing system. Cancer Sci. 2008 Nov;99(11):2230-7. doi: 10.1111/j.1349-7006.2008.00918.x.
25. Park JY, Wang PY, Matsumoto T, Sung HJ, Ma W, Choi JW, et al. p53 improves aerobic exercise capacity and augments

skeletal muscle mitochondrial DNA content. Circ Res. 2009 Sep 25;105(7):705-12, 11 p following 712. doi: 10.1161/CIRCRESAHA.109.205310.
26. Wen S, Gao J, Zhang L, Zhou H, Fang D, Feng S. p53 increase mitochondrial copy number via up-regulation of mitochondrial transcription factor A in colorectal cancer. Oncotarget. 2016 Nov 15;7(46):75981-75995. doi: 10.18632/oncotarget.12514.
27. Yoshida Y, Izumi H, Torigoe T, Ishiguchi H, Itoh H, Kang D, Kohno K. P53 physically interacts with mitochondrial transcription factor A and differentially regulates binding to damaged DNA. Cancer Res. 2003 Jul 1;63(13):3729-34.
28. He L, Lai H, Chen T. Dual-function nanosystem for synergetic cancer chemo-/radiotherapy through ROS-mediated signaling pathways. Biomaterials. 2015 May;51:30-42. doi: 10.1016/j.biomaterials.2015.01.063.
29. Bensaad K, Tsuruta A, Selak MA, Vidal MN, Nakano K, Bartrons R, et al. TIGAR, a p53-inducible regulator of glycolysis and apoptosis. Cell. 2006 Jul 14;126(1):107-20. doi: 10.1016/j.cell.2006.05.036.
30. Bensaad K, Cheung EC, Vousden KH. Modulation of intracellular ROS levels by TIGAR controls autophagy. EMBO J. 2009 Oct 7;28(19):3015-26. doi: 10.1038/emboj.2009.242.
31. Jiang X, Wang J. Down-regulation of TFAM increases the sensitivity of tumour cells to radiation via p53/TIGAR signalling pathway. J Cell Mol Med. 2019 Jul;23(7):4545-4558. doi: 10.1111/jcmm.14350.
32. Oshiro MM, Watts GS, Wozniak RJ, Junk DJ, Munoz-Rodriguez JL, Domann FE, Futscher BW. Mutant p53 and aberrant cytosine methylation cooperate to silence gene expression. Oncogene. 2003 Jun 5;22(23):3624-34. doi: 10.1038/sj.onc.1206545.
33. Gomes NP, Espinosa JM. Gene-specific repression of the p53 target gene PUMA via intragenic CTCF-Cohesin binding. Genes Dev. 2010 May 15;24(10):1022-34. doi: 10.1101/gad.1881010.
34. Qu H, Su Y, Yu L, Zhao H, Xin C. Wild-type p53 regulates OTOP2 transcription through DNA loop alteration of the promoter in colorectal cancer. FEBS Open Bio. 2018 Dec 20;9(1):26-34. doi: 10.1002/2211-5463.12554.
35. Wu B, Wang H, Zhang L, Sun C, Li H, Jiang C, Liu X. High expression of RAD18 in glioma induces radiotherapy resistance via down-regulating P53 expression. Biomed Pharmacother. 2019 Apr;112:108555. doi: 10.1016/j.biopha.2019.01.016.
36. Xie C, Wang H, Cheng H, Li J, Wang Z, Yue W. RAD18 mediates resistance to ionizing radiation in human glioma cells. Biochem Biophys Res Commun. 2014 Feb 28;445(1):263-8. doi: 10.1016/j.bbrc.2014.02.003.
37. Kunst HP, Rutten MH, de Mönnink JP, Hoefsloot LH, Timmers HJ, Marres HA, et al. SDHAF2 (PGL2-SDH5) and hereditary head and neck paraganglioma. Clin Cancer Res. 2011 Jan 15;17(2):247-54. doi: 10.1158/1078-0432.CCR-10-0420.
38. Kaelin WG Jr. SDH5 mutations and familial paraganglioma: somewhere Warburg is smiling. Cancer Cell. 2009 Sep 8;16(3):180-2. doi: 10.1016/j.ccr.2009.08.013.
39. Zong Y, Li Q, Zhang F, Xian X, Wang S, Xia J, et al. SDH5 Depletion Enhances Radiosensitivity by Regulating p53: A New Method for Noninvasive Prediction of Radiotherapy Response. Theranostics. 2019 Aug 14;9(22):6380-6395. doi: 10.7150/thno.34443.
40. Xie J, Li Y, Jiang K, Hu K, Zhang S, Dong X, et al. CDK16 Phosphorylates and Degrades p53 to Promote Radioresistance and Predicts Prognosis in Lung Cancer. Theranostics. 2018 Jan 1;8(3):650-662. doi: 10.7150/thno.21963.
41. Malumbres M, Harlow E, Hunt T, Hunter T, Lahti JM, Manning G, Morgan DO, et al. Cyclin-dependent kinases: a family portrait. Nat Cell Biol. 2009 Nov;11(11):1275-6. doi: 10.1038/ncb1109-1275.
42. Yanagi T, Krajewska M, Matsuzawa S, Reed JC. PCTAIRE1 phosphorylates p27 and regulates mitosis in cancer cells. Cancer Res. 2014 Oct 15;74(20):5795-807. doi: 10.1158/0008-5472.CAN-14-0872.
43. Yanagi T, Matsuzawa S. PCTAIRE1/PCTK1/CDK16: a new oncotarget? Cell Cycle. 2015;14(4):463-4. doi: 10.1080/15384101.2015.1006539.
44. Yanagi T, Tachikawa K, Wilkie-Grantham R, Hishiki A, Nagai K, Toyonaga E, et al. Lipid Nanoparticle-mediated siRNA Transfer Against PCTAIRE1/PCTK1/Cdk16 Inhibits In Vivo Cancer Growth. Mol Ther Nucleic Acids. 2016 Jun 28;5(6):e327. doi: 10.1038/mtna.2016.40.
45. Rouse J, Jackson SP. Interfaces between the detection, signaling, and repair of DNA damage. Science. 2002 Jul 26;297(5581):547-51. doi: 10.1126/science.1074740.
46. Demetriou SK, Ona-Vu K, Sullivan EM, Dong TK, Hsu SW, Oh DH. Defective DNA repair and cell cycle arrest in cells expressing Merkel cell polyomavirus T antigen. Int J Cancer. 2012 Oct 15;131(8):1818-27. doi: 10.1002/ijc.27440.
47. Yang J, Jing L, Liu CJ, Bai WW, Zhu SC. 53BP1 regulates cell cycle arrest in esophageal cancer model. Eur Rev Med Pharmacol Sci. 2019 Jan;23(2):604-612. doi: 10.26355/eurrev_201901_16874.
48. Chen W, Liu Q, Fu B, Liu K, Jiang W. Overexpression of GRIM-19 accelerates radiation-induced osteosarcoma cells apoptosis by p53 stabilization. Life Sci. 2018 Sep 1;208:232-238. doi: 10.1016/j.lfs.2018.07.015.
49. Yi H, Yan X, Luo Q, Yuan L, Li B, Pan W, et al. A novel small molecule inhibitor of MDM2-p53 (APG-115) enhances radiosensitivity of gastric adenocarcinoma. J Exp Clin Cancer Res. 2018 May 2;37(1):97. doi: 10.1186/s13046-018-0765-8.
50. Wang P, Sun W, Wang L, Gao J, Zhang J, He P. Correlations of p53 expression with transvaginal color Doppler ultrasound findings of cervical cancer after radiotherapy. J BUON. 2018 May-Jun;23(3):769-775.
51. Visconti R, Della Monica R, Grieco D. Cell cycle checkpoint in cancer: a therapeutically targetable double-edged sword. J Exp Clin Cancer Res. 2016 Sep 27;35(1):153. doi: 10.1186/s13046-016-0433-9.
52. Deckbar D, Jeggo PA, Löbrich M. Understanding the limitations of radiation-induced cell cycle checkpoints. Crit Rev Biochem Mol Biol. 2011 Aug;46(4):271-83. doi: 10.3109/10409238.2011.575764.
53. Schmitt CA. Senescence, apoptosis and therapy--cutting the lifelines of cancer. Nat Rev Cancer. 2003 Apr;3(4):286-95. doi: 10.1038/nrc1044.
54. Gabrielli B, Brooks K, Pavey S. Defective cell cycle checkpoints as targets for anti-cancer therapies. Front Pharmacol. 2012 Feb 2;3:9. doi: 10.3389/fphar.2012.00009.
55. Hematulin A, Sagan D, Sawanyawisuth K, Seubwai W, Wongkham S. Association between cellular radiosensitivity and G1/G2 checkpoint proficiencies in human cholangiocarcinoma cell lines. Int J Oncol. 2014 Sep;45(3):1159-66. doi: 10.3892/ijo.2014.2520.
56. Koniaras K, Cuddihy AR, Christopoulos H, Hogg A, O'Connell MJ. Inhibition of Chk1-dependent G2 DNA damage checkpoint radiosensitizes p53 mutant human cells. Oncogene. 2001 Nov 8;20(51):7453-63. doi: 10.1038/sj.onc.1204942.

57. Dillon MT, Good JS, Harrington KJ. Selective targeting of the G2/M cell cycle checkpoint to improve the therapeutic index of radiotherapy. Clin Oncol (R Coll Radiol). 2014 May;26(5):257-65. doi: 10.1016/j.clon.2014.01.009.
58. Lee JM, Bernstein A. p53 mutations increase resistance to ionizing radiation. Proc Natl Acad Sci U S A. 1993 Jun 15;90(12):5742-6. doi: 10.1073/pnas.90.12.5742.
59. Hematulin A, Meethang S, Utapom K, Wongkham S, Sagan D. Etoposide radiosensitizes p53-defective cholangiocarcinoma cell lines independent of their G_2 checkpoint efficacies. Oncol Lett. 2018 Mar;15(3):3895-3903. doi: 10.3892/ol.2018.7754.
60. Thakur DS. Topoisomerase II inhibitors in cancer Treatment. Int J Pharma Sci Nanotechnol. 2011;3:1173–1181.
61. Groselj B, Sharma NL, Hamdy FC, Kerr M, Kiltie AE. Histone deacetylase inhibitors as radiosensitisers: effects on DNA damage signalling and repair. Br J Cancer. 2013 Mar 5;108(4):748-54. doi: 10.1038/bjc.2013.21.
62. Ree AH, Dueland S, Folkvord S, Hole KH, Seierstad T, Johansen M, et al. Vorinostat, a histone deacetylase inhibitor, combined with pelvic palliative radiotherapy for gastrointestinal carcinoma: the Pelvic Radiation and Vorinostat (PRAVO) phase 1 study. Lancet Oncol. 2010 May;11(5):459-64. doi: 10.1016/S1470-2045(10)70058-9.
63. Chinnaiyan P, Cerna D, Burgan WE, Beam K, Williams ES, Camphausen K, Tofilon PJ. Postradiation sensitization of the histone deacetylase inhibitor valproic acid. Clin Cancer Res. 2008;14(17):5410-5. doi: 10.1158/1078-0432.CCR-08-0643.
64. Chen X, Wong P, Radany E, Wong JY. HDAC inhibitor, valproic acid, induces p53-dependent radiosensitization of colon cancer cells. Cancer Biother Radiopharm. 2009 Dec;24(6):689-99. doi: 10.1089/cbr.2009.0629.
65. Terranova-Barberio M, Pecori B, Roca MS, Imbimbo S, Bruzzese F, Leone A, et al. Synergistic antitumor interaction between valproic acid, capecitabine and radiotherapy in colorectal cancer: critical role of p53. J Exp Clin Cancer Res. 2017 Dec 6;36(1):177. doi: 10.1186/s13046-017-0647-5.
66. Brugarolas J, Chandrasekaran C, Gordon JI, Beach D, Jacks T, Hannon GJ. Radiation-induced cell cycle arrest compromised by p21 deficiency. Nature. 1995 Oct 12;377(6549):552-7. doi: 10.1038/377552a0.
67. Choo DW, Goh SH, Cho YW, Baek HJ, Park EJ, Motoyama N, et al. CHK2 is involved in the p53-independent radiosensitizing effects of valproic acid. Oncol Lett. 2017 Apr;13(4):2591-2598. doi: 10.3892/ol.2017.5792.
68. Shen YY, Yuan Y, Du YY, Pan YY. Molecular mechanism underlying the anticancer effect of simvastatin on MDA-MB-231 human breast cancer cells. Mol Med Rep. 2015 Jul;12(1):623-30. doi: 10.3892/mmr.2015.3411.
69. Hoque A, Chen H, Xu XC. Statin induces apoptosis and cell growth arrest in prostate cancer cells. Cancer Epidemiol Biomarkers Prev. 2008 Jan;17(1):88-94. doi: 10.1158/1055-9965.EPI-07-0531.
70. Hindler K, Cleeland CS, Rivera E, Collard CD. The role of statins in cancer therapy. Oncologist. 2006 Mar;11(3):306-15. doi: 10.1634/theoncologist.11-3-306.
71. Spampanato C, De Maria S, Sarnataro M, Giordano E, Zanfardino M, Baiano S, et al. Simvastatin inhibits cancer cell growth by inducing apoptosis correlated to activation of Bax and down-regulation of BCL-2 gene expression. Int J Oncol. 2012 Apr;40(4):935-41. doi: 10.3892/ijo.2011.1273.
72. Lim T, Lee I, Kim J, Kang WK. Synergistic Effect of Simvastatin Plus Radiation in Gastric Cancer and Colorectal Cancer: Implications of BIRC5 and Connective Tissue Growth Factor. Int J Radiat Oncol Biol Phys. 2015 Oct 1;93(2):316-25. doi: 10.1016/j.ijrobp.2015.05.023.
73. Lee JY, Kim MS, Ju JE, Lee MS, Chung N, Jeong YK. Simvastatin enhances the radiosensitivity of p53deficient cells via inhibition of mouse double minute 2 homolog. Int J Oncol. 2018 Jan;52(1):211-218. doi: 10.3892/ijo.2017.4192.
74. Vassilev LT, Vu BT, Graves B, Carvajal D, Podlaski F, Filipovic Z, et al. In vivo activation of the p53 pathway by small-molecule antagonists of MDM2. Science. 2004 Feb 6;303(5659):844-8. doi: 10.1126/science.1092472.
75. Yee-Lin V, Pooi-Fong W, Soo-Beng AK. Nutlin-3, A p53-Mdm2 Antagonist for Nasopharyngeal Carcinoma Treatment. Mini Rev Med Chem. 2018;18(2):173-183. doi: 10.2174/1389557516666170717125821.
76. Faccion RS, Bernardo PS, de Lopes GPF, Bastos LS, Teixeira CL, de Oliveira JA, et al. p53 expression and subcellular survivin localization improve the diagnosis and prognosis of patients with diffuse astrocytic tumors. Cell Oncol (Dordr). 2018 Apr;41(2):141-157. doi: 10.1007/s13402-017-0361-5.
77. Hoffman WH, Biade S, Zilfou JT, Chen J, Murphy M. Transcriptional repression of the anti-apoptotic survivin gene by wild type p53. J Biol Chem. 2002 Feb 1;277(5):3247-57. doi: 10.1074/jbc.M106643200.
78. Mirza A, McGuirk M, Hockenberry TN, Wu Q, Ashar H, Black S, et al. Human survivin is negatively regulated by wild-type p53 and participates in p53-dependent apoptotic pathway. Oncogene. 2002 Apr 18;21(17):2613-22. doi: 10.1038/sj.onc.1205353.
79. Stojanovic-Rundic S, Jankovic R, Micev M, Nikolic V, Popov I, Gavrilovic D, et al. p21 does, but p53 does not predict pathological response to preoperative chemoradiotherapy in locally advanced rectal cancer. J BUON. 2017 Nov-Dec;22(6):1463-1470.
80. Mata-Miranda M, Vázquez-Sapién GJ, Sánchez-Monroy V. [Generalities and applications of the stem cells]. Perinatol Reprod Hum. 2013;27(3):194-9. [Article in Spanish].
81. Alcalá-Pérez D. [Cancer stem cells: current concepts]. Rev Cent Dermatol Pascua. 2015; 24(2): 47-51. [Article in Spanish].
82. Krause M, Yaromina A, Eicheler W, Koch U, Baumann M. Cancer stem cells: targets and potential biomarkers for radiotherapy. Clin Cancer Res. 2011 Dec 1;17(23):7224-9. doi: 10.1158/1078-0432
83. de Araújo Farias V, O'Valle F, Lerma BA, Ruiz de Almodóvar C, López-Peñalver JJ, Nieto A, et al. Human mesenchymal stem cells enhance the systemic effects of radiotherapy. Oncotarget. 2015 Oct 13;6(31):31164-80. doi: 10.18632/oncotarget.5216.
84. Giuranno L, Wansleeben C, Iannone R, Arathoon L, Hounjet J, Groot AJ, Vooijs M. NOTCH signaling promotes the survival of irradiated basal airway stem cells. Am J Physiol Lung Cell Mol Physiol. 2019 Sep 1;317(3):L414-L423. doi: 10.1152/ajplung.00197.2019.
85. Zamulaeva IA, Selivanova EI, Matchuk ON, Krikunova LI, Mkrtchyan LS, Kulieva GZ, et al. Quantitative Changes in the Population of Cancer Stem Cells after Radiation Exposure in a Dose of 10 Gy as a Prognostic Marker of Immediate Results of the Treatment of Squamous Cell Cervical Cancer. Bull Exp Biol Med. 2019;168(1):156-159. doi: 10.1007/s10517-019-04667-x.
86. Chu K, Leonhardt EA, Trinh M, Prieur-Carrillo G, Lindqvist J, Albright N, Ling CC, Dewey WC. Computerized video time-lapse (CVTL) analysis of cell death kinetics in human bladder carcinoma cells (EJ30) X-irradiated in different phases

of the cell cycle. Radiat Res. 2002 Dec;158(6):667-77. doi: 10.1667/0033-7587(2002)158[0667:cvtlca]2.0.co;2.
87. Qiao L, Xu Z, Zhao T, Zhao Z, Shi M, Zhao RC, et al. Suppression of tumorigenesis by human mesenchymal stem cells in a hepatoma model. Cell Res. 2008 Apr;18(4):500-7. doi: 10.1038/cr.2008.40.
88. Li T, Song B, Du X, Wei Z, Huo T. Effect of bone-marrow-derived mesenchymal stem cells on high-potential hepatocellular carcinoma in mouse models: an intervention study. Eur J Med Res. 2013 Sep 30;18(1):34. doi: 10.1186/2047-783X-18-34.
89. Wu LW, Chen WL, Huang SM, Chan JY. Platelet-derived growth factor-AA is a substantial factor in the ability of adipose-derived stem cells and endothelial progenitor cells to enhance wound healing. FASEB J. 2019 Feb;33(2):2388-2395. doi: 10.1096/fj.201800658R.
90. Wu L, Tang Q, Yin X, Yan D, Tang M, Xin J, et al. The Therapeutic Potential of Adipose Tissue-Derived Mesenchymal Stem Cells to Enhance Radiotherapy Effects on Hepatocellular Carcinoma. Front Cell Dev Biol. 2019 Nov 12;7:267. doi: 10.3389/fcell.2019.00267.
91. Annett S, Robson T. Targeting cancer stem cells in the clinic: Current status and perspectives. Pharmacol Ther. 2018 Jul;187:13-30. doi: 10.1016/j.pharmthera.2018.02.001.
92. Pützer BM, Solanki M, Herchenröder O. Advances in cancer stem cell targeting: How to strike the evil at its root. Adv Drug Deliv Rev. 2017 Oct 1;120:89-107. doi: 10.1016/j.addr.2017.07.013.
93. Agliano A, Calvo A, Box C. The challenge of targeting cancer stem cells to halt metastasis. Semin Cancer Biol. 2017 Jun;44:25-42. doi: 10.1016/j.semcancer.2017.03.003.
94. Wu J, Ru NY, Zhang Y, Li Y, Wei D, Ren Z, et al. HAb18G/CD147 promotes epithelial-mesenchymal transition through TGF-β signaling and is transcriptionally regulated by Slug. Oncogene. 2011;30(43):4410-27. doi: 10.1038/onc.2011.149.
95. Tang J, Guo YS, Zhang Y, Yu XL, Li L, Huang W, et al. CD147 induces UPR to inhibit apoptosis and chemosensitivity by increasing the transcription of Bip in hepatocellular carcinoma. Cell Death Differ. 2012 Nov;19(11):1779-90. doi: 10.1038/cdd.2012.60.
96. Wu J, Li Y, Dang YZ, Gao HX, Jiang JL, Chen ZN. HAb18G/CD147 promotes radioresistance in hepatocellular carcinoma cells: a potential role for integrin β1 signaling. Mol Cancer Ther. 2015 Feb;14(2):553-63. doi: 10.1158/1535-7163.MCT-14-0618.
97. Xu J, Shen ZY, Chen XG, Zhang Q, Bian HJ, Zhu P, et al. A randomized controlled trial of Licartin for preventing hepatoma recurrence after liver transplantation. Hepatology. 2007 Feb;45(2):269-76. doi: 10.1002/hep.21465.
98. Bian H, Zheng JS, Nan G, Li R, Chen C, Hu CX, et al. Randomized trial of [131I] metuximab in treatment of hepatocellular carcinoma after percutaneous radiofrequency ablation. J Natl Cancer Inst. 2014 Sep 10;106(9):dju239. doi: 10.1093/jnci/dju239.
99. Fan XY, He D, Sheng CB, Wang B, Wang LJ, Wu XQ, et al. Therapeutic anti-CD147 antibody sensitizes cells to chemoradiotherapy via targeting pancreatic cancer stem cells. Am J Transl Res. 2019 Jun 15;11(6):3543-3554.
100. Konířová J, Cupal L, Jarošová Š, Michaelidesová A, Vachelová J, Davídková M, et al. Differentiation Induction as a Response to Irradiation in Neural Stem Cells In Vitro. Cancers (Basel). 2019 Jun 29;11(7):913. doi: 10.3390/cancers11070913.
101. Saha S, Aranda E, Hayakawa Y, Bhanja P, Atay S, Brodin NP, et al. Macrophage-derived extracellular vesicle-packaged WNTs rescue intestinal stem cells and enhance survival after radiation injury. Nat Commun. 2016 Oct 13;7:13096. doi: 10.1038/ncomms13096.
102. Clevers H, Nusse R. Wnt/β-catenin signaling and disease. Cell. 2012 Jun 8;149(6):1192-205. doi: 10.1016/j.cell.2012.05.012.
103. Bhanja P, Norris A, Gupta-Saraf P, Hoover A, Saha S. BCN057 induces intestinal stem cell repair and mitigates radiation-induced intestinal injury. Stem Cell Res Ther. 2018 Feb 2;9(1):26. doi: 10.1186/s13287-017-0763-3.
104. Wang Y, Probin V, Zhou D. Cancer therapy-induced residual bone marrow injury-Mechanisms of induction and implication for therapy. Curr Cancer Ther Rev. 2006 Aug 1;2(3):271-279. doi: 10.2174/157339406777934717.
105. Whelan TJ, Levine M, Julian J, Kirkbride P, Skingley P. The effects of radiation therapy on quality of life of women with breast carcinoma: results of a randomized trial. Ontario Clinical Oncology Group. Cancer. 2000 May 15;88(10):2260-6.
106. Raghunathan D, Khilji MI, Hassan SA, Yusuf SW. Radiation-Induced Cardiovascular Disease. Curr Atheroscler Rep. 2017 May;19(5):22. doi: 10.1007/s11883-017-0658-x.
107. Bertók L. Radio-detoxified endotoxin activates natural immunity: a review. Pathophysiology. 2005 Sep;12(2):85-95. doi: 10.1016/j.pathophys.2005.02.004.
108. Bertok L, Berczi I. Nomenclature and significance of innate/natural immune mechanisms and species-specific resistance. Adv Neuroimmune Biol. 2011;1:11–24. doi: 10.3233/NIB-2011-002.
109. Hegyesi H, Sándor N, Sáfrány G, Lovas V, Kovács Á, Takács A, et al. Radio-detoxified LPS alters bone marrow-derived extracellular vesicles and endothelial progenitor cells. Stem Cell Res Ther. 2019;10(1):313. doi: 10.1186/s13287-019-1417-4.
110. Huen MS, Chen J. The DNA damage response pathways: at the crossroad of protein modifications. Cell Res. 2008 Jan;18(1):8-16. doi: 10.1038/cr.2007.109.
111. Lengauer C, Kinzler KW, Vogelstein B. Genetic instabilities in human cancers. Nature. 1998 Dec 17;396(6712):643-9. doi: 10.1038/25292.
112. Reya T, Morrison SJ, Clarke MF, Weissman IL. Stem cells, cancer, and cancer stem cells. Nature. 2001 Nov 1;414(6859):105-11. doi: 10.1038/35102167.
113. Niwa O. Roles of stem cells in tissue turnover and radiation carcinogenesis. Radiat Res. 2010;174(6):833-9. doi: 10.1667/RR1970.1.
114. Rossi DJ, Jamieson CH, Weissman IL. Stems cells and the pathways to aging and cancer. Cell. 2008 Feb 22;132(4):681-96. doi: 10.1016/j.cell.2008.01.036.
115. Otsuka K, Iwasaki T. Effects of dose rates on radiation-induced replenishment of intestinal stem cells determined by Lgr5 lineage tracing. J Radiat Res. 2015 Jul;56(4):615-22. doi: 10.1093/jrr/rrv012.
116. Barker N, Ridgway RA, van Es JH, van de Wetering M, Begthel H, van den Born M, et al. Crypt stem cells as the cells-of-origin of intestinal cancer. Nature. 2009 Jan 29;457(7229):608-11. doi: 10.1038/nature07602.
117. Otsuka K, Suzuki K, Fujimichi Y, Tomita M, Iwasaki T. Cellular responses and gene expression profiles of colonic Lgr5+ stem cells after low-dose/low-dose-rate radiation exposure. J Radiat Res. 2018;59(suppl_2):ii18-ii22. doi: 10.1093/jrr/rrx078.
118. Brunner TB, Kunz-Schughart LA, Grosse-Gehling P, Baumann M. Cancer stem cells as a predictive factor in radiotherapy. Semin Radiat Oncol. 2012 Apr;22(2):151-74. doi: 10.1016/j.semradonc.2011.12.003.

119.Morrison R, Schleicher SM, Sun Y, Niermann KJ, Kim S, Spratt DE, et al. Targeting the mechanisms of resistance to chemotherapy and radiotherapy with the cancer stem cell hypothesis. J Oncol. 2011;2011:941876. doi: 10.1155/2011/941876.
120.Pawlik TM, Keyomarsi K. Role of cell cycle in mediating sensitivity to radiotherapy. Int J Radiat Oncol Biol Phys. 2004 Jul 15;59(4):928-42. doi: 10.1016/j.ijrobp.2004.03.005.
121.Peitzsch C, Kurth I, Kunz-Schughart L, Baumann M, Dubrovska A. Discovery of the cancer stem cell related determinants of radioresistance. Radiother Oncol. 2013 Sep;108(3):378-87. doi: 10.1016/j.radonc.2013.06.003.
122.Metheetrairut C, Adams BD, Nallur S, Weidhaas JB, Slack FJ. cel-mir-237 and its homologue, hsa-miR-125b, modulate the cellular response to ionizing radiation. Oncogene. 2017 Jan 26;36(4):512-524. doi: 10.1038/onc.2016.222.
123.Pajic M, Froio D, Daly S, Doculara L, Millar E, Graham PH, et al. miR-139-5p Modulates Radiotherapy Resistance in Breast Cancer by Repressing Multiple Gene Networks of DNA Repair and ROS Defense. Cancer Res. 2018 Jan 15;78(2):501-515. doi: 10.1158/0008-5472.CAN-16-3105.
124.Fabris L, Berton S, Citron F, D'Andrea S, Segatto I, Nicoloso MS, et al. Radiotherapy-induced miR-223 prevents relapse of breast cancer by targeting the EGF pathway. Oncogene. 2016 Sep 15;35(37):4914-26. doi: 10.1038/onc.2016.23.
125.Wilke CM, Hess J, Klymenko SV, Chumak VV, Zakhartseva LM, Bakhanova EV, et al. Expression of miRNA-26b-5p and its target TRPS1 is associated with radiation exposure in post-Chernobyl breast cancer. Int J Cancer. 2018 Feb 1;142(3):573-583. doi: 10.1002/ijc.31072.
126.Griñán-Lisón C, Olivares-Urbano MA, Jiménez G, López-Ruiz E, Del Val C, Morata-Tarifa C, et al. miRNAs as radio-response biomarkers for breast cancer stem cells. Mol Oncol. 2020 Mar;14(3):556-570. doi: 10.1002/1878-0261.12635.
127.Tekade RK, Sun X. The Warburg effect and glucose-derived cancer theranostics. Drug Discov Today. 2017 Nov;22(11):1637-1653. doi: 10.1016/j.drudis.2017.08.003.
128.Zhong JT, Zhou SH. Warburg effect, hexokinase-II, and radioresistance of laryngeal carcinoma. Oncotarget. 2017 Feb 21;8(8):14133-14146. doi: 10.18632/oncotarget.13044.
129.Pitroda SP, Wakim BT, Sood RF, Beveridge MG, Beckett MA, MacDermed DM, et al. STAT1-dependent expression of energy metabolic pathways links tumour growth and radioresistance to the Warburg effect. BMC Med. 2009 Nov 5;7:68. doi: 10.1186/1741-7015-7-68.
130.Harada H. Hypoxia-inducible factor 1-mediated characteristic features of cancer cells for tumor radioresistance. J Radiat Res. 2016 Aug;57 Suppl 1(Suppl 1):i99-i105. doi: 10.1093/jrr/rrw012.
131.Zhang TB, Zhao Y, Tong ZX, Guan YF. Inhibition of glucose-transporter 1 (GLUT-1) expression reversed Warburg effect in gastric cancer cell MKN45. Int J Clin Exp Med. 2015 Feb 15;8(2):2423-8.
132.Luo XM, Xu B, Zhou ML, Bao YY, Zhou SH, Fan J, Lu ZJ. Co-Inhibition of GLUT-1 Expression and the PI3K/Akt Signaling Pathway to Enhance the Radiosensitivity of Laryngeal Carcinoma Xenografts In Vivo. PLoS One. 2015 Nov 24;10(11):e0143306. doi: 10.1371/journal.pone.0143306.
133.Shen LF, Zhao X, Zhou SH, Lu ZJ, Zhao K, Fan J, Zhou ML. In vivo evaluation of the effects of simultaneous inhibition of GLUT-1 and HIF-1α by antisense oligodeoxynucleotides on the radiosensitivity of laryngeal carcinoma using micro 18F-FDG PET/CT. Oncotarget. 2017 May 23;8(21):34709-34726. doi: 10.18632/oncotarget.16671.
134.Bao YY, Zhou SH, Lu ZJ, Fan J, Huang YP. Inhibiting GLUT-1 expression and PI3K/Akt signaling using apigenin improves the radiosensitivity of laryngeal carcinoma in vivo. Oncol Rep. 2015 Oct;34(4):1805-14. doi: 10.3892/or.2015.4158.
135.Jiang T, Zhou ML, Fan J. Inhibition of GLUT-1 expression and the PI3K/Akt pathway to enhance the chemosensitivity of laryngeal carcinoma cells in vitro. Onco Targets Ther. 2018 Nov 6;11:7865-7872. doi: 10.2147/OTT.S176818.
136.Zhong JT, Yu Q, Zhou SH, Yu E, Bao YY, Lu ZJ, Fan J. GLUT-1 siRNA Enhances Radiosensitization Of Laryngeal Cancer Stem Cells Via Enhanced DNA Damage, Cell Cycle Redistribution, And Promotion Of Apoptosis In Vitro And In Vivo. Onco Targets Ther. 2019 Nov 5;12:9129-9142. doi: 10.2147/OTT.S221423.
137.Chowdhury M, Mihara K, Yasunaga S, Ohtaki M, Takihara Y, Kimura A. Expression of Polycomb-group (PcG) protein BMI-1 predicts prognosis in patients with acute myeloid leukemia. Leukemia. 2007 May;21(5):1116-22. doi: 10.1038/sj.leu.2404623
138.Vonlanthen S, Heighway J, Altermatt HJ, Gugger M, Kappeler A, Borner MM, et al. The bmi-1 oncoprotein is differentially expressed in non-small cell lung cancer and correlates with INK4A-ARF locus expression. Br J Cancer. 2001 May 18;84(10):1372-6. doi: 10.1054/bjoc.2001.1791.
139.Zhang FB, Sui LH, Xin T. Correlation of Bmi-1 expression and telomerase activity in human ovarian cancer. Br J Biomed Sci. 2008;65(4):172-7. doi: 10.1080/09674845.2008.11732824.
140.Song LB, Li J, Liao WT, Feng Y, Yu CP, Hu LJ, et al. The polycomb group protein Bmi-1 represses the tumor suppressor PTEN and induces epithelial-mesenchymal transition in human nasopharyngeal epithelial cells. J Clin Invest. 2009 Dec;119(12):3626-36. doi: 10.1172/JCI39374.
141.Ye L, Wang C, Yu G, Jiang Y, Sun D, Zhang Z, et al. Bmi-1 induces radioresistance by suppressing senescence in human U87 glioma cells. Oncol Lett. 2014 Dec;8(6):2601-2606. doi: 10.3892/ol.2014.2606.
142.Bruggeman SW, Hulsman D, Tanger E, Buckle T, Blom M, Zevenhoven J, et al. Bmi1 controls tumor development in an Ink4a/Arf-independent manner in a mouse model for glioma. Cancer Cell. 2007 Oct;12(4):328-41. doi: 10.1016/j.ccr.2007.08.032.
143.Wu C, Sun M, Liu L, Zhou GW. The function of the protein tyrosine phosphatase SHP-1 in cancer. Gene. 2003 Mar 13;306:1-12. doi: 10.1016/s0378-1119(03)00400-1.
144.Evren S, Wan S, Ma XZ, Fahim S, Mody N, Sakac D, et al. Characterization of SHP-1 protein tyrosine phosphatase transcripts, protein isoforms and phosphatase activity in epithelial cancer cells. Genomics. 2013 Nov-Dec;102(5-6):491-9. doi: 10.1016/j.ygeno.2013.10.001.
145.Amin S, Kumar A, Nilchi L, Wright K, Kozlowski M. Breast cancer cells proliferation is regulated by tyrosine phosphatase SHP1 through c-jun N-terminal kinase and cooperative induction of RFX-1 and AP-4 transcription factors. Mol Cancer Res. 2011 Aug;9(8):1112-25. doi: 10.1158/1541-7786.MCR-11-0097.
146.Sun Z, Pan X, Zou Z, Ding Q, Wu G, Peng G. Increased SHP-1 expression results in radioresistance, inhibition of cellular senescence, and cell cycle redistribution in nasopharyngeal carcinoma cells. Radiat Oncol. 2015 Jul 28;10:152.
147.Sabin RJ, Anderson RM. Cellular Senescence - its role in cancer and the response to ionizing radiation. Genome Integr.

2011 Aug 11;2(1):7. doi: 10.1186/2041-9414-2-7.
148.Coppé JP, Kauser K, Campisi J, Beauséjour CM. Secretion of vascular endothelial growth factor by primary human fibroblasts at senescence. J Biol Chem. 2006 Oct 6;281(40):29568-74. doi: 10.1074/jbc.M603307200.
149.Coppé JP, Desprez PY, Krtolica A, Campisi J. The senescence-associated secretory phenotype: the dark side of tumor suppression. Annu Rev Pathol. 2010;5:99-118. doi: 10.1146/annurev-pathol-121808-102144.
150.Kumari R, Jat P. Mechanisms of Cellular Senescence: Cell Cycle Arrest and Senescence Associated Secretory Phenotype. Front Cell Dev Biol. 2021 Mar 29;9:645593. doi: 10.3389/fcell.2021.645593.
151.Birch J, Gil J. Senescence and the SASP: many therapeutic avenues. Genes Dev. 2020 Dec 1;34(23-24):1565-1576. doi: 10.1101/gad.343129.120.
152.Wang L, Lankhorst L, Bernards R. Exploiting senescence for the treatment of cancer. Nat Rev Cancer. 2022 Jun;22(6):340-355. doi: 10.1038/s41568-022-00450-9.
153.Chen Z, Cao K, Xia Y, Li Y, Hou Y, Wang L, et al. Cellular senescence in ionizing radiation (Review). Oncol Rep. 2019 Sep;42(3):883-894. doi: 10.3892/or.2019.7209.
154.Patel NH, Sohal SS, Manjili MH, Harrell JC, Gewirtz DA. The Roles of Autophagy and Senescence in the Tumor Cell Response to Radiation. Radiat Res. 2020 Aug 1;194(2):103-115. doi: 10.1667/RADE-20-00009.
155.Rodier F, Coppé JP, Patil CK, Hoeijmakers WA, Muñoz DP, Raza SR, et al. Persistent DNA damage signalling triggers senescence-associated inflammatory cytokine secretion. Nat Cell Biol. 2009 Aug;11(8):973-9. doi: 10.1038/ncb1909. Epub 2009 Jul 13. Erratum in: Nat Cell Biol. 2009 Oct;11(10):1272. Dosage error in article text. PMID: 19597488; PMCID: PMC2743561.
156.Suzuki M, Boothman DA. Stress-induced premature senescence (SIPS)--influence of SIPS on radiotherapy. J Radiat Res. 2008 Mar;49(2):105-12. doi: 10.1269/jrr.07081.
157.Raffetto JD, Leverkus M, Park HY, Menzoian JO. Synopsis on cellular senescence and apoptosis. J Vasc Surg. 2001 Jul;34(1):173-7. doi: 10.1067/mva.2001.
158.Tsai KK, Stuart J, Chuang YY, Little JB, Yuan ZM. Low-dose radiation-induced senescent stromal fibroblasts render nearby breast cancer cells radioresistant. Radiat Res. 2009 Sep;172(3):306-13. doi: 10.1667/RR1764.1.
159.Mirzayans R, Scott A, Cameron M, Murray D. Induction of accelerated senescence by gamma radiation in human solid tumor-derived cell lines expressing wild-type TP53. Radiat Res. 2005 Jan;163(1):53-62. doi: 10.1667/rr3280.
160.Yu X, Liu Y, Yin L, Peng Y, Peng Y, Gao Y, et al. Radiation-promoted CDC6 protein stability contributes to radioresistance by regulating senescence and epithelial to mesenchymal transition. Oncogene. 2019;38(4):549-563. doi: 10.1038/s41388-018-0460-4.
161.Borlado LR, Méndez J. CDC6: from DNA replication to cell cycle checkpoints and oncogenesis. Carcinogenesis. 2008 Feb;29(2):237-43. doi: 10.1093/carcin/bgm268.
162.Liu Y, Hock JM, Van Beneden RJ, Li X. Aberrant overexpression of FOXM1 transcription factor plays a critical role in lung carcinogenesis induced by low doses of arsenic. Mol Carcinog. 2014 May;53(5):380-91. doi: 10.1002/mc.21989.
163.Young A, Berry R, Holloway AF, Blackburn NB, Dickinson JL, Skala M, et al. RNA-seq profiling of a radiation resistant and radiation sensitive prostate cancer cell line highlights opposing regulation of DNA repair and targets for radiosensitization. BMC Cancer. 2014 Nov 4;14:808. doi: 10.1186/1471-2407-14-
164.Kastenhuber ER, Lowe SW. Putting p53 in Context. Cell. 2017 Sep 7;170(6):1062-1078. doi: 10.1016/j.cell.2017.08.028.
165.Fischer M. Census and evaluation of p53 target genes. Oncogene. 2017;36(28):3943-3956. doi: 10.1038/onc.2016.502.
166.Williams AB, Schumacher B. p53 in the DNA-Damage-Repair Process. Cold Spring Harb Perspect Med. 2016 May 2;6(5):a026070. doi: 10.1101/cshperspect.a026070.
167.He Q, Au B, Kulkarni M, Shen Y, Lim KJ, Maimaiti J, et al. Chromosomal instability-induced senescence potentiates cell non-autonomous tumourigenic effects. Oncogenesis. 2018 Aug 15;7(8):62. doi: 10.1038/s41389-018-0072-4.

International Journal of Biomedicine 13(3) (2023) 46-53
http://dx.doi.org/10.21103/Article13(3)_RA4

REVIEW ARTICLE

INTERNATIONAL JOURNAL OF BIOMEDICINE

The Impact of PET/MRI Fusion on the Diagnostic Imaging Industry

Shrooq Aldahery*

Department of Applied Radiologic Technology, College of Applied Medical Sciences, University of Jeddah, Jeddah, Saudi Arabia

Abstract

The multimodal imaging technique has gained the spotlight in the present era due to its striking and immense applications. It is the combination of two or more modalities that complement one another to yield detailed information. Indubitably, it is an emerging and crucial technique due to its broad clinical and research applications. The diagnostic techniques with the dual modality are aligned for obtaining molecular data. Positron emission tomography (PET) is a progressive imaging technique in nuclear medicine. To flourish in the imaging industry, PET was combined with computed tomography (CT), but the fusion of the two provides some challenges, such as less soft tissue contrast and inefficiency of acquisition in simultaneous mode. As a result, another hybrid imaging technology, PET and MRI (PET/MRI), has been developed to provide more soft tissue contrast and less radiation dose exposure, leading this technique to be used extensively despite its shortcomings. This review study discusses the fusion of PET/MRI, technical challenges for their combination, commercially available models, and clinical applications observed in the wide areas of oncology, the cardiovascular system, the central nervous system, pediatrics, and inflammatory diseases. (**International Journal of Biomedicine. 2023;13(3):46-53.**)

Keywords: hybrid imaging • PET/MRI • technical challenges • dose advantage

For citation: Aldahery S. The Impact of PET/MRI Fusion on the Diagnostic Imaging Industry. International Journal of Biomedicine. 2023;13(3):46-53. doi:10.21103/Article13(3)_RA4

Abbreviations

CT, computed tomography; **FDG**, F-fluorodeoxyglucose; **MRI**, magnetic resonance imaging; **PMT**, photomultiplier tubes; **PET**, positron emission tomography; **TOF**, time-of-flight.

Background

Multimodal imaging has become increasingly significant for diagnosing diseases at the molecular level, leading to enormous advances in the medical imaging field. It is the combination of two or more techniques that complement each other to augment the efficacy. The diagnostic technique involves envisioning, characterizing, and assessing living organisms at basic cellular and molecular states. The conventional medical imaging modality assesses anatomical or functional characteristics. The anatomical evaluation is performed by computed tomography (CT) or magnetic resonance imaging (MRI), whereas functional evaluation is done by PET or MRI technique.[1] PET is the nuclear imaging technique with the basic principle of performing sensitive assays with even less radioligand concentration. It evaluates the functionality at the molecular basis from biological to pathophysiological process. It incorporates radiotracers such as 13N, 11C, 18F, and 150, which pass through the region of interest.[2] MRI utilizes magnetic fields and radio waves with different parameters to evaluate anatomical images with high resolution, physiological, biochemical, and metabolic activities of the body.[3,4]

The concept of fusion of PET/MRI was conceived by Simon Cherry and Paul Marsden in the 1990s to make use of the merits and demerits of the techniques. While they were performing an animal study, it was necessary to attain the anatomical information with soft tissue contrast provided by MRI and the molecular details by PET.[5] The PET and MRI

***Correspondence:** Dr. Shrooq Aldahery, staldahery@uj.edu.sa*

techniques are merged into a single modality to attain beneficial features simultaneously. The growth has been steady for the past 20 years as it has gained attention as a powerful tool used in clinical research. The necessity of fusion is highlighted as it can combat the pros and cons of conventional medical imaging. The pre-clinical study performed in the 1990s grasped attention, leading to the commercial launch.[6] This study demonstrates the potential of PET/MRI fusion, which paved the way for the growth of dual-modality imaging methods to strengthen them by considering the pluses and minuses of each technique.

Principle of the PET/MRI technique

PET technique is a painless, quantitative method that assesses the biological function by observing the flow of blood, neurotransmitters, radioactive tracers, and metabolites. In this technique, a radioactive tracer emitted after injection through the intravenous route is detected. The nucleus of the tracer releases a positron that causes a collision with electrons of the cell projecting photons which are examined by the camera present in the PET scan and are processed and converted to electrical signals, which takes about 10-40 min. It has applications in various fields, such as neurology, cardiology, cancer detection, atherosclerosis, and glucose consumption. PET technique offers broad advantages as it detects radiotracers in *in vivo* studies by considering sensitivity and quantitative precision. It employs molecular agents that display details of tissues and organs, leading this technique to have moderate space in the cancer field as it provides both diagnosis and cancer stages.[7] The last few decades have seen an immense revolution in scientific activity to modify and enhance the efficacy of PET technology. The advancement in this technique is the result of acquisition with the gating method, detectors integrated with enhanced geometry, and combination with other operational methods, such as MRI and CT, to magnify its potency. With its strength, there are also some shortcomings in this imaging modality; notably, the detection of photons is restricted due to the axial coverage from only 15 to 30cm; bounded temporal resolution thereupon causes risk and challenge to dynamic radiology with kinetic methodology.[8] Small-size tumors do not absorb the imaging tracer, which it lacks to be detected, and anatomical information of the body cannot be revealed with the PET technique. The total body-PET method provides distinctive features like increased resolution, detection sensitivity, expeditious method, large range of scans, and a low dose of tracer to offer better scan image quality to a profound understanding of disease and its stages, diagnosis, progress, or deterioration and prognosis of the illness.[4]

MRI is a painless diagnostic technique that postulates information about the body by using a strong magnetic field and radio waves to provide cross-sectional quality images. Due to the wide applications of this technique, it has broadened the horizon of imaging technology spectra. In this process of obtaining MR images, a patient is placed inside a huge magnetic area that causes the induction of a strong magnetic field externally. Due to this magnetic power, there is an alignment of nuclei of various atoms with the magnetic field, which, upon exposure to radio waves, produces energy that is analyzed by the system, creating an image.[9] MRI is often divided into structural MRI and functional MRI (fMRI). Structural MRI illustrates information about the anatomical structures, whereas fMRI explicates physiological activity. At the same time, MR image quality is determined by the interaction of appropriate parameters in each pulse sequence to obtain the maximum image quality to ensure high diagnostic accuracy in a reasonable scan time.[10]

MRI can provide 3D images with T1 and T2 relaxation times, which is cardinal for tumor assessment with high temporal and spatial resolution.[11] The grading of tumors is exceptionally stipulated by functional MRI as the advanced system applications, such as MR spectroscopy (MRS), perfusion-weighted imaging, and diffusion-weighted imaging.[12] However, MRI is contraindicated with patients with metallic objects in their bodies as they represent image distortion and safety issues in the subjects with implantations, and since bone does not give an MRI image, only bone marrow analyses are done.[9] One of the demerits noticed with MRI versus PET is that the sensitivity of functional information is less. Understanding PET and MRI functions is crucial, because when the modalities are combined, they complement each other and yield information simultaneously (Figure 1).

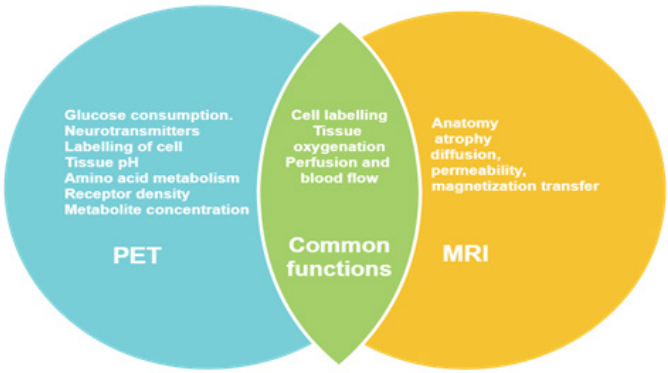

Fig. 1. *The functions of dual modality (PET/MRI) complement each other and can be acquired simultaneously.*

Predominant factors and merits of PET/MRI over PET/CT

The amalgamation of PET/MRI techniques has a fledgling and crucial impact in various fields, such as oncology, neurology, cardiology, and psychiatry. The concept of dual-modality was developed in the 1990s when the combination of PET/MRI and PET/CT was on track for development to expect a higher outcome. PET/CT has special applications, but shortcomings were noted. Many technical challenges in PET/CT technique set it back and initiated the spotlight on PET/MRI as it has fewer obstacles. The strengths of PET/MRI over PET/CT are low exposure to radiation, which reflects its safety, higher contrast with soft tissue, and it can be used to analyze any body part.[13] The imaging design of PET/CT is sequential, which causes it to obtain information from two systems; software is also installed to correct CT attenuation. Regardless of the same acquisition settings for both pediatrics and adults, the dose of CT in babies and children surpasses the dose given to adult subjects. Therefore, the benefit of replacing CT with MRI is underlined in pediatric patients. The approach to malignant cancer in pediatrics is of major concern and challenging due to the diagnostic imaging radiation dose. The preference for MRI over CT can reduce the radiation dose by almost 50%, which helps its use in children with cancer.[14] In

addition, the radiation dose is of consideration in patients with lymphoma as they have to be scanned multiple times, which exposes them to radiation of 23-26 mSv; in this order, the PET contributes about 5-7 mSv dose. Hence, replacing CT with MRI can abbreviate radiation exposure effectively. The other observed demerits of PET/CT are the probability of error due to the patient's motion during the examination, and the scanning process takes a long time. PET/MRI has beneficial outcomes in motion correction to obtain the information from MRI, and it can be used potentially in clinical and pre-clinical aspects.[3,15]

Manufacturing of Clinical PET/MRI integrated system

The first clinical integrated scanner, "BrainPET," was developed in 2007 by Siemens Healthcare after the pre-clinical studies revealed its effect. In the BrainPET design, the PET system was inserted into the MRI scanner, which was a 3-Telsa standard MRI scanner manufactured by Magnetom TIM Trio. It was based on simultaneous acquisition[16] (Figure 2).

Fig. 2. *Siemens MR-BrainPET prototype (PET insert into an MR scanner).*[15]

Further, Philips designed a whole-body PET/MRI model which has gained acceptance in Europe and endured with Conformité Européenne (CE), which certifies the standards, and it also received clearance by the Food and Drug Administration (FDA) (Section 510(k)) in the US (Figure 3). The model is based on the sequential design in which PET was placed adjacent to the MR scanner, 8 feet apart. A patient table is employed to obtain information in sequential order. A beneficial point has been obtained by modifying the state-of-the-art, time-of-flight (TOF)-PET which has caused the detectors of PET to work in the arena of MR scanners. Simultaneous data cannot be achieved with this technique.[17]

Fig. 3. *A whole-body sequential PET/MRI scanner (Philips Ingenuity TF PET/MRI).*[15]

General Electric (GE) designed a table in the year 2013 compatible with both PET and MRI, which led them to shift the patient between the scanners known as SIGNA PET/MR (Figure 4). The design of this product contains a component of MR which holds a bore of 60 cm 3-Tesla superconductive magnet, gradient coils, and transmitter. It is equipped so that the components of PET are placed between the body coil and gradient coil, which is shielded with radiofrequency. An appropriate temperature is maintained with the use of cold water. The performance of this design is explicit in terms of timing resolution, which is below 400 ps, energy resolution documented to be 10.3%, and scanner sensitivity is 23.3 kcps/MBq.[18]

Fig. 4. *SIGNA PET/MR (General Electric).*[15]

Biograph mMR is the first whole-body integrated scanner designed by Siemens in the year 2010 which has been granted the CE mark by Europe and received clearance from the FDA (Figure 5). This is based on Automatic Data processing (ADP) technology and has been advanced with gradient design by placing the PET detectors between a gradient coil and RF body coil. This design comprises a whole-body integrated scanner, which utilizes about a full 60cm bore magnet. The full gantry of PET is occupied by 56 detectors which make up eight rings, and the inner temperature of the detectors is maintained using cold water. The system's performance is measured using spatial, timing, and energy resolutions. The stated spatial resolution is 4.3 mm Full-width at Half Max (FWHM) from the field center at the distance of 1cm, timing resolution is 2.93 ms, and energy resolution is 14.5%. The sensitivity of the scanner noted is 15.0 kcps/MBq, and the data of the mMR scanner is obtained in 3D mode; the images of PET are obtained by the back projection that is filtered, or the statistics of Poisson distribution are followed.[19]

Fig. 5. *Siemens Biograph mMR whole-body scanner.* [15]

Technique challenges of PET/MRI fusion

The complexity in the design is caused by magnetic field consequences in physical challenges. The main objective is to obtain the integrated system without altering the functionality. The models are designed as sequential and simultaneous approaches. The sequential design is simple and economical, obtained by Philips Healthcare TF-PET/MRI. In the sequential approach, the software is co-registered, and the scanning procedure of PET and MRI is done one after another. This also gives a plus point for patients with claustrophobia, as this process is carried out in different modalities. In addition, in a sequential design, there is an additional shield with minimum exposure to the magnetic field. The drawback observed is the space, as it requires a larger area of 4.3×13m and causes motion artifacts to the organs, indicating its need for concurrent imaging. In the simultaneous approach, both modalities are constructed within the whole system to be placed in the same gantry. This design has two models; PET inserted MRI scanner and a fully integrated system. This model also has the benefit of less space.[20]

Due to its high potential, the obstacles to merging PET and MRI should be studied, and their compatibility must be assessed to impact the diagnostic imaging field. The hurdles to merging and maintaining PET and MRI with high performance are mentioned below (Figure 6):

1)The effect of PET on the MRI system
2)The effect of MRI on PET
3)Quantitative imaging
4)Space and time-bound

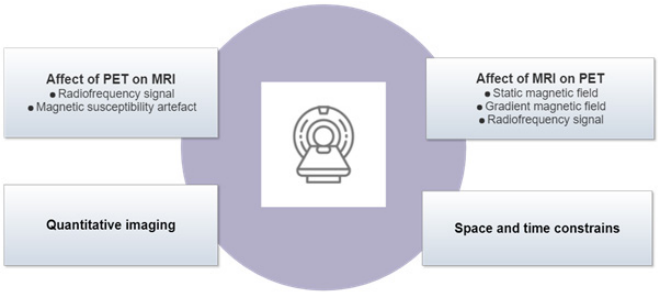

Fig. 6. *Technical challenges of combining PET/MRI.*

The PET detectors are located in the magnetic bore, affecting the magnetic quality due to rationales like interference of a radiofrequency signal (RF) and magnetic susceptibility artifact. The linear measure of the gradient field is influenced by the arrangement of PET components in the magnetic bore as it affects the magnitude and direction of magnetic flux that is supposed to be identical in the field. These minute changes can impact the susceptibility of the magnetic area. This variation can be rectified by shimming that presents homogeneity in the field.[21] The simultaneous TOF-PET/MRI contains a metal implant at the adjacent site that could emerge as the susceptibility artifact. Lead, and tungsten is the gamma-shielding substance in PET that produces an eddy current that causes distortion and intermittence. The homogeneity and occurrence of susceptibility artifacts could be maintained by employing non-magnetic materials.[17]

The RF signal is the other ground of technical challenge in PET/MRI systems. The stimulation of the MRI B1, which is applied perpendicular to the main magnetic field, causes the generation of an NMRI signal which is weak in characteristic; thereby, the coil in MRI is to be particularly sensitive, and the room of the procedure should be Faraday shielded. The received MRI image is distorted by the RF signal ranging between 120MHz- 3 T. This frequency is primarily present in digital technology like clock pulse, directing its need to be shielded to obtain a precise MR image. This precaution can prevent the non-linearity in the production of magnetic flux and eddy current.[22]

The effect of MRI on the PET system

The PET function is affected by the presence of a static magnetic field, a gradient magnetic field, and a radiofrequency signal as they interfere with photomultiplier tubes (PMT) and PET detectors. The weak feature of the static magnetic field will alter the functionality of PMT in block detectors as it deflects the flow of electrons from photocathode to dynode to anode chain. This occurs due to the Lorentz force, leading to loss or misinterpretation of diagnostic information. The resolution can be performed by shielding the PMT with steel or mu-metal with the exception of preventing it just from weak fields. The replacement of PMT can be done with Avalanche photodiode, a field insensitive-PMT, and position-sensitive PMTs but with the downside of intolerance to the tesla field in the MRI system. The approach to this obstacle is to expel the PMT from the system or to replace it with light detectors compatible with magnetic fields.[23]

To achieve larger skin depth at less frequency, the gradient magnetic fields are switched around 1kHz rate, but this alteration leads to the induction of eddy current, which increases the temperature and causes vibration of electronics in the PET. Therefore, the electronics with high frequency should be shielded with materials like copper or aluminum. The attribute of copper, such as its non-magnetic and non-ferromagnetic nature, protects by isolation with 99% of electronics present in PET. The gradient pattern reduces the system's sensitivity by 5% to 20%.[24] The solid-state photo detectors and electronics present near the coil should be of robust character. The robustness can be accomplished by redesigning the PET system.[4] Interference by RF is another technical obstacle that can affect the electronics situated in the magnetic bore, leading to a drop in the count of the PET rate and induction of a noise signal in the PET system resulting in heating and eddy current. The conducting shield is used for the PET detectors and electronics present in the magnetic bore that can minimize the interference of RF.[23]

Quantitative imaging of the PET/MRI system

In quantitative imaging, the attenuation is corrected by the linear attenuation coefficient at 511 keV. Attaining attenuation correction maps from emission data and MR image is complex and has brought attention to this arena. Many methods have been developed to combat this challenge, yet they have failed.[25]

Space and time constraint

The PET scanners are MRI-compatible and designed within the magnet's bore to obtain concurrent images. Acquisition

time is the paramount aspect for considering the system; notably, a CT system takes a shorter time of about 15s - 1min, while it might consume 20-40 min for different MR diagnostic images. The evolved PET technology containing a 3D scanner reduces the acquisition time to 3-15 min for brain imaging and 10-20 min for scanning the whole body.[4] Concerning the TOF, availability of 3D imaging, and longer axial field of view, the advanced technology of PET is more sensitive and accurate. The acquisition time varies with simultaneous and sequential models, which require longer imaging time, and in the latter system, the time depends on a slow acquisition system. In the sequential acquisition system, space should be contemplated as the design is compact, where the standalone systems have to be placed within a minimum area.[20]

Pre-clinical implementation of PET/MRI fusion technique

The amalgamation of PET/MRI modality is the desirable approach for pre-clinical examination as it provides soft tissue contrast with less vulnerability to radiation dose. CT is not the preferred approach to acquire anatomical details of laboratory animals except for lung and bone. The fusion offers a dose advantage over the CT technique, which requires a high radiation dose. In vascular-contrast imaging, the iodine is administered in substantial quantities to have better imaging quality regarding visual appearance and to differentiate soft tissues. These reasons provide PET/MRI as a first-hand approach for animal investigations.[21] The 7T PET/MRI animal scanner has exhibited promising results in the oncology field, which was also confirmed with a histopathological study. A PET/MRI scanner was used to scan a mouse with a CT26 colon tumor. Necrotic lesions were clearly distinguished with MRI curves obtained with a time-to-signal graph. This attainment would not have been achieved with exclusively PET, demonstrating the significance of the PET/MRI combination. MR contrasting agents and PET tracing agents, like [18F] fluoro-L-thymidine and [11C] methylmethionine, in adjunct diagnose tumor proliferation in the brain and spinal cord in the animal study.[26]

Clinical implementation of PET/MRI fusion technique

The promising growth of the fusion technique highlighted the need in the market to resolve its challenges for clinical implication. The integration of the PET/MRI system should be technically modified without altering the functionality of each modality. Apart from the primary use of anatomical and functional imaging, it offers various services in many fields, such as cancer, pediatrics, and central nervous and cardiovascular systems (Figure 7).[3]

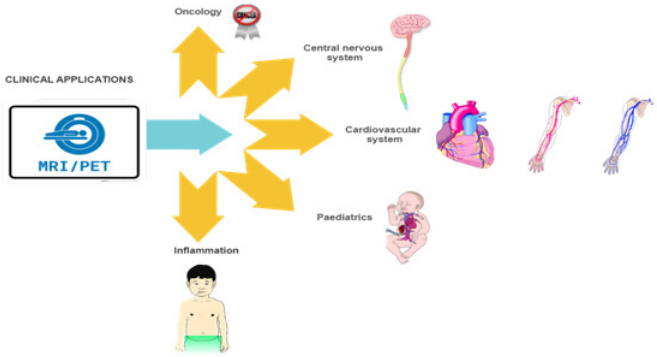

Fig. 7. *Clinical applications of dual-modality PET/MRI.*

Oncology

The PET/MRI technique offers the examination of tumors to a larger extent as it can differentiate soft tissue, which has availed the assessment of head, neck, rectal, prostate, and gynecological cancer in depth. Evaluation of reoccurrence after surgery and radiation is complex as radiation can cause fibrosis, scarring, and tissue distortion, which can be assessed with the PET/MRI process.[27] Along with soft tissue discrimination, MRI assists in T-staging cancer. Combining MRI with PET provides a way to determine cancer staging efficiently. Radiation dose is the chief concern, particularly in the pediatric population suffering from cancer, prompting an investigation to decrease the dose and ensure safety. An investigation on 15 children with multifocal malignant diseases showed that the effective dose of a PET/MR scan was only about 20% that of the equivalent PET/CT examination.[28] A comparative study between PET/CT and PET/MRI was conducted on 32 subjects suffering from different types of cancer by administering an 18F-fluorodeoxyglucose (FDG) single injection to determine which one has the better image outcome and time constraint. The study showed that simultaneous PET/MRI has better image quality, lower radiation dose, and less scanning time than PET/CT.[29] A similar finding on 80 subjects indicates the superiority and feasibility of PET/MRI in image quality.[30] This modality gives superior results in the head and neck region as they require high soft tissue contrast. The metabolic information provided by FDG-PET complements the MR scanning of head and neck tumors, indicating its benefit in this region.[31] Another study was conducted on 20 patients to determine the primary tumor and metastasizing of lymph nodes; the study revealed the supremacy of PET/MRI over MRI and PET in a standalone mode, which was also positively correlated with the histopathological examination.[32] Other investigations reported different results, indicating the statistically equivalent performance of both modalities, PET/MRI and PET/CT, in assessing head and neck tumors.[33] A contrary outcome was that no significant observation was determined regarding the functionality of both modalities, indicating further study in a large group of patients.[34]

The characteristic of lymphoma subtypes is exacerbated glucose metabolism, which can be primarily diagnosed at different stages and given follow-up treatment by PET 18F-FDG. An advancement in technology led to providing the effect of 18F-FDG-PET-MRI on image quality, where the reports indicated satisfactory image quality in addition to evaluating patients' response to lymphoma therapy.[32] The benefit of diagnosing with PET/MRI modality is also noted in benign prostatic hyperplasia, in which choline uptake is elevated and distinguished from tumor lesions.[35] This modality also provides a strong role in detecting prostate cancer and its staging. However, the suggestions demonstrate high complementary outcomes with 18F-choline-PET and diffusion-weighted MRI, but PET reported the presence of tumor lesions, and no such observation was shown with MRI diffusion-weighted imaging.[36] In addition, this fusion modality is efficient for assessing bone metastases, as revealed by a study conducted on 119 patients that found PET/MRI to be superior.[37]

Central nervous system

PET/MRI has neurological applications, which has widened the horizon to assess and implement it in the

diagnostic and clinical role. PET and MRI can be used to evaluate blood flow and oxygenation; their amalgamation is used to simultaneously measure functional activity. PET/MRI diagnostic power can provide an array of research and develop new targets for neurological diseases. Alzheimer's disease is one of the progressive neurological diseases affecting memory and cognitive development, which interferes with normal daily activities. The incidence rate is widely increasing in the world. The disease occurs due to an abnormal accumulation of proteins in the brain. The amyloid protein is accumulated around the brain, and the tau protein is aggregated within the brain, causing this form of dementia.[38] PET modality is used for qualitative and quantitative measurement of changes in the brain due to Alzheimer's disease. It evaluates alterations in the glucose metabolism in the brain and determines the disease's progression and therapeutic efficacy.[39] Structural MRI can assess the disease-affected morphological changes in the brain, and volumetric measurement has strengthened its potential as it can evaluate disease at the early stage. The findings observed are atrophy in the medial temporal lobe in mild cognitive impairment and Alzheimer's patients. The simultaneous development of PET/MRI has generated the area of comparison of alteration in morphology and metabolism, which has led to a better understanding of disease and therapy implications. An exploratory investigation conducted on Alzheimer's patients in 2010 demonstrated a decrease in hippocampus glucose metabolism, compared to the control group. The progress from the initial stage to the disease outcome is accurately determined by combining PET, MRI, and cerebrospinal fluid biomarkers. The development of advanced MRI techniques such as diffusion tensor imaging and arterial spin labeling can provide detailed information in addition to anatomical detail provided by MRI and metabolic details by PET, accentuating the significance of this dual modality.[40]

Neuro-oncology studies neoplasms in the brain and spinal cord, where the investigation and approach are complex. MRI is the optimal choice for imaging neoplasms in the cranial region. This technique provides anatomical information; added gadolinium enhances MRI, which can evaluate the blood flow and integrity of the blood-cerebrospinal fluid barrier.[41] It has significant limitations, such as the use of gadolinium contrast can disrupt the barrier and does not provide information on tumor activity in detail; classifying gliomas along with their proliferation is not well explored. Furthermore, the response of therapy is not determined with MRI.

The PET modality gives molecular details, such as the conversion of radio-labeled amino acids in the neoplasm and matrix metalloproteinase secretion. In combination the techniques complement each other and can help provide a detailed assessment, as demonstrated by different studies.[2,42] The efficacy of tumor assessment was found to be augmented more in PET/MRI than in PET/CT in a research study using C-methionine, Ga-DOTATOC with PET/MRI on 10 patients experiencing intracranial masses.[2] A study conducted on 28 patients suffering from gliomas illustrated the grading of tumors by fusion of simultaneous C-methionine PET and MR spectroscopy. It revealed that the partial correlation shows the differences in distribution, which can be employed for the surgical processes.[42] The merging of these techniques could provide more depth, such as sites for biopsy, the proliferation of cells, and separating the tumor cell to prevent inflammation and necrosis. In addition, combining PET and MRI with enhancers like gadolinium and tracer uptake somatostatin helps to plan the surgery and to monitor and determine the reoccurrence.[43]

Cardiovascular system

PET modality is considered the gold standard to evaluate the viability of the myocardium non-invasively. The MRI modality gives anatomical details that provide insight into a ventricular structure and function and diagnose myocardial infarction. Amalgamation can illustrate the cellular and molecular mechanisms behind infarction. The infarcted myocardium is described by MRI, followed by gadolinium, and the viability is examined by PET. Thus, the scars in the myocardium can be detected by the fusion of the mentioned techniques. The simultaneous acquisition of information by PET/MRI can be used to assess cardiovascular diseases. As the combination can bring forth anatomical and functional information, the probability of differentiation between epicardial stenosis and microvascular dysfunction increases.[43] PET/MRI has applications for detecting myocarditis and sarcoidosis. Several case studies have indicated the potential of fusion in cardiac sarcoidosis diagnosis, where early detection can manage fatal complications.[44,45] The apparent implication of PET/MRI in cardiac tumors is noted as its potential in the oncology field is fully investigated. Also, the identification of atherosclerotic plaque imaging can be identified using PET/MRI dual modality as its potential is observed in PET/CT.[46] Therefore, the fusion of PET/MRI has a strong application in cardiovascular imaging.

Pediatrics

Radiation dose is of significant concern in the pediatric population. The imaging techniques like PET/MRI fusion possess an excellent possibility for imaging pediatric patients with low radiation doses. The integration of MRI free from ionizing radiation and 15O or 11C nuclides having short half-lives provide doses in an acceptable pattern that has paved the way for fetus imaging in vivo. A study on 15 pediatric patients suffering from malignant diseases at multifocal sites demonstrated that the effective dose of a PET/MR scan was only about 20% that of the equivalent PET/CT examination; however, the PET/MRI takes longer, but its reliability and stability have been determined[28] (Figure 7).

Conclusion

The dual-modality method has evolved at a steady rate in the past 20 years to complement the anatomical and biological findings. The fusion of PET and MRI has offered a multitude of functions by providing anatomical, metabolic, and molecular information. This modality has been preferred over PET/CT or PET alone. The predominant suppressing factor is the lower soft tissue contrast presented by PET/CT. Another demerit is the inefficiency of developing a simultaneous acquisition model. PET/MRI has the upper hand

in providing soft tissue contrast, low exposure to radiation, and dynamism in acquisition models, which helps characterize tissues.. This substantiating approach has gained attention in clinical and pre-clinical research with widespread potential in cancer, the central nervous system, the cardiovascular system, pediatrics, and inflammatory diseases. Besides its magnificent applications, there are technical challenges, such as space and time constraint, quantitative imaging, the effect of PET use on MRI, and the impact of MRI use on PET. These shortcomings should be studied and improved by brainstorming notions for a better frame system. Furthermore, intensive research is required to tackle the obstacles and explore other potentials in clinical and pre-clinical departments to drive the impact of PET/MRI.

Competing Interests

The Author declares that there is no conflict of interest.

References

1. Martí-Bonmatí L, Sopena R, Bartumeus P, Sopena P. Multimodality imaging techniques. Contrast Media Mol Imaging. 2010 Jul-Aug;5(4):180-9. doi: 10.1002/cmmi.393.
2. Boss A, Bisdas S, Kolb A, Hofmann M, Ernemann U, Claussen CD, Pfannenberg C, Pichler BJ, Reimold M, Stegger L. Hybrid PET/MRI of intracranial masses: initial experiences and comparison to PET/CT. J Nucl Med. 2010 Aug;51(8):1198-205. doi: 10.2967/jnumed.110.074773.
3. Catana C, Guimaraes AR, Rosen BR. PET and MR imaging: the odd couple or a match made in heaven? J Nucl Med. 2013 May;54(5):815-24. doi: 10.2967/jnumed.112.112771.
4. Musafargani S, Ghosh KK, Mishra S, Mahalakshmi P, Padmanabhan P, Gulyás B. PET/MRI: a frontier in era of complementary hybrid imaging. Eur J Hybrid Imaging. 2018;2(1):12. doi: 10.1186/s41824-018-0030-6.
5. Shao Y, Cherry SR, Farahani K, Meadors K, Siegel S, Silverman RW, Marsden PK. Simultaneous PET and MR imaging. Phys Med Biol. 1997 Oct;42(10):1965-70. doi: 10.1088/0031-9155/42/10/010.
6. Pichler BJ, Kolb A, Nägele T, Schlemmer HP. PET/MRI: paving the way for the next generation of clinical multimodality imaging applications. J Nucl Med. 2010 Mar;51(3):333-6. doi: 10.2967/jnumed.109.061853.
7. Berger A. How does it work? Positron emission tomography. BMJ. 2003 Jun 28;326(7404):1449. doi: 10.1136/bmj.326.7404.1449.
8. Katal S, Eibschutz LS, Saboury B, Gholamrezanezhad A, Alavi A. Advantages and Applications of Total-Body PET Scanning. Diagnostics (Basel). 2022 Feb 7;12(2):426. doi: 10.3390/diagnostics12020426.
9. Katti G, Ara S, Shireen A. Magnetic Resonance Imaging (MRI) – A Review. *International Journal of Dental Clinics. 2011;3*.
10. Symms M, Jäger HR, Schmierer K, Yousry TA. A review of structural magnetic resonance neuroimaging. J Neurol Neurosurg Psychiatry. 2004 Sep;75(9):1235-44. doi: 10.1136/jnnp.2003.032714.
11. Olman CA, Harel N, Feinberg DA, He S, Zhang P, Ugurbil K, Yacoub E. Layer-specific fMRI reflects different neuronal computations at different depths in human V1. PLoS One. 2012;7(3):e32536. doi: 10.1371/journal.pone.0032536.
12. Fink JR, Muzi M, Peck M, Krohn KA. Multimodality Brain Tumor Imaging: MR Imaging, PET, and PET/MR Imaging. J Nucl Med. 2015 Oct;56(10):1554-61. doi: 10.2967/jnumed.113.131516.
13. Paspulati RM, Partovi S, Herrmann KA, Krishnamurthi S, Delaney CP, Nguyen NC. Comparison of hybrid FDG PET/MRI compared with PET/CT in colorectal cancer staging and restaging: a pilot study. Abdom Imaging. 2015 Aug;40(6):1415-25. doi: 10.1007/s00261-015-0474-0.
14. Jadvar H, Connolly LP, Fahey FH, Shulkin BL. PET and PET/CT in pediatric oncology. Semin Nucl Med. 2007 Sep;37(5):316-31. doi: 10.1053/j.semnuclmed.2007.04.001.
15. Catana C. Principles of Simultaneous PET/MR Imaging. Magn Reson Imaging Clin N Am. 2017 May;25(2):231-243. doi: 10.1016/j.mric.2017.01.002.
16. Schlemmer HP, Pichler BJ, Schmand M, Burbar Z, Michel C, Ladebeck R, Jattke K, Townsend D, Nahmias C, Jacob PK, Heiss WD, Claussen CD. Simultaneous MR/PET imaging of the human brain: feasibility study. Radiology. 2008 Sep;248(3):1028-35. doi: 10.1148/radiol.2483071927.
17. Zaidi H, Ojha N, Morich M, Griesmer J, Hu Z, Maniawski P, Ratib O, Izquierdo-Garcia D, Fayad ZA, Shao L. Design and performance evaluation of a whole-body Ingenuity TF PET-MRI system. Phys Med Biol. 2011 May 21;56(10):3091-106. doi: 10.1088/0031-9155/56/10/013.
18. Levin CS, Maramraju SH, Khalighi MM, Deller TW, Delso G, Jansen F. Design Features and Mutual Compatibility Studies of the Time-of-Flight PET Capable GE SIGNA PET/MR System. IEEE Trans Med Imaging. 2016 Aug;35(8):1907-14. doi: 10.1109/TMI.2016.2537811.
19. Delso G, Fürst S, Jakoby B, Ladebeck R, Ganter C, Nekolla SG, Schwaiger M, Ziegler SI. Performance measurements of the Siemens mMR integrated whole-body PET/MR scanner. J Nucl Med. 2011 Dec;52(12):1914-22. doi: 10.2967/jnumed.111.092726. Epub 2011 Nov 11. Erratum in: J Nucl Med. 2012 Mar;53(3):507.
20. Zaidi H, Del Guerra A. An outlook on future design of hybrid PET/MRI systems. Med Phys. 2011 Oct;38(10):5667-89. doi: 10.1118/1.3633909.
21. Pichler BJ, Wehrl HF, Kolb A, Judenhofer MS. Positron emission tomography/magnetic resonance imaging: the next generation of multimodality imaging? Semin Nucl Med. 2008 May;38(3):199-208. doi: 10.1053/j.semnuclmed.2008.02.001.
22. Yamamoto S, Takamatsu S, Murayama H, Minato K. A block detector for a multislice, depth-of-interaction MR-compatible PET. *IEEE Transactions on Nuclear Science. 2005;*52(1):33-37. doi: 10.1109/TNS.2004.843091.
23. Vandenberghe S, Marsden PK. PET-MRI: a review of challenges and solutions in the development of integrated multimodality imaging. Phys Med Biol. 2015 Feb 21;60(4):R115-54. doi: 10.1088/0031-9155/60/4/R115.
24. Pichler BJ, Judenhofer MS, Catana C, Walton JH, Kneilling M, Nutt RE, Siegel SB, Claussen CD, Cherry SR. Performance test of an LSO-APD detector in a 7-T MRI scanner for simultaneous PET/MRI. J Nucl Med. 2006 Apr;47(4):639-47.
25. Turkington TG. Attenuation correction in hybrid positron emission tomography. Semin Nucl Med. 2000 Oct;30(4):255-67. doi: 10.1053/snuc.2000.9542.

26. Jacobs AH, Thomas A, Kracht LW, Li H, Dittmar C, Garlip G, Galldiks N, Klein JC, Sobesky J, Hilker R, Vollmar S, Herholz K, Wienhard K, Heiss WD. 18F-fluoro-L-thymidine and 11C-methylmethionine as markers of increased transport and proliferation in brain tumors. J Nucl Med. 2005 Dec;46(12):1948-58.
27. Yoon DY, Hwang HS, Chang SK, Rho YS, Ahn HY, Kim JH, Lee IJ. CT, MR, US,18F-FDG PET/CT, and their combined use for the assessment of cervical lymph node metastases in squamous cell carcinoma of the head and neck. Eur Radiol. 2009 Mar;19(3):634-42. doi: 10.1007/s00330-008-1192-6.
28. Hirsch FW, Sattler B, Sorge I, Kurch L, Viehweger A, Ritter L, Werner P, Jochimsen T, Barthel H, Bierbach U, Till H, Sabri O, Kluge R. PET/MR in children. Initial clinical experience in paediatric oncology using an integrated PET/MR scanner. Pediatr Radiol. 2013 Jul;43(7):860-75. doi: 10.1007/s00247-012-2570-4.
29. Drzezga A, Souvatzoglou M, Eiber M, Beer AJ, Fürst S, Martinez-Möller A, Nekolla SG, Ziegler S, Ganter C, Rummeny EJ, Schwaiger M. First clinical experience with integrated whole-body PET/MR: comparison to PET/CT in patients with oncologic diagnoses. J Nucl Med. 2012 Jun;53(6):845-55. doi: 10.2967/jnumed.111.098608.
30. Quick HH, von Gall C, Zeilinger M, Wiesmüller M, Braun H, Ziegler S, Kuwert T, Uder M, Dörfler A, Kalender WA, Lell M. Integrated whole-body PET/MR hybrid imaging: clinical experience. Invest Radiol. 2013 May;48(5):280-9. doi: 10.1097/RLI.0b013e3182845a08.
31. Mak D, Corry J, Lau E, Rischin D, Hicks RJ. Role of FDG-PET/CT in staging and follow-up of head and neck squamous cell carcinoma. Q J Nucl Med Mol Imaging. 2011 Oct;55(5):487-99.
32. Platzek I, Beuthien-Baumann B, Schneider M, Gudziol V, Langner J, Schramm G, Laniado M, Kotzerke J, van den Hoff J. PET/MRI in head and neck cancer: initial experience. Eur J Nucl Med Mol Imaging. 2013 Jan;40(1):6-11. doi: 10.1007/s00259-012-2248-z.
33. Varoquaux A, Rager O, Poncet A, Delattre BM, Ratib O, Becker CD, Dulguerov P, Dulguerov N, Zaidi H, Becker M. Detection and quantification of focal uptake in head and neck tumours: (18)F-FDG PET/MR versus PET/CT. Eur J Nucl Med Mol Imaging. 2014 Mar;41(3):462-75. doi: 10.1007/s00259-013-2580-y.
34. Kubiessa K, Purz S, Gawlitza M, Kühn A, Fuchs J, Steinhoff KG, Boehm A, Sabri O, Kluge R, Kahn T, Stumpp P. Initial clinical results of simultaneous 18F-FDG PET/MRI in comparison to 18F-FDG PET/CT in patients with head and neck cancer. Eur J Nucl Med Mol Imaging. 2014 Apr;41(4):639-48. doi: 10.1007/s00259-013-2633-2.
35. Wetter A, Lipponer C, Nensa F, Beiderwellen K, Olbricht T, Rübben H, Bockisch A, Schlosser T, Heusner TA, Lauenstein TC. Simultaneous 18F choline positron emission tomography/magnetic resonance imaging of the prostate: initial results. Invest Radiol. 2013 May;48(5):256-62. doi: 10.1097/RLI.0b013e318282c654.
36. Quentin M, Schimmöller L, Arsov C, Rabenalt R, Antoch G, Albers P, Blondin D. Increased signal intensity of prostate lesions on high b-value diffusion-weighted images as a predictive sign of malignancy. Eur Radiol. 2014 Jan;24(1):209-13. doi: 10.1007/s00330-013-2999-3.
37. Eiber M, Takei T, Souvatzoglou M, Mayerhoefer ME, Fürst S, Gaertner FC, Loeffelbein DJ, Rummeny EJ, Ziegler SI, Schwaiger M, Beer AJ. Performance of whole-body integrated 18F-FDG PET/MR in comparison to PET/CT for evaluation of malignant bone lesions. J Nucl Med. 2014 Feb;55(2):191-7. doi: 10.2967/jnumed.113.123646.
38. Jack CR Jr. Alzheimer disease: new concepts on its neurobiology and the clinical role imaging will play. Radiology. 2012 May;263(2):344-61. doi: 10.1148/radiol.12110433.
39. Protas HD, Chen K, Langbaum JB, Fleisher AS, Alexander GE, Lee W, Bandy D, de Leon MJ, Mosconi L, Buckley S, Truran-Sacrey D, Schuff N, Weiner MW, Caselli RJ, Reiman EM. Posterior cingulate glucose metabolism, hippocampal glucose metabolism, and hippocampal volume in cognitively normal, late-middle-aged persons at 3 levels of genetic risk for Alzheimer disease. JAMA Neurol. 2013 Mar 1;70(3):320-5. doi: 10.1001/2013.jamaneurol.286.
40. Shaffer JL, Petrella JR, Sheldon FC, Choudhury KR, Calhoun VD, Coleman RE, Doraiswamy PM; Alzheimer's Disease Neuroimaging Initiative. Predicting cognitive decline in subjects at risk for Alzheimer disease by using combined cerebrospinal fluid, MR imaging, and PET biomarkers. Radiology. 2013 Feb;266(2):583-91. doi: 10.1148/radiol.12120010.
41. Song CI, Pogson JM, Andresen NS, Ward BK. MRI With Gadolinium as a Measure of Blood-Labyrinth Barrier Integrity in Patients With Inner Ear Symptoms: A Scoping Review. Front Neurol. 2021 May 20;12:662264. doi: 10.3389/fneur.2021.662264.
42. Bisdas S, Koh TS, Roder C, Braun C, Schittenhelm J, Ernemann U, Klose U. Intravoxel incoherent motion diffusion-weighted MR imaging of gliomas: feasibility of the method and initial results. Neuroradiology. 2013 Oct;55(10):1189-96. doi: 10.1007/s00234-013-1229-7.
43. Fraioli F, Punwani S. Clinical and research applications of simultaneous positron emission tomography and MRI. Br J Radiol. 2014 Jan;87(1033):20130464. doi: 10.1259/bjr.20130464.
44. White JA, Rajchl M, Butler J, Thompson RT, Prato FS, Wisenberg G. Active cardiac sarcoidosis: first clinical experience of simultaneous positron emission tomography--magnetic resonance imaging for the diagnosis of cardiac disease. Circulation. 2013 Jun 4;127(22):e639-41. doi: 10.1161/CIRCULATIONAHA.112.001217.
45. Schneider S, Batrice A, Rischpler C, Eiber M, Ibrahim T, Nekolla SG. Utility of multimodal cardiac imaging with PET/MRI in cardiac sarcoidosis: implications for diagnosis, monitoring and treatment. Eur Heart J. 2014 Feb;35(5):312. doi: 10.1093/eurheartj/eht335.
46. Ripa RS, Knudsen A, Hag AM, Lebech AM, Loft A, Keller SH, Hansen AE, von Benzon E, Højgaard L, Kjær A. Feasibility of simultaneous PET/MR of the carotid artery: first clinical experience and comparison to PET/CT. Am J Nucl Med Mol Imaging. 2013 Jul 10;3(4):361-71.

International Journal of Biomedicine 13(3) (2023) 54-58
http://dx.doi.org/10.21103/Article13(3)_RA5

REVIEW ARTICLE

INTERNATIONAL JOURNAL OF BIOMEDICINE

Acne Scar Management: Minoxidil as a Promising Approach or a Mirage?

Ramadan S. Hussein*, Salman Bin Dayel

Dermatology Unit, Department of Internal Medicine, College of Medicine, Prince Sattam Bin Abdulaziz University, Al-Kharj, Saudi Arabia

Abstract

Atrophic and hypertrophic scars can result from various conditions, such as acne, trauma, and surgery. Minoxidil, a medication used for the treatment of severe hypertension and hair loss, has been explored as a potential treatment for scars. This review aims to evaluate the current evidence regarding the role of minoxidil in the treatment of scars. Previously published reviews have primarily focused on the use of minoxidil in hair loss and have only briefly mentioned its potential use for scars. However, minoxidil may have a beneficial effect as an antifibrotic agent. Several studies have reported reduced collagen accumulation and fibrosis after treatment with minoxidil. The proposed mechanism of action is inhibition of the production of lysyl hydroxylases (LHs), which modify and cross-link proteins by converting lysine to hydroxylysine, making collagen more resistant to degradation. Minoxidil, as an LH inhibitor, has been shown to potentially benefit wound healing and regeneration in vitro by inhibiting the proliferation and migration of fibroblasts. To date, direct studies of the efficacy of minoxidil in treating acne scars have not been conducted; however, its inhibitory effects on fibroblast function and antifibrotic outcomes in some in vivo studies suggest that such use may be considered.(**International Journal of Biomedicine. 2023;13(3):54-58.**)

Keywords: acne • scar • treatment • minoxidil

For citation: Hussein RS, Dayel SB. Acne Scar Management: Minoxidil as a Promising Approach or a Mirage? International Journal of Biomedicine. 2023;13(3):54-58. doi:10.21103/Article13(3)_RA5

Introduction

Scars are a common skin condition resulting from various causes, such as acne, trauma, or surgery. Scars can be classified into two main categories based on the net change in collagen content: (1) Atrophic scars, characterized by collagen loss, are the most common type in the context of acne scars, affecting around 80% to 90% of individuals. Atrophic scars cause depressions or indentations on the skin surface, which can be both aesthetically and psychologically distressing. On the other hand, a smaller percentage of individuals develop hypertrophic scars and keloids, which involve an overgrowth of collagen. (2) Hypertrophic scars appear as raised, firm, pink formations with dense collagen bundles within the boundaries of the original injury site.[1]

Several treatment options have been explored to manage scars, including laser therapy, chemical peels, and dermal fillers. However, these treatments can be expensive and not suitable for all patients.[2] Minoxidil is a medication that is commonly used in dermatology to treat hair loss. It works by dilating blood vessels in the scalp, leading to enhanced circulation to the hair follicles and promoting hair growth.[3] However, it has also been suggested that minoxidil may have a potential role in treating scars. Previous reviews have mainly focused on the use of minoxidil for hair loss and have only briefly mentioned its potential antifibrotic role.[4,5]

This review aims to assess the existing evidence concerning the utilization of minoxidil in scar treatment. The review employs a narrative synthesis methodology and extensively searches various databases to identify pertinent studies. The inclusion criteria encompass in vitro experimental studies, randomized and non-randomized controlled trials, and observational studies that report the application of minoxidil in the treatment of fibrosis and scars.

The need for a treatment option that is both effective and safe for acne scars is significant, as it can significantly impact the quality of life of affected individuals. Scars can lead to significant psychological distress, affecting self-esteem and confidence.[6] Furthermore, managing acne scars can be challenging, with many expensive and invasive treatment

options. The potential use of minoxidil in treating scars is a promising avenue that warrants further investigation.

Scar pathogenesis

The wound-healing process involves various cells, chemical mediators, and extracellular matrix components. It advances through three distinct stages: inflammation, the formation of granulation tissue, and the remodeling of the matrix.[7]

During inflammation, the injury site undergoes vasoconstriction for hemostasis, followed by vasodilation and erythema. This stage activates various cells, such as macrophages, granulocytes, and lymphocytes. These cells release inflammatory mediators that prepare the wound site for the subsequent formation of granulation tissue,[8] which involves the repair of damaged tissues and the formation of new capillaries. Fibroblasts are stimulated to produce collagen, initially dominated by type III collagen and later shifted to type I collagen.[9]

During matrix remodeling, fibroblasts and keratinocytes play a crucial role in producing enzymes that shape the structure of the extracellular matrix. The balance between matrix metalloproteinases (MMPs) and tissue inhibitors of MMPs is essential. An imbalance in this ratio can lead to the formation of either atrophic or hypertrophic scars.(10) Atrophic scars occur when insufficient collagen factor deposition results in depressed areas. On the other hand, hypertrophic scars form when the healing response is overly robust, leading to the development of raised nodules comprised of fibrotic tissue (Table 1).

Table 1.

The steps involved in the pathogenesis of scars.

Step	Description
1.	Injury or damage to the skin.
2.	Inflammation as part of the normal wound-healing process.
3.	Migration of fibroblasts and other cells to the injury site, collagen production to form new tissue.
4.	Remodeling Atrophic scars: Decreased number of fibroblasts and collagen production, leading to tissue thinning. Hypertrophic scars: Overexpressed healing reaction, leading to the development of raised nodules comprised of fibrotic tissue

Acne scar types

Atrophic scars

Atrophic scars are a type of skin scarring that occurs as a result of loss of tissue during the wound healing process. Several types of atrophic scars include icepick, rolling, and boxcar scars. Individual scars can have characteristics of multiple types, and treatment options may need to be tailored to address the specific features of each scar.[11] Types of atrophic acne scars are presented in Table 2.[12]

Occasionally, patients may exhibit all three types of atrophic scars, making it difficult to distinguish between them. As a result, several authors have put forth various classifications and scales. One commonly utilized qualitative grading system is the one introduced by Goodman and Baron. This classification system defines four distinct grades that can be employed to characterize an acne scar (Table 3).[13]

Hypertrophic scars

Hypertrophic and keloidal scars are associated with excessive collagen accumulation and reduced collagenase activity. Hypertrophic scars are typically present as elevated, firm, pink formations with dense collagen bundles confined within the boundaries of the initial injury site. The histological characteristics of hypertrophic scars resemble those of other dermal scars. In contrast, keloids manifest as reddish-purple papules and nodules that extend beyond the original wound borders. Histologically, keloids display thick bundles of acellular collagen arranged in the whorls. These scars are more prevalent in individuals with darker skin tones and primarily occur on the trunk.[14]

Table 2.

Atrophic depressed acne scars according to Jacob et al.[12]

Acne Scars Subtype	Clinical Features and Treatment Options
Ice-pick	Narrow (<2 mm), deep, well-defined epithelial tracts that extend vertically into the deep dermis or subcutaneous tissue. Difficult to treat due to their depth and narrowness, but options such as chemical peels and laser resurfacing may be effective in reducing their appearance.
Rolling	Dermal tethering of skin that appears relatively normal, with a width typically exceeding 4 to 5 mm. Often caused by long-term inflammatory conditions such as acne and may respond to treatment options such as subcision, microneedling, or dermal fillers.
Boxcar	Depressions with round or oval shapes and distinct vertical edges, resembling scars from chickenpox (varicella). They can be shallow (diameter <3 mm) or deep (diameter >3 mm). Boxcar scars are often caused by severe acne and may respond to treatment options such as chemical peels, laser resurfacing, and dermal fillers.

Table 3.

Acne Scar Grading System (Goodman and Baron).[13]

Grade	Clinical Features
I	Macular or erythematous scars
II	Mild atrophic scars with decreased skin texture
III	Moderate atrophic scars with a visible depression
IV	Severe atrophic scars with deep depressions and sharp edges

Treatment of acne scars

Treatment Options for Atrophic Scars

Treatment options for atrophic scars have advanced in recent years, and several new and effective treatments have emerged. Here are some of the latest updates in the treatment of atrophic scars:

Microneedling is a technique that utilizes a device equipped with small needles to create tiny punctures in the skin. This process stimulates the production of collagen

and elastin, improving the appearance of atrophic scars. A systematic review and meta-analysis of 16 randomized controlled trials conducted in 2021 demonstrated the efficacy of microneedling as a treatment for atrophic acne scars, with minimal adverse effects reported.[15]

Platelet-rich plasma (PRP) therapy involves injecting the patient's own PRP into the affected area. Platelets contain growth factors that aid in tissue repair and regeneration. A review article from 2020, encompassing 13 studies, indicated that PRP therapy shows promise as a treatment for atrophic acne scars. However, further research is required to establish the optimal treatment protocol.[16]

Fractional laser resurfacing employs laser technology to create skin micro-wounds, stimulating collagen and elastin production. A systematic review and meta-analysis of 33 randomized controlled trials conducted in 2018 concluded that fractional laser resurfacing is an effective treatment for atrophic acne scars with a low risk of adverse effects.[17]

Chemical peels involve the application of a chemical solution to the skin, resulting in the exfoliation of the top layer and promoting the growth of new skin cells. A systematic review and meta-analysis of 24 randomized controlled trials conducted in 2019 established the effectiveness of chemical peels in treating atrophic acne scars. However, the optimal type and concentration of the chemical solution varied depending on the specific type of scar.[18]

Treatment Options for Hypertrophic Scars

Silicone gel is a transparent, quick-drying solution commonly used to prevent and treat hypertrophic acne scars. Its mechanism of action is not fully understood, but it is believed to increase hydration, protect the scar, and potentially affect the immune system. Clinical studies have shown a decreased scar thickness from 40% to 50%. Treatment duration varies depending on whether it is for existing scars or prevention.[19]

Intralesional steroid therapy involves injecting steroids directly into the scar tissue to reduce scar volume, thickness, and texture, as well as relieve itching and discomfort. The exact mechanisms are not fully understood, but they include anti-inflammatory properties and inhibition of collagen production. Steroid injections are usually preceded by anesthetic creams, and cryotherapy may be used to enhance drug dispersion. Adverse reactions may occur, such as hypopigmentation, skin atrophy, and infections.[20]

Cryotherapy using liquid nitrogen has the potential to greatly enhance the appearance of hypertrophic scars and keloids, possibly leading to their complete regression. By subjecting the affected area to low temperatures, cryotherapy slows down blood flow and induces thrombus formation, resulting in tissue necrosis. Cryotherapy can be combined with steroid injections to enhance effectiveness. Adverse reactions may include changes in pigmentation, skin atrophy, and pain.[21]

Pulsed dye laser (PDL) has shown promising outcomes in treating hypertrophic and keloidal scars. It reduces fibroblast proliferation, loosens collagen fibers, and decreases collagen type III deposition. PDL flattens and reduces scar volume, improves texture, and alleviates itching and pain. Multiple treatments may be necessary, and common side effects include temporary purpura and changes in pigmentation. PDL is more effective for patients with lighter skin types.[22]

Surgery options for hypertrophic scars include W-plasty to disrupt scar patterns and autologous skin grafts to close wounds with minimal tension. In facial defects requiring skin grafts, the retro- and preauricular areas, and the neck, are preferred as donor sites.[23]

Other treatment approaches may be considered, such as intralesional injection of 5-fluorouracil, radiotherapy, imiquimod, interferon, elastic compression, and bleomycin. However, their effectiveness is limited or impractical for various reasons, such as lack of clinical experience, high costs, or inefficacy. These approaches are generally more suitable for hypertrophic scars not caused by acne.[14]

Minoxidil as antifibrotic agent

Minoxidil was first introduced as an oral medication for the treatment of severe and recalcitrant hypertension in the 1970s.[24] Hypertrichosis was discovered as a side effect of chronic use of oral minoxidil in about one-fifth of patients. This observation prompted the development of a topical formulation to stimulate hair growth.[25] Topical minoxidil was FDA-approved specifically for androgenic alopecia (AGA) in 1988 as a first-line treatment for men with mild-to-moderate AGA,[26,27] subsequently for females. Topical minoxidil is used in both 2% and 5% foam and liquid solutions with varying efficacies for AGA in men and women.[28.29] Minoxidil downregulates the expression of the procollagen-lysine and 2-oxoglutarate 5-dioxygenases (PLODs) genes and their encoded catalyze lysyl hydroxylase (LH) proteins.[30] It was reported to reduce lysyl hydroxylase activity by decreasing the LH1 mRNA level.[31,32] Because the LHs modify and cross-link proteins by converting lysine to hydroxylysine, they make collagen more resistant to degradation.[33,34] Thus, limiting the supply of hydroxylysines for hydroxyallysine cross-link formation, minoxidil leads to antifibrotic effects.[32]

Zuurmond et al.[35] demonstrated that minoxidil treatment of cultured fibroblasts reduces LH1>>LH2b>LH3 mRNA levels depending on dose and time but has essentially no effect on the total number of pyridinoline ross-links in the collagen matrix. However, the collagen produced in the presence of minoxidil displayed some remarkable features: the hydroxylation of triple helical lysine residues was reduced to 50%, and lysylpyridinoline cross-linking was increased at the expense of hydroxylysylpyridinoline cross-linking, pointing out that the LH1 mRNA levels were the most sensitive to minoxidil treatment, and LH1 has a preference for triple helical lysine residues as substrate. The authors concluded that minoxidil is unlikely to serve as an antifibrotic agent, but confers characteristic features to the collagen matrix.

Shao et al.[36] found that the effects of minoxidil appear to be mediated at least partly through the TGF-β1/Smad3 and the MMPs/TIMPs pathways, resulting in reduced levels of lysylpyridinoline and hydroxylysylpyridinoline, resulting in a decrease in collagen biosynthesis.

In a study by Priestley et al.,[37] the effects of minoxidil in vitro were researched using fibroblasts grown from the lesional skin of patients with lichen sclerosus and morphea, and from the normal skin of healthy individuals. The proliferation of all fibroblast lines over 3 days was inhibited in

proportion to the concentration of minoxidil, being 20% or less of controls at 1mM. At 5mM, there was usually a net loss of cells. Secretion of glycosaminoglycans by normal fibroblasts showed a concentration-dependent reduction, being 25±6% of that of untreated cultures with 1mM minoxidil. In contrast, minoxidil at 0.1-1mM stimulated the proliferation of foreskin keratinocytes by up to 130%. The range of inhibitory effects of minoxidil on both normal and abnormal skin fibroblasts in vitro and stimulation of skin epithelial cells led the authors to conclude that minoxidil may provide proper topical treatment for keloids and other fibrosis.

Knitlova et al.[38] assessed the in vitro antifibrotic effects of minoxidil on clubfoot-derived cells. Minoxidil concentrations of 0.25 mM, 0.5 mM, and 0.75 mM inhibited cell proliferation in a concentration-dependent manner without causing a cytotoxic effect. Minoxidil in concentrations of ≥0.5 mM decreased collagen type I accumulation after 8 and 21 days in culture, demonstrating the potential antifibrotic effects in vivo.

A study by Freiha et al.[39] evaluated the effects of topical minoxidil 5% cream on full-thickness thermal skin burns in a Wistar rat model. The results showed that minoxidil reduced necrosis and increased wound contraction rates, resulting in positive results after one week of treatment regarding local antioxidant protection, keratinocyte migration, neo-capillarization, chronic inflammation, and fibrosis rate. However, after two weeks, the opposite results were observed.

Polo et al.[40] studied the capability of minoxidil to inhibit various fibroblast functions in vivo using an established animal model of wound contraction. Standardized cutaneous wounds were created on the dorsum of Sprague-Dawley rats. Minoxidil did not demonstrate significant inhibition of wound contraction rates that do not support the proposed use of minoxidil as an antifibrotic agent.

In conclusion, minoxidil has been shown to benefit wound healing and regeneration in vitro by inhibiting the proliferation and migration of fibroblasts. However, its potential as an antifibrotic agent for therapeutic use is still not demonstrated. It requires additional studies involving more study groups and more extended follow-up periods.

Competing Interests

The authors declare that they have no competing interests.

Acknowledgments

This study was supported by Prince Sattam bin Abdulaziz University (Project PSAU/2023/R/1444).

References

1. Tan J, Beissert S, Cook-Bolden F, Chavda R, Harper J, Hebert A, Lain E, Layton A, Rocha M, Weiss J, Dréno B. Impact of Facial Atrophic Acne Scars on Quality of Life: A Multi-country Population-Based Survey. Am J Clin Dermatol. 2022 Jan;23(1):115-123. doi: 10.1007/s40257-021-00628-1.
2. Connolly D, Vu HL, Mariwalla K, Saedi N. Acne Scarring-Pathogenesis, Evaluation, and Treatment Options. J Clin Aesthet Dermatol. 2017 Sep;10(9):12-23.
3. Gupta AK, Charrette A. Topical Minoxidil: Systematic Review and Meta-Analysis of Its Efficacy in Androgenetic Alopecia. Skinmed. 2015 May-Jun;13(3):185-9.
4. Choi N, Shin S, Song SU, Sung JH. Minoxidil Promotes Hair Growth through Stimulation of Growth Factor Release from Adipose-Derived Stem Cells. Int J Mol Sci. 2018 Feb 28;19(3):691. doi: 10.3390/ijms19030691.
5. Sung CT, Juhasz ML, Choi FD, Mesinkovska NA. The Efficacy of Topical Minoxidil for Non-Scarring Alopecia: A Systematic Review. J Drugs Dermatol. 2019 Feb 1;18(2):155-160.
6. Bhargava S, Cunha PR, Lee J, Kroumpouzos G. Acne Scarring Management: Systematic Review and Evaluation of the Evidence. Am J Clin Dermatol. 2018 Aug;19(4):459-477. doi: 10.1007/s40257-018-0358-5.
7. Cowin AJ, Brosnan MP, Holmes TM, Ferguson MW. Endogenous inflammatory response to dermal wound healing in the fetal and adult mouse. Dev Dyn. 1998 Jul;212(3):385-93. doi: 10.1002/(SICI)1097-0177(199807)212:3<385::AID-AJA6>3.0.CO;2-D.
8. Martin P, Leibovich SJ. Inflammatory cells during wound repair: the good, the bad and the ugly. Trends Cell Biol. 2005 Nov;15(11):599-607. doi: 10.1016/j.tcb.2005.09.002.
9. Baum CL, Arpey CJ. Normal cutaneous wound healing: clinical correlation with cellular and molecular events. Dermatol Surg. 2005 Jun;31(6):674-86; discussion 686. doi: 10.1111/j.1524-4725.2005.31612.
10. Midwood KS, Williams LV, Schwarzbauer JE. Tissue repair and the dynamics of the extracellular matrix. Int J Biochem Cell Biol. 2004 Jun;36(6):1031-7. doi: 10.1016/j.biocel.2003.12.003.
11. Gupta A, Kaur M, Patra S, Khunger N, Gupta S. Evidence-based Surgical Management of Post-acne Scarring in Skin of Color. J Cutan Aesthet Surg. 2020 Apr-Jun;13(2):124-141. doi: 10.4103/JCAS.JCAS_154_19.
12. Jacob CI, Dover JS, Kaminer MS. Acne scarring: a classification system and review of treatment options. J Am Acad Dermatol. 2001 Jul;45(1):109-17. doi: 10.1067/mjd.2001.113451.
13. Goodman GJ, Baron JA. Postacne scarring: a qualitative global scarring grading system. Dermatol Surg. 2006 Dec;32(12):1458-66. doi: 10.1111/j.1524-4725.2006.32354.x.
14. Fabbrocini G, Annunziata MC, D'Arco V, De Vita V, Lodi G, Mauriello MC, Pastore F, Monfrecola G. Acne scars: pathogenesis, classification and treatment. Dermatol Res Pract. 2010;2010:893080. doi: 10.1155/2010/893080.
15. Shen YC, Chiu WK, Kang YN, Chen C. Microneedling Monotherapy for Acne Scar: Systematic Review and Meta-Analysis of Randomized Controlled Trials. Aesthetic Plast Surg. 2022 Aug;46(4):1913-1922. doi: 10.1007/s00266-022-02845-3.

***Corresponding author**: Ramadan S. Hussein. Department of Internal Medicine, College of Medicine, Prince Sattam Bin Abdulaziz University, Al-Kharj, Saudi Arabia. E-mail: ramadangazeera@yahoo.com*

16. Long T, Gupta A, Ma S, Hsu S. Platelet-rich plasma in noninvasive procedures for atrophic acne scars: A systematic review and meta-analysis. J Cosmet Dermatol. 2020 Apr;19(4):836-844. doi: 10.1111/jocd.13331.
17. Lin L, Liao G, Chen J, Chen X. A systematic review and meta-analysis on the effects of the ultra-pulse CO2 fractional laser in the treatment of depressed acne scars. Ann Palliat Med. 2022 Feb;11(2):743-755. doi: 10.21037/apm-22-70.
18. Kontochristopoulos G, Platsidaki E. Chemical peels in active acne and acne scars. Clin Dermatol. 2017 Mar-Apr;35(2):179-182. doi: 10.1016/j.clindermatol.2016.10.011.
19. Berman B, Perez OA, Konda S, Kohut BE, Viera MH, Delgado S, Zell D, Li Q. A review of the biologic effects, clinical efficacy, and safety of silicone elastomer sheeting for hypertrophic and keloid scar treatment and management. Dermatol Surg. 2007 Nov;33(11):1291-302; discussion 1302-3. doi: 10.1111/j.1524-4725.2007.33280.x.
20. Atiyeh BS. Nonsurgical management of hypertrophic scars: evidence-based therapies, standard practices, and emerging methods. Aesthetic Plast Surg. 2007 Sep-Oct;31(5):468-92; discussion 493-4. doi: 10.1007/s00266-006-0253-y.
21. Layton AM, Yip J, Cunliffe WJ. A comparison of intralesional triamcinolone and cryosurgery in the treatment of acne keloids. Br J Dermatol. 1994 Apr;130(4):498-501. doi: 10.1111/j.1365-2133.1994.tb03385.x.
22. Keaney TC, Tanzi E, Alster T. Comparison of 532 nm Potassium Titanyl Phosphate Laser and 595 nm Pulsed Dye Laser in the Treatment of Erythematous Surgical Scars: A Randomized, Controlled, Open-Label Study. Dermatol Surg. 2016 Jan;42(1):70-6. doi: 10.1097/DSS.0000000000000582.
23. Wolfram D, Tzankov A, Pülzl P, Piza-Katzer H. Hypertrophic scars and keloids--a review of their pathophysiology, risk factors, and therapeutic management. Dermatol Surg. 2009 Feb;35(2):171-81. doi: 10.1111/j.1524-4725.2008.34406.x.
24. Campese VM. Minoxidil: a review of its pharmacological properties and therapeutic use. Drugs. 1981 Oct;22(4):257-78. doi: 10.2165/00003495-198122040-00001.
25. Panchaprateep R, Lueangarun S. Efficacy and Safety of Oral Minoxidil 5 mg Once Daily in the Treatment of Male Patients with Androgenetic Alopecia: An Open-Label and Global Photographic Assessment. Dermatol Ther (Heidelb). 2020 Dec;10(6):1345-1357. doi: 10.1007/s13555-020-00448-x.
26. Cranwell W, Sinclair R. Male androgenetic alopecia. In: KR Feingold, B Anawalt, A Boyce, et al, eds. Endotext. MDText.com, Inc.; 2016.
27. Rossi A, Anzalone A, Fortuna MC, Caro G, Garelli V, Pranteda G, Carlesimo M. Multi-therapies in androgenetic alopecia: review and clinical experiences. Dermatol Ther. 2016 Nov;29(6):424-432. doi: 10.1111/dth.12390.
28. Blume-Peytavi U, Hillmann K, Dietz E, Canfield D, Garcia Bartels N. A randomized, single-blind trial of 5% minoxidil foam once daily versus 2% minoxidil solution twice daily in the treatment of androgenetic alopecia in women. J Am Acad Dermatol. 2011 Dec;65(6):1126-1134.e2. doi: 10.1016/j.jaad.2010.09.724.
29. Price VH, Menefee E, Strauss PC. Changes in hair weight and hair count in men with androgenetic alopecia, after application of 5% and 2% topical minoxidil, placebo, or no treatment. J Am Acad Dermatol. 1999 Nov;41(5 Pt 1):717-21. doi: 10.1016/s0190-9622(99)70006-x.
30. Shao S, Zhang X, Duan L, Fang H, Rao S, Liu W, Guo B, Zhang X. Lysyl Hydroxylase Inhibition by Minoxidil Blocks Collagen Deposition and Prevents Pulmonary Fibrosis via TGF-β1/Smad3 Signaling Pathway. Med Sci Monit. 2018 Nov 27;24:8592-8601. doi: 10.12659/MSM.910761.
31. Hautala T, Heikkinen J, Kivirikko KI, Myllylä R. Minoxidil specifically decreases the expression of lysine hydroxylase in cultured human skin fibroblasts. Biochem J. 1992 Apr 1;283 (Pt 1)(Pt 1):51-4. doi: 10.1042/bj2830051.
32. Murad S, Walker LC, Tajima S, Pinnell SR. Minimum structural requirements for minoxidil inhibition of lysyl hydroxylase in cultured fibroblasts. Arch Biochem Biophys. 1994 Jan;308(1):42-7. doi: 10.1006/abbi.1994.1006.
33. van der Slot AJ, van Dura EA, de Wit EC, De Groot J, Huizinga TW, Bank RA, Zuurmond AM. Elevated formation of pyridinoline cross-links by profibrotic cytokines is associated with enhanced lysyl hydroxylase 2b levels. Biochim Biophys Acta. 2005 Jun 30;1741(1-2):95-102. doi: 10.1016/j.bbadis.2004.09.009.
34. Remst DF, Blaney Davidson EN, Vitters EL, Blom AB, Stoop R, Snabel JM, Bank RA, van den Berg WB, van der Kraan PM. Osteoarthritis-related fibrosis is associated with both elevated pyridinoline cross-link formation and lysyl hydroxylase 2b expression. Osteoarthritis Cartilage. 2013 Jan;21(1):157-64. doi: 10.1016/j.joca.2012.10.002.
35. Zuurmond AM, van der Slot-Verhoeven AJ, van Dura EA, De Groot J, Bank RA. Minoxidil exerts different inhibitory effects on gene expression of lysyl hydroxylase 1, 2, and 3: implications for collagen cross-linking and treatment of fibrosis. Matrix Biol. 2005 Jun;24(4):261-70. doi: 10.1016/j.matbio.2005.04.002.
36. Shao S, Fang H, Duan L, Ye X, Rao S, Han J, Li Y, Yuan G, Liu W, Zhang X. Lysyl hydroxylase 3 increases collagen deposition and promotes pulmonary fibrosis by activating TGFβ1/Smad3 and Wnt/β-catenin pathways. Arch Med Sci. 2019 Jan 16;16(2):436-445. doi: 10.5114/aoms.2018.81357.
37. Priestley GC, Lord R, Stavropoulos P. The metabolism of fibroblasts from normal and fibrotic skin is inhibited by minoxidil in vitro. Br J Dermatol. 1991 Sep;125(3):217-21. doi: 10.1111/j.1365-2133.1991.tb14743.x.
38. Knitlova J, Doubkova M, Plencner M, Vondrasek D, Eckhardt A, Ostadal M, Musilkova J, Bacakova L, Novotny T. Minoxidil decreases collagen I deposition and tissue-like contraction in clubfoot-derived cells: a way to improve conservative treatment of relapsed clubfoot? Connect Tissue Res. 2021 Sep;62(5):554-569. doi: 10.1080/03008207.2020.1816992.
39. Freiha M, Achim M, Gheban BA, Moldovan R, Filip GA. In Vivo Study of the Effects of Propranolol, Timolol, and Minoxidil on Burn Wound Healing in Wistar Rats. J Burn Care Res. 2023 Apr 26:irad057. doi: 10.1093/jbcr/irad057.
40. Polo M, Hill DP Jr, Carney G, Ko F, Wright TE, Robson MC. Minoxidil and wound contraction. Ann Plast Surg. 1997 Sep;39(3):292-8. doi: 10.1097/00000637-199709000-00012.

International Journal of Biomedicine 13(3) (2023) 59-65
http://dx.doi.org/10.21103/Article13(3)_OA1

ORIGINAL ARTICLE

Cardiology

INTERNATIONAL JOURNAL OF BIOMEDICINE

Dynamics of Non-Invasive Risk Factors of Sudden Cardiac Death after Myocardial Revascularization

Ergashali Ya. Tursunov*, Amayak G. Kevorkov, Ravshanbek D. Kurbanov, Nodir U. Zakirov, Alisher Sh. Rasulov

Republican Specialized Scientific and Practical Medical Center of Cardiology
Tashkent, Uzbekistan

Abstract

Background*:* An attempt was made to study the effect of surgical myocardial revascularization on the processes of electrical myocardium instability underlying the occurrence of life-threatening ventricular arrhythmias, as well as the possibility of its non-invasive assessment by studying heart rate variability (HRV) and heart rate turbulence (HRT), as well as the duration and dispersion of the QT interval. Based only on the presence of viable myocardium, it is often impossible to predict the positive impact of revascularization on a patient's prognosis, especially with reduced myocardial contractility. Moreover, given the well-studied relationship between myocardial remodeling and neurohormonal activation, non-invasive methods for assessing the autonomic regulation of cardiac activity can provide additional diagnostic information. Along with this, changes in these indicators and their prognostic role in patients with coronary artery disease after revascularization are subjects of discussion.

Methods and Results: All patients underwent a comprehensive clinical and biochemical blood test, transthoracic echocardiography, tissue Doppler echocardiography, ultrasound examination of brachiocephalic arteries, selective coronary angio- and ventriculography, as well as Holter monitoring. Results show that a year after the coronary intervention, there was a significant positive trend in the frequency and structure of ventricular arrhythmias. HRV indicators generally did not show significant dynamics. Only an increase in the values of the standard deviation of 5-minute average NN intervals (SDANN) and low-frequency power (LFP) indices was noted, indicating a gradual increase in the activity of the sympathetic part of the autonomic nervous system. HRT indicators also did not show significant dynamics. A significant increase was found in the number of patients with no signs of impaired HRT. The average duration of the QT interval decreased significantly. There was also a tendency to shorten the corrected QT interval; however, it was insignificant. In terms of dispersion, both the QT interval and its corrected index, no significant dynamics were recorded in the general group of patients.

Conclusion: Our study found that in patients with prior myocardial infarction, after revascularization, significant positive dynamics were recorded in life-threatening ventricular arrhythmias, but were unreliable for the indicators of autonomic regulation of cardiac activity, such as HRV and HRT.(**International Journal of Biomedicine. 2023;13(3):59-65.**)

Keywords: heart rate variability • heart rate turbulence • myocardial infarction • electrical myocardium instability

For citation:Tursunov EYa, Kevorkov AG, Kurbanov RD, Zakirov NU, Rasulov ASh. Dynamics of Non-Invasive Risk Factors of Sudden Cardiac Death after Myocardial Revascularization. International Journal of Biomedicine. 2023;13(3):59-65. doi:10.21103/Article13(3)_OA1

Abbreviations

CABG, coronary artery bypass graft; **CAD**, coronary artery disease; **CI**, circadian index; **EMI**, electrical myocardium instability; **EF**, ejection fraction; **HF**, heart failure; **HFP**, high-frequency power; **HRV**, heart rate variability; **HM**, Holter monitoring; **HRT**, heart rate turbulence; **LFP**, low-frequency power; **LVEF**, left ventricular ejection fraction; **LTVA**, life-threatening ventricular arrhythmias; **MI**, myocardial infarction; **PVC**, premature ventricular contractions; **PCI**, percutaneous intervention; **SCD**, sudden cardiac death; **SDANN**, standard deviation of 5-minute average NN intervals.

Introduction

Myocardial revascularization can significantly improve the long-term prognosis of patients with coronary artery disease (CAD). Currently, the indications for this intervention in the most severe patients are gradually expanding. Myocardial revascularization in patients with multivessel CAD significantly reduces the risk of death from fatal ventricular arrhythmias, progression of heart failure (HF), and acute myocardial infarction (MI).[1]

Even if there are indications for myocardial revascularization, it is necessary to choose the optimal method for its implementation: percutaneous intervention (PCI) or coronary artery bypass graft (CABG). It is important to consider that the best results to date have been obtained with auto-arterial bypass or angioplasty with implantation of drug-eluting stents; however, CABG can more often provide more complete myocardial revascularization than PCI.[2]

In recent years, there has been a peculiar evolution of endovascular interventions, largely due to the broader introduction into practice of the latest generation of drug-eluting stents, which led to a significant improvement in the results of PCI and made the level of PCI recommendations equal to CABG in patients with single-vessel disease (IA). In addition, PCI significantly improved its position in patients with two- and three-vessel lesions and SYNTAX scores less than 22. However, in patients with moderate and severe three-vessel disease (scores 23-32 or more), CABG remains the key method of revascularization.

Due to the great urgency of the problem of choosing the optimal method of revascularization in patients with CAD, attempts to compare the results of PCI and CABG continue. Based on the results of multicenter studies conducted in recent years, devoted to the study of this issue, 3 main conclusions can be drawn: (1) After CABG, there are excellent results in patient survival, especially with long-term follow-up;[3] (2) CABG leads to a decrease in the incidence of cardiovascular and cerebrovascular complications;[4-6] (3) There is a higher rate of repeat revascularization after PCI.

However, despite successful myocardial revascularization, a number of patients develop life-threatening ventricular arrhythmias already in the first year, and the symptoms of heart failure (HF) do not decrease or progress. This is due to the fact that in the pathogenesis of the development of life-threatening ventricular arrhythmias, myocardial ischemia is only one of the factors,[7] and thus, myocardial revascularization, reducing the effect of ischemia on the development of arrhythmia, has a limited effect on the substrate of ventricular arrhythmias in the form of cicatricial myocardial damage. In addition, the ongoing progress of the atherosclerotic process in the coronary arteries and the development of shunt or stent obstruction also affect the results of revascularization.[8]

One of the important tasks is the earliest detection of patients at high risk of developing various adverse events, primarily life-threatening ventricular arrhythmias. To date, non-invasive indicators have been proposed that are determined using Holter monitoring, particularly heart rate variability (HRV) and heart rate turbulence (HRT).[9] Based on numerous data, their effectiveness in assessing the risk of cardiovascular mortality and sudden cardiac death (SCD) in patients with CAD and HF has been demonstrated.

The currently existing models of stratifying patients by sudden-death risk groups usually provide for assessing changes in the systolic function of the left ventricle, and to a lesser extent, indicators characterizing the electrical instability of the myocardium. At the same time, the study of HRV, HRT, and QT interval dispersion to clarify the specific mechanisms of development and progression of life-threatening ventricular arrhythmias, especially in patients with acute MI, seems to be a promising direction.[10] Even more interesting is the study of the effect of myocardial revascularization on the dynamics of non-invasive indicators of myocardial electrical instability.

The aim of this study was to evaluate non-invasive risk factors for SCD in post-MI patients with preserved LVEF, as well as their correction after various methods of myocardial revascularization.

Materials and Methods

To study the possibilities of non-invasive assessment of electrical myocardium instability (EMI), we examined 239 patients aged 35 to 84 years (median age - 61 [55; 66] years) with a history of acute MI of various localization and with different natures of the lesion of the coronary bed, established based on the results of diagnostic selective coronary angiography.

Exclusion criteria were patients with impaired sinoauricular or atrioventricular conduction, or with no history of MI, hyperthermia, or the presence of diseases that significantly alter HRV (diabetes mellitus, hypo- or hyperthyroidism, extensive alcohol consumption, severe respiratory, renal, or hepatic insufficiency, cancer, etc.).

Upon admission to the hospital, all patients underwent a comprehensive clinical and biochemical blood test, transthoracic echocardiography, tissue Doppler echocardiography, ultrasound examination of brachiocephalic arteries, selective coronary angio- and ventriculography, as well as Holter monitoring using the CardioSens+ system (XAI-MEDICA, Ukraine). Monitoring was carried out in conditions of free movement of patients on standard therapy, which included antiplatelets, β-blockers, ACE inhibitors or ARBs, statins, nitrates (if necessary), and amiodarone (if necessary, in patients with potentially dangerous ventricular arrhythmias). Premature ventricular contractions (PVC) of III-V grades (Lown grading system)[11] and ≥10 PVC/hour were regarded as potentially dangerous ventricular arrhythmias.

The analysis of the obtained data included time and frequency domain methods of HRV, To, and Ts of HRT, as well as QT interval duration and dispersion.

Statistical analysis was performed using the statistical software «Statistica» (v13.0, StatSoft, USA). Baseline characteristics were summarized as frequencies and percentages for categorical variables. Continuous variables with normal distribution were presented as mean (standard deviation [SD]); non-normal variables were reported as

median (Me) (interquartile range [IQR]). A probability value of $P<0.05$ was considered statistically significant.

The study protocol was reviewed and approved by the Ethics Committee of the Republican Specialized Scientific and Practical Medical Center of Cardiology. All participants provided written informed consent.

Results

The clinical characteristics of the patients were compiled according to the results of the initial examination. The main group of patients consisted of men (82.8%) of ≥55 years (mean age 60.1±8.1 years), mostly with a history of anterior MI (57.7%) (Table 1). The presence of post-infarction aneurysm of the left ventricle was noted in 10.5% of cases. Also, it should be noted that 46.0% of patients were overweight and 40.1% were obese, with varying degrees of severity; thus, only 13.8% had normal body weight.

Table 1.

Clinical characteristics of the general group of patients (n=239).

Age, years		60.1±8.1	61 [55; 66]
Sex	Men Women	198 (82.8%) 41 (17.2%)	
BMI, kg/m ^{2}		29.1±4.6	29 [25.8; 31.6]
Normal body weight, n (%)		33 (13.8%)	
Overweight, n (%)		110 (46.0%)	
Obesity	Class I Class II Class III	82 (34.3%) 8 (3.3%) 6 (2.5%)	
MI localization	Anterior Posterior	138 (57.7%) 101 (42.3%)	
Left ventricular aneurysm		25 (10.5%)	

Table 2.

Dynamics of heart rate according to Holter monitoring data in the general group of patients (n=239) after 1 year of follow-up.

Parameter	Initial value		One year after of revascularization		*P*-value
	M±SD	Me[Q1;Q3]	M±SD	Me[Q1;Q3]	
Average HR, bpm	68.6±8.9	68.5[62;75]	72.7±9.3	71[67;77]	0.010
Maximum HR, bpm	101.1±14.7	100[90.5;112]	110.8±19.1	109[99;119]	0.008
Minimum HR, bpm	54.2±7.8	54[49;59.5]	55.1±9	53[49;60]	0.409
Daytime average HR, bpm	71.2±10.5	71[64.5;78.5]	76.5±10.1	74[69;82]	0.019
Nighttime average HR, bpm	69.2±57.4	65[59;71]	66.5±8.8	65[61;71]	0.229
CI	1.1±0.06	1.1[1.06;1.13]	1.15±0.08	1.15[1.1;1.2]	0.000

When assessing heart rate (Table 2), attention is drawn to the frequency, density, and categories of PVCs using Holter monitoring (Table 3), as well as to the relative rigidity of the baseline sinus rhythm, which is expressed in an insignificant difference between the average values of daytime and nighttime heart rate and, accordingly, in a decrease in the circadian index (CI).

PVCs noted in all subjects, as a whole, had a relatively unfavorable character (Table 3). Potentially dangerous ventricular arrhythmias were observed in almost 60% of the examined patients. When analyzing the structure of potentially dangerous ventricular arrhythmias, taking as a basis the maximum class of PVC registered in the patient, classes II and V of PVC were not observed in any of the examined patients, class III was detected in 19.9%, IVA in 26.9%, and IVB in 12.3%. When assessing the frequency of PVCs, frequent extrasystoles >10 PVCs/hour were detected in 48.5% of cases.

Table 3.

Dynamics of the frequency and structure of ventricular ectopic activity according to Holter monitoring data in the general group of patients (n=239).

Parameter		Initial value	One year after REV	Friedman ANOVA χ^2	*P*-value
PVC density, %		1.09±3.86	0.41±0.88	0.07	0.789
PDVA, n (%)		141(58.9%)	110 (46.0%)	31.0	0.000
Frequent (>10/hour) PVC, %		110(46.0%)	79 (33.1%)	31.0	0.000
PVC class (Lown), registered in a patient, n (%)	I	239(100%)	197 (82.4%)	42.0	0.000
	II	82(34.5%)	34 (14.2%)	48.0	0.000
	III	136(56.7 %)	107 (44.8%)	29.0	0.000
	IV A	91(38.0 %)	70 (29.3%)	21.0	0.000
	IV B	29(12.3 %)	14 (5.9%)	15.0	0.000
Highest registered PVC class (Lown), n (%)	0	0(0%)	42 (17.6 %)	42.0	0,000
	I	98(40.9%)	87 (36.4%)	11.0	0,001
	III	48(19.9%)	34 (14.2%)	14.0	0,000
	IV A	64(26.9%)	62 (25.9%)	2.0	0,157
	IV B	29(12.3%)	14 (5.9%)	15.0	0,000

REV -revascularization; PDVA -Potentially dangerous ventricular arrhythmias

HRV, assessed per day by both time and frequency methods, was characterized by a significant decrease in the values of indicators of both the total HRV and its components, as well as the predominance of the low-frequency component of HRV with an increase in the LFP/HFP ratio to 3.5, which indicates predominant sympathetic activity (Table 4).

Analysis of the HRT indicators did not reveal a decrease in the values of the To and Ts indicators, on average, for the group examined (Table 5). However, with an appropriate division of the patients, a quarter of them had HRT disorders, which allowed them to be classified either in category 1(19.0%) or category 2(5.9%) (Table 6).

The daily duration of both the QT interval and its corrected QTc index, calculated according to the Bazett formula, as a whole had normal values (Table 7).

Table 4.

Dynamics of HRV according to Holter monitoring data in the general group of patients (n=239).

Parameter	Initial value		One year after revascularization		*P*-value
	M±SD	Me [Q1; Q3]	M±SD	Me [Q1; Q3]	
SDNN, ms	41.4±14.8	39.3 [31.6; 47.8]	41.8±14.9	39.7 [32.5; 49.4]	0.237
SDANN, ms	80.6±25.8	79.7 [64.2; 96.7]	99.4±32.1	96.2 [78.6; 114.1]	0.013
rMSSD, ms	23.3±16.7	18.7 [14.3; 27.7]	20.9±9.6	18.2 [15.1; 26.1]	0.694
pNN50, %	5.1±8.1	1.8 [0.5; 6.1]	3.6±4.3	1.5 [0.7; 4.9]	0.694
HRV TI	9.1±2.8	9 [7.3; 10.7]	8.9±2.5	8.7 [7.3; 10.3]	0.694
TP, ms^2	2240.4±1624.4	1806.2 [1174.2; 2624.8]	2516.9±2058.6	1934.2 [1340; 3139.9]	0.435
ULF, ms^2	93.8±245	25.9 [11.5; 68.1]	102.2±176.4	45.7 [22.2; 80.2]	0.149
VLF, ms^2	1452.8±1058.8	1150.8 [786.5; 1826.9]	1593.3±1307.2	1288.1 [813.2; 2048.3]	0.435
LF, ms^2	445.8±366.8	333.7 [197.1; 566.9]	580.2±542	456.8 [253.3; 715.1]	0.006
LFnorm, %	67.3±12.9	70.4 [59.3; 76.4]	70.3±10	71.9 [63.7; 78.1]	0.237
HF, ms^2	247.5±335.9	137.7 [71.1; 309.3]	241.3±215.4	178.8 [90.8; 338.8]	0.088
HFnorm, %	32.3±12.7	29.5 [23.5; 40.2]	29.7±10	28.1 [21.9; 36.3]	0.237
LF/HF	3.5±2	3.1 [2.1; 4.5]	3.8±2.4	3.3 [2.4; 4.7]	0.358

Table 5.

Dynamics of HRT according to Holter monitoring data in the general group of patients (n=239).

Parameter	Initial value		One year after revascularization		*P*-value
	M±SD	Me [Q1; Q3]	M±SD	Me [Q1; Q3]	
To, %	-0.93±1.91	-0.81 [-2.2; 0.15]	-1.03±3.1	-0.99 [-1.72; -0.3]	0.689
Ts, ms/RRi	4.92±4.18	4.07 [1.59; 6.93]	6.97±8.91	4.95 [2.55; 8.2]	0.230

Table 6.

Dynamics of the category of decrease in HRT according to Holter monitoring data in the general group of patients (n=239).

		Initial value	After 1 year of observation	ANOVA χ^2	*P*-value
HRT category of decrease, n (%)	0	180 (75.1%)	213 (89.1%)	33.0	0.000
	1	45 (19.0%)	21 (8.8%)	24.0	0.000
	2	14 (5.9%)	5 (2.1%)	9.0	0.003

Table 7.

Dynamics of QT interval duration and dispersion according to Holter monitoring data in the general group of patients (n=239)

Parameter	Initial value		After 1 year of observation		*P*-value
	M±SD	Me[Q1;Q3]	M±SD	Me[Q1;Q3]	
QT, ms	396.4±39.5	396[368;424]	380.7±29.2	380[360;400]	0.011
QTc, ms	417.3±42.3	421[394;440]	413.8±25	411[394;433]	0.896
dQT, ms	91.7±44.9	84[64;108]	93.9±39.2	84[64; 16]	0.894
dQTc, ms	70±39.2	60[43;85]	74.7±38	61[45;96]	0.683

The QT interval dispersion (dQT) of the corrected QTc interval (dQTc), measured as the difference between the maximum and minimum values of the QT interval and QTc obtained from the analysis of the daily ECG recording, also did not show a significant increase (Table 7).

One year after the coronary intervention, the patients underwent HM again. The results showed that the heart rate, on average, increased somewhat (Table 2), so both the average and maximum heart rate, as well as the average daily heart rate, significantly increased. At the same time, both the minimum heart rate and the average nighttime heart rate slightly decreased, which, despite the absence of significant dynamics from these indicators, led to a significant increase in the CI.

When analyzing ventricular arrhythmias according to dynamic HM in the general group of patients, we found a significant positive trend in both the frequency and structure of PVC (Table 3). In particular, in 17.6% of patients, there were no signs of ventricular ectopic activity, and all previously diagnosed PVC classes, according to the Lown grading system, registered significant positive dynamics.

The majority of the HRV indicators did not show significant dynamics (Table 4) in the general group of patients. Only an increase in the values of the SDANN and LFP indicators

was noted, indicating a further increase in the activity of the sympathetic division of the autonomic nervous system.

HRT indicators also did not show significant dynamics, remaining within normal physiological values, on average (Table 5). However, with the appropriate division into groups, according to the category of HRS reduction (Table 6), the number of patients with no signs of HRS disorders and who were included in category 0 increased significantly from 75.1% to 89.1%, with a corresponding significant reduction in the number patients in categories 1 and 2.

The duration of the QT interval, according to HM in the general group of patients, significantly decreased (Table 7). There was also a tendency to shorten the corrected QT interval; however, it was not significant. In terms of dispersion, for both the QT interval and its corrected index, no significant dynamics were recorded in the general group of patients.

Discussion

The most common cause of SCD in patients with a history of life-threatening ventricular arrhythmias is monomorphic ventricular tachycardia with the transition to ventricular fibrillation, polymorphic ventricular tachycardia of the "torsades de pointed," and primary ventricular fibrillation. [12] It is now well known that myocardial ischemia is one of the important triggers of ventricular arrhythmias and, therefore, myocardial revascularization, eliminating the cause of ischemia and reducing the risk of complete occlusion of the coronary artery, can reduce the risk of developing life-threatening ventricular arrhythmias and improve prognosis. [2] In particular, myocardial revascularization significantly reduces the risk of developing life-threatening ventricular arrhythmias in the presence of damage to the trunk and proximal anterior descending artery and, in this case, is a necessary intervention.[13]

The main factors that most often provoke the development of life-threatening ventricular arrhythmias in CAD are myocardial ischemia, which acts as an arrhythmia trigger, and the presence of myocardial cicatricial changes after a past acute MI, acting as a substrate. Several studies[14,15] showed that this combination of trigger and substrate most often leads to the development of fatal ventricular arrhythmias. Acute ischemia caused even by complete occlusion of the coronary artery is much less likely to cause fatal ventricular arrhythmias in the absence of arrhythmia substrate in the form of myocardial cicatricial changes. On the contrary, in the presence of cicatricial changes in the myocardium, even a partial narrowing of the arterial lumen can already lead to ventricular tachycardia induction in most patients.[15]

With extensive areas of post-infarction myocardial damage affecting global LV systolic function, the amount of viable myocardium plays an important role in improving myocardial contractility after revascularization. Identifying a sufficient amount of viable myocardium [16] can often influence the decision on the possibility of revascularization, especially in patients with reduced LVEF.

Unfortunately, viable myocardial contractility after revascularization cannot be recovered in all cases. In 2004, Schinkel et al.[17] did not observe improvement in LV contractility after revascularization in about a third of patients with viable myocardium and, first of all, in patients with signs of severe post-infarction myocardial remodeling. In such a large study as STICH, the initial presence of a viable myocardium did not affect improvement in the survival of patients after surgical myocardial revascularization, compared with patients who received conservative therapy.[18] These results demonstrated that relying only on the presence of viable myocardium made it impossible to predict the positive effect of revascularization on the prognosis for patients, especially those with reduced myocardial contractility; and given the well-studied relationship between myocardial remodeling and the development of HF with neurohormonal activation, such non-invasive methods for assessing the autonomic regulation of cardiac activity using HM, such as HRV and HRT, can provide additional diagnostic information.

In patients with HF events and risk of ventricular tachycardia, the interaction of multidirectional regulatory mechanisms is probably important, which can be indirectly assessed using HRV and HRT. In various studies, the analysis of the HM data of patients immediately before the onset of ventricular tachycardia revealed signs of worsening HRV.[19]

With the help of the main parameters used in the analysis of HRV, one can first of all single out a group with a significant decrease in HRV and with formation of the so-called «rigid» rhythm, which, in itself, unequivocally, can be called a prognostically unfavorable sign. That is because in large studies a poor prognosis was demonstrated in this category of patients who underwent acute MI and a pronounced decrease in HRV. Thus, the possibility of using the HRV assessment technique to determine the risk of adverse events, primarily general and cardiovascular mortality, was confirmed.[20]

Numerous studies[20-24] have shown the role of HRV indicators as a prognostic criterion for mortality. SDNN is considered the indicator of a temporary method that is most often mentioned in the results of clinical trials and effectively determines the prognosis of mortality after acute MI. As for the study of the effect of revascularization on HRV parameters, based on the literature data, it can be concluded that myocardial revascularization, and, in particular, CABG, is accompanied by a decrease in HRV in the immediate postoperative period, and over the next 2-3 months there is an increase in indicators for HRV to preoperative levels, even in patients with low LVEF. Also, there is evidence of an association between low HRV and higher mortality in patients 3 years after CABG.[24]

Both characteristics of HRT are significantly affected by the level of LVEF. HR parameters are significantly reduced in patients with HF events, as well as those with structural heart lesions, even with intact EF. The prognostic value of the method has been demonstrated in such studies as MPIP, EMIAT, ISAR-HRT, and FINGER as a predictor of cardiac death, including SCD, and as a risk factor for ventricular arrhythmias (CARISMA study). According to the data, patients with pathological HRT category 2 have the most unfavorable prognosis. In the case of pathological HRT category 1, the prognosis was more often determined by the change in the Ts index.

A change in HRT affects the prognosis in patients with reduced EF and, importantly, increases the positive predictive value of reduced EF.[25] It is important that HRT determines the prognosis of cardiovascular mortality and SCD not only in patients with reduced LVEF, but also in patients without severe systolic dysfunction.[26] In particular, in the ISAR-Risk study, the levels of SCD and cardiovascular mortality in patients with severe autonomic dysfunction and in patients with preserved LVEF were similar to that with a significant decrease in EF of <30%.

The impact of surgical revascularization on HRT scores on subsequent adverse events has been researched in only a few studies. One of them proved the influence of the preoperative Ts value on mortality during the first year after CABG; another study[27] demonstrated a deterioration in HRT after surgery, which may have been associated with a change in baroreflex function and autonomic regulation after the surgical intervention. Indeed, the results of many studies testify to the deterioration of various indicators of autonomic regulation after major surgery. However, it is necessary to consider that the rate of recovery of autonomic regulation of cardiac activity and the degree of its decrease in patients may be different, which may reflect a different functional state of the patient and affect outcomes after surgery in different ways. Therefore, there is a need to further study the HRT dynamics at different times after myocardial revascularization and the impact of these changes on further prognosis.

Thus, literature data indicate that myocardial revascularization is an effective treatment for patients with CAD. HF, ventricular arrhythmias, and relapses of angina pectoris and MI are the main problems that determine an unfavorable outcome in the postoperative period in a number of patients. There is important evidence that violations of the autonomic regulation of the heart's activity and the heterogeneity of repolarization processes in the myocardium are integral indicators of morphofunctional changes that occur during the progression of CAD. The role of HRV and HRT indicators as predictors of SCD, mainly due to fatal ventricular arrhythmias and cardiovascular mortality, has been demonstrated. Along with this, changes in the above indicators and the prognostic role in patients with CAD on the background of revascularization are subjects of discussion because there are practically no works devoted to studying the effect of various methods of revascularization on the parameters of myocardial electrical instability, as one of the most important factors in the development of life-threatening ventricular arrhythmias, which is a predictor of SCD, especially in patients who have previously had MI.

The number of studies on the effect of myocardial revascularization on the indicators of autonomic regulation of cardiac activity and the possibility of their use as prognostic criteria before and after surgery is also insufficient, which determines the relevance of further research in this direction.

In conclusion, our study found that in patients with prior MI, after revascularization, significant positive dynamics were recorded in life-threatening ventricular arrhythmias, but were unreliable for the indicators of autonomic regulation of cardiac activity, such as HRV and HRT.

Competing Interests

The authors declare that they have no competing interests.

References

1. Velazquez EJ, Lee KL, Jones RH, Al-Khalidi HR, Hill JA, Panza JA, et al.; STICHES Investigators. Coronary-Artery Bypass Surgery in Patients with Ischemic Cardiomyopathy. N Engl J Med. 2016 Apr 21;374(16):1511-20. doi: 10.1056/NEJMoa1602001.
2. Kolh P, Kurlansky P, Cremer J, Lawton J, Siepe M, Fremes S. Transatlantic Editorial: A Comparison Between European and North American Guidelines on Myocardial Revascularization. Ann Thorac Surg. 2016 Jun;101(6):2031-44. doi: 10.1016/j.athoracsur.2016.02.062.
3. Jiang L, Xu L, Song L, Gao Z, Tian J, Sun K, Yu H, Xu B, Song L, Yuan J. Comparison of three treatment strategies for patients with triple-vessel coronary disease and left ventricular dysfunction. J Interv Cardiol. 2018 Jun;31(3):310-318. doi: 10.1111/joic.12497.
4. Park SJ, Ahn JM, Kim YH, Park DW, Yun SC, Lee JY, et al.; BEST Trial Investigators. Trial of everolimus-eluting stents or bypass surgery for coronary disease. N Engl J Med. 2015 Mar 26;372(13):1204-12. doi: 10.1056/NEJMoa1415447.
5. Gallo M, Blitzer D, Laforgia PL, Doulamis IP, Perrin N, Bortolussi G, Guariento A, Putzu A. Percutaneous coronary intervention versus coronary artery bypass graft for left main coronary artery disease: A meta-analysis. J Thorac Cardiovasc Surg. 2022 Jan;163(1):94-105.e15. doi: 10.1016/j.jtcvs.2020.04.010.
6. Serruys PW, Morice MC, Kappetein AP, Colombo A, Holmes DR, Mack MJ, Ståhle E, Feldman TE, van den Brand M, Bass EJ, Van Dyck N, Leadley K, Dawkins KD, Mohr FW; SYNTAX Investigators. Percutaneous coronary intervention versus coronary-artery bypass grafting for severe coronary artery disease. N Engl J Med. 2009 Mar 5;360(10):961-72. doi: 10.1056/NEJMoa0804626.
7. Andersen JA, Freeman P, Larsen JM, Andersen NH. Monomorphic ventricular tachycardia as the primary presentation of an anterior STEMI. Clin Case Rep. 2019 Jul 26;7(9):1680-1684. doi: 10.1002/ccr3.2324.
8. Marrakchi S, Laroussi L, Bennour E, Kammoun I, Kachboura S. Coronary PCI revascularization novel treatment of bundle branch reentrant ventricular tachycardia. J Cardiol Cases. 2019 Sep 20;20(5):151-154. doi: 10.1016/j.jccase.2019.08.003.
9. Gatzoulis KA, Tsiachris D, Arsenos P, Antoniou CK, Dilaveris P, Sideris S, et al. Arrhythmic risk stratification in post-myocardial infarction patients with preserved ejection fraction: the PRESERVE EF study. Eur Heart J. 2019 Sep 14;40(35):2940-2949. doi: 10.1093/eurheartj/ehz260.
10. Bui AH, Waks JW. Risk Stratification of Sudden Cardiac Death After Acute Myocardial Infarction. J Innov Card

***Corresponding author**: Ergashali Ya. Tursunov, Doctoral Student, Cardiac Arrhythmias Department, Republican Specialized Scientific and Practical Medical Center of Cardiology. Tashkent, Uzbekistan. E-mail: ergashali.tursunov.1990@mail.ru*

Rhythm Manag. 2018 Feb 15;9(2):3035-3049. doi: 10.19102/icrm.2018.090201.
11. Lown B, Wolf M. Approaches to sudden death from coronary heart disease. Circulation. 1971 Jul;44(1):130-42. doi: 10.1161/01.cir.44.1.130.
12. Priori SG, Blomström-Lundqvist C, Mazzanti A, Blom N, Borggrefe M, Camm J, et al. 2015 ESC Guidelines for the Management of Patients With Ventricular Arrhythmias and the Prevention of Sudden Cardiac Death. Rev Esp Cardiol (Engl Ed). 2016 Feb;69(2):176. doi: 10.1016/j.rec.2016.01.001.
13. Furukawa T, Moroe K, Mayrovitz HN, Sampsell R, Furukawa N, Myerburg RJ. Arrhythmogenic effects of graded coronary blood flow reductions superimposed on prior myocardial infarction in dogs. Circulation. 1991 Jul;84(1):368-77. doi: 10.1161/01.cir.84.1.368.
14. Kimura S, Bassett AL, Cameron JS, Huikuri H, Kozlovskis PL, Myerburg RJ. Cellular electrophysiological changes during ischemia in isolated, coronary-perfused cat ventricle with healed myocardial infarction. Circulation. 1988 Aug;78(2):401-6. doi: 10.1161/01.cir.78.2.401.
15. Rizzello V, Poldermans D, Boersma E, Biagini E, Schinkel AF, Krenning B, et al. Opposite patterns of left ventricular remodeling after coronary revascularization in patients with ischemic cardiomyopathy: role of myocardial viability. Circulation. 2004 Oct 19;110(16):2383-8. doi: 10.1161/01.CIR.0000145115.29952.14.
16. Saidova MA, Belenkov IuN, Akchurin RS, Sergienko VB, Khodareva EN, Kostrova VV. [Viable myocardium: comparative evaluation of surgical and pharmacological treatment of patients with ischemic heart disease, post-infarct cardiosclerosis and chronic cardiac failure]. Ter Arkh. 2002;74(2):60-4. [Article in Russian].
17. Schinkel AF, Poldermans D, Rizzello V, Vanoverschelde JL, Elhendy A, Boersma E, Roelandt JR, Bax JJ. Why do patients with ischemic cardiomyopathy and a substantial amount of viable myocardium not always recover in function after revascularization? J Thorac Cardiovasc Surg. 2004 Feb;127(2):385-90. doi: 10.1016/j.jtcvs.2003.08.005.
18. Bonow RO, Maurer G, Lee KL, Holly TA, Binkley PF, Desvigne-Nickens P, et al.; STICH Trial Investigators. Myocardial viability and survival in ischemic left ventricular dysfunction. N Engl J Med. 2011 Apr 28;364(17):1617-25. doi: 10.1056/NEJMoa1100358.
19. Huikuri HV, Valkama JO, Airaksinen KE, Seppänen T, Kessler KM, Takkunen JT, Myerburg RJ. Frequency domain measures of heart rate variability before the onset of nonsustained and sustained ventricular tachycardia in patients with coronary artery disease. Circulation. 1993 Apr;87(4):1220-8. doi: 10.1161/01.cir.87.4.1220.
20. Huikuri HV, Stein PK. Clinical application of heart rate variability after acute myocardial infarction. Front Physiol. 2012 Feb 27;3:41. doi: 10.3389/fphys.2012.00041.
21. Bigger JT Jr, Fleiss JL, Steinman RC, Rolnitzky LM, Kleiger RE, Rottman JN. Correlations among time and frequency domain measures of heart period variability two weeks after acute myocardial infarction. Am J Cardiol. 1992 Apr 1;69(9):891-8. doi: 10.1016/0002-9149(92)90788-z.
22. Kleiger RE, Miller JP, Bigger JT Jr, Moss AJ. Decreased heart rate variability and its association with increased mortality after acute myocardial infarction. Am J Cardiol. 1987 Feb 1;59(4):256-62. doi: 10.1016/0002-9149(87)90795-8.
23. Tsuji H, Larson MG, Venditti FJ Jr, Manders ES, Evans JC, Feldman CL, Levy D. Impact of reduced heart rate variability on risk for cardiac events. The Framingham Heart Study. Circulation. 1996 Dec 1;94(11):2850-5. doi: 10.1161/01.cir.94.11.2850.
24. Lakusic N, Mahovic D, Sonicki Z, Slivnjak V, Baborski F. Outcome of patients with normal and decreased heart rate variability after coronary artery bypass grafting surgery. Int J Cardiol. 2013 Jun 20;166(2):516-8. doi: 10.1016/j.ijcard.2012.04.040.
25. Cygankiewicz I, Zareba W, Vazquez R, Vallverdu M, Cino J, Cinca J, et al. Relation of heart rate turbulence to severity of heart failure. Am J Cardiol. 2006 Dec 15;98(12):1635-40. doi: 10.1016/j.amjcard.2006.07.042.
26. Mäkikallio TH, Barthel P, Schneider R, Bauer A, Tapanainen JM, Tulppo MP, Schmidt G, Huikuri HV. Prediction of sudden cardiac death after acute myocardial infarction: role of Holter monitoring in the modern treatment era. Eur Heart J. 2005 Apr;26(8):762-9. doi: 10.1093/eurheartj/ehi188.
27. Cygankiewicz I, Wranicz JK, Bolinska H, Zaslonka J, Jaszewski R, Zareba W. Prognostic significance of heart rate turbulence in patients undergoing coronary artery bypass grafting. Am J Cardiol. 2003 Jun 15;91(12):1471-4, A8. doi: 10.1016/s0002-9149(03)00402-8.

International Journal of Biomedicine 13(3) (2023) 66-71
http://dx.doi.org/10.21103/Article13(3)_OA2

ORIGINAL ARTICLE

Cardiology

INTERNATIONAL JOURNAL OF BIOMEDICINE

Blood Pressure Variability: Marker or Predictor of Cardiovascular Risk?

D. Yuldasheva, G. A. Khamidullaeva*

Republican Specialized Center of Cardiology
Tashkent, Uzbekistan

Abstract

***Background*:** Regardless of the mean blood pressure (BP) value, short-term and long-term BP variability (BPV) are associated with the development and progression of target organ damage and predictors of cardiovascular complications and mortality. The purpose of the present study was to evaluate the prognostic significance of increased BPV in patients with arterial hypertension (AH).

Methods and Results: The study consisted of two stages. In the first stage, a retrospective analysis of 365 ABPM (24-hour ambulatory blood pressure monitoring) results was carried out. As a result of the analysis, 271 patients aged 56.1±10.0 years with uncontrolled AH Grades 1-3 (ESC/ESH, 2018) were included in this study. Depending on the values of BPV, AH patients were divided into two groups: Group 1 consisted of patients with normal BPV (n=145), and Group 2 consisted of patients with increased BPV (n=126). The second stage included 91 patients with uncontrolled hypertension without permanent antihypertensive therapy who had increased SBPV.

We found statistically significant differences in BP between the AH patients with normal BPV and increased BPV. Thus, in the group with normal BPV, compared with increased BPV, the parameters of the average 24-h systolic BP (SBP), daytime SBP, and nighttime SBP were statistically lower (141±14.6 vs. 147.2±20.2 mmHg, $P<0.004$; 142.8±15.1 vs. 148.4±20.7 mmHg, $P<0.01$; and 136.2±15.5 vs. 143.8±21.4 mmHg, $P<0.001$; respectively).

A statistically significant moderate direct correlation was found between the average 24-h SBP and the average 24-h and daytime SBP variability (SBPV) ($r_s=0.49$ and $r_s=0.40$ respectively, $P<0.001$ in all cases). A statistically significant moderate to weak direct correlation also was found between the average daytime SBP, and the average 24-h and daytime SBPV ($r_s=0.45$ and $r_s=0.37$, respectively, $P<0.001$ in all cases). A moderate direct correlation was found between nighttime SBP and 24-hour SBPV ($r_s=0.52$, $P<0.001$) and between nighttime SBP and daytime SBPV ($r_s=0.42$, $P<0.001$). Weak direct correlations were found between the average 24-h SBPV and central SBP (SBPc) ($r_s=0.34$, $P<0.001$), as well as between the average 24-h and daytime SBPV and central pulse pressure (PPc) ($r_s=0.33$ and $r_s=0.32$, respectively, $P<0.001$ in all cases). A weak direct correlation was found between carotid intima-media thickness (CIMT) and the average 24-h and daytime SBPV ($r_s=0.37$ [$P<0.001$] and $r_s=0.3$ [$P=0.04$]).

Conclusion: The increased SBPV is associated with impaired diurnal blood pressure profile (DBPP) and structural and functional changes in blood vessels, in particular, an increase in SBPc and PP in the aorta, and CIMT thickening, which characterizes increased BPV as a predictor of vascular remodeling in patients with uncontrolled AH.(**International Journal of Biomedicine. 2023;13(3):66-71.**)

Keywords: arterial hypertension • blood pressure variability • 24-hour ambulatory blood pressure monitoring • target organ damage

For citation: Yuldasheva AD, Khamidullaeva GA. Blood Pressure Variability: Marker or Predictor of Cardiovascular Risk? International Journal of Biomedicine. 2023;13(3):66-71. doi:10.21103/Article13(3)_OA2

Abbreviations

ABPM, 24-hour ambulatory blood pressure monitoring; **AH**, arterial hypertension; **ARV**, average real variability; **BP**, blood pressure; **BPV**, BP variability; **BMI**, body mass index; **CIMT**, carotid intima-media thickness; **DBP**, diastolic BP; **DBPP**, diurnal blood pressure profile; **DBPV**, DBP variability; **GFR**, glomerular filtration rate; **IVST**, interventricular septal thickness; **LVDD**, LV diastolic dysfunction; **LVH**, left ventricular hypertrophy; **MAU**, microalbuminuria; **PP**, pulse pressure; **PPc**, central pulse pressure; **PWV**, pulse wave velocity; **PWT**, posterior wall thickness; **SBPV**, SBP variability; **SBP**, systolic BP; **uACR**, urine albumin-creatinine ratio.

Introduction

High blood pressure (BP) is a leading risk factor for cardiovascular disease. BP shows marked fluctuations in the short and long term.[1] Such fluctuations over time, expressed in appropriate terms of descriptive statistics (standard deviation, coefficient of variation), are called BP variability (BPV). Regardless of the mean BP value, short-term and long-term BPV are associated with the development and progression of target organ damage and predictors of cardiovascular complications and mortality.[2,3]

For a long time, BPV was considered as a random variable that does not deserve attention when working with a patient. The impetus for the beginning of BPV study was the introduction into clinical practice of the technique of daily monitoring of blood pressure (ABPM) in the 1970s. One of the first works concerning the study of BP variability dates back to the early 1990s when Italian scientist Frattola and colleagues,[4] using invasive 24-hour BP monitoring, demonstrated the relationship between increased BPV and the severity of target organ damage. All markers of target organ damage (microalbuminuria, increased PWV, left ventricular hypertrophy, and atherosclerotic plaques in the carotid arteries) are independent predictors of death from cardiovascular disease.

In 2000, *Circulation* published an article by Dirk Sander and co-authors[5] devoted to the study of the association of BPV with the risk of early progression of atherosclerosis in patients with hypertension. In 2010, a number of publications appeared with the results of the ASCOT BPLA study on BPV, in which, for the first time, BP was assessed not by the results of ABPM but within and between visits. Thus, in *The Lancet*, the results of an analysis of BPV, conducted by Professor Peter Rothwell,[6,7] were published, according to which high long-term variability in systolic blood pressure (SBP) has a much more pronounced direct relationship with the frequency of cerebrovascular and coronary events than the average level of SBP in the brachial artery.

The purpose of the present study was to evaluate the prognostic significance of increased BPV in patients with arterial hypertension (AH).

Materials and Methods

The study consisted of two stages. In the first stage, a retrospective analysis of 365 ABPM results was carried out. As a result of the analysis, 271 patients aged 56.1±10.0 years with uncontrolled AH Grades 1-3 (ESC/ESH, 2018) were included in this study.

Exclusion criteria were symptomatic hypertension, acute coronary syndrome, chronic heart failure (NYHA FC>III), cardiac arrhythmia, history of stroke and myocardial infarction, diabetes, renal impairment, severe co-morbidities.

Office BP was measured using a mercury sphygmomanometer, according to Korotkov's method. BP was measured 3 times, and the means of these measurements were used in the analyses. The 24-hour ABPM was performed using a BR-102 plus (SCHILLER, Switzerland). BP was measured during the daytime (07:00–23:00) every 30 min and at night (23:00–07:00) every 60 min. The interpretation of the results was based on generally accepted recommendations for ABPM quality criteria: monitoring duration of at least 23 hours, 50 successful measurements, and no "gaps" in the record lasting more than 1 hour.

Depending on the values of BPV, AH patients were divided into two groups: Group 1 consisted of patients with normal BPV (n=145), and Group 2 consisted of patients with increased BPV (n=126). When creating groups with increased and normal variability in SBP and DBP, we conditionally set the threshold levels of daytime SBP variability (SBPV) – 15 mmHg, daytime DBP variability (DBPV) – 14 mmHg, and nighttime SBPV and DBPV – 15 mmHg and 12 mmHg, respectively.

The second stage included 91 patients with uncontrolled hypertension without permanent antihypertensive therapy who had increased SBPV, according to ABPM. The mean age of the patients was 52.8±11.9 years.

The pulse contour analysis was carried out using the SphygmoCor device (AtCor Medical, Australia), which obtains peripheral arterial pressure waveforms by applying an arterial applanation tonometer to the wrist. Such indicators as the central SBP (SBPc), central DBP (DBPc), central PP (PPc), and PWV were analyzed.

All patients underwent echocardiography with the determination of the left ventricular mass index (LVMI), ultrasound examination of the carotid intima-media thickness (CIMT), as well as the determination of the level of microalbuminuria (MAU), blood creatinine, and glomerular filtration rate (GFR) calculation according to the CKD-EPI equation.

Statistical analysis was performed using the statistical software package SPSS version 26.0 (SPSS Inc, Armonk, NY: IBM Corp). The normality of distribution of continuous variables was tested by the Kolmogorov-Smirnov test with the Lilliefors correction and Shapiro-Wilk test. Baseline characteristics were summarized as frequencies and percentages for categorical variables and as mean± standard deviation (SD) for continuous variables. For data with normal distribution, inter-group comparisons were performed using Student's t-test. Spearman's rank correlation coefficient (r_s) was calculated to measure the strength and direction of the relationship between two variables. A probability value of $P<0.05$ was considered statistically significant.

The study protocol was reviewed and approved by the Ethics Committee of the Republican Specialized Centre of Cardiology. All participants provided written informed consent.

Results

At the first stage, after analyzing the data of 271 ABPM in patients with uncontrolled hypertension, we obtained a wide range of characteristics of SBPV and DBPV. In 153(56.4%) patients, an increased average 24-h SBPV of 16.1±4.4mm was noted. Increased average 24-h DBPV (12.6±3.4 mmHg) was noted in 84(31%) patients.

In the group with increased BPV, the average daytime SBPV and DBPV were 19.1±4.2 and 13.8±3.6 mmHg, respectively. The average nighttime SBPV and DBPV were 15.5±6.1 and 12.4±7.7 mmHg. We found statistically significant differences between the AH patients with normal BPV and increased BPV. Thus, in the group with normal BPV, compared with increased BPV, the parameters of the average 24-h SBP, daytime SBP, and nighttime SBP were lower by 6mmHg (141±14.6 vs. 147.2±20.2 mmHg; $P<0.004$), 6 mmHg (142.8±15.1 vs. 148.4±20.7 mmHg; $P<0.01$), and 7 mmHg (136.2±15.5 vs. 143.8±21.4 mmHg; $P<0.001$), respectively.

In addition, between the groups with normal BPV and increased BPV, there were statistically significant differences in the degree of nocturnal fall in SBP: 5.4±10.7 mmHg and 2.9±8.3 mmHg, respectively ($P<0.03$) (Table 1). There was a greater tendency for higher values of the daytime and nighttime load of SBP and DBP in the group with increased BPV than in the group with normal BPV. The value of pulse pressure (PP) also prevailed in the group with increased BPV, compared with normal BPV (62±14.3 mmHg versus 59.6±11.7 mmHg, but without statistically significant differences (Table 1).

When assessing nocturnal BP decrease (dipping) in AH patients with normal and increased BPV, it turned out that most patients in both groups had an unfavorable daily BP index. In all patients, the pathological variants of DBPP were found, among which a "non-dipper" variant prevailed (51% of cases in the group with normal BPV and 42.8% in the group with increased BPV). In the group with normal BPV, 25.5% of cases had the optimal degree of nocturnal SBP reduction (dipper), while in the group with increased BPV it was 19.8%. In the group with normal BPV, there were 1.6 times fewer people with a steady increase in night SBP (night-peaker) than in the group with increased BPV (22.7% and 36.5%, respectively), which has an important prognostic value. Patients with an increased degree of nocturnal SBP reduction (over dipper) were 0.60% and 0.79%, respectively. No statistically significant differences were found when comparing the indicators of nocturnal BP-dipping.

The second stage analysis, where 91 patients with uncontrolled hypertension and increased SBPV were examined, showed that a high cardiovascular risk characterized the patients. Thus, more than 80% of patients had increased body weight and obesity, half were diagnosed with LV hypertrophy and LV diastolic dysfunction, and 60% were diagnosed with increased PWV and thickening of CIMT (Table 2).

Evaluation of BPV during the office BP measurement showed that the number of patients with a difference in SBP of more than 5 mmHg between the first and second measurements amounted to 15(16.4%) patients. Between the second and third measurements, the difference was also

Table 1.
ABPM indicators considering BPV.

Parameter	Normal BPV		Increased BPV		*P*-value
	M±SD	95% CI	M±SD	95% CI	
Average 24-h SBP, mmHg	141±14.6	139-143	147.2±20.2	143.7-150.7	0.004
Average 24-h DBP, mmHg	83.3±12.07	81-85	85.6±13.4	83.2-87.9	0.138
Average daytime SBP, mmHg	142.8±15.1	140-145	148.4±20.7	144.7-152	0.01
Average daytime DBP, mmHg	84.9±12.6	82.9-86.9	86.9±13.7	84.5-89.3	0.211
Average nighttime SBP, mmHg	136.2±15.5	133.7-138.72	143.8±21.4	140.1-147.6	0.0001
Average nighttime DBP, mmHg	78.7±11.8	76.8-80.6	81.6±14.4	79.1-84.1	0.069
Nocturnal SBP fall,%	5.4±10.7	3.7-7.2	2.9±8.3	1.4-4.4	0.03
Nocturnal DBP fall,%	7.4±8.9	6-9	6.3±9.6	4.6-8.05	0.328
Daytime SBP load, %	57.6±25.3	53.5-61.7	62.3±22.2	58.4-66.2	0.107
Daytime DBP load, %	39.1±30.7	34.1-44.1	43.1±29.1	38-48.2	0.273
Nighttime SBP load, %	83.4±19.7	80.2-86.6	86.2±18.8	82.9-89.5	0.234
Nighttime DBP load, %	48.8±32	43.6-53.9	51.5±32.7	45.8-57.2	0.493
PP, mmHg	59.6±11.7	57.7-61.53	62±14.3	59.5-64.5	0.129

observed in 16(17.5%) patients, and between the first and third measurements - in 50(55%) patients. In 10(11%) patients, we did not find a difference >5 mmHg between measurements.

Table 2.

Clinical characteristics of AH patients (n=91) with increased SBPV

Parameter		
SBP, mmHg (M±SD / 95% CI)	161.3±14.5	157.3-165.3
DBP, mmHg (M±SD / 95% CI)	93.1±10.6	90.1-96.04
BMI >30 kg/m^2, (n / %)	48	52.7%
BMI >25<30 kg/m^2, (n / %)	25	27.4%
LVH, (n / %)	31	34%
LVDD, (n / %)	16	17.5%
PWV >10 m/sec, (n / %)	31	34%
CIMT ≥0.9 mm, (n / %)	28	30.7%

In AH patients with increased BPV, the assessment of the relationship between BP and ABPM data on the Chaddock scale revealed a statistically significant moderate direct correlation between the average 24-h SBP and the average 24-h and daytime SBPV (r_s=0.49 and r_s=0.40 respectively, *P*<0.001 in all cases). A statistically significant moderate to weak direct correlation also was found between the average daytime SBP, and the average 24-h and daytime SBPV (r_s=0.45 and r_s=0.37, respectively, *P*<0.001 in all cases). A moderate direct correlation was found between nighttime SBP and 24-hour SBPV (r_s=0.52, *P*<0.001) and between nighttime SBP and daytime SBPV (r_s=0.42, *P*<0.001). Weak direct correlations were also found between the average 24-h SBPV and SBPc (r_s=0.34, *P*<0.001), as well as between the average 24-h and daytime SBPV and PPc (r_s=0.33 and r_s=0.32, respectively, *P*<0.001 in all cases). A weak direct correlation was found between CIMT and the average 24-h and daytime SBPV (r_s=0.37 [*P*<0.001] and r_s=0.3 [*P*=0.04]). We did not find statistically significant correlations between the increased SBPV, parameters of the functional state of the kidneys, and indicators of the structural state of the left ventricle. It should also be emphasized that increased nighttime SBPV was also not significantly associated with the studied parameters (Table 3).

Table 3.

Correlation analysis between increased SBPV, ABPM data, and target organ damage parameters.

Parameter	Average 24-h SBPV		Average daytime SBPV		Average nighttime SBPV	
	r_s	*P*	r_s	*P*	r_s	*P*
Average 24-h SBP	0.49	<0.001	0.40	<0.001	0.037	0.724
Average daytime SBP	0.45	<0.001	0.37	<0.001	0.015	0.884
Average nighttime SBP	0.52	<0.001	0.42	<0.001	0.11	0.289
SBPc	0.34	0.001	0.33	0.001	0.08	0.443
DBPc	0.16	0.118	0.17	0.1	-0.1	0.36
PPc	0.33	0.002	0.32	0.001	0.14	0.131
PWV	-0.193	0.06	-0.2	0.06	-0.07	0.5
CIMT	0.37	<0.001	0.3	0.04	0.2	0.06
IVST	0.22	0.03	0.18	0.07	-0.33	0.755
PWT	0.071	0.5	0.04	0.65	-0.026	0.8
LVMI	0.071	0.5	0.03	0.75	0.055	0.6
uACR	0.02	0.8	0.05	0.63	0.003	0.974
GFR	-0.12	0.2	-0.14	0.16	-0.045	0.67
Creatinine	0.14	0.17	0.244	0.18	0.15	0.14
MAU	-0.21	0.845	-0.46	0.65	-0.023	0.83

Discussion

The relationship between increased BPV and cardiovascular diseases has been shown in previous studies.[8-11] A number of studies reported significant associations between high average real variability (ARV) and the presence and progression of subclinical organ damage.[12-16]

In our patients with uncontrolled AH and increased SBPV, the average 24-h, daytime and nighttime SBP values were higher than in AH patients with normal SBPV. It can be assumed that impaired BPV is associated with an additional increase in SBP and significantly increases the risk of damage to target organs. Analysis of DBPP showed that in the AH patients with increased SBPV, there was a significantly low rate of nighttime SBP reduction, thereby placing an additional load on the target organs.

In addition, data from a number of studies indicate that increased SBP is associated with the progression of atherosclerosis. Thus, in a well-known meta-analysis,[17] after adjusting for demographic indicators, a correlation was found between SBP and the progression of atherosclerosis. After adjusting for age, patients' PWV was shown to increase by 1.14 m/s for every 20 mmHg increase in SBP. However, the correlation between mean BP or DBP and PWV was weak, while it was negative in our study. Many investigators have studied potential mechanisms for the relationship between BPV and poor cardiovascular outcomes. First, BPV may be a marker of arterial stiffness associated with reduced compliance of large elastic arteries. In a study by Tursunova et al.,[18] increased daytime SBPV and PP variability in patients with isolated systolic AH correlated with an increase in arterial stiffness, compared with patients with systolic-diastolic AH, and an increased vascular stiffness (carotid-femoral PWV >10 m/s) increased the risk of developing LV concentric hypertrophy and concentric remodeling, which adversely affected the prognosis.[19]

Our data on the relationship between BPV and kidney damage are consistent with a prospective study by Hung et al.,[20] which included 300 Han Chinese participants with hypertension (mean age of 63.5 years) and investigated whether short-term BPV is correlated with hypertensive nephropathy. Five different BPV parameters were derived from ambulatory BP monitoring (ABPM), including standard deviation (SD), weighted SD (wSD), coefficient of variation (CoV), successive variation (SV), and ARV. The renal event was defined as >50% reduction in baseline eGFR. The Cox proportional hazard regression (HR) model to assess the independent effects of BPV showed that 24-h SBP (HR=1.105; 95% CI=1.020-1.197, *P*=0.015) and 24-h DBP (HR=1.162; 95% CI=1.004-1.344, *P*=0.044) were independently associated with renal events. However, BPV parameters were only associated with renal events univariately, but not after adjusting for baseline characteristics, 24-h mean BP, and office BP.

In this study, we found a direct correlation between CIMT and the average 24-h and daytime SBPV. This is consistent with a study by Xiong et al.[15] who provided the evidence that, for the subjects from the southern area of China, all of the indices of SBPV for daytime and 24 h had significant correlation with CIMT.

Short-term variability of 24-hour SBP showed an independent, although moderate, relation to aortic stiffness in hypertension in a study by Schillaci et al.[16] These results were consistent with our findings.

Conclusion

Our data showed that increased BPV is associated with impaired diurnal blood pressure profile and structural and functional changes in blood vessels, in particular, an increase in SBPc and PP in the aorta, and CIMT thickening, which characterizes increased BPV as a predictor of vascular remodeling in patients with uncontrolled AH. A well-controlled 24-h and daytime SBPV should be prioritized in managing AH.

Competing Interests

The authors declare that they have no competing interests.

References

1. Lewington S, Clarke R, Qizilbash N, Peto R, Collins R; Prospective Studies Collaboration. Age-specific relevance of usual blood pressure to vascular mortality: a meta-analysis of individual data for one million adults in 61 prospective studies. Lancet. 2002 Dec 14;360(9349):1903-13. doi: 10.1016/s0140-6736(02)11911-8. Erratum in: Lancet. 2003 Mar 22;361(9362):1060.
2. Stevens SL, Wood S, Koshiaris C, Law K, Glasziou P, Stevens RJ, McManus RJ. Blood pressure variability and cardiovascular disease: systematic review and meta-analysis. BMJ. 2016 Aug 9;354:i4098. doi: 10.1136/bmj.i4098.
3. Parati G, Bilo G, Kollias A, Pengo M, Ochoa JE, Castiglioni P, et al. Blood pressure variability: methodological aspects, clinical relevance and practical indications for management - a European Society of Hypertension position paper ∗. J Hypertens. 2023 Apr 1;41(4):527-544. doi: 10.1097/HJH.0000000000003363.
4. Frattola A, Parati G, Cuspidi C, Albini F, Mancia G. Prognostic value of 24-hour blood pressure variability. J Hypertens. 1993 Oct;11(10):1133-7. doi: 10.1097/00004872-199310000-00019.
5. Sander D, Kukla C, Klingelhöfer J, Winbeck K, Conrad B. Relationship between circadian blood pressure patterns and progression of early carotid atherosclerosis: A 3-year follow-up study. Circulation. 2000 Sep 26;102(13):1536-41. doi: 10.1161/01.cir.102.13.1536.
6. Rothwell PM, Howard SC, Dolan E, O'Brien E, Dobson JE, Dahlöf B, Sever PS, Poulter NR. Prognostic significance of

***Corresponding author**: Prof. Gulnoz A. Khamidullaeva, PhD, ScD. The Republican Specialized Center of Cardiology, Tashkent, Uzbekistan. E-mail: gulnoz0566@mail.ru*

visit-to-visit variability, maximum systolic blood pressure, and episodic hypertension. Lancet. 2010 Mar 13;375(9718):895-905. doi: 10.1016/S0140-6736(10)60308-X.
7. Rothwell PM, Howard SC, Dolan E, O'Brien E, Dobson JE, Dahlöf B, Poulter NR, Sever PS; ASCOT-BPLA and MRC Trial Investigators. Effects of beta blockers and calcium-channel blockers on within-individual variability in blood pressure and risk of stroke. Lancet Neurol. 2010 May;9(5):469-80. doi: 10.1016/S1474-4422(10)70066-1.
8. Mehlum MH, Liestøl K, Kjeldsen SE, Julius S, Hua TA, Rothwell PM, Mancia G, Parati G, Weber MA, Berge E. Blood pressure variability and risk of cardiovascular events and death in patients with hypertension and different baseline risks. Eur Heart J. 2018 Jun 21;39(24):2243-2251. doi: 10.1093/eurheartj/ehx760.
9. Palatini P, Saladini F, Mos L, Fania C, Mazzer A, Cozzio S, Zanata G, Garavelli G, Biasion T, Spinella P, Vriz O, Casiglia E, Reboldi G. Short-term blood pressure variability outweighs average 24-h blood pressure in the prediction of cardiovascular events in hypertension of the young. J Hypertens. 2019 Jul;37(7):1419-1426. doi: 10.1097/HJH.0000000000002074.
10. de Havenon A, Fino NF, Johnson B, Wong KH, Majersik JJ, Tirschwell D, Rost N. Blood Pressure Variability and Cardiovascular Outcomes in Patients With Prior Stroke: A Secondary Analysis of PRoFESS. Stroke. 2019 Nov;50(11):3170-3176. doi: 10.1161/STROKEAHA.119.026293.
11. Mena LJ, Felix VG, Melgarejo JD, Maestre GE. 24-Hour Blood Pressure Variability Assessed by Average Real Variability: A Systematic Review and Meta-Analysis. J Am Heart Assoc. 2017 Oct 19;6(10):e006895. doi: 10.1161/JAHA.117.006895.
12. Filomena J, Riba-Llena I, Vinyoles E, Tovar JL, Mundet X, Castañé X, Vilar A, López-Rueda A, Jiménez-Baladó J, Cartanyà A, Montaner J, Delgado P; ISSYS Investigators. Short-Term Blood Pressure Variability Relates to the Presence of Subclinical Brain Small Vessel Disease in Primary Hypertension. Hypertension. 2015 Sep;66(3):634-40; discussion 445. doi: 10.1161/HYPERTENSIONAHA.115.05440.
13. Leoncini G, Viazzi F, Storace G, Deferrari G, Pontremoli R. Blood pressure variability and multiple organ damage in primary hypertension. J Hum Hypertens. 2013 Nov;27(11):663-70. doi: 10.1038/jhh.2013.45.
14. Mulè G, Calcaterra I, Costanzo M, Morreale M, D'Ignoto F, Castiglia A, Geraci G, Rabbiolo G, Vaccaro F, Cottone S. Average real variability of 24-h systolic blood pressure is associated with microalbuminuria in patients with primary hypertension. J Hum Hypertens. 2016 Mar;30(3):164-70. doi: 10.1038/jhh.2015.66.
15. Xiong H, Wu D, Tian X, Lin WH, Li C, Zhang H, Cai Y, Zhang YT. The relationship between the 24 h blood pressure variability and carotid intima-media thickness: a compared study. Comput Math Methods Med. 2014;2014:303159. doi: 10.1155/2014/303159.
16. Schillaci G, Bilo G, Pucci G, Laurent S, Macquin-Mavier I, Boutouyrie P, Battista F, Settimi L, Desamericq G, Dolbeau G, Faini A, Salvi P, Mannarino E, Parati G. Relationship between short-term blood pressure variability and large-artery stiffness in human hypertension: findings from 2 large databases. Hypertension. 2012 Aug;60(2):369-77. doi: 10.1161/HYPERTENSIONAHA.112.197491.
17. Oganov RG, Deev AD, Gorbunov VM. [Comparative informativeness of various methods of analyzing the results of daily monitoring of blood pressure in evaluating the effectiveness of antihypertensive therapy]. Cardiovascular Therapy and Prevention. 2003;1:17–25. [Article in Russian].
18. Tursunova NB, Nizamov UI, Kurbanov RD, Khamidullaeva GA, Abdullaeva GJ, Shek AB. The relationship between the parameters of blood pressure variability and arterial wall stiffness in patients with arterial hypertension. International Journal of Biomedicine. 2019;9(3):197-201.
19. Mancia G, Fagard R, Narkiewicz K, Redón J, Zanchetti A, Böhm M, et al.; Task Force Members. 2013 ESH/ESC Guidelines for the management of arterial hypertension: the Task Force for the management of arterial hypertension of the European Society of Hypertension (ESH) and of the European Society of Cardiology (ESC). J Hypertens. 2013 Jul;31(7):1281-357. doi: 10.1097/01.hjh.0000431740.32696.cc.
20. Hung MH, Huang CC, Chung CM, Chen JW. 24-h ambulatory blood pressure variability and hypertensive nephropathy in Han Chinese hypertensive patients. J Clin Hypertens (Greenwich). 2021 Feb;23(2):281-288. doi: 10.1111/jch.14108.

International Journal of Biomedicine 13(3) (2023) 72-78
http://dx.doi.org/10.21103/Article13(3)_OA3

ORIGINAL ARTICLE

Cardiology

INTERNATIONAL JOURNAL OF BIOMEDICINE

The 4q25/*PITX2* SNP rs6817105 and Atrial Fibrillation in Uzbek Patients with Arterial Hypertension

G. M. Radzhabova[1], G. Zh. Abdullaeva[1*], D. V. Zakirova[2], M. T. Pulatova[1], N. Kh. Sherbadalova[1], M. N. Khatamova[1], Z. T. Mashkurova[1], N. N. Ibrokhimov[2], A. A. Abdullaev[2], M. A. Sadulloeva[1]

[1]*Republican Specialized Center of Cardiology*
[2]*Center for Advanced Technologies*
Tashkent, Uzbekistan

Abstract

Background: Atrial fibrillation (AF) is one of the most common cardiac arrhythmias and a major predictor of morbidity and mortality. In recent years, genome-wide association studies (GWAS) have identified common genetic variants associated with a higher risk of AF. The aim of our research was to study the possible association of the 4q25/*PITX2* SNP rs6817105 with the risk of developing AF in patients with arterial hypertension (AH) in the Uzbek population.

***Methods and Results*:** The study included 142 AH (Grades 1-3; ESC/ESH, 2018) patients of Uzbek nationality who were initially diagnosed with paroxysmal form (15[10.6%]), persistent form (43[30.3%]), and permanent form of AF (84[59.1%]). The mean age of these patients was 64.8±10.9 years. AF was verified using ECG Holter monitoring. The control group (n=88) consisted of AH patients without AF with a mean age of 56.5±12.3 years. Echocardiography was carried out according to the recommendations of the American Society of Echocardiography in M- and B-modes. We genotyped SNP rs6817105 (T>C) and examined the relationships among rs6817105 genotype, clinical characteristics, and echocardiographic parameters in AH patients with AF and non-AF AH patients (controls).

In AH patients with AF and AH patients without AF, the 4q25/*PITX2* SNP rs6817105 genotype distribution was as follows: CC=72(50.7%), CT=60(42.3%), TT=10(7.0%) [χ^2=45.690; *P*=0.000], and CC=34(38.6%), CT=37(42.1%), TT=17(19.3%) [χ^2=7.932; *P*=0.019], respectively. The rs6817105 minor C allele frequency was significantly higher in AH patients with AF than in non-AF AH patients (71.8% vs. 59.7%, *P*=0.007). Analysis of the multiplicative model for the rs6817105 SNP showed a significant risk of AF in the carriage of the C allele (OR=1.72, 95% CI: 1.16-2.56, *P*=0.007). The dominant and additive models for the rs6817105 SNP showed a significant risk of AF with the carriage of the CC+CT genotypes (OR=3.16, 95% CI: 1.37-7.27, *P*=0.005) and the homozygous CC genotype (OR=1.63, 95% CI: 0.95-2.81, *P*=0.008), respectively. The allelic distribution showed that the carriage of the C allele was dominant in permanent and persistent AF (110/68.75% vs. 50/31.25% for the T allele [(χ2=22.50, *P*=0.000], and 64(74.42%) vs. 22(25.58%) for the T allele [χ^2=20.512, *P*=0.000], respectively). Among AH patients with paroxysmal AF, the C allele prevailed to the greatest extent: 20(90.9%) vs. 2(9.1%) for the T allele (χ^2=14.727, *P*=0.000), indicating a significant accumulation of the C allele and CC genotype among patients with paroxysmal AF. In general, in AH patients with AF, carriers of the CC genotype, the left atrial volume index (LAVI) was significantly higher than the carriers of the CT and TT genotypes: 46.8±13.9 ml/m^2 vs. 40.4±13.0 ml/m^2 and 36.1±11.0 ml/m^2, respectively (*P*=0.0083).

Conclusion: The present study is the first molecular genetic study investigating the association of 4q25/*PITX2* SNP rs6817105 in AH patients with AF in the Uzbek population. Our results indicate the rs6817105 minor C allele and CC genotype are associated with the risk of developing AF in AH patients of Uzbek nationality. The highest accumulation of the rs6817105 minor C allele and CC genotype is found in paroxysmal AF. In carriers of the rs6817105 CC genotype, the LAVI was significantly larger than in carriers of the CT and TT genotypes.(**International Journal of Biomedicine. 2023;13(3):72-78.**)

Keywords: atrial fibrillation • rs6817105 • arterial hypertension • left atrial volume index

For citation: Radzhabova GM, Abdullaeva GZh, Zakirova DV, Pulatova MT, Sherbadalova NKh, Khatamova MN, Mashkurova ZT, Ibrokhimov NN, Abdullaev AA, Sadulloeva MA. The 4q25/*PITX2* SNP rs6817105 and Atrial Fibrillation in Uzbek Patients with Arterial Hypertension. International Journal of Biomedicine. 2023;13(3):72-78. doi:10.21103/Article13(3)_OA3

Abbreviations

AH, arterial hypertension; **AF**, atrial fibrillation; **BP**, blood pressure; **DBP**, diastolic BP; **GWAS**, genome-wide association studies; **IVST**, interventricular septal thickness; **LVMI**, left ventricular mass index; **LVH**, left ventricular hypertrophy; **LAD**, left atrial dimension; **LAV**, left atrial volume; **LAVI**, left atrial volume index; **LVESD**, left ventricular end-systolic dimension; **LVEDD**, left ventricular end-diastolic systolic dimension; **PWT**, posterior wall thickness; **SBP**, systolic BP; **SNP**, single nucleotide polymorphism.

Introduction

Arterial hypertension (AH) is one of the main factors causing a high risk of cardiovascular complications and mortality. Overall, according to ESH/ESC data for 2018, the prevalence of hypertension is 30%-45% of the general population, with a sharp increase with age. Today, 15%-40% of the adult population suffers from hypertension worldwide, and in people over 65 years of age, hypertension has been detected in 30%-50% of cases. Of patients with hypertension, 76% are at risk of dying within 10 years.[1] The existence of a relationship between high blood pressure (BP) and the risk of developing new-onset atrial fibrillation (AF) has been demonstrated.[2] Experimental evidence suggests that electrical and structural remodeling changes in the hypertensive heart may predispose to AF.[3]

AF is one of the most common cardiac arrhythmias and a major predictor of morbidity and mortality. AF is a polygenic and polyetiological disease. Of no minor importance are racial and ethnic differences in the prevalence of AF in the general population, noted in several studies. Factors that increase the risk of developing AF include age, hypertension, cardiomyopathy, valvular disease, and genetic predisposition. According to the literature, there is a familial form of AF, indicating the importance of genetic factors in the development of AF. Thus, mutations of various genes associated with ion channels have been identified, but it should be noted that such findings are extremely rare.[4]

In recent years, GWAS have identified common genetic variants associated with a higher risk of AF. The first GWAS for AF identified a chromosome 4q25 locus conferring the risk of AF in Icelanders.[5] To date, GWAS have identified ≈140 genetic loci associated with AF,[6] located near genes coding for ion channels, developmental transcription factors, structural remodeling, and cytoskeletal proteins.[7] Among them, variants at 4q25, located upstream of the *PITX2* gene, demonstrate a strong association with AF in European and Japanese populations. GWAS have reported a strong association of the SNP rs6817105 (T>C) on chromosome 4q25 with AF.[8-10]

The paired-related homeobox (*PITX2*) gene is the nearest gene to the 4q25 AF-associated SNPs and is the most likely target for these 4q25 AF susceptibility variants.[11] The *PITX2* gene encoding for the transcription factor PITX2 (paired-like homeodomain transcription factor 2), one of the homeobox transcription factors, is a main player in the regulation of asymmetric organogenesis. The *PITX2*, the closest gene to rs6817105, is a critical mediator of left-side morphogenesis.[12-15] *PITX2* regulates left-right differentiation (including sinoatrial node restriction to the right atrium), and deficiency leads to structural and electrical remodeling of the heart, which may lead to AF through different mechanisms.[7,16] Cardiac expression of *PITX2* is almost exclusively restricted to the left atrium in the normal adult heart.[17] The left atrium and sleeves of the pulmonary vein are potential substrates for AF development, and the pulmonary vein is often the origin of ectopic foci in AF patients.[18]

In mice models, reduced expression of PITX2c during development results in AF inducibility upon stimulation, which implicates a developmental role of this gene in AF susceptibility.[17,19,20] A number of researchers have observed that reduction in PITX2 resulted in potassium and calcium channel gene dysregulation, ultimately leading to a shortening of the atrial action potential, a depolarized resting membrane potential, and a predisposition to AF.[18,20,21]

Tomomori et al.[8] found that the rs6817105 minor C allele frequency (MAF) was significantly higher in AF patients than in non-AF controls (66% vs. 47%, OR 2.12, $P=4.9\times10^{-26}$). Sinus node dysfunction was independently associated with the rs6817105 C allele in these AF patients, and left atrium enlargement was independently associated with the rs6817105 minor C allele in AF patients. The maximum sinus node recovery time (SNRT) and corrected SNRT (CSRT) increased with the number of minor C alleles and were longest in patients with the CC genotype.

Unfortunately, studies on the search for molecular genetic predictors of AF in AH patients in the Uzbek population are rare. Previously, a group of researchers studied only the association of the *ATFB5* SNP rs2200733 with the risk of developing AF in people of Uzbek nationality.[22]

The aim of our research was to study the possible association of the 4q25/*PITX2* SNP rs6817105 with the risk of developing AF in patients with hypertension in the Uzbek population.

Materials and Methods

The study included 142 AH (Grades 1-3; ESC/ESH, 2018) patients of Uzbek nationality who were initially diagnosed with paroxysmal form (15[10.6%]), persistent form (43[30.3%]), and permanent form of AF (84[59.1%]). The mean age of these patients was 64.8±10.9 years. The control group (n=88) consisted of AH patients without AF with a mean age of 56.5±12.3 years. The presence of AF was ruled out based on the history, the absence of symptoms of AF on physical examination, and a normal electrocardiogram at the time of inclusion in the study.

AF was classified as paroxysmal, persistent, and permanent in accordance with the ACC/AHA/ESC guidelines for AF.[23] The diagnosis of AF was based on ECG findings and/or Holter ECG data according to standard diagnostic criteria.[24] AF was verified using ECG Holter monitoring (LABTECH Cardiospy, Hungary).

Office BP was measured using a mercury sphygmomanometer, according to Korotkov's method. BP was measured 3 times, and the means of these measurements were used in the analyses. Echocardiography was carried out according to the recommendations of the American Society of Echocardiography in M- and B-modes[25] using Philips Clearview-350 «Affiniti 30» Ultrasound Machine (the Netherlands). The following parameters were measured and calculated: IVST, PWT, LVEDD, LVESD, LAD, LAVI, and LVM (LVM was calculated using the formula R. Devereux. (1994) LVM was indexed to body surface area (LVMI). LVM was calculated using the formula R. Devereux.[26] Left ventricular hypertrophy (LVH) was defined as LVMI of >95g/m^2 (for women) and >115g/m^2 (for men).[1]

Exclusion criteria were symptomatic hypertension, valvular heart disease, acute coronary syndrome, chronic heart failure (NYHA FC>III), cardiac arrhythmia, history of stroke and myocardial infarction, diabetes, renal impairment, severe co-morbidities, orthostatic hypotension, artificial pacemaker, QT>480 ms, documented, previous episodes of persistent ventricular arrhythmia, WPW syndrome, Brugada syndrome, bradycardia (HR less than 60 bpm), blood clots in the LA, thyroid dysfunction, sinus node dysfunction, SSS, second-third-degree AV block.

To perform genotyping of blood samples for rs6817105 SNP, genomic DNA was isolated from whole blood using the ArtDNA MiniSpin kit (ArtBioTech LLC, BY) according to the manufacturer's standard protocol. The quantity and quality of DNA were determined on a NanoDrop 2000 spectrophotometer (Thermo Scientific™ Wilmington, DE, USA).

PCR was performed on the QuantStudio 5 Dx Real-Time PCR System (Applied Biosystems, USA). The reaction was carried out in a volume of 10µl using the TaqMan® Genotyping Assays kit (Thermo Fisher Scientific, USA) according to the manufacturer's standard protocol. The reaction mixture contained of 10ng genomic DNA, 5µl TaqMan Genotyping Master Mix, 0.5µl TaqMan Genotyping Assays. Sample genotyping results were analyzed using the Thermo Fisher Scientific Design & Analysis 2.6.0 2021 program and entered for primary processing in Microsoft Excel-2019.

Statistical analysis was performed using the statistical software «Statistica» (v10.0, StatSoft, USA). Baseline characteristics were summarized as frequencies and percentages for categorical variables and as mean± standard deviation (SD) for continuous variables. Multiple comparisons were performed with one-way ANOVA and Tukey HSD post-hoc test. Genetic markers for HWE were tested. One-way table (chi-square goodness-of-fit test) was used to test categorical probabilities when one categorical variable had more than two levels. Four genetic models were analyzed (https://calc.pcr24.ru/index.php): the dominant model, the recessive model, the multiplicative model, and the additive model (the Cochran-Armitage trend test). Odds ratios (ORs) and 95% confidence intervals (CIs) were calculated. A probability value of $P \leq 0.05$ was considered statistically significant.

The study protocol was reviewed and approved by the Ethics Committee of the Republican Specialized Centre of Cardiology. All participants provided written informed consent.

Results

The distribution of polymorphic markers of the 4q25/*PITX2* SNP rs6817105 in AH patients with AF and non-AF AH patients was in HWE (Table1). In AH patients with AF and AH patients without AF, the 4q25/*PITX2* SNP rs6817105 genotype distribution was as follows: CC=72(50.7%), CT=60(42.3%), TT=10(7.0%) [χ^2=45.690; P=0.000], and CC=34(38.6%), CT=37(42.1%), TT=17(19.3%) [χ^2=7.932; P=0.019], respectively. An analysis of the frequency distribution of the rs6817105 alleles showed that the carriage of the C allele was dominant in AH patients with AF (71.8% vs. 28.2% for the T allele; χ^2=78.546, P=0.000), compared to non-AF AH patients (59.7% vs. 40.3% for the T allele; χ^2=6.568, P=0.010). Thus, the rs6817105 minor C allele frequency was significantly higher in AH patients with AF than in non-AF AH patients (71.8% vs. 59.7%, P=0.007).

Table 1.

The distribution of polymorphic markers of the 4q25/PITX2 SNP rs6817105 in AH patients with AF (case) and non-AF AH patients (control).

Genotype	Case	HWE	χ^2	P	Control	HWE	χ^2	P	Allele	Frequency of alleles	
										Case	Control
TT	0.070	0.079			0.193	0.163			T	0.282	0.403
CT	0.423	0.405	0.13	0.72	0.420	0.481	0.74	0.39	C	0.718	0.597
CC	0.507	0.516			0.386	0.356					

Analysis of the multiplicative model for the rs6817105 SNP showed a significant risk of AF in the carriage of the C allele (OR=1.72, 95% CI: 1.16-2.56, P=0.007) (Table 2).

Table 2.

Genetic predisposition to TRH (the genetic models).

Inheritance model	Allele, Genotype	Case	Control	χ^2	P	OR (95%CI)
		n=142	n=88			
Multiplicative model (χ^2 test, df=1)	T	0.282	0.403	7.30	0.007	0.58 (0.39-0.86)
	C	0.718	0.597			1.72 (1.16-2.56)
Additive model ([CATT], xi=[0,1,2], df=1)	TT	0.070	0.193	7.004	0.008	0.32 (0.14-0.73)
	CT	0.423	0.420			1.01 (0.59-1.73)
	CC	0.507	0.386			1.63 (0.95-2.81)
Dominant model (χ^2 test, df=1)	TT	0.070	0193	7.90	0.005	0,32 (0.14-0.73)
	CT+CC	0.930	0.807			3.16 (1.37-7.27)
Recessive model (χ^2 test, df=1)	TT+CT	0.493	0.614	3.18	0.07	0.61 (0,36-1.05)
	CC	0.507	0.386			1.63 (0.95-2.81)

The dominant and additive models for the rs6817105 SNP showed a significant risk of AF with the carriage of the CC+CT genotypes (OR=3.16, 95% CI: 1.37-7.27, *P*=0.005) and the homozygous CC genotype (OR=1.63, 95% CI: 0.95-2.81, *P*=0.008), respectively (Table 2).

Subsequently, the frequency distribution of the rs6817105 genotypes and alleles was analyzed considering the form of AF (Figures 1 and 2).

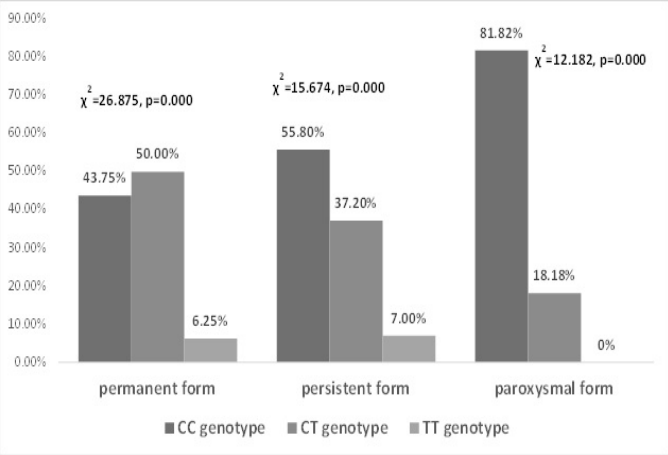

Fig. 1. *Frequency distribution of the 4q25/PITX2 SNP rs6817105 genotypes in AH patients considering the form of AF.*

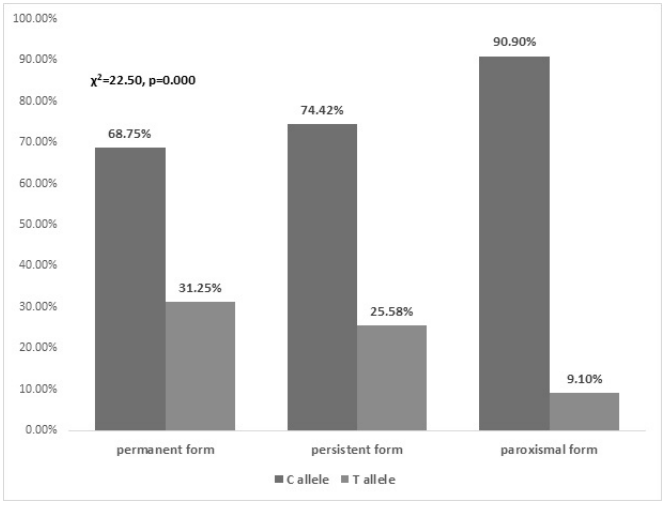

Fig. 2. *Frequency distribution of the 4q25/PITX2 SNP rs6817105 alleles in AH patients considering the form of AF.*

Among AH patients with permanent, persistent, and paroxysmal AF, the genotype distribution was as follows: CC=35(43.75%), CT=40(50%), TT=5(6.25%) (χ^2=26.875, *P*=0.000); CC=24(55.8%), CT=16(37.2%), TT=3(7.0%) (χ^2=15.674, *P*=0.000); CC=9(81.82%), CT=2(18.18%), TT=0 (χ^2=12.182, *P*=0.002), respectively.

The allelic distribution showed that the carriage of the C allele was dominant in permanent and persistent AF (110/68.75% vs. 50/31.25% for the T allele [(χ^2=22.50, *P*=0.000], and 64(74.42%) vs. 22 (25.58%) for the T allele [χ^2=20.512, *P*=0.000], respectively). Among AH patients with paroxysmal AF, the C allele prevailed to the greatest extent: 20(90.9%) vs. 2(9.1%) for the T allele (χ^2=14.727, *P*=0.000), indicating a significant accumulation of the C allele and CC genotype among patients with paroxysmal AF.

We also analyzed the initial clinical data (age, duration of AH, SBP, DBP, LAVI, LVMI) in AH patients with various AF forms, considering the rs6817105 SNP. In general, in AH patients with AF, carriers of the CC genotype, the LAVI was significantly higher than the carriers of the CT and TT genotypes: 46.8±13.9 ml/m^2 vs. 40.4±13.0 ml/m^2 and 36.1±11.0 ml/m^2, respectively (*P*=0.0083) (Table 3). A similar analysis was carried out among AH patients with paroxysmal and persistent AF. These patients were combined into one group (n=54) due to the small size of the presented sample. There were no significant differences in clinical characteristics (age, duration of hypertension, SBP, DBP, IOLR, LVMI) among rs6817105 genotypes in the patient group (Table 4). However, there was a trend toward an increase in the values of LAVI in carriers of the CC genotype.

Table 3.

Clinical characteristics of AH patients with AF considering the 4q25/PITX2 SNP rs6817105 genotypes (n=129).

Variable	Genotype			One-Way ANOVA
	CC (n=69) [1]	CT (n=50) [2]	TT (n=10) [3]	*P*-value
Age, yrs.	64.7±10.2	65.0±10.1	61.7±12.3	0.6483
AH duration, yrs.	12.8±9.1	15.4±10.8	15.3±16.4	0.3780
SBP, mmHg	146.9±25.9	143.4±26.2	147.5±26.0	0.7477
DBP, mmHg	90.4±11.03	88.6±12.9	91.8±14.6	0.6262
LAVI, ml/m^2	46.8±13.9	40.4±13.0	36.1±11.0	0.0083*
LVMI, g/m^2	280.2±104.6	269.6±101.7	230.5±75.8	0.3458

**Tukey HSD post-hoc test: $P_{[1-2]}$=0.0296, $P_{[1-3]}$=0.0507*

A similar analysis was carried out among AH patients with permanent AF (n=75). There were also no significant differences in clinical characteristics (Table 5).

Thus, the results obtained indicate the rs6817105 minor C allele and CC genotype are associated with the risk of developing AF in AH patients of Uzbek nationality. The highest accumulation of the rs6817105 minor C allele and CC genotype is found in paroxysmal AF. In carriers of the rs6817105 CC genotype, the LAVI was significantly larger than in carriers of the CT and TT genotypes.

Table 4.

Clinical characteristics of AH patients with paroxysmal and persistent AF considering the 4q25/PITX2 SNP rs6817105 genotypes (n=54).

Variable	Genotype			One-Way ANOVA
	CC (n=34)	CT (n=15)	TT (n=5)	*P*-value
Age, yrs.	62.2±10.8	61±9.49	53±14.4	0.2152
AH duration, yrs.	11.4±7.4	12.5±9.6	13.8±11.3	0.7989
SBP, mmHg	150.5±25.9	146±28.4	156±28.8	0.7457
DBP, mmHg	92.6±9.6	87.6±16.7	94±15.1	0.3856
LAVI, ml/m^2	37.4±11.8	33.0±9.1	28.9±2.24	0.1578
LVMI, g/m^2	143.0±60.2	128.6±38.9	111.6±25.7	0.3864

Table 5.

Clinical characteristics of AH patients with permanent AF considering the 4q25/PITX2 SNP rs6817105 genotypes (n=75).

Variable	Genotype			One-Way ANOVA
	CC (n=35)	CT (n=35)	TT (n=5)	*P*-value
Age, yrs.	67.2±9.1	66.5±10.1	65.8±7.5	0.9270
AH duration, yrs.	14.3±10.3	16.6±11.1	16.2±19.3	0.6927
SBP, mmHg	143.4±25.7	142.4±25.6	146.0±23.0	0.9533
DBP, mmHg	88.2±12.0	89.0±11.5	91.0±12.4	0.8722
LAVI, ml/m^2	50.4±14.4	48.2±12.0	41.2±12.7	0.3327
LVMI, g/m^2	141.7±44.2	139.0±41.9	131.1±34.1	0.8652

Discussion

The rapid development of scientific technologies has made it possible to identify new cellular and molecular levels of AH pathogenesis. To date, sufficient factual material has been accumulated on the involvement of candidate genes in the development of AH, damage to target organs, and cardiovascular complications. On the one hand, left ventricular myocardial remodeling underlies electrophysiological changes in the heart of a patient with hypertension, triggering cardiac arrhythmias, including AF. On the other hand, the literature presents gene mutations (in particular, *SCN5A*, *KCNQ*, *ATFB5*, *PITX2* gene polymorphisms), which can cause heart rhythm disturbances, including AF. Many loci associated with the development of AF have been identified to date.[27] AF is often promoted by certain combinations of genes, including the genes encoding components of renin-angiotensin-aldosterone and endothelial systems. Detection of left atrial dilatation can provide additional information and is a prerequisite for the diagnosis of diastolic dysfunction. It has been shown that LAVI>34 ml/m^2 is an independent predictor of death, heart failure, AF, and ischemic stroke.

We investigated relationships between 4q25/*PITX2* SNP rs6817105 polymorphic markers and clinical and functional parameters in Uzbek patients with AH and AF. Our results indicate a significantly greater accumulation of the rs6817105 minor C allele and CC genotype among AH patients with AF than among AH patients without AF. In AH patients with AF, carriers of the CC genotype, the LAVI was significantly higher than the carriers of the CT and TT genotypes: 46.8±14.9 ml/m^2 vs. 40.4±13.0 ml/m^2 and 36.5±11.6 ml/m^2, respectively (P=0.020). The multiplicative model for the rs6817105 SNP showed a significant risk of AF in the carriage of the C allele (OR=1.72, 95% CI: 1.16-2.56, P=0.007). The additive and recessive models for the rs6817105 SNP showed a significant risk of AF with the carriage of the homozygous CC genotype (OR=1.63, 95% CI: 0.95-2.81, P=0.008).

In recent years, GWAS have identified common genetic variants associated with a higher risk of AF in populations of European ancestry.[9,28-30] However, ethnic differences exist in the frequency of AF-related SNPs between European and Asian populations.[31,32]

The present study is the first molecular genetic study investigating the association of 4q25/*PITX2* SNP rs6817105 in AH patients with AF in the Uzbek population. Our results regarding the 4q25/PITX2 SNP rs6817105 in AF development are consistent with the previous observations.[8,33-35] We verified that the 4q25/PITX2 SNP rs681710 is associated with AF and showed that a carriage of the minor C allele and CC genotype results in left atrial enlargement.

Conclusions

- Our results indicate the rs6817105 minor C allele and CC genotype are associated with the risk of developing AF in AH patients of Uzbek nationality.
- The highest accumulation of the rs6817105 minor C allele and CC genotype is found in paroxysmal AF.
- In carriers of the rs6817105 CC genotype, the LAVI was significantly larger than in carriers of the CT and TT genotypes.

Competing Interests

The authors declare that they have no competing interests.

References

1. Williams B, Mancia G, Spiering W, Agabiti Rosei E, Azizi M, Burnier M, Clement DL, Coca A, et al.; ESC Scientific Document Group. 2018 ESC/ESH Guidelines for the management of arterial hypertension. Eur Heart J. 2018

September 1;39(33):3021-3104. doi: 10.1093/eurheartj/ehy339. Erratum in: Eur Heart J. 2019 Feb 1;40(5):475.
2. Van Gelder IC, Crijns HJ, Tieleman RG, Brugemann J, De Kam PJ, Gosselink AT, et al.; Chronic atrial fibrillation. Success of serial cardioversion therapy and safety of oral anticoagulation. Arch Intern Med. 1996 December;156(22):2585-2592. doi: 10.1001/archinte.156.22.2585.
3. Go O, Rosendorff C. Hypertension and atrial fibrillation. Curr Cardiol Rep. 2009 November;11(6):430-435. doi: 10.1007/s11886-009-0062-4.
4. Andalib A, Brugada R, Nattel S. Atrial fibrillation: evidence for genetically determined disease. Curr Opin Cardiol. 2008 May;23(3):176-83. doi: 10.1097/HCO.0b013e3282fa7142.
5. Gudbjartsson DF, Arnar DO, Helgadottir A, Gretarsdottir S, Holm H, Sigurdsson A, et al. Variants conferring risk of atrial fibrillation on chromosome 4q25. Nature. 2007 Jul 19;448(7151):353-7. doi: 10.1038/nature06007.
6. Roselli C, Rienstra M, Ellinor PT. Genetics of Atrial Fibrillation in 2020: GWAS, Genome Sequencing, Polygenic Risk, and Beyond. Circ Res. 2020 Jun 19;127(1):21-33. doi: 10.1161/CIRCRESAHA.120.316575
7. Schulz C, Lemoine MD, Mearini G, Koivumäki J, Sani J, Schwedhelm E, et al. *PITX2* Knockout Induces Key Findings of Electrical Remodeling as Seen in Persistent Atrial Fibrillation. Circ Arrhythm Electrophysiol. 2023 Mar;16(3):e011602. doi: 10.1161/CIRCEP.122.011602.
8. Tomomori S, Nakano Y, Ochi H, Onohara Y, Sairaku A, Tokuyama T, et al. Chromosome 4q25 Variant rs6817105 Bring Sinus Node Dysfunction and Left Atrial Enlargement. Sci Rep. 2018 Oct 1;8(1):14565. doi: 10.1038/s41598-018-32453-8.
9. Ellinor PT, Lunetta KL, Albert CM, Glazer NL, Ritchie MD, Smith AV, et al. Meta-analysis identifies six new susceptibility loci for atrial fibrillation. Nat Genet. 2012 Apr 29;44(6):670-5. doi: 10.1038/ng.2261.
10. Christophersen IE, Rienstra M, Roselli C, Yin X, Geelhoed B, Barnard J, et al.; METASTROKE Consortium of the ISGC; Neurology Working Group of the CHARGE Consortium; Dichgans M, Ingelsson E, Kooperberg C, Melander O, Loos RJF, Laurikka J, et al.; AFGen Consortium. Large-scale analyses of common and rare variants identify 12 new loci associated with atrial fibrillation. Nat Genet. 2017 Jun;49(6):946-952. doi: 10.1038/ng.3843. Epub 2017 Apr 17. Erratum in: Nat Genet. 2017 Jul 27;49(8):1286.
11. Aguirre LA, Alonso ME, Badía-Careaga C, Rollán I, Arias C, Fernández-Miñán A, et al. Long-range regulatory interactions at the 4q25 atrial fibrillation risk locus involve PITX2c and ENPEP. BMC Biol. 2015 Apr 17;13:26. doi: 10.1186/s12915-015-0138-0.
12. Shiratori H, Yashiro K, Shen MM, Hamada H. Conserved regulation and role of Pitx2 in situs-specific morphogenesis of visceral organs. Development. 2006 Aug;133(15):3015-25. doi: 10.1242/dev.02470.
13. Lin CR, Kioussi C, O'Connell S, Briata P, Szeto D, Liu F, et al. Pitx2 regulates lung asymmetry, cardiac positioning and pituitary and tooth morphogenesis. Nature. 1999 Sep 16;401(6750):279-82. doi: 10.1038/45803.
14. Franco D, Sedmera D, Lozano-Velasco E. Multiple Roles of Pitx2 in Cardiac Development and Disease. J Cardiovasc Dev Dis. 2017 Oct 11;4(4):16. doi: 10.3390/jcdd4040016.
15. Welsh IC, Thomsen M, Gludish DW, Alfonso-Parra C, Bai Y, Martin JF, Kurpios NA. Integration of left-right Pitx2 transcription and Wnt signaling drives asymmetric gut morphogenesis via Daam2. Dev Cell. 2013 Sep 30;26(6):629-44. doi: 10.1016/j.devcel.2013.07.019.
16. van Ouwerkerk AF, Hall AW, Kadow ZA, Lazarevic S, Reyat JS, Tucker NR, Nadadur RD, Bosada FM, Bianchi V, Ellinor PT, Fabritz L, Martin JF, de Laat W, Kirchhof P, Moskowitz IP, Christoffels VM. Epigenetic and Transcriptional Networks Underlying Atrial Fibrillation. Circ Res. 2020 Jun 19;127(1):34-50. doi: 10.1161/CIRCRESAHA.120.316574. Epub 2020 Jun 18. Erratum in: Circ Res. 2020 Aug 28;127(6):e143-e146.
17. Kirchhof P, Kahr PC, Kaese S, Piccini I, Vokshi I, Scheld HH, et al. PITX2c is expressed in the adult left atrium, and reducing Pitx2c expression promotes atrial fibrillation inducibility and complex changes in gene expression. Circ Cardiovasc Genet. 2011 Apr;4(2):123-33. doi: 10.1161/CIRCGENETICS.110.958058.
18. Syeda F, Kirchhof P, Fabritz L. PITX2-dependent gene regulation in atrial fibrillation and rhythm control. J Physiol. 2017 Jun 15;595(12):4019-4026. doi: 10.1113/JP273123.
19. Wang J, Klysik E, Sood S, Johnson RL, Wehrens XH, Martin JF. Pitx2 prevents susceptibility to atrial arrhythmias by inhibiting left-sided pacemaker specification. Proc Natl Acad Sci U S A. 2010 May 25;107(21):9753-8. doi: 10.1073/pnas.0912585107.
20. Chinchilla A, Daimi H, Lozano-Velasco E, Dominguez JN, Caballero R, Delpón E, et al. PITX2 insufficiency leads to atrial electrical and structural remodeling linked to arrhythmogenesis. Circ Cardiovasc Genet. 2011 Jun;4(3):269-79. doi: 10.1161/CIRCGENETICS.110.958116.
21. Syeda F, Holmes AP, Yu TY, Tull S, Kuhlmann SM, Pavlovic D, et al. PITX2 Modulates Atrial Membrane Potential and the Antiarrhythmic Effects of Sodium-Channel Blockers. J Am Coll Cardiol. 2016 Oct 25;68(17):1881-1894. doi: 10.1016/j.jacc.2016.07.766.
22. Abdullaeva GJ, Abdullaev AA, Kevorkov AG, Abduvalieva GA, Zakirov NU, Kurbanov RD. Interrelation between rs2200733 polymorphism of ATFB5 gene and atrial fibrillation in Uzbek patients. Turk Kardiyol Dern Ars. 2021 July; 49(5):404-409. doi: 10.5543/tkda.2021.08434.
23. Kirchhof P, Benussi S, Kotecha D, Ahlsson A, Atar D, Casadei B, et al. ESC Scientific Document Group. 2016 ESC Guidelines for the management of atrial fibrillation developed in collaboration with EACTS. Eur Heart J. 2016 Oct 7;37(38):2893-2962. doi: 10.1093/eurheartj/ehw210.
24. European Heart Rhythm Association; European Association for Cardio-Thoracic Surgery; Camm AJ, Kirchhof P, Lip GY, Schotten U, Savelieva I, Ernst A, et al. Guidelines for the management of atrial fibrillation: the Task Force for the Management of Atrial Fibrillation of the European Society of Cardiology (ESC). Eur Heart J. 2010 Oct;31(19):2369-429. doi: 10.1093/eurheartj/ehq278. Epub 2010 Aug 29. Erratum in: Eur Heart J. 2011 May;32(9):1172.
25. Sahn DJ, Demaria A, Kisslo J, Weyman A. Recommendation regarding quantitation in M-mode echocardiography: Results of a survey of echocardiographic measurements. Circulation. 1978 December;58(6):1072-1083.

***Corresponding author**: Guzal Zh. Abdullaeva, PhD, ScD. Department of Arterial Hypertension, Republican Specialized Center of Cardiology. Tashkent, Uzbekistan. E-mail: guzal-abdullaeva@bk.ru*

doi: 10.1161/01.cir.58.6.1072.
26. Devereux RB, Reichek N. Echocardiographyic determination of left ventricular mass in man. Anatomic validation of the method. Circulation. 1977 April; 55(4):613-618. doi: 10.1161/01.cir.55.4.613.
27. Shul'man VA, Nikulina SYu, Isachenko OO, Aksyutina NV, Romanenko SN, Maksimov VN, et al. [Genetic aspects of atrial fibrillation]. J Arrhythmology. 2006;(46):57-60. [Article in Russian].
28. Kääb S, Darbar D, van Noord C, Dupuis J, Pfeufer A, Newton-Cheh C, et al. Large scale replication and meta-analysis of variants on chromosome 4q25 associated with atrial fibrillation. Eur Heart J. 2009 Apr;30(7):813-9. doi: 10.1093/eurheartj/ehn578.
29. Benjamin EJ, Rice KM, Arking DE, Pfeufer A, van Noord C, Smith AV, et al. Variants in ZFHX3 are associated with atrial fibrillation in individuals of European ancestry. Nat Genet. 2009 Aug;41(8):879-81. doi: 10.1038/ng.416
30. Ellinor PT, Lunetta KL, Glazer NL, Pfeufer A, Alonso A, Chung MK, et al. Common variants in KCNN3 are associated with lone atrial fibrillation. Nat Genet. 2010 Mar;42(3):240-4. doi: 10.1038/ng.537.
31. Li C, Wang F, Yang Y, Fu F, Xu C, Shi L, et al. Significant association of SNP rs2106261 in the ZFHX3 gene with atrial fibrillation in a Chinese Han GeneID population. Hum Genet. 2011 Mar;129(3):239-46. doi: 10.1007/s00439-010-0912-6.
32. Chang SH, Chang SN, Hwang JJ, Chiang FT, Tseng CD, Lee JK, et al. Significant association of rs13376333 in KCNN3 on chromosome 1q21 with atrial fibrillation in a Taiwanese population. Circ J. 2012;76(1):184-8. doi: 10.1253/circj.cj-11-0525.
33. Lee KT, Yeh HY, Tung CP, Chu CS, Cheng KH, Tsai WC, et al. Association of RS2200733 but not RS10033464 on 4q25 with atrial fibrillation based on the recessive model in a Taiwanese population. Cardiology. 2010; 116(3): 151-156. doi: 10.1159/000318172.
34. Ferrán A, Alegret JM, Subirana I, Aragonès G, Lluis-Ganella C, Romero-Menor C, Planas F, Joven J, Elosua R. Association between rs2200733 and rs7193343 genetic variants and atrial fibrillation in a Spanish population, and meta-analysis of previous studies. Rev Esp Cardiol (Engl Ed). 2014 Oct;67(10):822-9. doi: 10.1016/j.rec.2013.12.019.
35. Thum T, Gross C, Fiedler J, Fischer T, Kissler S, Bussen M, et al. MicroRNA-21 contributes to myocardial disease by stimulating MAP kinase signalling in fibroblasts. Nature. 2008 Dec 18;456(7224):980-4. doi: 10.1038/nature07511.

International Journal of Biomedicine 13(3) (2023) 79-83
http://dx.doi.org/10.21103/Article13(3)_OA4

ORIGINAL ARTICLE

Metabolic Syndrome

INTERNATIONAL JOURNAL OF BIOMEDICINE

Relationship of Cytokine Status Parameters with the Lipid Peroxidation-Antioxidant Defense System in Obese Adolescents

Marina A. Darenskaya[1], Lyubov V. Rychkova[1], Natalya V. Semenova[1], Zhanna V. Prokhorova[1], Olga A. Tugarinova[2], Tatyana A. Mityukova[3], Anastasia A. Basalai[3], Olga E. Poluliakh[3], Lyubov I. Kolesnikova[1]

[1]*Scientific Centre for Family Health and Human Reproduction Problems, Irkutsk, Russian Federation*
[2]*Tarbagatai Central District Hospital, Ministry of Health of the Republic of Buryatia, Ulan-Ude, Russian Federation*
[3]*Institute of Physiology of the National Academy of Sciences, Minsk, Republic of Belarus*

Abstract

The aim of this study was to identify the relationships between cytokine status, lipid peroxidation (LPO) products, and total antioxidant activity (TAA) in obese adolescent boys and girls.

Methods and Results: The study included 29 boys and 33 girls with an established diagnosis of exogenous-constitutional obesity of the first degree. Twenty-eight healthy adolescent boys and 24 adolescent girls made up control groups.

The concentration of cytokines (IL-6, IL-8, IL-4, and IL-10) was assessed by enzyme immunoassay. The content of LPO products (conjugated dienes [CDs], ketodienes and conjugated trienes [KD-CT], Schiff bases [SB], thiobarbituric acid reactants [TBARs], total antioxidant activity (TAA) was evaluated. Spectrophotometric methods were used. The data obtained indicated a statistically significant increase in the level of IL-6 (P=0.018) and the IL-6/IL10 ratio (P=0.033) in obese boys, compared with the control. There was also an increase in the content of LPO products in this group relative to the control group: KD-CT (P=0.043) and SB (P=0.021). In the group of obese girls, there was an increase in IL-6 values (P=0.018), a decrease in IL-4 (P=0.040), and an increase in CDs (P=0.035) and KD-CT (P=0.044). The following correlations were found in the control group of boys: CDs–KD-CT (r=0.91; P=0.001), TBARS–IL-8 (r=0.73; P=0.027), and SB–IL-4 (r=0.79; P=0.011); there were no statistically significant correlations between study parameters in obese boys. The following correlations were recorded in the girls of the control group: CDs–KD-CT (r=0.99; P<0.0001), TAA–IL-10 (r=-0.80; P=0.033), TAA–IL-4 (r=-0.78; P=0.040); in obese girls, it was SB–IL-4 (r=-0.67; P=0.048).

Conclusion: Data analysis showed high activity of proinflammatory cytokines and LPO products in obese adolescents, regardless of gender, with a reduced concentration of anti-inflammatory factors and correlations between parameters of inflammation and OS in girls. An important component of the pathogenetic approach in treating obesity should be the control of these parameters.(**International Journal of Biomedicine. 2023;13(3):79-83.**)

Keywords: interleukins • adolescents • lipid peroxidation • obesity

For citation: Darenskaya MA, Rychkova LV, Semenova NV, Prokhorova ZV, Tugarinova OA, Mityukova TA, Basalai AA, Poluliakh OE, Kolesnikova LI. Relationship of Cytokine Status Parameters with the Lipid Peroxidation-Antioxidant Defense System in Obese Adolescents. International Journal of Biomedicine. 2023;13(3):79-83. doi:10.21103/Article13(3)_OA4

Abbreviations

BMI, body mass index; **BW**, body weight; **CD**, conjugated dienes; **IL**, interleukins; **KD-CT**, ketodienes and conjugated trienes; **LPO**, lipid peroxidation; **OS**, oxidative stress; **ROS**, reactive oxygen species; **SB**, Schiff bases**; SDS BMI**, standard deviation score of body mass index; **TAA**, total antioxidant activity; **TBARs**, thiobarbituric acid reactants; **TNF-α**, tumor necrosis factor-α.

Introduction

The high prevalence of cardiovascular diseases leads to an increase in disability of the able-bodied population, which prioritizes the creation of new principles for treating and preventing obesity in children and adolescents.[1,2] In developed countries, up to a quarter of the adolescent population is overweight, and 15% are obese.[3] The structure of obesity consists of various forms, among which the exogenous-constitutional form occupies a special place in terms of prevalence (up to 75%-97%).[4]

Obesity is currently considered as a chronic inflammatory process, which is accompanied by the activation of proinflammatory cytokines, such as IL-6, IL-1, and TNFα, known mediators of the early stage of inflammation, as well as IL-8, γ-interferon, IL-18, IL-1.[5,6] Inflammation in obesity is manifested by cellular infiltration, changes in microcirculation, a shift in adipokine secretion and adipose tissue metabolism, and the accumulation of nonspecific markers of inflammation in the blood, which reflect the severity of the process.[7]

Oxidative stress (OS) is also an important component of the pathogenesis of obesity and its possible complications.[2,8,9] Experimental studies have shown a stimulating effect of OS on the proliferation and differentiation of preadipocytes, as well as an increase in the size of adipocytes.[10] It has been found that in obesity, the production of reactive oxygen species (ROS) increases, and the hunger center is activated due to increased oxidative processes.[11-13] OS in obesity is stimulated by factors such as hyperglycemia, elevated lipid levels, chronic increased activity of muscle tissue to maintain excess BW, impaired respiratory function of mitochondria.[14] The consequence of the OS progression in obesity is an increase in the content of cytotoxic compounds, which include endogenous aldehydes acting as damage mediators.[10] Despite the ongoing studies, the relationship between the parameters of the inflammatory process and OS parameters has not been sufficiently studied in obese adolescents.

The aim of this study was to identify the relationships between cytokine status, LPO products, and TAA in obese adolescent boys and girls.

Materials and Methods

The study included 29 boys (average age of 13.39±1.85 years) and 33 girls (average age of 14.56±2.01 years) with an established diagnosis of exogenous-constitutional obesity of the first degree. Twenty-eight healthy adolescent boys (average age of 13.96±1.5 years) and 24 adolescent girls (average age of 14.37±1.5 years) made up control groups. Criteria for inclusion in groups with exogenous-constitutional obesity degree 1 were excess BW of more than 95 percentile for a certain gender, height, and age; exclusion of acute or exacerbation of chronic diseases at the beginning of the examination or one month before it; permanent residence of a teenager in the territory of this municipality. Height, body weight (BW), and waist circumference were measured, and BMI (kg/m^2) was calculated. The puberty stage was determined according to Tanner. Overweight was considered to be a BMI >85th percentile for a given gender and age, and obesity was considered to be a BMI >95th percentile.[15] Exclusion criteria were physical development delay, BW deficiency, genetic and symptomatic forms of obesity, and taking medications that potentially affect BW.

All adolescents were subjected to general clinical examination, including anamnestic data collection, physical examination, anthropometric data analysis, blood pressure measurement, nutritional status assessment, determination of blood lipid profile, and glucose tolerance testing.

The study was carried out in accordance with the Helsinki Declaration of the World Medical Association (1964, ed. 2013) and approved by the Committee on Biomedical Ethics under the Scientific Center for Family Health and Human Reproduction (Extract from the meeting No. 5 as of 05.16.2016).

The study material was blood plasma and serum. Blood was collected in accordance with the existing requirements in the morning on an empty stomach from the cubital vein.

The concentration of pro-inflammatory cytokines (IL-6, IL-8) and anti-inflammatory interleukins (IL-4 and IL-10) was assessed by enzyme immunoassay using monoclonal antibody panels (JSC "Vector-Best", Novosibirsk, Russia). Measurements were performed on a microplate photometer (Multiskan Ascent, Finland). The IL-6/IL-10 ratio, reflecting the balance of pro- and anti-inflammatory cytokines, was also calculated.

The content of LPO products (conjugated dienes [CDs], ketodienes and conjugated trienes [KD-CT] and Schiff bases [SB]) was determined by the Volchegorsky method.[16] The level of thiobarbituric acid reactants (TBARs) was determined fluorimetrically by the method of Gavrilov et al.[17] Total antioxidant activity (TAA) was evaluated by the method of Klebanov et al.[18] Measurements were carried out on a spectrophotometer SF-2000 (Novosibirsk, Russia).

Statistical analysis was performed using STATISTICA 10.0 software package (Stat-Soft Inc, USA). The normality of distribution of continuous variables was tested by the Kolmogorov-Smirnov test with the Lilliefors correction and Shapiro-Wilk test. Differences of continuous variables departing from the normal distribution, even after transformation, were tested by the Mann-Whitney U-test. Pearson's Correlation Coefficient (r) was used to determine the strength of the relationship between the two continuous variables. A probability value of $P<0.05$ was considered statistically significant.

The study was conducted in accordance with ethical principles of the WMA Declaration of Helsinki (1964, ed. 2013) and approved by the Ethics Committee at the Scientific Centre for Family Health and Human Reproduction Problems (Irkutsk, Russia). Written informed consent was obtained from all participants (patients or parents/guardians of each patient).

Results and Discussion

The data obtained indicated a statistically significant increase in the level of IL-6 ($P=0.018$) and the IL-6/IL10 ratio ($P=0.033$) in obese boys, compared with the control (Figure 1).

There was also an increase in the content of LPO products in this group relative to the control group: KD-CT (P=0.043) and SB (P=0.021). In the group of obese girls, there was an increase in IL-6 values (P=0.018), a decrease in IL-4 (P=0.040), and an increase in CDs (P=0.035) and KD-CT (P=0.044) (Figure 2).

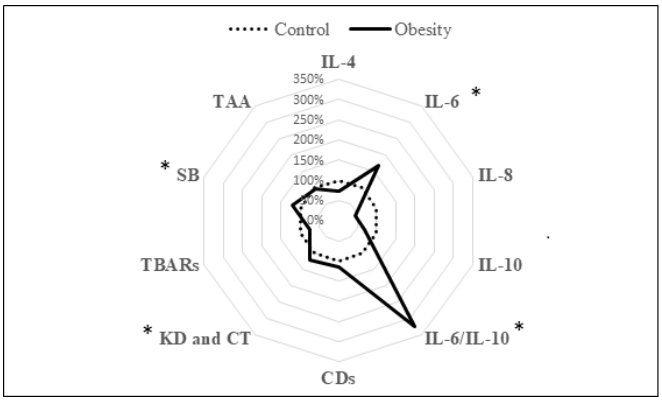

Fig. 1. *Cytokine status parameters, TAA and LPO products in obese boys; 100% - control group; *- statistically significant differences between group with obesity and control group (P<0.05).*

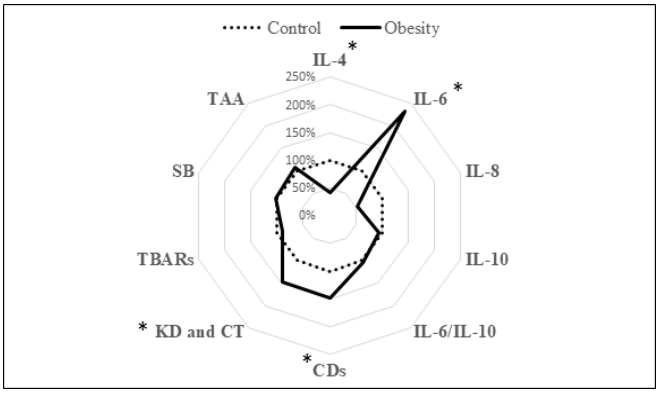

Fig. 2. *Cytokine status parameters, TAA and LPO products in obese girls; 100% - control group; *- statistically significant differences between group with obesity and control group (P<0.05).*

The following correlations were found in the control group of boys: CDs–KD-CT (r=0.91; P=0.001), TBARS–IL-8 (r=0.73; P=0.027), and SB–IL-4 (r=0.79; P=0.011); there were no statistically significant correlations between study parameters in obese boys. The following correlations were recorded in the girls of the control group: CDs–KD-CT (r=0.99; P<0.0001), TAA–IL-10 (r=-0.80; P=0.033), TAA–IL-4 (r=-0.78; P=0.040); in obese girls, it was SB–IL-4 (r=-0.67; P=0.048) (Table 1).

Our study found a significant increase in the values of the proinflammatory IL-6 and the IL-6/IL10 ratio in obese boys, as well as a marked increase in IL-6 level and a decrease in IL-4 level in obese girls.

Increased OS and inflammation often characterize obesity due to the infiltration of adipocytes by immune cells.[14] The inflammatory process is a physiological reaction of the organism to various kinds of stimuli.[7] The resulting response usually leads to the restoration of systemic metabolic homeostasis. In obesity, there is an increase in inflammatory reactions in metabolically active areas, such as adipose tissue, liver, and immune cells.[6] In addition, there is a sharp increase in the level of circulating proinflammatory cytokines, adipokines, and other inflammatory markers.[19] In this context, a certain contribution to the inflammatory nature of obesity is made by TNFα, IL-6, fibrinogen, C-reactive protein, and plasminogen activator inhibitor-1 or resistin, confirming the relationship between inflammation and obesity.[14] It was found that a wide range of mediators of the proinflammatory response are produced by macrophages of adipose tissue together with adipocytes.[20] A potential cause of inflammation in obesity may be hypoxia of adipose tissue, which occurs due to hypertrophy of adipocytes. A disproportionate increase in cell size lengthens the distance over which oxygen must diffuse, which can lead to a hypoxic state in enlarged adipocytes.[19,20]

Table 1.

Correlations* between the parameters in study groups of adolescents.

Control (boys)	Obesity (boys)	Control (girls)	Obesity (girls)
CDs–KD-CT (r=0.91)	-	CDs–KD-CT (r=0.99)	SB–IL-4 (r=-0.67)
TBARS–IL-8 (r=0.73)	-	TAA–IL-10 (r=-0.80)	-
SB–IL-4 (r=0.79)	-	TAA–IL-4 (r=-0.78)	-

* - *Table shows only statistically significant correlations.*

The production of highly reactive ROS is considered one of the most important adverse cellular reactions in response to excessive amounts of nutrients in obesity.[21] The growth of ROS production disrupts the balance between pro-oxidant and antioxidant factors, leading to the dominance of the pro-oxidant state and OS.[22-25] OS, in turn, damages cellular structures and causes an inflammatory response.[20] In addition, OS in obesity is closely associated with insulin resistance and metabolic syndrome.[10,11] Significant markers of OS in obesity are various products of LPO.[26] The latter has a pronounced damaging effect on the structural components of the cells, DNA synthesis, proliferative processes. and other factors.[10] We found higher values of KD-CT and SB in obese adolescent boys, and CDs and KD-CT in obese girls, which may have adverse consequences in the long term.

Correlation analysis showed the presence of close interrelations of inflammatory factors and OS in the control groups; however, a different picture was recorded with obesity. Thus, no correlations were found in boys, which indicated an imbalance of the existing mechanisms in the conditions of pathology. The only negative dependence was registered in obese girls – the end products of LPO (SB) and IL-4. This relationship may indicate the dominance of proinflammatory factors in this group, mediated by the action of OS products. There are studies

which show that the state of inflammation and OS phenomena interact closely in conditions of obesity.[14] Common genetic mechanisms that potentiate inflammation and OS mechanisms have been identified.[20]

Conclusion

In our study, data analysis showed high activity of proinflammatory cytokines and LPO products in obese adolescents, regardless of gender, with a reduced concentration of anti-inflammatory factors and correlations between parameters of inflammation and OS in girls. An important component of the pathogenetic approach in treating obesity should be the control of these parameters.

This work was carried out using the equipment of the Center for the Development of Advanced Personalized Health Technologies, Scientific Centre for Family Health and Human Reproduction Problems, Irkutsk.

Competing Interests

The authors declare that they have no competing interests.

References

1. Spinelli A, Buoncristiano M, Kovacs VA, Yngve A, Spiroski I, Obreja G, et al. Prevalence of Severe Obesity among Primary School Children in 21 European Countries. Obes Facts. 2019;12(2):244-258. doi: 10.1159/000500436.
2. Darenskaya MA, Rychkova LV, Balzhirova DB, Semenova NV, Nikitina OA, Lesnaya A, et al. The level of lipid peroxidation products and medium-molecular-weight peptides in adolescents with obesity. International Journal of Biomedicine. 2023;13(2):292-295. doi: 10.21103/Article13(2)_OA17
3. O'Connor TG, Williams J, Blair C, Gatzke-Kopp LM, Francis L, Willoughby MT. Predictors of Developmental Patterns of Obesity in Young Children. Front Pediatr. 2020 Mar 24;8:109. doi: 10.3389/fped.2020.00109.
4. Marseglia L, Manti S, D'Angelo G, Nicotera A, Parisi E, Di Rosa G, Gitto E, Arrigo T. Oxidative stress in obesity: a critical component in human diseases. Int J Mol Sci. 2014 Dec 26;16(1):378-400. doi: 10.3390/ijms16010378.
5. Rohm TV, Meier DT, Olefsky JM, Donath MY. Inflammation in obesity, diabetes, and related disorders. Immunity. 2022 Jan 11;55(1):31-55. doi: 10.1016/j.immuni.2021.12.013.
6. Wu H, Ballantyne CM. Metabolic Inflammation and Insulin Resistance in Obesity. Circ Res. 2020 May 22;126(11):1549-1564. doi: 10.1161/CIRCRESAHA.119.315896.
7. Palma G, Sorice GP, Genchi VA, Giordano F, Caccioppoli C, D'Oria R, Marrano N, Biondi G, Giorgino F, Perrini S. Adipose Tissue Inflammation and Pulmonary Dysfunction in Obesity. Int J Mol Sci. 2022 Jul 1;23(13):7349. doi: 10.3390/ijms23137349.
8. Darenskaya MA, Kolesnikova LI, Rychkova LV, Kravtsova OV, Semenova NV, Kolesnikov SI. Relationship between lipid metabolism state, lipid peroxidation and antioxidant defense system in girls with constitutional obesity. AIMS Molecular Science. 2021;8(2):117-126. doi: 10.3934/molsci.2021009
9. Darenskaya MA, Gavrilova OA, Rychkova LV, Kravtsova OV, Grebenkina LA, Osipova EV, et al. The assessment of oxidative stress intensity in adolescents with obesity by the integral index. International Journal of Biomedicine. 2018;8(1):37-41. doi: 10.21103/Article8(1)_OA5
10. Manzoor MF, Arif Z, Kabir A, Mehmood I, Munir D, Razzaq A, Ali A, Goksen G, Coşier V, Ahmad N, Ali M, Rusu A. Oxidative stress and metabolic diseases: Relevance and therapeutic strategies. Front Nutr. 2022 Oct 17;9:994309. doi: 10.3389/fnut.2022.994309.
11. Raut SK, Khullar M. Oxidative stress in metabolic diseases: current scenario and therapeutic relevance. Mol Cell Biochem. 2023 Jan;478(1):185-196. doi: 10.1007/s11010-022-04496-z.
12. Darenskaya MA, Rychkova LV, Kolesnikov SI, Semenova NV, Nikitina OA, Brichagina AS, et al. Biochemical Status of Obese Male Adolescents of Different Ethnicity: Discriminant Analysis in the Identification of the Most Informative Indicators. Bull Exp Biol Med. 2022 Aug;173(4):459-463. doi: 10.1007/s10517-022-05579-z.
13. Darenskaya MA, Rychkova LV, Kolesnikov SI, Kravtsova OV, Semenova NV, Brichagina AS, Kolesnikova LI. Changes in lipid peroxidation system during standard therapy for exogenous constitutional obesity in adolescents of different sex. Questions of children's nutrition. 2022;20(1):5-11. doi: 10.20953/1727-5784-2022-1-5-11
14. Zuo L, Prather ER, Stetskiv M, Garrison DE, Meade JR, Peace TI, Zhou T. Inflammaging and Oxidative Stress in Human Diseases: From Molecular Mechanisms to Novel Treatments. Int J Mol Sci. 2019 Sep 10;20(18):4472. doi: 10.3390/ijms20184472.
15. Styne DM, Arslanian SA, Connor EL, Farooqi IS, Murad MH, Silverstein JH, Yanovski JA. Pediatric Obesity-Assessment, Treatment, and Prevention: An Endocrine Society Clinical Practice Guideline. J Clin Endocrinol Metab. 2017 Mar 1;102(3):709-757. doi: 10.1210/jc.2016-2573.
16. Volchegorskiĭ IA, Nalimov AG, Iarovinskiĭ BG, Lifshits RI. [Comparison of various approaches to the determination of the products of lipid peroxidation in heptane-isopropanol extracts of blood]. Vopr Med Khim. 1989 Jan-Feb;35(1):127-31. [Article in Russian].
17. Gavrilov VB, Gavrilova AR, Mazhul' LM. [Methods of determining lipid peroxidation products in the serum using a thiobarbituric acid test]. Vopr Med Khim. 1987 Jan-Feb;33(1):118-22. [Article in Russian].
18. Klebanov GI, Babenkova IV, Teselkin IuO, Komarov OS, Vladimirov IuA. [Evaluation of the antioxidative activity of blood plasma using yolk lipoproteins]. Lab Delo. 1988;(5):59-62. [Article in Russian].
19. Smith MM, Minson CT. Obesity and adipokines: effects on sympathetic overactivity. J Physiol. 2012 Apr 15;590(8):1787-801. doi: 10.1113/jphysiol.2011.221036.
20. Bondia-Pons I, Ryan L, Martinez JA. Oxidative stress

***Corresponding author:** Prof. Marina A. Darenskaya, PhD, ScD. Scientific Centre for Family Health and Human Reproduction Problems, Irkutsk, the Russian Federation. E-mail: marina_darenskaya@inbox.ru*

and inflammation interactions in human obesity. J Physiol Biochem. 2012 Dec;68(4):701-11. doi: 10.1007/s13105-012-0154-2.
21. Povarova OV, Gorodetskaya EA, Kalenikova EI, Medvedev OS. [Metabolic markers and oxidative stress in the pathogenesis of obesity in children]. Russian Bulletin of Perinatology and Pediatrics. 2020;65(1):22-29. doi:10.21508/1027-4065-2020-65-1-22-29. [Article in Russian].
22. Kolesnikova LI, Darenskaya MA, Kolesnikov SI. [Free radical oxidation: a pathophysiologist's view]. Bulletin of Siberian Medicine. 2017;16(4):16-29. doi: 10.20538/1682-0363-2017-4-16–29. [Article in Russian].
23. Darenskaya MA, Rychkova LV, Semenova NV, Belkova NL, Kolesnikova LI. The role of oxidative stress and changes in the composition of the gut microbiota in the genesis of adolescent obesity. International Journal of Biomedicine. 2022;12(3):344-348. doi: 10.21103/Article12(3)_RA3
24. Vona R, Gambardella L, Cittadini C, Straface E, Pietraforte D. Biomarkers of Oxidative Stress in Metabolic Syndrome and Associated Diseases. Oxid Med Cell Longev. 2019 May 5;2019:8267234. doi: 10.1155/2019/8267234.
25. Darenskaya MA, Rychkova LV, Kolesnikov SI, Kravtsova OV, Semenova NV, Brichagina A, et al. Oxidative stress index levels in Asian adolescents with exogenous-constitutional obesity. International Journal of Biomedicine. 2022;12(1):142-146. doi: 10.21103/Article12(1)_OA16
26. Rychkova LV, Darenskaya MA, Semenova NV, Kolesnikov SI, Petrova AG, et al. Oxidative stress intensity in children and adolescents with a new coronavirus infection. International Journal of Biomedicine. 2022;12(2):242-246. doi: 10.21103/Article12(2)_OA7

International Journal of Biomedicine 13(3) (2023) 84-90
http://dx.doi.org/10.21103/Article13(3)_OA5

ORIGINAL ARTICLE

Diabetes Mellitus

INTERNATIONAL JOURNAL OF BIOMEDICINE

Depression, Anxiety and Stress Among Patients with Type 2 Diabetes Mellitus in Primary Health Care in Kosovo

Mehmedali Gashi[1], Sanije Hoxha-Gashi[1.2*], Sefedin Muçaj[1.2]

[1]*Faculty of Medicine, University of Pristina "Hasan Prishtina", Pristina, Kosovo*
[2]*National Institute of Public Health of Kosovo, Pristina, Kosovo*

Abstract

Background: At a global level, over 300 million people are estimated to suffer from depression, equivalent to 4.4% of the world's population. The presence of depression, anxiety, and stress (DAS) has major consequences for individuals with diabetes. The aim of this study was to determine the prevalence of DAS among adult patients with T2DM in primary health care (PHC) settings in Kosovo and to determine any association between DAS, sociodemographic characteristics, and other risk factors.

Methods and Results: This cross-sectional study was conducted in seven Main Family Medicine Centers in Kosovo (Prishtina, Mitrovica, Peja, Prizren, Ferizaj, Gjilan, and Gjakova) from November 2022 to February 2023. The study included 596 adult patients above 18 years of age who were diagnosed with T2DM at least one year ago. By gender, more respondents were female ((F 55.4% vs. M 44.6%); adults aged 30-59 accounted for 38.4%, aged 60+ – 57.7%. Anxiety was the most common type of psychological distress among the subjects (82.0%), depression was second with a prevalence of 74% and stress third with a prevalence of 43.0%. Females were predominant among respondents regarding the three forms of mental health problems: Depression (F 75.8% vs. M 71.8%), Anxiety (F 86.1% vs. M 77.1%), and Stress (F 48.5% vs. M 36.1%)

Subjects with only primary education were more likely to be depressed (79.6%, *P*=0.007; OR=1.689, 95% CI: 1.153 – 2.477). HbA1C >6.5% was found to be strongly associated with depression (76.4%, *P*=0.002; OR=2.071, 95% CI: 1.305 – 3.284). Female gender and the presence of comorbidities were found to be significantly associated with anxiety. Female gender, level of education, history of DM in the family, presence of comorbidities, and HbA1c >6.5% were significantly associated with stress.

Conclusion: Our study showed that the prevalence of DAS is high in patients with T2DM. Periodic screening of patients with diabetes in PHC settings for early signs of psychological distress using easy and inexpensive validated screening tools like the DASS-21 questionnaire is recommended.(**International Journal of Biomedicine. 2023;13(3):84-90.**)

Key words: depression • anxiety • and stress • diabetes mellitus • Kosovo adults

For citation: Gashi M, Hoxha-Gashi S, Muçaj S. Depression, Anxiety and Stress Among Patients with Type 2 Diabetes Mellitus in Primary Health Care in Kosovo. International Journal of Biomedicine. 2023;13(3):84-90. doi:10.21103/Article13(3)_OA5

Abbreviations

DM, diabetes mellitus; **DAS**, depression, anxiety, and stress; **PHC**, primary health care; **T2DM**, type 2 diabetes mellitus.

Introduction

Diabetes is a common chronic disease worldwide. Its prevalence is increasing and is expected to be 783 million by 2045.[1] According to the Kosovo STEPS surveys, the prevalence of diabetes mellitus (DM) in 2011[2] among 15-64 year-olds was 7.7% (95% CI: 6.0% – 9.7%), and 7.9% (95% CI: 6.9% – 9.0%) among 18-69 year-olds. In 2019 the prevalence was higher among females than among males.[2,3] Diabetes is the leading noncommunicable disease in Kosovo, according to annual reports from the Department of Statistics at the National Institute of Public Health of Kosovo.[4] Type 2 diabetes mellitus (T2DM) affects more than 90% of diabetics. After cardiovascular diseases and cancers, the most common cause of premature death among Kosovo residents is diabetes.[5] Several studies have suggested a complex and bidirectional association between depression, anxiety, and stress (DAS) and chronic diseases, especially T2DM.[6-8] Therefore, patients

with T2DM can be at greater risk for depression and anxiety.[9] Previous research has examined the prevalence and association of DAS among T2DM patients in different countries.[10-18] In Kosovo, we have no data on the prevalence of DAS in adults and even less in DM patients. The Republic of Kosovo has an area of 10,905.25km^2. Kosovo has 38 municipalities, with 1,469 settlements organized according to the country's laws. According to the estimate of the Statistics Agency of Kosovo (SAK) for 2021, the total population in Kosovo is 1,773,971. Kosovo is characterized by a new population structure, where the average age is 30.2 years.[19] Healthcare services in Kosovo are organized through a network of health institutions organized at three levels: Primary Health Care (PHC), Secondary Health Care, and Tertiary Health Care. PHC is the gateway for citizens of the Republic of Kosovo to the health system.[20,21]

The aim of this study was to determine the prevalence of DAS among adult patients with T2DM in PHC settings in Kosovo and to determine any association between DAS, sociodemographic characteristics, and other risk factors.

Materials and Methods

This cross-sectional study was conducted in seven Main Family Medicine Centers in Kosovo (Prishtina, Mitrovica, Peja, Prizren, Ferizaj, Gjilan, and Gjakova) from November 2022 to February 2023.

Inclusion criteria: adult patients above 18 years of age who were diagnosed with T2DM at least one year ago. Exclusion criteria: patients under 18 and those previously diagnosed with mental illness or cognitive impairment.

The sample size was calculated using Kish's formula: Sample size = $z^2 \times p \times (1-p)/c^2$), where z=1.96 for 95% confidence interval (CI), p=prevalence (the possible prevalence of DAS in patients with diabetes as 50% (as we do not have similar research in Kosovo), and c=desired level of precision (4%).

The response rate was expected to be 85%; the desired sample was 700 patients. Therefore, 700 questionnaires were distributed proportionally in seven Main Family Medicine Centers. From 700 questionnaires, we have reactive feedback from 596, or 85.1%.

Data were collected by distributing a self-administered questionnaire consisting of two parts. The first part contains the sociodemographic data of each patient and the current status of DM, indicated by findings such as duration of diabetes, regularity of follow-up (every 3 to 6 months based on the patient's condition), the most recent HbA1c, current regimen for diabetes management and diabetes complications. Factors affecting the severity of DM were also recorded, such as comorbidities, complications, and family history of DM. The second part contains questions about DAS using the DAS Scale (DASS-21) questionnaire.[22]

The DASS-21 is the short form of the DASS-42, a self-report scale designed to measure the negative emotional states of DAS. This scale is suitable for clinical settings for diagnosis and outcome monitoring and for non-clinical settings as a mental health screener.

Statistical analysis was performed using the statistical software package SPSS version 22.0 (SPSS Inc, Armonk, NY: IBM Corp). For descriptive analysis, results are presented as mean ± standard deviation (SD). Odds ratio (OR) with 95% confidence interval (CI) was also calculated. For data with normal distribution, inter-group comparisons were performed using Student's t-test. Differences of continuous variables departing from the normal distribution were tested by the Mann-Whitney *U*-test. Group comparisons with respect to categorical variables are performed using chi-square test. A probability value of $P<0.05$ was considered statistically significant.

Results

The distribution of respondents by socio-demographic characteristics and selected variables is presented in Table 1. This study included 596 patients with T2DM. By gender, more respondents were female (F 55.4% vs. M 44.6%); adults aged 30-59 accounted for 38.4%, aged 60+ – 57.7%. Rural residents accounted for 35.9%, and residents with primary school – 42.8%. unemployed – 72.5%, married – 77.7%, residents with three and more children – 66.5%. Family history of DM was found in 61.1%, and co-morbidity in 68.3%. HbA1C >6.5% was found in 84.1% of respondents.

Anxiety was the most common type of psychological distress among the subjects (82.0%), depression was second with a prevalence of 74% and stress third with a prevalence of 43.0%. The prevalence of the three forms of psychological distress based on severity is summarized in Table 2. Females were predominant among respondents regarding the three forms of mental health problems: Depression (F 75.8% vs. M 71.8%), Anxiety (F 86.1% vs. M 77.1%), and Stress (F 48.5% vs. M 36.1%) (Tables 3-5).

On bivariate analysis, depression was found to be significantly associated with levels of education and HbA1c. Subjects with only primary education were more likely to be depressed (79.6%, $P=0.0072$; OR=1.689, 95% CI: 1.153 – 2.477). HbA1C >6.5% was found to be strongly associated with depression (76.4%, $P=0.002$; OR=2.071, 95% CI: 1.305 – 3.284) (Table 3).

Female gender and the presence of comorbidities were found to be significantly associated with anxiety. Females appeared to have more anxiety (86.1%; $P=0.004$; OR=1.837 (95% CI: 1.204 –2.804). Of those with comorbidities, 84.5% of the respondents also scored positive for anxiety ($P=0.022$, OR=1.657, 95% CI: 1.076 – 2.55)) (Table 4).

Female gender, level of education, history of DM in the family, presence of comorbidities, and HbA1c >6.5% were significantly associated with stress. Females appeared to have more stress (48.5%, $P=0.0024$; OR=1.667, 95% CI: 1.198 – 2.320). Subjects with only primary education were more likely to be stressed (52.5%, $P<0.0001$; OR=1.988, 95% CI: 1.428 – 2.768). HbA1C >6.5% was found to be strongly associated with stress (45.3%, $P=0.008$; OR=1.885, 95% CI: 1.177 – 3.019) (Table 5).

Of those with comorbidities, 46.7% of the respondents also scored positive for stress ($P=0.007$, OR=1.632, 95% CI: 1.142 – 2.332). Subjects with a family history of DM were less likely to be stressed (39.6%, $P=0.036$; OR=0.701, 95% CI: 0.503 – 0.978).

Table 1.

Distribution of respondents by socio-demographic characteristics and selected variables.

Variable	Total number of patients (n=596)	
	n	%
Gender		
Male	266	44.6
Female	330	55.4
Age, years		
<30	23	3.9
30-59	229	38.4
60+	344	57.7
Mean ± SD	60.3 ± 13.0	
Residence		
City	382	64.1
Village	214	35.9
Level of education		
Primary school	255	42.8
Secondary school	211	35.4
University/College	130	21.8
Current Job status		
Employed	164	27.5
Unemployed	432	72.5
Marital status		
Married	463	77.7
Single	44	7.4
Widow(er)	80	13.4
Separated	9	1.5
Number of children		
1-2	141	23.7
3-4	245	41.1
5-6	128	21.5
>6	23	3.9
No children	59	9.9
History of DM in family		
Yes	364	61.1
No	232	38.9
Co-morbidity		
Yes	407	68.3
No	189	31.7
HbA1C		
> 6.5%	501	84.1
≤6.5%	95	15.9

Table 2.

Severity of depression, anxiety and stress symptoms among the participants

Mental disorder	n	%
Depression		
Normal	155	26.0
Mild	56	9.4
Moderate	168	28.2
Severe	115	19.3
Exetremely severe	102	17.1
Anxiety		
Normal	107	18.0
Mild	32	5.4
Moderate	129	21.6
Severe	71	11.9
Exetremely severe	257	43.1
Stress		
Normal	340	57.0
Mild	60	10.1
Moderate	70	11.7
Severe	94	15.8
Exetremely severe	32	5.4

Table 3.

Association between depression status and socio-demographic and other variables

Variable	Depression				Chi-square test OR (95% CI)
	Yes		No		
	n	%	n	%	
Total	441	74.0	155	26.0	
Gender					
F	250	75.8	80	24.2	*P*=0.274 1.227 (0.850 to 1.771)
M	191	71.8	75	28.2	
Age, years					
<30	15	65.2	8	34.8	*P*=0.399* 1.172 (0.810 to 1.695)
30-59	167	72.9	62	27.1	
60+	259	75.3	85	24.7	
Mean ± SD	60.3 ± 13.2		60.0 ± 13.8		
* 60+ vs. <60					
Residency					
City	288	75.4	94	24.6	*P*=0.298 1.222 (0.838 to 1.781)
Village	153	71.5	61	28.5	

Table 3 (continued).

Association between depression status and socio-demographic and other variables

Variable	Depression				Chi-square test OR (95% CI)
	Yes		No		
	n	%	n	%	
Total	441	74.0	155	26.0	
Level of education					
Primary school	203	79.6	52	20.4	*P*=0.007* 1.689 (1.153 to 2.477)
Secondary school	153	72.5	58	27.5	
University/College	85	65.4	45	34.6	
* Primary vs. Secondary + University					
Current job status					
Employed	122	74.4	42	25.6	*P*=0.892 1.029 (0.682 to 1.552)
Unemployed	319	73.8	113	26.2	
Marital status					
Married	346	74.7	117	25.3	*P*=0.445* 1.183 (0.769 to 1.82)
Single	34	77.3	10	22.7	
Widow(er)	54	67.5	26	32.5	
Separated	7	77.8	2	22.2	
* Married vs. Single + Widow(er) + Separated					
Having children					
Yes	396	73.7	141	26.3	*P*=0.674 0.874 (0.465 to 1.641)
No	45	76.3	14	23.7	
History of DM in family					
Yes	263	72.3	101	27.7	*P*=0.226 0.790 (0.540 to 1.157)
No	178	76.7	54	23.3	
Co morbidity					
Yes	311	76.4	96	23.6	*P*=0.049 1.470 (1.002 to 2.157)
No	130	68.8	59	31.2	
HbA1C					
> 6.5%	383	76.4	118	23.6	*P*=0.002 2.071 (1.305 to 3.284)
≤6.5%	58	61.1	37	38.9	

Table 4.

Association between anxiety status and socio-demographic and other variables

Variable	Anxiety				Chi-square test OR (95% CI)
	Yes		No		
	n	%	n	%	
Total	489	82.0	107	18.0	
Gender					
F	284	86.1	46	13.9	*P*=0.004 1.837 (1.204 to 2.804)
M	205	77.1	61	22.9	

Table 4 (continued).

Association between anxiety status and socio-demographic and other variables

Variable	Anxiety				Chi-square test OR (95% CI)
	Yes		No		
	n	%	n	%	
Total	489	82.0	107	18.0	
Age, years					
<30	20	87.0	3	13.0	*P*=0.628* 0.900 (0.588 to 1.378)
30-59	189	82.5	40	17.5	
60+	280	81.4	64	18.6	
Mean ± SD	60.1 ± 13.3		61.1 ± 13.7		
* 60+ vs. <60					
Residency					
City	318	83.2	64	16.8	*P*=0.308 1.249 (0.814 to 1.919)
Village	171	79.9	43	20.1	
Level of education					
Primary school	216	84.7	39	15.3	*P*=0.145* 1.38 (0.895 to 2.126)
Secondary school	171	81.0	40	19.0	
University/College	102	78.5	28	21.5	
* Primary vs. Secondary + University					
Current job status					
Employed	138	84.1	26	15.9	*P*=0.411 1.225 (0.755 to 1.987)
Unemployed	351	81.3	81	18.8	
Marital status					
Married	378	81.6	85	18.4	*P*=0.630* 0.881 (0.527 to 1.474)
Single	39	88.6	5	11.4	
Widow(er)	65	81.3	15	18.8	
Separated	7	77.8	2	22.2	
* Married vs. Single + Widow(er) + Separated					
Having children					
Yes	437	81.4	100	18.6	*P*=0.204 0.588 (0.259 to 1.334)
No	52	88.1	7	11.9	
History of DM in family					
Yes	293	80.5	71	19.5	*P*=0.217 0.758 (0.488 to 1.177)
No	196	84.5	36	15.5	
Co-morbidity					
Yes	344	84.5	63	15.5	*P*=0.022 1.657 (1.076 to 2.55)
No	145	76.7	44	23.3	
HbA1C					
> 6.5%	414	82.6	87	17.4	*P*=0.391 1.269 (0.736 to 2.188)
≤6.5%	75	78.9	20	21.1	

Table 5.

Association between stress status and socio-demographic and other variables

Variable	Stress				Chi-square test
	Yes		No		
	n	%	n	%	OR (95% CI)
Total	256	43.0	340	57.0	
Gender					
F	160	48.5	170	51.5	*P*=0.002 1.667 (1.198 to 2.320)
M	96	36.1	170	63.9	
Age, years					
<30	9	39.1	14	60.9	*P*=0.968* 1.007 (0.725 to 1.398)
30-59	99	43.2	130	56.8	
60+	148	43.0	196	57.0	
Mean ± SD	60.3 ± 13.6		60.2 ± 13.2		
* 60+ vs. <60					
Residency					
City	160	41.9	222	58.1	*P*=0.482 0.886 (0.632 to 1.241)
Village	96	44.9	118	55.1	
Level of education					
Primary school	134	52.5	121	47.5	*P*<0.0001* 1.988 (1.428 to 2.768)
Secondary school	81	38.4	130	61.6	
University/College	41	31.5	89	68.5	
* Primary vs. Secondary + University					
Current Job status					
Employed	64	39.0	100	61.0	*P*=0.233 0.800 (0.554 to 1.154)
Unemployed	192	44.4	240	55.6	
Marital status					
Married	195	42.1	268	57.9	*P*=0.442* 0.859 (0.583 to 1.266)
Single	19	43.2	25	56.8	
Widow(er)	37	46.3	43	53.8	
Separated	5	55.6	4	44.4	
* Married vs. Single + Widow(er) + Separated					
Having children					
Yes	228	42.5	309	57.5	*P*=0.462 0.817 (0.477 to 1.4)
No	28	47.5	31	52.5	
History of DM in family					
Yes	144	39.6	220	60.4	*P*=0.036 0.701 (0.503 to 0.978)
No	112	48.3	120	51.7	
Co-morbidity					
Yes	190	46.7	217	53.3	*P*=0.007 1.632 (1.142 to 2.332)
No	66	34.9	123	65.1	
HbA1C					
> 6.5%	227	45.3	274	54.7	*P*=0.008 1.885 (1.177 to 3.019)
≤6.5%	29	30.5	66	69.5	

Discussion

Many studies show that comorbid depression, anxiety and/or stress in diabetics not only increases disease severity, complications, work impairment, and poor quality of life, but it is also connected with greater use of medical services and much higher healthcare expenses. It is critical for developing nations to quantify the prevalence of DAS among patients with diabetes to commence early treatment, improve clinical outcomes, and reduce resource utilization and cost. Our study is the first in PHC in Kosovo with T2DM and has shown a high prevalence of DAS at 74.0%, 82.0%, and 43.0%, respectively. These values are higher than in many developed countries.[23-28] In a study by Khuwaja et al.,[24] 57.9% (95% CI: 54.7% – 61.2%) and 43.5% (95% CI: 40.3% – 46.8%) of study participants had anxiety and depression, respectively. Our study was done in the end stage of the pandemic, which can be one of the factors for the high prevalence of DAS among diabetic patients. In the study of Arenliu-Qosaj et al.[29] about the prevalence of perceived DAS in healthcare workers in Kosovo during the COVID-19 pandemic, most healthcare workers (71.6%) reported a mild, moderate, or severe mental health burden.

Some of the other reasons for the high prevalence of DAS in T2DM patients, compared to other countries, are (1) the lack of health insurance, which means that most of these patients cover the costs of services such as medications, laboratory tests, analysis of complications out of pocket – from the family budget; (2) the health system of Kosovo is not sufficiently developed: it lacks a health information system, databases for patients with diabetes and DAS, screenings for certain diseases, including diabetes and DAS, the capacity to treat the complications of diabetes as well as for regular 6-monthly or annual visits of these patients.

There are other factors that make life difficult for patients with diabetes: PHC is not developed enough to manage these patients successfully; the level of health education of patients in Kosovo is unsatisfactory; the general economic and social situation in the country is poor; the rate of unemployment is high. The nature of DM itself contributes to the problem: the chronicity of the disease, its duration, the presence of complications (acute and chronic but more chronic), the need to take insulin several times a day, every day (invasive methods of receiving therapy, piercing with a needle). Changes in the family structure in Kosovo have resulted in a lack of family care for patients, especially the elderly (migration of the population outside the country, a part of the family leaving the home for various reasons and leaving the elderly alone, without care), posttraumatic stress after the war, and more.

In a study by Bensbaa et al.[28] in Maroko, a low educational level was strongly correlated with depression in T2DM patients, with a threshold P-value of 0.01. Also, in our study depression was found to be significantly associated with level of education. Subjects with only primary education were more likely to be depressed (79.6%, *P*=0.007; OR=1.689, 95% CI: 1.153 – 2.477) and were more likely to be stressed (52.5%, *P*<0.0001; OR=1.988, 95% CI: 1.428 – 2.768) than those with secondary education + University. The prevalence of anxiety

in previous literature was higher than that of depression, and this is comparable to our study results.

A study by Mukrim et al.[23] in Northern Saudi Arabia showed that the prevalence reached approximately 45.6% for anxiety, 18.7% for stress, and 37.4% for depression.

In a study by Cardenas et al.[12] in Ecuador, the prevalence of depression, anxiety, and stress was 31.7%, 33.7%, and 25.0%, respectively. Male gender was associated with a decreased risk for DAS. A higher level of education was associated with low risk for DAS. The high prevalence of DAS was associated with major risk factors, such as female gender and low-level education, like our study. The presence of DAS has major consequences for individuals with diabetes.[32,33] However, several studies have shown that depression can be well treated in individuals with diabetes. Increased awareness of depression in diabetes care is needed. This can be achieved by including screening instruments for depression as part of regular diabetes care.[34]

Conclusion

Our study showed that the prevalence of DAS is high in patients with T2DM. Anxiety was the most common type of psychological distress among the subjects (82.0%), depression was second with a prevalence of 74% and stress third with a prevalence of 43.0%. Periodic screening of patients with diabetes in PHC settings for early signs of psychological distress using easy and inexpensive validated screening tools like the DASS-21 questionnaire is recommended.

Limitations of the study

The major limitation of the present study is that the data were cross-sectional, which does not allow for studying the cause-and-effect relationship.

Ethical considerations

Ethical Approval for this research was received from the Ethics Committee of Medical Faculty, University of Prishtina, number 2689. Written informed consent was obtained from all participants.

Competing Interests

The authors declare that they have no competing interests.

References

1. International Diabetes Federation (IDF). IDF Diabetes Atlas 2021. IDF Atlas 10th edition. International Diabetes Federation; 2021. Available from: https://diabetesatlas.org/atlas/tenth-edition/
2. Gashi S. Prevalence of chronic diseases risk factors and specific health determinants in a transitional country-The case of Kosova. School of Medicine, University of Zagreb. Dissertation, Zagreb 2018
3. Ramadani N, Hoxha-Gashi S, Muçaj S, Hoxha A, Jerliu N, Kern J. Trends in Prediabetes and Diabetes Prevalence in Kosovo: A Comparison of the Results of Steps Survey From 2011 and 2019. International Journal of Biomedicine. 2023;13(1):47- 53. doi: 10.21103/Article13(1)_OA4
4. National Institute of Public Health of Kosova. Department of Health Statistics. Health statistics report. Report of survey on risk factors for chronic disease. Prishtina. 2011-2021.
5. Statistical Office of Kosova. Causes of death in Kosovo 2018 and 2019. Pristina, December 2020
6. Atlantis E, Ghassem Pour S, Girosi F. Incremental predictive value of screening for anxiety and depression beyond current type 2 diabetes risk models: a prospective cohort study. BMJ Open. 2018 Jan 23;8(1):e018255. doi: 10.1136/bmjopen-2017-018255.
7. Scott KM, Lim C, Al-Hamzawi A, Alonso J, Bruffaerts R, Caldas-de-Almeida JM, Florescu S, de Girolamo G, Hu C, de Jonge P, Kawakami N, Medina-Mora ME, Moskalewicz J, Navarro-Mateu F, O'Neill S, Piazza M, Posada-Villa J, Torres Y, Kessler RC. Association of Mental Disorders With Subsequent Chronic Physical Conditions: World Mental Health Surveys From 17 Countries. JAMA Psychiatry. 2016 Feb;73(2):150-8. doi: 10.1001/jamapsychiatry.2015.2688.
8. Druss BG, Walker ER. Mental disorders and medical comorbidity. The Synthesis Project. Robert Wood Johnson Foundation. 2011;21:7–15
9. Al-Mohaimeed AA. Prevalence and factors associated with anxiety and depression among type 2 diabetes in Qassim: A descriptive cross-sectional study. J Taibah Univ Med Sci. 2017 May 31;12(5):430-436. doi: 10.1016/j.jtumed.2017.04.002.
10. Tan KC, Chan GC, Eric H, Maria AI, Norliza MJ, Oun BH, Sheerine MT, Wong SJ, Liew SM. Depression, anxiety and stress among patients with diabetes in primary care: A cross-sectional study. Malays Fam Physician. 2015 Aug 31;10(2):9-21.
11. Vidyulatha J, Pramodkumar TA, Pradeepa R, Poongothai S, Thenmozhi S, Venkatesan U, Jebarani S, Anjana RM, Mohan V. Association of stress, depression, and anxiety among individuals with microvascular complications in type 2 diabetes. Journal of Diabetology. 2022 Jul 1;13(3):294-300.
12. Cárdenas L, Cabezas MDC, Muñoz A, Proaño JL, Miño C, Aguirre N. Prevalence and risk factors of depression, anxiety, and stress in an Ecuadorian outpatient population with type II diabetes mellitus: A cross-sectional study (STROBE). Medicine (Baltimore). 2022 Sep 30;101(39):e30697. doi: 10.1097/MD.0000000000030697.
13. Mikaliūkštienė A, Žagminas K, Juozulynas A, Narkauskaitė L, Sąlyga J, Jankauskienė K, Stukas R, Šurkienė G. Prevalence and determinants of anxiety and depression symptoms in patients with type 2 diabetes in Lithuania. Med Sci Monit. 2014 Feb 4;20:182-90. doi: 10.12659/MSM.890019.
14. Khaledi M, Haghighatdoost F, Feizi A, Aminorroaya A. The prevalence of comorbid depression in patients with type 2 diabetes: an updated systematic review and meta-analysis

***Corresponding author**: Prof. Ass. Dr. Sanije Hoxha – Gashi, Faculty of Medicine, University of Prishtina "Hasan Prishtina"; National Institute of Public Health of Kosovo, Prishtina, Kosovo. E-mail: sanije.gashi@uni-pr.edu*

on huge number of observational studies. Acta Diabetol. 2019 Jun;56(6):631-650. doi: 10.1007/s00592-019-01295-9.
15. Hohls JK, König HH, Quirke E, Hajek A. Anxiety, Depression and Quality of Life-A Systematic Review of Evidence from Longitudinal Observational Studies. Int J Environ Res Public Health. 2021 Nov 16;18(22):12022. doi: 10.3390/ijerph182212022.
16. Pouwer F, Schram MT, Iversen MM, Nouwen A, Holt RIG. How 25 years of psychosocial research has contributed to a better understanding of the links between depression and diabetes. Diabet Med. 2020 Mar;37(3):383-392. doi: 10.1111/dme.14227.
17. Liu X, Haagsma J, Sijbrands E, Buijks H, Boogaard L, Mackenbach JP, Erasmus V, Polinder S. Anxiety and depression in diabetes care: longitudinal associations with health-related quality of life. Sci Rep. 2020 May 20;10(1):8307. doi: 10.1038/s41598-020-57647-x.
18. Woon LS, Sidi HB, Ravindran A, Gosse PJ, Mainland RL, Kaunismaa ES, Hatta NH, Arnawati P, Zulkifli AY, Mustafa N, Leong Bin Abdullah MFI. Depression, anxiety, and associated factors in patients with diabetes: evidence from the anxiety, depression, and personality traits in diabetes mellitus (ADAPT-DM) study. BMC Psychiatry. 2020 May 12;20(1):227. doi: 10.1186/s12888-020-02615-y.
19. Kosovo Agency of Statistics. Statistics Yearbook of Republic of Kosova, Prishtina, 2021
20. Ministry of Health, Republic of Kosova. Plani i Veprimit per percaktimin e kritereve per regjistrin e banoreve per Kujdesin Paresor Shendetesor, Prishtine, Decembar 2022.
21. Ministry of Health. Administrative Instruction (Health) UA 04/2020 Primary Health Care, Prishtina, 20.11.2020
22. Lovibond, S.H.; Lovibond, P.F. (1995). Manual for the Depression Anxiety Stress Scales (2nd ed.). Sydney: Psychology Foundation (Available from The Psychology Foundation, Room 1005 Mathews Building, University of New South Wales, NSW 2052, Australia
23. Mukrim ME, Alshammari NM, Alshammari WM, Alshammari MS, Alshammari YN, Alshammari AS, Alshammari MS. Prevalence of depression, anxiety, and stress among diabetes mellitus patients in Arar, Northern Saudi Arabia. Age. 2019;62:22-3.
24. Khuwaja AK, Lalani S, Dhanani R, Azam IS, Rafique G, White F. Anxiety and depression among outpatients with type 2 diabetes: A multi-centre study of prevalence and associated factors. Diabetol Metab Syndr. 2010 Dec 20;2:72. doi: 10.1186/1758-5996-2-72.
25. Lin EH, Rutter CM, Katon W, Heckbert SR, Ciechanowski P, Oliver MM, Ludman EJ, Young BA, Williams LH, McCulloch DK, Von Korff M. Depression and advanced complications of diabetes: a prospective cohort study. Diabetes Care. 2010 Feb;33(2):264-9. doi: 10.2337/dc09-1068.
26. Tovilla-Zárate C, Juárez-Rojop I, Peralta Jimenez Y, Jiménez MA, Vázquez S, Bermúdez-Ocaña D, Ramón-Frías T, Genis Mendoza AD, García SP, Narváez LL. Prevalence of anxiety and depression among outpatients with type 2 diabetes in the Mexican population. PLoS One. 2012;7(5):e36887. doi: 10.1371/journal.pone.0036887.
27. Lin EH, Heckbert SR, Rutter CM, Katon WJ, Ciechanowski P, Ludman EJ, Oliver M, Young BA, McCulloch DK, Von Korff M. Depression and increased mortality in diabetes: unexpected causes of death. Ann Fam Med. 2009 Sep-Oct;7(5):414-21. doi: 10.1370/afm.998.
28. Bensbaa S, Agerd L, Boujraf S, Araab C, Aalouane R, Rammouz I, Ajdi F. Clinical assessment of depression and type 2 diabetes in Morocco: Economical and social components. J Neurosci Rural Pract. 2014 Jul;5(3):250-3. doi: 10.4103/0976-3147.133576.
29. Arenliu Qosaj F, Weine SM, Sejdiu P, Hasani F, Statovci S, Behluli V, Arenliu A. Prevalence of Perceived Stress, Anxiety, and Depression in HCW in Kosovo during the COVID-19 Pandemic: A Cross-Sectional Survey. Int J Environ Res Public Health. 2022 Dec 12;19(24):16667. doi: 10.3390/ijerph192416667.
30. Das-Munshi J, Stewart R, Ismail K, Bebbington PE, Jenkins R, Prince MJ. Diabetes, common mental disorders, and disability: findings from the UK National Psychiatric Morbidity Survey. Psychosom Med. 2007 Jul-Aug;69(6):543-50. doi: 10.1097/PSY.0b013e3180cc3062.
31. Tovilla-Zárate C, Juárez-Rojop I, Peralta Jimenez Y, Jiménez MA, Vázquez S, Bermúdez-Ocaña D, Ramón-Frías T, Genis Mendoza AD, García SP, Narváez LL. Prevalence of anxiety and depression among outpatients with type 2 diabetes in the Mexican population. PLoS One. 2012;7(5):e36887. doi: 10.1371/journal.pone.0036887.
32. Williams JW Jr, Katon W, Lin EH, Nöel PH, Worchel J, Cornell J, Harpole L, Fultz BA, Hunkeler E, Mika VS, Unützer J; IMPACT Investigators. The effectiveness of depression care management on diabetes-related outcomes in older patients. Ann Intern Med. 2004 Jun 15;140(12):1015-24. doi: 10.7326/0003-4819-140-12-200406150-00012.
33. Pouwer F, Beekman AT, Lubach C, Snoek FJ. Nurses' recognition and registration of depression, anxiety and diabetes-specific emotional problems in outpatients with diabetes mellitus. Patient Educ Couns. 2006 Feb;60(2):235-40. doi: 10.1016/j.pec.2005.01.009.
34. Hermanns N, Kulzer B, Krichbaum M, Kubiak T, Haak T. How to screen for depression and emotional problems in patients with diabetes: comparison of screening characteristics of depression questionnaires, measurement of diabetes-specific emotional problems and standard clinical assessment. Diabetologia. 2006 Mar;49(3):469-77. doi: 10.1007/s00125-005-0094-2.

International Journal of Biomedicine 13(3) (2023) 91-95
http://dx.doi.org/10.21103/Article13(2)_OA6

ORIGINAL ARTICLE

Ophthalmology

INTERNATIONAL JOURNAL OF BIOMEDICINE

Association Between Central Corneal Thickness and Intraocular Pressure in Patients with Refractive Anomalies and Emmetropes

Mimoza Ismaili*

Department of Ophthalmology, Faculty of Medicine, University of Pristina "Hasan Prishtina", Prishtina, Kosovo

Abstract

Background: The aim of this study was to determine the relationship between central corneal thickness (CCT) and intraocular pressure (IOP) in patients with refractive anomalies and emmetropes.

Methods and Results: This retrospective study was conducted in the Department of Ophthalmology at the University Clinical Center. The study included 330 respondents, with a total of 660 eyes, divided into two groups. The test group (TG) included 180 respondents with refractive anomalies (65 respondents with hypertropia, 65 with myopia, and 50 with astigmatism); the control group (CG) included 150 respondents with uncorrected visual acuity – 6/6 in both eyes. All respondents included in the research were aged 18–40, with an average age of 22.9 years. The values of CCT in TG was around 499.3–577.1 μm. From 360 eyes in the TG with refractive anomalies, the highest IOP values were found in the astigmatic group (20.6 mmHg) and the lowest values in the myopic group (15.3 mmHg) (P<0.001) and were statistically higher compared to the CG (P<0.001 in both cases). We found a statistically significant, moderate positive correlation between the values of CCT and IOP in the hypermetropic group (r_s=0.655, 95% CI: 0.540 to 0.745, P<0.0001) and a statistically significant low negative correlation (r_s=-0.209, 95% CI: -0.373 to -0.033, P=0.0165) between the values of CCT and IOP in the myopic group. Also, a statistically significant low negative correlation (r_s=-0.304, 95% CI: -0.510 to -0.152, P=0.0005) was found between the values of CCT and IOP in the astigmatism group.

Conclusion: The results of our study show that increasing the CCT values in the hypermetropic group leads to an increase in the IOP values. Therefore, these findings can be used as a reference for our population, which would assist in the early diagnosis of ocular hypertension. (**International Journal of Biomedicine. 2023;13(3):91-95.**)

Keywords: central corneal thickness • refractive anomaly • intraocular pressure

For citation:Ismaili M. Association Between Central Corneal Thickness and Intraocular Pressure in Patients with Refractive Anomalies and Emmetropes. International Journal of Biomedicine. 2023;13(3):91-95. doi:10.21103/Article13(3)_OA6

Abbreviations

CCT, central corneal thickness, **DS**, diopter sphere; **DC**, diopter cylinder; **GAT**, Goldmann applanation tonometry; **IOP**, intraocular pressure.

Introduction

Central corneal thickness (CCT), a crucial indicator of a healthy cornea, helps to evaluate corneal diseases.[1] CCT, as well as intraocular pressure (IOP), is important for assessing glaucoma, considering that low CCT will lead to the underestimation of intraocular pressure and interfere with the prognosis of glaucoma.[2] IOP is a key element in the management of glaucoma, and it should, therefore, be measured using a reliable technique with a high degree of accuracy. Though Goldman applanation tonometry (GAT) is the most widely used and current "gold standard" for IOP measurements, readings of IOP measurements made with GAT are affected by CCT.[3,4]

Refractive errors constitute one of the most common causes of visual impairment affecting all age groups.[5] Refractive error is another factor associated with CCT in adults and children, with high myopic refractive errors reported to have reduced CCT compared, to those with greater hyperopic refraction.[6-9]

The aim of this study was to determine the relationship between CCT and IOP in patients with refractive anomalies and emmetropes.

Materials and Methods

This retrospective study was conducted in the Department of Ophthalmology at the University Clinical Center. The study included 330 respondents, with a total of 660 eyes, divided into two groups. The test group (TG) included 180 respondents with refractive anomalies (65 respondents with hypertropia, 65 with myopia, and 50 with astigmatism); the control group (CG) included 150 respondents with uncorrected visual acuity – 6/6 in both eyes. All respondents included in the research were aged 18–40, with an average age of 22.9 years.

Data collection

Emmetropic respondents were selected after a detailed examination. Refractive anomalies were presented by the spherical equivalent refraction calculated as sphere plus half of the cylindrical error. The respondents were classified according to the spherical power into three major groups: emmetropic group (+0.25 to −0.25 D), myopic group (≥−0.50D), and hypermetropic group(≥+0.50D); furthermore, according to the cylindrical equivalent some respondents were classified into the astigmatism group (≥−0.5 DC to + ≥0.5 DC). The hypermetropia and myopia groups were divided into three subgroups based on refractive power: mild (≤3.00 DS), moderate (3.00-6.00 DS), and high (>6.00 DS).

Based on the focus of the main meridians in the astigmatic group, the respondents were classified into these subgroups: myopic astigmatism, hypermetropic astigmatism, compound astigmatism, and mixed astigmatism. Myopic astigmatism was determined in respondents who had a negative (sphere and cylinder) error of ≥-0.50DC, and hypermetropic astigmatism was determined in respondents who had a positive (sphere and cylinder) error of ≥+0.50DC.

In the subgroup of myopic compound astigmatism, respondents were classified into the group where both the sphere and cylinder had negative diopters (≥ −0.50D and ≥ −0.50DC), as well as the group of compound hypermetropic astigmatism (≥ +0.50D and ≥ +0.50DC). Meanwhile, the mixed astigmatism group included respondents with a positive sphere (+0.50D) and a negative cylinder (-0.50DC), or the opposite.

Inclusion criteria, respondents with the following: previously undiagnosed refractive anomalies, need for correction of refractive anomalies, normal corneal topography, no ocular disease, no previous eye surgery, and no previous correction with glasses.

Exclusion criteria, patients with the following: glaucoma and previous corneal refractive surgery procedures; IOP>21 mmHg; evidence of other anterior segment pathology, including corneal opacities, keratoconus, corneal oedema, presbyopia, amblyopia, staphyloma; best visual acuity of 6/6 (also expressed as 20/20 or 1.0); diabetes mellitus or other acute or chronic diseases possibly affecting the corneal thickness; no history of contact lens wear; encroached pterygium; refusal to give consent.

Procedure

Data collected from respondents with refractive anomalies were retrospectively collected for 360 eyes examined over a period of two years, thereafter compared with data from normal eyes. After informed consent was obtained, the respondents underwent a complete ophthalmic examination and anterior segment evaluation biomicroscopy. Visual acuity was measured at 6 meters (20 feet) using a Snellen chart.

IOP measurement by GAT: three measurements were taken, and the average was calculated, optic axis length measurement with ultrasound A scan, corneal curvature measurement with the automated keratometry, and 90D cycloplegia fundus exam.

CTT measurement was initially performed on all respondents with refractive anomalies as well as the CG. CCT was measured by ultrasonic pachymetry, five CCT measurements were taken, and the average was used for analysis. The visual acuity was determined using mydriatic points, then under the influence of the mydriatic, with Hydrochloride Cyclopentolate (one drop of 1% solution). A cyclopentolate drop was instilled two times at an interval of 10 minutes, and refraction was carried out after 45 minutes after the first instillation. Cycloplegia was considered complete if the pupil was dilated to 6 mm or more and no light reflex was present. On completion of testing the right eye, the acuity of the left eye was measured. Results were the same when the left eye was analyzed; thus, right-eye data were presented.

Statistical analysis was performed using the statistical software package SPSS version 22.0 (SPSS Inc, Armonk, NY: IBM Corp). For the descriptive analysis, results are presented as mean (M) ± standard deviation (SD). For data with normal distribution, inter-group comparisons were performed using Student's t-test. A non-parametric Kruskal-Wallis test was used to compare median values among ≥3 groups, followed by Dunn's test to identify which groups are different. Categorical variables were analyzed using the chi-square test with Yates' correction or, alternatively, Fisher's exact test. Spearman's rank correlation coefficient (r_s) was calculated to measure the strength and direction of the relationship between two variables. A probability value of $P<0.05$ was considered statistically significant.

Results

By categorizing respondents by gender, we found no difference with a significant statistical value. Most of the surveyed respondents (75.2%) from the four groups were between 20–29 years. All respondents included in the research were aged 18–40, with a mean age of 22.9±4.0 years. According to age, we found statistically significant differences between the groups ($P=0.0002$). Respondents with astigmatism were younger than the group with hypermetropia ($P<0.01$) and myopia ($P<0.01$) (Table 1).

The values of CCT in TG was around 499.3–577.1 μm. We found a statistically significant difference between the CCT of the three groups—hypermetropia, myopia, and astigmatism—and the CG ($P<0.001$) (Table 2). Also,

compared with the CG, we obtained a statistically significant difference in the IOP value in all groups with refractive anomalies (P<0.0001) (Table 3). From 360 eyes in the TG with refractive anomalies, the highest IOP values were found in the astigmatic group (20.6 mmHg) and the lowest values in the myopic group (15.3 mmHg) (P<0.001) and were statistically higher compared to the CG (P<0.001 in both cases) (Table 3).

Table 1.

General characteristics of study patients

	Hypermetropic group n=65	Myopic group n=65	Astigmatism group n=50	Control group n=150	*P*-value
Gender, n (%)					
F	45(69.2)	41(63.1)	32(64.0)	94(62.7)	0.824
M	20(30.8)	24(36.9)	18(36.0)	56(37.3)	
Age, mean±SD (year)	23.8±4.9	24.2±5.6	21.6±2.1	22.3±2.7	0.0002
Age group (year) n (%)					
< 20	11(16.9)	12(18.5)	10 20.0)	30(20.0)	0.0057
20-29	47(72.3)	43(66.2)	40(80.0)	118(78.7)	
≥30	7(10.8)	10(15.4)	-	2(1.3)	

Table 2.

Central corneal thickness by groups

CCT (µm)	n	Mean ±SD	*P*-value
Hypermetropia	65	561.5±25.3	Hypermetropia High vs.Con., P<0.05 Moderate vs.Con., P<0.001 Low vs.Con., P<0.001
high	7	569.5±23.2	
moderate	15	577.1±40.2	
low	43	559.7±21.5	
Myopia	65	517.9±37.3	Myopia High vs. Con., P<0.001 Moderate vs. Con., P<0.001 Low vs. Con., P<0.001
high	5	507.3±50.8	
moderate	9	499.3±41.8	
low	51	526.0±34.5	
Astigmatism	50	528.3±35.3	Astigmatism Hypermetrop.vs. Con.,P>0.05 Myopic vs. Con., P<0.001 Mixed vs. Con., P>0.05 Compound vs. Cont., P<0.001
hypermetropic	10	547.8±27	
myopic	21	518.2±24.6	
mixed	11	549.4±41.5	
compound	8	514.1±36	
Control (Con.)	150	553.3±18.5	
Kruskal Wallis test		P<0.001	
Dunn's test Hypermetropia vs. Myopia [P<0.001]; Hypermetropia vs. Astigmatism [P<0.001]; Hypermetropia vs. Control [P>0.05]; Myopia vs. Astigmatism [P>0.05]; Myopia vs. Control [P<0.001]; Astigmatism vs.Control [P<0.001].			

IOP, mmHg	Group			
	Hypermetropia	Myopia	Astigmatism	Control
n	65	65	50	150
Mean	19.9	15.3	20.6	12.3
SD	5.0	4.7	4.9	3.0
Min	10	10	10	10
Max	26.5	24.5	29	21
Kruskal Wallis test P<0.0001				
Dunn's test Hypertropia vs. Myopia [P<0.001]; Hypertropia vs. Astigmatism [P>0.05]; Hypertropia vs. Control [P<0.001]; Myopia vs. Astigmatism [P<0.001] Myopia vs. Control [P<0.001]; Astigmatism vs. Control [P<0.001]				

We have analyzed the degree of correlation between the values of CCT (µm) and IOP (mmHg) in the hypermetropic group, where a statistically significant, moderate positive correlation was found (r_s=0.655, 95% CI: 0.540 to 0.745, P<0.0001), (Figure 1). A statistically significant low negative correlation (r_s=-0.209, 95% CI: -0.373 to -0.033, P=0.0165) was found between the values of CCT and IOP in the myopic group (Figure 2). Also, a statistically significant low negative correlation (r_s=-0.304, 95% CI: -0.510 to -0.152, P=0.0005) was found between the values of CCT and IOP in the astigmatism group (Figure 3). No significant correlation (r_s=0.074, 95% CI: -0.042 to 0.189, P=0.197) was determined between the values of CCT and IOP in the CG (Figure 4).

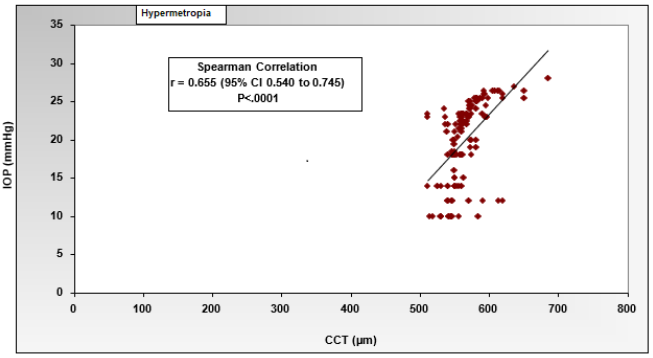

Fig. 1. *Correlation between CCT and IOP in the hypermetropic group.*

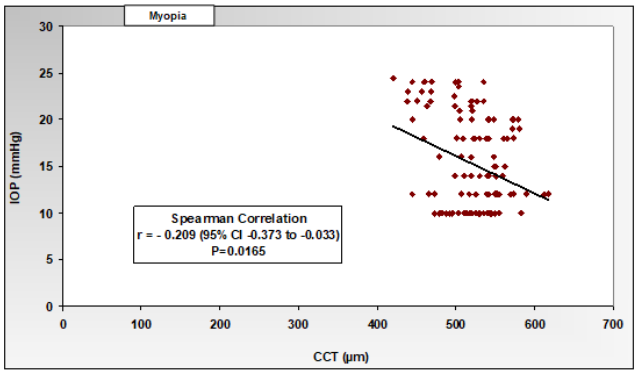

Fig. 2. *Correlation between CCT and IOP in the myopic group.*

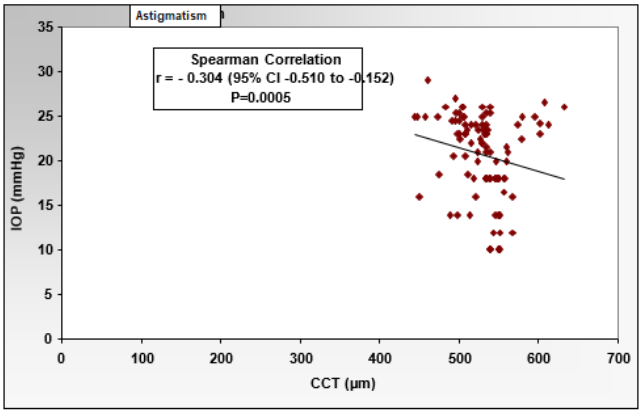

Fig. 3. *Correlation between CCT and IOP in the astigmatism group.*

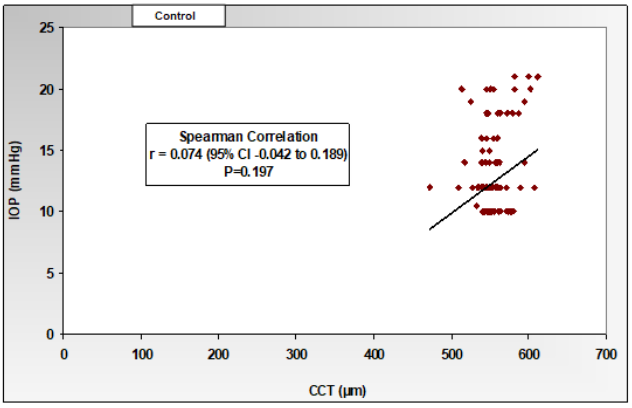

Fig. 4. *Correlation between CCT and IOP in the control group.*

Discussion

In a study by Juwayli et al.,[10] the average age of the myopic study group was 32.3±5.61years, while in the hypermetropic group - 35±6.59 years, ranging from 20 to 40 years. Women dominated in both groups; there were 25 myopic and 25 hyperopic eyes.[10] In our study, the average age was 22.9, range 18-40, and it also included astigmatic respondents (Table 1). A study by Qayum et al.[11] found that CCT was associated with IOP in both genders. These results were consistent with our findings.

We also found a statistically significant difference between the CCT values of the three groups—hypermetropic, myopic, and astigmatic—and the CG (P<0.001) (Table 2). In the hypermetropic group, the mean value of CCT was higher than in the CG (emmetrope). Many researchers have reported a correlation between CCT and IOP measurements using the GAT method. An increasing number of new methods for IOP measurement have become the object of many studies, which compare them with the GAT method, which is still considered to be the standard method.[12]

In this study, using GAT methods, we found that the average IOP value of our respondents was 12.3 mmHg.[13] This is consistent with other studies. Ehlers et al.[14] showed a 5 mm mmHg increase in IOP for every 70-µm increase in CCT, while a study by Wei et al.[15] reported a 0.32 mmHg increase in IOP for every 10-µm increase in CCT.

Many studies found a positive association between IOP and CCT measured by applanation and a possible overestimation. Numerous studies have shown that patients diagnosed with ocular hypertension have significantly thicker corneas than normal subjects.[16,17] But in our study, the respondents did not have a positive history of glaucoma. From 360 eyes in the TG with refractive anomalies, the highest IOP values were found in the astigmatic group (20.6 mmHg) and the lowest values in the myopic group (15.3 mmHg) (P<0.001) and were statistically higher compared to the CG (P<0.001 in both cases) (Table 3).

A study by Hoffmann et al.[8] with the pachymetry method showed that a normal range of the values of CCT was around 520–550 µm. They concluded that variability in CCT measurement could be a reason for error with GAT, where thick cornea may cause an overestimation of IOP values. Also, the results of our study show that these reasons can affect the IOP values measured with the GAT method.

The relationship between refractive anomalies and IOP is another area of discrepancy. Some studies have suggested that myopia may be associated with the risk of primary open-angle glaucoma and hypermetropia with a possible risk of ocular hypertension.[18] Most of the studies have focused mainly on myopic and hypermetropic eyes, but we have also included astigmatic eyes in our study.

Regarding the relationship between IOP and refractive errors, a study conducted in Wisconsin[16] showed that myopes were 60% more likely to develop glaucoma than emmetropes. A study by Nomura et al.[19] found a positive relationship between IOP and increasing degrees of myopia; unlike our results, a correlation was found between IOP and the myopic group, regardless of the degree of myopia. Such results have been encountered in other studies, such as a study by Mana, who found a weak but significant correlation between GAT-IOP and corneal astigmatism.[20] Meanwhile, our study found a statistically significant low negative correlation between the values of CCT and IOP in the astigmatic group (Figure 1). We obtained a statistically significant difference between the values of the CCT and IOP of the hypermetropic, myopic, and astigmatic groups, compared with the CG (P<0.001) (Figures 1-4). In our results, of the 360 eyes in the TG, the highest IOP values were found in the astigmatic group (20.6 mmHg), while the lowest values were in the myopic group (15.3 mmHg).

In conclusion, the results of our study show that increasing the CCT values in the hypermetropic group leads to an increase in the IOP values. Also, these results showed that the mean IOP measured by the applanation tonometer was 12.3 mmHg in control, and the highest IOP values were found in the astigmatic group (20.6 mmHg). Therefore, these findings can be used as a reference for our population, which would assist in the early diagnosis of ocular hypertension.

Acknowledgments

I would like to express my gratitude to my colleagues and our hospital staff for their constant support and guidance throughout the study period.

Competing Interests

The author declares that there is no conflict of interest.

References

1. Gab-Alla AA. Reversal of Myopic Correction for Patients Intolerant to LASIK. J Ophthalmol. 2021 Dec 15;2021:7113676. doi: 10.1155/2021/7113676.
2. Gordon MO, Beiser JA, Brandt JD, Heuer DK, Higginbotham EJ, Johnson CA, Keltner JL, Miller JP, Parrish RK 2nd, Wilson MR, Kass MA. The Ocular Hypertension Treatment Study: baseline factors that predict the onset of primary open-angle glaucoma. Arch Ophthalmol. 2002 Jun;120(6):714-20; discussion 829-30. doi: 10.1001/archopht.120.6.714.
3. Brandt JD, Beiser JA, Kass MA, Gordon MO. Central corneal thickness in the Ocular Hypertension Treatment Study (OHTS). Ophthalmology. 2001 Oct;108(10):1779-88. doi: 10.1016/s0161-6420(01)00760-6.
4. Cockburn DM. Effects of corneal thickness on IOP measurement. Clin Exp Optom. 2004 May;87(3):185-6.
5. Abdull MM, Sivasubramaniam S, Murthy GV, Gilbert C, Abubakar T, Ezelum C, Rabiu MM; Nigeria National Blindness and Visual Impairment Study Group. Causes of blindness and visual impairment in Nigeria: the Nigeria national blindness and visual impairment survey. Invest Ophthalmol Vis Sci. 2009 Sep;50(9):4114-20. doi: 10.1167/iovs.09-3507.
6. Aslan L, Aslankurt M, Yüksel E, Özdemir M, Aksakal E, Gümüşalan Y, Özdemir G. Corneal thickness measured by Scheimpflug imaging in children with Down syndrome. J AAPOS. 2013 Apr;17(2):149-52. doi: 10.1016/j.jaapos.2012.10.020.
7. Hashemi H, Asgari S, Mehravaran S, Emamian MH, Shariati M, Fotouhi A. The distribution of corneal thickness in a 40- to 64-year-old population of Shahroud, Iran. Cornea. 2011 Dec;30(12):1409-13. doi: 10.1097/ICO.0b013e31822018dd.
8. Hoffmann EM, Lamparter J, Mirshahi A, Elflein H, Hoehn R, Wolfram C, Lorenz K, Adler M, Wild PS, Schulz A, Mathes B, Blettner M, Pfeiffer N. Distribution of central corneal thickness and its association with ocular parameters in a large central European cohort: the Gutenberg health study. PLoS One. 2013 Aug 1;8(8):e66158. doi: 10.1371/journal.pone.0066158.
9. Uçakhan OO, Gesoğlu P, Ozkan M, Kanpolat A. Corneal elevation and thickness in relation to the refractive status measured with the Pentacam Scheimpflug system. J Cataract Refract Surg. 2008 Nov;34(11):1900-5. doi: 10.1016/j.jcrs.2008.07.018.
10. Juwayli RMM, Farag AAR, Shalaby AAEA. Correlation between Refractive Errors and Intraocular Pressure after Adjusting by Central Corneal Thickness. The Egyptian Journal of Hospital Medicine. 2021 January;82(3):581-586.
11. Qayum SH. Correlation between Central Corneal thickness and Intraocular Pressure measured with Goldmann Applanation Tonometer (GAT) in healthy individuals. JMSCR. 2019;7(5) May.
12. Osman EA, Gikandi PW, Al-Jasser AA, Alotaibi M, Mousa A. Comparison of Goldmann Applanation, Noncontact Air Puff, and Tono-Pen XL Tonometry in Normal Controls versus Glaucoma Patients at a University Hospital in Riyadh, Saudi Arabia. Middle East Afr J Ophthalmol. 2018 Jan-Mar;25(1):8-13. doi: 10.4103/meajo.MEAJO_291_16.
13. Shafiq I. Influence of Central Corneal Thickness (CCT) on Intraocular Pressure (IOP) Measured with Goldmann Applanation Tonometer (GAT) in Normal Individuals. Pak J Ophthalmol. 2008;24(4).
14. Ehlers N, Bramsen T, Sperling S. Applanation tonometry and central corneal thickness. Acta Ophthalmol (Copenh). 1975 Mar;53(1):34-43. doi: 10.1111/j.1755-3768.1975.tb01135.x.
15. Wei W, Fan Z, Wang L, Li Z, Jiao W, Li Y. Correlation analysis between central corneal thickness and intraocular pressure in juveniles in Northern China: the Jinan city eye study. PLoS One. 2014 Aug 22;9(8):e104842. doi: 10.1371/journal.pone.0104842.
16. Johnson M, Kass MA, Moses RA, Grodzki WJ. Increased corneal thickness simulating elevated intraocular pressure. Arch Ophthalmol. 1978 Apr;96(4):664-5. doi: 10.1001/archopht.1978.03910050360012.
17. Whitacre MM, Stein RA, Hassanein K. The effect of corneal thickness on applanation tonometry. Am J Ophthalmol. 1993 May 15;115(5):592-6. doi: 10.1016/s0002-9394(14)71455-2.
18. Wong TY, Klein BE, Klein R, Knudtson M, Lee KE. Refractive errors, intraocular pressure, and glaucoma in a white population. Ophthalmology. 2003 Jan;110(1):211-7. doi: 10.1016/s0161-6420(02)01260-5.
19. Nomura H, Ando F, Niino N, Shimokata H, Miyake Y. The relationship between intraocular pressure and refractive error adjusting for age and central corneal thickness. Ophthalmic Physiol Opt. 2004 Jan;24(1):41-5. doi: 10.1046/j.1475-1313.2003.00158.x.
20. Hagishima M, Kamiya K, Fujimura F, Morita T, Shoji N, Shimizu K. Effect of corneal astigmatism on intraocular pressure measurement using ocular response analyzer and Goldmann applanation tonometer. Graefes Arch Clin Exp Ophthalmol. 2010 Feb;248(2):257-62. doi: 10.1007/s00417-009-1202-7.

Correspondence:
Dr. Sci. Mimoza Ismaili, drmimozaismaili@gmail.com

International Journal of Biomedicine 13(3) (2023) 96-100
http://dx.doi.org/10.21103/Article13(3)_OA7

ORIGINAL ARTICLE

Ophthalmology

INTERNATIONAL JOURNAL OF BIOMEDICINE

Association Between Central Corneal Thickness and Axial Length in Patients with Refractive Anomalies and Emmetropes

Mimoza Ismaili

Department of Ophthalmology, Faculty of Medicine, University of Pristina "Hasan Prishtina", Prishtina, Kosovo

Abstract

Background: This study aimed to determine the correlation between central corneal thickness (CCT) and axial length (AL) in patients with refractive anomalies and emmetropes.

Methods and Results: The study included 330 respondents, with a total of 660 eyes, divided into two groups. The test group (TG) included 180 respondents with refractive anomalies (65 respondents with hypertropia, 65 with myopia, and 50 with astigmatism); the control group (CG) included 150 respondents with uncorrected visual acuity – 6/6 in both eyes.

The CCT values were higher in the hypermetropic group compared to the myopic group (561.5±25.3 vs. 517.9±37.3 mm, $P<0.001$), astigmatism group (561.5±25.3 vs. 528.3±35.3 mm, $P<0.001$) and the CG (561.5±25.3 vs. 553.3±18.5 mm, $P<0.001$).

From 360 eyes in the TG with refractive anomalies, the lowest AL values were found in the hypermetropic group (21.7±1.0 mm) compared to the myopic group ($P<0.001$), the astigmatism group ($P<0.001$), and the CG ($P<0.001$). Similar differences were also found for the right eyes (OD): hypermetrops tend to have shorter AL than the astigmatic group ($P<0.001$), myopic group ($P<0.001$), and the CG (emmetrope) ($P<0.001$).

Conclusion: The mean CCT value in the hyperopic group was higher than in the emmetropic group, while the CCT value of the myopic and astigmatic group was lower than that of the emmetropic group. AL values were the lowest in the hypermetropic group than in the myopic, astigmatic, and control groups.(**International Journal of Biomedicine. 2023;13(3):96-100.**)

Keywords: central corneal thickness • refractive anomaly • axial length

For citation:Ismaili M. Association between Central Corneal Thickness and Axial Length in Patients with Refractive Anomalies and Emmetropes. International Journal of Biomedicine. 2023;13(3):96-100. doi:10.21103/Article13(3)_OA7

Introduction

Central corneal thickness (CCT) is an important indicator of corneal health status. It is an essential tool in assessing and managing corneal diseases and helps estimate the corneal barrier and endothelial pump function.[1] Refractive errors refer to an optical defect in which the optical system cannot sharply focus parallel rays of light on the retina when the accommodation is at rest.[2-4]The most common refractive errors are myopia, hyperopia, and astigmatism.[5] The global magnitude of refractive errors is not reliably reported, but it is estimated that more than 2.3 billion people worldwide are affected by this ocular condition.[6]

***Correspondence:**

Dr. Sci. Mimoza Ismaili, drmimozaismaili@gmail.com

Experimental, epidemiological, and clinical research has shown that both environmental and genetic factors influence refractive development.[7] The axial length (AL) is known to be shorter in hyperopes and longer in myopes than in emmetropic eyes.[8] Compared with other ocular components, such as the cornea and crystalline lens, the AL is typically regarded as the primary determinant of refractive error.[9] The AL is the distance from the corneal surface to an interference peak corresponding to the retinal pigment epithelium/Bruch's membrane; this is expressed in millimeters,[10,11] and AL is one of the key variables determining the eye's refractive status. AL grows beyond the length at which emmetropia occurs, leading to myopia. Before emmetropia, short AL tends to keep hyperopia.[12] Among these components, AL received the most attention since it is a main parameter for both myopia and hypermyopia.[13]

This study aimed to determine the correlation between CCT and AL in patients with refractive anomalies and emmetropes.

Materials and Methods

The study included 330 respondents, with a total of 660 eyes, divided into two groups. The test group included 180 respondents with refractive anomalies (65 respondents with hypertropia, 65 with myopia, and 50 with astigmatism); the control group (CG) included 150 respondents with uncorrected visual acuity – 6/6 in both eyes.

All respondents included in the research were aged 18–40, with an average age of 22.9 years.

Data collection

Emmetropic respondents were selected after a detailed examination. Refractive anomalies were presented by the spherical equivalent refraction calculated as sphere plus half of the cylindrical error. The respondents were classified according to the spherical power into three major groups: emmetropic group (+0.25 to −0.25 D), myopic group (≥−0.50D), and hypermetropic group(≥+0.50D); furthermore, according to the cylindrical equivalent some respondents were classified into the astigmatism group (≥−0.5 DC to + ≥0.5 DC). The hypermetropia and myopia groups were divided into three subgroups based on refractive power: mild (≤3.00 DS), moderate (3.00-6.00 DS), and high (>6.00 DS).

Based on the focus of the main meridians in the astigmatic group, the respondents were classified into these subgroups: myopic astigmatism, hypermetropic astigmatism, compound astigmatism, and mixed astigmatism. Myopic astigmatism was determined in respondents who had a negative (sphere and cylinder) error of ≥-0.50DC, and hypermetropic astigmatism was determined in respondents who had a positive (sphere and cylinder) error of ≥+0.50DC.

In the subgroup of myopic compound astigmatism, respondents were classified into the group where both the sphere and cylinder had negative diopters (≥ −0.50D and ≥ −0.50DC), as well as the group of compound hypermetropic astigmatism (≥ +0.50D and ≥ +0.50DC). Meanwhile, the mixed astigmatism group included respondents with a positive sphere (+0.50D) and a negative cylinder (-0.50DC), or the opposite.

Inclusion criteria, respondents with the following: previously undiagnosed refractive anomalies, need for correction of refractive anomalies, normal corneal topography, no ocular disease, no previous eye surgery, and no previous correction with glasses.

Exclusion criteria, patients with the following: glaucoma and previous corneal refractive surgery procedures; IOP>21mmHg; evidence of other anterior segment pathology, including corneal opacities, keratoconus, corneal oedema, presbyopia, amblyopia, staphyloma; best visual acuity of 6/6 (also expressed as 20/20 or 1.0); diabetes mellitus or other acute or chronic diseases possibly affecting the corneal thickness; no history of contact lens wear; encroached pterygium; refusal to give consent.

Procedure

Data collected from respondents with refractive anomalies were retrospectively collected for 360 eyes examined over a period of two years, thereafter compared with data from normal eyes. After informed consent was obtained, the respondents underwent a complete ophthalmic examination and anterior segment evaluation biomicroscopy. Visual acuity was measured at 6 meters (20 feet) using a Snellen chart.

IOP measurement by Goldmann applanation tonometry (GAT): three measurements were taken, and the average was calculated, optic axis length measurement with ultrasound A scan, corneal curvature measurement with the automated keratometry, and 90D cycloplegia fundus exam.

CTT measurement was initially performed on all respondents with refractive anomalies as well as the CG. CCT was measured by ultrasonic pachymetry, five CCT measurements were taken, and the average was used for analysis. The visual acuity was determined using mydriatic points, then under the influence of the mydriatic, with Hydrochloride Cyclopentolate (one drop of 1% solution). A cyclopentolate drop was instilled two times at an interval of 10 minutes, and refraction was carried out after 45 minutes after the first instillation. Cycloplegia was considered complete if the pupil was dilated to 6 mm or more and no light reflex was present. On completion of testing the right eye, the acuity of the left eye was measured. Results were the same when the left eye was analyzed; thus, right-eye data were presented.

Statistical analysis was performed using the statistical software package SPSS version 22.0 (SPSS Inc, Armonk, NY: IBM Corp). For the descriptive analysis, results are presented as mean (M) ± standard deviation (SD). For data with normal distribution, inter-group comparisons were performed using Student's t-test. A non-parametric Kruskal-Wallis test was used to compare median values among ≥3 groups, followed by Dunn's test to identify which groups are different. Categorical variables were analyzed using the chi-square test with Yates' correction or, alternatively, Fisher's exact test. Spearman's rank correlation coefficient (r_s) was calculated to measure the strength and direction of the relationship between two variables. A probability value of $P<0.05$ was considered statistically significant.

Results

Most of the respondents in all groups were females, without significant differences between groups (P=0.824). In all groups, the respondents were younger than 40, although the control and astigmatism groups were younger than the others (P=0.0002), (Table 1).

We found a statistically significant difference between the CCT values of the three groups—hypermetropia, myopia, and astigmatism—and the CG ($P<0.001$) (Table 2). But we found no statistically significant difference between the CCT values in the hypermetropic and mixed astigmatism groups, compared with the CG ($P>0.05$).

In the group of respondents with hypermetropia, we found a statistically significant difference in the CCT values in the subgroups of high, moderate, and low hypermetropia, compared to the CG (569.5±23.2 vs. 553.3±18.5 mm [$P<0.05$], 577.1±40.2 vs. 553.3±18.5 mm [$P<0.001$], and 559.7±21.5 vs. 553.3±18.5 mm [$P<0.001$], respectively). In the group with myopia, we found statistically significant differences

in the CCT values in the subgroups of high, moderate, and low myopia, compared to the CG (507.3±50.8 vs. 553.3±18.5 mm [P<0.001], 499.3±41.8 vs. 553.3±18.5 mm [P<0.001], and 526.0±34.5 vs. 553.3±18.5 mm [P<0.001], respectively) (Table 2). In the group with astigmatism, we found a statistically significant difference between the CCT values in the myopic and compound subgroups of astigmatism, compared with the CG (518.2±24.6 vs. 553.3±18.5 mm and 514.1±36.0 vs. 553.3±18.5 mm, P<0.001 in both cases) (Table 2). About 24.5% of the myopic eyes and 16% of the astigmatic eyes had CCT less than 500 µm.

Table 1.

General characteristics of study patients

	Hypermetropic group n=65	Myopic group n=65	Astigmatism group n=50	Control group n=150	P-value
Gender. n (%)					
F	45(69.2)	41(63.1)	32(64.0)	94(62.7)	0.824
M	20(30.8)	24 36.9)	18(36.0)	56(37.3)	
Age (year)					
Mean ± SD	23.8±4.9	24.2±5.6	21.6±2.1	22.3±2.7	0.0002
Rank	18-40	18-39	17-28	18-30	

Table 2.

Central corneal thickness by groups

CCT (µm)	n	Mean ±SD	P-value
Hypermetropia	65	561.5±25.3	Hypermetropia
high	7	569.5±23.2	High vs.Con., P<0.05
moderate	15	577.1±40.2	Moderate vs.Con., P<0.001
low	43	559.7±21.5	Low vs.Con., P<0.001
Myopia	65	517.9±37.3	Myopia
high	5	507.3±50.8	High vs. Con., P<0.001
moderate	9	499.3±41.8	Moderate vs. Con., P<0.001
low	51	526.0±34.5	Low vs. Con., P<0.001
Astigmatism	50	528.3±35.3	Astigmatism
hypermetropic	10	547.8±27	Hypermetrop.vs. Con., P>0.05
myopic	21	518.2±24.6	Myopic vs. Con., P<0.001
mixed	11	549.4±41.5	Mixed vs. Con., P>0.05
compound	8	514.1±36	Compound vs. Cont., P<0.001
Control (Con.)	150	553.3±18.5	
Kruskal Wallis test		P<0.001	

Dunn's test

Hypermetropia vs. Myopia [P<0.001];
Hypermetropia vs. Astigmatism [P<0.001];
Hypermetropia vs. Control [P>0.05];
Myopia vs. Astigmatism [P>0.05];
Myopia vs. Control [P<0.001];
Astigmatism vs.Control [P<0.001].

Table 3.

AL (OD) values in groups with refractive anomalies

AL (mm)	Group			
	Hypermetropia	Myopia	Astigmatism	Control
n	65	65	50	150
Mean	21.6	23.2	23.0	23.1
SD	0.9	1.1	1.1	0.3
Min	19.0	21.0	20.8	22.0
Max	23.3	26.3	25.2	24.9
Kruskal Wallis test P<0.0001				

Dunn's test

Hypermetropia vs. Myopia [P<0.001]; Hypermetropia vs. Astigmatism [P<0.001]; Hypermetropia vs. Control [P<0.001]; Myopia vs. Astigmatism [P>0.05]; Myopia vs. Control [P>0.05]; Astigmatism vs. Control [P>0.05]

From 360 eyes in the TG with refractive anomalies, the lowest AL values were found in the hypermetropic group (21.7±1.0 mm) compared to the myopic group (P<0.001), the astigmatism group (P<0.001), and the CG (P<0.001). Similar differences were also found for the right eyes (OD) (Table 3): hypermetrops tend to have shorter AL than the astigmatic group (P<0.001), myopic group (P<0.001), and the CG (emmetrope) (P<0.001) (Table 3).

Moreover, we found a significant correlation between CCT and AL in the hypermetropic and astigmatism groups but no significant correlation between the myopic group and the CG (Figures 1-4).

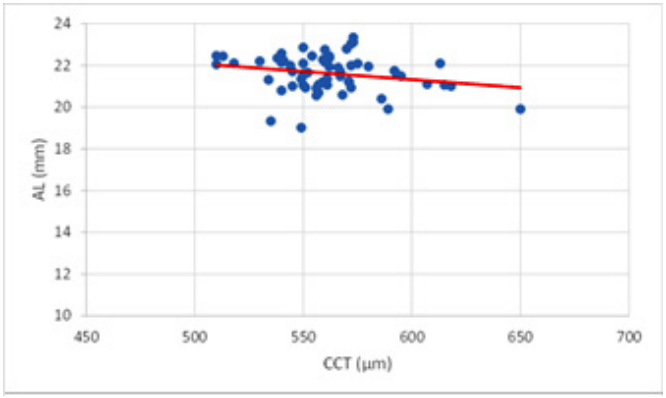

Fig. 1. *Correlation between CCT and AL in the hypermetropic group.*

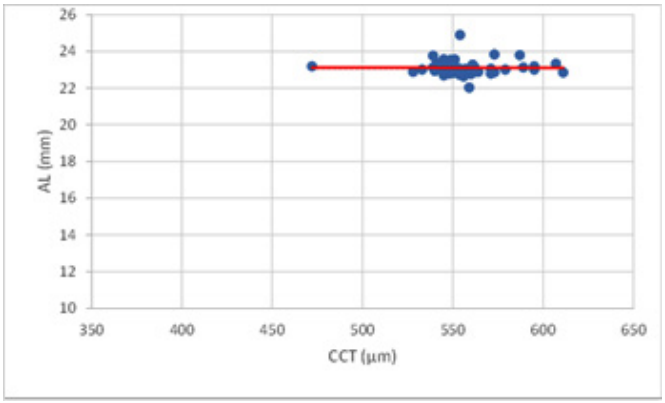

Fig. 2. *Correlation between CCT and AL in the myopic group.*

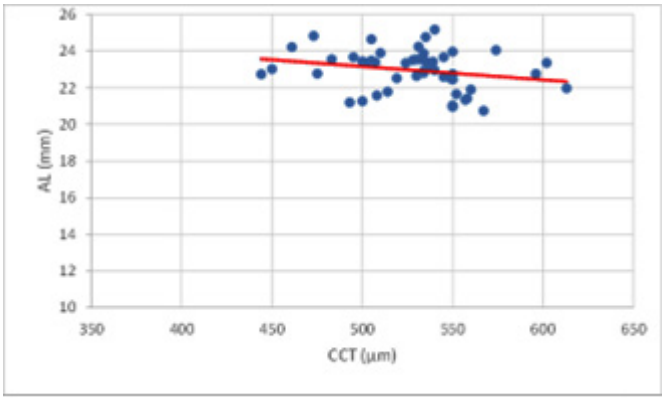

Fig. 3. *Correlation between CCT and AL in the astigmatism group.*

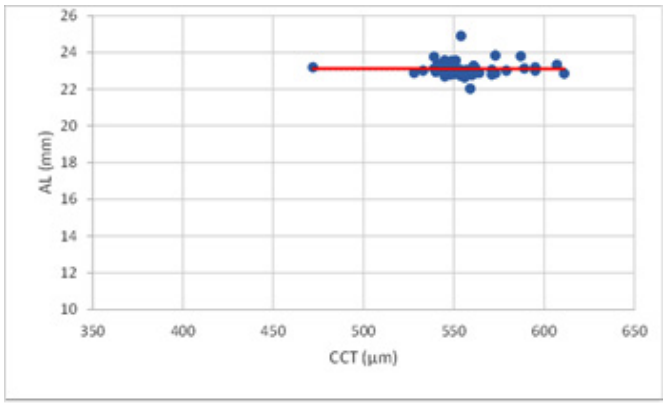

Fig. 4. *Correlation between CCT and AL in the control group.*

Discussion

In this study, the mean age was 22.9 years, ranging from 18 to 40 years, because people of these ages represent refractive stability. The respondents were distributed into three age subgroups:18-40 years in the hypermetropic group, 18-39 years in the myopic group, 17-28 years in the astigmatic group, and 18-30 years in the emmetropic group. Respondents with astigmatism were younger than the hypermetropic (P<0.01) and myopic (P<0.01) groups. In all groups, females dominated, without a significant difference between the groups.

In a study by Juwayli et al.,[14] the average age of the myopic study group was 32.3± 5.61years, while in the hypermetropic group - 35± 6.59 years, ranging from 20 to 40 years. Women dominated in both groups. Their results are similar to those of our study. The results of a study by Mourad et al.[15] with the mean age for all patients of 33.75 years, most of them females, were also similar to our study results. However, the mean age in our study group was 22.9.

In a study by Iyamu et al.,[16] there was a statistically significant negative correlation between CCT and age, and that was a 5.0µm decrease in CCT for every 10-year increase in age. Their finding does not correspond with our study.

Our results confirmed our initial hypotheses. The first hypothesis is that the value of CCT in hypermetropic respondents is higher than in the emmetropic group. The second hypothesis is that CCT's value in myopic respondents is lower than in the emmetropic group. The third hypothesis, the value of the CCT in respondents with astigmatism depends on the type of astigmatic equivalents.

Our findings showed that the median CCT in the hypermetropic group was 564.8 µm, in the myopic group - 521.3 µm, and in the astigmatism group - 530.3 µm, compared to the emmetropic group with 552.3 µm. As a result, a correlation was found between CCT and refractive anomalies, as CCT was statistically higher in the hypermetropic group than in the myopic and astigmatism groups (P<0.001). About 24.5% of myopic and 16% of astigmatic eyes had CCT less than 500 µm.

The correlation between the CCT and refractive anomalies is questionable. Thus, as in our study, Shisheng et al.[17] suggested a positive correlation between these two parameters; but Liu et al.[18] found no significant correlation.

Bradfield et al.[19] found that the CCT is 1µm thinner than average for every degree of increased myopic refractive anomaly. In our study, we found such a correlation, but we did not determine the degree of the anomaly. A study by Kadhim et al.[20] that measured the CCT by ultrasound pachymeter found significantly thinner corneas in myopia (539.5 nm) than emmetropia (550.47 nm). Our study had similar results. Saxena et al.,[21] who used the same CCT evaluation methodology, found a thinner CCT in myopic individuals than in hyperopic. We had the same finding in our study.

A study by Nomura et al.[22] found a median CCT for hyperopia of 512.5 nm and for emmetropia of 516 nm. Their conclusion is contrary to our study results because we found CCT to be thicker in the hypermetropic group than in the emmetropic one. According to a study by Hashmani et al.,[23] astigmatism significantly correlates with CCT. These findings are in accordance with our study.

Mourad et al.[15] studied the association between CCT and axial errors of refraction, but unlike our study, the CCT was obtained by pentacam. They found the CCT is higher in the emmetropia than in myopia and hypermetropia groups. This result does not correspond with our study outcome because we found a higher CCT value in a hypermetropic group than in other study groups.

The other findings of our study were related to the correlation between CCT parameters and AL in respondents with refractive anomalies. In our study, AL values for both eyes were the lowest in the hypermetropic group, with an average of 21.7±1.0 mm statistically significant difference (P<0.001) than in the myopic group (23.3 mm), astigmatism group (23.1 mm), and the CG (23.1 mm), (P<0.001). So far, there is no consensus in terms of CCT correlation with other ocular parameters, including the AL.[16]

Chang et al.[24] found that the mean CCT in myopic adults was 533µm and is thinner in more myopic eyes with longer AL. Our results showed that CCT values were lower in the myopic group, with longer AL, but not in more myopic eyes. According to Bhardwaj et al.,[25] myopes tend to have longer AL, and hypermetropes tend to have a shorter AL than emmetropes and astigmatics up to particular age. This is in accordance with our results, although in different study age groups.

Unlike other studies, Iyamu et al.[16] found no correlation between CCT and AL in adult Nigerians. Neither did Shimmyo et al.,[26] who studied the ocular parameters of 1084 eyes. Meanwhile, we found a significant correlation between CCT and AL in the myopic and astigmatism groups, but no significance in the hypermetropic group and the CG.

In conclusion, the mean CCT value in the hyperopic group was higher than in the emmetropic group, while the CCT value of the myopic and astigmatic group was lower than that of the emmetropic group. In about 24.5% of the myopic eyes and 16% of the astigmatic eyes, the CCT was lower than 500 μm. AL values were the lowest in the hypermetropic group than in the myopic, astigmatic, and control groups.

Ethical Approval

This study was approved by the Health Research Ethics Committee at the University of Pristina (Ref. Nr.12072). Informed consent was obtained from all participants before collecting the data.

Competing Interests

The author declares that there is no conflict of interest.

References

1. Ehlers N, Bramsen T, Sperling S. Applanation tonometry and central corneal thickness. Acta Ophthalmol (Copenh). 1975 Mar;53(1):34-43. doi: 10.1111/j.1755-3768.1975.tb01135.x.
2. Jobke S, Kasten E, Vorwerk C. The prevalence rates of refractive errors among children, adolescents, and adults in Germany. Clin Ophthalmol. 2008 Sep;2(3):601-7. doi: 10.2147/opth.s2836.
3. Opubiri I, Adio A, Megbelayin E. Refractive error pattern of children in South-South Nigeria: A tertiary hospital study. Sky J Med & Med Sci. 2013;1:10-4.
4. Rai S, Thapa HB, Sharma MK, Dhakhwa K, Karki R. The distribution of refractive errors among children attending Lumbini Eye Institute, Nepal. Nepal J Ophthalmol. 2012 Jan-Jun;4(1):90-5. doi: 10.3126/nepjoph.v4i1.5858.
5. Holden BA, Sulaiman S, Knox K. The challenge of providing spectacles in the developing world. Community Eye Health. 2000;13(33):9-10.
6. Wojciechowski R. Nature and nurture: the complex genetics of myopia and refractive error. Clin Genet. 2011 Apr;79(4):301-20. doi: 10.1111/j.1399-0004.2010.01592.x.
7. Remón L, Monsoriu JA, Furlan WD. Influence of different types of astigmatism on visual acuity. J Optom. 2017 Jul-Sep;10(3):141-148. doi: 10.1016/j.optom.2016.07.003.
8. Shobita N, Selvam VP, Shah VJ, Radha J ,Vijayraghavan V, et al. Correlation of Central Corneal Thickness with Refractive Errorsand Corneal Curvature in the South Indian Population. Acta Scientific Ophthalmology. 2021;4(4):31-38.
9. Mutti DO, Hayes JR, Mitchell GL, Jones LA, Moeschberger ML, Cotter SA, et al.; CLEERE Study Group. Refractive error, axial length, and relative peripheral refractive error before and after the onset of myopia. Invest Ophthalmol Vis Sci. 2007 Jun;48(6):2510-9. doi: 10.1167/iovs.06-0562.
10. Hitzenberger CK. Optical measurement of the axial eye length by laser Doppler interferometry. Invest Ophthalmol Vis Sci. 1991 Mar;32(3):616-24.
11. Schmid GF, Papastergiou GI, Nickla DL, Riva CE, Lin T, Stone RA, Laties AM. Validation of laser Doppler interferometric measurements in vivo of axial eye length and thickness of fundus layers in chicks. Curr Eye Res. 1996 Jun;15(6):691-6. doi: 10.3109/02713689609008911.
12. He X, Zou H, Lu L, Zhao R, Zhao H, Li Q, Zhu J. Axial length/corneal radius ratio: association with refractive state and role on myopia detection combined with visual acuity in Chinese schoolchildren. PLoS One. 2015 Feb 18;10(2):e0111766. doi: 10.1371/journal.pone.0111766.
13. Young TL, Metlapally R, Shay AE. Complex trait genetics of refractive error. Arch Ophthalmol. 2007 Jan;125(1):38-48. doi: 10.1001/archopht.125.1.38.
14. Juwayli RMM, Farag AAR, Shalaby AAEA. Correlation between Refractive Errors and Intraocular Pressure after Adjusting by Central Corneal Thickness. The Egyptian Journal of Hospital Medicine. 2021 January;82(3):581-586.
15. Mourad MS, Rayhan RA, Moustafa M, Hassan AA. Correlation between central corneal thickness and axial errors of refraction. J Egypt Ophthalmol Soc. 2019;112:52-60.
16. Iyamu E, Iyamu JE, Amadasun G. Central corneal thickness and axial length in an adult Nigerian population. Journal of Optometry. 2013;6(3):154–160.
17. Shisheng Z,Cuiping L, Jingcai L.Analysis of Factors Correlated with Corneal Shape in Myopia. Chinese Journal of Optometry Ophthalmology and Visual Science. 2002;4:43–45.
18. Liu Z, Pflugfelder SC. The effects of long-term contact lens wear on corneal thickness, curvature, and surface regularity. Ophthalmology. 2000 Jan;107(1):105-11.
19. Pediatric Eye Disease Investigator Group; Bradfield YS, Melia BM, Repka MX, Kaminski BM, Davitt BV, Johnson DA, et al. Central corneal thickness in children. Arch Ophthalmol. 2011 Sep;129(9):1132-8.
20. Kadhim YJ, Farhood QK. Central corneal thickness of Iraqi population in relation to age, gender, refractive errors, and corneal curvature: a hospital-based cross-sectional study. Clin Ophthalmol. 2016 Nov 25;10:2369-2376.
21. Saxena AK, Bhatnagar A, Thakur S. Central Corneal Thickness. Important Considerate in Ophthalmic Clinic. Austin J Clin Ophthalmol. 2017;4:1076**.**
22. Nomura H, Ando F, Niino N, Shimokata H, Miyake Y. The relationship between intraocular pressure and refractive error adjusting for age and central corneal thickness. Ophthalmic Physiol Opt. 2004 Jan;24(1):41-5.
23. Hashmani N, Hashmani S, Hanfi AN, Ayub M, Saad CM, Rajani H, et al. Effect of age, sex, and refractive errors on central corneal thickness measured by Oculus Pentacam®. Clin Ophthalmol. 2017 Jun 30;11:1233-1238.
24. Chang SW, Tsai IL, Hu FR, Lin LL, Shih YF. The cornea in young myopic adults. Br J Ophthalmol. 2001 Aug;85(8):916-20. doi: 10.1136/bjo.85.8.916.
25. Bhardwaj V, Rajeshbhai GP. Axial length, anterior chamber depth-a study in different age groups and refractive errors. J Clin Diagn Res. 2013 Oct;7(10):2211-2. doi: 10.7860/JCDR/2013/7015.3473.
26. Shimmyo M, Orloff PN. Corneal thickness and axial length. Am J Ophthalmol. 2005 Mar;139(3):553-4. doi: 10.1016/j.ajo.2004.08.061.

International Journal of Biomedicine 13(3) (2023) 101-104
http://dx.doi.org/10.21103/Article13(3)_OA8

ORIGINAL ARTICLE

Radiology

INTERNATIONAL JOURNAL OF BIOMEDICINE

Risk Factors for Nonalcoholic Fatty Liver Disease among Patients Referred to Radiological Departments at Hail Hospitals, KSA

Mahasin G. Hassan*

Department of Radiological Sciences, College of Health and Rehabilitation Sciences, Princess Nourah bint Abdulrahman University, Riyadh, Saudi Arabia

Abstract

***Background*:** Nonalcoholic fatty liver disease (NAFLD) incidence and prevalence have increased globally. The gravity of this chronic disease comes from its ability to progress to cirrhosis and hepatocellular carcinoma, which are rising rapidly. Genetic, demographic, environmental, and clinical factors are significant in the occurrence of NAFL. This study aimed to assess risk factors that affect the occurrence of NAFLD.

***Methods and Results*:** This cross-sectional study was carried out at hospitals in the Hail Region, KSA. It included 160 patients: 76 were considered as control (normal liver), and 84 suffered from fatty liver (according to a US image). Sonography was carried out using a US scanner with curvilinear transducers having a frequency of 3.5MHz. The following data were obtained: age, BMI, clinical history, including long-term medication of more than 3 months (oral antidiabetic medications, hormone replacement therapy for hyperthyroidism, and antihypertensive drug), type 2 diabetes (T2D), viral hepatitis, liver span, lipidemia, metabolic disorders, and weight loss. The prevalence of NAFLD increases significantly among patients taking medications for a long time and T2D patients (P<0.001). Hepatomegaly is one of the most common physical examination findings of NAFLD (P<0.001).

Conclusion: A periodic US examination is helpful because it can reveal fatty infiltration of the liver in the early stages to avoid fatal complications, especially for patients with long-term medication or T2D. Other studies with larger sample sizes and different known risk factors are needed to discover all risk factors for the KSA population. (**International Journal of Biomedicine. 2023;13(3):101-104.**)

Keywords: nonalcoholic fatty liver disease • risk factors • ultrasound

For citation:Hassan MG. Risk Factors for Nonalcoholic Fatty Liver Disease among Patients Referred to Radiological Departments at Hail Hospitals, KSA. International Journal of Biomedicine. 2023;13(3):101-104. doi:10.21103/Article13(3)_OA8

Abbreviations

BMI, body mass index; **HRT**, hormone replacement therapy; **LS**, liver span; **NAFLD**, nonalcoholic fatty liver disease; **NW**, normal weight; **T2D**, type 2 diabetes; **US**, ultrasound.

Introduction

Nonalcoholic fatty liver disease (NAFLD) incidence and prevalence have increased globally.[1] The prevalence in Asia is equal to that in the West. The gravity of this chronic disease comes from its ability to progress to cirrhosis and hepatocellular carcinoma, which are rising rapidly.[2-4] Genetic, demographic, environmental, and clinical factors are significant in the occurrence of NAFLD.[1] Certain genetic factors have revealed their role in the occurrence of NAFLD, e.g., patatin-like phospholipase domain-containing 3 (*PNPLA3*) gene, sorting and assembly machinery component 50 (*SAMM50*) gene, and centrosomal protein of 192 kDa (*CEP192*) gene.[1,4] An unhealthy lifestyle, obesity, and weight loss are major risk factors. The tendency to contract NAFLD increases with age, reaching a peak at the age of 60, and is higher among males than females. The global increase in the incidence of NAFLD is associated with rising obesity, T2D, and metabolic syndrome.[1,5]

Correspondence:

Dr. Mahasin G. Hassan, Ph.D, mghassan@pnu.edu.sa

Different noninvasive modalities are used to detect NAFLD, like US and MRI.[6] US is the method of choice because of its low cost and availability. Different techniques have been developed nowadays to increase the accuracy of this modality. Quantitative US and US with artificial intelligence are new techniques for identifying NAFLD in high-risk patients.[6,7] Sonographically, fatty liver disease is characterized by increased echogenicity, vascular blurring, and enlargement.[8] During clinical examinations. it has been observed that NAFLD is discovered suddenly, and many patients are suffering from fatty liver without knowing it.

This study aimed to assess risk factors that affect the occurrence of NAFLD.

Materials and Methods

This cross-sectional study was carried out at hospitals in the Hail Region, KSA, on 160 patients who came to the radiological departments for an abdominal ultrasound. Sonography was carried out using a US scanner with curvilinear transducers having a frequency of 3.5 MHz. US scanning was performed according to AIUM guidelines for an abdominal ultrasound.[9]

The following data were obtained: age, BMI, clinical history, including long-term medication of more than 3 months, T2D, viral hepatitis, liver span, lipidemia (the level of cholesterol more than 240 mg/dL or triglycerides more than 240 mg/dL), and weight loss. In addition, the presence of sickle cell anemia, cystic fibrosis, maple syrup urine disease, Gaucher's disease, or hemochromatosis was assessed. These data were retrieved from the PACS.

A designed data collection sheet containing all the study variables was used. This study included 160 patients: 76 were considered as control (normal liver), and 84 suffered from fatty liver (according to a US image).

The sonographic diagnosis of fatty liver depends on parenchymal brightness (increased echogenicity than the normal liver). There are three patterns: diffuse, characterized by overall hyperechogenicity (n=77); focal, characterized by focal hyperechogenicity (n=5); and focal fatty sparing, characterized by hypoechoic areas within hyperechoic parenchyma (n=2). In addition, the LS (≤13 cm or >13cm) was assessed.

Statistical analysis was performed using the statistical software package SPSS version 23.0 (SPSS Inc, Armonk, NY: IBM Corp). Baseline characteristics were summarized as frequencies and percentages for categorical variables. Continuous variables with normal distribution were presented as mean and standard deviation (SD). The frequencies of categorical variables were compared using Pearson's chi-squared test. A probability value of $P<0.05$ was considered statistically significant.

Results

Table 1 shows the age, BMI mean, and standard deviation. Patients were classified into three groups according to age; 18-30 years, 31-60 years, and 61-97 years. The sample was classified into three groups according to BMI: normal weight (NW), overweight and obese. The association between age groups, BMI, liver span, and NAFLD were assessed using a chi-square test (Tables 2-4).

Table 1.

Basic characteristics.

Variable	Minimum	Maximum	Mean	SD
Age	16.00	97.00	47.5250	20.81121
BMI	18.50	81.00	39.4100	13.99385

Table 2.

Association between age and BMI, and NAFLD

	Age groups (P=0.160)			BMI groups (P=0.145)		
	1-30 yr.	31-60 yr.	61-97 yr.	NW	Overweight	Obese
Normal	20	40	16	8	10	58
Fatty liver	26	32	26	14	18	52
Total	46	72	42	22	28	110

Table 3.

Association between known risk factors and the presence of NAFLD.

		Normal	Fatty liver	Total	P-value
Long-term medication	Yes	4	30	34	0.000
	No	72	54	126	
T2D	Yes	0	18	18	0.000
	No	76	66	142	
Viral hepatitis	Yes	4	8	12	0.307
	No	72	76	148	
Lipidemia	Yes	2	4	6	0.771*
	No	74	80	154	

* *Pearson's chi-squared test with the Yates' correction*

Table 4.

Association between liver span and NAFLD.

Liver span, cm	Normal	Fatty liver	Total	P-value
≤ 13	76	62	138	0.000
>13	0	22	22	
Total	76	84	160	

Figure 1 shows the distribution of risk factors among patients with NAFLD. There were five patients with a high level of cholesterol and one with a high triglyceride level.

No patients suffered from sickle cell anemia, cystic fibrosis, Gaucher's disease, or hemochromatosis (Figure 2).

There were 34 patients who had been taking medication for a long time (antidiabetic medications - 16, hormone replacement therapy (HRT) for hyperthyroidism - 10, and antihypertensive drug - 8).

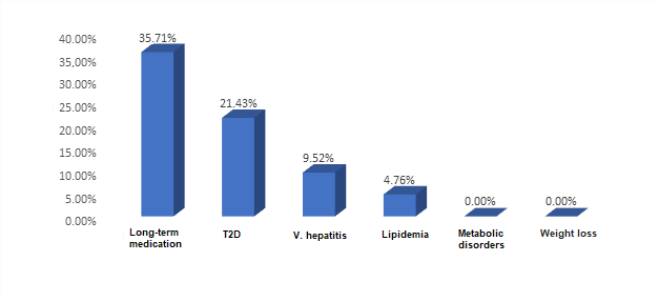

Fig. 1. *Distribution of NAFLD risk factors*

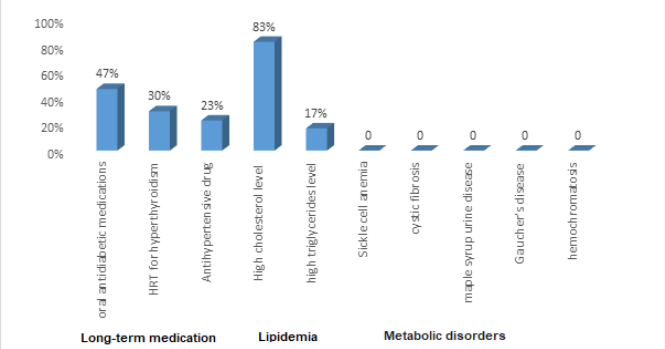

Fig. 2. *Long-term medication, lipidemia and metabolic disorders.*

Discussion

Different studies have been carried out to assess risk factors in certain populations or regions. For example, a previous study found that increased BMI is the main risk factor.[10] Another study found that risk factors include gender, hypertension, body fat ratio, blood triglycerides, and fasting blood glucose.[11] In this study, the ages of patients ranged between 16 and 97 years. Patients between 31-60 years had the highest prevalence of the disease. The results show no significant association between the disease and age (P=0.160). The prevalence of obesity (BMI >30 kg/m^2) among all patients (sample) was higher (68.75%) than the other BMI groups, and these patients had the highest prevalence (61.9%) of NAFLD; however, there was no significant association (P=0.145). The study found that taking medications for a long time and T2D were the main factors affecting NAFLD (P<0.001).

Previously, it was shown that some long-term medications induce fatty liver. These medications include corticosteroids, antidepressants and the antipsychotic medications tamoxifen, amiodarone, and methotrexate.[12] In this study, long-term medications included oral antidiabetic medications, HRT for hyperthyroidism, and antihypertensive drugs. This study also showed the relationship between long-term medications and NAFLD. T2D is usually present together with NAFLD[13] which was also confirmed by this study. Lipidemia was not associated with NAFLD, apparently due to insufficient samples in this study.

One of the clinical and sonographic manifestations of fatty liver is hepatomegaly. With US, hepatomegaly is assessed by measuring LS. LS differs according to region and population. According to a study conducted in Saudi Arabia, the LS was 12.5 cm among males and 11.9 cm among females.[14] In this study, 13 cm was the cutoff point,[15] used as an upper limit for normal LS. The study showed a significant association between fatty liver and hepatomegaly (P<0.001).

Conclusion

The prevalence of NAFLD increases significantly among patients taking medications for a long time (oral antidiabetic medications, HRT for hyperthyroidism, and antihypertensive drug) and T2D patients. NAFLD is discovered suddenly, and in this regard, a periodic US examination is helpful because it can reveal fatty infiltration of the liver in the early stages to avoid fatal complications, especially for patients with long-term medication or T2D. Hepatomegaly is one of the most common physical examination findings of NAFLD. Other studies with larger sample sizes and different known risk factors are needed to discover all risk factors for the KSA population.

Competing Interests

The Author declares that there is no conflict of interest.

Acknowledgments

Special thanks are extended to my students, Alanoud Almasood and Sada Alshammary, for their help and assistance with data collection.

References

1. Huh Y, Cho YJ, Nam GE. Recent Epidemiology and Risk Factors of Nonalcoholic Fatty Liver Disease. J Obes Metab Syndr. 2022 Mar 30;31(1):17-27. doi: 10.7570/jomes22021.
2. Ching-Yeung Yu B, Kwok D, Wong VW. Magnitude of Nonalcoholic Fatty Liver Disease: Eastern Perspective. J Clin Exp Hepatol. 2019 Jul-Aug;9(4):491-496. doi: 10.1016/j.jceh.2019.01.007.
3. Feng G, Li XP, Niu CY, Liu ML, Yan QQ, Fan LP, Li Y, Zhang KL, Gao J, Qian MR, He N, Mi M. Bioinformatics analysis reveals novel core genes associated with nonalcoholic fatty liver disease and nonalcoholic steatohepatitis. Gene. 2020 Jun 5;742:144549. doi: 10.1016/j.gene.2020.144549.
4. Cai C, Song X, Yu C. Identification of genes in hepatocellular carcinoma induced by nonalcoholic fatty liver disease. Cancer Biomark. 2020;29(1):69-78. doi: 10.3233/CBM-190169.
5. Maurice J, Manousou P. Nonalcoholic fatty liver disease.

Clin Med (Lond). 2018 Jun;18(3):245-250. doi: 10.7861/clinmedicine.18-3-245.
6. Tahmasebi A, Wang S, Wessner CE, Vu T, Liu JB, Forsberg F, et al. Ultrasound-Based Machine Learning Approach for Detection of Nonalcoholic Fatty Liver Disease. J Ultrasound Med. 2023 Feb 20. doi: 10.1002/jum.16194.
7. Pirmoazen AM, Khurana A, Loening AM, Liang T, Shamdasani V, Xie H, El Kaffas A, Kamaya A. Diagnostic Performance of 9 Quantitative Ultrasound Parameters for Detection and Classification of Hepatic Steatosis in Nonalcoholic Fatty Liver Disease. Invest Radiol. 2022 Jan 1;57(1):23-32. doi: 10.1097/RLI.0000000000000797.
8. Khov N, Sharma A, Riley TR. Bedside ultrasound in the diagnosis of nonalcoholic fatty liver disease. World J Gastroenterol. 2014 Jun 14;20(22):6821-5. doi: 10.3748/wjg.v20.i22.6821.
9. AIUM practice guideline for the performance of an ultrasound examination of the abdomen and/or retroperitoneum. J Ultrasound Med. 2012 Aug;31(8):1301-12. doi: 10.7863/jum.2012.31.8.1301.
10. Lin Y, Feng X, Cao X, Miao R, Sun Y, Li R, Ye J, Zhong B. Age patterns of nonalcoholic fatty liver disease incidence: heterogeneous associations with metabolic changes. Diabetol Metab Syndr. 2022 Nov 28;14(1):181. doi: 10.1186/s13098-022-00930-w.
11. Hu XY, Li Y, Li LQ, Zheng Y, Lv JH, Huang SC, Zhang W, Liu L, Zhao L, Liu Z, Zhao XJ. Risk factors and biomarkers of non-alcoholic fatty liver disease: an observational cross-sectional population survey. BMJ Open. 2018 Apr 5;8(4):e019974. doi: 10.1136/bmjopen-2017-019974.
12. LiverTox: Clinical and Research Information on Drug-Induced Liver Injury [Internet]. Bethesda (MD): National Institute of Diabetes and Digestive and Kidney Diseases; 2012. Nonalcoholic Fatty Liver. [Updated 2019 May 4]. Available from: https://www.ncbi.nlm.nih.gov/books/NBK547860/
13. Dharmalingam M, Yamasandhi PG. Nonalcoholic Fatty Liver Disease and Type 2 Diabetes Mellitus. Indian J Endocrinol Metab. 2018 May-Jun;22(3):421-428. doi: 10.4103/ijem.IJEM_585_17.
14. Kheiralla OAM, Babikr WG, Elbadry AH. Sonographic Average Value Of Normal Liver Span Among Saudi Adults Referred To Najran University Hospital." *IOSR-JDMS*, 2016;15(5):27-34.
15. Dean D. Abdominal Ultrasound, and Instrumentation. Part 1, Module 4, 1st ed. The Burwin institute of diagnostic medical ultrasound. 2005, Luneburg; Canada.

International Journal of Biomedicine 13(3) (2023) 105-109
http://dx.doi.org/10.21103/Article13(3)_OA9

ORIGINAL ARTICLE

Radiology

INTERNATIONAL JOURNAL OF BIOMEDICINE

Hepatic Iron Deposition Quantification in Patients with β-Thalassemia Using Magnetic Resonance Imaging

Faten A. Nasser[1], Rehab Hussien[2], Mahasin G. Hassan[3*], Tasneem S. A. Elmahdi[4], Ali Alsaadi[1,5], Enas M. Fallatah[1]

[1]*Department of Radiology, Madina Maternity and Children Hospital, Al-Madina Al-Munawara, Saudi Arabia*
[2]*Department of Diagnostic Radiology, College of Medical Applied Sciences, University of Hail, Hail, Saudi Arabia*
[3]*Department of Radiological Sciences, College of Health and Rehabilitation Sciences, Princess Nourah bint Abdulrahman University, Riyadh, Saudi Arabia*
[4]*College of Health Sciences, Alrayan Colleges, Madina, Saudi Arabia*
[5]*Department of Radiology, King Salman Medical City, Madina, Saudi Arabia*

Abstract

Background: Detection and quantification of liver iron overload are significant to initiate treatment and monitoring of iron overload. This study aimed to quantify liver iron deposits in β-thalassemia major patients using MRI T2* and its correlation with age and heart iron deposition.

Methods and Results: This retrospective study included 54 records of patients between 5-16 years of age with hepatic iron deposition due to β-thalassemia major. Data were collected from MRI reports in Picture Archiving and Communication Systems-Radiology Information System (PACS-RIS) and serum ferritin (SF) test results obtained from Hospital Information Systems and written into a dedicated datasheet. The information was recorded on a data collection sheet. The datasheet included all the required data, demographic data, lab results, T2* mapping for iron deposition in the liver and heart, and liver measurements.

All subjects had high SF (from 1120 to 9850 ng/ml) with an average of 4317.93±2779.9 ng/ml. Age and SF correlated positively (r=0.368, *P*=0.0006). A negative correlation was observed between SF and liver T2* (r=-0578, *P*=0.000), whereas between liver T2* and heart T2* correlation had a positive direction (r=0.329, *P*=0.015)

Conclusion: MRI provides accurate, non-invasive, valid, and repeatable techniques, which are more acceptable to patients for assessing iron load. Furthermore, MRI T2* methods measure iron overload within the target organ precisely.(**International Journal of Biomedicine. 2023;13(3):105-109.**)

Keywords: iron deposition • ferritin • β-thalassemia • MRI

For citation: Nasser FA, Hussien R, Hassan MG, Elmahdi TSA, Alsaadi A, Fallatah EM. Hepatic Iron Deposition Quantification in Patients with β-Thalassemia Using Magnetic Resonance Imaging. International Journal of Biomedicine. 2023;13(3):105-109. doi:10.21103/Article13(3)_OA9

Introduction

Hemochromatosis is a metabolic disorder that causes excess iron deposition, which leads to iron accumulation in the body's organs, especially in the liver, heart, and pancreas, causing dysfunction or severe health complications.[(1)] Hemochromatosis was first described in 1865 by the French physician Armand Trousseau as "bronze diabetes."[(2)] The hereditary nature of hemochromatosis was demonstrated by Marcel Simon and colleagues in the 1970's.[(3)] Secondary hemochromatosis is the result of another disease or condition that creates iron overload.

Hereditary hemochromatosis (HH) is an autosomal recessive disease caused by mutations in the "high iron Fe"(*HFE*) gene. Two of the 37 allelic variants of *HFE* described to date

(C282Y and H63D) are significantly correlated with HH.[4] Homozygosity for the C282Y mutation was found in 52–100% of previous studies on clinically diagnosed probands.[5] Today, approximately 0.4% of Caucasians carry a homozygous[6,7] and approximately 6% a heterozygous *HFE* C282Y mutation.[7] The C282Y mutation causes excessive systemic iron accumulation.[8,9] Normal iron absorption happens in the proximal small intestine, 1–2 mg daily. However, this absorption rate may increase to 4–5 mg daily with progressive accumulation of 15–40 g of iron in patients with hereditary hemochromatosis. Despite this high prevalence, the mutation causes a clinically relevant phenotype only in a minority of cases.[10] HH is observed mostly in people of northern European origin, with a prevalence of approximately 1 per 220–250 persons, while it is less prevalent in patients of African descent.[6,11-12] Some rare forms of HH are increasingly found in patients clinically characterized as HH and negative for C282Y homozygosity in *HFE*.[13] They present with phenotypically proven hepatic iron overload with no other explanation. These forms are distributed in Asian populations, where they may represent the main non-hematological cause of hereditary iron overload.[14-16]

Secondary hemochromatosis is mostly related to multiple red blood cell transfusions in patients with red blood cell disorders involving β-thalassemia major, myelodysplastic syndromes, aplastic anemia, and sickle cell disease.[17] Our study focused attention on thalassemia. β-thalassemia syndromes are the most common inherited hemoglobinopathies caused by a genetic deficiency in beta-globin. Although regular blood transfusion has increased the survival rate among thalassemia patients, treatment of the disease itself could lead to a chain of syndromes, such as iron deposits, that lead to organ dysfunction, which sometimes may cause death.[18]

The liver is one of the main sources of iron storage. Therefore, the detection of liver iron overload initiates treatment and prevents complications. A liver biopsy has been a standard reference for detecting and quantifying liver iron content. Still, its invasive nature limits its implementation, and its accuracy is greatly affected by hepatic inflammation, fibrosis, and uneven iron distribution. Also, serum ferritin (SF) has been used as a surrogate marker, but it is not reliable because its level may be affected by inflammation, vitamin C deficiency, oxidative stress, hepatic dysfunction, or malignancy.[19]

Alternatively, the MRI T2* technique is a valid, non-invasive, and reproducible method for evaluating tissue iron loading and, therefore, more acceptable to patients. It measures iron load within the objective organ by measuring the effect of local distortion of magnetic fields caused by excess iron in tissues. Iron concentrations are based on measurements of proton transverse magnetization decay rates, relaxometry (R2 or R2*), as great signal decay rates indicate great iron absorption.[20,21]

In 2005, Wood et al.[21] measured the R2* from a single, mild hepatic segment by drawing ROI boundaries of the liver, and excluding hilar vessels from obtaining an R2* map by using the gradient-recalled-multi-echo (GRE MR) imaging technique with a single breath-hold for each echo GRE sequence.

In 2019 Sobhani et al.[19] assessed the role of multi-echo T2*-weighted image (T2*WI) in MRI quantification of hepatic iron deposition in patients with β-thalassemia major. They explained that patients with high SF are likelier to have higher liver or cardiac iron load.

Thalassemia is an inherited disease that causes many complications, and the treatment of the disease itself could lead to a chain of syndromes, which sometimes may cause death. Despite this, there is a shortage of regional studies to establish regional references.

This study aimed to quantify liver iron deposits in β-thalassemia major patients using MRI T2* and its correlation with age and heart iron deposition.

Materials and Methods

The study included 54 records of patients between 5-16 years of age with hepatic iron deposition due to β-thalassemia major. Patients diagnosed with another hemochromatosis type or MRI contraindicated for him were excluded. The study was carried out at the Medina Maternity and Children Hospital in Al Medina Almonawara from Dec 2021 to May, 2022.

Study design, data collection, and analysis

In this descriptive and retrospective study, patients underwent MRI with a 1.5-T machine (GE, Healthcare) using a body coil or cardiac coil, respiratory triggering or navigators, and peripheral gating. All patients received frequent blood transfusions and chelation therapy (Deferasirox), a dose of approximately 750-1500 mg per day, through 170 days. The demographic data were extracted from patients' documents. Patients underwent liver and cardiac MRIs.

Data were collected from MRI reports in Picture Archiving and Communication Systems-Radiology Information System (PACS-RIS) and SF test results obtained from Hospital Information Systems and written into a dedicated datasheet. The information was recorded on a data collection sheet. The datasheet included all the required data, demographic data, lab results, T2* mapping for iron deposition, and liver measurements.

Statistical analysis was performed using the statistical software package SPSS version 23.0 (SPSS Inc, Armonk, NY: IBM Corp). Baseline characteristics were summarized as frequencies and percentages for categorical variables. Minimum, maximum, and mean±SD were used for summarizing the data. A scatterplot was used to show the relationship between two quantitative variables measured for the same individuals. Pearson's Correlation Coefficient (r) was used to determine the strength of the relationship between the two continuous variables. A probability value of $P<0.05$ was considered statistically significant.

Ethical approvals were obtained from the The institutional review board (IRB) at King Salman bin Abdulaziz Medical City (IRB number: 040-22).

Results

Of the 54 pediatric β-thalassemia major patients between 5 and 16 years of age, the largest group was the 9-12 years, representing 48.1% (Table 1). All subjects had high SF (from 1120 to 9850 ng/ml) with an average of 4317.93± 2779.9 ng/ml (Table 2). Age and SF correlated positively (r=0.368, P=0.0006)

(Table 3). There was a significant positive correlation between age and liver size (r=0.303, *P*=0.026) (Table 3). No correlation was found between liver T2* and age (P=0.662) (Table 3). A negative correlation was observed between SF and liver T2* (r=-0578, *P*=0.000) (Table 3, Figure 1), whereas between liver T2* and heart T2* correlation had a positive direction (r=0.329, *P*=0.015) (Table 3, Figure 2).

Table 1.

The age groups of the patients

Age group	N	Percentage (%)
5 – 8 yrs.	13	24.1
9 – 12 yrs.	26	48.1
13-16 yrs.	15	27.8
Total	54	100

Table 2.

Testing parameters

	Mean	Maximum	Minimum	Variance	SD
Age	2.04	3.00	1.00	0.53	0.73
Weight, kg	30.82	56.00	13.00	94.34	9.71
Ferritin, ng/ml	4317.93	9850.00	1120.00	7728225.88	2779.9
T2* liver	2.49	8.00	0.30	3.83	1.96
T2*heart	24.05	45.70	4.00	131.13	11.45
Liver size, cm	16.74	20.50	12.11	5.86	2.42

Table 3.

Pearson correlations between the variables of the study.

Correlations		SF	Liver size	T2* liver
Age	Pearson Correlation	0.368	0.303	- 0.069
	P-value	0.006	0.026	0.622
SF	Pearson Correlation			-0.578
	P-value			0.000
T2* heart	Pearson Correlation			0.329
	P-value			0.015

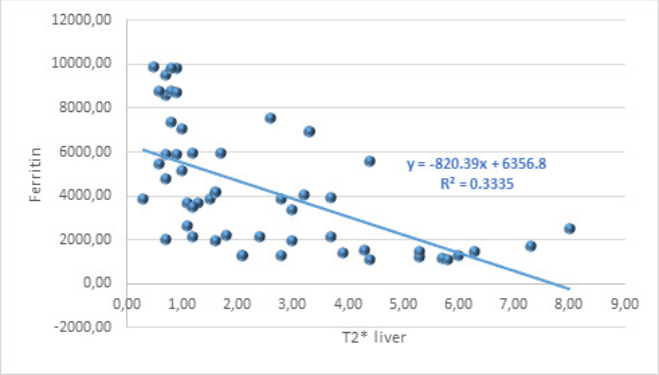

Fig. 1. *Scatter plot with a fit line of SF with T2* liver.*

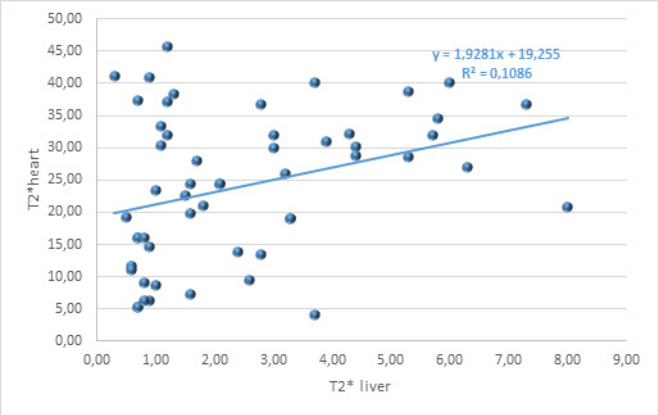

Fig. 2. *Scatter plot with a fit line of T2* heart with T2* liver.*

Discussion

Iron overload in β-thalassemia major patients occurs because the rate of iron entering the body is considerably greater than the rate of clearance, leading to excess iron discharge into the blood. The body has no mechanism for eliminating excess iron, so it is collected and stored in crystalline form within ferritin and hemosiderin. This study's primary objective was quantifying hepatic iron deposition in patients with β-thalassemia by multi-echo T2* weighted sequence through the relaxometry method where short Time to Echo (TE) (0.9 - 11 ms) was used with a breath-hold. Then MRI images were transferred to a post-processing program (GE Cardiac VX) for MRI analytical software. The region of interest (ROI) of about 1-2cm or more was placed in the greater part of the liver parenchyma to measure the signal intensity for each TE.

This study, conducted on β-thalassemia major patients of a range of ages from 5 to16 years, has presented various results for iron overload (mild, moderate, severe). This study followed the method of Wood et al.,[21] which used a multi-echo T2*-weighted sequence with short TEs and a breath-hold for hepatic iron quantification. While short TE is considered key to detecting iron concentration, especially in defining severe iron overload in the liver;[22] also, a long TE makes respiratory motion artifacts appear in images.[23]

Our study showed a moderate positive correlation between age and SF (Table 3). This explains that as age increases, blood transfusions increase and thus lead to increased iron deposits. On the contrary, Bandyopadhyay et al.[23] performed a similar study which demonstrated that patients at a younger age had more elevated ferritin levels, which illustrates that these differences were due to improper chelation regimens or that the patients had not obtained chelation treatment. Furthermore, they observed no significant correlation between the age and liver T2*, similar to our study findings. This explains the heterogeneous distribution of depository iron.

A moderate negative correlation (r=-0.578) was observed between SF level and liver T2*, like Azarkeivan et al.,[24] S Kaban & Ç Damar,[25] and El Sherif et al.[26] This result shows that patients with high SF are more likely to have a

higher liver iron load. A high SF level in the blood may be evidence of iron loading within the body in general; however, the excess iron load distribution among the various organs occurs randomly in the body. Variations in the concentration of iron may usually be related to the chelation protocol.[27] Ferritin level decreases by a factor of 820.39 when liver T2* increases by 1. Heart T2* value increases by a factor of 1.9281 when liver T2* increases by 1.

In our study, there is a positive correlation (r=0.329, *P*=0.015) between liver T2* and heart T2*, while most previous studies, like Kolnagou et al.,[28] showed no correlation between heart T2* and liver T2*. In contrast, El Sherif et al.[26] demonstrated a moderate negative correlation between hepatic and cardiac iron deposition.

The variations in results may be because of distinctions in clinical data, genetic and study population, sample size, SF levels, chelation protocols, and iron deposits in different organs.

Conclusion

Our results indicate negative correlations between iron concentration measurement by liver T2* and SF. There is no significant correlation between age and iron concentration in liver T2*, despite the notable correlation between the age and SF test, illustrating that as age increases, the blood transfusions increase, thus leading to increased iron deposits in the body. The study showed that the iron deposition in the liver is considered an indication of iron deposition in other organs, like the heart, as the study's hypothesis stated. MRI provides accurate, non-invasive, valid, and repeatable techniques, which are more acceptable to patients for assessing iron load. Furthermore, MRI T2* methods measure iron overload within the target organ precisely. Monitoring and follow-up of iron overload using MRI T2* for all hemochromatosis patients is helpful for early detection of any potential complication. Conducting the study on large sample size and other organs is recommended.

Competing Interests

The authors declare that they have no competing interests.

References

1. McDowell LA, Kudaravalli P, Sticco KL. Iron Overload. 2022 Apr 28. In: StatPearls [Internet]. Treasure Island (FL): StatPearls Publishing; 2023 Jan–. PMID: 30252387
2. Trousseau A. Glycosurie, diabète sucré. Clinique médicale de l'Hôtel-Dieu de Paris, 2nd edition, Paris, 1865, 2: 663-698.
3. Simon M, Alexandre JL, Bourel M, Le Marec B, Scordia C. Heredity of idiopathic haemochromatosis: a study of 106 families. Clin Genet. 1977 May;11(5):327-41. doi: 10.1111/j.1399-0004.1977.tb01324.x.
4. Pointon JJ, Wallace D, Merryweather-Clarke AT, Robson KJ. Uncommon mutations and polymorphisms in the hemochromatosis gene. Genet Test. 2000;4(2):151-61. doi: 10.1089/10906570050114867.
5. Hanson EH, Imperatore G, Burke W. HFE gene and hereditary hemochromatosis: a HuGE review. Human Genome Epidemiology. Am J Epidemiol. 2001 Aug 1;154(3):193-206. doi: 10.1093/aje/154.3.193.
6. Adams PC, Reboussin DM, Barton JC, McLaren CE, Eckfeldt JH, McLaren GD, et al.; Hemochromatosis and Iron Overload Screening (HEIRS) Study Research Investigators. Hemochromatosis and iron-overload screening in a racially diverse population. N Engl J Med. 2005 Apr 28;352(17):1769-78. doi: 10.1056/NEJMoa041534.
7. European Association For The Study Of The Liver. EASL clinical practice guidelines for HFE hemochromatosis. J Hepatol. 2010 Jul;53(1):3-22. doi: 10.1016/j.jhep.2010.03.001.
8. Radford-Smith DE, Powell EE, Powell LW. Haemochromatosis: a clinical update for the practising physician. Intern Med J. 2018 May;48(5):509-516. doi: 10.1111/imj.13784.
9. Porter JL, Rawla P. Hemochromatosis. 2023 Mar 31. In: StatPearls [Internet]. Treasure Island (FL): StatPearls Publishing; 2023 Jan–. PMID: 28613612.
10. Hollerer I, Bachmann A, Muckenthaler MU. Pathophysiological consequences and benefits of *HFE* mutations: 20 years of research. Haematologica. 2017 May;102(5):809-817. doi: 10.3324/haematol.2016.160432.
11. Bacon BR, Adams PC, Kowdley KV, Powell LW, Tavill AS; American Association for the Study of Liver Diseases. Diagnosis and management of hemochromatosis: 2011 practice guideline by the American Association for the Study of Liver Diseases. Hepatology. 2011 Jul;54(1):328-43. doi: 10.1002/hep.24330.
12. Phatak PD, Bonkovsky HL, Kowdley KV. Hereditary hemochromatosis: time for targeted screening. Ann Intern Med. 2008 Aug 19;149(4):270-2. doi: 10.7326/0003-4819-149-4-200808190-00009.
13. Porto G, Brissot P, Swinkels DW, Zoller H, Kamarainen O, Patton S, et al. EMQN best practice guidelines for the molecular genetic diagnosis of hereditary hemochromatosis (HH). Eur J Hum Genet. 2016 Apr;24(4):479-95. doi: 10.1038/ejhg.2015.128.
14. Lok CY, Merryweather-Clarke AT, Viprakasit V, Chinthammitr Y, Srichairatanakool S, Limwongse C, et al. Iron overload in the Asian community. Blood. 2009 Jul 2;114(1):20-5. doi: 10.1182/blood-2009-01-199109.
15. Hayashi H, Wakusawa S, Motonishi S, Miyamoto K, Okada H, Inagaki Y, Ikeda T. Genetic background of primary iron overload syndromes in Japan. Intern Med. 2006;45(20):1107-11. doi: 10.2169/internalmedicine.45.1876.
16. McDonald CJ, Wallace DF, Crawford DH, Subramaniam VN. Iron storage disease in Asia-Pacific populations: the importance of non-HFE mutations. J Gastroenterol Hepatol. 2013 Jul;28(7):1087-94. doi: 10.1111/jgh.12222.
17. Labranche R, Gilbert G, Cerny M, Vu KN, Soulières D, Olivié D, et al. Liver Iron Quantification with MR Imaging: A Primer for Radiologists. Radiographics. 2018 Mar-Apr;38(2):392-412. doi: 10.1148/rg.2018170079.

Correspondence:
Dr. Mahasin G. Hassan, Ph.D, mghassan@pnu.edu.sa

18. Awad FM, Alshazly SA. Hepatic iron deposition in patients with sickle cell disease: Role of breath-hold multiecho T2*-weighted MRI sequence. Egypt J Radiol Nucl Med. 2014;45(3):651–5.
19. Sobhani S, Rahmani F, Rahmani M, Askari M, Kompani F. Serum ferritin levels and irregular use of iron chelators predict liver iron load in patients with major beta thalassemia: a cross-sectional study. Croat Med J. 2019 Oct 31;60(5):405-413. doi: 10.3325/cmj.2019.60.405.
20. Paisant A, Boulic A, Bardou-Jacquet E, Bannier E, d'Assignies G, Lainé F, Turlin B, Gandon Y. Assessment of liver iron overload by 3 T MRI. Abdom Radiol (NY). 2017 Jun;42(6):1713-1720. doi: 10.1007/s00261-017-1077-8.
21. Wood JC, Enriquez C, Ghugre N, Tyzka JM, Carson S, Nelson MD, Coates TD. MRI R2 and R2* mapping accurately estimates hepatic iron concentration in transfusion-dependent thalassemia and sickle cell disease patients. Blood. 2005 Aug 15;106(4):1460-5. doi: 10.1182/blood-2004-10-3982.
22. Shah N, Mishra A, Chauhan D, Vora C, Shah NR. Study on effectiveness of transfusion program in thalassemia major patients receiving multiple blood transfusions at a transfusion centre in Western India. Asian J Transfus Sci. 2010 Jul;4(2):94-8. doi: 10.4103/0973-6247.67029.
23. Bandyopadhyay U, Kundu D, Sinha A, Banerjee K, Bandyopadhyay R, Mandal T, Ray D. Conservative management of Beta-thalassemia major cases in the sub-division level hospital of rural West Bengal, India. J Nat Sci Biol Med. 2013 Jan;4(1):108-12. doi: 10.4103/0976-9668.107269.
24. Azarkeivan A, Hashemieh M, Akhlaghpoor S, Shirkavand A, Yaseri M, Sheibani K. Relation between serum ferritin and liver and heart MRI T2* in beta thalassaemia major patients. East Mediterr Health J. 2013 Aug;19(8):727-32.
25. Kaban S, Damar Ç. Interrelationship between liver T2*-weighted magnetic resonance imaging and acoustic radiation force impulse elastography measurement results and plasma ferritin levels in children with β-thalassemia major. J Clin Ultrasound. 2022 Jan;50(1):108-116. doi: 10.1002/jcu.23095.
26. El Sherif AM, Ibrahim AS, Elsayed MA, Abdelhakim AS, Ismail AM. The impact of magnetic resonance imaging in the assessment of iron overload in heart and liver in transfusion-dependent thalassemic children: Minia experience. Egypt J Radiol Nucl Med. 2021;52, 264. doi: 10.1186/s43055-021-00645-4 52, 264
27. Johnston JD. Non-invasive assessment of hepatic iron stores by MRI. Ann Clin Biochem. 2004 May;41(Pt 3):254. doi: 10.1258/000456304323019695.
28. Kolnagou A, Natsiopoulos K, Kleanthous M, Ioannou A, Kontoghiorghes GJ. Liver iron and serum ferritin levels are misleading for estimating cardiac, pancreatic, splenic and total body iron load in thalassemia patients: factors influencing the heterogenic distribution of excess storage iron in organs as identified by MRI T2*. Toxicol Mech Methods. 2013 Jan;23(1):48-56. doi: 10.3109/15376516.2012.727198.

International Journal of Biomedicine 13(3) (2023) 110-116
http://dx.doi.org/10.21103/Article13(3)_OA10

ORIGINAL ARTICLE

Surgery

INTERNATIONAL JOURNAL OF BIOMEDICINE

Predictive Factors of Mortality in Patients with Nonvariceal Upper Gastrointestinal Bleeding

Edite Sadiku[1*], Kliti Hoti[2], Aureta Bruci[1], Stela Tac[1], Aurora Bruci[2], Bledar Kraja[1]

[1]*University Hospital Center "Mother Teresa", Gastrohepatology, Tirana, Albania*
[2]*University of Medicine, Faculty of Public Health, Tirana, Albania*

Abstract

Background: Nonvariceal upper gastrointestinal bleeding (NVUGIB) is one of the most common medical emergencies and often represents a life-threatening event. The aim of this study is to find potential predictive factors associated with 30-day mortality in patients with NVUGIB.

***Methods and Results*:** Our prospective study was conducted in Mother Teresa Hospital between May 2022 and December 2022. A total of 224 patients (aged >18 years) with NVUGIB were included in the study. Demographical and clinical characteristics, endoscopic findings, and laboratory tests were reviewed during a 30-day follow-up period. Logistic regression was employed to identify the independent predictors of mortality.

The mean age of the 224 patients enrolled in the study was 63.21±16.3 years and most patients (72.8%) were male. One hundred fifty (66.9%) patients had comorbidities. The most common endoscopic diagnoses underlying NVUGIB episodes were duodenal ulcers (53.1%). Recurrent bleeding was recorded in 50(22.3%) patients. Out of 224 patients included in the study, 24(10.7%) died within 30 days of admission, 20(8.9%) died during hospitalization, and 4(1.8%) died after discharge. The mean age of death was 76.42±12.59 years; 95.8% of deaths were associated with one or more major comorbidities. In the multivariate logistic regression, after the exclusion of confounding factors, low red blood cell (RBC) (*P*=0.043, OR=0.413, CI 95%: 0.176-0.974), warfarin (*P*=0.036, OR=10.547, CI 95%: 1.165-95.462), and Rockall score (RS) >5 (*P*=0.034, OR=4.107, CI 95%: 1.114-15.139) were found to be independent predictive factors for mortality.

Conclusion: The 30-day mortality rate remained high after NVUGIB, especially during hospitalization. Low RBC, warfarin, and RS>5 were independent factors of mortality in patients with NVUGIB.(**International Journal of Biomedicine. 2023;13(3):110-116.**)

Keywords: nonvariceal upper gastrointestinal bleeding • mortality • predictive factors

For citation: Sadiku E, Hoti K, Bruci A, Tac S, Bruci A, Kraja B. Predictive Factors of Mortality in Patients with Nonvariceal Upper Gastrointestinal Bleeding. International Journal of Biomedicine. 2023;13(3):110-116. doi:10.21103/Article13(3)_OA10

Abbreviations

BP, blood pressure; **BUN**, blood urea nitrogen; **GIB**, gastrointestinal bleeding; **GBS**, Glasgow-Blatchford score; **HR**, heart rate; **INR**, international normalized ratio; **NVUGIB**, nonvariceal upper gastrointestinal bleeding; **NSAIDs**, nonsteroidal anti-inflammatory drugs; **RBC**, red blood cell; **RS**, Rockall score; **WBC**, white blood cells.

Introduction

Nonvariceal upper gastrointestinal bleeding (NVUGIB) is a common medical condition that results in significant morbidity, mortality, and cost of medical care.[1,2] Mortality rates reported for NVUGIB range from 2% to 13.2% and vary in different countries.[3] Despite advances in endoscopic treatments and the decrease in the incidence of *H. pylori*, mortality remains high, and it might be due to increasing age, comorbidities, and health care systems, which confound the effects of therapy improvements.[3,4] Multiorgan failure, cardiopulmonary conditions, and terminal malignancies are the most common causes in these patients.[5,6] Comorbidities, hypotension, tachycardia, low hemoglobin, endoscopic findings, and administration of anticoagulants and nonsteroidal anti-inflammatory drugs are seen as risk factors for mortality in NVUGIB.[5-10]

The aim of this study is to find potential predictive factors associated with 30-day mortality in patients with NVUGIB.

Materials and Methods

Our prospective study was conducted in Mother Teresa Hospital between May 2022 and December 2022. A total of 224 patients (aged >18 years) with NVUGIB were included in the study. Exclusion criteria were patients who did not undergo endoscopy, patients with variceal bleeding, and patients who have not been followed up to one month after hospitalization. All participants provided written informed consent.

The study data were obtained from the anamnesis, physical examination, and clinical records of the patients. The following information was documented prospectively: *Patient data* (age, gender, date of admission); *History data* (presentation of symptoms, previous history of gastrointestinal bleeding or peptic ulcer disease); *Social history* (current smoking status, alcohol consumption); *Physical examination findings* (nasogastric lavage, rectal examination and initial hemodynamic status); *Initial laboratory data* (complete blood count, urinalysis, creatinine, platelet count and prothrombin time, transaminases, total bilirubin, electrolytes); *Comorbidities,* including hypertension, diabetes mellitus, cardiovascular diseases, cerebrovascular disease, heart failure, atrial fibrillation, liver cirrhosis (determined by clinical, laboratory and radiological data, without biopsy), malignancies; *Medications* (antiplatelet agents, vitamin K antagonists, NSAIDs, steroids, protein pump inhibitors); *Endoscopic findings: the* identification of the bleeding lesion, stigmata of recent hemorrhage at ulcer base according to the Forrest classification[7] (active bleeding, visible vessel, or adherent clots were classified as "high risk," whereas flat spot and clean based ulcer as "low risk").

Proton pump inhibitors were administered intravenously to all patients. Each patient's bleeding risk was assessed by the Rockall score (RS) and Glasgow-Blatchford score (GBS) systems.

The endoscopic hemostatic technique used, as well as the presence of rebleeding, the need for surgery, and for hospital stay, were also described. Patients were followed by daily visits during hospitalization or until discharge or death. Hemodynamically unstable patients received intravenous crystalloid solutions and blood according to individual requirements. All endoscopic procedures were performed in the endoscopy unit by a gastroenterologist of the Gastroenterology Service.

Outcomes

The outcomes evaluated were the frequency of death, rebleeding, and need for surgery. Such outcomes were monitored from the admission to the hospital or the onset of bleeding for in-hospital patients up to 30 days after the endoscopic examination. The primary outcome was mortality within 30 days of admission. Patients were advised to return for examination at 4 and 12 weeks after discharge.

i) Mortality within 30 days:

- *Intrahospital*: deaths occurring in hospital after diagnosis and treatment of bleeding.

- *After discharge*: deaths occurring after discharge from the hospital, diagnosis, and treatment of the bleeding.

ii) Recurrence of bleeding within 30 days:

- Recurrence of bleeding was defined as the onset of new hematemesis or hematochezia with hypovolemic shock or a greater than 2 g/dL drop in hemoglobin levels after a 24-hour period with stable vital signs within 30 days of admission. All bleeding episodes were confirmed by endoscopy.

iii) Unidentified cause of hemorrhage: the presence of blood in the stomach without finding a cause.

To ensure the completeness of 30-day follow-up information, patients were contacted by phone.

Statistical analysis was performed using the statistical software package SPSS version 25.0 (SPSS Inc, Armonk, NY: IBM Corp). Baseline characteristics were summarized as frequencies and percentages for categorical variables and as mean (M) ± standard deviation (SD) for continuous variables. For data with normal distribution, inter-group comparisons were performed using Student's t-test. Group comparisons with respect to categorical variables are performed using chi-square test. A probability value of $P<0.05$ was considered statistically significant. All variables were subject to univariate logistic regression, and odds ratios (ORs) were calculated between non-survived and survived groups, with a 95% confidence interval (CI). Variables were included in binary logistic regression if the corresponding *P*-value was less than 0.05. Binary logistic regression analysis was used to develop a multivariate model to determine the risk factors of death among critically ill patients.

Results

Patient characteristics are reported in Table 1. The mean age of the 224 patients enrolled in the study was 63.21±16.3 years and most patients (72.8%) were male. On admission, the most common symptom was melena (96.5%), followed by hematemesis (47.8%) and hematochezia (1.7%). One hundred fifty (66.9%) patients had comorbidities, the most common being hypertension (n=122), followed by atrial fibrillation (n=34), heart failure (n=32), and diabetes mellitus (n=32). One hundred forty-nine (66.5%) patients were taking medications, including aspirin - 68(30.4%), NSAIDs - 21(9.3%), clopidogrel - 11(4.9%), vitamin K antagonists - 8(3.6%), and rivaroxaban (Xarelto) - 15(6.7%). A total of 26(11.6%) patients were referred for previous history of gastrointestinal bleeding, of which 7 had undergone surgical intervention. Smoking and alcohol use were observed only in men, among whom 69(30.8%) patients were smokers, and 67(29.9%) were alcohol users until the day of hospitalization. Fifty-three patients presented with tachycardia (heart rate > 100 bpm) and 41 with hypotension (systolic blood pressure < 90 mmHg) (Table 2).

The mean serum level of hemoglobin upon admission was 8.5 g/dL. All patients underwent digital-rectal examination with patient approval, resulting in 187(83.5%) patients with melena, 7(3.1%) with hematochezia. A nasogastric tube was

performed on 90 patients, of whom 58 patients were positive. The mean number of units of packed RBCs transfused was 2.23±1.73. The mean total RS was 2.64±1.77, and 72(32.1%) patients had a score ≥5, indicating a high risk of mortality. The mean GBS was 11.75±2.06.

Table 1.

Characteristics of the NVUGIB patients (n=224)

Factor	Value [n (%), M±SD]
Male sex	163 (72.8)
Age, year	63.21±16.3
Hematemesis	117 (47.8)
Melena	216 (96.5)
Hematochezia	4 (1.78)
Heavy alcoholics	72 (39.1)
Current smokers	68 (37.0)
History of GIB	26 (11.6)
Comorbidities	150 (66.9)
Hypertension	122 (54.4)
Atrial fibrillation	34 (15.1)
Diabetes mellitus	32 (14.2)
Liver cirrhosis	2 (0.89)
Chronic kidney disease	13 (5.8)
Cerebrovascular disease	9 (4.0)
Heart failure	32 (14.2)
Cardiovascular disease	10(4.5)
Metastatic malignancy	8 (3.6)
Use of medication	149 (66.5)
Antiplatelet agents	79 (35.2)
NSAIDs	21 (9.3)
Vitamin K antagonist	8 (3.6)
Rivaroxaban (Xarelto)	15 (6.7)

In our study (Table 3), 142 endoscopies were performed within 12h, 45 within 12 to 24h, 22 within 24 to 48h, and 15 over 48h. The most common endoscopic diagnoses underlying NVUGIB episodes were duodenal ulcers (53.1%), followed by gastric ulcers (19.2%), erosive gastritis (7.1%), and esophageal ulcers (5.8%). Of 224 patients, 80.5% were high-risk stigmata (Forrest 1 - 38.4%, Forrest 2A - 18.3%, Forrest 2B - 23.8%) and 70(31.3%) underwent endoscopic treatment.

Clinical outcomes

Recurrent bleeding was recorded in 50(22.3%) patients, whereas emergency surgery was deemed necessary in only 10 cases. Forty-seven cases were in the first week. The mean hospital stay was 7.7±3.4 days. Of the 224 patients included in the study, 24(10.7%) died within one month of admission, whereas 20(8.9%) died during hospitalization, and 4(1.8%) died after discharge from the hospital. Among patients who died within 30 days, 17 died during the first 7 days. The mean age of death was 76.42±12.59 years; 95.8% of deaths were associated with one or more major comorbidities. Of all the patients, 14 underwent surgery.

Table 2.

Clinical and laboratory data of the patients, at admission (n=224)

Factor	Value [n (%), M±SD]
Initial vital sign	
BP, mmHg	108.67±16.8
Heart rate, bpm	90.02±15.3
Hypotension (SBP < 90 mmHg)	41 (18.3)
Tachycardia (heart rate > 100 bpm	53 (23.7)
Initial laboratory data	
Hemoglobin, g/dL	8.97±2.95
RBC × 10^6/L	3.07±1.03
WBC, K/uL	11.5±6.2
Platelets, K/uL	258±133.9
Blood nitrogen urea, mg/dL	77.5±45.2
Prothrombin time (PT), sec	76.5± 23.5
INR	1.71±2.23
Positive nasogastric tube aspiration	58/90 (64.4)
Melena	187/224 (83.5)
Hematochezia	7/224 (3.1)
Mean transfusion requirement, no. of unit	2.23±1.73
GBS	11.75±2.06
RS	2.64±1.77

Predictive factors for 30-day mortality in NVUGIB

In the univariate analysis, significant risk factors for 30-day mortality were age (P=0.000), tachycardia (P=0.002), hypertension (P=0.039), chronic kidney disease (P=0.025), heart failure (P=0.037), diabetes mellitus (P=0.033), malignancies (P=0.004), low RBC (P=0.040), leukocytosis (P=0.021), increased urea (P=0.001), aspirin (P=0.031), warfarin (P=0.015), hospital stay (P=0.000), RS≥5 (P=0.000), and GBS>12 (P=0.010) (Table 4).

Low RBC (P=0.043 OR=0.413, CI 95%: 0.176-0.974), warfarin (P=0.036, OR= 10.547, CI 95%: 1.165-95.462), and RS>5 (P=0.034, OR=4.107, CI 95%: 1.114-15.139) were found to be independent predictive factors for mortality in the multivariate logistic regression (Table 5).

Table 3.
Endoscopic features and clinical outcomes of patients with NVUGIB (n = 224)

Factor	Value [n (%)]
Urgent endoscopy(<12h)	142 (63.4)
Endoscopy findings	
Duodenal ulcer	119 (53.1)
Gastric ulcer	43 (19.2)
Erosive gastritis	16 (7.1)
Esophageal ulcer	13 (5.8)
Neoplasia	16 (7.1)
Mallory-Weiss syndrome	5 (2.2)
Angiodysplasia	1 (0.4)
Dieulafoy's lesion	2 (0.8)
No evidence of upper GIB	3 (1.3)

Table 3 (continued).
Endoscopic features and clinical outcomes of patients with NVUGIB (n = 224)

Factor	Value [n (%)]
Forrest classification	
I	63/164 (38.4)
IIa	30/164 (18.3)
IIb	39/164 (23.8)
IIc	19/164 (11.5)
III	13/164 (8.0)
Outcomes	
Rebleeding	50 (22.3)
Death	24 (10.7)
During hospitalization	20 (8.9)
Hospital stay, day	7.7±3.4

Table 4.
Univariate analysis of clinical variables for mortality in patients with NVUGIB.

Factor	Univariate analysis			
	30-Day death (+) (n = 24)	30-Day death (–) (n = 200)	*P*-value	OR (95% CI)
Age, yrs.	76.42±12.59	61.63±16.09	**0.000**	1.093 (1.046 -1.142)
Hematemesis	13 (54.2)	94 (47.0)	0.508	1.333 (0.570-3.117)
Melena	23 (95.8)	193 (96.5)	0.868	0.834 (0.098-7.086)
Alcohol	5 (20.8)	62 (31.0)	0.309	0.586 (0.209-1.640)
Current smoker	10 (41.7)	59 (29.5)	0.226	1.707 (0.718-4.060)
History of GIB	1 (4.1)	25 (12.5)	0.081	0.164 (0.021-1.246)
Comorbidities				
Hypertension	18 (75.0)	104 (52.0)	**0.039**	2.769 (1.055-7.266)
Atrial fibrillation	6 (25.0)	28 (14.0)	0.163	2.048 (0.748-5.603)
Diabetes mellitus	7 (29.2)	25 (12.5)	**0.033**	2.882 (1.087-7.641)
Chronic kidney disease	4 (16.7)	3 (1.5)	**0.025**	4.244 (1.198-15.033)
Cerebrovascular disease	3 (12.5)	6 (3.0)	0.318	1.593 (0.639-3.975)
Heart failure	7 (29.1)	25 (12.5)	**0.037**	2.076 (1.053-7.432)
Cardiovascular disease	2 (8.3)	8 (4.0)	0.099	1.468 (0.930-2.317)
Metastatic malignancy	4 (16.7)	4 (2.0)	**0.004**	2.355 (1.320-4.202)
Aspirin	12 (5.0)	56 (28.0)	**0.031**	2.571 (1.091-6.062)
Warfarin	3 (12.5)	4 (2.0)	**0.015**	7.000 (1.466-33.416)
Hypotension (SBP < 90 mmHg)	7 (29.2)	34 (17.0)	0.152	2.010 (0.774-5.221)
Tachycardia (HR >100 bpm)	12 (50.0)	41 (20.5)	**0.002**	3.878 (1.624-9.263)
Hemoglobin, g/dL	7.66 ±2.39	8.65±2.81	0.102	0.868 (0.733-1.028)
RBC × 10^6/L	2.67± 0.84	3.12±1.05	**0.040**	0.599 (0.368-0.978)
WBC, K/uL	11.7±6.8	10.4±5.8	**0.021**	1.065 (1.009-1.123)
Platelets, K/uL	279.0±115.47	255.47±136.0	0.417	1.001 (0.998-1.004)
BNU, mg/dL	108.88±58.43	73.75±42.05	**0.001**	1.014 (1.006-1.022)
Prothrombin time (PT), sec	61.35±29.40	78.11±22.27	**0.004**	0.977 (0.961-0.992)
Positive nasogastric tube	9 (37.5)	81 (4.1)	0.387	2.059 (0.401-10.560)
Positive rectal examination	21 (91.7)	166 (86.0)	0.124	0.479 (0.188-1.223)
Transfusion requirement, no. of unit	2.29±2.18	2.22±1.68	0.848	1.024 (0.804-1.304)

Table 4 (continued).

Univariate analysis of clinical variables for mortality in patients with NVUGIB.

Factor	Univariate analysis			
	30-Day death (+) (n = 24)	**30-Day death (–) (n = 200)**	***P*-value**	**OR (95% CI)**
GBS >12	17 (70.8)	84 (42.0)	**0.010**	3.354 (1.331-8.448)
RS >5	18 (75.0)	54 (27.0)	**0.000**	8.111 (3.059-21.509)
Urgent endoscopy(<12h)	15 (62.5)	127 (63.5)	0.893	0.895 (0.178-4.507)
Endoscopy findings				
Peptic ulcer disease	18 (75.0)	144 (72)	0.853	1.103 (0.390-3.120)
Non-Peptic ulcer disease	5 (21.0)	41 (20.5)	0.830	1.133 (0.362-3.549)
Neoplasia	1 (4.1)	15 (7.5)	0.555	0.536 (0.068-4.250)
Forrest classification				
I	8 (33.3)	55 (27.5)	0.440	1.487 (0.543-4.067)
IIA	2 (8.3)	28 (14.0)	0.369	0.497 (0.108-2.283)
IIB	5 (20.8)	34 (17.0)	0.870	1.104 (0.338-3.605)
Rebleeding	7 (29.2)	43 (21.5)	0.397	1.503 (0.586-3.859)
Hospital stay, day	7.04	6.76	**0.000**	0.704 (0.579-0.856)

Table 5.

Logistic Regression Model to determine the predictors of mortality.

Factor	*P*-value	OR	95% CI	
			Lower	Upper
Age	0.066	1.053	0.997	1.113
RBC × 10^6/uL	**0.043**	0.413	0.176	0.974
WBC, K/uL	0.635	1.017	0.948	1.092
BUN, mg/dL	0.686	1.003	0.990	1.015
Heart rate > 100 bpm	0.223	2.134	0.631	7.220
Hypertension	0.472	0.591	0.141	2.479
Heart failure	0.798	0.831	0.201	3.438
Aspirin	0.066	3.519	0.920	13.467
Warfarin	**0.036**	10.547	1.165	95.462
GBS >12	0.592	0.655	0.139	3.079
RS>5	**0.034**	4.107	1.114	15.139
Hospital stay, day	0.056	0.700	0.566	0.864

Discussion

NVUGIB is one of the most common medical emergencies and often represents a life-threatening event. The results of this study have differences from and similarities to other studies. Acute NVUGIB remains a common medical problem associated with high morbidity, 30-day mortality, and healthcare costs.[1] The incidence of acute upper gastrointestinal bleeding in the Western world is 103 per 100,000 adults annually, with a mortality of about 2%-10%.[4]

Our study enrolled 224 patients with a mean age of 63.21±16.3 years. Our patients were younger than those in Greek (66±15),[11] Italian (68±16),[12] and Canadian (66±17)[13] studies and older than in the Turkish study (57.75±18.85).[13] Male patients accounted for 72.8% of participants—the same model as in Western studies.

In our study, 66.9% of patients had comorbidities, the most common of which were hypertension (122[54.4%]), followed by atrial fibrillation (34[15.1%]), diabetes mellitus (32[14.2%]), and heart failure (32[14.2%]). The same results have been seen in different studies.

As for the use of medications, in our study, the prevalence of aspirin use was 30.3%, 9.8% for vitamin K antagonists, 9.3% for NSAIDs, 6.6% for rivaroxaban (Xarelto), and 4.9% for clopidogrel. Compared to other studies,[12-14] it turned out that we had a higher use of aspirin and lower of NSAIDs.

At admission, the most frequent clinical presentation was melena (96.5%), 47.8% with hematemesis, and 1.7% with hematochezia. In our study, there was no significant correlation with mortality, while in the Turkish study,[14] hematemesis was one of the predictors of patient management and clinical outcomes of NVUGIB.

The most frequent source of bleeding was peptic ulcers, among which duodenal ulcers (53.1%) prevailed, followed by gastric ulcers (19.2%) and erosive gastritis (7.1%). The frequency was similar to that of previous studies conducted at the Gastrohepatology Department in Mother Teresa Hospital in 2015[15] and 2019.[16] Compared to Western studies [13,17] we had a higher percentage of peptic ulcers, similar to the Turkish study.[14] This result is due to the lack of investigation and the failure to eradicate H. pylori, knowing that its eradication has been associated with a decrease of peptic ulcers.

Also, there was a high percentage of high-risk stigmata lesions (Forrest 1 - 38.4%, Forrest 2A - 18.3%, Forrest 2B - 23.8%, and Forrest 3 - 8.0%), unlike in Western studies. [12-14] This may be for several reasons, including low socio-economic conditions and patient negligence. Also, the study

was conducted in a tertiary center, and the referral of active bleeding and severe cases is higher even from the regional hospitals.

Regarding the endoscopy time in our study, 63.4% were done within 12 hours, and 20.0% within 12-24 hours. This result was similar to the Korean study (65.8%) of Lee et al.[18] In other studies, most endoscopies are performed within 24 hours.[12,13] In many studies and gastroenterology societies, endoscopy is not recommended within 12 hours because no change in the outcomes has been observed.[19-21] And in our study, no significant correlation was found between the time of endoscopy and mortality.

The recurrence of bleeding in our study was 22.3%, which was higher than in the Italian, Canadian, and Turkish studies (3.2%, 14.1%, and 9.0%, respectively).[12-14] All the episodes were during the hospitalization and mostly within 24 hours. The high percentage is due to the limited endoscopic treatment procedures and the high rate of high-risk stigmata ulcerative lesions. Also, no significant correlation was found between rebleeding and mortality. In some other studies, rebleeding was considered an independent predictive factor for mortality.[11,22] The number of surgical interventions (10) was higher than in the Italian and Turkish studies (1.3% and 2.6%, respectively). [12,14] This is due to the limited endoscopic procedures.

Out of 224 patients included in the study, 24(10.7%) died within 30 days of admission, 20(8.9%) died during hospitalization, and 4(1.8%) died after discharge.

The mortality rate was higher than that in Western countries such as the USA and most of Europe, and similar to mortality in Denmark (10.5%-11%).[3] This may be because the study was done in a tertiary hospital center, where the patients' conditions may be more severe and contribute to poor clinical outcomes and higher mortality rates. The higher mortality rate occurred in the first week (70.8%), and 29.2% had a recurrence of bleeding. These findings were similar to the findings of studies conducted in Italy.[12] The mean age of death was 76.42±12.59, the same as studies in Italy (76.6±14.0)[12] and Canada (72±12.6),[13] in which advanced age was also an independent predictive factor for mortality.

Studies in the literature refer to comorbidities as independent risk factors not only for gastrointestinal bleeding but also for mortality.[23] They are also important factors in scoring systems for patient risk assessment.[24]

In our study, 95.8% of deaths were associated with one or more major comorbidities. The most frequent comorbidities were hypertension, atrial fibrillation, heart failure, chronic kidney disease, and malignancies.

Also, many studies have identified many risk factors for mortality in NUVGIB, such as hypotension, tachycardia, advanced age, comorbidities, coagulopathy, low hemoglobin, anticoagulants, and antiplatelets.[23,25] Some of these risk factors have also been identified in our study. In the univariate analysis, significant risk factors for 30-day mortality were age (P=0.000), tachycardia (P=0.002), hypertension (P=0.039), chronic kidney disease (P=0.025), heart failure (P=0.037), diabetes mellitus (P=0.033), malignancies (P=0.004), low RBC (P=0.040), leukocytosis (P=0.021), increased urea (P=0.001), aspirin (P=0.031), warfarin (P=0.015), hospital stay (P=0.000), RS≥5 (P=0.000), and GBS>12 (P=0.010).

In many studies, leukocytosis has been associated with a poor prognosis and mortality. It has been hypothesized that the reason leukocytosis could lead to mortality could be an infectious or inflammatory condition.[26] Regarding medications, aspirin and warfarin were found to be risk factors for mortality. Aspirin is thought to increase mortality due to the increased severity of ulcer and hemorrhagic lesions and antiplatelet effects.[8] Warfarin is known as a risk factor for mortality,[27] which we also found in our study; and it is thought that it may be due to its anticoagulant effects and irregular monitoring of PT and INR. In the Multivariate logistic regression, after the exclusion of confounding factors, low RBC (P=0.043, OR=0.413, CI 95%: 0.176-0.974), warfarin (P=0.036, OR=10.547, CI 95%: 1.165-95.462), and RS>5 (P=0.034, OR=4.107, CI95%: 1.114-15.139) were found to be independent predictive factors for mortality. Similar results were observed in different studies.[12, 17,22]

In our study, both RS and GBS scores were calculated for all the patients on the basis of clinical and endoscopic variables.[28] Thirty-day mortality rates tended to be higher in patients with a high RS>5 and GBS >12 in univariate analysis. Also, RS was identified as an independent predictor of mortality. It is important to identify these factors because they can be used before endoscopy to identify high-risk patients, for whom a high level of care is needed to prevent adverse outcomes.

Our study has some limitations: First, our study was realized in a short period and had a small sample size. This could lead to bias. Second, although *H. pylori* is the main cause of peptic ulcers and its eradication reduces the possibility of rebleeding, the patients were not tested.[29,30]

In conclusion, our study shows that the 30-day mortality rate remained high after NVUGIB, especially during hospitalization. Low RBC, warfarin, and RS>5 were independent factors of mortality in patients with NVUGIB. These findings show that high-risk patients should be carefully monitored to prevent adverse outcomes.

Competing Interests

The authors declare that they have no competing interests.

References

1. Wuerth BA, Rockey DC. Changing Epidemiology of Upper Gastrointestinal Hemorrhage in the Last Decade: A Nationwide Analysis. Dig Dis Sci. 2018 May;63(5):1286-1293. doi: 10.1007/s10620-017-4882-6.

2. Kim BS, Li BT, Engel A, Samra JS, Clarke S, Norton ID, Li AE. Diagnosis of gastrointestinal bleeding: A practical guide for clinicians. World J Gastrointest Pathophysiol. 2014 Nov 15;5(4):467-78. doi: 10.4291/wjgp.v5.i4.467.

***Correspondence:** Edite Sadiku, MD, PhD. E-mail: editesadiku@gmail.com*

3. Jairath V, Martel M, Logan RF, Barkun AN. Why do mortality rates for nonvariceal upper gastrointestinal bleeding differ around the world? A systematic review of cohort studies. Can J Gastroenterol. 2012 Aug;26(8):537-43. doi: 10.1155/2012/862905.
4. Stanley AJ, Laine L. Management of acute upper gastrointestinal bleeding. BMJ. 2019 Mar 25;364:l536. doi: 10.1136/bmj.l536.
5. Sung JJ, Tsoi KK, Ma TK, Yung MY, Lau JY, Chiu PW. Causes of mortality in patients with peptic ulcer bleeding: a prospective cohort study of 10,428 cases. Am J Gastroenterol. 2010 Jan;105(1):84-9. doi: 10.1038/ajg.2009.507.
6. Laine L, Peterson WL. Bleeding peptic ulcer. N Engl J Med. 1994 Sep 15;331(11):717-27. doi: 10.1056/NEJM199409153311107.
7. Forrest JA, Finlayson ND, Shearman DJ. Endoscopy in gastrointestinal bleeding. Lancet. 1974 Aug 17;2(7877):394-7. doi: 10.1016/s0140-6736(74)91770-x.
8. Mose H, Larsen M, Riis A, Johnsen SP, Thomsen RW, Sørensen HT. Thirty-day mortality after peptic ulcer bleeding in hospitalized patients receiving low-dose aspirin at time of admission. Am J Geriatr Pharmacother. 2006 Sep;4(3):244-50. doi: 10.1016/j.amjopharm.2006.09.006.
9. Thomsen RW, Riis A, Christensen S, McLaughlin JK, Sørensen HT. Outcome of peptic ulcer bleeding among users of traditional non-steroidal anti-inflammatory drugs and selective cyclo-oxygenase-2 inhibitors. Aliment Pharmacol Ther. 2006 Nov 15;24(10):1431-8. doi: 10.1111/j.1365-2036.2006.03139.x.
10. Klein A, Gralnek IM. Acute, nonvariceal upper gastrointestinal bleeding. Curr Opin Crit Care. 2015 Apr;21(2):154-62. doi: 10.1097/MCC.0000000000000185.
11. Papatheodoridis G, Akriviadis E, Evgenidis N, Kapetanakis A, Karamanolis D, Kountouras J, et al. Greek results of the "ENERGIB" European study on non-variceal upper gastrointestinal bleeding. Ann Gastroenterol. 2012;25(4):327-332.
12. Marmo R, Koch M, Cipolletta L, Capurso L, Pera A, Bianco MA, et al. Predictive factors of mortality from nonvariceal upper gastrointestinal hemorrhage: a multicenter study. Am J Gastroenterol. 2008 Jul;103(7):1639-47; quiz 1648. doi: 10.1111/j.1572-0241.2008.01865.x.
13. Barkun A, Sabbah S, Enns R, Armstrong D, Gregor J, Fedorak RN, et al.; RUGBE Investigators. The Canadian Registry on Nonvariceal Upper Gastrointestinal Bleeding and Endoscopy (RUGBE): Endoscopic hemostasis and proton pump inhibition are associated with improved outcomes in a real-life setting. Am J Gastroenterol. 2004 Jul;99(7):1238-46. doi: 10.1111/j.1572-0241.2004.30272.x.
14. Mungan Z. An observational European study on clinical outcomes associated with current management strategies for non-variceal upper gastrointestinal bleeding (ENERGIB-Turkey). Turk J Gastroenterol. 2012;23(5):463-77. doi: 10.4318/tjg.2012.0402.
15. Sadiku E. et al. Causes and Treatment of Acute Upper Gastrointestinal Bleeding in Adults. Our experience. Tirana, 2015.
16. Simaku E. et al. [Shkaqet dhe trajtimi I hemorragjive te siperme gastrointestinale, eksperienca jone]. Tirana, 2019. [Article in Albanian].
17. Quentin V, Remy AJ, Macaigne G, Leblanc-Boubchir R, Arpurt JP, Prieto M, et al.; Members of the Association Nationale des Hépato-gastroentérologues des Hôpitaux Généraux (ANGH) SANGHRIA Study Group. Prognostic factors associated with upper gastrointestinal bleeding based on the French multicenter SANGHRIA trial. Endosc Int Open. 2021 Sep 16;9(10):E1504-E1511. doi: 10.1055/a-1508-5871.
18. Lee YJ, Min BR, Kim ES, Park KS, Cho KB, Jang BK, et al. Predictive factors of mortality within 30 days in patients with nonvariceal upper gastrointestinal bleeding. Korean J Intern Med. 2016 Jan;31(1):54-64. doi: 10.3904/kjim.2016.31.1.54.
19. Siau K, Hodson J, Ingram R, Baxter A, Widlak MM, Sharratt C, et al.. Time to endoscopy for acute upper gastrointestinal bleeding: Results from a prospective multicentre trainee-led audit. United European Gastroenterol J. 2019 Mar;7(2):199-209. doi: 10.1177/2050640618811491.
20. Gralnek IM, Stanley AJ, Morris AJ, Camus M, Lau J, Lanas A, et al. Endoscopic diagnosis and management of nonvariceal upper gastrointestinal hemorrhage (NVUGIH): European Society of Gastrointestinal Endoscopy (ESGE) Guideline - Update 2021. Endoscopy. 2021 Mar;53(3):300-332. doi: 10.1055/a-1369-5274.
21. Laine L, Barkun AN, Saltzman JR, Martel M, Leontiadis GI. ACG Clinical Guideline: Upper Gastrointestinal and Ulcer Bleeding. Am J Gastroenterol. 2021 May 1;116(5):899-917. doi: 10.14309/ajg.0000000000001245. Erratum in: Am J Gastroenterol. 2021 Nov 1;116(11):2309.
22. González-González JA, Vázquez-Elizondo G, García-Compeán D, Gaytán-Torres JO, Flores-Rendón ÁR, Jáquez-Quintana JO, et al. Predictors of in-hospital mortality in patients with non-variceal upper gastrointestinal bleeding. Rev Esp Enferm Dig. 2011 Apr;103(4):196-203.. doi: 10.4321/s1130-01082011000400005. [Article in English, Spanish].
23. Leontiadis GI, Molloy-Bland M, Moayyedi P, Howden CW. Effect of comorbidity on mortality in patients with peptic ulcer bleeding: systematic review and meta-analysis. Am J Gastroenterol. 2013 Mar;108(3):331-45; quiz 346. doi: 10.1038/ajg.2012.451.
24. de Groot N, van Oijen M, Kessels K, Hemmink M, Weusten B, Timmer R, et al. Prediction scores or gastroenterologists' Gut Feeling for triaging patients that present with acute upper gastrointestinal bleeding. United European Gastroenterol J. 2014 Jun;2(3):197-205. doi: 10.1177/2050640614531574.
25. Hajiagha Mohammadi AA, Reza Azizi M. Prognostic factors in patients with active non-variceal upper gastrointestinal bleeding. Arab J Gastroenterol. 2019 Mar;20(1):23-27. doi: 10.1016/j.ajg.2019.01.001.
26. Moledina SM, Komba E. Risk factors for mortality among patients admitted with upper gastrointestinal bleeding at a tertiary hospital: a prospective cohort study. BMC Gastroenterol. 2017 Dec 20;17(1):165. doi: 10.1186/s12876-017-0712-8.
27. Xu Y, Siegal DM. Anticoagulant-associated gastrointestinal bleeding: Framework for decisions about whether, when and how to resume anticoagulants. J Thromb Haemost. 2021 Oct;19(10):2383-2393. doi: 10.1111/jth.15466.
28. Klein A, Gralnek IM. Acute, nonvariceal upper gastrointestinal bleeding. Curr Opin Crit Care. 2015 Apr;21(2):154-62. doi: 10.1097/MCC.0000000000000185.
29. Huang TC, Lee CL. Diagnosis, treatment, and outcome in patients with bleeding peptic ulcers and Helicobacter pylori infections. Biomed Res Int. 2014;2014:658108. doi: 10.1155/2014/658108.
30. Popa DG, Obleagă CV, Socea B, Serban D, Ciurea ME, Diaconescu M, et al. Role of *Helicobacter pylori* in the triggering and evolution of hemorrhagic gastro-duodenal lesions. Exp Ther Med. 2021 Oct;22(4):1147. doi: 10.3892/etm.2021.10582.

International Journal of Biomedicine 13(3) (2023) 117-122
http://dx.doi.org/10.21103/Article13(3)_OA11

ORIGINAL ARTICLE

Sports Medicine

INTERNATIONAL JOURNAL OF BIOMEDICINE

Investigating the Role of Proximal Femoral Morphology in Noncontact ACL Injuries: A Comparative Study

Dijon Musliu[1,2], Jeton Shatri[1,3], Sadi Bexheti[1], Ardita Kafexholli[3], Redon Jashari[4], Agron Mahmuti[5], Lavdim Berisha[5], Ardian Karakushi[5], Qerim Kida[5]

[1]*Faculty of Medicine, Institute of Anatomy, University of Prishtina "Hasan Prishtina", Prishtina, Kosovo*
[2]*Clinic of Orthopedics, University Clinical Center of Kosovo, Prishtina, Kosovo*
[3]*Clinic of Radiology, University Clinical Center of Kosovo, Prishtina, Kosovo*
[4]*Health Science Department, Universum College, Prishtina, Kosovo*
[5]*Royal Medical Hospital, Prishtina, Kosovo*

Abstract

Background: Non-contact anterior cruciate ligament (ACL) injury is a common and debilitating injury among athletes, with high recurrence rates and long-term consequences. Identifying individuals at risk of ACL injury can help prevent or reduce the severity of these injuries. The present study aimed to assess the alpha angle in ACL rupture patients in both the injured (ipsilateral) and non-affected (contralateral) extremities, compared to a control group.

***Methods and Results*:** This case-control study included 105 subjects (78.1% male and 21.9% female) aged between 15 and 45 years of both sexes involved in sports. The case group consisted of 54 patients with sport-related, noncontact ACL ruptures identified by MRI. Fifty-one patients, 10(19.6%) of whom were female, with no ACL rupture, were included in the study as a control group. Hip radiographs were taken in all the subjects using the modified Dunn View with the patient in the supine position, hip flexed 45° and abducted 20°. OsiriX software was used to obtain the measurements. Most injuries were caused by football (58.1%), followed by jumping sports (23.8%) and skiing (18.1%). The mean alpha angle was 49.27° (SD=4.93) for subjects without ACL rupture and 54.84° (SD=6.17) for subjects with ACL rupture, and the difference was statistically significant (P<0.001). Results also showed a statistically significant difference in the alpha angle on the ipsilateral (54.84° [SD=6.17]) and contralateral (49.48° [SD=7.04]) hips of the case subjects (P<0.001). The logistic regression analysis indicated a statistically significant difference in alpha angle between the case and control groups and between hips of the same subject with an OR of 1.12 (P=0.041) and 1.2 (P=0.000), respectively.

***Conclusion*:** Alterations in proximal femur morphology should be considered a potential risk factor for ACL injury, and alpha angle can be a significant predictor of ACL injury. We recommend that young athletes actively participating in sports have their hip alpha angle measured so those with higher alpha angle can follow special prevention programs.**(International Journal of Biomedicine. 2023;13(3):117-122.)**

Keywords: anterior cruciate ligament • alpha angle • femoroacetabular impingement

For citation: Musliu D, Shatri J, Bexheti S, Kafexholli A, Jashari R, Mahmuti A, Berisha L, Karakushi A, Kida Q. Investigating the Role of Proximal Femoral Morphology in Noncontact ACL Injuries: A Comparative Study. International Journal of Biomedicine. 2023;13(3):117-122. doi:10.21103/Article13(3)_OA11

Abbreviations

ACL, anterior cruciate ligament; **FAI**, femoroacetabular impingement; **NWI**, notch width index.

Introduction

The anterior cruciate ligament (ACL) constitutes one of the major stabilizers of the knee joint, and it is the most injured ligament of this joint.[1] The injury consists of a rupture of the ligament, which usually happens at sports practitioners and, in most cases, is noncontact.[2]

Various risk factors that predispose one to an ACL rupture have been described. Multiple studies have reported that sex (female gender is more predisposed to an ACL injury),

femoral intercondylar notch width (smaller dimensions), ACL volume, joint laxity, neuromuscular factors, and higher posterior slope of the tibial plateau are risk factors.[2,3]

Different studies indicate that certain individuals are more susceptible to experiencing an ACL rupture.[4,5] Moreover, those who have previously sustained such an injury still have a high risk for re-rupture. While there is a gender bias toward ACL injury, with females having up to an eight times higher risk of sustaining an injury, the number of males affected is higher, mainly due to their greater involvement in sports.[6]

Numerous studies have reported that abnormalities of the joints adjacent to the knee impact the knee and limb kinematics, thus raising the chances for an ACL rupture.[7,8]

In the proximal femur, these bony abnormalities have been found to mostly cause hip impingement. Depending on the cause, hip impingement can be of three types: cam, pincer, and mixed. The pincer type occurs when the bone abnormality is located in the acetabulum, whereas bony abnormalities in the femoral head produce the first type.[9]

In young and active patients, femoroacetabular impingement (FAI) has already been confirmed as a major risk for early osteoarthritis.[10] Furthermore, recent studies suggest a correlation between hip biomechanical alternations and knee injuries, with some reporting the relationship between these radiographic alternations and a higher risk of ACL injury.[11]

The present study aimed to assess the alpha angle in ACL rupture patients in both the injured (ipsilateral) and non-affected (contralateral) extremities, compared to a control group. According to our hypothesis, the affected side of the patients with an ACL tear will have a greater hip alpha angle than both the control group and the contralateral hip. We wish to go deeper into the relationship between ACL tears and hip morphology and offer insights that may have significant clinical implications and could help in the prevention regimens of ACL injuries.

Materials and Methods

This case-control study included 105 subjects (78.1% male and 21.9% female) aged between 15 and 45 years of both sexes involved in sports. The case group consisted of 54 patients with sport-related, noncontact ACL ruptures identified by MRI and verified arthroscopically by the same surgeon. Measurements taken from the same patient's hips are regarded as dependent observations. Fifty-one patients, 10 of whom were female, with no ACL rupture, were included in the study as a control group. Subjects in the control group were matched by age and by the side of the injured knee. Exclusion criteria for both groups were previous hip or knee surgery, previous fractures, developmental hip dysplasia, or other hip issues on either side. Patients were categorized according to the type of sport during the injury: football, skiing, basketball (while falling from a jump), volleyball, or handball.

A priori power analysis was conducted using G*Power v.3.1 (Universitat Düsseldorf, Germany) and determined that at least 51 subjects were required in each case and control group for 80% power based on an effect size of 0.5.

For the dependent observations, a more robust study was desired. Therefore, we computed the effect size based on previous studies.[12] Using the G*Power v.3.1, our effect size was calculated at 0.45, and with 95% power, the total sample size was 54.

For the hip radiographs to be taken, informed consent had to be signed by each patient in the study. In hip X-rays, the alpha angle is assessed to determine the cam impingement. In the case group, the alpha angle was measured in both hips, and the injured side was matched with a hip radiograph in the control group. According to Smith et al.,[13] the modified Dunn View radiograph gives the most sensitive view for assessing the cam morphology by measuring the alpha angle. We took the modified Dunn View radiograph with the patient in the supine position, hip flexed 45° and abducted 20°.

We used OsiriX software to obtain the measurements. OsiriX's oval and angle tool was employed to draw a precise circle around the femoral head. This instrument shows two lines that connect at the oval's center, which makes it possible to measure angles precisely. The alpha angle was determined with the lines pointing away from the center of the femoral head, one through the anatomical axis of the femoral neck in the middle of its narrowest part and the other toward the point where the bone margin of the femoral head deviates from the circle.[2,13] This methodology ensured accurate and reliable measurement of the alpha angle for this study (Figure 1).

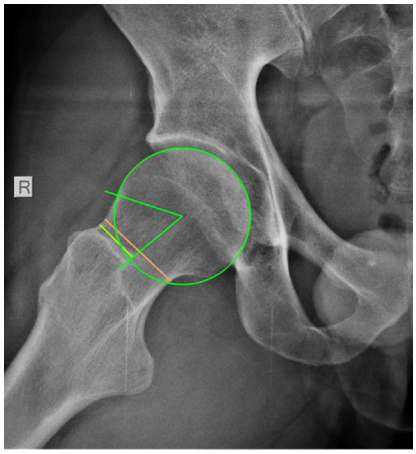

Fig. 1. *The alpha angle measurement on Dunn View hip X-ray, using the oval and angle instrument in OsiriX software.*

One orthopedic surgeon and one radiologist, blinded to the diagnosis of the injured side, evaluated the radiographs and measured the alpha angle.

Statistical analysis was performed using the statistical software package SPSS version 25.0 (SPSS Inc, Armonk, NY: IBM Corp). For the descriptive analysis, results are presented as mean (M) ± standard deviation (SD). To assess the accuracy of the measurements, we used the intraclass

correlation coefficient (ICC). The two-sample t-test and paired t-test were used to compare data with normal distribution. The independent samples T-test was used to compare the alpha angle means between the case and control groups, whereas the dependent samples T-test was employed to compare the difference between two dependent means of alpha angle in the hips of case subjects. Group comparisons with respect to categorical variables are performed using chi-square test. Pearson's correlation coefficient (r) was used to determine the strength of the relationship between the two continuous variables. Logistic regression analysis was used to determine the predictive ability of alpha angle on ACL injury. A probability value of $P<0.05$ was considered statistically significant.

Results

Most injuries were caused by football (58.1%), followed by jumping sports (23.8%) and skiing (18.1%). The mean age of all subjects was 27.2 years, with a minimum age of 15.0 years and a maximum age of 45.0 years (Table 1).

Table 1.

Characteristics of subjects.

	Case	Control	*P*-value
N	54	51	
Age	15-45 (mean 23.5)	15-45 (mean 31.01)	<0.001
Gender M/F	40/14	42/9	NS
Mechanism Football	33		NS
Jumping	12		
Skiing	9		

To examine the relationship between alpha angle and ACL injury, we compared the alpha angle of the subjects with and without ACL rupture. Results supported our hypothesis that a higher alpha angle is associated with an increased risk of ACL injury. Specifically, we found that the mean alpha angle was 49.27° for subjects without ACL rupture and 54.84° for subjects with ACL rupture, and the difference was statistically significant ($P<0.001$) (Table 2).

Table 2.

Group statistics between case and control subjects regarding the alpha angle (°).

	ACL Rupture Present	N	Mean	SD	SEM	*P*-value
Alpha angle measurements statistics	Yes (Ipsilateral hip)	54	54.84	6.17	.84	n/a
	No (Control-Group)	51	49.27	4.93	.69	<0.001
	No (Contralateral hip)	54	49.48	7.04	.95	<0.001

Results also showed a statistically significant difference in a paired samples T-test for dependent observations, comparing the alpha angle on the ipsilateral and contralateral hips of the case subjects. ($P<0.001$) (Table 2).

This finding supports our hypothesis that changes in proximal femur morphology, such as higher alpha angle, are associated with an increased risk for an ACL rupture, even between the hips of the same subject. To further explore the relationship between alpha angle and ACL injury, we conducted a two-tailed Pearson correlation analysis at the 0.001 level between the hip alpha angle and ACL injury of the case patients. Results showed a moderately strong relationship between the variables.

We conducted a logistic regression analysis to determine alpha angle's predictive ability on ACL injury (Table 3). Results revealed an OR of 1.2 ($P=0.000$), with a B coefficient of 0.185, indicating that for every degree of increased alpha angle, there is a 20% increase in the risk of an ACL injury.

Table 3.

Logistic Regression – Variables in the equation between case (ipsilateral/contralateral hip alpha angle) and control groups.

	B	S.E	Wald	Df	Sig	OR
Control subjects Alpha Angle	.185	.045	17.067	1	.000	1.20
Contralateral hip Alpha angle	.120	.059	4.162	1	.041	1.12

Interestingly, odds ratio (OR) was positive even when we compared both hips of case subjects, albeit at a slightly lower rate (OR=1.12, $P=0.041$). These findings suggest that alpha angle is a significant predictor of ACL injury even between the extremities of the same patient.

To test for potential confounding factors, we conducted a Kruskal-Wallis test to examine the relationship between the mechanism of injury (football, skiing, jumping) and alpha angle. Results showed no significant differences between the mechanism of injury and alpha angle. Additionally, we tested for a correlation between age and alpha angle, but the results showed a negative correlation that was not statistically significant. In this regard, more data and research are needed to establish significant results.

ICC was calculated to assess the reliability of hip alpha angle measurements made by two observers for three groups: cases, controls, and contralateral hip of the case group. The ICC was calculated using a two-way random effects model and absolute agreement consistency. The ICC values for cases, controls, and contralateral hip of the case group were 0.94 (95% CI = 0.90–0.96), 0.93 (95% CI = 0.88–0.96), and 0.98 (95% CI = 0.997–0.999), respectively, indicating excellent reliability.

Discussion

There are a few previous studies that have taken under consideration the relationship between alpha angle and ACL injury. Our data correspond with these findings. Lopes et al.[2] found that subjects with a noncontact ACL injury had a larger alpha angle in their ipsilateral hip. They also considered hip mobility and found that despite the increase in the alpha angle there was no evidence of decreased hip mobility. Higher alpha angle for the patients with an ACL injury, compared to those in the control group, was reported by Bagherifard et al[14] But in their study, they reported that the ACL injury group also showed a decrease in the hip range of motion parameters of internal rotation, abduction, and adduction, as well as the sum of internal and external rotation, contrary to what Lopes et al.[2] reported. The study by VandenBerg et al.[15] also supports the idea that restricted hip rotation range of motion (ROM) is associated with an increased risk of ACL injury. These results suggest a correlation between cam and pincer FAI morphology and ACL injury, which correlates with our findings. Another study found that decreased hip flexion and internal rotation can create compensatory knee tensions, increasing the risk of ACL rupture. The changes in hip motion were associated with cam-type impingement or decreased femoral offset.[16]

Furthermore, the results of our study are consistent with those of Philippon et al.[12] that patients with ACL injury had greater hip alpha angle than those with non-ACL injury. Alpha angle larger than 60° is associated with a decreased hip ROM, particularly internal rotation, and an increased risk of ACL injury. This association was observed in males and females, but the odds were higher in males. Schaver et al.[17] reached similar conclusions, with an association between higher alpha angle and patients undergoing ACL reconstruction. They defined the cam morphology at an alpha angle >60°.

Contrary to these studies, which described a limitation of their own AP radiographs, we took the radiographs in Dunn View to measure the alpha angle, but the results seem similar.[12,14,17] Our study aimed not to define the cam morphology but to look at proximal femur morphology by investigating the differences between different degrees of alpha angle and the correlation with ACL injury. The mean alpha angle of 54.84°, as measured in our case subjects, stands between the values reported so far as a definition of cam impingement.[18]

There is an agreement among researchers that alterations in all joints, above and below the knee, play an important role in ACL injury.[12] There have been many reports regarding the distal femur anatomic landmarks and not only their potential impact on ACL injury. Such factors as the intercondylar notch being narrower and the β angle and lateral tibial plateau being larger were described by Shen et al.[19] as associated with a higher risk for ACL injury. The same landmarks, as well as an increased alpha angle, have been studied by Barnum et al.[20] with similar results, resulting in a higher risk for ACL injury. The increased posterior tibial slope may promote ACL injury by increasing anterior tibial motion relative to the femur or by creating torsional loads. The notch width index (NWI) is also linked to ACL injury, with narrower NWI in ACL injury cases, compared to controls. NWI is advantageous in eliminating influences of height, weight, sex, individual differences, and measurement errors.[21]

ACL volume and femoral intercondylar notch width were reported by Whitney et al.[22] to be significant independent predictors of ACL injuries in both the female and male groups. A decrease in each predictor was associated with an increased likelihood of injury in men. In contrast, in females, the thickness of the bony ridge at the anteromedial outlet of the femoral notch was also a significant predictor. Meanwhile, Polamalu et al.,[23] through statistical shape modeling, revealed significant differences in bony morphological features associated with ACL injuries, with variations in the angle between the long axis, condylar axis, and mechanical axis of the distal femur location. A smaller angle between the long and condylar axes may increase contact area and stability, thus reducing the risk of ACL injury. K. Çimen and colleagues[24] compared distal femur and proximal tibia anatomy; even though they didn't find significant differences in the NWI, they found significant differences in the tibial eminence width index when comparing the ACL-injured group to those with an intact ACL. Moreover, Duparc et al.[25] have described the index of cumulative torsions as a regulatory ticket for the limb, with femoral torsion being extremely variable. The increased tibial and femoral torsions have also been described to increase the risk of an ACL injury.[26,27]

Our study's limitation is that we have not considered pincer morphology, and AP radiographs were not taken to limit the patients' exposure. The femoral head-neck offset ratio was not measured and observed since the mean of the alpha angle expressed the degree of femoral deformity. Another limitation may be the small number of subjects, even though the power analysis was done before the study. Furthermore, we did not compare the distal femur morphology, but this should be done in the future to reduce the potential confounding factors and to define even further the role of the alpha angle and proximal femur morphology in ACL rupture.

Conclusion

The present study investigated the relationship between alpha angle and ACL injury in 105 subjects. The results revealed a significant association between a higher alpha angle and increased risk of ACL injury, with the mean alpha angle being significantly higher in subjects with ACL rupture than those without. The logistic regression analysis further supported this finding, indicating a statistically significant difference in alpha angle between the case and control groups and between hips of the same subject with an OR of 1.12 and 1.2, respectively. Overall, our results indicate that alterations in proximal femur morphology should be considered a potential risk factor for ACL injury, and alpha angle can be a significant predictor of ACL injury. We recommend that

young athletes actively participating in sports have their hip alpha angle measured so those with higher alpha angle can follow special prevention programs.

Ethical Approval

The study was conducted in accordance with the Declaration of Helsinki and approved by the Ethics Committee of the Faculty of Medicine, University of Prishtina "Hasan Prishtina" of May 18, 2021. All participants provided written informed consent.

Competing Interests

The authors declare that they have no competing interests.

Data availability statements

The data that support the findings of this study are available from the Council of Medical Faculty, University of Prishtina "Hasan Prishtina" upon reasonable request. Contact person: Qerim Kida, E-mail: qerimkida@gmail.com

References

1. Levine JW, Kiapour AM, Quatman CE, Wordeman SC, Goel VK, Hewett TE, Demetropoulos CK. Clinically relevant injury patterns after an anterior cruciate ligament injury provide insight into injury mechanisms. Am J Sports Med. 2013 Feb;41(2):385-95. doi: 10.1177/0363546512465167.
2. Lopes OV Jr, Tragnago G, Gatelli C, Costa RN, de Freitas Spinelli L, Saggin PRF, Kuhn A. Assessment of the alpha angle and mobility of the hip in patients with noncontact anterior cruciate ligament injury. Int Orthop. 2017 Aug;41(8):1601-1605. doi: 10.1007/s00264-017-3482-6.
3. Uhorchak JM, Scoville CR, Williams GN, Arciero RA, St Pierre P, Taylor DC. Risk factors associated with noncontact injury of the anterior cruciate ligament: a prospective four-year evaluation of 859 West Point cadets. Am J Sports Med. 2003 Nov-Dec;31(6):831-42. doi: 10.1177/03635465030310061801.
4. Webster KE, Feller JA. Exploring the High Reinjury Rate in Younger Patients Undergoing Anterior Cruciate Ligament Reconstruction. Am J Sports Med. 2016 Nov;44(11):2827-2832. doi: 10.1177/0363546516651845.
5. Schweizer N, Strutzenberger G, Franchi MV, Farshad M, Scherr J, Spörri J. Screening Tests for Assessing Athletes at Risk of ACL Injury or Reinjury-A Scoping Review. Int J Environ Res Public Health. 2022 Mar 1;19(5):2864. doi: 10.3390/ijerph19052864.
6. Al-Saeed O, Brown M, Athyal R, Sheikh M. Association of femoral intercondylar notch morphology, width index and the risk of anterior cruciate ligament injury. Knee Surg Sports Traumatol Arthrosc. 2013 Mar;21(3):678-82. doi: 10.1007/s00167-012-2038-y.
7. Tainaka K, Takizawa T, Kobayashi H, Umimura M. Limited hip rotation and non-contact anterior cruciate ligament injury: a case-control study. Knee. 2014 Jan;21(1):86-90. doi: 10.1016/j.knee.2013.07.006.
8. Gomes JL, de Castro JV, Becker R. Decreased hip range of motion and noncontact injuries of the anterior cruciate ligament. Arthroscopy. 2008 Sep;24(9):1034-7. doi: 10.1016/j.arthro.2008.05.012.
9. Trigg SD, Schroeder JD, Hulsopple C. Femoroacetabular Impingement Syndrome. Curr Sports Med Rep. 2020 Sep;19(9):360-366. doi: 10.1249/JSR.0000000000000748.
10. Amanatullah DF, Antkowiak T, Pillay K, Patel J, Refaat M, Toupadakis CA, Jamali AA. Femoroacetabular impingement: current concepts in diagnosis and treatment. Orthopedics. 2015 Mar;38(3):185-99. doi: 10.3928/01477447-20150305-07.
11. Ellera Gomes JL, Palma HM, Ruthner R. Influence of hip restriction on noncontact ACL rerupture. Knee Surg Sports Traumatol Arthrosc. 2014 Jan;22(1):188-91. doi: 10.1007/s00167-012-2348-0.
12. Philippon M, Dewing C, Briggs K, Steadman JR. Decreased femoral head-neck offset: a possible risk factor for ACL injury. Knee Surg Sports Traumatol Arthrosc. 2012 Dec;20(12):2585-9. doi: 10.1007/s00167-012-1881-1.
13. Smith KM, Gerrie BJ, McCulloch PC, Lintner DM, Harris JD. Comparison of MRI, CT, Dunn 45° and Dunn 90° alpha angle measurements in femoroacetabular impingement. Hip Int. 2018 Jul;28(4):450-455. doi: 10.5301/hipint.5000602.
14. Bagherifard A, Jabalameli M, Yahyazadeh H, Shafieesabet A, Gharanizadeh K, Jahansouz A, Khanlari P. Diminished femoral head-neck offset and the restricted hip range of motion suggesting a possible role in ACL injuries. Knee Surg Sports Traumatol Arthrosc. 2018 Feb;26(2):368-373. doi: 10.1007/s00167-017-4589-4.
15. VandenBerg C, Crawford EA, Sibilsky Enselman E, Robbins CB, Wojtys EM, Bedi A. Restricted Hip Rotation Is Correlated With an Increased Risk for Anterior Cruciate Ligament Injury. Arthroscopy. 2017 Feb;33(2):317-325. doi: 10.1016/j.arthro.2016.08.014.
16. Bedi A, Warren RF, Wojtys EM, Oh YK, Ashton-Miller JA, Oltean H, Kelly BT. Restriction in hip internal rotation is associated with an increased risk of ACL injury. Knee Surg Sports Traumatol Arthrosc. 2016 Jun;24(6):2024-31. doi: 10.1007/s00167-014-3299-4.
17. Schaver AL, Grezda K, Willey MC, Westermann RW. Radiographic Cam Morphology of the Hip May Be Associated with ACL Injury of the Knee: A Case-Control Study. Arthrosc Sports Med Rehabil. 2021 Jun 24;3(4):e1165-e1170. doi: 10.1016/j.asmr.2021.05.004.
18. Fraitzl CR, Kappe T, Pennekamp F, Reichel H, Billich C. Femoral head-neck offset measurements in 339 subjects: distribution and implications for femoroacetabular impingement. Knee Surg Sports Traumatol Arthrosc. 2013 May;21(5):1212-7. doi: 10.1007/s00167-012-2042-2
19. Shen L, Jin ZG, Dong QR, Li LB. Anatomical Risk Factors of Anterior Cruciate Ligament Injury. Chin Med J (Engl). 2018 Dec 20;131(24):2960-2967. doi: 10.4103/0366-6999.247207.

***Corresponding author**: Qerim Kida, Royal Medical Hospital, Prishtina, Kosovo. E-mail: qerimkida@gmail.com*

20. Barnum MS, Boyd ED, Vacek P, Slauterbeck JR, Beynnon BD. Association of Geometric Characteristics of Knee Anatomy (Alpha Angle and Intercondylar Notch Type) With Noncontact ACL Injury. Am J Sports Med. 2021 Aug;49(10):2624-2630. doi: 10.1177/03635465211023750.
21. Li Z, Li C, Li L, Wang P. Correlation between notch width index assessed via magnetic resonance imaging and risk of anterior cruciate ligament injury: an updated meta-analysis. Surg Radiol Anat. 2020 Oct;42(10):1209-1217. doi: 10.1007/s00276-020-02496-6.
22. Whitney DC, Sturnick DR, Vacek PM, DeSarno MJ, Gardner-Morse M, Tourville TW, Smith HC, Slauterbeck JR, Johnson RJ, Shultz SJ, Hashemi J, Beynnon BD. Relationship Between the Risk of Suffering a First-Time Noncontact ACL Injury and Geometry of the Femoral Notch and ACL: A Prospective Cohort Study With a Nested Case-Control Analysis. Am J Sports Med. 2014 Aug;42(8):1796-805. doi: 10.1177/0363546514534182.
23. Polamalu SK, Musahl V, Debski RE. Tibiofemoral bony morphology features associated with ACL injury and sex utilizing three-dimensional statistical shape modeling. J Orthop Res. 2022 Jan;40(1):87-94. doi: 10.1002/jor.24952.
24. Çimen K, Otağ İ, Oztemür Z. The relationship of distal femur and proximal tibia morphology with anterior cruciate ligament injuries. Surg Radiol Anat. 2023 Apr;45(4):495-501. doi: 10.1007/s00276-023-03097-9.
25. Duparc F, Thomine JM, Simonet J, Biga N. Femoral and tibial bone torsions associated with medial femoro-tibial osteoarthritis. Index of cumulative torsions. Orthop Traumatol Surg Res. 2014 Feb;100(1):69-74. doi: 10.1016/j.otsr.2013.12.014.
26. Meyer EG, Haut RC. Anterior cruciate ligament injury induced by internal tibial torsion or tibiofemoral compression. J Biomech. 2008 Dec 5;41(16):3377-83. doi: 10.1016/j.jbiomech.2008.09.023.
27. Alpay Y, Ezici A, Kurk MB, Ozyalvac ON, Akpinar E, Bayhan AI. Increased femoral anteversion related to infratrochanteric femoral torsion is associated with ACL rupture. Knee Surg Sports Traumatol Arthrosc. 2020 Aug;28(8):2567-2571. doi: 10.1007/s00167-020-05874-0.

International Journal of Biomedicine 13(3) (2023) 123-126
http://dx.doi.org/10.21103/Article13(3)_OA12

ORIGINAL ARTICLE

Microbiology

INTERNATIONAL JOURNAL OF BIOMEDICINE

Co-occurrence of Carbapenemase Genes *bla*$_{NDM}$, *bla*$_{VIM}$, *bla*$_{KPC}$, and *bla*$_{OXA-48}$ in *Pseudomonas aeruginosa* Clinical Isolates

Salma Mohamed[1*], Zainab Ahmed[2], Tajalseer Mubarak[2], Sara Mohamed[3], Rayan Mohamed[2], Hassan Higazi[1], Sara Ali[1]

[1]*Department of Medical Laboratory Science, Faculty of Health Sciences, Gulf Medical University, United Arab Emirates*
[2]*Department of Microbiology, Faculty of Medical Laboratory Science, University of Science and Technology, Sudan*
[3]*Deparment of Internal Medicine, Faculty of Medicine, Al Neelain University, Sudan*

Abstract

Pseudomonas aeruginosa, a gram-negative bacterium, is notorious for its innate resistance to many antibiotics. Carbapenems are broad-spectrum antibiotics often used to treat severe *P. aeruginosa* infections. However, the emergence and proliferation of carbapenem-resistant *P. aeruginosa* (CRPA) strains have become a grave global health concern. This study examined the co-occurrence of four major carbapenemase genes, namely *bla*$_{NDM}$, *bla*$_{VIM}$, *bla*$_{KPC}$, and *bla*$_{OXA-48}$, in clinical isolates of *P. aeruginosa*.

Using standard microbiological methods,150 *P. aeruginosa* clinical isolates were collected and identified, and antimicrobial susceptibility testing was conducted following Clinical and Laboratory Standards Institute guidelines. Polymerase chain reaction (PCR) with gene-specific primers was used to detect the presence of carbapenemase genes.

Among the 150 P. aeruginosa clinical isolates, 62(41.3%) were found to be carbapenem-resistant. The most detected carbapenemase genes were *bla*$_{KPC}$ (49%), *bla*$_{NDM}$ (31%), *bla*$_{OXA-48}$ (22%), and *bla*$_{VIM}$ (9%). Notably 13(12.9%) isolates carried two carbapenemase genes. The combination of *bla*$_{KPC}$ and *bla*$_{NDM}$ genes was found in eight isolates, two isolates carried *bla*$_{KPC}$ and *bla*$_{VIM,}$ and three isolates carried *bla*$_{OXA-48}$ and *bla*$_{NDM}$. Four isolates (6.5%) harbored three carbapenemase genes. Co-occurrence of *bla*$_{NDM}$, *bla*$_{VIM}$, *bla*$_{KPC}$, and *bla*$_{OXA-48}$ was observed in four isolates (2.8%).

Our findings highlight the alarming prevalence of carbapenemase genes, particularly *bla*$_{NDM}$ and *bla*$_{KPC}$, in clinical isolates of *P. aeruginosa*. The co-occurrence of multiple carbapenemase genes in the same isolate raises concerns about the potential for horizontal gene transfer and dissemination of multidrug-resistant *P. aeruginosa* strains in clinical settings. Further research is needed to elucidate the molecular mechanisms underlying the co-occurrence of carbapenemase genes and their impact on the clinical outcomes of *P. aeruginosa* infections. Urgent measures, such as enhanced surveillance, infection control protocols, and antibiotic stewardship programs, are imperative to combat the emergence and spread of CRPA strains.(**International Journal of Biomedicine. 2023;13(3):123-126.**)

Keywords: *Pseudomonas aeruginosa* • carbapenemase • *bla*$_{NDM}$ • *bla*$_{VIM}$ • *bla*$_{KPC}$ • *bla*$_{OXA-48}$ • clinical isolates

For citation:Mohamed S, Ahmed Z, Mubarak T, Mohamed S, Mohamed R, Higazi H, Ali S. Co-occurrence of Carbapenemase Genes *bla*$_{NDM}$, *bla*$_{VIM}$, *bla*$_{KPC}$ and *bla*$_{OXA-48}$ in *Pseudomonas aeruginosa* Clinical Isolates. International Journal of Biomedicine. 2023;13(3):123-126. doi:10.21103/Article13(3)_OA12

Introduction

Pseudomonas aeruginosa is a gram-negative opportunistic pathogen that commonly causes nosocomial infections, particularly in immunocompromised patients and those with chronic illnesses.(1) *P. aeruginosa* infections are often difficult to treat due to its intrinsic resistance to many antibiotics, and carbapenems are considered as the last-resort antibiotics for treating severe *P. aeruginosa* infections. However, the emergence and spread of CRPA strains have become a global health threat, limiting treatment options, and posing challenges in infection control practices.(2

Carbapenem resistance in *P. aeruginosa* is often mediated by the acquisition of carbapenemase genes, which encode enzymes that can hydrolyze carbapenem antibiotics. Several types of carbapenemase genes have been identified in

P. aeruginosa, including bla_{NDM}, bla_{VIM}, bla_{KPC}, and bla_{OXA-48}, which are commonly found in other gram-negative bacteria as well.[3] These carbapenemase genes are often carried on mobile genetic elements, such as plasmids and integrons, which can facilitate their horizontal transfer among bacteria, leading to the dissemination of carbapenem resistance in clinical settings.[4]

While the presence of individual carbapenemase genes in *P. aeruginosa* has been widely reported, there are limited studies investigating the co-occurrence of multiple carbapenemase genes in the same isolate.[5] The co-occurrence of carbapenemase genes may have important clinical implications, as it can potentially lead to increased antibiotic resistance, treatment failures, and higher mortality rates. Therefore, understanding the prevalence and characteristics of co-existing carbapenemase genes in *P. aeruginosa* clinical isolates is crucial for the effective management of CRPA infections.[6,7]

In this study, we aimed to investigate the co-occurrence of four major carbapenemase genes, namely $bla_{NDM,}$ bla_{VIM}, bla_{KPC}, and bla_{OXA-48}, in *P. aeruginosa* clinical isolates collected from different hospitals.

Materials and Methods

Bacterial isolates

A total of 150 *P. aeruginosa* clinical isolates were collected from different hospitals in diverse geographical regions in Khartoum state. The isolates were obtained from various clinical specimens, including blood, respiratory samples, urine, and wound swabs (Table 1). The isolates were identified as *P. aeruginosa* using standard microbiological methods.

Table 1.

Samples distribution

Sample	Number	Prevalence (%)
Urine	30	20
Sputum	30	20
Blood	10	6.7
Wound swab	80	53.3

Antimicrobial susceptibility testing

The antimicrobial susceptibility of *P. aeruginosa* isolates was determined by the disc diffusion method according to the Clinical and Laboratory Standards Institute (CLSI) guidelines.[8] The antibiotics evaluated included imipenem and meropenem. The interpretation of susceptibility was based on the CLSI breakpoints.

Detection of carbapenemase genes by real-time PCR

Genomic DNA was extracted from *P. aeruginosa* isolates using a commercial DNA extraction kit following the manufacturer's instructions.[9] The presence of carbapenemase genes, including bla_{NDM}, bla_{VIM}, bla_{KPC}, and bla_{OXA-48}, was detected by PCR using gene-specific primers (Table 2).[10-12] The real-time PCR amplification was performed in a thermal cycler under the following conditions: The test reaction was set to a total volume of 25 µl. 5 µl master mix, 1 µl of forward and reverse primers, the amount of Eva green dye used in the reaction varied per the amplicon size; for bla_{KPC} a volume of 2 µl of the Eva green was used, 1.5 µl for bla_{OXA-48} and bla_{VIM} and 1 µl Eva green was used for bla_{NDM} as it was the smallest amplicon size. 0.3 µl of the DNA template was used and the rest of the reaction's volume was double distilled water.

Using the SaCycler-96 system (Sacacae Biotechnologies), real-time PCR protocol was carried out as follows. Hot start 94C° for 10 min, the number of cycles 40, and the loop steps were as follows: denaturation at 94C° for 45 seconds, annealing at 52C° for 45 seconds and elongation at 72C° for 30 seconds, which included the fluorescent data at acquisition 533 nm filter, a final elongation step was set to be at 72C° for 10 min. After the end of the polymerization cycles, the melting curve step was added to start from 65C° gradually increasing by 0.1 C/s to 95C, with the fluorescence data acquisition every 1 second.

Results

Among the 150 P. aeruginosa clinical isolates, 62(41.3%) were found to be carbapenem-resistant. The most detected carbapenemase genes were bla_{KPC} (49%), bla_{NDM} (31%), bla_{OXA-48} (22%), and bla_{VIM} (9%) (Figure 1). Notably 13(12.9%) isolates carried two carbapenemase genes. The combination of bla_{KPC} and bla_{NDM} genes was found in eight isolates, two isolates carried bla_{KPC} and $bla_{VIM,}$ and three isolates carried bla_{OXA-48} and bla_{NDM}. Four isolates (6.5%) harbored three carbapenem

Table 2.

Details of primers used, including sequence, annealing temperature, and product size.

Gene	Primer	Sequence	GC%	Tm C°	M.W µg/µmol	Final Con. µM	Amp size bp
bla_{OXA-48}	OXA-48-F	5'-GCGTGGTTAAGGATGAACAC-3'	42.1	50.8	5855.9	0.2	177
	OXA-48-R	5'-CATCAAGTTCAACCCAACCG-3'	42.1	50.8	5865.5	0.2	
bla_{KPC}	KPC-Fm	5'-CGTCTAGTTCTGCTGTCTTG-3'	50	52.6	5492.6	0.2	785
	KPC-Rm	5'-CTTGTCATCCTTGTTAGGCG-3'	58.3	63	7224.7	0.2	
bla_{VIM}	VIM-F	5'-GATGGTGTTTGGTCGCATA-3'	50.0	55.4	6024.0	0.2	382
	VIM-R	5'-CGAATGCGCAGCACCAG-3'	65.0	57.4	6160.1	0.2	
bla_{NDM}	NDM-F	5'-GGTTTGGCGATCTGGTTTTC-3'	55.6	54.9	5463.6	0.2	82
	NDM-R	5'-CGGAATGGCTCATCACGATC-3'	47.6	55.6	5463.6	0.2	

resistance genes. Co-occurrence of bla_{NDM}, bla_{VIM}, bla_{KPC}, and bla_{OXA-48} was observed in four isolates (2.8%) (Table 3).

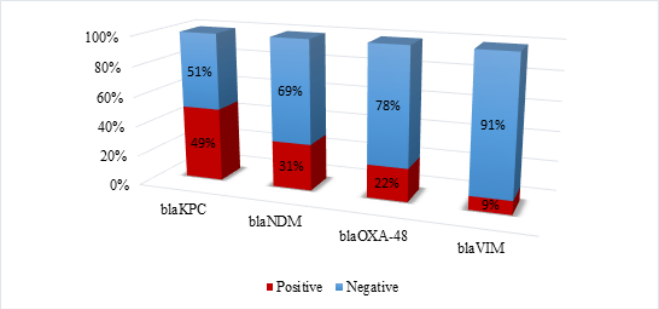

Fig. 1. *Percentage of positive test results for Carbapenemase genes in selected samples: bla_{KPC}, bla_{NDM}, bla_{OXA-48}, and bla_{VIM}.*

Table 3.

Carbapenemase genes prevalence: comparative analysis of isolate data

Carbapenemase Gene	Number of isolates	Prevalence (%)
bla_{NDM}	28	31
bla_{VIM}	22	9
bla_{KPC}	12	49
bla_{OXA-48}	18	22
Gene Combinations		
bla_{KPC} + bla_{VIM}	2	7
bla_{NDM} + bla_{KPC}	8	26
bla_{NDM} + bla_{OXA-48}	3	1

Discussion

The study results revealed that carbapenem resistance among Pseudomonas aeruginosa clinical isolates was high, with 41.3% (62 out of 150) being resistant to carbapenems. This finding is concerning as carbapenems are often considered as the last-resort antibiotics for treating serious infections caused by multidrug-resistant bacteria.

Further analysis of the carbapenemase genes showed an interesting trend of bla_{KPC} being the most detected gene, and bla_{VIM} being the least detected gene. The bla_{KPC} gene is commonly associated with resistance to carbapenem that is found in Enterobacteriaceae, such as *Klebsiella pneumoniae* and *Escherichia coli*.[13,14] However, it is less commonly associated with *Pseudomonas aeruginosa*, which are known to have intrinsic resistance to carbapenems due to their efflux pumps and impermeable outer membrane. Therefore, when bla_{KPC} is being frequently detected in *Pseudomonas aeruginosa*, it indicates a concerning trend of horizontal gene transfer or acquisition of this resistance gene from other bacteria.[15,16]

On the other hand, bla_{VIM} is a class B metallo-β-lactamase gene that confers resistance to carbapenems and is more commonly found in *Pseudomonas* species. However, the fact that it is being detected less frequently could be for several reasons, such as geographical variations in the prevalence of bla_{VIM}-positive *Pseudomonas* strains.

Interestingly, the study also identified isolates that carried more than one carbapenem resistance gene. Approximately 12.9% of the isolates (13 out of 101) carried two carbapenem resistance genes. The most common combination was bla_{KPC} and bla_{NDM}, which was found in eight isolates. Other combinations included bla_{KPC} and bla_{VIM}, as well as bla_{OXA-48} and bla_{NDM}, which were present in 2 and 3 isolates, respectively. Additionally, 6.5% of the isolates (4 out of 62) harbored three carbapenem resistance genes. Notably, four isolates (2.8%) were found to co-exist with all four carbapenemase genes, namely bla_{KPC} and bla_{VIM}, as well as bla_{OXA-48} and bla_{NDM}.

The co-occurrence of resistance genes in *Pseudomonas* strains is concerning as it indicates the presence of multiple mechanisms of carbapenem resistance in the same bacterial isolate and raises concerns about the potential for horizontal gene transfer, which can contribute to the rapid spread of carbapenem resistance among bacterial populations, making treatment options more limited and increasing the risk of treatment failure.

The findings of this study have important implications for clinical practice and highlight the need for continuous surveillance of carbapenem resistance in *P. aeruginosa* isolates. Understanding the prevalence and diversity of carbapenemase genes in *P. aeruginosa* can aid in the development of appropriate treatment strategies and infection control measures to mitigate the spread of carbapenem resistance in healthcare settings. Further research is warranted to better understand the mechanisms underlying the emergence and dissemination of carbapenem resistance in *P. aeruginosa*, and to explore potential strategies to combat this growing threat to public health.

In conclusion, it is important to note that antibiotic resistance is a complex and dynamic phenomenon, and continuous monitoring and surveillance are crucial in understanding the trends and patterns of resistance genes in bacterial populations. This information can help guide antibiotic stewardship efforts and infection control strategies to mitigate the spread of antibiotic-resistant bacteria.

Acknowledgments

We thank the National Ribat University, Al Neelain University, and the Army Hospital for making their facilities available for our practical work.

Competing Interests

The authors declare that they have no competing interests.

References

1. Heidari R, Farajzadeh Sheikh A, Hashemzadeh M, Farshadzadeh Z, Salmanzadeh S, Saki M. Antibiotic resistance, biofilm production ability and genetic diversity

of carbapenem-resistant Pseudomonas aeruginosa strains isolated from nosocomial infections in southwestern Iran. Mol Biol Rep. 2022 May;49(5):3811-3822. doi: 10.1007/s11033-022-07225-3.
2. Büchler AC, Shahab SN, Severin JA, Vos MC, Voor In 't Holt AF. Outbreak investigations after identifying carbapenem-resistant Pseudomonas aeruginosa: a systematic review. Antimicrob Resist Infect Control. 2023 Apr 3;12(1):28. doi: 10.1186/s13756-023-01223-1.
3. Spicer L, Campbell D, Johnson JK, Longo C, Balbuena T, Ewing T, et al. Characterization of carbapenem-resistant gram-negative bacteria collected in the Sentinel Surveillance Program, 2018–2019. 2022;2(S1):s52-s.
4. Olaniran OB, Adeleke OE, Donia A, Shahid R, Bokhari H. Incidence and Molecular Characterization of Carbapenemase Genes in Association with Multidrug-Resistant Clinical Isolates of Pseudomonas aeruginosa from Tertiary Healthcare Facilities in Southwest Nigeria. Curr Microbiol. 2021 Dec 14;79(1):27. doi: 10.1007/s00284-021-02706-3.
5. ElBaradei, A. Co-occurrence of blaNDM-1 and blaOXA-48 among carbapenem resistant Enterobacteriaceae isolates causing bloodstream infections in Alexandria, Egypt. Egyptian Journal of Medical Microbiology, 2022; 31(3): 1-7. doi: 10.21608/ejmm.2022.247169
6. Demirci-Duarte S, Unalan-Altintop T, Gulay Z, Sari Kaygisiz AN, Cakar A, Gur D. In vitro susceptibility of OXA-48, NDM, VIM and IMP enzyme- producing Klebsiella spp. and Escherichia coli to fosfomycin. J Infect Dev Ctries. 2020 Apr 30;14(4):394-397. doi: 10.3855/jidc.12456.
7. Pragasam AK, Veeraraghavan B, Shankar BA, Bakthavatchalam YD, Mathuram A, George B, Chacko B, Korula P, Anandan S. Will ceftazidime/avibactam plus aztreonam be effective for NDM and OXA-48-Like producing organisms: Lessons learnt from In vitro study. Indian J Med Microbiol. 2019 Jan-Mar;37(1):34-41. doi: 10.4103/ijmm.IJMM_19_189.
8. Sahu C, Jain V, Mishra P, Prasad KN. Clinical and laboratory standards institute versus European committee for antimicrobial susceptibility testing guidelines for interpretation of carbapenem antimicrobial susceptibility results for Escherichia coli in urinary tract infection (UTI). J Lab Physicians. 2018 Jul-Sep;10(3):289-293. doi: 10.4103/JLP.JLP_176_17.
9. Barbaro A, Cormaci P, La Marca A. DNA extraction from soil by EZ1 advanced XL (Qiagen). Forensic Sci Int. 2019 Jun;299:161-167. doi: 10.1016/j.forsciint.2019.04.004.
10. Mohamed SER, Alobied A, Hussien WM, Saeed MI. blaOXA-48 Carbapenem Resistant Pseudomonas aeruginosa Clinical Isolates in Sudan. Journal of Advances in Microbiology. 2018;10(4):1-5.
11. Mohamed S, Alobied A, Saeed MI, Hussien WMJS. New Delhi Metallo-β-lactamase (NDM)-mediated Carbapenem-resistant Pseudomonas aeruginosa clinical isolate in Sudan. Journal of Advances in Microbiology. 2018;1(3):1-5.
12. Mohamed S, Ahmed Z, Mubarak T, Mohamed S, Higazi H, Ali S. Detection of the blaVIM-2 Gene in Carbapenem-Resistant Acinetobacter baumannii Clinical Isolates in Sudan. International Journal of Biomedicine. 2022;12(4):636-639. doi:10.21103/Article12(4)_OA21
13. Zhang R, Liu L, Zhou H, Chan EW, Li J, Fang Y, Li Y, Liao K, Chen S. Nationwide Surveillance of Clinical Carbapenem-resistant Enterobacteriaceae (CRE) Strains in China. EBioMedicine. 2017 May;19:98-106. doi: 10.1016/j.ebiom.2017.04.032.
14. Logan LK, Weinstein RA. The Epidemiology of Carbapenem-Resistant Enterobacteriaceae: The Impact and Evolution of a Global Menace. J Infect Dis. 2017 Feb 15;215(suppl_1):S28-S36. doi: 10.1093/infdis/jiw282.
15. Wozniak A, Figueroa C, Moya-Flores F, Guggiana P, Castillo C, Rivas L, Munita JM, García PC. A multispecies outbreak of carbapenem-resistant bacteria harboring the blaKPC gene in a non-classical transposon element. BMC Microbiol. 2021 Apr 9;21(1):107. doi: 10.1186/s12866-021-02169-3.
16. Huddleston JR. Horizontal gene transfer in the human gastrointestinal tract: potential spread of antibiotic resistance genes. Infect Drug Resist. 2014 Jun 20;7:167-76. doi: 10.2147/IDR.S48820.

***Corresponding author:** *Dr. Salma Elnour Rahma Mohamed, Ph.D. Department of Medical Laboratory Science, Faculty of Health Sciences, Gulf Medical University, Ajman, United Arab Emirates. E-mail: dr.sara@gmu.ac.ae*

International Journal of Biomedicine 13(3) (2023) 127-130
http://dx.doi.org/10.21103/Article13(3)_OA13

ORIGINAL ARTICLE

Microbiology

INTERNATIONAL JOURNAL OF BIOMEDICINE

The Aminoglycoside Resistance Genes, *pehX*, *bla*$_{\text{CTX-M}}$, *bla*$_{\text{AmpC}}$, and *npsB* among *Klebsiella oxytoca* Stool Samples

Mohanad H. Hussein[1], Hasan A. Aal Owaif[2*], Sura A. Abdulateef[3]

[1]*Department of Molecular and Medical Biotechnology, College of Biotechnology, Al-Nahrain University, Baghdad, Iraq*
[2]*Department of Plant Biotechnology, College of Biotechnology, Al-Nahrain University, Baghdad, Iraq*
[3]*Department of Applied Sciences, University of Technology-Iraq*

Abstract

Background*: Klebsiella oxytoca* may cause various infections, including respiratory, urinary, and bloodstream infections, often with multidrug-resistant strains posing challenges in treatment. The aim of this study was for molecular identification of *K. oxytoca* and to assess the existence of aminoglycoside resistance genes in biofilm and in toxin-producing and AmpC-positive isolates.

Methods and Results: A total of 400 non-duplicate stool samples were collected from patients with colitis from 2019 to 2020 and were immediately cultured onto McConkey and blood agar (Merk, Germany). Antibiotic discs and Mueller-Hinton agar (MHA) culture medium (Merck, Germany) were used for antimicrobial susceptibility testing. The disk diffusion was done for susceptibility examination of them using CLSI 2020. Phenotypic detection of AmpC enzymes and biofilm formation were also determined. The PCR was performed to detect polygalacturonase (*pehX*) gene, *bla*$_{\text{CTX-M}}$ gene, *npsB* toxin-encoding gene, *bla*$_{\text{AmpC}}$ gene, and the *aac(6')-lb* and *aac(3')-IIa* AMEs genes.

A total of 100 *K. oxytoca* were identified from stool samples. Most isolates were not susceptible to tetracycline, cotrimoxazole, or cefoxitin disks. Moreover, most were susceptible to amikacin and piperacillin-tazobactam disks. Among 100 isolates, 54% produced the AmpC enzyme in the combined disk method. Among them, 30 isolates were resistant to gentamicin. Strong biofilm formation was determined in 66% of isolates, and 30% of them produced moderate biofilms. Moreover, 4% of the isolates had weak biofilms. Among the 60 gentamicin-resistant *K. oxytoca*, 32 isolates had strong biofilms, and 11 isolates produced moderate ones. The *pehX* was used for the molecular identification of K. oxytoca; the results showed the presence of this gene in all isolates. The majority (98%) of *K. oxytoca* amplified the *npsB* toxin-encoding gene. The rate of *bla*$_{\text{CTX-M}}$, *bla*$_{\text{AmpC}}$, *aac(6')-lb*, and *aac(3)-IIa* genes were 62%, 45%, 12%, 24%, respectively.

Conclusion: In our study, more than half of *K. oxytoca* showed MDR phenotype. Moreover, half of the isolates carried the *bla*$_{\text{AmpC}}$ and *bla*$_{\text{CTX-M}}$ genes. Strong biofilm formation was observed in more than 60% of them.(**International Journal of Biomedicine. 2023;13(3):127-130.**)

Keywords: *Klebsiella oxytoca* • aminoglycoside resistance • biofilm

For citation:Hussein MH, Owaif HAA, Abdulateef SA. The Aminoglycoside Resistance Genes, *pehX*, *bla*$_{\text{CTX-M}}$, *bla*$_{\text{AmpC}}$, and *npsB* among *Klebsiella oxytoca* Stool Samples. International Journal of Biomedicine. 2023;13(3):127-130. doi:10.21103/Article13(3)_OA13

Abbreviations

AMEs, aminoglycoside modifying enzymes; **ESBLs**, extended-spectrum beta-lactamases; **MDR**, multidrug resistance; **PCR**, polymerase chain reaction

Introduction

Klebsiella oxytoca may cause various infections, including respiratory, urinary, and bloodstream infections, often with multidrug-resistant strains posing challenges in treatment. The genus *Klebsiella*, like *Escherichia, Salmonella, Shigella, Haemophilus*, and some other Gram-negative bacteria, belongs to the domain of *Proteobacteria* and the

branch of *Gammaproteobacteria* (class III).[1-3] This bacterium multiplies by disturbing the microbial balance of intestinal flora and causes colitis.[4] Colonization of skin and mucous membranes is the first step[5] in the pathogenicity of *K. oxytoca*. This opportunistic pathogen can generate a thick layer of biofilm as one of its important virulence factors, enabling the bacteria to attach to living or abiotic surfaces, contributing to drug resistance. The thickness of the biofilm layer extends from a simple cell layer around a bacterium to a thick layer surrounding the bacterial community. In this biofilm layer, a complex network of channels allows bacteria to access the environment. One of the benefits of this outer layer is the ability to absorb the nutrients needed and concentrate them for bacterial metabolism.[6] Biofilms make bacteria resistant to various agents, such as antibiotics, environmental stress conditions, and phagocytosis of host immune cells.[7,8] The presence of these surface components enables the bacterium to attach to various surfaces, including tissues, catheters, and other injectable medical devices. The first reported bacterial enzyme to degrade penicillin was Amp-C beta-lactamase in *E. coli*. In 1965 Swedish researchers began a genetic and systematic study of penicillin-resistant *E. coli*. The sequence of the *AmpC* gene of *E. coli* was reported in 1981. It was different from the TEM-1 beta-lactamase sequence and contained serine at its active site. AmpC β-lactamases belong to Ambler class C and Bush-Jacoby-Medeiros functional group 1.[9,10] When the functional classification scheme was published in 1995, chromosomally determined AmpC β-lactamases in Enterobacteriaceae and a few other families were known.[11,12] Aminoglycosides are important antibiotics against multidrug-resistant Gram-negative bacteria. However, resistance to these drugs has limited the choices. The aim of this study was for molecular identification of *K. oxytoca* and to assess the existence of aminoglycoside resistance genes in biofilm and in toxin-producing and AmpC-positive isolates.

Materials and Methods

A total of 400 non-duplicate stool samples were collected from patients with colitis from 2019 to 2020 and were immediately cultured onto McConkey and blood agar (Merk, Germany). Various biochemical tests were performed to confirm *K. oxytoca* isolates, in addition to the molecular test. Antibiotic discs and Mueller-Hinton agar (MHA) culture medium (Merck, Germany) were used for antimicrobial susceptibility testing. The disk diffusion was done for susceptibility examination using CLSI 2020. Antibiotic discs used were cefoxitin 30 µg (FOX), ceftazidime 30 µg (CAZ), cefotaxime 30 µg (CTX), cefepime 50 µg (FEP), meropenem 10 µg (MEM), gentamicin 10 µg (G), tetracycline 30 µg (TE), cotrimoxazole 25 µg (SXT), piperacillin-tazobactam 30 µg (PITZ), co-amoxiclav 30 µg (AMC), imipenem 10 µg (IPM), amikacin 30 µg (AN) and ciprofloxacin 30 µg (CP) (MAST, UK).[13-15]

To detect Amp-C beta-lactamase enzyme, we used ceftazidime, cefotaxime, and cefoxitin 30 µg (FOX) + clavulanic acid 10 µg and cefoxitin 30 µg plus and without boronic acid 400 µg. After incubation for 24 hours at 37°C, in the combined disk test, the diameter of the growth inhibition zone differed by 5 mm, compared to cefoxitin singly. This finding showed a positive result. Biofilm formation was performed by the microtitre-plate method and determined using an ELISA reader at OD490.

The PCR was performed to detect polygalacturonase (*pehX*) gene, $bla_{\text{CTX-M}}$ gene, *npsB* toxin-encoding gene, bla_{AmpC} gene, and the *aac(6')-lb* and *aac(3')-IIa* AMEs genes (Table 1).

Table 1.

Primer sequence.

Primer	Sequence: 5' → 3'	Amplicon size (bp)	Ref.
$bla_{\text{CTX-M}}$	F: TTTGCGATGTGCAGTACCAGTAA R: CGATATCGTTGGTGGTGCCATA	544	[16]
pehX	F: GGACTACGCCGTCTATCGTCAAG R: TAGCCTTTATCAAGCGGATACTGG	513	[17]
npsB	F: CCCGTTGGCCGCTCATCACCTAT R: GCGCCGCACAATTTCCCTTCCTC	470	[18]
bla_{AmpC}	F: TGGCCAGAACTGACAGGCAAA R: TTTCTCCTGAACGTGGCTGGC	462	[19]
aac(6')-Ib	F: TATGAGTGGCTAAATCGAT R: CCCGCTTTCTCGTAGCA	395	[20]
aac(3)-IIa	F: GGCAATAACGGAGGCGCTTCAAAA R: TTCCAGGCATCGGCATCTCATACG	563	[20]

Ref - Reference

Results

A total of 100 *K. oxytoca* were identified from stool samples. Most isolates were not susceptible to tetracycline, cotrimoxazole, or cefoxitin disks. Moreover, most were susceptible to amikacin and piperacillin-tazobactam disks (Table 2).

Table 2.

The antibiotic resistance profile.

Disk/Resistance (n = 100)	Susceptibility (n = %)	Intermediate (n = %)	Resistance (n = %)
CAZ	46	0.0	54
FEP	41	0.0	59
CTX	54	5	41
AMC	41	8	51
IPM	52	8	40
MEM	53	9	38
PITZ	68	2	30
FOX	63	0.0	37
AN	67	3	30
G	60	4	36
CP	41	4	56
TE	34	0.0	66
SXT	29	2	69

Among 100 isolates, 54% produced the AmpC enzyme in the combined disk method. Among them, 30 isolates

were resistant to gentamicin. Strong biofilm formation was determined in 66% of isolates, and 30% of them produced moderate biofilms. Moreover, 4% of the isolates had weak biofilms. Among the 60 gentamicin-resistant *K. oxytoca*, 32 isolates had strong biofilms, and 11 isolates produced moderate ones. The *pehX* was used for the molecular identification of *K. oxytoca*; the results showed the presence of this gene in all isolates (Figure 1). The majority (98%) of *K. oxytoca* amplified the *npsB* toxin-encoding gene. Therefore, nearly all the isolates were toxin-producing strains (Figure 2). The rate of bla_{CTX-M}, bla_{AmpC}, *aac(6')-lb*, and *aac(3)-IIa* genes were 62%, 45%, 12%, 24%, respectively. Table 3 shows the relation between biofilm formation, resistance genes, and MDR phenotype.

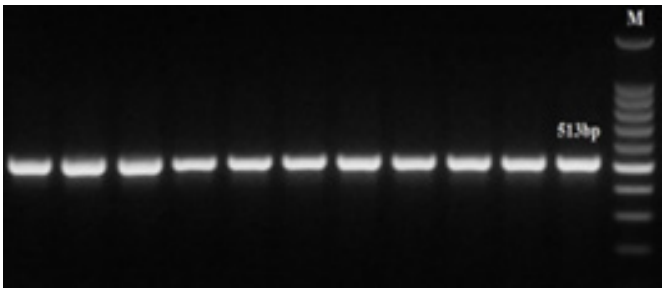

Fig. 1. *The pehX gene with 513bp size, M: 100bp DNA marker.*

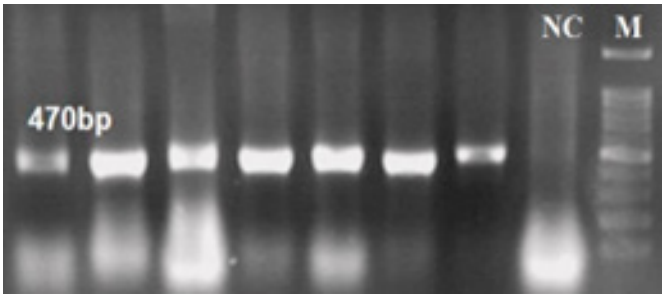

Fig. 2. *The npsB toxin gene with 470bp size, NC: negative control, M: 100bp DNA marker.*

Table 3.

The relation between biofilm formation, resistance genes and MDR phenotype.

Characteristics	bla_{CTX-M}	bla_{AmpC}	Resistance profile
Strong biofilm	35%	27%	CAZ, FEP, AMC, G, FOX, CP, SXT, TE, CTX
aac(6')-lb	6%	8%	CAZ, FEP, AMC, G, FOX, CP, SXT, TE, AN, PITZ, IPM, CTX
aac(3)-IIa	18%	16%	CAZ, FEP, AMC, G, FOX, CP, SXT, TE, AN, PITZ, IPM, MER, FEP, CTX

Discussion

We observed that 25% of stool samples were positive for *K. oxytoca* and confirmed by the presence of the *pehX* gene, 98% of which carried the *npsB* toxin-encoding gene. Most isolates were not susceptible to tetracycline, cotrimoxazole, or cefoxitin disks. However, most of them were susceptible to amikacin and piperacillin-tazobactam disks. In Cheng's study, the prevalence of K. oxytoca was that 2.1%, and 31.6% of these isolates contained toxins.[21] Also, none of the *K. oxytoca* isolates were reported from samples of hemorrhagic colitis. In 2010, Conejo et al.[22] conducted a study on multidrug-resistant *K. oxytoca* carrying the bla_{IMP-8} gene associated. A total of 9 out of 52 hospitalized patients in Spain were infected with this bacterium. In 2011, the first report was from *K. oxytoca*, new ESBLs called OXY-2, which was able to hydrolyze cefotaxime and ceftazidime.[23] This family of new broad-spectrum beta-lactamases was identified after the first report of CTX-M enzymes in 1986 in Japan and in 1989 in Germany, Argentina, France, and Italy. CTX-M beta-lactamases have now been identified in most Enterobacteriaceae species. At least 65 types of CTX-M have been identified in 5 families based on their amino acid sequences.[7,8] Recently, species with resistance to cephalosporins have been increasing rapidly, so the total samples isolated in Bulgaria, Cyprus, Romania, and Portugal, 28%, 16%, 16%, and 12%, respectively, produced ESBLs.[9,24]

In this study, 66% and 45% of isolates were contained bla_{CTX-M} and bla_{AmpC} genes, respectively. The prevalence of AmpC enzyme in *E. coli* and *K. pneumoniae* strains was 17.1% in China. In the United States, 4% of *E. coli* collected from 25 US states carried the AmpC enzyme.[25-28] In a study in India, 37.5% of *E. coli* isolates, and 24.1% of *K. pneumonia* isolates had the AmpC gene. In a study of 173 *E. coli* and *Klebsiella* isolates in the United Kingdom, 49% of *E. coli* and 55% of *Klebsiella* isolates contained the AmpC beta-lactamase enzyme, which is highly prevalent in this country.[29,30] However, biofilm formation and AMEs genes have not been investigated. We observed that 16% and 8% of AmpC-bearing *K. oxytoca* carried the *aac(3)-IIa* and *aac(6)-Ib* genes, respectively. Moreover, 27% of them were strong biofilm producers. Among 100 isolates, 54% produced the AmpC enzyme in the combined disk method. Among them, 30 isolates were resistant to gentamicin.

In conclusion, more than half of *K. oxytoca* showed MDR phenotype. Moreover, half of the isolates carried the bla_{AmpC} and bla_{CTX-M} genes. Strong biofilm formation was observed in more than 60% of them, of which 27% carried the *blaAmpC* gene, 22% carried the *aac(3)-IIa* gene, and 6% had the *aac(6)-Ib* gene. It is suggested to implement combination therapy for MDR isolates.

Competing Interests

The authors declare that they have no competing interests.

References

1. Beaugerie L, Metz M, Barbut F, et al. Klebsiella oxytoca as an agent of antibiotic-associated hemorrhagic colitis. Clin Gastroenterol Hepatol. 2003;1(5):370-376. doi: 10.1053/s1542-3565(03)00183-6.
2. Joainig MM, Gorkiewicz G, Leitner E, et al. Cytotoxic Effects of Klebsiella oxytoca Strains Isolated from Patients with Antibiotic-associated Hemorrhagic Colitis or Other Diseases Caused by Infections and from Healthy Subjects. J Clin Microbiol. 2010;48(3):817-824. doi:10.1128/JCM.01741-09.
3. Ghasemian A, Mobarez AM, Peerayeh SN, et al. Report

of Plasmid-mediated Colistin Resistance in Klebsiella oxytoca from Iran. Rev Res Med Microbiol. 2018;29(2):59-63. doi:10.1097/MRM.0000000000000134.
4. Ghasemian A, Mobarez AM, Peerayeh SN, et al. Expression of Adhesin Genes and Biofilm Formation among Klebsiella oxytoca Clinical Isolates from Patients with Antibiotic-associated Hemorrhagic Colitis. J Med Microbiol. 2019;68(7):978-985. doi: 10.1099/jmm.0.000965.
5. Bradford PA. Extended-spectrum beta-lactamases in the 21st century: characterization, epidemiology, and detection of this important resistance threat. Clin Microbiol Rev. 2001 Oct;14(4):933-51, table of contents. doi: 10.1128/CMR.14.4.933-951.2001.
6. Di Domenico EG, Farulla I, Prignano G, et al. Biofilm is a Major Virulence Determinant in Bacterial Colonization of Chronic Skin Ulcers Independently from the Multidrug Resistant Phenotype. Int J Mol Sci. 2017;18(5):1077. doi: 10.3390/ijms18051077.
7. Stahlhut SG, Struve C, Krogfelt KA, Reisner A. Biofilm Formation of Klebsiella pneumoniae on Urethral Catheters Requires Either Type 1 or Type 3 Fimbriae. FEMS Immunol Med Microbiol. 2012;65(2):350-359.doi: 10.1111/j.1574-695X.2012.00965.x.
8. Oydanich M, Dingle TC, Hamula CL, et al. Retrospective Report of Antimicrobial Susceptibility Observed in Bacterial Pathogens Isolated from Ocular Samples at Mount Sinai Hospital, 2010 to 2015. Antimicrob Resist Infect Control. 2017;6:29. doi.org/10.1186/s13756-017-0185-0.
9. Jacoby GA. AmpC β-Lactamases. Clin Microbiol Rev. 2009;22(1):161-182. doi: 10.1128/CMR.00036-08.
10. Shahid M, Sobia F, Singh A, et al. AmpC β-lactamases and Bacterial Resistance: An Updated Mini Review. Rev Med Microbiol. 2009;20(3):41-55. doi: 10.1097/MRM.0b013e328331ad83.
11. Bush K, Jacoby GA, Medeiros AA. A functional classification scheme for beta-lactamases and its correlation with molecular structure. Antimicrob Agents Chemother. 1995 Jun;39(6):1211-33. doi: 10.1128/AAC.39.6.1211.
12. Rayamajhi N, Kang SG, Lee DY, et al. Characterization of TEM-, SHV- and AmpC-type β-lactamases from Cephalosporin-resistant Enterobacteriaceae Isolated from Swine. Int J Food Microbiol. 2008;124(2):183-187. doi: 10.1016/j.ijfoodmicro.2008.03.009.
13. Clinical and Laboratory Standards Institute (CLSI). Performance Standards for Antimicrobial Susceptibility Testing. Approved Standard. CLSI Document M100, 2020.
14. Ahmed AM, Nakano H, Shimamoto T. The First Characterization of Extended-spectrum β-lactamase-producing Salmonella in Japan. J Antimicrob Chemother. 2004;54(1):283-284. doi: 10.1093/jac/dkh300. Epub 2004 Jun 9.
15. Aal Owaif HA, Mhawesh AA, Abdulateef SA. The role of BipA in the regulation of K1 capsular polysaccharide production of uropathogenic Escherichia coli. Ann Trop Med Public Health. 2019;22 (Special Issue):S254. doi: 10.36295/ASRO.2019.220924.
16. Shrief R, Hassan RH, Zaki MES, Rizk MA. Molecular Study of Klebsiella Oxytoca Associated with Urinary Tract Infection in Children. Open Microbiol J. 2022;16:1-8. doi:10.2174/18742858-v16-e2201070.
17. Kovtunovych G, Lytvynenko T, Negrutska V, Lar O, Brisse S, Kozyrovska N. Identification of Klebsiella oxytoca using a specific PCR assay targeting the polygalacturonase pehX gene. Res Microbiol. 2003;154(8):587-592. doi: 10.1016/S0923-2508(03)00148-7.
18. Ghasemian A, Mobarez AM, Peerayeh SN, Bezmin Abadi AT. The association of surface adhesin genes and the biofilm formation among Klebsiella oxytoca clinical isolates. New Microbes New Infect. 2019;27:36-39. doi: 10.1016/j.nmni.2018.07.001.
19. Liu X, Liu Y. Detection and genotype analysis of AmpC β-lactamase in Klebsiella pneumoniae from tertiary hospitals. Exp Ther Med. 2016;12:480-484. doi: 10.3892/etm.2016.3295.
20. Ghotaslou R, Sefidan FY, Akhi MT, Asgharzadeh M, Asl YM. Dissemination of Genes Encoding Aminoglycoside-Modifying Enzymes and armA Among Enterobacteriaceae Isolates in Northwest Iran. Microb Drug Resist. 2017;23(7):826-832. doi: 10.1089/mdr.2016.0224.
21. Cheng VCC, Yam W-C, Tsang L-L, et al. Epidemiology of Klebsiella oxytoca-associated Diarrhea Detected by Simmons Citrate Agar Supplemented with Inositol, Tryptophan and Bile Salts. J Clin Microbiol. 2012;50(5):1571-1579. doi: 10.1128/JCM.00163-12.
22. Conejo MC, Domínguez MC, López-Cerero L. Isolation of Multidrug-resistant Klebsiella oxytoca Carrying blaIMP-8, associated with OXY Hyperproduction, in the Intensive Care Unit of a Community Hospital in Spain. J Antimicrob Chemother. 2010;65(5):1071-1073. doi: 10.1093/jac/dkq063.
23. Younes A, Hamouda A, Amyes SFB. First Report of A Novel Extended-spectrum Beta-lactamase KOXY-2 Producing Klebsiella oxytoca that Hydrolyses Ceftazidime. J Chemother. 2011;23(3):127-130. doi: 10.1179/joc.2011.23.3.127.
24. Wong D, van Duin D. Novel Beta-lactamase Inhibitors: Unlocking Their Potential in Therapy. Drugs. 2017;77(6):615-628. doi: 10.1007/s40265-017-0725-1.
25. Shibu P, McCuaig F, McCartney AL, et al. Improved Molecular Characterization of the Klebsiella oxytoca Complex Reveals the Prevalence of the Kleboxymycin Biosynthetic Gene Cluster. Microb Genom. 2021;7(7):000592. doi: 10.1099/mgen.0.000592.
26. Iroha IR, Okeh EN, Moses IB, et al. Prevalence and Antibiotic Susceptibility Patterns of Extended Spectrum Beta-Lactamase-producing Klebsiella oxytoca Isolated from Urine Samples of Patients Visiting Private Laboratories in Abakaliki Metropolis. Afr J Microbiol Res. 2019;13(28):538-543. doi: 10.5897/AJMR2019.9154.
27. Kumar D, Anjum N, Singh S, et al. A Study on Prevalence, Virulence Factors and Antibiotic Susceptibility of Klebsiella oxytoca Isolates in a Tertiary Care Centre. Asian Pac J Health Sci. 2019;6(1):28-32. doi:10.21276/apjhs.2019.6.1.4.
28. AL-Khikani FHO, Abadi RM, Ayit AS. Emerging Carbapenemase Klebsiella oxytoca with Multidrug Resistance Implicated in Urinary Tract Infection. Biomed Biotechnol Res J. 2020;4:148-151. doi:10.4103/bbrj.bbrj_165_19.
29. Zhang Y, Zhou H, Shen X-Q, et al. Plasmid-borne armA Methylase Gene, Together with blaCTX-M-15 and blaTEM-1, in a Klebsiella oxytoca Isolate from China. J Med Microbiol. 2008;57(Pt10):1273-1276. doi: 10.1099/jmm.0.2008/001271-0.
30. Abdulateef SA, Hussein MH, Al-Saffar AZ. In vitro Cytotoxic and Genotoxic of Lipopolysaccharide Isolated from Klebsiella pneumoniae AS1 on MCF-7 Human Breast Tumor Cell Line. International Journal of Drug Delivery Technology.2021;11(1):184-189. doi: 10.25258/ijddt.11.1.34.

Correspondence:
Dr. Hasan A. Aal Owaif, hasan.abdulhadi@nahrainuniv.edu.iq

International Journal of Biomedicine 13(3) (2023) 131-136
http://dx.doi.org/10.21103/Article13(3)_OA14

ORIGINAL ARTICLE

Microbiology

INTERNATIONAL JOURNAL OF BIOMEDICINE

Gender Differences on Prevalence of Uropathogens and Their Antimicrobial Resistance: Results from a Single-Center Study in Peja Region, Kosovo

Ilirjana Loxhaj[1,2], Sanije Hoxha-Gashi[3,4*], Sunchica Petrovska[1], Sadushe Loxha[3]

[1]*University "Ss.Cyril and Methodius", Faculty of Medicine, Skopje, North Macedonia*
[2]*Regional Hospital of Peja, Kosovo*
[3]*Faculty of Medicine, University of Pristina "Hasan Prishtina", Pristina, Kosovo*
[4]*National Institute of Public Health of Kosovo, Pristina, Kosovo*

Abstract

Background: Urinary tract infection (UTI) is the world's second most common bacterial infection, behind respiratory tract infections, affecting people of all ages worldwide. It is the most common bacterial infection among females. The present study aimed to determine the local bacterial species distribution of UTI isolates between males and females in the Peja region.

Methods and Results: This cohort longitudinal, prospective-retrospective study was conducted in the microbiological laboratories of Peja region, Kosovo. The research includes all urine samples tested for gram-negative bacteria during three years, 2018-2020. The comparison of male and female samples in terms of the type of bacteria isolated showed that the urinary infection in female patients was caused by *E. coli*, significantly more often than in male patients (86.31% vs. 62.87%, *P*=0.0000), while in the samples from male patients, *Klebsiella* spp. (12.05% vs. 3.68%, *P*=0.0000), P. aeruginosa (7.49% vs. 1.59%, *P*=0.0000), and *Acinetobacter* spp. (7.82% vs. 1.59%, *P*=0.0000), were detected significantly more often than female isolates. The prevalence of *Proteus* spp. was similar in male and female isolates (6.19% vs. 5.03%, *P*=0.3926). The results of the statistical analysis showed a statistically significant difference in the resistance of *E. coli* to the analyzed antibiotics depending on the gender of the patients. *E. coli* showed significantly higher resistance in male patients than in female patients to 12 of the 13 antibiotics that were used: ampicillin, amikacin, gentamicin, cefalexin, cefuroxime, cefotaxime, ceftazidime, ofloxacin, imipenem, piperacillin, nitrofurantoin, and trimethoprim/sulfamethoxazole. In both genders, *E. coli* showed the lowest resistance to imipenem and the highest resistance to ampicillin.

Conclusion: Not only does the prevalence of uropathogens gram-negative bacteria differ by gender (greater frequency among women) but their antibiotic resistance also differs by gender (higher resistance among male patients). (**International Journal of Biomedicine. 2023;13(3):131-136.**)

Keywords: urinary tract infection • gram-negative bacteria • gender • antibiotic resistance

For citation: Loxhaj I, Hoxha-Gashi S, Petrovska S, Loxha S. Gender Differences on Prevalence of Uropathogens and Their Antimicrobial Resistance: Results from a Single-Center Study in Peja Region, Kosovo. International Journal of Biomedicine. 2023;13(3):131-136. doi:10.21103/Article13(3)_OA14

Introduction

Urinary tract infections (UTIs) are frequent worldwide, and the pattern of antibiotic resistance differs by region. A UTI is a medical illness marked by pathogenic bacteria in the urine, bladder, urethra, kidney, and prostate.[1] It is the world's second most common bacterial infection, behind respiratory tract infections, affecting people of all ages worldwide.[2] It is the most common bacterial infection among females. An estimated 50.0% of women will get a UTI at least once, and UTIs are most common in people aged 16 to 64.[3] Recurrence of urinary infections is common in women. Recurring UTIs in women are defined as at least 2 UTIs occurring within a 6-month period or at least 3 UTIs in 12 months. The frequency of recurring UTIs in women is estimated to be 25%-50% of all infections.[4-7] Recurrent UTIs, on the other hand, demand several clinical visits and antibiotic therapy.[8] UTI therapy is estimated to account for 15% of all antibiotic use in humans.

Because of the rise of drug-resistant uropathogens, managing UTIs has become a public health priority.[9] Because UTIs are not reportable infections, it is impossible to assess their prevalence correctly. The situation may be exacerbated because, in most outpatient settings, a positive urine culture result is not necessary to make a diagnosis based on symptoms.[10] However, studies show that, despite UTI symptoms, women do not seek medical attention. As a result, the real picture of UTIs is likely to be understated in the literature.[11] A large proportion of uncontrolled antibiotic usage has contributed to the emergence of resistant bacterial infections. Resistance rates to the most common prescribed drugs used in treating UTIs vary considerably in different areas. Estimating local etiology and susceptibility profile could support the most effective empirical treatment.[12] So far, there has not been extensive research in the Peja region on differences in urine bacteriology characteristics and susceptibility patterns between males and females.

The present study aimed to determine the local bacterial species distribution of UTI isolates between males and females in the Peja region, their susceptibility pattern to antibiotics, and to get fundamental, appropriate antimicrobial therapies. One of the main tasks was to determine gender differences in the prevalence of uropathogens and their antimicrobial resistance in urine samples.

This cohort longitudinal, prospective-retrospective study was conducted in the microbiological laboratories at the Regional Hospital in Peja and the Regional Center of Public Health in Peja.

Materials and Methods

The research includes all urine samples tested for gram-negative bacteria in the Peja region during three years, 2018-2020. The epidemiological method was used to collect and analyze the data, focusing on gram-negative pathogenic bacteria and their medication resistance.

Exclusion criteria: isolates from patients under 18; patients with more than two species of bacteria, and isolates of *Candida* spp.[13]

The procedures of bacteriological examination of urine samples and determination of susceptibility to antibiotics are described in detail in another paper.[14]

Statistical analysis was performed using the statistical software package SPSS version 22.0 (SPSS Inc, Armonk, NY: IBM Corp). Baseline characteristics were summarized as frequencies and percentages for categorical variables and as mean ± standard deviation (SD) for continuous variables. For data with normal distribution, inter-group comparisons were performed using Student's t-test. The frequencies of categorical variables were compared using chi-square test with Yates' correction or Fisher's exact test (2-tail), when appropriate. A probability value of $P<0.05$ was considered statistically significant.

Results

A total of 12791 urine samples were analyzed in the study, of which 2316(18.11%) were positive for the growth of gram-negative pathogenic strains, and 10475(81.89%) were negative. From positive cases (n=2316) male were 307(13.26%) and female – 2009(86.74%). The patients from the group with gram-negative isolates were aged 19 to 95 years, with an average age of 54.4±18.1 years. Female patients were more often aged 19 to 40 and 41 to 60 years, while male patients were more often older than 61 years (P=0.0000). The average age of male patients was 63.6±17 years, and that of female patients was 52.9±18 years. According to the results of statistical analysis, male patients were significantly older (P=0.0000) (Table 1).

Table 1.

Patients by gender and age groups.

Age-group, years	Total n (%)	Gender		*P*-value
		Male n (%)	Female n (%)	
19 – 40	595 (25.7%)	45 (14.66)	550 (27.38)	0.0000
41 – 60	707 (30.5%)	49 (15.96)	658 (32.75)	
≥ 61	1014 (43.8%)	213 (69.38)	801 (39.87)	
mean±SD	54.4 ± 18.1	63.58 ± 16.99	52.99 ± 17.9	0.0000
min – max	19 – 95	19 – 95	19 – 95	

The comparison of male and female samples in terms of the type of bacteria isolated showed that the urinary infection in female patients was caused by *E. coli*, significantly more often than in male patients (86.31% vs. 62.87%, P=0.0000), while in the samples from male patients, *Klebsiella* spp. (12.05% vs. 3.68%, P=0.0000), *P. aeruginosa* (7.49% vs. 1.59%, P=0.0000), and *Acinetobacter* spp. (7.82% vs. 1.59%, P=0.0000), were detected significantly more often than female isolates. The prevalence of *Proteus* spp. was similar in male and female isolates (6.19% vs. 5.03%, p=0.3926), (Table 2).

Table 2.

Prevalence of gram-negative bacteria by gender.

Bacteria		n	Gender		*P*-value
			Male n (%)	Female n (%)	
E. coli	No	389	114 (37.13)	275 (13.69)	0.0000
	Yes	1927	193 (62.87)	1734 (86.31)	
Klebsiella spp.	No	2205	270 (87.95)	1935 (96.32)	0.0000
	Yes	111	37 (12.05)	74 (3.68)	
Proteus spp.	No	2196	288 (93.81)	1908 (94.97)	0.3926
	Yes	120	19 (6.19)	101 (5.03)	
P. aeruginosa	No	2261	284 (92.51)	1977 (98.41)	0.0000
	Yes	55	23 (7.49)	32 (1.59)	
Acinetobacter spp.	No	2260	283 (92.18)	1977 (98.41)	0.0000
	Yes	56	24 (7.82)	32 (1.59)	

Table 3 shows the distribution of resistant isolates from the *E. coli* strain depending on the gender of the patients. The results of the statistical analysis showed a statistically significant difference in the resistance of *E. coli* to the analyzed antibiotics depending on the gender of the patients. *E. coli* showed significantly higher resistance in male patients than in female patients to 12 of the 13 antibiotics that were used: ampicillin, amikacin, gentamicin, cefalexin, cefuroxime, cefotaxime, ceftazidime, ofloxacin, imipenem, piperacillin, nitrofurantoin, and trimethoprim/sulfamethoxazole. In both genders, *E. coli* showed the lowest resistance to imipenem and the highest resistance to ampicillin.

Table 3.

Distribution of resistant (R) E. coli strain isolates by gender.

Resistance / *E. coli*				
Antibiotic	Gender			*P-value*
	Total	Male R / n / (%)	Female R / n / (%)	
Ampicilin	911	111 / 187 / (59.36)	800 / 1685 / (47.48)	0.0020
Amikacin	30	9 / 157 / (5.73)	21 / 1334 / (1.57)	0.0013*
Gentamicin	163	34 / 185 / (18.38)	129 / 1639 / (7.87)	0.0000
Tobramicin	16	2 / 25 / (8)	14 / 325 / (4.31)	0.7226*
Cefalexin	327	50 / 119 / (42.02)	277 / 1098 / (25.23)	0.0001
Cefuroxime	95	15 / 26 / (57.69)	80 / 326 / (24.54)	0.0002
Cefotaxime	75	12 / 25 / (48)	63 /319 / (19.75)	0.0010
Ceftazidime	62	9 / 22 / (40.91)	53 / 283 / (18.73)	0.0267*
Ofloxacin	79	11 / 19(57.89)	68 /266 / (25.56)	0.0024
Imipenem	22	5 / 130 / (3.85)	17 / 118 / (1.43)	0.0035
Piperacillin	207	29 / 60 / (48.33)	178 / 578 / (30.8)	0.0057
Nitrofurantoin	142	39 / 184 / (21.2)	103 / 1633 / (6.31)	0.0000
Trimethoprim /Sulfamethoxazole	682	87 / 178 / (48.88)	595 / 1632 / (36.46)	0.0012

**Yates' P-value*

In both genders, *Klebsiella* spp. showed the highest resistance to ampicillin and the lowest to imipenem (Table 4).

Table 5 shows the distribution of resistant isolates from the *Proteus* spp. strain depending on the gender of the patients. A statistically significant difference in the gender distribution of resistant isolates of *Proteus* spp. was not found. In the group of male patients, *Proteus* spp. showed no resistance to 7 of the 13 tested antibiotics, the highest resistance was shown to nitrofurantoin. In the group of female patients, the lowest resistance of *Proteus* spp. was registered to amikacin, then to ofloxacin and imipenem, and the highest to nitrofurantoin and ampicillin.

Table 6 shows the distribution of resistant isolates from the *Pseudomonas aeruginosa* strain depending on the gender of the patients. Resistance of *Pseudomonas aeruginosa* to amikacin, gentamicin, ofloxacin, and imipenem was significantly higher in male patients than in female patients. *Pseudomonas aeruginosa* was non-significantly more often resistant to cefalexin in female than in male patients. In the group of men, 100% resistance was registered to cefuroxime, cefotaxime, and ofloxacin. In the group of female patients, *Pseudomonas aeruginosa* showed no resistance to 2 (tobramycin and ofloxacin) of the 13 tested antibiotics and low resistance to amikacin and imipenem.

Table 4.

Distribution of resistant (R) Klebsiella spp. strain isolates by gender.

Resistance / *Klebsiella* spp.				
Antibiotic	Gender			*P*-value
	Total	Male R / n / (%)	Female R / n / (%)	
Ampicilin	92	34 / 35 / (97.14)	58 / 74 / (78.38)	0.0117
Amikacin	2	2 / 31 / (6.45)	0 / 68 / 0	0.0958^
Gentamicin	16	11 / 36 / (30.56)	5 / 73 / (6.85)	0.0010
Tobramicin	7	2 / 18 / (11.11)	5 / 44 / (11.36)	0.6792*
Cefalexin	47	19 / 25 / (76)	28 / 65 / (43.08)	0.0051
Cefuroxime	30	15 / 19 / (78.95)	15 / 44 / (34.09)	0.0011
Cefotaxime	29	14 / 19 / (73.68)	15 / 45 / (33.33)	0.0030
Ceftazidime	26	12 / 16 / (75)	14 / 39 / (35.9)	0.0083
Ofloxacin	17	12 / 17 / (70.59)	5 / 34 / (14.71)	0.0001
Imipenem	8	3 / 31 / (9.68)	5 / 68 / (7.35)	1.0*
Piperacillin	55	27 / 32 / (84.38)	28 / 66 / (42.42)	0.0001
Nitrofurantoin	30	12 / 29 / (41.38)	18 / 65 / (27.69)	0.1885
Trimethoprim /Sulfamethoxazole	57	20 / 27 / (74.07)	37 / 70 / (52.86)	0.0571

** Yates' P-value, ^Fisher's Exact Test (two-tailed)*

Table 5.

Distribution of resistant (R) Proteus spp. strain isolates by gender.

Resistance / *Proteus* spp.				
Antibiotic	Gender			*P*-value
	Total	Male R / n / (%)	Female R / n / (%)	
Ampicilin	61	9 / 19 / (47.37)	52 / 97 / (53.61)	0.618
Amikacin	2	0 / 15 / 0	2 / 77 / (2.6)	1^
Gentamicin	18	4 / 19 / (21.05)	14 / 97 / (14.43)	0.7024*
Tobramicin	4	0 / 4 / 0	4 / 20 / (20)	1^
Cefalexin	20	2 / 11 / (18.18)	18 / 70 / (25.71)	0.8719*
Cefuroxime	5	0 / 5	5 / 21 / (23.81)	0.5451^
Cefotaxime	3	0 / 5	3 / 20 / (15)	1^
Ceftazidime	3	0 / 4	3 / 19 / (15.79)	1^
Ofloxacin	1	0 / 4	1 / 19 / (5.26)	1^
Imipenem	4	0 / 15	4 / 74 / (5.41)	1^
Piperacillin	16	3 / 11 / (27.27)	13 / 64 / (20.31)	0.9025*
Nitrofurantoin	60	12 / 17 / (70.59)	48 / 85 / (56.47)	0.2802
Trimethoprim / Sulfamethoxazole	50	7 / 17 / (41.18)	43 / 93 / (46.24)	0.7004

**Yates' P-value, ^Fisher's Exact Test (two-tailed)*

Table 6.

Distribution of resistant (R) Pseudomonas aeruginosa strain isolates by gender.

Resistance / *Pseudomonas aeruginosa*				
Antibiotic	Gender			*P*-value
	Total	Male R / n / (%)	Female R / n / (%)	
Ampicilin	41	17 / 19 / (89.47)	24 / 27 / (88.89)	0.6757*
Amikacin	6	5 / 17 / (29.41)	1 / 28 / (3.57)	0.0434*
Gentamcin	12	8 / 22 / (36.36)	4 / 32 / (12.5)	0.0382
Tobramicin	1	1 / 5 / (20)	0 / 9 / 0	0.3571^
Cefalexin	22	7 / 9 / (77.78)	15 / 18 / (83.33)	0.8602*
Cefuroxime	7	3 / 3 / (100)	4 / 6 / (66.67)	0.4500^
Cefotaxime	7	3 / 3 / (100)	4 / 7 / (57.14)	0.4750^
Ceftazidime	9	5 / 6 / (83.33)	4 / 9 / (44.44)	0.3328*
Ofloxacin	2	2 / 2 / (100)	0 / 5 / 0	0.0476^
Imipenem	8	7 / 22 / (31.82)	1 / 24 / (4.17)	0.0373*
Piperacillin	20	11 / 19 / (57.89)	9 / 23 / (39.13)	0.2255
Nitrofurantoin	37	17 / 22 / (77.27)	20 / 27 / (74.07)	0.7958
Trimethoprim / Sulfamethoxazole	39	14 / 18 / (77.78)	25 / 30 / (83.33)	0.9244*

**Yates' P-value, ^Fisher's Exact Test (two-tailed)*

Table 7.

Distribution of resistant (R) Acinetobacter spp. strain isolates by gender.

Resistance / *Acinetobacter* spp.				
Antibiotic	Gender			*P*-value
	Total	Male R / n / (%)	Female R / n / (%)	
Ampicilin	38	21 / 24 / (87.5)	17 / 32 / (53.13)	0.0064
Amikacin	6	6 / 17 / (35.29)	0 / 22 / 0	0.0038^
Gentamcin	21	14 / 22 / (63.64)	7 / 32 / (21.88)	0.0020
Tobramicin	No resistance			
Cefalexin	15	9 / 14 / (64.29)	6 / 12 / (50)	0.4624
Cefuroxime	1	0 / 1 / 0	1 / 2 / (50)	1^
Cefotaxime	1	0 / 1 / 0	1 / 2 / (50)	1^
Ceftazidime	1	0 / 1 / 0	1 / 2 / (50)	1^
Ofloxacin	2	0 / 1 / 0	2 / 2 / (100)	0.3333^
Imipenem	1	0 / 16 / 0	1 / 22 / (4.55)	1^
Piperacillin	15	6 / 14 / (42.86)	9 / 21 / (42.86)	1.0
Nitrofurantoin	30	17 / 20 / (85)	13 / 28 / (46.43)	0.0065
Trimethoprim / Sulfamethoxazole	32	19 / 23 / (82.61)	13 / 28 / (46.43)	0.0078

**Yates' P-value, ^Fisher's Exact Test (two-tailed)*

Table 7 shows the distribution of resistant isolates from the *Acinetobacter* spp. strain depending on the gender of the patients. *Acinetobacter* spp. showed significantly higher resistance in male patients than in female patients to ampicillin, amikacin, gentamicin, nitrofurantoin, and trimethoprim/sulfamethoxazole. *Acinetobacter* spp did not show resistance to tobramicin in both sexes, to cefuroxime, cefotaxime, ceftazidime, ofloxacin, and imipenem in male patients, and to amikacin in female patients. This bacterium showed high resistance to ampicillin and trimethoprim/sulfamethoxazole in male patients, to ampicillin in female patients.

Discussion

In this work, we described the relationships between gender. isolated bacterial agents and antibiotic resistance of UTIs. The comparison of male and female samples in terms of the type of bacteria isolated showed that the urinary infection in female patients significantly more often than in male patients was caused by *E. coli* (86.31% vs. 62.87%, *P*=0.0000), while in the samples from male patients, *Klebsiella* spp., *P. aeruginosa*, and *Acinetobacter* spp. were detected significantly more often than female isolates (12.05% vs. 3.68% [*P*=0.0000], 7.49% vs. 1.59% [*P*=0.0000], and 7.82% vs. 1.59% [*P*=0.0000], respectively). The prevalence of *Proteus* spp. was similar in male and female isolates (6.19% vs. 5.03%, *P*=0.3926). Similar to a study conducted by Raka et al.[15] in Kosovo in 2001. In a study by Amin et al.[16] in Iran, of the total number of positive cultures for UTI, 68% were in females and 32% in males. The most frequently isolated bacteria was *E.coli*, with 59.0% (F 75.5% vs. M 24.5), and the second was *Klebsiella* with 11.6% (F 67.7 % vs. M 32.3%). In this study, *Klebsiella* was more frequent among females.

A study in Italy [17] found that among the 2741 urine samples, 1702(62.1%) and 1309(37.9%) were negative and positive for bacterial growth, respectively. Of 1309 patients with infection, 760(73.1%) were females, and 279(26.9%) were males. The three most isolated pathogenic strains were *E.coli* (72.2%), *Klebsiella pneumoniae* (12.4%), and *Proteus mirabilis* (9.0%). And other studies found that UTIs are twice more likely to occur in women than men over all age groups [18] and account for 1.2% of all office visits by women.[19] A third of women are diagnosed with a UTI before the age of 24 years, and half develop at least one episode by 35 years of age. [20] Several predisposing factors might contribute to the higher prevalence of UTIs among women.[21,22] It is well recognized that UTI is more prevalent in females than in males, and our data corroborate this generalization and correspond with a previous study conducted by Deshpande et al.[23]

Similarly, our observation on the prevalence of uropathogens is consistent with other prior reports.[24] We found that women of reproductive age are the most susceptible to UTIs. Vaginal colonization with pathogens and sexual activity have been identified as risk factors for UTI in women of this age group in previous studies.[25-27] Besides, the prevalence of UTI was also high in post-menopausal women. This phenomenon might be a result of genito-urinary atrophy and vaginal prolapse after menopause that alters the vaginal pH, decreasing the normal vaginal flora. This condition allows for gram-negative bacteria to grow as uropathogens.[28]

The results of our study showed a statistically significant difference in the resistance of *E.coli* to the analyzed

antibiotics, depending on the gender of the patients, higher resistance in male patients than in female patients to 12 of the 13 used antibiotics (ampicillin, amikacin, gentamicin, cefalexin, cefuroxime, cefotaxime, ceftazidime, ofloxacin, imipenem, piperacillin, nitrofurantoin, and trimethoprim/sulfamethoxazole) we used. In both sexes, *E.coli* showed the lowest resistance to imipenem (3.85% and 1.43%, respectively, in male and female patients) and the highest resistance to ampicillin (59.36% and 47.48%, respectively, in male and female patients)..

Similar to our study, in a study by Gu et al.,[29] higher susceptibility trends were observed in females than in males regarding major gram-negative bacteria *E. coli* and *K. pneumoniae*. In other studies,[30-32] *E. coli* isolated from males showed resistance to the majority of antibiotics.

Conclusion

Results of our study showed that not only does the prevalence of uropathogens gram-negative bacteria differ by gender (greater frequency among women) but their antibiotic resistance also differs by gender (higher resistance among male patients).

Limitations of the Study

Limitations are the same as published elsewhere. Finally, this is a single-center study, and further multi-center and prospective studies are required.

Ethical Considerations

Study approval was obtained from the Committee on Ethical Issues, Kosovo Doctors Chamber nr. 16/2022.

Competing Interests

The authors declare that they have no competing interests.

References

1. Sammon JD, Sharma P, Rahbar H, Roghmann F, Ghani KR, Sukumar S, Karakiewicz PI, Peabody JO, Elder JS, Menon M, Sun M, Trinh QD. Predictors of admission in patients presenting to the emergency department with urinary tract infection. World J Urol. 2014 Jun;32(3):813-9. doi: 10.1007/s00345-013-1167-3.
2. Prestinaci F, Pezzotti P, Pantosti A. Antimicrobial resistance: a global multifaceted phenomenon. Pathog Glob Health. 2015;109(7):309-18. doi: 10.1179/2047773215Y.0000000030.
3. Tandogdu Z, Wagenlehner FM. Global epidemiology of urinary tract infections. Curr Opin Infect Dis. 2016 Feb;29(1):73-9. doi: 10.1097/QCO.0000000000000228.
4. Foxman B. Recurring urinary tract infection: incidence and risk factors. Am J Public Health. 1990 Mar;80(3):331-3. doi: 10.2105/ajph.80.3.331.
5. Geerlings SE. Clinical Presentations and Epidemiology of Urinary Tract Infections. Microbiol Spectr. 2016 Oct;4(5). doi: 10.1128/microbiolspec.UTI-0002-2012.
6. Gupta K, Trautner BW. Diagnosis and management of recurrent urinary tract infections in non-pregnant women. BMJ. 2013 May 29;346:f3140. doi: 10.1136/bmj.f3140.
7. Scholes D, Hooton TM, Roberts PL, Stapleton AE, Gupta K, Stamm WE. Risk factors for recurrent urinary tract infection in young women. J Infect Dis. 2000 Oct;182(4):1177-82. doi: 10.1086/315827.
8. Al-Badr A, Al-Shaikh G. Recurrent Urinary Tract Infections Management in Women: A review. Sultan Qaboos Univ Med J. 2013 Aug;13(3):359-67. doi: 10.12816/0003256.
9. Bader MS, Loeb M, Brooks AA. An update on the management of urinary tract infections in the era of antimicrobial resistance. Postgrad Med. 2017 Mar;129(2):242-258. doi: 10.1080/00325481.2017.1246055.
10. Almukhtar SH. Urinary tract infection among women aged (18–40) years old in Kirkuk City, Iraq. Open Nurs J. 2018;12. doi: 10.2174/1874434601812010248
11. Abou Heidar NF, Degheili JA, Yacoubian AA, Khauli RB. Management of urinary tract infection in women: A practical approach for everyday practice. Urol Ann. 2019 Oct-Dec;11(4):339-346. doi: 10.4103/UA.UA_104_19.
12. Gharavi MJ, Zarei J, Roshani-Asl P, Yazdanyar Z, Sharif M, Rashidi N. Comprehensive study of antimicrobial susceptibility pattern and extended spectrum beta-lactamase (ESBL) prevalence in bacteria isolated from urine samples. Sci Rep. 2021 Jan 12;11(1):578. doi: 10.1038/s41598-020-79791-0.
13. Mulliqi-Osmani Gj, Raka L. Mostrimi në mikrobiologjinë klinike, Prishtinë. 2013;43-47(83).
14. Loxhaj I, Hoxha-Gashi S, Petrovska S, Loxha S. Prevalence of Isolated Bacteria from Urinary Tracts and Antibiotic Resistance Trend in Peja Region, Kosovo. International Journal of Biomedicine. 2023;13(2):313-320. doi:10.21103/ Article13(2)_OA22
15. Raka L, Mulliqi-Osmani G, Berisha L, Begolli L, Omeragiq S, Parsons L, Salfinger M, Jaka A, Kurti A, Jakupi X. Etiology and susceptibility of urinary tract isolates in Kosova. Int J Antimicrob Agents. 2004 Mar;23 Suppl 1:S2-5. doi: 10.1016/j.ijantimicag.2003.09.009.
16. Mehdinejad M, Pourdangchi Z, Amin M. Study of bacteria isolated from urinary tract infections and determination of their susceptibility to antibiotics. Jundishapur Journal of Microbiology. 2009;2(3):118-123
17. Maione A, Galdiero E, Cirillo L, Gambino E, Gallo MA, Sasso FP, Petrillo A, Guida M, Galdiero M. Prevalence, Resistance Patterns and Biofilm Production Ability of Bacterial Uropathogens from Cases of Community-Acquired Urinary Tract Infections in South Italy. Pathogens. 2023 Mar 29;12(4):537. doi: 10.3390/pathogens12040537.
18. Foxman B. Urinary tract infection syndromes: occurrence, recurrence, bacteriology, risk factors, and disease burden. Infect Dis Clin North Am. 2014 Mar;28(1):1-13. doi: 10.1016/j.idc.2013.09.003.

***Corresponding author**: Prof. Ass. Dr. Sanije Hoxha – Gashi, Faculty of Medicine, University of Prishtina "Hasan Prishtina"; National Institute of Public Health of Kosovo, Prishtina, Kosovo. E-mail: sanije.gashi@uni-pr.edu*

19. Schappert SM. Ambulatory care visits of physician offices, hospital outpatient departments, and emergency departments: United States, 1995. Vital Health Stat 13. 1997 Jun;(129):1-38. PMID: 9198408.
20. Foster RT Sr. Uncomplicated urinary tract infections in women. Obstet Gynecol Clin North Am. 2008 Jun;35(2):235-48, viii. doi: 10.1016/j.ogc.2008.03.003.
21. Grigoryan L, Trautner BW, Gupta K. Diagnosis and management of urinary tract infections in the outpatient setting: a review. JAMA. 2014 Oct 22-29;312(16):1677-84. doi: 10.1001/jama.2014.12842.
22. August SL, De Rosa MJ. Evaluation of the prevalence of urinary tract infection in rural Panamanian women. PLoS One. 2012;7(10):e47752. doi: 10.1371/journal.pone.0047752.
23. Deshpande KD, Pichare AP, Suryawanshi NM, Davane MS, Article O. Antibiogram of gram negative uropathogens in hospitalized. Int J Recent Trends Sci Technol. 2011;1(2):56–60.
24. Sharifian M, Karimi A, Tabatabaei SR, Anvaripour N. Microbial sensitivity pattern in urinary tract infections in children: a single center experience of 1,177 urine cultures. Jpn J Infect Dis. 2006 Dec;59(6):380-2.
25. Haque R, Akter ML, Salam MA. Prevalence and susceptibility of uropathogens: a recent report from a teaching hospital in Bangladesh. BMC Res Notes. 2015 Sep 5;8:416. doi: 10.1186/s13104-015-1408-1.
26. Abou Heidar NF, Degheili JA, Yacoubian AA, Khauli RB. Management of urinary tract infection in women: A practical approach for everyday practice. Urol Ann. 2019 Oct-Dec;11(4):339-346. doi: 10.4103/UA.UA_104_19.
27. Medina M, Castillo-Pino E. An introduction to the epidemiology and burden of urinary tract infections. Ther Adv Urol. 2019 May 2;11:1756287219832172. doi: 10.1177/1756287219832172.
28. Muhammad A, Khan SN, Ali N, Rehman MU, Ali I. Prevalence and antibiotic susceptibility pattern of uropathogens in outpatients at a tertiary care hospital. New Microbes New Infect. 2020 Jun 13;36:100716. doi: 10.1016/j.nmni.2020.100716.
29. Gu J, Chen X, Yang Z, Bai Y, Zhang X. Gender differences in the microbial spectrum and antibiotic sensitivity of uropathogens isolated from patients with urinary stones. J Clin Lab Anal. 2022 Jan;36(1):e24155. doi: 10.1002/jcla.24155.
30. Linhares I, Raposo T, Rodrigues A, Almeida A. Frequency and antimicrobial resistance patterns of bacteria implicated in community urinary tract infections: a ten-year surveillance study (2000-2009). BMC Infect Dis. 2013 Jan 18;13:19. doi: 10.1186/1471-2334-13-19.
31. Chatterjee N, Ghosh RR, Chatterjee M, Chattopadhyay S. Correlation of demographic profile and antibiotic resistance in patients with urinary tract infection attending a teaching hospital in Kolkata. J Med Sci Clin Res. 2014;2(11):2806-2816.
32. Hossain A, Hossain SA, Fatema AN, Wahab A, Alam MM, Islam MN, Hossain MZ, Ahsan GU. Age and gender-specific antibiotic resistance patterns among Bangladeshi patients with urinary tract infection caused by *Escherichia coli*. Heliyon. 2020 Jun 8;6(6):e04161. doi: 10.1016/j.heliyon.2020.e04161.

International Journal of Biomedicine 13(3) (2023) 137-142
http://dx.doi.org/10.21103/Article13(3)_OA15

ORIGINAL ARTICLE

Dermatology

INTERNATIONAL JOURNAL OF BIOMEDICINE

Dermatoglyphs in People with Down Syndrome and People with Normal Karyotype: A Comparison of Quantitative Characteristics

Jehona Kolgeci-Istogu[1,2], Besa Gacaferri Lumezi[1*], Mentor Sopjani[1], Labinot Istogu[2], Dhurata Kolgeci[1]

[1]*Medical Faculty, University of Prishtina, Prishtina, Kosovo*
[2]*Martha-Maria Hospital, Nuremberg, Germany*

Abstract

Background: All types of chromosomal aberrations have an impact on the development of dermatoglyphs, which changes both their quantitative and qualitative characteristics. This study aims to compare the quantitative characteristics of dermatoglyphs between individuals with Down syndrome and those with normal karyotypes in the Kosova Albanian population.

Methods and Results: The quantitative characteristics of digitopalmar dermatoglyphs were analyzed on 104 individuals (54 men and 50 women) with Down syndrome from Kosova's Albanian population. The dermatoglyphs of 403 Albanians from Kosova with normal karyotypes (the control group) were also analyzed quantitatively. Using the method devised by Cummins and Midlo, dermatoglyph traces were obtained and analyzed. We analyzed the quantitative features of both the dermatoglyphs of the fingers and the dermatoglyphs of the palms of the hands. Moorhead and Seabright's peripheral blood culture technique was utilized to analyze the karyotypes of individuals with Down syndrome.

A total of 40 dermatoglyphic variables were analyzed. When the quantitative dermatoglyphic features of men with Down syndrome and the control group were compared, significant differences were discovered in 20 of the dermatoglyphic variables. Significant differences were discovered in 21 of the dermatoglyphic variables when the features of women with Down syndrome and the control group were compared. One of the most distinctive characteristics of Down syndrome was the breadth of the atd angle, which should be taken into consideration. Compared to the control group's males and females, the males and females with Down syndrome exhibit wider atdT angles (161.91° vs. 92.60° [P<0.0001] and 165.48° vs. 94.75° [P<0.0001], respectively).

Conclusion: The size of atd angles is the factor that most closely identifies people with Down syndrome.(**International Journal of Biomedicine. 2023;13(3):137-142.**)

Keywords: Down syndrome • dermatoglyphs • atd angle • epidermal ridge

For citation: Kolgeci-Istogu J, Lumezi BG, Sopjani M, Istogu L, Kolgeci D. Dermatoglyphs in People with Down Syndrome and People with Normal Karyotype: A Comparison of Quantitative Characteristics. International Journal of Biomedicine. 2023;13(3):137-142. doi:10.21103/Article13(3)_OA15

Abbreviations

FRC, finger ridge count; **rc**, ridge count; **PRC**, palmar ridge count; **PIR**, pattern intensity right; **PIL**, pattern intensity left; **TPII**, total pattern intensity index

Introduction

Dermatoglyphics is the study of naturally occurring epidermal ridges found on the fingertips and toes, as well as the palms of the hands and soles of the feet.(1) They begin to form during the sixth or seventh week of intrauterine development, with their final formation occurring between the nineteenth and twenty-first weeks. After their formation, dermatoglyphs do not alter throughout an individual's lifetime. This characteristic elevated the significance of dermatoglyphics in biomedical research.(2-4)

During studies, the most common dermatoglyphic figures are the arc, ulnar loop, radial loop, twist, incidental twist, and triradius, all located near the figures. Always

present on the tips of the digits are dermatoglyphic markings. One can count the epidermal ridges on the ulnar loop, radial loop, pleats, and accidental folds. The digital triradius, marked with the letters a, b, c, and d, is located at the base of digits 2, 3, 4, and 5. During dermatoglyphic analysis, it is possible to enumerate embryonic ridges between the triradius a-b, b-c, and c-d. The axial triradius is located in the proximal portion of the hand's palm and is denoted by the letter t. From the intersection of the triradius a, t, and d with straight lines, the "atd" angle, which represents a distinct dermatoglyphic measurable variable, can be derived.

The quantitative characteristics of dermatoglyphs can be analyzed based on the specifications.[5,6] The quantitative characteristics of dermatoglyphs are investigated by analyzing the epidermal ridges on the digits and palms of the hands. One digit is analyzed for its number of epidermal ridges and triradius. In the palms of the hands, the number of epidermal ridges between the triradius a-b, b-c, and c-d of the right hand and the left hand, as well as the size of the atd angle, are analyzed.[7,8]

The genes of the human genome govern the development of quantitative dermatoglyphic characteristics. Multiple genes appear implicated, so the inheritance pattern is not straightforward. Numerous studies have demonstrated that people with chromosomal aberrations (Down syndrome, Edwards' syndrome, Turner's syndrome, etc.) have dermatoglyphs that differ significantly from those of healthy individuals.[9-12] Not only do chromosomal aberrations significantly decrease the quality of human life, they also influence the development of quantitative human dermatoglyphic characteristics.[13]

In the general population, Down syndrome (DS) is the most prevalent chromosomal disorder. The incidence of infants born with this syndrome is 1 in 700.[14] Through cytogenetic analysis, it has been determined that there are three cytogenetic forms of Down syndrome. The cytogenetic form of trisomy 21 is found in approximately 94% of patients with Down syndrome. Trisomy 21 with translocation affects approximately 4% of people with Down syndrome. Approximately 2% of individuals with Down syndrome have the mosaic variant of trisomy 21.[15]

When the dermatoglyphs of people with Down syndrome free trisomy of chromosome 21, trisomy 21 with translocation, and the mosaic form of trisomy 21 were compared, no significant differences were found. All three Down syndrome forms possess dermatoglyphs that are characteristic of Down syndrome.[16] However, the dermatoglyphic features in individuals with Down syndrome significantly differ from those in healthy individuals.[17] The ulnar loop is present in approximately 80% of the digits of individuals with Down syndrome, whereas it is present in about 60% of the fingers of healthy individuals. Men with DS have approximately 130 epidermal ridges on their fingertips, whereas healthy men have approximately 145. The sum of the atd angles in both hands of individuals with Down syndrome ranges between 137° and 163°, whereas in healthy individuals, it ranges between 85° and 97°.

In the Albanian population of Kosova, no dermatoglyphic research has been conducted on individuals with Down syndrome. In this study, we investigated the dermatoglyphs of individuals with Down syndrome who are part of the Albanian population of Kosova. We compared them to individuals from the same population without chromosomal abnormalities. Our study concluded that people with Down syndrome in the Albanian population of Kosova have the same quantitative changes in the dermatoglyphs as people with DS in other populations.

This study aims to compare the quantitative characteristics of dermatoglyphs between individuals with Down syndrome and those with normal karyotypes in the Kosova Albanian population.

Materials and Methods

The quantitative characteristics of digitopalmar dermatoglyphs were analyzed on 104 individuals (54 men and 50 women) with Down syndrome from Kosova's Albanian population. The dermatoglyphs of 403 Albanians from Kosova with normal karyotypes were also analyzed quantitatively. This group serves as the control group. Using the method devised by Cummins and Midlo,[18] dermatoglyphic traces were obtained and analyzed.

During the research, the quantitative features of both the dermatoglyphs of the fingers (FRC: Finger Ridge Count) and the dermatoglyphs of the palms of the hands (PRC: Palmar Ridge Count) were analyzed.

The following quantitative characteristics of dermatoglyphs were analyzed in the fingers: Right hand – FRC of Finger 1 (FRR1), Finger 2 (FRR2), Finger 3 (FRR3), Finger 4 (FRR4), and Finger 5 (FRR5); Left hand – FRC of Finger 1 (FRL1), Finger 2 (FRL2), Finger 3 (FRL3), Finger 4 (FRL4), and Finger 5 (FRL5); Total FRC Right (TFRR (1-5)); Total FRC Left (TFRL (1-5)); Total FRC (TFRC); the number of triradius in the fingers of the right hand – Pattern Intensity Right (PIR): PIR1, PIR2, PIR3, PIR4, and PIR5 and the number of triradius in the fingers of the left hand - Pattern Intensity Left (PIL): PIL1, PIL2, PIL3, PIL4, and PIL5; Total PIR (1-5 R) (TPIR1-5R); Total PIL (1-5 L) (TPIL1-5L); the total number of triradius for the 5 fingers of the right hand (TPIR – Total PIR); the total number of triradius for the 5 fingers of the left hand (TPIL– Total PIL), as well as the total number of triradius in all 10 fingers of the right and left hand, i.e., Total Pattern Intensity Index (TPII).

In the palms of the hands, we analyzed the following patterns: the number of epidermal ridges between the digital triradius a,b,c, and d of the right hand (a-b rc R, b-c rc R and c-d rc R) and of the left hand (a-b rc L, b-c rc L and c-d rc L), the total number of epidermal ridges in the interdigital regions for the right and left hand – Total PRC on the right hand (TPRR), Total PRC on the left hand (TPRL), the total number of epidermal ridges between triradius a and b on both hands (Total Palmar Ridge - TPR 1), the total number of epidermal ridges between triradii b and c on both hands (TPR2), the total number of epidermal ridges between the triradii c and d in both hands (TPR3), the size of the atd angle in the right hand (atd R) and in the left hand (atd L) as well as the size of the atd angle in both hands (atd T).

Moorhead and Seabright's peripheral blood culture technique[19] was utilized to analyze the karyotypes of individuals with Down syndrome.

Statistical analysis was performed using the statistical software package SPSS version 21.0 (SPSS Inc, Armonk, NY: IBM Corp). The normality of distribution of continuous variables was tested by the Kolmogorov-Smirnov test with the Lilliefors correction and Shapiro-Wilk test. For the descriptive analysis, results are presented as mean (M) ± standard deviation (SD). For data with normal distribution, inter-group comparisons were performed using Student's t-test. Differences of continuous variables departing from the normal distribution, even after transformation, were tested by the Mann-Whitney U-test. A probability value of $P<0.05$ was considered statistically significant.

The study protocol was reviewed and approved by the Ethics Committee of the University of Prishtina.

Results

Analyses of the quantitative characteristics of dermatoglyphs were conducted on two groups of people. The first cohort consisted of 104 individuals with Down syndrome. The second group consists of 403 individuals with a normal karyotype (the control group).

Three distinct forms of trisomy 21 were present in the karyotypes of individuals with Down syndrome. There were 93 cases of free trisomy of chromosome 21 with 47,XY,+21 karyotype (males) and 47,XX,+21 karyotype (females) (Figure 1), 10 cases of trisomy 21 with translocation (Figure 2), and only one case of trisomy 21 mosaic form.

Among individuals with Down syndrome who had karyotypes with different types of trisomy 21, no significant differences in the quantitative features of the dermatoglyphs were observed; therefore, all these individuals comprised the group of people with Down syndrome.

The quantitative characteristics of the dermatoglyphs of the digits of men with Down syndrome and men with a normal karyotype are compared in Table 1. The results of the Mann-Whitney test (U') indicate a significant difference between men with Down syndrome and the control group for the number of epidermal ridges on FRR2 ($P<0.001$), and on FRR5 ($P<0.011$) of the right hand, while on the left hand for the number of epidermal ridges on FRL1 ($P=0.003$), and for FRL3 ($P=0.0014$), as well as for the TFRL variable of the left hand ($P=0.042$).

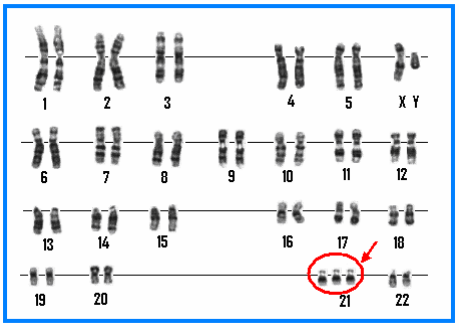

Fig. 1. *Karyotype of the child with free trisomy of chromosome 21 (47,XY,+21).*

Table 1.

The quantitative characteristics of the dermatoglyphs of the fingers between men with Down syndrome and men with a normal karyotype.

Variable	Down syndrome Male (n=54)		Control group Male (n=201)		Mann-Whitney test or T-test	*P*-value
	Mean	SD	Mean	SD		
FRR1	18.24	6.15	17.10	5.72	U'=5939.5	0.287
FRR2	12.37	4.89	9.17	6.16	U'=3860	0.001
FRR3	11.96	3.69	10.17	5.17	U'=4590.0	0.082
FRR4	11.46	4.52	13.09	5.55	U'=4130.0	0.071
FRR5	10.22	4.16	11.16	4.60	U'=4668.0	0.011
TFRR	64.26	17.27	60.70	20.41	t=1.173	0.242
FRL1	16.85	6.80	14.35	5.73	U'=6860.5	0.003
FRL2	11.74	4.93	8.17	5.99	U'=7270.5	0.0001
FRL3	12.59	3.70	9.80	5.46	U'=6961.0	0.0014
FRL4	11.85	4.44	12.91	5.49	U'=6366.0	0.051
FRL5	9.83	4.54	10.95	4.28	U'=6274.0	0.078
TFRL	62.87	16.74	56.18	20.57	U'=6405.5	0.042
TFRC	127.13	32.12	116.88	39.70	t=1.749	0.0816
PIR1	1.17	0.42	1.45	0.56	U'=6961.0	0.0012
PIR2	1.00	0.27	1.22	0.58	U'=6571.0	0.0149
PIR3	1.02	0.14	1.12	0.45	U'=6006.0	0.209
PIR4	1.13	0.34	1.49	0.53	U'=7380.0	<0.0001
PIR5	1.07	0.33	1.18	0.38	U'=5979.0	0.232
TPIR	5.39	0.94	6.46	1.70	U'=7585.5	<0.0001
PIL1	1.09	0.40	1.32	0.56	U'=6613.5	0.0119
PIL2	1.04	0.27	1.21	0.59	U'=6357.0	0.0479
PIL3	1.02	0.14	1.11	0.49	U'=5954.5	0.2554
PIL4	1.24	0.43	1.35	0.51	U'=6030.0	0.2005
PIL5	1.07	0.33	1.19	0.50	U'=5928.5	0.272
TPIL	5.46	1.02	6.18	1.82	U'=6825.5	0.0035
TPII	10.85	1.73	12.64	3.32	U'=7386.5	<0.0001

The TFRC in males with Down syndrome was 127.13, while it was 116.88 in males from the control group. Even though the TFRC of men with Down syndrome was higher than that of men in the control group, the t-test reveals no significant difference ($P=0.0816$).

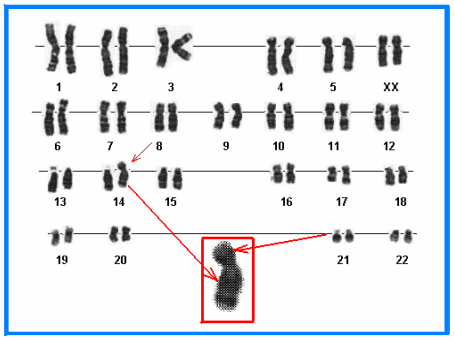

Fig. 2. *Child with trisomy 21 with Robertson's translocation between chromosomes 14 and 21: 46,XX, rob (14;21) (q10;q10), +21 mat.*

The test results (Table 1) reveal significant differences between men with Down syndrome and the control group for the number of triradius on the PIR1(*P*=0.0012), PIR2 (*P*=0.0149), PIR4 (*P*<0.0001), TPIR (*P*<0.0001), PIL1 (*P*=0.0119), PIL2 (*P*=0.0479), TPIL (*P*=0.0035), and for the total number of triradius in both hands TPII (*P*<0.0001).

In Table 2, the quantitative characteristics of palmar dermatoglyphs are compared between men with Down syndrome and men with normal karyotypes. The results of the U' test show a significant difference between men with Down syndrome and the control group for the number of epidermal ridges between the triradius a and b of the right hand (a-b rc R) (*P*=0.0189) and for the number of epidermal ridges between the triradius c and d of the right hand (c-d rc R) (c-d rc R) (*P*=0.0002), as well as for the number of epidermal ridges for the variable TPR3 (*P*=0.025).

In the U′ test between men with Down syndrome and the control group, significant differences were observed for the size of the atd angle right (atd R) (*P*<0.0001) and the atd angle left (atd L) (*P*<0.0001), and the total atd angle for both hands (atdT) (*P*<0.0001) (Table 2).

Table 2.

The quantitative characteristics of palmar dermatoglyphs between males with Down syndrome and men with a normal karyotype.

Variable	Down syndrome Male (n=54)		Control group Male (n=201)		Mann-Whitney test or T-test	*P*-value
	Mean	SD	Mean	SD		
a-b rc R	35.07	7.99	37.29	5.51	t=2.363	0.0189
b-c rc R	24.63	6.16	25.30	5.52	U'=5806.0	0.431
c-d rc R	37.61	8.43	33.83	6.17	U'=7251.5	0.0002
TPRR	97.31	16.90	96.42	12.02	t=0.443	0.657
a-g rc L	38.00	6.79	38.72	5.58	U'=5718.0	0.546
b-c rc L	23.98	6.44	24.82	5.13	U'=6119.0	0.151
c-d rc L	33.26	9.75	32.85	6.19	U'=5834.0	0.3982
TPRL	95.24	17.93	96.39	12.12	t=0.553	0.581
TPRC	192.56	32.92	192.81	23.37	t=0.064	0.949
TPR 1	73.07	13.38	76.01	10.18	t=1.753	0.0808
TPR 2	48.61	11.57	49.86	10.54	t=0.757	0.449
TPR 3	70.87	15.45	66.68	11.18	t=2.242	0.025
atd R	81.07	14.68	46.44	9.03	U'=10492	<0.0001
atd L	80.83	18.96	46.15	8.54	U'=10028	<0.0001
atd T	161.91	30.13	92.60	16.71	U'=10569	<0.0001

In Table 3, the quantitative characteristics of finger dermatoglyphs are compared between women with Down syndrome and women with normal karyotypes. The U' test revealed statistically significant differences between women with Down syndrome and the control group in terms of the number of epidermal ridges on FFF1 (*P*=0.001), FRR3 (*P*=0.0013), and FRR4 of the right hand (*P*=0.019). For the left hand, there were significant differences in the number of epidermal ridges on FRL1 (*P*<0.0001), FRL2 (*P*=0.0005), FRL3 (*P*=0.0003), and the TFRL variable (*P*=0.0045). The TFRC in females with Down syndrome was 126.16, whereas it was 111.37 in the control group (*P*=0.0419). The U' test (Table 3) revealed significant differences between females with Down syndrome and the control group in terms of the number of PIR2 (*P*=0.021) and the TPIR (*P*=0.0278).

Table 3.

The quantitative features of the dermatoglyphs of the fingers between women with Down syndrome and women with a normal karyotype.

Variable	Down syndrome Female (n=50)		Control group Female (n=202)		Mann-Whitney test or T-test	*P*-value
	Mean	SD	Mean	SD		
FRR1	17.46	5.78	14.63	5.50	U'=3540.0	0.001
FRR2	11.74	3.84	9.89	6.11	U'=4309.5	0.108
FRR3	12.18	3.83	9.76	5.00	U'=3567.0	0.0013
FRR4	11.04	5.10	13.04	5.39	U'=3970.0	0.019
FRR5	9.28	4.55	10.47	5.00	U'=5801.0	0.104
TFRR	61.70	15.90	57.78	22.00	U'=5447.0	0.390
FRL1	17.32	5.84	12.85	5.33	U'=7450.5	<0.0001
FRL2	12.24	5.08	8.87	6.35	U'=6645.5	0.0005
FRL3	13.64	4.49	10.01	5.87	U'=6725.5	0.0003
FRL4	12.00	5.29	12.24	5.49	U'=5256.0	0.656
FRL5	9.26	3.89	10.22	4.88	U'=5796.0	0.1062
TFRL	64.46	18.54	54.19	22.67	U'=6363.0	0.0045
TFRC	126.16	32.75	111.37	43.99	U'=5989.5	0.0419
PIR1	1.26	0.53	1.34	0.55	U'=5445.0	0.348
PIR2	1.04	0.35	1.25	0.60	U'=6065.0	0.021
PIR3	1.02	0.25	1.08	0.38	U'=5344.5	0.505
PIR4	1.20	0.45	1.36	0.53	U'=5829.0	0.085
PIR5	1.08	0.44	1.10	0.33	U'=5120.0	0.875
TPIR	5.60	1.39	6.13	1.64	U'=6061.5	0.0278
PIL1	1.24	0.52	1.31	0.56	U'=5386.0	0.459
PIL2	1.08	0.40	1.15	0.67	U'=5430.0	0.403
PIL3	1.08	0.34	1.08	0.45	U'=5088.5	0.9319
PIL4	1.22	0.51	1.29	0.52	U'=5388.0	0.455
PIL5	1.14	0.35	1.12	0.37	U'=5146.5	0.828
TPIL	5.76	1.51	5.95	1.84	U'=5457.5	0.376
TPII	11.36	2.72	12.08	3.27	U'=5827.0	0.0921

In Table 4, the quantitative characteristics of palmar dermatoglyphs are compared between women with Down syndrome and women with normal karyotypes. The U' test showed significant differences between females of the two studied groups for the ridge count of the right hand (b-c rc R, *P*=0.0316; c-d rc R, *P*<0.0001) and the total palmar ridge count of the right hand (TPRR) (*P*=0.016). In the left hand of women, the U' test showed significant differences in the TPRL variable (*P*=0.0199) and the TPRC variable (*P*=0.0043). Significant

differences were also revealed for TPR2 (P=0.0421) and TPR3 (P=0.0008). Through the U' test, significant differences were observed between the women with Down syndrome and the women of the control group for the size of the atd angle right [atdR] (P<0.0001), atd angle left [atdL] (P<0.0001), and total atd angle for both hands (atdT) (P<0.0001) (Table 4).

Table 4.

The quantitative characteristics of palmar dermatoglyphs of women with Down syndrome and women with a normal karyotype.

Variable	Down syndrome Female (n=50)		Control group Female (n=202)		Mann-Whitney test or T-test	*P*-value
	Mean	SD	Mean	SD		
a-b rc R	35.92	5.96	37.00	5.24	U'=5418.5	0.4251
b-c rc R	27.48	6.10	25.41	5.24	U'=6042.5	0.0316
c-d rc R	38.94	7.03	33.70	6.77	U'=7127.5	<0.0001
TPRR	102.34	13.42	96.11	12.09	t=3.192	0.016
a-g rc L	39.28	5.91	37.98	5.13	U'=5838.5	0.087
b-c rc L	26.14	5.48	24.90	5.43	U'=5671.0	0.178
c-d rc L	34.92	7.47	32.78	6.28	U'=5909.0	0.0628
TPRL	100.34	13.86	95.64	12.39	t=2.342	0.0199
TPRC	202.68	25.75	191.75	23.58	t=2.88	0.0043
TPR1	75.20	10.49	74.98	9.48	U'=5324.5	0.5527
TPR2	53.62	10.97	50.30	10.10	t=2.043	0.0421
TPR3	73.86	12.35	66.49	12.23	U'=6606.5	0.0008
atdR	82.02	12.47	47.31	8.50	U'=9828.0	<0.0001
atdL	83.46	13.76	47.45	8.40	U'=9789.5	<0.0001
atdT	165.48	24.40	94.75	16.29	U'=10569.0	<0.0001

Discussion

All types of chromosomal aberrations have an impact on the development of dermatoglyphs, which changes both their quantitative and qualitative characteristics. It is generally believed that autosomal chromosome aberrations alter the frequency of finger folds and the triradius of hands, whereas sex chromosome aberrations alter the number of embryonic ridges.[20-22] Down syndrome is characterized by an increase in the frequency of ulnar folds on the fingers, a widening of the atd angles in both hands (up to 163°), and a decrease in total finger ridge count (TFRC).

Contrary to the findings of other authors, our study revealed that the TFRC variable was higher in people with Down syndrome than in people without the condition, for both men (127.13 vs. 116.88, P=0.0816) and women (126.13 vs. 111.37, P=0.0419).

According to the findings of our study, men and women with Down syndrome had wider atdT angles in both hands than men and women in the control group: 161.91° vs. 92.60° in men (P<0.0001) (Table 2) and 165.48° vs. 94.75° in women (P<0.0001) (Table 4).

The findings in our work for the atdR, atdL, and atdT for males and females with Down syndrome are generally similar to the values found in other populations. In our study, significant differences were discovered for 40 dermatoglyphic variables when the quantitative characteristics of cases with Down syndrome and control cases were compared (Tables 1-4). Significant differences were found in 14 dermatoglyphic variables between men with Down syndrome and men with a normal karyotype when comparing the quantitative characteristics of the fingers (FRR2, FRR 5, FRL 1, FRL 2, FRL 3, TFRL, PIR 1, PIR 3, PIR 4, TPIR, PIL 1, PIL 2, TPIL, and the TPII) (Table 1).

Six dermatoglyphic variables (a-b rc R, c-d rc R, TPR 3, atd R, atd L, and atd T) on the palms of the hands of males from the two groups were found to be significantly different (Table 2).

Ten dermatoglyphic variables (FRR 1, FRR 3, FRR 4, FRL 1, FRL 2, FRL 3, TFRL, TFRC, PIR 2, and TPIR) were found to be significantly different between females with Down syndrome and those with a normal karyotype (Table 3).

When the palms of the hands of females in the two groups were compared, 11 of the dermatoglyphic variables (b-c rc R, c-d rc R, TPRR, a-b rc L, TPRL, TPRC, TPR 2, TPR 3, atd R, atd L, and atd T) showed significant differences (Table 4).

It appears that the genes necessary for the development of dermatoglyphs are related to chromosome 21, based on the presence of 40 dermatoglyphic variables with significant differences. The presence of the additional chromosome 21 in the karyotype of people with Down syndrome is the reason for these notable variations in the quantitative characteristics of the dermatoglyphs.

According to our research findings, the size of atd angles is the factor that most closely identifies people with Down syndrome. So, when developing techniques for screening for Down syndrome, the atd angle should be considered.

A diagnosis of Down syndrome can be made with an accuracy of up to 88% when the atd angle is the sole diagnostic criterion.[23] It is possible to make the diagnosis of Down syndrome with a reliability (probability) of up to 90% if the other factors that are distinctive to Down syndrome are also taken into account.[24]

We believe that the dermatoglyphic approach can be utilized as an additional way of diagnosing children with Down syndrome, especially in low-income countries. This would be a quick-to-implement, orienting diagnosis of the child suspected of having Down syndrome for further karyotype analysis that will lead to the establishment of the definitive diagnosis and the identification of the type of trisomy 21. Dermatoglyphic analysis is one of the cheapest, fastest, and non-invasive diagnostic techniques.[25]

Conclusions

The following conclusions were reached after comparing the dermatoglyphs of Down syndrome sufferers with those of the control group:

1. Compared to the control group's males and females, the males and females with Down syndrome exhibit wider atdT angles (161.91° vs. 92.60° [P<0.0001] and 165.48° vs. 94.75° [P<0.0001], respectively).

2. One of the most distinctive characteristics of Down syndrome is the breadth of the atd angle, which should be taken into consideration while developing procedures for detecting the condition.

3. The values of the TFRC variables of the males (127.13) and females (126.16) with Down syndrome were higher than those of the males (116.88) and females (111.37) in the control group.

4. When the quantitative dermatoglyphic features of men with Down syndrome and the control group were compared, significant differences were discovered in 20 of the dermatoglyphic variables. Significant differences were discovered in 21 of the dermatoglyphic variables when the features of women with Down syndrome and the control group were compared. The trisomy 21 condition in people with Down syndrome is the cause of these notable differences.

Competing Interests

The authors declare that they have no competing interests.

References

1. Sharma A, Sood V, Singh P, Sharma A. Dermatoglyphics: A review on fingerprints and their changing trends of use. CHRISMED J Health Res. 2018;5(3):167-172.
2. Nayak SB, Velan J, Shern NL, Zoung LF, Jeyarajan A, Aithal AP. Correlation between dermatoglyphic pattern of right thumb; learning methodologies; and academic performance of medical students. J Datta Meghe Inst Med Sci Univ. 2017;12(3):177-180.
3. Sharma M K, Jhawar P, Sharma H, Sharma S, Kalavatia I. Dermatoglyphics an attempt to predict Downs syndrome. Int J Biol Med Res. 2012;3(2):1631-1635.
4. Masjkey D, Bhattacharya S, Dhungel S, Jha CB, Shrestha S, Ghimire SR, Rai D. Utility of phenotypic dermal indices in the detection of Down syndrome patients. Nepal Med Coll J. 2007 Dec;9(4):217-21.
5. Ghodsi Z, Shahri NM, Ahmadi SK. Quantitative and qualitative study of Dermatoglyphic patterns in albinism. Current Research Journal of Biological Sciences. 2012;4(4):385-388.
6. Rosa A, Arquimbau R, Fananas L. Quantitative and qualitative palmar dermatoglyphics in the Mediterranean population of Delta de L'ebre (Spain). Int J Anthropol. 1998;13:89-96.
7. Cvjeticanin M, Jajic Z, Burgic N. Quantitative analysis of digitopalmar dermatoglyphics in forty female ankylosing spondylitis patients. International Journal of Current Research. 2018;10(09):73791-73798.
8. Cvjeticanin M, Jajic Z, Hadzigrahic N. Quantitative analysis of digitopalmar dermatoglyphics in fifty female psoriatic monoarthritis patients. Imperial Journal of Interdisciplinary Research (IJIR). 2016; 2:10101-10105.
9. Tarca A. Dermal prints pathology in Down syndrome. JURNAL DE MEDICINĂ PREVENTIVĂ. 2001;9(1):18-23.
10. Hassanzadeh N M, Raoofian R, Abutorabi R, Hosseini HB. Dermatoglyphic assessment in Down and Klinefelter syndrome. Jran J Med Sci. 2007;32(2):105-109.
11. Sontakke BR, Ghosh SK, Pal AK. Dermatoglyphics of fingers and palm in Klinefelter's syndrome. Nepal Med Coll J. 2010 Sep;12(3):142-4.
12. Bhalla AK, Marwaha RK, Sharma A, Trehan A, Muralidharan R, Bagga R. Dermatoglyphics in Turner syndrome. Int J Anthropol. 2005;20(1-2):111-125.
13. Theisen A, Shaffer LG. Disorders caused by chromosome abnormalities. Appl Clin Genet. 2010 Dec 10;3:159-74. doi: 10.2147/TACG.S8884.
14. Danopoulos S, Deutsch GH, Dumortier C, Mariani TJ, Al Alam D. Lung disease manifestations in Down syndrome. Am J Physiol Lung Cell Mol Physiol. 2021 Nov 1;321(5):L892-L899. doi: 10.1152/ajplung.00434.2020.
15. Kolgeci S, Kolgeci J, Azemi M, Shala-Beqiraj R, Gashi Z, Sopjani M. Cytogenetic study in children with down syndrome among kosova Albanian population between 2000 and 2010. Mater Sociomed. 2013;25(2):131-5. doi: 10.5455/msm.2013.25.131-135.
16. Kolgeci S, Kolgeci J, Azemi M, Daka A, Shala-Beqiraj R, Kurtishi I, Sopjani M. Dermatoglyphics and Reproductive Risk in a Family with Robertsonian Translocation 14q;21q. Acta Inform Med. 2015 Jun;23(3):178-83. doi: 10.5455/aim.2015.23.179-183.
17. Santhosh K. Role of Dermatoglyphics as a Diagnostic Tool in Syndromes and Systemic Disorders. Int J Dentistry Oral Sci. 2021;08(5):2390-2400
18. Gasiorowski A, Hajn V. Dermatoglyphic analysis of palm prints by the method according to Cummins et Midlo. Biologica. 2002;39(40):153-161.
19. Verma RS, Babu A, Hill G. Human Chromosomes: Principles and Techniques. Second Edition, New York, 1995:72-133.
20. Hossain MM, Ashrafuzzaman M, Jahan I, Lugova H, Samad N, Das P, Haque M. An Adaptive Approach to Detection of Dermatoglyphic Patterns of Bangladeshi People with Down Syndrome Using Fingerprint Classification. Advances in Human Biology. 2021;11(3):255-261
21. Cam FS, Gul D, Tunca Y, Fistik T. Analysis of the dermatoglyphics in Turkish patients with Klinefelter's syndrome. Hereditas. 2008;145:163-166.
22. Matsuyama N, Ito Y. The frequency of fingerprint type in parents of children with Trisomy 21 in Japan. J Physiol Anthropol. 2006 Jan;25(1):15-21. doi: 10.2114/jpa2.25.15.
23. PENROSE LS. The distal triradius t on the hands of parents and sibs of mongol imbeciles. Ann Hum Genet. 1954 Jul;19(1):10-38. doi: 10.1111/j.1469-1809.1954.tb01260.x.
24. Plato CC, Cereghino JJ, Steinberg FS. Palmar dermatoglyphics of Down's syndrome: revisited. Pediatr Res. 1973 Mar;7(3):111-8. doi: 10.1203/00006450-197303000-00002.
25. Parveen R, Rahman MS, Ahmed M, Azim MA, Momena Z, Salman MN. Dermatoglyphic Assessment in Male Down Syndrome. Community Based Medical Journal. 2002;11(2):144–151.

***Corresponding author:** Besa Gacaferri Lumezi, Associate Professor, Dermatologist, E-mail: besa.gacaferi@uni-pr.edu*

International Journal of Biomedicine 13(3) (2023) 143-147
http://dx.doi.org/10.21103/Article13(3)_OA16

ORIGINAL ARTICLE

Dentistry

INTERNATIONAL JOURNAL OF BIOMEDICINE

A Morphologic Approach of Lip Prints in a Sample of Albanian Population in Kosovo

Miranda Sejdiu Abazi[1], Erik Musliu[2*], Saranda Sejdiu Sadiku[3*], Egzon Veliu[4], Rina Prokshi[4]

[1]*Department of Dentistry, UBT - College of Higher Education Institution, Pristina, Kosovo*
[2]*Department of Dentistry, Alma Mater Europaea Campus College "REZONANCA", Pristina, Kosovo*
[3]*Department of Pharmacy, Faculty of Medicine, University of Pristina, Pristina, Kosovo*
[4]*Department of Dentistry, Faculty of Medicine, University of Pristina, Pristina, Kosovo*

Abstract

Background: Cheiloscopy (lip-print studies) is an important tool for the identification of human bodies in social and criminal issues. Lip prints present the labial mucosa with characteristic grooves and lines specific to every person. The purpose of this study was to analyze the lip prints among an adolescent sample of the Albanian population in Kosovo, to determine the most prevalent lip-print pattern in both genders, and to determine if there are any differences between male and female lip prints.

Methods and Results: A total of 100 adolescents aged from 12 to 18 were randomly selected from schools in southeastern Kosovo. The lip prints were classified according to Suzuki and Tsuchihashi's classification (1970). For the analysis, the lips were divided into four quadrants: right upper quadrant, left upper quadrant, right lower quadrant, and left lower quadrant. The analysis was done using a magnifying glass.

In the present study, the slightly prevalent lip-print pattern among all subjects was Type II (25.0%), followed by Type I (20.0%), Type III (17.0%), Type IV (16.0%), Type I′ (16.0%), and Type V (6.0%). The lip prints of Type IV were slightly more common in female subjects (24.0%), followed by Type II (20.0%), Type I (18.0%), Type III (18.0%), Type I′ (12.0%), and Type V (8.0%). Type II was slightly more common in male subjects (30.0%), followed by Type I (22.0%), Type I′ (20/0%), Type III (16.0%), Type IV (8.0%), and Type V (8.0%). However, some differences between the sexes, with a tendency toward the predominance of Type IV in women and Type II in men, were not statistically significant, and there was no significant difference between the lip patterns by quadrants in women and men. (**International Journal of Biomedicine. 2023;13(3):143-147.**)

Keywords: lip prints • cheiloscopy • forensic dentistry

For citation: Abazi MS, Musliu E, Sadiku SS, Veliu E,Prokshi R. A Morphologic Approach of Lip Prints in a Sample of Albanian Population in Kosovo. International Journal of Biomedicine. 2023;13(3):143-147. doi:10.21103/Article13(3)_OA16

Introduction

The biological phenomenon of systems of furrows on the red part of human lips was first noted by anthropologists. R. Fischer was the first to describe it in 1902. Lip prints are unique, like fingerprints, for individuals. Apart from identifying and evidential use, lip prints may also be used in detection work, being the source of criminalistic information.[1] No lip-print pattern is the same, even in identical twins.[2,3] Personal identification as an integral part of forensic science is an important and challenging task. Many methods are employed for identification. Lip grooves are a very good source for identification processes. This is a simple technique, a reliable, non-invasive, time-friendly mode that can be used successfully in human identification.[4-6] Braga et al.[7] concluded that no pair of lip-print patterns relate to each other. Domiaty et al.[2] showed that the lip-print pattern is unique for each individual, even in twins.

Saraswathi et al.[3] studied the lip prints of different individuals in different parts of the lips. Each pair of lips

Correspondence:
Dr. Erik Musliu, E-mail: eriku222@hotmail.com
Dr. Saranda Sejdiu Sadiku, E-mail: sarandassejdiu@gmail.com

was divided into four compartments (quadrants), with two compartments on each lip, and were allotted the digits 1-4 in a clockwise sequence starting from the subject's upper right. In the overall study, no individual had a single type of lip print in all four compartments, and no two or more individuals had a similar type of lip-print pattern. It was found that an intersecting pattern was most common, both among males and females, having 39.5% and 36.5%, respectively. However, in the fourth quadrant, a branched pattern was common (24%).

The primary objective of the study by Remya et al.[8] was to determine the uniqueness of lip prints, to identify the most common type, and to determine the gender difference in the lip-print pattern. Lip prints collected were classified based on the classification scheme proposed by Suzuki and Tsuchihashi [9] into six types (Type I: A clear-cut groove running vertically across the lip; Type I′: Partial-length groove of Type I; Type II: A branched groove; Type III: An intersected groove; Type IV: A reticular pattern; Type V: Other patterns). The majority of the study population from Kerala State, India,[8] belonged to Type IV (26%) and Type I' (23.5%). Type V (7.5%) was the minor type. Type II (33%) was common in females, and Type IV (38%)was common in males, with statistically significant differences (P<0.001). No two lip prints of the same type matched each other. The authors concluded that the lip print pattern of an individual is unique, and that there is a sex-related difference.

The purpose of this study was to analyze the lip prints among an adolescent sample of the Albanian population in Kosovo, to determine the most prevalent lip-print pattern in both genders, and to determine if there are any differences between male and female lip prints.

Materials and Methods

A total of 100 adolescents aged from 12 to 18 were randomly selected from schools in southeastern Kosovo. All surveyed were healthy, without inflammation, deformities, surgical scars, or active lesions on the lips, and without hypersensitivity to cosmetic products. Materials for data collection included red color lipstick, cellophane tape, white paper A4, tissue paper to remove the lipstick, and scissors (Figure 1). Lip impressions were taken with red lipstick by Flor Mar. The lips were rubbed with tissue paper, and the lipstick was applied with cotton wool on the upper and lower lip. A piece of cellophane tape was positioned on the lips without pressure, and lip prints were taken with cellophane tape in the relaxed position of the lips. Each paper with a lip print was coded (Figure 2). For the analysis, the lips were divided into four quadrants: right upper quadrant (RUQ), left upper quadrant (LUQ), right lower quadrant (RLQ), and left lower quadrant (LLQ). The analysis was done using a magnifying glass. The lip prints were classified according to Suzuki and Tsuchihashi's classification.[11]

Statistical analysis was performed using the statistical software package SPSS version 23.0 (SPSS Inc, Armonk, NY: IBM Corp).

The study protocol was reviewed and approved by the Faculty of Dentistry Ethics Committee at Ss. Cyril and Methodius University in Skopje (N #02-150115) and the Ethics Committee of the Dental Chamber of Kosovo, Republic of Kosovo (N #19). All participants provided written informed consent. All participants provided written informed consent.

Fig. 1. *Technique for data collection.*

Fig. 2. *Lip print patterns.*

Results

In the present study, the slightly prevalent lip-print pattern among all subjects was Type II (25.0%), followed by Type I (20.0%), Type III (17.0%), Type IV (16.0%), Type I′ (16.0%), and Type V (6.0%). The lip prints of Type IV were slightly more common in female subjects (24.0%), followed by Type II (20.0%), Type I (18.0%), Type III (18.0%), Type I′ (12.0%), and Type V (8.0%). Type II was slightly more common in male subjects (30.0%), followed by Type I (22.0%), Type I′ (20/0%), Type III (16.0%), Type IV (8.0%), and Type V (8.0%). There was no significant difference in the lip patterns between male and female subjects (Fisher's exact test = 6.864, P=0.233 / Monte Carlo Sig. (2-sided) / 0.222 – 0.244 /) (Table 1).

Table 1.

Patterns of lip prints in female and male subjects.

Gender		Lip prints						Total
		Type I	Type I′	Type II	Type III	Type IV	Type V	
Female	n	9	6	10	9	12	4	50
	%	18.0%	12.0%	20.0%	18.0%	24.0%	8.0%	100%
Male	n	11	10	15	8	4	2	50
	%	22.0%	20.0%	30.0%	16.0%	8.0%	4.0%	100%
Total	n	20	16	25	17	16	6	100
	%	20.0%	16.0%	25.0%	17.0%	16.0%	6.0%	100%

The lip pattern in female subjects (Table 2) in four different lip quadrants was as follows: In RUQ, Type IV was slightly more common (28.0%), followed by Type II (20.0%), Type III (18.0%), Type I (14.0%), and Type I′ (14.0%), and Type V was the rarest (8.0%). In LUQ, Type IV was slightly more common (24.0%), followed by Type II (20.0%), Type III (20.0%), Type I (14.0%), Type V (12.0%), and Type I′ was the rarest (10.0%). In LLQ, Type I was slightly more common (24.0%), followed by Type II (24.0%), Type IV (22.0%), Type III (12.0%), Type I′ (10.0%), and Type V was the rarest (8.0%). In RLQ, Type II was slightly more common (28.0%), followed by Type IV (22.0%), Type III (16.0%), Type I′ (14.0%), Type I (12.0%), and Type V (8.0%) was the rarest. There was no significant difference between lip-print patterns by quadrants in female subjects (Fisher's exact test = 6.387, *P*=0.979) / Monte Carlo Sig. (2-sided) / 0.976 – 0.983 /).

Table 2.

Patterns of lip prints in female subjects.

Lip print		Quadrants				Total
		RUQ	LUQ	LLQ	RLQ	
Type I	n	7	7	12	6	32
	%	14.0%	14.0%	24.0%	12.0%	16.0%
Type I′	n	7	5	5	7	24
	%	14.0%	10.0%	10.0%	14.0%	12.0%
Type II	n	10	10	12	14	46
	%	20.0%	20.0%	24.0%	28.0%	23.0%
Type III	n	8	10	6	8	32
	%	16.0%	20.0%	12.0%	16.0%	16.0%
Type IV	n	14	12	11	11	48
	%	28.0%	24.0%	22.0%	22.0%	24.0%
Type V	n	4	6	4	4	18
	%	8.0%	12.0%	8.0%	8.0%	9.0%
Total	n	50	50	50	50	200
	%	100.0%	100.0%	100.0%	100.0%	100.0%

The lip patterns in male subjects (Table 3) in four different lip quadrants was somewhat different than those in female subjects. In RUQ, Type I′ was slightly more common (24.0%), followed by Type I (22.0%), Type II (18.0%), Type III (18.0%), Type IV (12, 0%), and Type V was the rarest (6.0%). In LUQ, Type II was slightly more common (22.0%), followed by Type I (18.0%), Type I′ (18.0%), Type III (18.0%), Type IV (18.0%), and Type V was the rarest (6.0%). In LLQ, Type II was also slightly more common (28.0%), followed by Type I (20.0%), Type I′ (20.0%), Type III (16.0%), Type IV (10,0%), and Type V was the rarest (6,0%). In RLQ, Type II was also slightly more common (32,0%), followed by Type I (24,0%), Type III (18,0%), Type I′ (14,0%), Type IV (8,0%), and Type V was the rarest (4.0%). There was no significant difference between lip-print patterns by quadrants in male subjects (Fisher's exact test = 6.970, *P*=0.967 / Monte Carlo Sig. (2-sided) / 0.962 – 0.971 /).

Table 3.

Patterns of lip prints in male subjects

Lip print		Quadrants				Total
		RUQ	LUQ	LLQ	RLQ	
Type I	n	11	9	10	12	42
	%	22.0%	18.0%	20.0%	24.0%	21.0%
Type I′	n	12	9	10	7	38
	%	24.0%	18.0%	20.0%	14.0%	19.0%
Type II	n	9	11	14	16	50
	%	18.0%	22.0%	28.0%	32.0%	25.0%
Type III	n	9	9	8	9	35
	%	18.0%	18.0%	16.0%	18.0%	17.5%
Type IV	n	6	9	5	4	24
	%	28.0%	24.0%	22.0%	22.0%	24.0%
Type V	n	3	3	3	2	11
	%	6.0%	6.0%	6.0%	4.0%	5.5%
Total	n	50	50	50	50	200
	%	100.0%	100.0%	100.0%	100.0%	100.0%

Discussion

In the present study, the slightly prevalent lip-print pattern among all subjects was Type II (25.0%), followed by Type I (20.0%), Type III (17.0%), Type IV (16.0%), Type I′ (16.0%), and Type V (6.0%).

Various studies have shown different predominant lip patterns among the population. The most prevalent lip-print pattern in the Iranian population, according to a study conducted by Moshfeghi et al.,[10] was Type V (33.16%), and less prevalent was Type III (2.60%). In contrast to this result, Manikya et al.[11] noted that in Kerala and Manipuri populations Type III was the most prevalent (45% and 38%, respectively). According Šimović et al.,[12] in the Croatian population, Type II (40.0%) was predominant in females, while in males, the predominant pattern was Type III (35.0%). Haroun et al.,[13] in a sample of the Sudanese population, found that the prevalent

lip print pattern was Type I′. In the North Indian population, Type I (32.33%) appears to be the most predominant lip pattern, according to a study conducted by Randhawa et al.[14]

The most common type among Pondicharry males was Type III, whereas, in females, it was Type II, according to a study conducted by Kumar et al.[15]. Negi et al.[16] found that in the North Indian population, the branched pattern (Type II) in males and the vertical pattern (Type I) in females were the predominant lip print patterns.

In a study by Malik et al.,[17] performed on the Indian population, Types I and I' were most common in females, but Types IV and V were seen most commonly in males. Around 48 of 50 females and 45 of 50 males were correctly recognized based on lip prints. The authors concluded that lip prints can be used to determine gender. A study by Sharma et al.[18] aimed to ascertain whether lip prints hold the potential to determine the sex of an individual from the configuration. The study included 40 students of Subharati Dental College, 20 males and 20 females, aged between 20 and 30 years. The results obtained showed no two lip prints matched with each other, Type I (I′) was most seen in females, whereas Type IV was seen most in males. According to that study, 18 of 20 females were correctly recognized as females, and 17 of 20 males were correctly identified as males, based on their lip prints. Thus, the authors concluded that lip prints are unique to an individual and hold the potential for recognizing the sex of an individual. A study by Nagalaxmi et al.[19] showed the uniqueness of the lip prints and rugae patterns, with the lip prints showing a sensitivity of 81.7% in predicting sex. A study by Tandon et al. [20] also showed that lip prints can aid in gender determination.

In contrast, Sandhu et al.[21] showed that among the Punjabi population, Type I pattern was found to be predominant in both males (51.02%) and females (43.47%), and there was no statistically observed difference between males and females in individual lip-print types. These data are consistent with our results regarding no difference between males and females in the character of lip prints.

A study conducted at Kasturba Medical College (Mangalore, India) [22] among 200 (100 North Indians and 100 South Indians) randomly selected medical students between 18-25 years showed that Type II was the most commonly occurring lip-print pattern and Type V was the rarest. In addition, Type I and Type I' lip patterns were more common in males, and Type II, followed by Type III, Type IV, and Type V patterns were more common in females. At the same time, the revealed differences were typical for LUQ. Type III and Type IV patterns were predominant in North Indians, while Type II was predominant in South Indians. Results of the study showed that lip prints were related to sex and geographical distribution of the individual.

A study by Ghimire et al.[23] included a total of 200 Nepalese undergraduate students. Type I pattern was predominant in all four quadrants among males. In females also Type I was predominant in LUQ, LLQ and RLQ, whereas in RUQ, Type II pattern was predominant.

The quadrant-wise predominant lip-print patterns among male and female Indian and Malaysian dental students were assessed in a study by Durbakula et al.[24] The dominant lip pattern in all four quadrants for Indians was Type II, and for Malaysians, it was Type I'; the differences were statistically significant (P<0.05).

Among the Goan population,[25] the predominant pattern in all four quadrants was Type V followed by Type I' in RUQ, LUQ, and LLQ and Type I in RLQ. The distribution of patterns was not affected by sex. Thus, it is possible to note the ethnic features in the distribution of lip patterns; concerning gender differences, the existing data are contradictory.

In the present study, the most common lip pattern among subjects was Type II. However, some differences between the sexes, with a tendency toward the predominance of Type IV in women and Type II in men, were not statistically significant, and there was no significant difference between the lip patterns by quadrants in women and men.

Competing Interests

The authors declare that they have no competing interests.

References

1. Reddy LVK. Lip prints: An overview in forensic dentistry. J Adv Dental Research. 2011;2(1):17-20.
2. El Domiaty MA, Al-gaidi SA, Elayat AA, Safwat MD, Galal SA. Morphological patterns of lip prints in Saudi Arabia at Almadinah Almonawarah province. Forensic Sci Int. 2010 Jul 15;200(1-3):179.e1-9. doi: 10.1016/j.forsciint.2010.03.042.
3. Saraswathi T, Mishra G, Ranganathan K. Study of lip prints. Journal of Forensic Dental Sciences. 2009.1(1):28–31
4. Gandikota C, Venkata YP, Challa P, Juvvadi SR, Mathur A. Comparative study of palatal rugae pattern in class II div 1 and class I individuals. J Pharm Bioallied Sci. 2012 Aug;4(Suppl 2):S358-63. doi: 10.4103/0975-7406.100271.
5. Maheswari TNU, Gnanasundaram N. Role of Lip prints in Personal Identification and criminalization. Anil Aggrawal's Internet Journal of Forensic Medicine and Toxicology. 2011;12(1)
6. Caldas IM, Magalhães T, Afonso A. Establishing identity using cheiloscopy and palatoscopy. Forensic Sci Int. 2007 Jan 5;165(1):1-9. doi: 10.1016/j.forsciint.2006.04.010.
7. Braga S, Pereira ML, Sampaio-Maia B, Caldas IM. Characterization of lip prints in a Portuguese twins' population. J Forensic Odontostomatol. 2020 Sep 30;38(2):40-46.
8. Remya S, Priyadarshini T, Umadethan B, Gopalan MK, Nadankutty J. Cheiloscopy – A Study of Lip Prints for Personal Identification. IOSR Journal of Dental and Medical Sciences. 2016;15(2):101-103.
9. Suzuki K, Tsuchihashi Y. New attempt of personal identification by means of lip print. J Indian Dent Assoc. 1970 Jan;42(1):8-9.
10. Moshfeghi M, Beglou A, Mortazavi H, Bahrololumi N. Morphological patterns of lip prints in an Iranian population. J Clin Exp Dent. 2016 Dec 1;8(5):e550-e555. doi: 10.4317/jced.52921.
11. Manikya S, Sureka V, Prasanna MD, Ealla K, Reddy S, Bindu PS. Comparison of Cheiloscopy and Rugoscopy in Karnataka, Kerala, and Manipuri Population. J Int Soc Prev

Community Dent. 2018 Sep-Oct;8(5):439-445. doi: 10.4103/jispcd.JISPCD_223_18.
12. Šimović M, Pavušk I, Muhasilović S, Vodanović M. Morphologic Patterns of Lip Prints in a Sample of Croatian Population. Acta Stomatol Croat. 2016 Jun;50(2):122-127. doi: 10.1564/asc50/2/4.
13. Haroun AM, Awooda EM. Morphologic patterns of lip prints in a sample of Sudanese population: A cross-sectional study. International Journal of Preventive and Clinical Dental Research. 2021;8(2):31-34.
14. Randhawa K, Narang RS, Arora PC. Study of the effect of age changes on lip print pattern and its reliability in sex determination. J Forensic Odontostomatol. 2011 Dec 1;29(2):45-51.
15. Kumar GS, Vezhavendhan N, Vendhan P. A study of lip prints among Pondicherry population. J Forensic Dent Sci. 2012 Jul;4(2):84-7. doi: 10.4103/0975-1475.109894.
16. Negi A, Negi A. The connecting link! Lip prints and fingerprints. J Forensic Dent Sci. 2016 Sep-Dec;8(3):177. doi: 10.4103/0975-1475.195117.
17. Malik R, Goel S. Cheiloscopy - A deterministic aid for forensic sex determination. J of Ind Acad of oral Med and Radiology. 2011;23(1):17–19.
18. Sharma P, Saxena S, Rathod V. Cheiloscopy: The study of lip prints in sex identification. Journal of Forensic Dental Sciences. 2009;1(1):24–27.
19. Nagalaxmi V, Ugrappa S, M NJ, Ch L, Maloth KN, Kodangal S. Cheiloscopy, Palatoscopy and Odontometrics in Sex Prediction and Dis-crimination - a Comparative Study. Open Dent J. 2015 Jan 6;8:269-79. doi: 10.2174/1874210601408010269.
20. Tandon A, Srivastava A, Jaiswal R, Patidar M, Khare A. Estimation of gender using cheiloscopy and dermatoglyphics. Natl J Maxillofac Surg. 2017 Jul-Dec;8(2):102-105. doi: 10.4103/njms.NJMS_2_17.
21. Sandhu SV, Bansal H, Monga P, Bhandari R. Study of lip print pattern in a Punjabi population. J Forensic Dent Sci. 2012 Jan;4(1):24-8. doi: 10.4103/0975-1475.99157.
22. Rastogi P, Parida A. Lip prints–an aid in identification. Australian Journal of Forensic Sciences. 2011. 1-8. doi:10.1080/00450618.2011.610819
23. Ghimire N, Nepal P, Upadhyay S, Budhathoki SS, Subba A, Kharel B. Lip print pattern: an identification tool. *Health Renaissance*, 2013.11(3), 229-233.
24. Durbakula K, Kulkarni S, Prabhu V, Jose M, Prabhu RV. Study and comparison of lip print patterns among Indian and Malaysian dental students. *J* Cranio Max Dis. 2015;4:5-11.
25. Prabhu RV, Dinkar A, Prabhu V. A study of lip print pattern in Goan dental students - A digital approach. J Forensic Leg Med. 2012 Oct;19(7):390-5. doi: 10.1016/j.jflm.2012.04.012.

International Journal of Biomedicine 13(3) (2023) 148-153
http://dx.doi.org/10.21103/Article13(3)_OA17

ORIGINAL ARTICLE

Experimental Surgery

INTERNATIONAL JOURNAL OF BIOMEDICINE

Vertical Bone Augmentation Using Two Bioactive Glasses in a Rabbit Tibia Model: A Comparative Study with Literature Review

Timur V. Melkumyan[1,2*], Nuritdin Kh. Kamilov[1], Zurab S. Khabadze[2], Maria K. Makeeva[2,3], Gerhard K. Seeberger[4], Sargis S. Gevorgyan[2], Angela D. Dadamova[1]

[1]*Tashkent State Dental Institute, Tashkent, Uzbekistan*
[2]*Peoples' Friendship University of Russia (RUDN University), Moscow, Russia*
[3]*Sechenov University, Moscow, Russia*
[4]*Order of Physicians and Dentists of the Province of Cagliari, Sardinia, Italy*

Abstract

Background: Recently, synthetic materials based on bioactive glasses have been in special demand in dental implantology, which, according to the mechanism of their action, are not only osteo-conductors, but also osteo-inductors. Of even greater interest is the fact that the biological degradation of these materials causes alkalization of the area and inhibits the growth of many pathogens. Considering the unique properties of this group of osteoplastic fillers and the problems associated with healing after guided bone regeneration, this study aimed to compare the effectiveness of using bioactive glasses S53P4 and 45S5 when performing vertical bone augmentation in an experiment applying a rabbit tibia model.

Methods and Results: Six adult outbred rabbits aged from 1.5 to 2 years and weighing from 2.5 kg to 3.2 kg were used in the study. A titanium mesh was used to perform a true vertical guided bone regeneration technique. In each animal, two titanium tents were placed: one on the left tibia and one on the right tibia. On the left limb, empty spaces were filled with bioactive synthetic bone filler NovaBone® Morsels (USA); on the right limb, we used a mixture of bioactive glass Bonalive® granules CMF (Finland) and mineralized bone MedPark Bone-D XB (Bovine Xenograft, South Korea) in a ratio of 1:1. The quantity and quality of regenerated tissues were assessed after 8-10 weeks. The NovaBone application has allowed a gain of 2.6±2.67 mm in extra-skeletal hard tissue growth. No signs of guided bone regeneration were observed in all cases of application of an osteoplastic mixture of Bonalive and Bone-D XB granules.

Conclusion: Within the limits of this study, it was found that the use of a mixture of bioactive glass Bonalive (S53P4) with bovine hydroxyapatite in a 1:1 ratio was not effective in vertically guided bone regeneration, but the application of NovaBone (45S5) could promote a new bone formation.(**International Journal of Biomedicine. 2023;13(3):148-153.**)

Keywords: bioactive glasses • vertical bone augmentation • rabbit tibia model

For citation: Melkumyan TV, Kamilov NKh, Khabadze ZS, Makeeva MK, Seeberger GK, Gevorgyan SS, Dadamova AD. Vertical Bone Augmentation Using Two Bioactive Glasses in a Rabbit Tibia Model: A Comparative Study with Literature Review. International Journal of Biomedicine. 2023;13(3):148-153. doi:10.21103/Article13(3)_OA17

Introduction

Dental implantation has become a traditional and affordable method of mouth rehabilitation for a large number of patients. One of the main conditions for achieving satisfactory and stable results at the stage of healing and implant loading is considered to be an adequate volume of the alveolar ridge, which is necessary for the correct placement of the infrastructure. Therefore, to avoid serious clinical problems, the existing horizontal and vertical bone deficiency must be replenished using various tissue regeneration techniques.[1-8]

Guided bone regeneration (GBR) is one of the most widespread and studied methods for restoring lost bone. It has been established that the favorable formation of a new bone may occur in the absence of ingrowth of fibrous tissue and epithelium, while the migration of osteogenic cells into the site of a bone defect is maintained.[9-11] Therefore, the increase in the desired volume of bone tissue is difficult to predict due to the significant difference in the rate of osteogenesis and fibrogenesis.

In accordance with many studies, the success rate of the GBR technique depends on a positive coincidence of the following factors: primary wound closure, biocompatibility and bioactivity of a bone graft, volumetric maintenance of augmented part, and negligible connective tissue ingrowth.[9,10] However, from a practical viewpoint, it comes to the quality of materials used, operator skills, and individual response of the patient.

It is believed that osteogenesis, osteo-induction, and osteo-conduction are the three main mechanisms of bone regeneration. To date, none of the known osteoplastic materials works in three directions, except for autogenous bone, which contains osteoblasts and necessary proteins and minerals for bone formation.[12-14] However, the main disadvantages associated with using autologous bone are additional surgery in the donor site, difficulty obtaining a sufficient amount of graft, morbidity, high resorption rate, and, not infrequently, the poor quality of transplant tissue.[15-18] In this regard, the development of new materials for predictable bone regeneration when applying a simultaneous or staged approach of implant placement in an augmented alveolar ridge remains relevant.

Recently, synthetic bone grafts based on bioactive glasses have been in special demand in implant dentistry. In terms of mechanism of action, they are both osteo-conductors and osteo-inductors. Among the other unique properties of these bone substitutes is a multi-component chemical composition, which can be modified by adding certain oxides to the basic formula to impart distinctive properties to the graft. Also, these substitutes have the ability to form a strong bond with bone and chemical type of resorption without the participation of osteoclasts. A beneficial bacteriostatic feature of bioactive glasses is due to the increased pH at time of interaction with tissue fluid.[19-22]

The basic formula of any bioactive glass is mainly presented by oxides of SiO_2, Na_2O, CaO, and P_2O_5 in various proportions. This composition is considered traditional and is typical for the first generation of grafts, such as 45S5 and S53P4.[23]

Considering the significant advantages of bioactive glasses compared to other synthetic bone substitutes, since their discovery by Larry Hench, many experimental and clinical studies have been carried out to identify the opportunities for their field application.[21-23]

A review of scientific databases revealed a lot of knowledge on bioactive materials with the 45S5 composition at the preclinical and clinical stages of application. According to the results of several observations, they contributed to a significant increase in the volume of the alveolar ridge when using the GBR technique despite minor postoperative complications.[21,22]

Primary wound closure is among the main prerequisites for the successful outcome of bone grafting in the case of alveolar ridge augmentation. However, the technical sensitivity of surgery, along with the low regenerative capacity of injured soft tissues and the patient›s morbidity at the early stages of the healing period, may be the reason for wound dehiscence followed by suppuration and loss of the augmented site. That is why using bioactive bone grafts with pronounced antibacterial properties could help reduce the risk of infectious complications.[24-28]

Previously, it was found that bioactive osteoplastic material S53P4 may inhibit the growth of many aerobic and anaerobic pathogenic microorganisms and can integrate with living tissues after implantation through stimulation of a new bone formation.[29-32]

This study aimed to compare the effectiveness of using bioactive glasses S53P4 and 45S5 when performing vertical bone augmentation in an experiment applying a rabbit tibia model.

Materials and Methods

Six adult outbred rabbits aged from 1.5 to 2 years and weighing from 2.5 kg to 3.2 kg were used in the study. Before and after surgery, the rabbits were kept separately in a room for experimental animals where the required temperature and humidity were maintained. The animals were fed with a standard laboratory diet.

All experiments were performed in accordance with the Guidelines for the Care and Use of Laboratory Animals (Laboratory Animal Resources Institute, 1996). The aim and methods of the research did not require the euthanasia of the animals at the end of the experiment. The study protocol was reviewed and approved by the Ethics Committee of the Tashkent State Dental Institute.

A titanium mesh (Oss Builder, Tutanium Membrane OB3 Vertical 20[BW]×11[BL]×11[LL], Osstem Implant, Korea) was used to perform a true vertical guided bone regeneration technique. It was trimmed and bent in a standard manner to get the desired fit in each case. The shape of the experimental titanium tent resembled a rectangular basket (dimensions 10-11[L]×5-6[W]×6-7[H] mm), which was fixed on the inner surface of the tibia upside down using four titanium screws (1-1.2/3-4 mm, CONMET) (Fig. 1).

Therefore, in each animal, two titanium tents were placed: one on the left tibia and one on the right tibia. On the left limb, empty spaces were filled with bioactive synthetic bone filler NovaBone® Morsels (USA) (Fig. 2); on the right limb, we used a mixture of bioactive glass Bonalive® granules CMF (Finland) and mineralized bone MedPark Bone-D XB (Bovine Xenograft, South Korea) in a ratio of 1:1 (Fig. 3a, b).

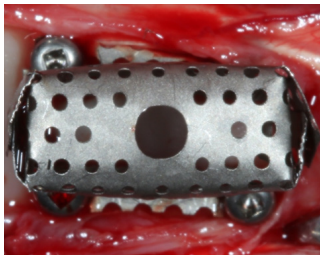

Fig. 1. *Titanium tent mounted on the inner surface of rabbit tibia.*

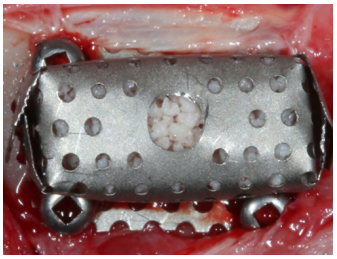

Fig. 2. *Titanium tent filled with NovaBone granules.*

Fig. 3a. *Mixture of Bonalive and Bone-D XB granules.*

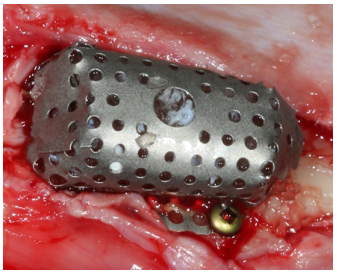

Fig. 3b. *Augmented site filled with a mixture of Bonalive and Bone-D XB granules.*

Surgery was conducted under general intravenous anesthesia with 1% etaminal sodium solution in a dosage of 3ml/kg of body weight through the ear vein. The limbs

around the site of surgery were shaved and disinfected with a 5% alcohol solution of iodine. Soft tissues were additionally infiltrated with 2-4 ml of 2% lidocaine hydrochloride solution before making a full-thickness incision.

The median incision was made longitudinally to the axis of the limb on the inner surface of the tibia down the knee joint by 1-1.5cm. The incision length in each case varied between 4 and 5cm. After the skin-periosteal flaps were elevated and mobilized, a flat cortical surface of the tibia was exposed, and the titanium tent was securely screw retained. Augmented spaces were filled with osteoplastic materials in accordance with the study protocol. Flaps were repositioned and wounds closed in each case with interrupted sutures using absorbent suture material (Vicryl 4/0).

Reentry surgery was performed after 8-10 weeks. A trephine drill with an outer diameter of 5 mm was used to collect hard tissue samples from the augmented site. A biopsy was made under constant irrigation with saline solution at a handpiece rotation speed of 1200 rpm. The height of the obtained bone cylinders was measured in millimeters. The bone gains up from the cortex border were considered. For each sample, four measurements were made (Fig. 4 a, b). After that, tissue samples were fixed in a 10% neutral buffered formalin solution followed by decalcification, washing, and drying. Samples were then embedded in paraffin in accordance with the standard procedure. Sections of 4-6μm thickness were prepared from paraffin blocks and stained with hematoxylin and eosin. Light microscopy of tissues was performed using a Leitz HM-LUX microscope (Germany).

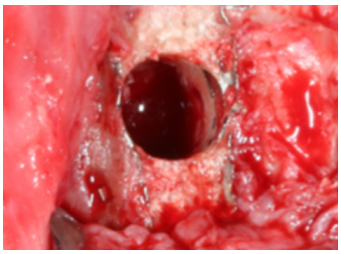

Fig. 4a. *Bone defect after tissue sampling from the augmented site of the tibia (NovaBone).*

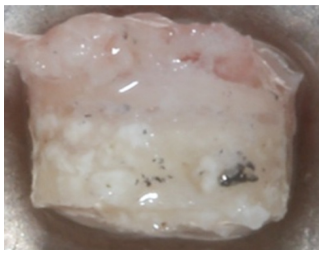

Fig. 4b. *A tissue sample taken from the augmented site of rabbit tibia (NovaBone).*

Statistical analysis was performed using StatSoft Statistica v6.0. For descriptive analysis, results are presented as mean±standard deviation (SD). The Mann-Whitney U Test was used to compare the differences between the two independent groups. A probability value of $P<0.05$ was considered statistically significant.

Results

At the time of reentry surgery, the general health condition of the animals was assessed as normal. In cases of using NovaBone, skin palpation over the augmented site of the tibia had no signs of pathology. In all animals, protruding portions of the left limbs were dense and immobile. However, examination of augmented sites on opposite limbs revealed fluctuation, and cold abscesses were diagnosed in three out of six cases. After drainage of cysts, the altered and granulomatous tissues were excised along with the titanium membranes, and wounds were thoroughly washed with a 0.05% chlorhexidine solution. No signs of guided bone regeneration were observed. In the remaining three cases of application of an osteoplastic mixture of Bonalive and Bone-D XB granules, there were fibrous and granulomatous tissues noted, nor was there any visual or histological evidence of a new bone formation. At the same time, vertically guided bone regeneration performed on the tibia was positive in all six animals after application of NovaBone bioactive granules (Fig. 5a). Despite no precedents of a complete graft maturation into a dense mineralized tissue, the average new bone gain was 2.6±2.67mm (Fig. 5b).

Microscopic examination of stained sections showed the presence of mature, viable bone tissue with a uniform distribution of osteocytes (Fig. 6a). Some sections showed residual biodegradable fragments of NovaBone granules surrounded by osteoid and woven bone (Fig. 6b).

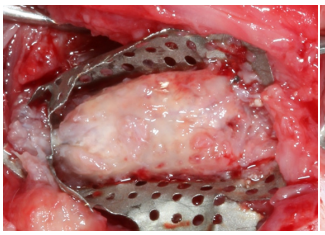

Fig. 5a. *Augmented portion of rabbit tibia (NovaBone).*

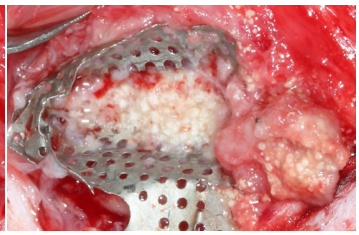

Fig. 5b. *Regenerated bone and graft particles in granulomatous tissue (NovaBone).*

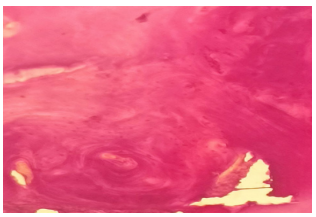

Fig. 6a. *Histological slice taken from the augmented site (H&E, ×40): non-mineralized osteoid and newly formed bone (NovaBone).*

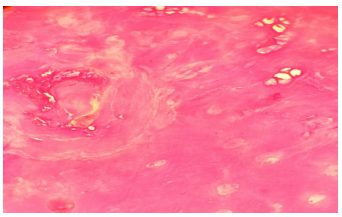

Fig. 6b. *Histological slice taken from the augmented site (H&E, ×20): fragments of graft surrounded by the osteoid matrix and woven bone (NovaBone).*

Discussion

The present study tested an extra-skeletal guided bone regeneration technique using a rabbit tibia model to assess the osteo-promotive capacity of applied bioactive glasses. Despite the difference in the mechanisms of ossification during embryonic development, the geometry of rabbit tibia and atrophied jawbone is very similar, which allows us to simulate a complicated clinical situation corresponding to the third class of alveolar ridge defects according to the Sibert classification.[33]

The main source of blood supply to the augmented site of the alveolar ridge is the residual bone. The surrounding soft tissues also take part in transporting nutrients and growth factors, but to a much lesser extent. The latter are associated

with periosteal trauma during flap elevation and mobilization, the presence of a barrier membrane, and soft tissue edema at the initial stages of healing.[34-36]

Thus, the probability of incomplete bone graft remodeling into viable hard tissue during guided bone regeneration remains significantly high. According to the results of most studies, the amount of new bone gain ranges from 30%-70% of the total volume of the graft.[37-40]

In the present study, the NovaBone application has allowed a gain of 2.6±2.67 mm in extra-skeletal hard tissue growth. Generation of new bone was mainly noted around fixing screws and along the lower border of the titanium membrane. The unreacted portion of the osteoplastic graft was replaced by granulomatous and granulation tissues containing remnants of filler particles. A similar type of regeneration was noted earlier in other studies.[38-40]

On the other hand, the necessary gain in bone volume also depends on the type of membrane. It maintains the space for directed bone tissue growth despite using the particulate graft. For this purpose, commercially available titanium membranes were used in the present study. They were trimmed and bent into a three-dimensional structure resembling an inverted basket. It was retained with the help of four titanium screws on a flat surface of the tibia and filled with bone graft substitute.[40-41] Additional holes in the tibia cortex to induce bleeding from the marrow space were not made.

Titanium meshes are non-resorbable membranes and are widely used in oral and reconstructive surgery. They serve to increase the volume of the alveolar ridge as well. The most common titanium meshes are perforated and have a thickness of more than 100 μm, which gives sufficient rigidity to the structure and makes it possible to protect the internal space from external mechanical impact.[15,16,41,42]

The issue of perforation size in titanium membranes remains disputable. According to some studies, the presence of the 40-60 μm pores promotes the free transport of nutrients to the augmented site but does not prevent the ingrowth of fibrous tissue. Other data indicate the optimal perforation size of 20 μm because it still facilitates a free diffusion of tissue fluid and cell migration while obstructing connective tissue and epithelium invasion. Experimental studies have also been conducted on non-perforated hemispherical titanium caps, which have been used for vertical bone regeneration. Despite the paucity of data, most of these studies concluded in favor of non-perforated membranes due to the more significant growth of hard tissue.[42,43]

In the present study, titanium membranes of 0.3 mm thickness with a pore diameter of 0.5–1 mm were used. During the entire observation period, there was no incidence of titanium tent exposure. However, with respect to the new bone gain, there were significant differences between the bone substitutes. It was revealed that a mixture of Bonalive bioactive glass with bovine hydroxyapatite in a 1:1 ratio did not contribute to the formation of new bone and, in 50% of cases, was accompanied by the formation of cold abscesses, despite the results of previous microbiological studies indicating the bacteriostatic properties of this material.[29-32] At the same time, the use of NovaBone alone in all animals demonstrated the absence of infectious complications and the formation of new mineralized tissue. However, a complete transformation of the synthetic graft into a living bone was not achieved.

Thus, within the limits of this study, it was found that the use of a mixture of bioactive glass Bonalive (S53P4) with bovine hydroxyapatite in a 1:1 ratio was not effective in vertically guided bone regeneration, but the application of NovaBone (45S5) could promote a new bone formation.

Competing Interests

The authors declare that they have no competing interests.

References

1. Liaw K, Delfini RH, Abrahams JJ. Dental Implant Complications. Semin Ultrasound CT MR. 2015 Oct;36(5):427-33. doi: 10.1053/j.sult.2015.09.007. Epub 2015 Oct 9. PMID: 26589696.

2. Brägger U, Aeschlimann S, Bürgin W, Hämmerle CH, Lang NP. Biological and technical complications and failures with fixed partial dentures (FPD) on implants and teeth after four to five years of function. Clin Oral Implants Res. 2001 Feb;12(1):26-34. doi: 10.1034/j.1600-0501.2001.012001026.x. PMID: 11168268.

3. Klimecs V, Grishulonoks A, Salma I, Neimane L, Locs J, Saurina E, Skagers A. Bone Loss around Dental Implants 5 Years after Implantation of Biphasic Calcium Phosphate (HAp/βTCP) Granules. J Healthc Eng. 2018 Dec 5;2018:4804902. doi: 10.1155/2018/4804902. PMID: 30631412; PMCID: PMC6304842.

4. Varon-Shahar E, Shusterman A, Piattelli A, Iezzi G, Weiss EI, Houri-Haddad Y. Peri-implant alveolar bone resorption in an innovative peri-implantitis murine model: Effect of implant surface and onset of infection. Clin Implant Dent Relat Res. 2019 Aug;21(4):723-733. doi: 10.1111/cid.12800. Epub 2019 Jun 20. PMID: 31219661.

5. Noelken R, Al-Nawas B. Bone regeneration as treatment of peri-implant disease: A narrative review. Clin Implant Dent Relat Res. 2023 Aug;25(4):696-709. doi: 10.1111/cid.13209. Epub 2023 May 17. PMID: 37199027.

6. Melkumyan TV, Seeberger GK, Khabadze ZS, Kamilov NKh, Makeeva MK, Dashtieva MU, Sheraliea SSh, Dadamova AD. Air Abrasion of Titanium Dental Implants with Water-Soluble Powders: An In Vitro Study. International Journal of Biomedicine. 2022;12(3):428-432.

7. Beschnidt SM, Cacaci C, Dedeoglu K, Hildebrand D, Hulla H, Iglhaut G, Krennmair G, Schlee M, Sipos P, Stricker A, Ackermann KL. Implant success and survival rates in daily dental practice: 5-year results of a non-interventional study using CAMLOG SCREW-LINE implants with or without platform-switching abutments. Int J Implant Dent. 2018 Nov 2;4(1):33. doi: 10.1186/s40729-018-0145-3. PMID: 30386925; PMCID: PMC6212375.

***Corresponding author:** *Prof. Timur V. Melkumyan, PhD, ScD. Tashkent State Dental Institute Tashkent, Uzbekistan. Peoples' Friendship University of Russia (RUDN University), Moscow, Russia. E-mail: t.dadamov@gmail.com*

8. Canullo L, Caneva M, Tallarico M. Ten-year hard and soft tissue results of a pilot double-blinded randomized controlled trial on immediately loaded post-extractive implants using platform-switching concept. Clin Oral Implants Res. 2017 Oct;28(10):1195-1203. doi: 10.1111/clr.12940. Epub 2016 Aug 8. PMID: 27502452.
9. Paul N, Jyotsna S, Keshini MP. Alveolar Ridge Augmentation Using Autogenous Bone Graft and Platelet-Rich Fibrin to Facilitate Implant Placement. Contemp Clin Dent. 2022 Jan-Mar;13(1):90-94. doi: 10.4103/ccd.ccd_154_20. Epub 2022 Mar 23. PMID: 35466292; PMCID: PMC9030314.
10. Soldatos N, Al Ramli R, Nelson-Rabe L, Ferguson B, Soldatos K, Weltman R. Vertical ridge augmentation (VRA) with the use of a cross-linked resorbable membrane, tenting screws, and a combination grafting technique: a report of three cases. Quintessence Int. 2021;0(0):328-339. doi: 10.3290/j.qi.a45424. PMID: 33117997.
11. Melkumyan T. V. Kamilov N. Kh., Daurova F. Yu. Dadamova A. D. Evaluation of vertical guided bone regeneration using a particulate form of experimental bioactive glass in rabbit: a case report with literature review. International Journal of Biomedicine. 2021;11(3):308-314.
12. Diomede F, Marconi GD, Fonticoli L, Pizzicanella J, Merciaro I, Bramanti P, Mazzon E, Trubiani O. Functional Relationship between Osteogenesis and Angiogenesis in Tissue Regeneration. Int J Mol Sci. 2020 May 3;21(9):3242. doi: 10.3390/ijms21093242. PMID: 32375269; PMCID: PMC7247346.
13. Liu J, Kerns DG. Mechanisms of guided bone regeneration: a review. Open Dent J. 2014 May 16;8:56-65. doi: 10.2174/1874210601408010056. PMID: 24894890; PMCID: PMC4040931.
14. Mendoza-Azpur G, de la Fuente A, Chavez E, Valdivia E, Khouly I. Horizontal ridge augmentation with guided bone regeneration using particulate xenogenic bone substitutes with or without autogenous block grafts: A randomized controlled trial. Clin Implant Dent Relat Res. 2019 Aug;21(4):521-530. doi: 10.1111/cid.12740. Epub 2019 Mar 18. PMID: 30884111.
15. Jung RE, Fenner N, Hämmerle CH, Zitzmann NU. Long-term outcome of implants placed with guided bone regeneration (GBR) using resorbable and non-resorbable membranes after 12-14 years. Clin Oral Implants Res. 2013 Oct;24(10):1065-73. doi: 10.1111/j.1600-0501.2012.02522.x.
16. Ronda M, Rebaudi A, Torelli L, Stacchi C. Expanded vs. dense polytetrafluoroethylene membranes in vertical ridge augmentation around dental implants: a prospective randomized controlled clinical trial. Clin Oral Implants Res. 2014 Jul;25(7):859-66. doi: 10.1111/clr.12157. Epub 2013 Apr 8. PMID: 23560678.
17. Khojasteh A, Kheiri L, Motamedian SR, Khoshkam V. Guided Bone Regeneration for the Reconstruction of Alveolar Bone Defects. Ann Maxillofac Surg. 2017 Jul-Dec;7(2):263-277. doi: 10.4103/ams.ams_76_17. PMID: 29264297; PMCID: PMC5717906.
18. Elnayef B, Porta C, Suárez-López Del Amo F, Mordini L, Gargallo-Albiol J, Hernández-Alfaro F. The Fate of Lateral Ridge Augmentation: A Systematic Review and Meta-Analysis. Int J Oral Maxillofac Implants. 2018 May/Jun;33(3):622-635. doi: 10.11607/jomi.6290. PMID: 29763500.
19. Shamsoddin E, Houshmand B, Golabgiran M. Biomaterial selection for bone augmentation in implant dentistry: A systematic review. J Adv Pharm Technol Res. 2019 Apr-Jun;10(2):46-50. doi: 10.4103/japtr.JAPTR_327_18. PMID: 31041181; PMCID: PMC6474167.
20. Garcia DC, Mingrone LE, de Sá MJC. Evaluation of Osseointegration and Bone Healing Using Pure-Phase β - TCP Ceramic Implant in Bone Critical Defects. A Systematic Review. Front Vet Sci. 2022 Jul 12;9:859920. doi: 10.3389/fvets.2022.859920. PMID: 35909673; PMCID: PMC9327785.
21. Tomas M, Čandrlić M, Juzbašić M, Ivanišević Z, Matijević N, Včev A, Cvijanović Peloza O, Matijević M, Perić Kačarević Ž. Synthetic Injectable Biomaterials for Alveolar Bone Regeneration in Animal and Human Studies. Materials (Basel). 2021 May 26;14(11):2858. doi: 10.3390/ma14112858. PMID: 34073551; PMCID: PMC8197881.
22. Zhao F, Yang Z, Xiong H, Yan Y, Chen X, Shao L. A bioactive glass functional hydrogel enhances bone augmentation via synergistic angiogenesis, self-swelling and osteogenesis. Bioact Mater. 2022 Oct 3;22:201-210. doi: 10.1016/j.bioactmat.2022.09.007. PMID: 36246665; PMCID: PMC9535384.
23. Skallevold HE, Rokaya D, Khurshid Z, Zafar MS. Bioactive Glass Applications in Dentistry. Int J Mol Sci. 2019 Nov 27;20(23):5960. doi: 10.3390/ijms20235960. PMID: 31783484; PMCID: PMC6928922.
24. Wang YY, Chatzistavrou X, Faulk D, Badylak S, Zheng L, Papagerakis S, Ge L, Liu H, Papagerakis P. Biological and bactericidal properties of Ag-doped bioactive glass in a natural extracellular matrix hydrogel with potential application in dentistry. Eur Cell Mater. 2015 Jun 20;29:342-55. doi: 10.22203/ecm.v029a26. PMID: 26091732.
25. Bellantone M, Williams HD, Hench LL. Broad-spectrum bactericidal activity of Ag(2)O-doped bioactive glass. Antimicrob Agents Chemother. 2002 Jun;46(6):1940-5. doi: 10.1128/AAC.46.6.1940-1945.2002. PMID: 12019112; PMCID: PMC127232.
26. Fernandes HR, Gaddam A, Rebelo A, Brazete D, Stan GE, Ferreira JMF. Bioactive Glasses and Glass-Ceramics for Healthcare Applications in Bone Regeneration and Tissue Engineering. Materials (Basel). 2018 Dec 12;11(12):2530. doi: 10.3390/ma11122530. PMID: 30545136; PMCID: PMC6316906.
27. Baino F, Fiorilli S, Vitale-Brovarone C. Bioactive glass-based materials with hierarchical porosity for medical applications: Review of recent advances. Acta Biomater. 2016 Sep 15;42:18-32. doi: 10.1016/j.actbio.2016.06.033. Epub 2016 Jun 28. PMID: 27370907.
28. Cannio M, Bellucci D, Roether JA, Boccaccini DN, Cannillo V. Bioactive Glass Applications: A Literature Review of Human Clinical Trials. Materials (Basel). 2021 Sep 20;14(18):5440. doi: 10.3390/ma14185440. PMID: 34576662; PMCID: PMC8470635.
29. Van Gestel NA, Geurts J, Hulsen DJ, van Rietbergen B, Hofmann S, Arts JJ. Clinical Applications of S53P4 Bioactive Glass in Bone Healing and Osteomyelitic Treatment: A Literature Review. Biomed Res Int. 2015;2015:684826. doi: 10.1155/2015/684826. Epub 2015 Oct 4. PMID: 26504821; PMCID: PMC4609389.
30. Steinhausen E, Lefering R, Glombitza M, Brinkmann N, Vogel C, Mester B, Dudda M. Bioactive glass S53P4 vs. autologous bone graft for filling defects in patients with

chronic osteomyelitis and infected non-unions - a single center experience. J Bone Jt Infect. 2021 Jan 12;6(4):73-83. doi: 10.5194/jbji-6-73-2021. PMID: 34084694; PMCID: PMC8132459.
31. Tarek Al Malat, Martin Glombitza, Janosch Dahmen, Peter-Michael Hax, Eva Steinhausen. The Use of Bioactive Glass S53P4 as Bone Graft Substitute in the Treatment of Chronic Osteomyelitis and Infected Non-Unions – a Retrospective Study of 50 Patients. Z Orthop Unfall 2018; 156(02): 152-159 DOI: 10.1055/s-0043-124377
32. Kaya S, Cresswell M, Boccaccini AR. Mesoporous silica-based bioactive glasses for antibiotic-free antibacterial applications. Mater Sci Eng C Mater Biol Appl. 2018 Feb 1;83:99-107. doi: 10.1016/j.msec.2017.11.003. Epub 2017 Nov 10. PMID: 29208293.
33. Zhang Z, Gan Y, Guo Y, Lu X, Li X. Animal models of vertical bone augmentation (Review). Exp Ther Med. 2021 Sep;22(3):919. doi: 10.3892/etm.2021.10351.
34. Garcia J, Dodge A, Luepke P, Wang HL, Kapila Y, Lin GH. Effect of membrane exposure on guided bone regeneration: A systematic review and meta-analysis. Clin Oral Implants Res. 2018 Mar;29(3):328-338. doi: 10.1111/clr.13121. Epub 2018 Jan 24. PMID: 29368353.
35. Urban IA, Monje A, Lozada JL, Wang HL. Long-term Evaluation of Peri-implant Bone Level after Reconstruction of Severely Atrophic Edentulous Maxilla via Vertical and Horizontal Guided Bone Regeneration in Combination with Sinus Augmentation: A Case Series with 1 to 15 Years of Loading. Clin Implant Dent Relat Res. 2017 Feb;19(1):46-55. doi: 10.1111/cid.12431. Epub 2016 May 30. PMID: 27238406.
36. Thomas MV, Puleo DA. Infection, inflammation, and bone regeneration: a paradoxical relationship. J Dent Res. 2011 Sep;90(9):1052-61. doi: 10.1177/0022034510393967. Epub 2011 Jan 19. PMID: 21248364; PMCID: PMC3169879.
37. Lee JS, Lee JS, Kang MH, Jung UW, Choi SH and Cho KS: Proof-of-concept study of vertical augmentation using block-type allogenic bone grafts: A preclinical experimental study on rabbit calvaria. J Biomed Mater Res B Appl Biomater 106: 2700-2707, 2018.
38. Tamimi F, Torres J, Al-Abedalla K, Lopez-Cabarcos E, Alkhraisat MH, Bassett DC, Gbureck U and Barralet JE: Osseointegration of dental implants in 3D-printed synthetic onlay grafts customized according to bone metabolic activity in recipient site. Biomaterials 35: 5436-5445, 2014.
39. Kim JW, Jung IH, Lee KI, Jung UW, Kim CS, Choi SH, Cho KS and Yun JH: Volumetric bone regenerative efficacy of biphasic calcium phosphate-collagen composite block loaded with rhBMP-2 in vertical bone augmentation model of a rabbit calvarium. J Biomed Mater Res A 100: 3304-3313, 2012.
40. Sam G, Pillai BR. Evolution of Barrier Membranes in Periodontal Regeneration-"Are the third Generation Membranes really here?". J Clin Diagn Res. 2014 Dec;8(12):ZE14-7. doi: 10.7860/JCDR/2014/9957.5272. Epub 2014 Dec 5. PMID: 25654055; PMCID: PMC4316361.
41. Rakhmatia YD, Ayukawa Y, Furuhashi A, Koyano K. Current barrier membranes: titanium mesh and other membranes for guided bone regeneration in dental applications. J Prosthodont Res. 2013 Jan;57(1):3-14. doi: 10.1016/j.jpor.2012.12.001. Epub 2013 Jan 21. PMID: 23347794.
42. Hasegawa H, Kaneko T, Endo M, Kanno C, Yamazaki M, Yaginuma S, Igarashi H, Honma H, Masui S, Suto M, Sakisaka Y, Ishihata H. Comparing the Efficacy of a Microperforated Titanium Membrane for Guided Bone Regeneration with an Existing Mesh Retainer in Dog Mandibles. Materials (Basel). 2021 Jun 17;14(12):3358. doi: 10.3390/ma14123358. PMID: 34204390; PMCID: PMC8234924.
43. Murai M, Sato S, Fukase Y, Yamada Y, Komiyama K, Ito K. Effects of different sizes of beta-tricalcium phosphate particles on bone augmentation within a titanium cap in rabbit calvarium. Dent Mater J. 2006 Mar;25(1):87-96. doi: 10.4012/dmj.25.87. PMID: 16706302.

International Journal of Biomedicine 13(3) (2023) 154-161
http://dx.doi.org/10.21103/Article13(3)_OA18

ORIGINAL ARTICLE

Medicinal Plants

INTERNATIONAL JOURNAL OF BIOMEDICINE

In vivo Evaluation of the Antiviral Effects of Arabian Coffee (*Coffea arabica*) and Green Tea (*Camellia sinensis*) Extracts on Influenza A Virus

Sarah Alfaifi[1], Rania Suliman[2*], Mona Timan Idriss[3,4], Abeer S Aloufi[1], Ebtesam Alolayan[5], Maaweya Awadalla[6], Alhassan Aodah[7], Omar Abu Asab[7], Jarallah Al-Qahtani[8], Nahla Mohmmed[9], Bandar Alosaimi[6]

[1]*Department of Biology, College of Science, Princess Nourah bint Abdulrahman University, Riyadh, Saudi Arabia*
[2]*Department of Clinical Laboratory Sciences, Prince Sultan Military College of Health Sciences, Dhahran, Saudi Arabia*
[3]*Department of Pharmaceutics, Faculty of Pharmacy, Imperial University College, Khartoum, Sudan*
[4]*Department of Medical Sciences and Preparation Year, Northern College of Nursing, Arar, Saudi Arabia*
[5]*Department of Zoology, King Saud University, Riyadh, Saudi Arabia*
[6]*Research Center, King Fahad Medical City, Riyadh, Saudi Arabia*
[7]*Life Science & Environment Research Institute, King Abdulaziz City for Science and Technology, Riyadh, Saudi Arabia*
[8]*Department of Histopathology, King Fahad Military Medical Complex, Dhahran, Saudi Arabia*
[9]*Department of Clinical Microbiology, Virology, Umeå University, Umeå, Sweden*

Abstract

This in vivo study was conducted to evaluate the antiviral activity of Arabian coffee (*Coffea arabica*) and green tea (*Camellia sinensis*) extracts against the influenza virus. High-performance liquid chromatography (HPLC) was used to determine the active components in each extract, and eighty experimental mice were treated. Electrophoresis was performed to detect protein expression, and reverse transcription-polymerase chain reaction (RT-PCR) was used to analyze gene expression and quantify viral RNA. Lung tissue histopathology was processed to observe pathological signs. Oral administration of all extracts reduced the viral quantification in mice lungs by 61.6% in the early phase of infection, measured by PCR. From the extracts tested, unroasted green Arabica coffee (AC) extract in protective groups showed remarkable body weight stability of 16.76 g, a survival rate of 100%, and healthier lung tissue, compared to other groups. The antiviral effects of the tested AC and GT (green tea) revealed that AC extracts induced veridical effects, increased body weight, and improved survival rate. Those natural extracts may interfere with viral replication and reduce virus infection. The observed anti-influenza activity demonstrated by reduced symptoms and increased survival rate in animal models suggests that AC extracts might be used as a promising prophylactic agent against influenza viral infections. The active compound in the unroasted green AC extract requires further in vitro analysis as to which viral proteins are targeted by the natural extract and which molecular mechanism this antiviral inhibition is interfering with.(**International Journal of Biomedicine. 2023;13(3):154-161.**)

Keywords: Influenza A virus • *Coffea arabica* • *Camellia sinensis* • RT-PCR • HPLC

For citation: Alfaifi S, Suliman R, Idriss MT, Aloufi AS, Alolayan E, Awadalla M, Aodah A, Asab OA, Al-Qahtani J, Mohmmed N, Alosaimi B. In vivo Evaluation of the Antiviral Effects of Arabian coffee (*Coffea arabica*) and Green Tea (*Camellia sinensis*) Extracts on Influenza A Virus. International Journal of Biomedicine. 2023;13(3):154-161. doi:10.21103/Article13(3)_OA18

Abbreviations

HPLC, high-performance liquid chromatography; **RT-PCR**, reverse transcription-polymerase chain reaction; **AC**, Arabica coffee; **GT**, green tea; **CGA**, chlorogenic acid

Introduction

Influenza A is a flu-causing pathogen that infects the respiratory system and has resulted in global pandemics such as the 1918 flu pandemic and the more recent 2009 swine flu pandemic.[1] The emerging variants of viruses are antiviral resistant and pose threats to existing drugs, leading to a demand for the discovery of therapeutic natural products to control and prevent viral infections.[2] Medicinal plants are the major source of novel therapeutic agents.[3] Recently, there have been numerous examples of remedies that originated from natural products,[4,5] and that have been widely used in the treatment of many diseases.[6] Many studies report that chlorogenic acid (CGA) has a wide antiviral effect against different viruses, including HIV,[7,8] adenovirus, hepatitis B virus,[9] and herpes simplex viruses,[10] and also inhibits inflammation caused by viral infection[5] and reduces serum hepatitis B virus level in vivo.[11] Numerous studies examined the effect of using GT and coffee after infection. However, they were mostly in vitro, with only a few studies in vivo.

Some medicinal plant extracts contain many beneficial constituents, such as CGA, catechins, and caffeine, that have many protective properties, such as being antioxidant, anti-inflammatory, and antimicrobial, and are important in preventing respiratory infections.[6,7,12] *Coffea arabica* and *Camellia sinensis* have a high content of CGA and caffeic acid, in common with several traditional Chinese medicines.[9,13] They are one example of natural plants with a rich source of biologically active compounds and have shown different biological effects, not only as antioxidants and anti-inflammatories, but as antifungal and anti-hyperglycemic agents.[14,15]

Green tea (GT) has organic effects and contains effective components that promote health, such as catechins, theanine, and caffeine. In previous studies, it has shown antioxidant and anti-inflammatory properties. The most significant health benefit relevant to this study is its inhibitory effect on viruses, especially influenza, by inhibiting the activity of viral RNA to prevent replication and affect the Hemagglutinin gene.[5,10] Arabica coffee (AC) extracts have effective antiviral compounds. In green, unroasted AC, there is a high content of CGA, and brown-roasted AC contains caffeine. These components have been found to inhibit RNA viruses – more sensitive than DNA viruses – in a concentration used in hot drinks.[9,16]

The chemical structure and bioactive compounds of the tea and coffee inform about the inhibitory activity on viruses. CGAs are a family of esters formed between quinic acid and cinnamic acids, such as caffeic, ferulic, and p-coumaric acids.[17,18] Of CGAs, 5′-caffeoylquinic acid is the most abundant isomer in coffee. It has been observed that CGAs influence the inhibitory activity of neuraminidase, which effectively inhibits H1N1 and H3N2 in mice.[19] Caffeine is a methylxanthine (1,3,7-trimethylxanthine) that is structurally related to adenosine and acts primarily as an adenosine receptor antagonist with psychotropic and anti-inflammatory activities.[20,21] In an in vivo study, increased doses of caffeine led to a decrease in viral protein expression and acted as a protective effect against the lethal challenge of Enterovirus A71.[22] Catechins are polyphenols that exhibit different amounts of phenolic rings attached by two or more hydroxyl groups. An in vivo study showed that mice treated with catechins enhanced CD8+ mediated adaptive immunity, reducing proinflammatory cytokine gene expression in the lungs and thus inhabiting influenza virus and SARS-CoV-1.[23,24]

Saudi Arabia was hit by outbreaks of influenza virus A-H1N1 from 2009 to 2011 and again from 2014 to 2016. This was also worsened by the MERS coronavirus epidemic in 2012.[25,14] Since coffee and tea in Saudi Arabia are consumed in high quantities daily, and different roasting procedures might result in different compounds, this study was therefore conducted to explore the effect of AC and GT extracts in drinkable forms as a natural antiviral compound against influenza A virus infection in mice.

Materials and Methods

Animal Study and Influenza A virus Infection

The study was carried out on eighty pathogen-free BALBc adult female mice provided by the animal house of King Saud University with an average weight of 17–20 g and aged from five to six weeks old. They were all housed in clean and properly ventilated cages under the same environmental conditions, with free access to food and water throughout the experiment. They were acclimatized to their environment at least two weeks before starting the experiment.

The mice were divided into three major groups (protective, infected, control) and then sub-divided into three subgroups with 10 mice in each sub-group: Group 1 was described as ‘protective pre-infection’ (Subgroup 1a included mice treated with GT extracts, Subgroup 1b had mice treated with roasted brown AC extracts, and Subgroup 1c included mice treated with unroasted green AC extracts). Group 2 was infected with the influenza virus (Subgroup 2a included mice treated with GT extracts post-infection, Subgroup 2b had mice treated with roasted brown AC extract post-infection, and Subgroup 2c included mice treated with unroasted green AC extracts post-infection). Group 3 consisted of control groups: (a. negative control group consisting of asymptomatic mice, and b. infected mice). All mice, except for the normal control group, were infected by aerosol transmission. The influenza A infection dose used in this study was 106 TCID50 (50% tissue culture infectious dose), A/Denver/1/57(H1N1). The 1.5ml of purified aerosol was delivered to individual mice in each group, with one mouse in their cage for 10 minutes. Influenza symptoms were checked daily.

Sample Preparation for Caffeine, CGA, and Catechin Determination

Three natural extracts (GT, brown AC, and green AC) were purchased from a local market. Each sample was prepared every day in a drinkable concentration. The green tea and brown

and green AC samples were first ground. About 3 g of ground samples were added to 100 ml of distilled water, placed over a heater (100 °C), and then given to the mice. Extraction was carried out for 30 minutes. Then the solution was cooled. Next, 1 ml of each extraction and 1ml of acetonitrile were added to each tube, vortexed for 1.5-minute, and then filtered through a disposable syringe filter (Chromafil Xtra PA-45/25) into HPLC vials for analysis, 10µ from each vial.[5]

High-performance liquid chromatography (HPLC)

Separation of caffeine, CGA, and catechin was carried out by HPLC (Waters Alliance 2695 HPLC Separations Module-SN: J18SM4916A-COO, the U.S.) using Xbrige waters C18 250mm×4.6mm×5.0um HPLC column at wavelength detection 210nm. The mobile phase condition was a gradient of 0.5% phosphoric acid in water mixed with methanol (70:30) v/v at a 0.55mL/min flow rate. The injection volume was 10µL; the retention time for catechins, CGA, and caffeine was 6.8 min, 7.5 min, and 8.8 min, respectively. Quantification was determined using peak area and calculated from a five-point standard curve; standard curve points were prepared by dilution in methanol.

Preparation of Stock and Working Solution

Caffeine, catechin, and CGA stock solutions were prepared by taking 1 ml of stock and 9 ml of distilled water. The working standards of the stock solution 0.1, 0.25, 0.5, 1.0, and 1.5 ml were prepared by serial dilution with methanol (Tables 1, 2, 3). The content of caffeine, catechin, and CGA of the GT, and brown and green AC samples were calculated by interpolation within the regression equation of the best line of fit. The results were then presented in mg/ml.

Histopathology Tissue Processing

Fixation and Clearing

The first step was a fixation to denature the protein to render the cells and their components resistant. It was started by using formalin for two hours containing 70% ethanol and then 80% ethanol for two hours. The next step was 90% and 95% ethanol for two hours. For clearing, we used xylene for two hours, washed it with alcohol, and then two more hours of xylene.[16]

Embedding the Tissue

After fixation, the tissue was supported by using paraffin wax to facilitate tissue cutting by using an embedding machine (Thermo Electron Corporation Shandon Histocentre SN:1293060904048, COO; the U.S.). Paraffin wax was dispensed, and the tissue was oriented in the mold, fixed to the bottom using the tamping tool, and then a cassette was placed on top of the mold and filled with wax. To solidify the paraffin wax, the tissue block was placed on a cold plate. Paraffin Section Cutting Sections were prepared by microtome (Thermo electron corporation Shandon-Finesse me+, SN: FN2076M0611, COO; the U.S.), starting with ERMA disposable Microtome Blades Patho Cutter-HP-R by trimming the surface of the block, then cutting 3–5µm thickness slices. The slices were placed in a water bath at 7 °C temperature, then slipped down the slide, removed vertically from the water, and left to dry in an oven for 10 minutes.[26]

Hematoxylin and Eosin Stain Tissue (H&E)

This step is carried out by following regressive HE stains. The slide sections are dipped into xylene baths for 5 minutes to hydrate the lung sections by decreasing the concentration of alcohol baths by 95% then 70% for 1 minute each, washed with distilled water, and then stained in Gill II hematoxylin for 3 minutes. The slide sections are then washed through running water for 2 minutes, then in distilled water and dipped in eosin for 4 minutes, then dehydrated in 95% EtOH. To remove excess eosin, slides were immersed in graded alcohols and then xylene. Once dehydration was completed, a drop of polystyrene mountant was applied, and a coverslip.[16,26]

RNA Extraction

RNA was extracted according to the manufacturer's instructions of the RNA extraction kit of QIAGEN. All centrifuge steps were carried out at room temperature. The wash buffers AW1 and AW2 were prepared; 25ml of 96%-100% ethanol was added to AW1, and 30ml of 96%-100% ethanol was added to AW2. A fresh lysis buffer AVL was prepared and added to 10µl 21 of 1-mercaptoethanol for every 1ml of lysis buffer. Tissue samples obtained from mice were caused to lyze by adding buffer AVL to motivate highly denaturing conditions, to ensure isolation of intact viral RNA, and, most importantly, to inactivate RNases. Buffer AW1 was added, followed by buffer AW2 mixed gently by the vortex. 700µl of the sample was then transferred to the spin cartridge and centrifuged at 12,000g for 15 seconds at room temperature. The used filter was discarded, then RNA was eluted in a special RNase-free buffer AVE to prevent microbial growth. Pure viral RNA was obtained and stored until used.[27]

Amplification of H1N1 Gene

Amplification was performed according to the thawing system (Applied Biosystems, Thermo Fisher Scientific Veriti 96 well thermal cycler, SN:2990234516, COO: Singapore) component and mixed by inverting several times the specific primer used to detect the presence of the H1N1 virus. Except for RNA, the following components were mixed: 25µl of SuperScript III One-Step Reaction Mix (2X), 2µl SuperScript III One-Step Enzyme Mix (25X), 2µl of Forward Primer (10µM), 2µl of Reverse Primer (10µM), 14µl of Nuclease-free H2O, and 5V of total RNA (up to 1µg), with a total volume of 50µl. The RNA template was added last, and the reactions started immediately.[28,29] We amplified two PCR products using four primers. The first product had a length of 1264bp. The second amplicon or PCR product was 913bp long. Together they overlapped and covered the entire hemagglutinin gene length of 1710 bp.

Gel Electrophoresis

The PCR products were visualized in 1% agarose gel, by mixing 1g agarose in 100ml 1×TAE buffer. The solution was boiled in a microwave for one minute. The solution was not over-boiled so that the buffer and the final percentage of agarose in the gel were not affected (Table 5). For the final concentration, 0.2-0.5µg/ml ethidium bromide was added to show the bands bound to RNA under ultraviolet light. A gel tray with a well comb was prepared at room temperature. The agarose gel without bubbles was poured into the gel tray without bubbles. Solidification was completed within 20–30 minutes. The loading buffer was then added to each sample. As it contained glycerol, it increased the density of samples to prevent diffusing. The gel box was filled with a 1×running buffer. Five microliters of 1Kb plus the DNA

ladder molecular marker and the PCR product were loaded on the gel. Gel electrophoresis was performed at 120V and 100mA for 60 minutes. Gel (Owl™ Easy Cast™ B1A Mini Gel Electrophoresis Systems, SN:300163431, COO: United States) pictures were recorded by Bio-Rad (Cheick touch Imaging Systems, SN:732BR1055, COO; Singapore).[30]

Statistical analysis was performed using the statistical software package SPSS version 26.0 (SPSS Inc, Armonk, NY: IBM Corp). The Kaplan-Meier (KM) method was used to analyze 'time-to-event' data. A probability value of $P<0.05$ was considered statistically significant.

Ethical Considerations

The proposal for research was approved by the Institutional Review Board, Faculty of Science, Princess Nourah Bint Abdulrahman University, IRB Registration number with KACST, KSA: H-01-R-059 and IRB Log Number: 19-0212. Research procedures were carried out in accordance with national and institutional regulations. Animal welfare, housing, husbandry, and pain management procedures complied with the relevant European Animal Research Association legislation.

Results

Qualification Analysis of All Extracts by HPLC

The HPLC quantification analysis method showed good separation peaks for caffeine, catechin, and CGA in different retention times (Figure 1). The quantification measurement of the components in GT, green AC, and brown AC by HPLC analysis using a PDA detector was carried out (Figure 2). Caffeine concentration has the highest value in GT rather than in green AC or AC (Table 1). CGA concentration was highest in green AC, while catechin was highest in GT.

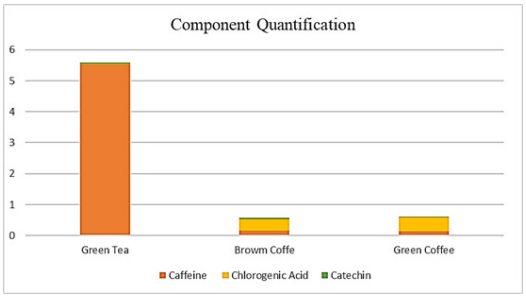

Fig. 1. *Chromatogram for active ingredient separation using HPLC.*

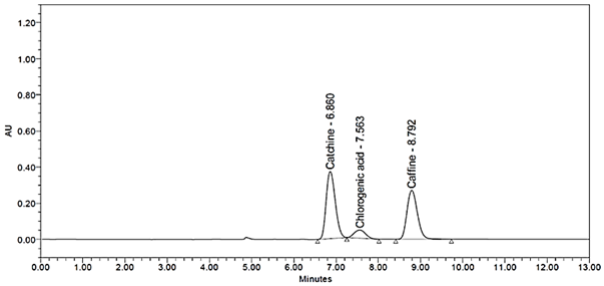

Fig. 2. *Component quantification in green tea, brown coffee, and green coffee by HPLC.*

Table 1.

Caffeine, Chlorogenic acid, and Catechin peak area and concentration of green tea, brown and green coffee.

Name of sample		Concentration (µg/mL)	Peak area	Final amount (mg/ml)
Caffeine	Green Tea	3.915	120891	0.026
	Brown Coffee	56.732	357725	0.38
	Green Coffee	66.534	420198	0.44
Chlorogenic acid	Green Tea	827.680	1954683	5.518
	Brown Coffee	23.180	525512	0.155
	Green Coffee	22.075	499020	0.147
Catechin	Green Tea	7.199	1193816	0.048
	Brown Coffee	5.196	155516	0.034
	Green Coffee	4.619	136058	0.031

Effect of Extracts on Influenza Virus

Subgroup 1c mice showed marked improved pulmonary sections manifested by fewer lesions of inflammatory cells (black arrow) and healthy lung tissue histopathology (Figures 3 a, b, and c).

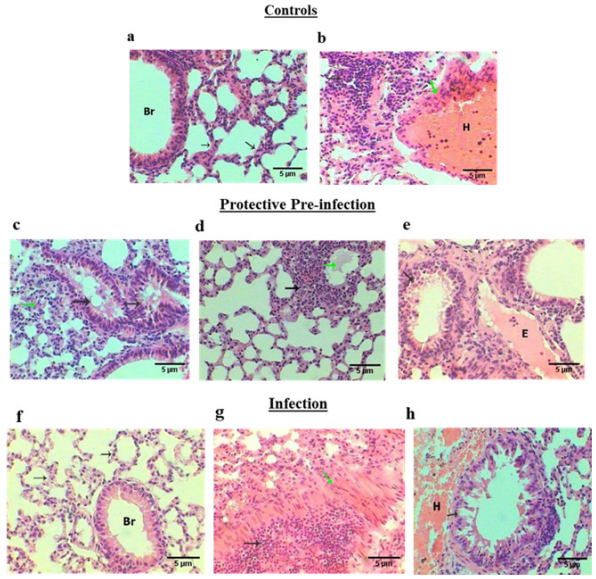

Fig. 3. *(a) Negative control lung tissue. Bronchiole (Br), alveolar intersepta (black arrows) (H&E stain: 400 X). (b) Positive control lung tissue. Hemorrhage (H), hyaline membrane (green arrow) (H&E stain: 400x). (c) Protective GC lung tissue. Inflammatory cells (black arrow), edema (green arrow) (H&E stain: 400x). (d) Protective GT lung tissue. Hyperplasia (black arrow), edema (E) (H&E stain: 400x). (e) Protective BC lung tissue. Collapsed bronchioles (black arrows), leukocytic exudate (green arrow) (H&E stain: 400x). (f) Treated with GT lung tissue. Bronchiole (Br), alveolar intersepta (black arrows) (H&E stain: 400x). (g) Treated with BC lung tissue. Inflammation (black arrow), hyaline membrane (green arrow) (H&E stain: 400x). (h) Treated with GC lung tissue. Hemorrhage (H) destructed bronchiole cells (black arrow) (H&E stain: 400x).*

In addition to steady body weight, there was a slight rise in lung weight and a stable survival rate (100%) compared to the positive and negative controls (Table 2). Subgroup 1b mice displayed some pathological changes represented by hyperplasia (black arrow) of bronchioles columnar epithelia, in addition to the formation of hyaline membranes and edema (Figure 3 (e). There was steady body weight, a slight rise in lung weight, and a small decrease in survival rate (80%) compared to the positive and negative controls. Subgroup 1a mice showed marked pathological alterations characterized by collapsed bronchioles (black arrow) filled with edema, as well as exudate of leukocytic infiltration (green arrow) (Figure 3 (d). Steady body weight, a slight rise in lung weight, and a stable survival rate (100%) were observed when compared with the positive and negative controls. Polyphenolic compounds present in all these extracts, particularly catechin, and CGA, are known to have strong anti-influenza activity by inhibiting various steps in the virus life cycle. Thus, unroasted green AC extracts showed the strongest antiviral activity, compared with roasted brown AC and GT.

Table 2.

The measurement of body weight and lung weight in grams and the survival rate (%) of each group.

Group	Subgroup	Body weight (g)	Lung weight (g)	Survival rate (%)
Protective group	1a) green tea	16.76	0.30	100
	1b) brown coffee	15.70	0.36	80
	1c) green coffee	16.73	0.33	100
Control group	a.) negative control	16.31	0.34	90
	b.) positive control	12.21	0.41	30
Infected group	2a) green tea	13.88	0.34	40
	2b) brown coffee	15.94	0.41	80
	2c) green coffee	16.27	0.37	80

Subgroup 2c mice showed improvement, manifested by completely opened bronchioles and thin healthy alveolar septa (black arrow) (Figure 3 (h). However, Subgroup 2b mice showed severe alterations represented by thick alveolar septa due to the exudate of inflammatory cells, the formation of wide hyaline membranes, and great aggregations of inflammatory cells (black arrow) (Figure 3 (g). Furthermore, Subgroup 2a mice revealed adverse effects manifested by the destruction of the bronchiolar columnar epithelia (black arrow), in addition to wide areas of hemorrhage (Figure 3 (f).

Experimental Use of Mice

Protective pre-infection subgroups were treated for two weeks before the infection with GT, brown AC, and green AC extracts. These mice were healthy and hyper-activated after the infection. The bodies of the mice were weighed daily. Lung weight was taken on day seven after infection initiation (Table 2). We noticed from Days 2–5 that the mice experienced slight weight loss, hair redness, lack of energy, and eye and nose irritation (Figure 4 (a).

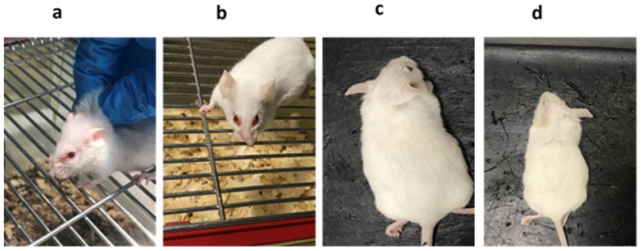

Fig. 4. *Experimental Animals*: **(a)** *Mice infected with H1N1-protective group.* **(b)** *Mice infected with H1N1-infected group.* **(c)** *Negative control-healthy mouse.* **(d)** *Positive control infected with H1N1.*

In infected subgroups, symptoms appeared within 2-5 days: significant weight loss, hair redness, and eye and nose irritation (Figure 4 (b). In addition, there was an energy reduction, and the number of deaths increased sharply in infected groups. The mice were weighed daily, and lung weight was taken on Day 7 after infection initiation (Table 2).

PCR and Gel Electrophoresis

In addition to the results of lung tissue observations, survival rate analysis, and clinical observations, PCR products were not detected in Group 1. Supplementary Figure 1 shows negative PCR results for the H1N1 hemagglutinin (HA) gene analyzed for Subgroups 1a-c. For gel band quantification, we further analyzed the thickness of each band in Group 2 using ImageJ software (Table 3). The extracts showed the potent inhibition effect of influenza virus replication in the lungs of infected mice.

The HA gene for H1N1 influenza viruses with expected PCR product (1264 bp) for Subgroups 1a-c and HA gene for

Table 3.

Quantifying Hemagglutinin gene (HA) bands in infected groups showing the thickness of each band by using ImageJ software.

Quantification of the *HA* gene bands								
	Green Tea	Brown Coffee	Green Coffee	Green Tea	Brown coffee	Green Coffee	Positive Control	Negative Control
ImageJ quantification	395055	232472	212829	212829	345785	337908	881860	128180

H1N1 influenza viruses with PCR product (1264 bp) for Subgroups 2a-c (Figure 1). In Group 2, we observed flu-like clinical signs. Following this observation, extracts were given, and weight loss, respiratory symptoms, and survival rates were recorded. In agreement with findings from the lung tissue when observing inflammatory cells, PCR results also showed bands HA (1264 bp) representing the effect of treating mice with the extract after the onset of clinical symptoms (Figure 1).

Discussion

In this study, we reported that HPLC quantification analysis showed the highest caffeine catechin contest was in GT; these findings are in agreement with a study by Lee et al.[31] that found GT inhibited the influenza A-H1N1 in chicken egg and mice models but did not reduce the symptoms. The study addressed the effect of GT as an antiviral, with evidence of inhibiting the influenza virus A H1N1 in the early phase of the virus's life cycle. Supporting the current study, in the Subgroup 1a mice with protective pre-infection GT use, GT had the highest caffeine and catechin, whereas, in a study by Lee et al.,[31] GT catechin inhibited initial entry of the influenza virus.

Our findings suggest an association between treatment in the protective pre-infection Subgroups 1a-c and stable body weight and a decrease in symptoms, as histopathology showed healthy lung tissue with a few inflammatory cells in protective groups. However, treatment after infection did not present this association. Using quantitative reverse transcription PCR, Lee with colleagues[31] found inhibitory effects in neuraminidase and strong inhibitory activity on hemagglutinin in the protective pre-infection GT group.

In 2014, Utsunomyia et al.[32] studied the effect of reagents caffeic acid, quinic acid, and CGA on the multiplication of the influenza A virus. They found that the infected cells were suppressed after receiving the reagents in the early stage of the infection. The degree of suppression became less prominent with the delay of the reagent to the infected cell culture. These results help to explain the results from the current study, as the protective pre-infection subgroups presented with a healthier body and lung weight, a higher survival rate, decreased inflammation of cells in lung tissue, and negative bands in gel electrophoresis of the virus in the lungs and infected groups experienced a decrease in body weight and an increase in lung weight. The relationship between lung tissue weight before and after treatment showed an increase in infected lung weight due to an increased number of inflamed cells and serous fluid. Histopathology showed apparent inflammation in lung tissue and positive clear bands in gel electrophoresis.

These findings are likely to be due to the coffee components strongly interfering with the multiplication of the influenza A virus. When added in the early stage of infection, coffee extract interacts with certain enzymes necessary for preparing viral RNA and affects the formation of progeny virus to a limited extent when added after the onset of RNA replication.[32] The reagents that used Utsunomyia with colleagues [32] were chemically modified, not natural extracts with multiple effective components. There was no in vivo experiment in their study to test the effect of these reagents on live infections and the subsequent effects on health. CGA seems to have the ability to reduce significant symptoms and increase the survival rate.

Most research involving natural extraction illustrates an antiviral effect in different proteins in the structure of the virus. Components also acted as inhibitors in the first stage of the life cycle of the virus. However, similar studies have examined the antiviral effect after infection; most have been in vitro, and only a few in vivo.[33] Our findings demonstrate that natural extraction plays an important role as an anti-influenza with minimal side effects, most likely due to the inhibitory effects of catechins, which could be interpreted as suppressed viral replication activity. The replication is thus halted by preventing the release of the virus.[34] CGA on NS1 (nonstructural protein 1) is a protective viral protein that regulates the host gene expression and disarms interferon.[35]

This research concluded that natural extraction has an important and effective role in reducing the symptoms of infections and increasing survival rates. The results show that GT is the most effective, reducing both the viral quantity in the lungs and pathological signs in histology. GT tea showed a strong effect on survival rates and reduced symptoms, especially in the protective groups. Despite these promising results of correlations between natural extraction, reduced symptoms of the influenza virus, and increased survival rate with minimal side effects, questions remain unanswered as to which viral proteins are targeted by natural extract and which molecular mechanisms the antiviral inhibition is interfering with. More studies need to address different concentrations of natural extracts and compare them with active molecules using GC-Ms spectrometry.

The study highlighted the protective effect of green tea and Arabica coffee on the influenza virus in vivo. To better understand the implication of these results, future studies should focus on the impact of green tea and Arabica coffee on influenza viruses and other respiratory viruses in vitro, addressing the effects on the virus life-cycle in order to determine the direct medicinal impacts of natural extraction on the structure of viruses or indirectly on the immune system.

Competing Interests

The authors declare that they have no competing interests.

Acknowledgments

The authors acknowledge the assistance provided by the Infectious Diseases Vaccines Chair at King Saud University and King Abdulaziz City for Science and Technology, Life Science & Environment Research Institute labs. The authors are also thankful for the training provided by Mr. Saad Alamri and Mr. Murad Alshehry at King Fahd Medical City.

References

1. Cianci R, Newton EE, Pagliari D. Efforts to Improve the Seasonal Influenza Vaccine. Vaccines (Basel). 2020 Nov 3;8(4):645. doi: 10.3390/vaccines8040645.
2. Idriss MT, Abdelgadir AA, Nour AH. In Vitro Antiviral Activity of Rooibos Tea (Aspalathus linearis) Leaves Aqueous Extract against Influenza Virus. Trop J Nat Prod Res, 2021.
3. Calixto JB. The role of natural products in modern drug discovery. An Acad Bras Cienc. 2019;91 Suppl 3:e20190105. doi: 10.1590/0001-3765201920190105.
4. Newman DJ, Cragg GM. Natural Products as Sources of New Drugs from 1981 to 2014. J Nat Prod. 2016 Mar 25;79(3):629-61. doi: 10.1021/acs.jnatprod.5b01055.
5. Garigliany MM, Desmecht DJ. N-acetylcysteine lacks universal inhibitory activity against influenza A viruses. J Negat Results Biomed. 2011 May 9;10:5. doi: 10.1186/1477-5751-10-5.
6. Dias DA, Urban S, Roessner U. A historical overview of natural products in drug discovery. Metabolites. 2012 Apr 16;2(2):303-36. doi: 10.3390/metabo2020303.
7. Gamaleldin E, et al. Neuraminidase inhibition of Dietary chlorogenic acids and Gamaleldin Elsadig Karar M, Matei MF, Jaiswal R, Illenberger S, Kuhnert N. Neuraminidase inhibition of Dietary chlorogenic acids and derivatives - potential antivirals from dietary sources. Food Funct. 2016 Apr;7(4):2052-9. doi: 10.1039/c5fo01412c.
8. Chiang LC, Chiang W, Chang MY, Ng LT, Lin CC. Antiviral activity of Plantago major extracts and related compounds in vitro. Antiviral Res. 2002 Jul;55(1):53-62. doi: 10.1016/s0166-3542(02)00007-4.
9. Khan MT, Ather A, Thompson KD, Gambari R. Extracts and molecules from medicinal plants against herpes simplex viruses. Antiviral Res. 2005 Aug;67(2):107-19. doi: 10.1016/j.antiviral.2005.05.002. Erratum in: Antiviral Res. 2005 Sep;67(3):169.
10. Ramírez-Aristizabal LS, Ortíz A, Restrepo-Aristizabal MF, Salinas-Villada JF. Comparative study of the antioxidant capacity in green tea by extraction at different temperatures of four brands sold in Colombia. Vitae. 2007;24(2).
11. Madsen A, Cox RJ. Prospects and Challenges in the Development of Universal Influenza Vaccines. Vaccines (Basel). 2020 Jul 6;8(3):361. doi: 10.3390/vaccines8030361.
12. Ngom RBV, Foyet HS. In vitro antibacterial, non-cytotoxic and antioxidant activities of *Boscia Senegalensis* and T*apinanthus Dodoneifolius,* plants used by pastoralists in Cameroon". Pastoralism. 2022;12(13).
13. Li W, Xing L, Fang L, Wang J, Qu H. Application of near infrared spectroscopy for rapid analysis of intermediates of Tanreqing injection. J Pharm Biomed Anal. 2010 Nov 2;53(3):350-8. doi: 10.1016/j.jpba.2010.04.011.
14. Takahashi T, Kokubo R, Sakaino M. Antimicrobial activities of eucalyptus leaf extracts and flavonoids from Eucalyptus maculata. Lett Appl Microbiol. 2004;39(1):60-4. doi: 10.1111/j.1472-765X.2004.01538.x.
15. Ghisalberti EL. Bioactive acylphloroglucinol derivatives from Eucalyptus species. Phytochemistry. 1996 Jan;41(1):7-22. doi: 10.1016/0031-9422(95)00484-x.
16. Morton J, Snider TA. Guidelines for collection and processing of lungs from aged mice for histological studies. Pathobiol Aging Age Relat Dis. 2017 Apr 21;7(1):1313676. doi: 10.1080/20010001.2017.1313676.
17. Naveed M, Hejazi V, Abbas M, Kamboh AA, Khan GJ, Shumzaid M, Ahmad F, Babazadeh D, FangFang X, Modarresi-Ghazani F, WenHua L, XiaoHui Z. Chlorogenic acid (CGA): A pharmacological review and call for further research. Biomed Pharmacother. 2018 Jan;97:67-74. doi: 10.1016/j.biopha.2017.10.064.
18. Trugo LC. COFFEE | Analysis of Coffee Products. *Encyclopedia of Food Sciences and Nutrition (Second Edition),2003;*1498–1506. doi.org: 10.1016/b0-12-227055-x/00271-6
19. Muchtaridi M, Lestari D, Khairul Ikram NK, Gazzali AM, Hariono M, Wahab HA. Decaffeination and Neuraminidase Inhibitory Activity of Arabica Green Coffee (*Coffea arabica*) Beans: Chlorogenic Acid as a Potential Bioactive Compound. Molecules. 2021 Jun 4;26(11):3402. doi: 10.3390/molecules26113402.
20. van Dam RM, Hu FB, Willett WC. Coffee, Caffeine, and Health. N Engl J Med. 2020 Jul 23;383(4):369-378. doi: 10.1056/NEJMra1816604.
21. National Center for Biotechnology Information. PubChem Compound Summary for CID 2519, Caffeine. Retrieved September 11, 2022. Available from https://pubchem.ncbi.nlm.nih.gov/compound/
22. Yu J, Zhang W, Huo W, Meng X, Zhong T, Su Y, Liu Y, Liu J, Wang Z, Song F, Zhang S, Li Z, Yu X, Yu X, Hua S. Regulation of host factor γ-H2AX level and location by enterovirus A71 for viral replication. Virulence. 2022 Dec;13(1):241-257. doi: 10.1080/21505594.2022.2028482.
23. Fan FY, Sang LX, Jiang M. Catechins and Their Therapeutic Benefits to Inflammatory Bowel Disease. Molecules. 2017 Mar 19;22(3):484. doi: 10.3390/molecules22030484.
24. Yang CC, Wu CJ, Chien CY, Chien CT. Green Tea Polyphenol Catechins Inhibit Coronavirus Replication and Potentiate the Adaptive Immunity and Autophagy-Dependent Protective Mechanism to Improve Acute Lung Injury in Mice. Antioxidants (Basel). 2021 Jun 7;10(6):928. doi: 10.3390/antiox10060928.
25. Smee DF, Hurst BL, Wong MH. Effects of TheraMax on influenza virus infections in cell culture and in mice. Antivir Chem Chemother. 2011 Jul 4;21(6):231-7. doi: 10.3851/IMP1744.
26. Fukushi M, Ito T, Oka T, Kitazawa T, Miyoshi-Akiyama T, Kirikae T, Yamashita M, Kudo K. Serial histopathological examination of the lungs of mice infected with influenza A virus PR8 strain. PLoS One. 2011;6(6):e21207. doi: 10.1371/journal.pone.0021207.
27. Bachman J. Reverse-transcription PCR (RT-PCR). Methods Enzymol. 2013;530:67-74. doi: 10.1016/B978-0-12-420037-1.00002-6.

***Corresponding author:** Dr. Rania Suliman, Department of Clinical Laboratory Sciences, Prince Sultan Military College of Health Sciences, Dhahran, Saudi Arabia. E-mail: rsuliman@psmchs.edu.sa*

28. Waters DL, Shapter FM. The polymerase chain reaction (PCR): general methods. Methods Mol Biol. 2014;1099:65-75. doi: 10.1007/978-1-62703-715-0_7.
29. Naeem A, Elbakkouri K, Alfaiz A, Hamed ME, Alsaran H, AlOtaiby S, Enani M, Alosaimi B. Antigenic drift of hemagglutinin and neuraminidase in seasonal H1N1 influenza viruses from Saudi Arabia in 2014 to 2015. J Med Virol. 2020 Mar 11;92(12):3016–27. doi: 10.1002/jmv.25759.
30. Poddar SK. Influenza virus types and subtypes detection by single step single tube multiplex reverse transcription-polymerase chain reaction (RT-PCR) and agarose gel electrophoresis. J Virol Methods. 2002 Jan;99(1-2):63-70. doi: 10.1016/s0166-0934(01)00380-9.
31. Lee HJ, Lee YN, Youn HN, Lee DH, Kwak JH, Seong BL, Lee JB, Park SY, Choi IS, Song CS. Anti-influenza virus activity of green tea by-products in vitro and efficacy against influenza virus infection in chickens. Poult Sci. 2012 Jan;91(1):66-73. doi: 10.3382/ps.2011-01645.
32. Utsunomiya H, Ichinose M, Ikeda K, Uozaki M, Morishita J, Kuwahara T, Koyama AH, Yamasaki H. Inhibition by caffeic acid of the influenza A virus multiplication in vitro. Int J Mol Med. 2014 Oct;34(4):1020-4. doi: 10.3892/ijmm.2014.1859.
33. Craig AP, Fields C, Liang N, Kitts D, Erickson A. Performance review of a fast HPLC-UV method for the quantification of chlorogenic acids in green coffee bean extracts. Talanta. 2016 Jul 1;154:481-5. doi: 10.1016/j.talanta.2016.03.101.
34. Cheng SS, Huang CG, Chen YJ, Yu JJ, Chen WJ, Chang ST. Chemical compositions and larvicidal activities of leaf essential oils from two eucalyptus species. Bioresour Technol. 2009 Jan;100(1):452-6. doi: 10.1016/j.biortech.2008.02.038.
35. Lima FJ, Brito TS, Freire WB, Costa RC, Linhares MI, Sousa FC, Lahlou S, Leal-Cardoso JH, Santos AA, Magalhães PJ. The essential oil of Eucalyptus tereticornis, and its constituents alpha- and beta-pinene, potentiate acetylcholine-induced contractions in isolated rat trachea. Fitoterapia. 2010 Sep;81(6):649-55. doi: 10.1016/j.fitote.2010.03.012.

International Journal of Biomedicine 13(3) (2023) 162-164
http://dx.doi.org/10.21103/Article13(3)_CR1

CASE REPORT

INTERNATIONAL JOURNAL OF BIOMEDICINE

Parapharyngeal Acinic Cell Carcinoma: A Case Report of a Rare Extra-Parotid Occurrence

Rinë Limani[1], Fahredin Veselaj[2*], Zgjim Limani[3], Labinota Kondirolli[4], Brikenë Blakaj Gashi[4]

[1]*Department of Anatomical Pathology, Faculty of Medicine, University of Prishtina "Hasan Prishtina", Prishtina, Kosovo*
[2]*Department of Surgery, Faculty of Medicine, University of Prishtina "Hasan Prishtina", Prishtina, Kosovo*
[3]*Deartment of Othorinolaryngology, Head and Neck Surgery, Faculty of Medicine, University of Prishtina "Hasan Prishtina", Prishtina, Kosovo*
[4]*Faculty of Medicine, University of Prishtina "Hasan Prishtina", Prishtina, Kosovo*

Abstract

Parapharyngeal space (PPS) tumors are among the most challenging tumors of the head and neck region to diagnose and treat. Acinic cell carcinoma (ACC) is an extremely rare extra-parotid malignant neoplasm of the PPS. Herewith, we report a case of extra-parotid, low-grade solid pattern ACC diagnosed in a 55-year-old male who presented with a left parapharyngeal bulge. Despite its rare occurrence, ACC of the PPS should be included in the differential diagnosis of PPS tumors.(**International Journal of Biomedicine. 2023;13(3):162-164.**)

Keywords: pharapharyngeal space • acinic cell carcinoma • extra-parotid

For citation:Limani R, Veselaj F, Limani Z, Kondirolli L, Gashi BB. Parapharyngeal Acinic Cell Carcinoma: A Case Report of a Rare Extra-Parotid Occurrence. International Journal of Biomedicine. 2023;13(3):162-164. doi:10.21103/Article13(3)_CR1

Introduction

Acinic cell carcinoma (ACC) is a malignant neoplasm of the salivary glands, most commonly occurring in the parotid gland. ACC of the minor salivary glands is rare, constituting between 3% and 12% of salivary gland ACCs, with the majority presenting in the minor salivary glands of the palate.(1) ACC is slightly more common in women in their 50s and 60s than in other groups in the population. Previous radiation exposure and familial predisposition are among the most common risk factors for ACC.(1) ACC of the PPS separate from the parotid gland is extremely rare.

***Corresponding author:** Fahredin Veselaj, MD, Ph.D, Department of Surgery, Faculty of Medicine University of Prishtina "Hasan Prishtina", Prishtina, Kosovo. E-mail: fahredin.veselaj@uni-pr.edu*

Case Presentation

A 55-year-old male patient presented with a complaint of a left peritonsillar mass. He had no risky habits, and his family history was irrelevant. On clinical examination, a left parapharyngeal bulge was present. Neck and nasal examinations were unremarkable. On laryngoscopy examination, the larynx was unremarkable as well. Computed tomography (CT) revealed a regular, well-defined mass with a slightly heterogeneous enhancement on the left post-styloid PPS (Figure 1A). The transcervical approach was chosen for surgical excision. Tumor excision revealed a well-encapsulated, soft, rubbery, grayish-white, homogenously solid mass measuring 6×4.5×2.3cm. No invasion of the surrounding structures was seen. Representative sections were taken for histological examination. On histological examination, hematoxylin and eosin-stained slides revealed

a low-grade malignant epithelial tumor composed of well-differentiated basophilic acinar cells with granulated to vacuolar cytoplasm and eccentric nucleus (Figure 1B). There was no vascular or perineural invasion. Surgical margins were free of the tumor. The final histological diagnosis was low-grade ACC solid type.

Discussion

PPS tumors have a nonspecific clinical presentation. They can present as a mass or swelling in the neck or throat, with difficulties in swallowing, breathing, changes in voice or speech, pain in the ear or jaw, or facial weakness.[2] Imaging studies such as CT scans and MRI are used for initial diagnosis; nevertheless, a biopsy followed by surgical resection is necessary to confirm the diagnosis.[2] PPS tumors constitute approximately 0.5% to 1.5% of all head and neck tumors.[3,4] The most common tumors of the PPS are benign tumors such as pleomorphic adenomas of the salivary gland, followed by paragangliomas and neurogenic tumors.[5]

Furthermore, salivary gland neoplasms are the most frequently found primary malignant tumors.[5,6] Salivary neoplasms in PPS may arise from the deep lobe of the parotid gland, ectopic salivary rests, or minor salivary glands of the lateral pharyngeal wall.[5-7] ACC is a rare type of salivary gland tumor in the PPS.[6] In imaging studies, anteromedially parapharyngeal fat displacement by the tumor is a feature that favors extra-parotid tumor origin in PPS.[8]

WHO defines ACC as a malignant epithelial neoplasm of the salivary glands in which at least some neoplastic cells demonstrate serous acinar cell differentiation characterized by cytoplasmic zymogen secretory granules.[9] ACC grows slowly over time, and it usually presents clinically only when it becomes large enough to be detected. ACC is a low-grade neoplasm that was initially considered as a benign tumor entity. It has four histological growth patterns, such as solid, multicystic, papillary-cystic, and follicular.[9] The most frequent histological patterns are solid, composed of well-differentiated polygonal acinar cells with well-defined cytoplasmic borders, and microcystic with prominent cellular vacuolization and intercellular cystic change. Whereas the rarest patterns are the papillary, composed of papilla covered by hobnailed cells, intercalated duct-like cells, and cells with eosinophilic cytoplasm with indistinct cell borders, and the follicular pattern comprised of closely packed cystic spaces lined by flattened epithelium and filled with eosinophilic colloid-like material reminiscent of thyroid follicles.[9]A mixture of patterns is frequent.

ACC of the PPS separate from the parotid gland is extremely rare. In our thorough investigation, when excluding deep parotid lobe ACCs, we encountered only seven reported cases of ACC in the PPS separate from the parotid gland reported in the literature.[6,10-14]

Our case was a solid pattern ACC, presenting in a 55-year-old male. We encountered no invasion of the surrounding structures, as well as no intravascular or perineural invasion. The tumor, in our case, was separate from the parotid gland, indicating that it could be arising from the minor salivary glands of the PPS. ACC on histology comes into close differential diagnosis with other salivary and head and neck masses, such as salivary metastasis of thyroid carcinoma, which are thyroglobulin positive, salivary oncocytoma, composed of eosinophilic non–serous cells, mucoepidermoid carcinoma positive for p63 and mammary analog secretory carcinoma that lacks PAS-positive secretory granules and is vimentin and adipophilin positive.[15,16] In addition to the characteristic morphological presentation, in our case, we also report no positivity for thyroglobulin, p63, vimentin, and adipophilin. Normal salivary gland is also a potential differential diagnosis with ACC.

Nevertheless, our case lacked its normal lobular architecture. Of the reported cases in the literature, all but one case of ACC,[13] separate from the parotid in PPS, were low-grade tumors with no recurrence and metastasis. We also report a low-grade extra- parotid ACC in PPS.

Nevertheless, ACCs of salivary glands have an unpredictable course. Local recurrence has been reported, as have occasional, distant metastasis to the lungs and the bones via hematogenous spread and metastasis to regional lymph nodes. The reported mortality of ACC at 5 years is less than 10%. ACCs of the PPS, because of their rarity and clinical presentation, are challenging to be diagnosed and treat.[17]

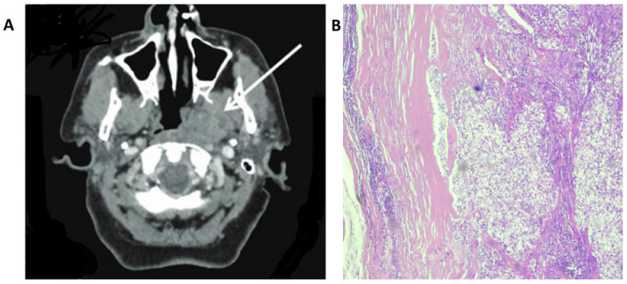

Figure 1. *A. Computed Tomography (CT) presents a regular, well-defined mass with a slightly heterogeneous enhancement on the left post-styloid PPS. B. Histological section of hematoxylin and eosin stained low-grade malignant epithelial tumor, composed of well-differentiated basophilic acinar cells with granulated to vacuolar cytoplasm and eccentric nucleus (X 100).*

Treatment consists of surgical removal of the tumor, which may require complex surgical techniques to preserve important structures, depending on the location of the tumor, including the carotid artery, jugular vein, and cranial nerves. Radiation therapy and chemotherapy may also be used in some cases, alone or in combination with surgery.[7,8] Our case was treated only with surgical resection, as we encountered no invasion beyond the tumor capsule, and the histological features were of no high grade. Moreover, there was no vascular or perineural invasion. However, there are reports of low-grade ACC behaving aggressively; therefore, we opted for treatment with radiation therapy and chemotherapy despite the low-grade morphology.[6,10-13]

In conclusion, extra-parotid ACC of PPS is an extremely rare tumor that should be considered in the differential diagnosis of PPS tumors. Surgical excision ACC is curative

in low-grade tumors with no invasion of the surrounding structures. However, its surgical management is challenging because of the location and relationship with nearby structures, and therefore radiation therapy and chemotherapy are often adjunct treatments to surgical resection.

Competing Interests

The authors declare that they have no competing interests.

References

1. Babu SS, Sunil S, Prathap A, Mathew AL. Acinic cell carcinoma of the posterior buccal mucosa: A rare case report. J Cancer Res Ther. 2020 Apr-Jun;16(3):675-679. doi: 10.4103/jcrt.JCRT_399_18.
2. Jiang C, Wang W, Chen S, Liu Y. Management of Parapharyngeal Space Tumors: Clinical Experience with a Large Sample and Review of the Literature. Curr Oncol. 2023 Jan 11;30(1):1020-1031. doi: 10.3390/curroncol30010078.
3. Galli J, Rolesi R, Gallus R, Seccia A, Pedicelli A, Bussu F, Scarano E. Parapharyngeal Space Tumors: Our Experience. J Pers Med. 2023 Feb 2;13(2):283. doi: 10.3390/jpm13020283.
4. Shahab R, Heliwell T, Jones AS. How we do it: a series of 114 primary pharyngeal space neoplasms. Clin Otolaryngol. 2005 Aug;30(4):364-7. doi: 10.1111/j.1365-2273.2005.00993.x.
5. Riffat F, Dwivedi RC, Palme C, Fish B, Jani P. A systematic review of 1143 parapharyngeal space tumors reported over 20 years. Oral Oncol. 2014 May;50(5):421-30. doi: 10.1016/j.oraloncology.2014.02.007.
6. van Hees T, van Weert S, Witte B, René Leemans C. Tumors of the parapharyngeal space: the VU University Medical Center experience over a 20-year period. Eur Arch Otorhinolaryngol. 2018 Apr;275(4):967-972. doi: 10.1007/s00405-018-4891-x.
7. Hughes KV 3rd, Olsen KD, McCaffrey TV. Parapharyngeal space neoplasms. Head Neck. 1995 Mar-Apr;17(2):124-30. doi: 10.1002/hed.2880170209.
8. Chen Z, Chen YL, Yu Q, Zhou SH, Bao YY, Shang DS, Ruan LX. Excision of tumors in the parapharyngeal space using an endoscopically assisted transoral approach: a case series and literature review. J Int Med Res. 2019 Mar;47(3):1103-1113. doi: 10.1177/0300060518816190.
9. El-Naggar AK, JKC C, Grandis JR, Takata T, Grandis J, Slootweg P (eds). WHO Classification of Head and Neck Tumours, 4th Edition, Volume 9. Lyon, IARC; 2017.
10. Yokoyama M, Nomura Y, Semba T. Acinic cell carcinoma of the parapharyngeal space: case report. Head Neck. 1993 Jan-Feb;15(1):67-9. doi: 10.1002/hed.2880150115.
11. Nguyen J, Palacios E, Horam E, Neitzschman H. Unusual parapharyngeal acinic cell carcinoma. Ear Nose Throat J. 2012 Jan;91(1):16-20. doi: 10.1177/014556131209100105. Erratum in: Ear Nose Throat J. 2012 Feb;91(2):53.
12. Lien KH, Young CK, Chin SC, Liao CT, Huang SF. Parapharyngeal space tumors: a serial case study. J Int Med Res. 2019 Aug;47(8):4004-4013. doi: 10.1177/0300060519862659.
13. Segovia VPK, Alonzo DM, Ong EAV. Parapharyngeal Acinic Cell Carcinoma: Initially Managed as a Case of Peritonsillar Abscess. Int J Head Neck Surg. 2022;13(3):88–9
14. Kumral TL, Uyar Y, Yildrim G, Berkiten G, Salturk Z. Parafarengeal Bölgede Ekstra-Parotidea Asinik Hücreli Karsinom. ENTcase. 2016;2(1):28-32
15. Tumors of the Salivary Glands, Atlas of Tumor Pathology: Third Series. Fascicle 17 G. L. Ellis and P. L. Auclair. Armed Forces Institute of Pathology, Washington D.C. ISBN: 1 881041 26 3 (Printed). 1996.
16. Kumar U. Acinic Cell Carcinoma Papillary-Cystic Variant: Diagnostic Pitfalls in Fine Needle Aspiration Cytology. J Clin Diagn Res. 2017 May;11(5):ED05-ED06. doi: 10.7860/JCDR/2017/21347.9772.
17. Cha W, Kim MS, Ahn JC, Cho SW, Sunwoo W, Song CM, Kwon TK, Sung MW, Kim KH. Clinical analysis of acinic cell carcinoma in parotid gland. Clin Exp Otorhinolaryngol. 2011 Dec;4(4):188-92. doi: 10.3342/ceo.2011.4.4.188.

International Journal of Biomedicine 13(3) (2023) 165-168
http://dx.doi.org/10.21103/Article13(3)_CR2

CASE REPORT

INTERNATIONAL JOURNAL OF BIOMEDICINE

Exploring the Role of MRI in the Detection of Atypical Liver Hemangiomas and Exclusion of Metastases

Floren Kavaja, Fahredin Veselaj*

Faculty of Medicine, University of Prishtina "Hasan Prishtina"
Prishtina, Kosovo

Abstract

Background: In this article, we highlight the importance of utilizing multiple imaging modalities, including CT, MRI, and abdominal Doppler ultrasound, to accurately differentiate between atypical liver hemangiomas (LH) and metastases.

Case report: We introduce a 57-year-old male patient who presented with severe abdominal pain. Initial CT scan findings showed hypodense liver lesions and a well-defined hypodense mass in the sub-diaphragmatic region, raising suspicion for metastatic liver lesions, and prompting further evaluation. To differentiate between atypical hemangiomas and metastases, an MRI scan was performed, revealing a hyperintense signal on T2-weighted images and a hypointense signal on T1-weighted images, consistent with the characteristics of LH. These characteristic signal intensities aided in ruling out metastatic liver lesions, which typically present with a more solid and homogeneous appearance. Contrast-enhanced MRI played a crucial role in confirming the diagnosis. The liver lesions demonstrated moderate vascularization during the early phase of contrast enhancement, followed by progressive centripetal filling during the portal venous and delayed phases. This enhancement pattern is consistent with the slow flow within the dilated vascular spaces of liver hemangiomas. The lesion in the right liver lobe is almost completely filled with contrast, further supporting the diagnosis of hemangioma. Abdominal Doppler ultrasound can provide additional information regarding the vascularity of liver lesions. In this case, the Doppler examination likely helped to further confirm the presence of a hemangioma, as these lesions typically demonstrate increased vascularity compared to metastatic lesions.

Conclusion: The comprehensive imaging evaluation utilizing CT, MRI, and abdominal Doppler ultrasound allowed for the confident differentiation of atypical liver hemangiomas from metastatic liver lesions in this case. This emphasizes the importance of a multimodal imaging approach in cases of liver lesions with overlapping features, leading to improved patient management and outcomes.(**International Journal of Biomedicine. 2023;13(3):165-168.**)

Keywords: liver hemangiomas • liver metastases • MRI • CT • Doppler ultrasound

For citation: Kavaja F, Veselaj F. Exploring the Role of MRI in the Detection of Atypical Liver Hemangiomas and Exclusion of Metastases. International Journal of Biomedicine. 2023;13(3):165-168. doi:10.21103/Article13(3)_CR2

Introduction

Liver hemangiomas (LH) are the most common benign tumors, often discovered accidentally during routine checkups. These lesions present abnormal proliferation of blood vessels, varying in size, and are typically solitary, although multiple hemangiomas can be present in a few cases.[1]

Most LH are asymptomatic and do not require any treatment. However, larger hemangiomas may cause symptoms such as pain or discomfort in the upper abdomen, especially when compressing tissues nearby.[2,3]

Imaging plays a crucial role in the diagnosis of LH. Ultrasound is often the initial imaging modality, providing valuable information regarding the lesion's size, location, and vascularity. However, more definitive and accurate characterization of LH is achieved through cross-sectional imaging techniques such as computed tomography (CT) and magnetic resonance imaging (MRI).[4-6]

MRI, in particular, is highly sensitive and specific for detecting LH. T1-weighted images typically demonstrate a hyperintense signal, whereas T2-weighted images show a heterogeneous, hypointense to hyperintense signal.

***Corresponding author**: Ass. Dr. Fahredin Veselaj, Ph.D. Faculty of Medicine, University of Prishtina "Hasan Prishtina". Prishtina, Kosovo. E-mail: fahredin.veselaj@uni-pr.edu*

Gadolinium-based contrast agents can be used to further enhance the visualization of LH, with rapid enhancement during the arterial phase and progressive centripetal filling during the portal venous and delayed phases. This enhancement pattern results from the slow flow within the dilated vascular spaces of the hemangioma.

LH typically display a characteristic "cavernous" appearance on MRI, with a tangled network of thin-walled blood vessels. This can be visualized as areas of high signal intensity on T2-weighted images.[5,6] Metastases, on the other hand, often present with a more solid and homogeneous appearance. This discrepancy in internal architecture can contribute to the differentiation between LH and metastases.[7]

In contrast, metastatic liver lesions often exhibit a different enhancement pattern, with variable enhancement during different phases depending on the primary tumor type. This disparity in enhancement patterns can be valuable in differentiating LH from metastases.[7] Yet clinical correlation, including the patient's medical history and the presence of primary tumors, provides valuable information to aid in the differentiation process.

MRI's ability to capture the characteristic enhancement patterns, assess the internal architecture, and evaluate the signal intensity characteristics of liver lesions makes it a valuable imaging modality in differentiating LH from metastases. The combination of these features with clinical correlation enhances the accuracy of diagnosis and facilitates appropriate treatment planning for patients.[8]

Case Presentation

We hereby present the case of a 57-year-old male who presented with severe abdominal pain. He is an active smoker, previously diagnosed with peptic ulcers and chronic gastritis.

Initially, the patient underwent a CT scan (Fig.1-3), where the liver presented with a homogenous hypodense lesion in the VII-VIII segment, measuring 3.5×2.5×3 cm, which discretely imbibes contrast but does not homogenate it in the late phase. Another similar hypodense lesion was also found on the IV segment. The stomach was presented with thickened walls. In the sub-diaphragmatic region, between the small stomach curve and the left lobe of the liver and pancreas, there was a hypodense, well-defined mass measuring 5.5×4×6 cm. There were also pre-aortal lymph nodes measuring 1 0mm and advanced left lumbar spine scoliosis.

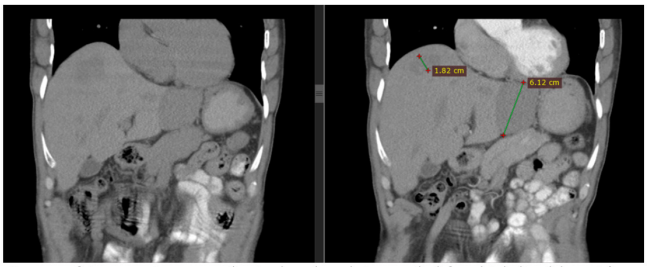

Fig. 1. *Left image: Native CT scan showing hypodense lesions on the left and right liver lobes. Right image: After intravenous contrast application, there is no pathological contrast concentration in the arterial phase.*

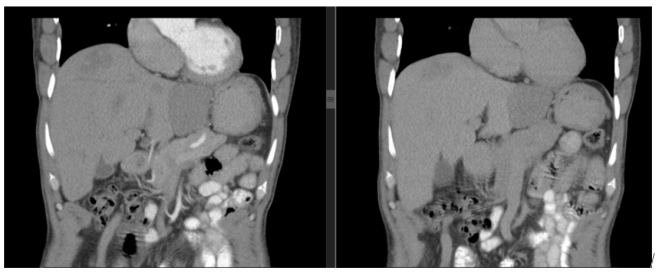

Fig. 2. *Left image: After intravenous contrast application, there is no pathological contrast concentration in the arterial phase. Right image: Venous phase without pathological contrast concentration too.*

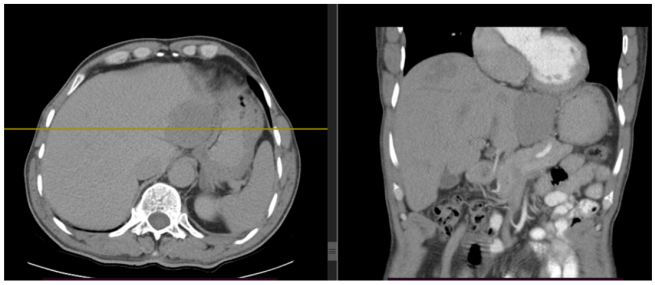

Fig. 3. *Left image: Native CT. Right image: Post-contrast CT.*

Afterward, a gastroscopy revealed hyperemic stomach walls, leading to a diagnosis of chronic gastritis and peptic ulcer. The patient was treated with proton pump inhibitors and sucralfate for three weeks.

An MRI scan (Fig.4-8) was performed to further define the aforementioned findings and differentiate whether liver lesions were atypical hemangiomas or metastasis. The left liver lobe presented with a 49×62 mm lesion with a hyperintense signal on T2 and hypointense in T1 sequences. A small lesion was presented on the right lobe measuring 30×14 mm, with the same MRI characteristics as the previous one. After intravenous contrast application, the lesion showed moderate vascularization in the early phase. In contrast, in the later phase, the lesion in the right liver lobe was almost completely filled with contrast, while in the left lobe, there was centripetal imbibition suggesting hemangioma.

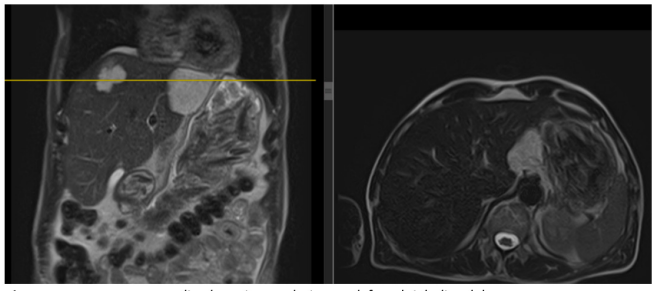

Fig. 4. *T2 sequences revealing hyperintense lesions on left and right liver lobes.*

Additionally, an abdominal echo-Doppler examination was conducted to reaffirm the diagnosis of atypical hemangioma.

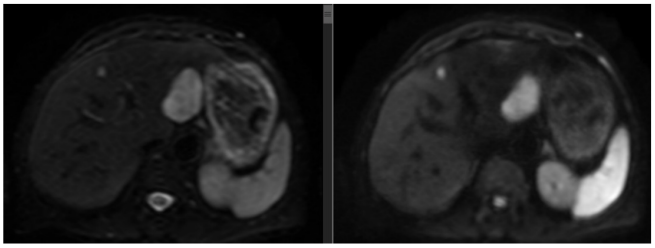

Fig. 5. *DWI sequences revealing restricted diffusion hyperintense lesions on left and right liver lobes.*

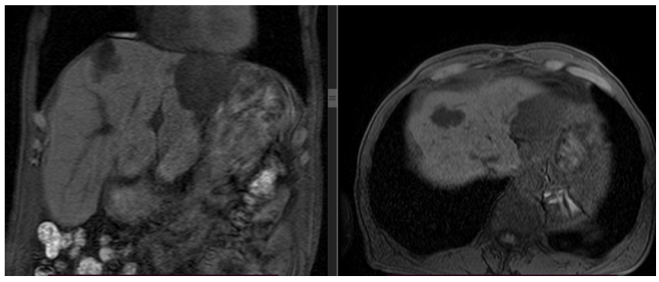

Fig. 6. *In dynamic post-contrast T1 sequence, lesions appear with hypointensity.*

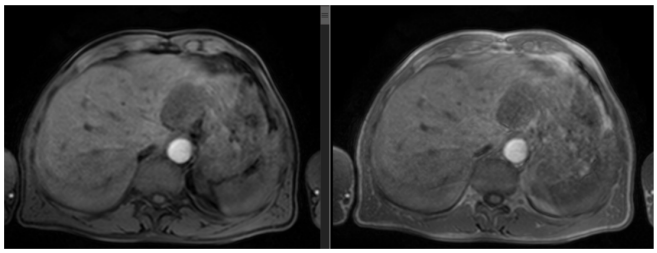

Fig. 7. *After intravenous contrast application on the WFS sequence, there are discrete signs of contrast concentration of the lesion.*

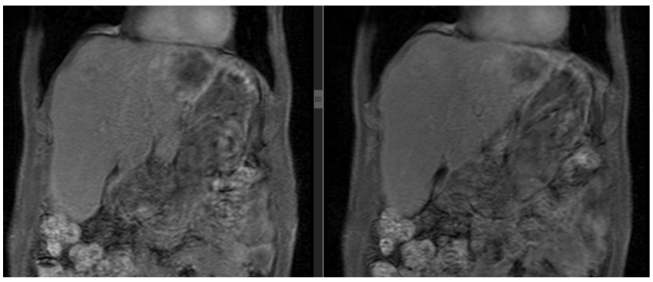

Fig. 8. *The pre-dynamic sequence, 30 minutes after intravenous contrast application, showed that the right liver lobe lesion is almost homogenized. In contrast, the left lobe lesion shows a progressive centripetal typical for hemangioma.*

Discussion

LH pose diagnostic challenges due to their appearance and potential overlap with metastatic lesions. In this case report, our 57-year-old male patient presented with severe abdominal pain. Initial CT scan findings showed hypodense liver lesions in segments IV and VII-VIII, as well as a well-defined hypodense mass in the sub-diaphragmatic region. These findings raised suspicion for metastatic liver lesions, prompting further evaluation.[9]

To differentiate between atypical hemangiomas and metastases, an MRI scan was performed. In this case, the MRI scan revealed a hyperintense signal on T2-weighted images and a hypointense signal on T1-weighted images, consistent with the characteristics of LH. These characteristic signal intensities aided in ruling out metastatic liver lesions, which typically present with a more solid and homogeneous appearance.[9,10]

Furthermore, contrast-enhanced MRI played a crucial role in confirming the diagnosis. The liver lesions demonstrated moderate vascularization during the early phase of contrast enhancement, followed by progressive centripetal filling during the portal venous and delayed phases. This enhancement pattern is consistent with the slow flow within the dilated vascular spaces of LH. The lesion in the right liver lobe is almost completely filled with contrast, further supporting the diagnosis of hemangioma.[10,11]

Abdominal Doppler ultrasound can provide additional information regarding the vascularity of liver lesions. In this case, the Doppler examination likely helped to further confirm the presence of a hemangioma, as these lesions typically demonstrate increased vascularity compared to metastatic lesions.[10]

Overall, this case report highlights the importance of utilizing multiple imaging modalities, including CT, MRI, and abdominal Doppler ultrasound, to accurately differentiate between LH and metastases.[11-14] The characteristic MRI findings, such as the hyperintense signal on T2-weighted images and the dynamic contrast enhancement pattern, were instrumental in ruling out metastatic liver lesions and confirming the diagnosis of atypical hemangiomas. This case emphasizes the value of MRI as a reliable imaging tool for detecting and characterizing LH, aiding in appropriate treatment planning and management decisions for patients.[9-11]

Conclusion

This case report emphasizes the importance of employing a multimodal imaging approach for the accurate diagnosis and differentiation of LH from metastatic liver lesions. The initial CT scan findings raised suspicion for metastatic liver lesions due to the presence of hypodense liver lesions in multiple segments and a well-defined sub-diaphragmatic mass. However, the subsequent MRI scan was pivotal in confirming the diagnosis of atypical hemangiomas. Furthermore, the additional use of abdominal echo-Doppler examination helped to confirm the diagnosis by revealing increased vascularity in the liver lesions, a characteristic feature of hemangiomas.

This case highlights the crucial role of MRI, with its excellent soft tissue contrast, in detecting and characterizing LH. By providing detailed information on signal intensity, and enhancement patterns, MRI aids in distinguishing hemangiomas from metastatic liver lesions, leading to accurate diagnosis and appropriate treatment planning.

In summary, the comprehensive imaging evaluation utilizing CT, MRI, and abdominal Doppler ultrasound allowed

for the confident differentiation of atypical LH from metastatic liver lesions in this case. This emphasizes the importance of a multimodal imaging approach in cases of liver lesions with overlapping features, leading to improved patient management and outcomes.

Competing Interests

The authors declare that they have no competing interests.

References

1. Bajenaru N, Balaban V, Săvulescu F, Campeanu I, Patrascu T. Hepatic hemangioma -review-. J Med Life. 2015;8 Spec Issue(Spec Issue):4-11. PMID: 26361504; PMCID: PMC4564031.
2. Horowitz JM, Venkatesh SK, Ehman RL, Jhaveri K, Kamath P, Ohliger MA, et al. Evaluation of hepatic fibrosis: a review from the society of abdominal radiology disease focus panel. Abdom Radiol (NY). 2017 Aug;42(8):2037-2053. doi: 10.1007/s00261-017-1211-7.
3. Zhang W, Huang ZY, Ke CS, Wu C, Zhang ZW, Zhang BX, Chen YF, Zhang WG, Zhu P, Chen XP. Surgical Treatment of Giant Liver Hemangioma Larger Than 10 cm: A Single Center's Experience With 86 Patients. Medicine (Baltimore). 2015 Aug;94(34):e1420. doi: 10.1097/MD.0000000000001420.
4. Werner JA, Dünne AA, Folz BJ, Rochels R, Bien S, Ramaswamy A, Lippert BM. Current concepts in the classification, diagnosis and treatment of hemangiomas and vascular malformations of the head and neck. Eur Arch Otorhinolaryngol. 2001 Mar;258(3):141-9. doi: 10.1007/s004050100318.
5. Tateyama A, Fukukura Y, Takumi K, Shindo T, Kumagae Y, Kamimura K, Nakajo M. Gd-EOB-DTPA-enhanced magnetic resonance imaging features of hepatic hemangioma compared with enhanced computed tomography. World J Gastroenterol. 2012 Nov 21;18(43):6269-76. doi: 10.3748/wjg.v18.i43.6269.
6. Zheng JG, Yao ZM, Shu CY, Zhang Y, Zhang X. Role of SPECT/CT in diagnosis of hepatic hemangiomas. World J Gastroenterol. 2005 Sep 14;11(34):5336-41. doi: 10.3748/wjg.v11.i34.5336.
7. Lombardo DM, Baker ME, Spritzer CE, Blinder R, Meyers W, Herfkens RJ. Hepatic hemangiomas vs metastases: MR differentiation at 1.5 T. AJR Am J Roentgenol. 1990 Jul;155(1):55-9. doi: 10.2214/ajr.155.1.2112864.
8. akayama Y, Nishie A, Okamoto D, Fujita N, Asayama Y, Ushijima Y, Yoshizumi T, Yoneyama M, Ishigami K. Differentiating Liver Hemangioma from Metastatic Tumor Using T2-enhanced Spin-echo Imaging with a Time-reversed Gradient-echo Sequence in the Hepatobiliary Phase of Gadoxetic Acid-enhanced MR Imaging. Magn Reson Med Sci. 2022 Jul 1;21(3):445-457. doi: 10.2463/mrms.mp.2020-0151.
9. Nouira K, Allani R, Bougamra I, Bouzaidi K, Azaiez O, Mizouni H, Messaoud MB, Menif E. Atypical small hemangiomas of the liver: hypervascular hemangiomas. Int J Biomed Sci. 2007 Dec;3(4):302-4. PMID: 23675058; PMCID: PMC3614658.
10. Sivrioglu AK, Kafadar C. Differentiation between hepatic hemangioma and metastases on diffusion-weighted MRI. Clin Imaging. 2016 Jan-Feb;40(1):183. doi: 10.1016/j.clinimag.2015.09.018.
11. Hui C, Sum R. Hepatic GIST metastases: an illustrative case series. BJR Case Rep. 2022 Jan 10;8(2):20210166. doi: 10.1259/bjrcr.20210166.
12. Coenegrachts K. Magnetic resonance imaging of the liver: New imaging strategies for evaluating focal liver lesions. World J Radiol. 2009 Dec 31;1(1):72-85. doi: 10.4329/wjr.v1.i1.72.
13. Matos AP, Velloni F, Ramalho M, AlObaidy M, Rajapaksha A, Semelka RC. Focal liver lesions: Practical magnetic resonance imaging approach. World J Hepatol. 2015 Aug 8;7(16):1987-2008. doi: 10.4254/wjh.v7.i16.1987.
14. Mamone G, Di Piazza A, Carollo V, Cannataci C, Cortis K, Bartolotta TV, Miraglia R. Imaging of hepatic hemangioma: from A to Z. Abdom Radiol (NY). 2020 Mar;45(3):672-691. doi: 10.1007/s00261-019-02294-8.

International Journal of Biomedicine 13(3) (2023) 169-171
http://dx.doi.org/10.21103/Article13(3)_CR3

CASE REPORT

INTERNATIONAL JOURNAL OF BIOMEDICINE

Management of Impacted Lower Second Molar with Extra Alveolar Tads: A Case Report

Miranda Sejdiu Abazi[1], Arben Abazi[2], Saranda Sejdiu Sadiku[3]

[1]*Department of Dentistry, UBT – College of Higher Education and Institution, Pristina, Kosovo*
[2]*Department of Dentistry, Faculty of Medicine, University of Pristina, Pristina, Kosovo*
[3]*Department of Pharmacy, Faculty of Medicine, University of Pristina, Pristina, Kosovo*

Abstract

The aim of this case report is to present an orthodontic technique combined with skeletal anchorage (TADs) in the retromolar region to pull out a right horizontally impacted mandibular second molar (MM2) beneath the third molar (MM3). This treatment approach was performed by extracting the adjacent MM3 lying over the MM2. A miniscrew was inserted in the retromolar region. It required minimal surgical exposure—mucosal incision, crown uncovering, and attaching a bondable button for uprighting MM2 with an elastic chain. Disimpaction was done for several days without any side effects.(**International Journal of Biomedicine. 2023;13(3):169-171.**)

Keywords: impacted mandibular second molar • temporary anchorage device • fixed appliance

For citation: Abazi MS, Abazi A, Sadiku SS. Management of Impacted Lower Second Molar with Extra Alveolar Tads: A Case Report. International Journal of Biomedicine. 2023;13(3):169-171. doi:10.21103/Article13(3)_CR3

Introduction

The teeth erupt when the root is three-quarters developed. The impaction means that the teeth failed to erupt within a physiological time frame, which is mainly detected late after a routine dental examination.(1)

Management of impacted teeth is very challenging in dentistry. The most prevalent impacted teeth are the third molars .(2,3) The prevalence of an impacted second molar is reported to be under 2%,(4,5) the most common being mesioangular impacted second molars.(5-7) Performing surgical procedures exposing an impacted mandibular second molar (MM2) is safe and reduces treatment time, and the treatment outcome differs from case to case.(8,9) Treatment procedures using temporary anchorage devices (TADs) combined with a surgical approach effectively treat impacted molars.(10) Miniscrews inserted in the ramus of the mandible are reliable in uprighting of horizontally impacted molars and should engage in bone an average of 3 mm.(11)

Case Presentation

A 21-year-old female patient presented to our private clinic for orthodontic treatment. After the clinical evaluation, a panoramic cephalometric was ordered. The image showed the impaction of the right MM2, which was lying beneath the MM3. The patient was unaware of such impaction. The panoramic radiograph presented an impacted MM2 on the right side. The angulation was measured between the long axis of the MM2 and MM with a cephalometric protractor (Figure 1).

Fig. 1. *The angulation of MM2.*

The treatment goal was to treat the impaction and alignment of the teeth. The patient signed an informed consent before treatment therapy. She was informed of procedures, treatment plans, and the advantages and disadvantages of the therapy. Initially, orthodontic fixed appliances, FORESTADENT (Germany) sprint brackets, were used with slot size 22. After the teeth were aligned, the patient was referred to a surgeon to extract MM3. After two weeks, we proceeded to insert a titanium miniscrew (FORESTADENT, Germany) with a length of 8 mm and diameter of 2 mm, manually in the retromolar area, and on the same day, minimal surgery was done - a mucosal incision (Figure 2).

***Fig. 2**. Insertion of a miniscrew in the retromolar area.*

After three weeks, a bondable button was inserted in the distal surface of MM2. A Dentaurum power chain, without pause, was inserted to pull out the impacted molar. The patient was observed twice per month, every month, until the tooth presented in the mouth. After MM2 was pulled, the button was removed, and the tube was placed for further alignment and leveling of MM2 with a continuous wire technique (Figures 3-5). The impaction was corrected in 59 days. The miniscrew was removed after 48 days. Currently, the MM2 is in the process of leveling (Figure 6).

Discussion

The present work described the effectiveness of uprighting of MM2 with extra-alveolar insertion of TADs and elimination of factors such as MM3 that prevented the eruption of MM2. Early diagnosis and early treatment is the primary key to a better prognosis for uprighting the impacted molars.[12] Uprighting of tipped and impacted molar benefits better hygiene, improving functional and periodontal occlusion, and quality of life.[13] Mandibular uprighting treatment with TADs leads to rapid, more predictable results of disimpaction, with fewer side effects.[11] Lee et al.[14] in their study design with direct miniscrew anchorage, concluded that this technique is simple to apply with a positive outcome; even the MM3 could be left in situ, or if it is extracted, the miniscrew could be inserted on the same day.

Lorente and colleagues[15] believe that a miniscrew inserted mesially to an impacted tooth may be the treatment of choice for deeply impacted molars with any angulation.

We can conclude that placement of the miniscrew in the extra-alveolar region is easy and quickly performed and has a great effect on the horizontal disimpaction of the MM2 without any side effects.

Competing Interests

The authors declare that they have no competing interests.

References

1. Kaczor-Urbanowicz K, Zadurska M, Czochrowska E. Impacted Teeth: An Interdisciplinary Perspective. Adv Clin Exp Med. 2016 May-Jun;25(3):575-85. doi: 10.17219/acem/37451.
2. Bhat M, Hamid R, Mir A. Prevalence of impacted teeth in adult patients: A radiographic study. Int J Appl Dent Sci 2019:5(1):10-12.
3. Soh NHBC, Kumar S, Arthi. Prevalence of Impacted Teeth Among Dental Patients - An Institutional Study. European

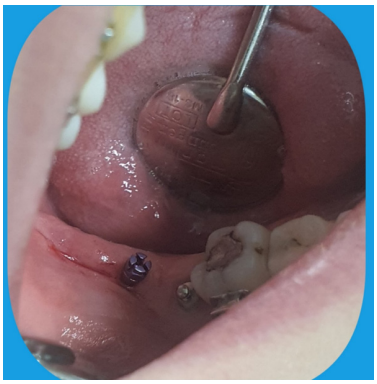

***Fig. 3.** Intraoral view of the miniscrew and bondable button in MM2.*

***Fig.4-5**. The inserted super-elastic archwire was in the tube for uprighting the impacted second molar.*

***Fig. 6.** Alignment and leveling of MM2.*

Journal of Molecular & Clinical Medicine. 2020;7(1):1943-1951.
4. Patil S, Maheshwari S. Prevalence of impacted and supernumerary teeth in the North Indian population. J Clin Exp Dent. 2014 Apr 1;6(2):e116-20. doi: 10.4317/jced.51284.
5. Cassetta M, Altieri F, Di Mambro A, Galluccio G, Barbato E. Impaction of permanent mandibular second molar: a retrospective study. Med Oral Patol Oral Cir Bucal. 2013 Jul 1;18(4):e564-8. doi: 10.4317/medoral.18869.
6. Shapira Y, Finkelstein T, Shpack N, Lai YH, Kuftinec MM, Vardimon A. Mandibular second molar impaction. Part I: Genetic traits and characteristics. Am J Orthod Dentofacial Orthop. 2011 Jul;140(1):32-7. doi: 10.1016/j.ajodo.2009.08.034.
7. Turley PK. The management of mesially inclined/impacted mandibular permanent second molars. J World Fed Orthod. 2020 Oct;9(3S):S45-S53. doi: 10.1016/j.ejwf.2020.09.004.
8. Selvido DI, Wongsirichat N, Arirachakaran P, Rokaya D, Wongsirichat N. Surgical Management of Impacted Lower Second Molars: A Comprehensive Review. Eur J Dent. 2022 Jul;16(3):465-477. doi: 10.1055/s-0041-1739443.
9. Kravitz ND, Yanosky M, Cope JB, Silloway K, Favagehi M. Surgical Uprighting of Lower Second Molars. J Clin Orthod. 2016 Jan;50(1):33-40.
10. Altieri F, Guarnieri R, Mezio M, Padalino G, Cipollone A, Barbato E, Cassetta M. Uprighting Impacted Mandibular Second Molar Using a Skeletal Anchorage: A Case Report. Dent J (Basel). 2020 Nov 18;8(4):129. doi: 10.3390/dj8040129.
11. Tamer İ, Öztaş E, Marşan G. Up-to-Date Approach in the Treatment of Impacted Mandibular Molars: A Literature Review. Turk J Orthod. 2020 May 21;33(3):183-191. doi: 10.5152/TurkJOrthod.2020.19059.
12. Shpack N, Finkelstein T, Lai YH, Kuftinec MM, Vardimon A, Shapira Y. Mandibular Permanent Second Molar Impaction Treatment Options and Outcome. Open Journal of Dentistry and Oral Medicine.2013;1(1):9-14. doi: 10.13189/ojdom.2013.010103
13. Yeh JC, Chao CW, Wu YT, Chou CC, Kao CT. Management of Tipped and Impacted Mandibular Second Molars. Taiwanese Journal of Orthodontics. 2018;30(4):Article 6.
14. Lee KJ, Park YC, Hwang WS, Seong EH. Uprighting mandibular second molars with direct miniscrew anchorage. J Clin Orthod. 2007 Oct;41(10):627-35.
15. Lorente C, Lorente P, Perez-Vela M, Esquinas C, Lorente T. Management of Deeply Impacted Molars with the Miniscrew-Supported Pole Technique. J Clin Orthod. 2018 Nov;52(11):589-97.

***Corresponding author:** *Dr. Sci. Miranda Sejdiu Abazi. Department of Dentistry, UBT – College of Higher Education and Institution, Pristina, Kosovo. E-mail: dr.miranda.sejdiu@gmail.com*

International Journal of Biomedicine 13(3) (2023) 172-174
http://dx.doi.org/10.21103/Article13(3)_ShC

SHORT COMMUNICATION

INTERNATIONAL JOURNAL OF BIOMEDICINE

Asymptomatic Bacteriuria among Pregnant Women Attending Antenatal Care in Sudan

Sara Mohammed Ali[1,2*], Rolla Abdalkader Ahmed Nasser[2], Naima Jama Adam[3], Athar Saed Jama[3], Salma Elnour Rahma Mohamed[1], Hassan Hijazi[1], Sahar Mohammed Seed Ahmed[2]

[1]*College of Health Sciences, Medical Laboratory Sciences Program, Gulf Medical University, Ajman, United Arab Emirates*
[2]*Faculty of Medical Laboratory Sciences, Department of Microbiology, Omdurman Ahlia University, Omdurman, Sudan*
[3]*Faculty of Medical Laboratory Sciences, Department of Microbiology, International University of Africa, Khartoum, Sudan*

Abstract

Background: Asymptomatic bacteriuria is common during pregnancy due to the apparent reduction in immunity of pregnant women, which appears to encourage the growth of both commensal and non-commensal microorganisms. The objective of this study was to determine the frequency of asymptomatic bacteriuria and identify the causative organisms among pregnant women.

Methods and Results: This cross-sectional study was carried out at Ibrahim Malik Teaching Hospital and Bashaier University Hospital from April to July 2019 to assess the prevalence of asymptomatic bacteriuria among pregnant women. Fifty urine specimens were collected from pregnant women who didn't show any signs or symptoms of urinary tract infection. Clean-catch mid-stream urine was collected into a sterile, universal container. Bacteriological culture and bacterial identification were carried out. The prevalence of asymptomatic bacteriuria in pregnant women in this study was 12%. *Escherichia coli* and *Staphylococcus aureus* were the most frequently isolated organisms: 2/6(33.3%) and 2/6(33.3%), respectively, followed by *Proteus species* 1/6(16.7%) and *Klebsiella pneumonia* 1/6(16.7%). Asymptomatic bacteriuria tended to increase from the first to the third trimester (1/8.3%, 2/11.1%, and 3/15%, respectively), but without statistical significance (P=0.845). We also found a trend to increase in the prevalence of asymptomatic bacteriuria with decreasing age: 2(15.4%) in the age group of 18-25 years, 3(11.5%) in the age group of 26-33 years, and only 1(9.1%) in the age group of 34-41 years (P=0.890).

Conclusion: Periodic urine cultures should be performed routinely throughout pregnancy, especially during the first and third trimesters, to identify any unsuspecting unsuspected infection. Bacterial counts are of the most importance and should be done routinely. This measure will significantly reduce maternal and obstetric complications associated with pregnancy.(**International Journal of Biomedicine. 2023;13(3):172-174.**)

Keywords: asymptomatic bacteriuria • pregnancy • urine cultures

For citation: Ali SM, Nasser RAA, Adam NJ, Jama AS, Mohamed SER, Hijazi H, Ahmed SMS. Asymptomatic Bacteriuria among Pregnant Women Attending Antenatal Care in Sudan. International Journal of Biomedicine. 2023;13(3):172-174. doi:10.21103/Article13(3)_ShC

Introduction

Asymptomatic bacteriuria is defined by a mid-stream sample of urine showing bacterial growth >10^5CFU/mL in two consecutive samples in women without urinary tract infection (UTI) symptoms.[1,2] Asymptomatic bacteriuria is common during pregnancy due to the apparent reduction in immunity of pregnant women, which appears to encourage the growth of both commensal and non-commensal microorganisms.[3] UTI causes symptoms such as frequent urination, painful urination, or pelvic pain. Asymptomatic bacteriuria does not cause any noticeable symptoms.[4] Bacteria cause UTIs typically when

they are introduced into the urinary tract during intercourse or when wiping after a bowel movement. The bacterium *E. coli* is responsible for most cases of asymptomatic bacteriuria. Other bacterial species can also cause colonization, including *Klebsiella pneumoniae*, *Proteus mirabilis*, *Pseudomonas aeruginosa*, *Staphylococcal species*, *Enterococci,* and group B *Streptococcus*. [5]

Physiological increases in plasma volume during pregnancy decrease urine concentration, and up to 70% of pregnant women develop glucosuria, which encourages bacterial growth in the urine.[6] In non-pregnant women, asymptomatic bacteriuria rarely causes serious problems. However, this infection can progress upward in pregnant women, causing acute urethritis, cystitis, and pyelonephritis.[7] Asymptomatic bacteriuria is associated with an increased risk of intrauterine growth retardation and low birth-weight infants.[8] Pregnancy enhances the progression from asymptomatic to symptomatic bacteriuria, which could lead to pyelonephritis and adverse obstetric outcomes, such as prematurity, low birth weight, and preterm labor. Preterm labor is a common cause of serious complications, including death, in newborn babies.[9] According to the WHO, up to 45% of pregnant women with untreated asymptomatic bacteriuria will develop pyelonephritis. Untreated asymptomatic bacteriuria leads to the development of symptomatic cystitis in approximately 30% of patients and can lead to the development of pyelonephritis in up to 50%.

It is important to identify factors that increase infection to avoid the consequences and further complications of bacteriuria in pregnant women through early detection and treatment, as the American College of Obstetricians and Gynecologists recommends.[10] However, a routine urine culture test is not carried out for antenatal women in many hospitals in developing countries, including Sudan, probably due to cost implication and time factor for culture results.

The objective of this study was to determine the frequency of asymptomatic bacteriuria and identify the causative organisms among pregnant women.

Materials and Methods

This cross-sectional study was carried out at Ibrahim Malik Teaching Hospital and Bashaier University Hospital from April to July 2019 to assess the prevalence of asymptomatic bacteriuria among pregnant women.

Fifty urine specimens were collected from pregnant women who didn't show any signs or symptoms of UTI. Clean-catch mid-stream urine was collected into a sterile, universal container. Wet preparation and direct Gram stain were done for all specimens. Culture on Cysteine Lactose Electrolyte Deficient agar (CLED) using a calibrated loop drop delivering 0.002ml of urine, which was incubated aerobically at 37°C overnight. Colonial morphology, indirect Gram stains, and biochemical tests, including Kligler iron agar, indole production test, urease test, citrate utilization test, methyl red test, catalase test, coagulase test, and DNase test were done.

Statistical analysis was performed using the statistical software package SPSS version 21.0 (SPSS Inc, Armonk, NY: IBM Corp). Baseline characteristics were summarized as frequencies and percentages. Group comparisons were performed using the chi-square test. A probability value of $P<0.05$ was considered statistically significant.

Results and Discussion

Of the 50 women, 12(24%) were in the first trimester, 18(36%) in the second, and 20(40%) in the third trimester. Asymptomatic bacteriuria tended to increase from the first to the third trimester (1/8.3%, 2/11.1%, and 3/15%, respectively), but without statistical significance (P=0.845).

According to age, pregnant women were distributed as follows: the age group of 18-25 (n=13), the age group of 26-33 years (n=26), and the age group of 34-41 years (n=11). We found a trend to increase in the prevalence of asymptomatic bacteriuria with decreasing age. The asymptomatic bacteriuria prevalence was as follows: 2(15.4%) in the age group of 18-25 years, 3(11.5%) in the age group of 26-33 years, and only 1(9.1%) in the age group of 34-41 years (P=0.890).

Wet preparation showed Pus cells >5 per high power field in 6/50(12%) cases. Colony counts yielding bacterial growth of 10^5CFU/ml or more of pure isolates were considered significant for infection. Gram's staining reaction showed 4 Gram-negative rods and 2 Gram-positive cocci. *Escherichia coli* and *Staphylococcus aureus* were the most frequently isolated organisms: 2/6(33.3%) and 2/6(33.3%), respectively, followed by *Proteus species* 1/6(16.7%) and *Klebsiella pneumonia* 1/6(16.7%).

The prevalence of asymptomatic bacteriuria in pregnant women in this study was 12%. This is slightly lower than the 13% from the study by Ibrahim et al.[11] performed in 2018 in Kosti (Sudan). The most prevalent organism observed in our study was *Escherichia coli* 2/6(33.3%) and *Staphylococcus aureus* 2/6(33.3%). This finding agrees with a study by Sujatha and Nawan done in India.[9]

In this study, the differences in asymptomatic bacteriuria according to the trimesters were insignificant, which agrees with the findings reported by other researchers. In contrast, Kosti Teaching Hospital found increasing prevalence with gestational age.[11]

This study showed a trend to increase asymptomatic bacteriuria prevalence with decreasing age but without statistical differences. In contrast, some studies observed a much higher prevalence of asymptomatic bacteriuria in younger pregnant women.[12,13] Other studies found a progressive rise in bacteriuria prevalence with age.[14,15]

Conclusion

Routine urinalysis is imprecise for the identification of pyuria and bacteriuria. Periodic urine cultures should be performed routinely throughout pregnancy, especially during the first and third trimesters, to identify any unsuspected infection. Bacterial counts are of the most importance and should be done routinely. This measure will significantly reduce maternal and obstetric complications associated with pregnancy.

Competing Interests

The authors declare that they have no competing interests.

References

1. Kass EH. Asymptomatic infections of the urinary tract. Trans Assoc Am Physicians.1956:69:56.
2. Imade PE, Izekor PE, Eghafona NO, Enabulele OI, Ophori E. Asymptomatic bacteriuria among pregnant women. N Am J Med Sci. 2010 Jun;2(6):263-6. doi: 10.4297/najms.2010.2263.
3. Ali R, Afzal U, Kausar S. Asymptomatic Bacteriuria Among Pregnant Women. Annals of Punjab Medical College *(*APMC). 2011;5(2):155-158
4. Cope M, Cevallos ME, Cadle RM, Darouiche RO, Musher DM, Trautner BW. Inappropriate treatment of catheter-associated asymptomatic bacteriuria in a tertiary care hospital. Clin Infect Dis. 2009 May 1;48(9):1182-8. doi: 10.1086/597403.
5. Badran YA, El-Kashef TA, Abdelaziz AS, Ali MM. Impact of genital hygiene and sexual activity on urinary tract infection during pregnancy. Urol Ann. 2015 Oct-Dec;7(4):478-81. doi: 10.4103/0974-7796.157971. Retraction in: Urol Ann. 2019 Jul-Sep;11(3):338.
6. Manjula NG, Girish C, Math GC, Patil A, Gaddad SM, Shivannavar CT. Incidence of Urinary Tract Infections and Its Aetiological Agents among Pregnant Women in Karnataka Region," Advances in Microbiology, 2013;3(6):473-478. doi: .4236/aim.2013.36063.
7. Okwu M, Imade O, Akpoka O A, Olley M, Ashi-ingwu B. Prevalence of Asymptomatic Bacteriuria among Pregnant Women Attending Antenatal Clinics in Ovia North East Local Government Area, Edo State, Nigeria. Iran J Med Microbiol 2021; 15 (2) :227-231
8. Hantush Zadeh S, Khosravi D, Shahbazi F, Kaviani Jebeli Z, Ahmadi F, Shirazi M. Idiopathic urinary findings and fetal growth restriction in low risk pregnancy. Eur J Obstet Gynecol Reprod Biol. 2013 Nov;171(1):57-60. doi: 10.1016/j.ejogrb.2013.08.037.
9. Sujatha R, Nawani M. Prevalence of asymptomatic bacteriuria and its antibacterial susceptibility pattern among pregnant women attending the antenatal clinic at kanpur, India. J Clin Diagn Res. 2014 Apr;8(4):DC01-3. doi: 10.7860/JCDR/2014/6599.4205.
10. Kalinderi K, Delkos D, Kalinderis M, Athanasiadis A, Kalogiannidis I. Urinary tract infection during pregnancy: current concepts on a common multifaceted problem. J Obstet Gynaecol. 2018 May;38(4):448-453. doi: 10.1080/01443615.2017.1370579.
11. Ibrahim OMA, Azoz MEH, Eldeen AAM, Mohammed Ibrahim Alsadig MI, Alagab MBA, Elmugabil A. Asymptomatic Bacteriuria in Pregnant Women at Kosti Teaching Hospital, Kosti-White Nile State (Sudan). Int J Curr Microbiol App Sci. 2018;7(6): 925-930. doi: 10.20546/ijcmas.2018.706.110
12. Gayathree L, Shetty S, Deshpande SR, Venkatesha DT. Screening for Asymptomatic Bacteriuria in Pregnancy: An Evaluation of Various Screening Tests at The Hassan District Hospital, India. Journal of Clinical and Diagnostic Research [serial online]. 2010 August;4:2702-2706.
13. Rohini UV, Reddy GS, Kandati J, Ponugoti M. Prevalence and associate risk factors of asymptomatic bacteriuria in pregnancy with bacterial pathogens and their antimicrobial susceptibility in a tertiary care hospital. Int J Reprod Contracept Obstet Gynecol. 2017;6:558-62.
14. Tan CK, Ulett KB, Steele M, Benjamin WH, Jr, Ulett GC. Prognostic value of semi-quantitative bacteruria counts in the diagnosis of group B streptococcus urinary tract infection: a 4-year retrospective study in adult patients. BMC Infect Dis. 2012;12:273. doi: 10.1186/1471-2334-12-273.
15. Wilson ML, Gaido L. Laboratory diagnosis of urinary tract infections in adult patients. Clin Infect Dis. 2004 Apr 15;38(8):1150-8. doi: 10.1086/383029.

***Corresponding author**: Sara Mohammed Ali, College of Health Sciences, Medical Laboratory Sciences Program, Gulf Medical University. Ajman, United Arab Emirates. E-mail: dr.sara@gmu.ac.ae*

IJBM

INTERNATIONAL JOURNAL OF BIOMEDICINE

Instructions for Authors

International Journal of Biomedicine **(IJBM)** publishes peer-reviewed articles on aspects of basic, applied, and translational research on biology and medicine. International Journal of Biomedicine welcomes submissions of the following types of paper: Original articles, Reviews, Perspectives, Viewpoints, and Case Reports.

All research studies involving animals must have been conducted following animal welfare guidelines such as *the National Institutes of Health (NIH) Guide for the Care and Use of Laboratory Animals*, or equivalent documents. Studies involving human subjects or tissues must adhere to the *Declaration of Helsinki and Title 45, US Code of Federal Regulations, Part 46, Protection of Human Subjects*, and must have received approval from the appropriate institutional committee charged with oversight of human studies. Informed consent must be obtained.

Pre-submissions

Authors are welcome to send an abstract or draft manuscript to obtain a view from the Editor about the suitability of their paper. Our Editors will do a quick review of your paper and advise if they believe it is appropriate for submission to our journal. It will not be a full review of your manuscript.

Manuscript Submission

Manuscript submissions should conform to the guidelines set forth in the Recommendations for the Conduct, Reporting, Editing and Publication of Scholarly Work in Medical Journals (ICMJE Recommendations), available from www.ICMJE.org.

Original works will be accepted with the understanding that they are contributed solely to the Journal, are not under review by another publication, and have not previously been published except in abstract form.

All manuscripts must be submitted through the International Journal of Biomedicine`s online submission system (www.ijbm.org/submission.php). Manuscripts must be typed, double-spaced using a 14-point font, including references, figure legends, and tables. Leave 1-inch margins on all sides. Assemble the manuscript in this order: Title Page, Abstract, Key Words, Text (Introduction, Methods, Results, and Discussion), Acknowledgments, Sources of Funding, Disclosures, References, Tables, Figures, and Figure Legends. References, figures, and tables should be cited in numerical order according to first mention in the text.

The preferred order for uploading files is as follows: Cover letter, Full Manuscript PDF (PDF containing all parts of the manuscript including references, legends, figures and tables), Manuscript Text File (MS Word), Figures (each figure and its corresponding legend should be presented together), and Tables. Files should be labeled with appropriate and descriptive file names (e.g., SmithText.doc, Fig1.eps, Table3.doc). Text, Tables, and Figures should be uploaded as separate files. (Multiple figure files can be compressed into a Zip file and uploaded in one step; the system will then unpack the files and prompt the naming of each figure. See www.WinZip.com for a free trial.)

Authors who are unable to provide an electronic version or have other circumstances that prevent online submission must contact the Editorial Office prior to submission to discuss alternate options (editor@ijbm.org).

Cover Letter

The cover letter should be saved as a separate file for upload. In it, the authors should (1) state that the manuscript, or parts of it, have not been and will not be submitted elsewhere for publication; (2) state that all authors have read and approved the manuscript; and (3) disclose any financial or other relations that could lead to a conflict of interest. If a potential conflict exists, its nature should be stated for each author. When there is a stated potential conflict of interest a footnote will be added indicating the author's equity interest in or other affiliation with the identified commercial firms.

The corresponding author should be specified in the cover letter. All editorial communications will be sent to this author. A short paragraph telling the editors why the authors think their paper merits publication priority may be included in the cover letter.

Types of articles

Original articles

Original articles present the results of original research. These manuscripts should present well-rounded studies reporting innovative advances that further knowledge about a topic of importance to the fields of biology or medicine. These can be submitted as either a full-length article (no more than 6,000 words, 4 figures, 4 tables) or a Short Communication (no more than 2,500 words, 2 figures, 2 tables). An original

article may be Randomized Control Trial, Controlled Clinical Trial, Experiment, Survey, and Case-control or Cohort study.

Case Reports

Case reports describe an unusual disease presentation, a new treatment, a new diagnostic method, or a difficult diagnosis. The author must make it clear what the case adds to the field of medicine and include an up-to-date review of all previous cases in the field. These articles should be no more than 5,000 words with no more than 6 figures and 3 tables. Case Reports should consist of the following headings: Abstract (no more than 100 words), Introduction, Case Presentation (clinical presentation, observations, test results, and accompanying figures), Discussion, and Conclusions.

Reviews

Reviews analyze the current state of understanding on a particular subject of research in biology or medicine, the limitations of current knowledge, future directions to be pursued in research, and the overall importance of the topic. Reviews could be non-systematic (narrative) or systematic. Reviews can be submitted as a Mini-Review (no more than 2,500 words, 3 figures, and 1 table) or a long review (no more than 6,000 words, 6 figures, and 3 tables). Reviews should contain four sections: Abstract, Introduction, Topics (with headings and subheadings, and Conclusions and Outlook.

Perspectives

Perspectives are brief, evidenced-based and formally structured essays covering a wide variety of timely topics of relevance to biomedicine. Perspective articles are limited to 2,500 words and usually include ≤10 references, one figure or table. Perspectives contain four sections: Abstract, Introduction, Topics (with headings and subheadings), Conclusions and Outlook.

Viewpoints

Viewpoint articles include academic papers, which address any important topic in biomedicine from a personal perspective than standard academic writing. Maximum length is 1,200 words, ≤70 references, and 1 small table or figure.

Manuscript Preparation

Title Page

The first page of the manuscript (title page) should include (1) a full title of the article, (2) a short title of less than 60 characters with spaces, (3) the authors' names, academic degrees, and affiliations, (4) the total word count of the manuscript (including Abstract, Text, References, Tables, Figure Legends), (5) the number of figures and tables, and (6) the name, email address, and complete address of corresponding author.

Disclaimers. An example of a disclaimer is an author's statement that the views expressed in the submitted article are his or her own and not an official position of the institution or funder.

Abstract

The article should include a brief abstract of no more than 200 words. Limit use of acronyms and abbreviations. Define at first use with acronym or abbreviation in parentheses. The abstract should be structured with the following headings: Background, Methods and Results, and Conclusions. The Background section should describe the rationale for the study. Methods and Results should briefly describe the methods and present the significant results. Conclusions should succinctly state the interpretation of the data. Authors should supply a list of up to four key words not appearing in the title, which will be used for indexing. The key words should be listed immediately after the Abstract. Use terms from the Medical Subject Headings (MeSH) list of Index Medicus when possible.

Main text in the IMRaD format

Introduction should describe the purpose of the study and its relation to previous work in the field; it should not include an extensive literature review.

Methods should be concise but sufficiently detailed to permit repetition by other investigators. Previously published methods and modifications should be cited by reference. A subsection on statistics should be included in the Methods section.

Results should present positive and relevant negative findings of the study, supported when necessary by reference to Tables and Figures.

Discussion should interpret the results of the study, with emphasis on their relation to the original hypotheses and to previous studies. The importance of the study and its limitations should also be discussed.

The IMRaD format does not include a separate Conclusion section. The conclusion is built into the Discussion. More information on the structure and content of these sections can be found in the Recommendations for the Conduct, Reporting, Editing and Publication of Scholarly Work in Medical Journals (ICMJE Recommendations), available from www.ICMJE.org.

Acknowledgments, Sources of Funding, and Disclosures

Acknowledgments : All contributors who do not meet the criteria for authorship should be listed in an acknowledgments section. Examples of those who might be acknowledged include a person who provided purely technical help, writing assistance, or a department chairperson who provided only general support. Authors should declare whether they had assistance with study design, data collection, data analysis, or manuscript preparation. If such assistance was available, the authors should disclose the identity of the individuals who provided this assistance and the entity that supported it in the published article.

Sources of Funding: All sources of financial support for the study should be cited on the title page, including federal or state agencies, nonprofit organizations, and pharmaceutical or other commercial sources.

Disclosure and conflicts of interest: All authors must disclose any financial or other relations that could lead to a conflict of interest. If a potential conflict exists, its nature should be stated for each author. All sources of financial support for the study should be cited, including federal or state agencies, nonprofit organizations, and pharmaceutical or other commercial sources. Please use ICMJE Form for Disclosure of Potential Conflicts of Interest (http://www.icmje.org/conflicts-of-interest/).

References

References should follow the standards summarized in the NLM's International Committee of Medical Journal Editors (ICMJE) Recommendations for the Conduct,

Reporting, Editing and Publication of Scholarly Work in Medical Journals: Sample References webpage (www.nlm.nih.gov/bsd/uniform_requirements.html) and detailed in the NLM's Citing Medicine, available from www.ncbi.nlm.nih.gov/books/NBK7256/. MEDLINE abbreviations for journal titles (www.ncbi.nlm.nih.gov/nlmcatalog/journals) should be used.

References should be presented in the Vancouver style. The first six authors should be listed in each reference citation (if there are more than six authors, "et al" should be used following the sixth). Periods are not used in authors' initials or journal abbreviations. Examples of journal reference style:

Journal Article: Serruys PW, Ormiston J, van Geuns RJ, de Bruyne B, Dudek D, Christiansen E, et al. A Polylactide Bioresorbable Scaffold Eluting Everolimus for Treatment of Coronary Stenosis: 5-Year Follow-Up. J Am Coll Cardiol. 2016;67(7):766-76. doi: 10.1016/j.jacc.2015.11.060.

Book: Murray PR, Rosenthal KS, Kobayashi GS, Pfaller MA. Medical Microbiology. 4th ed. St. Louis: Mosby; 2002.

Chapter in Edited Book: Meltzer PS, Kallioniemi A, Trent JM. Chromosome alterations in human solid tumors. In: Vogelstein B, Kinzler KW, editors. The Genetic Basis of Human Cancer. New York: McGraw-Hill; 2002:93–113.

References should be numbered consecutively in the order in which they are first mentioned in the text. Identify references in text, tables, and legends by Arabic numerals in parentheses and listed at the end of the article in citation order.

Tables

Tables should be comprehensible without reference to the text and should not be repetitive of descriptions in the text. Every table should consist of two or more columns; tables with only one column will be treated as lists and incorporated into the text. All tables must be cited in the text and numbered in order of appearance. Tables should include a short title. Place explanatory matter in footnotes, not in the heading. Explain all nonstandard abbreviations in footnotes, and use symbols to explain information if needed. Each table submitted should be double-spaced, each on its own page. Each table should be saved as its own file as a Word Document. Explanatory matter and source notations for borrowed tables should be placed in the table footnote.

Figures and Legends

All illustrations (line drawings and photographs) are classified as figures. All figures should be cited in the text and numbered in order of appearance. Figures should be provided in .tiff, .jpeg or .eps formats. Color images must be at least 300 dpi. Gray scale images should be at least 300 dpi. Line art (black and white or color) and combinations of gray scale images and line art should be at least 1,000 dpi. The optimal size of lettering is 12 points. Symbols should be of a similar size. Figures should be sized to fit within the column (86 mm) or the full text width (180 mm). Line figures must be sharp, black and white graphs or diagrams, drawn professionally or with a computer graphics package. Legends should be supplied for each figure and should be brief and not repetitive of the text. Any source notation for borrowed figures should appear at the end of the legend. Figures should be uploaded as individual files.

Units of Measurement

Measurements of length, height, weight, and volume should be reported in metric units (meter, kilogram, or liter) or their decimal multiples. Temperatures should be in degrees Celsius. Blood pressures should be in millimeters of mercury. All measurements must be given in SI or SI-derived units. Drug concentrations may be reported in either SI or mass units, but the alternative should be provided in parentheses where appropriate.

Style and Language

The journal accepts manuscripts written in English. Spelling should be US English only. The language of the manuscript must meet the requirements of academic publishing. Reviewers may advise rejection of a manuscript compromised by grammatical errors. Non-native speakers of English may choose to use a copyediting service.

Abbreviations and Symbols

Use only standard abbreviations; use of nonstandard abbreviations can be confusing to readers. Avoid abbreviations in the title of the manuscript. The spelled-out abbreviation followed by the abbreviation in parenthesis should be used on first mention unless the abbreviation is a standard unit of measurement.

Drugs should be referred to by their generic names. If proprietary drugs have been used in the study, refer to these by their generic name, mentioning the proprietary name, and the name and location of the manufacturer, in parentheses.

Permissions

To use tables or figures borrowed from another source, permission must be obtained from the copyright holder, usually the publisher. Authors are responsible for applying for permission for both print and electronic rights for all borrowed materials and are responsible for paying any fees related to the applications of these permissions. This is necessary even if you are an author of the borrowed material. It is essential to begin the process of obtaining permission early, as a delay may require removing the copyrighted material from the article. The source of a borrowed table should be noted in a footnote and of a borrowed figure in the legend. It is essential to use the exact wording required by the copyright holder. A copy of the letter granting permission, identified by table or figure number, should be sent along with the manuscript. A permission request form is provided for the authors use in requesting permission from copyright holders.

Page Proofs

Page proofs are sent from the Publisher electronically and must be returned within 72 hours to avoid delay in publication. Generally, peer review is completed within 4-5 weeks.

It is important to note that when citing an article from IJBM, the correct citation format is **International Journal of Biomedicine.**

IJBM

INTERNATIONAL JOURNAL OF BIOMEDICINE

International Journal of Biomedicine (IJBM) is an open access journal. IJBM publishes peer-reviewed articles on aspects of basic, applied, and translational research in biology and medicine. The main purpose of IJBM is to establish a scientific platform for targeted promotion of new scientific ideas and biomedical technologies focused on the applied aspects of biomedicine.

The journal publishes articles on:

Internal Medicine
Cardiology
Pulmonology
Endocrinology
Neurology
Hepatology
Gastroenterology
Nephrology
Ophthalmology
Otorhinolaryngology
Radiology
Surgery
Obstetrics and Gynecology
Pediatrics
Dermatology and STD
Clinical Immunology
Oncology
Genomics and Proteomics
Population Genetics
Epidemiology and Population Health
Reproductive Health
Adolescent Health
Cell Biology
Experimental Biology
Biotechnology
Dentistry
Infectious Diseases
Sports Medicine

Authors are invited to submit:

Original clinical and experimental research studies
Review articles
Case reports
Perspectives